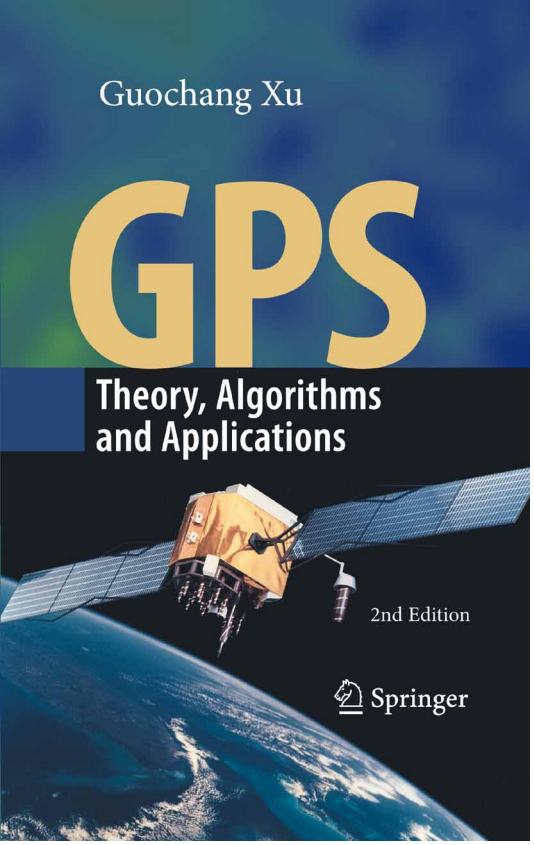

Ketabton.com

(c) ketabton.com: The Digital Library

(c) ketabton.com: The Digital Library

Guochang Xu

GPS

Theory, Algorithms and Applications

Second Edition

With 59 Figures

Springer

(c) ketabton.com: The Digital Library

Author

Guochang Xu, **Dr.-Ing.**
GeoForschungsZentrum Potsdam (GFZ)
Department 1: Geodesy and Remote Sensing
Potsdam, Germany

Library of Congress Control Number: 2007929855

ISBN 978-3-540-72714-9 **Springer Berlin Heidelberg New York**
ISBN 978-3-540-67812-0 (first edition) **Springer Berlin Heidelberg New York**

This work is subject to copyright. All rights are reserved, whether the whole or part of the material is concerned, specifically the rights of translation, reprinting, reuse of illustrations, recitations, broadcasting, reproduction on microfilm or in any other way, and storage in data banks. Duplication of this publication or parts thereof is permitted only under the provisions of the German Copyright Law of September 9, 1965, in its current version, and permission for use must always be obtained from Springer. Violations are liable to prosecution under the German Copyright Law.

Springer is a part of Springer Science+Business Media
springer.com
© Springer-Verlag Berlin Heidelberg 2003, 2007
All rights reserved

The use of general descriptive names, registered names, trademarks, etc. in this publication does not imply, even in the absence of a specific statement, that such names are exempt from the relevant protective laws and regulations and therefore free for general use.

Cover illustration: Copyright © Boeing. All rights reserved.

Cover design: WMXDesign, Heidelberg
Typesetting: Stasch · Bayreuth (stasch@stasch.com)
Production: Christine Adolph
Printing: Krips bv, Meppel
Binding: Stürtz GmbH, Würzburg

Printed on acid-free paper 30/2133/CA – 5 4 3 2 1 0

(c) ketabton.com: The Digital Library

To
Liping, Jia, Yuxi and Pan

(c) ketabton.com: The Digital Library

Preface to the Second Edition

After the first edition of this book was published at the end of 2003, I was very happy to put the hard work of book writing behind me and concentrate myself with my small team on the development of a multi-functional GPS/Galileo software (MFGsoft). The experiences from the practice and the implementation of the theory and algorithms into the high standard software gave me a strong feeling that I would very much like to revise and to supplement the original book, to modify parts of the contents and to report on the new progress and knowledge. Furthermore, with the EU Galileo system now being realised and the Russian GLONASS system under development; the GPS theory and algorithms should be re-described so that they are also valid for the Galileo and GLONASS systems. Therefore, I am grateful to all of the readers of this book, whose interest made it possible so that the Springer asked me to complete this second edition.

I remember that I was in a hurry during the last check of the layout of the first edition. The description of a numerical solution of the variation equation in Sect. 11.5.1 was added to the book at the last minute in a limited extension of exactly one page. Traditionally, the variation equations in orbits determination (OD) and geopotential mapping as well as OD Kalman filtering are solved by integration, which is complicated and computing intensive. In the OD history, this is the first time that the variation equation will not be integrated, but solved by a linear algebra equation system. However, this was mentioned neither in the preface nor at the beginning of the chapter. The high precision of this algebra method is verified by a numerical test.

The problems discussed in Chap. 12 of the first edition are mostly solved and now described by the so-called independent parameterisation theory, which points out that in undifferenced and differencing algorithms the independent ambiguity vector is the double differencing one. Using this parameterisation method, the GPS observation equations are regular ones and can be solved without using any a priori information. Many conclusions may be derived from this new knowledge. For example, the synchronisation of the GPS clocks may not be realised by the carrier phase observables because of the linear correlations between the clock error parameters and the ambiguities. The equivalence principle is extended to show that the equivalences are not only valid between the undifferenced and differencing algorithms, but also valid between uncombined and combining algorithms as well as their mixtures. That is the GPS data processing algorithms are equivalent under the same parameterisation of the observation model. Different algorithms are beneficial for different data processing purposes. One of the consequences of the equivalence theory is that a so-called secondary data processing algorithm is developed. In other words, the complete GPS positioning problem may be separated into two steps (first to transform the data to the secondary

(c) ketabton.com: The Digital Library

observables and then to process the secondary data). Another consequence of the equivalence is that any GPS observation equations can be separated into two sub-equations and this is very advantageous in practice. Further more, it shows that the combinations under the traditional parameterisation are inexact algorithms compared with the combinations under the independent parameterisation.

Supplemented contents include a more detailed introduction, not only concerning the GPS but also the development of the EU Galileo system and Russian GLONASS system as well as the combination of the GPS, GLONASS and Galileo systems. So this book will cover the theory, algorithms and applications of the GPS, GLONASS and Galileo systems. The equivalence of the GPS data processing algorithms and the independent parameterisation of the GPS observation models are discussed in detail. Other new contents include the concept of forming optimal networks, the application of the diagonalisation algorithm, the adjustment models of the radiation pressure and atmospheric drag, as well as the discussions and comments of what are currently, in the author's opinion, the key research problems. The application of the theory and algorithms to the development of the GPS/Galileo software is also outlined. The contents concerning the ambiguity search are reduced while the contents of the ionosphere-free ambiguity fixing are cancelled out, although it is reported by Lemmens (2004) as new. Some of the contents of the sections have also been reordered. In this way I hope this edition may be better served as a reference and handbook of GPS/Galileo research and applications.

The extended contents are partly the results of the development of MFGsoft and have been subjected to an individual review. Prof. Lelgemann of the TU Berlin, Prof. Yuanxi Yang of the Institute of Surveying and Mapping in Xian, Prof. Ta-Kang Yeh of the ChingYun University of Taiwan and Prof. Yunzhong Shen of TongJi University are thanked for their valuable reviews. I am grateful to Prof. Jiancheng Li and Dr. Zhengtao Wang of Wuhan University as well as Mr. Tinghao Xiao of Potsdam University for their cooperation in the software development from 2003 to 2004 at the GFZ.

I wish to sincerely thank Prof. Dr. Markus Rothacher for his support and trust during my research activities at the GFZ. Dr. Jinghui Liu of the educational department of the Chinese Embassy in Berlin, Prof. Heping Sun and Jikun Ou of IGG in Wuhan and Prof. Qin Zhang of ChangAn University are thanked for their friendly support during my scientific activities in China. The Chinese Academy of Sciences is thanked for the Outstanding Overseas Chinese Scholars Fund. During this work, several interesting topics have been carefully studied by some of my students. My grateful thanks go to Ms. Daniela Morujao of Lisbon University, Ms. Jamila Bouaicha of TU Berlin, Dr. Jiangfeng Guo and Ms. Ying Hong of IGG in Wuhan, Mr. Guanwen Huang of ChangAn University. I am also thankful for the valuable feedback from readers and from students through my professorships at ChangAn University and the IGG CAS.

Guochang Xu
June 2007

(c) ketabton.com: The Digital Library

Preface to the First Edition

The contents of this book cover static, kinematic and dynamic GPS theory, algorithms and applications. Most of the contents come from the source code descriptions of the Kinematic/Static GPS Software (KSGsoft), which was developed in GFZ before and during the EU AGMASCO project. The principles described here have been mostly applied in practice and are carefully revised in theoretical aspect. A part of the contents is worked out as a theoretic basis and applied to the developing quasi real time GPS orbit determination software in GFZ.

The original purpose of writing such a book is indeed to have it for myself as a GPS handbook and as a reference for a few of my friends and students who worked with me in Denmark. The desire to describe the theory in an exact manner comes from my mathematical education. My extensive geodetic research experiences have lead to a detailed treatment of most topics. The completeness of the contents reflects my habit as a software designer.

Some of the results of the research efforts carried out in GFZ are published here for the first time. One example is the unified GPS data processing method using selectively eliminated equivalent observation equations. Methods such as the zero-, single-, double-, triple-, and user defined differential GPS data processing are unified in a unique algorithm. The method has both the advantages of un-differential and differential methods; i.e., the un-correlation property of the original observations is still kept, and the unknown number may be greatly reduced. Another example is the general criterion and its equivalent criterion for integer ambiguity search. Using the criterion the search can be carried out in ambiguity, coordinate or both domains. The optimality and uniqueness properties of the criterion are proved. Further examples are the diagonalisation algorithm of the ambiguity search problem, the ambiguity-ionospheric equations for ambiguity and ionosphere determination, as well as the use of the differential Doppler equation as system equation in Kalman filter, etc.

The book includes twelve chapters. After a brief introduction, the coordinate and time systems are described in the second chapter. Because the orbits determination is also an important topic of this book, the third chapter is dedicated to the Keplerian satellite orbits. The fourth chapter deals with the GPS observables, including code range, carrier phase and Doppler measurements.

The fifth chapter covers all physical influences of the GPS observations, including ionospheric effects, tropospheric effects, relativistic effects, Earth tide and ocean loading tide effects, clock errors, antenna mass centre and phase centre corrections, multipath effects, anti-spoofing and historical selective availability, as well as instrumental biases. Theories, models and algorithms are discussed in detail.

(c) ketabton.com: The Digital Library

The sixth chapter first covers the GPS observation equations, such as their formation, linearisation, related partial derivatives, as well as linear transformation and errors propagation. Then useful data combinations are discussed, where, especially, a concept of ambiguity-ionospheric equations and the related weight matrix are introduced. The equations include only ambiguity and ionosphere as well as instrumental error parameters and can also be solved independently in kinematic applications. Traditional differential GPS observation equations, including the differential Doppler equations, are also discussed in detail. The method of selectively eliminated equivalent observation equations is proposed to unify the un-differential and differential GPS data processing methods.

The seventh chapter covers all adjustment and filtering methods, which are suitable and needed in GPS data processing. The main adjustment methods described are classical, sequential and block-wise, as well as conditional least squares adjustments. The key filtering methods discussed are classical and robust as well as adaptively robust Kalman filters. The a priori constraints method, a priori datum method and quasi-stable datum method are also discussed for dealing with the rank deficient problems. The theoretical basis of the equivalently eliminated equations is derived in detail.

The eighth chapter is dedicated to cycle slip detection and ambiguity resolution. Several cycle slip detection methods are outlined. Emphasises are given in deriving a general criterion for integer ambiguity search in ambiguity, coordinate or both domains. The criterion is derived from conditional adjustment; however, the criterion has nothing to do with any condition in the end. An equivalent criterion is also derived, and it shows that the well-known least squares ambiguity search criterion is just one of the terms of the equivalent criterion. A diagonalisation algorithm and its use for ambiguity search are proposed. The search can be done within a second after the normal equation is diagonalised. Ambiguity function method and the method of float ambiguity fixing are outlined.

The ninth chapter describes the GPS data processing in static and kinematic applications. Data pre-processing is outlined. Emphasises are given to the solving of ambiguity-ionospheric equations and single point positioning, relative positioning as well as velocity determination using code, phase and combined data. The equivalent undifferential and differential data processing methods are discussed. A method of Kalman filtering using velocity information is described. The accuracy of the observational geometry is outlined at the end of the chapter.

The tenth chapter comprises the concepts of the kinematic positioning and flight state monitoring. The usage of the IGS station, multiple static references, height information of the airport, kinematic troposphere model, and the known distances of the multiple antennas on the aircraft are discussed in detail. Numerical examples are also given.

The eleventh chapter deals with the topic of perturbed orbit determination. Perturbed equations of satellite motion are derived. Perturbation forces of the satellite motion are discussed in detail including the perturbations of the Earth's gravitational field, Earth tide and ocean tide, the Sun, the Moon and planets, solar radiation pressure, atmospheric drag as well as coordinate perturbation. Orbit correction is outlined based on the analysis solution of C_{20} perturbation. Precise orbit determination is discussed, including its principle and related derivatives as well as numerical integration and interpolation algorithms.

(c) ketabton.com: The Digital Library

The final chapter is a brief discussion about the future of GPS and comments on some remaining problems.

The book has been subjected to an individual review of chapters, sections or according to its contents. I am grateful to reviewers Prof. Lelgemann of the Technical University (TU) Berlin, Prof. Leick of the University of Maine, Prof. Rizos of the University of New South Wales (UNSW), Prof. Grejner-Brzezinska of Ohio State University, Prof. Yuanxi Yang of the Institute of Surveying and Mapping in Xian, Prof. Jikun Ou of the Institute of Geodesy and Geophysics (IGG) in Wuhan, Prof. Wu Chen of Hong Kong Polytechnic University, Prof. Jiancheng Li of Wuhan University, Dr. Chunfang Cui of TU Berlin, Dr. Zhigui Kang of the University of Texas at Austin, Dr. Jinling Wang of UNSW, Dr. Yanxiong Liu of GFZ, Mr. Shfaqat Khan of KMS of Denmark, Mr. Zhengtao Wang of Wuhan Univerity, Dr. Wenyi Chen of the Max-Planck Institute of Mathematics in Sciences (Leipzig, Germany), et al. The book has been subjected to a general review by Prof. Lelgemann of TU Berlin. A grammatical check of technical English writing has been performed by Springer-Verlag Heidelberg.

I wish to sincerely thank Prof. Dr. Dr. Ch. Reigber for his support and trust throughout my scientific research activities at GFZ. Dr. Niels Andersen, Dr. Per Knudsen, and Dr. Rene Forsberg at KMS of Denmark are thanked for their support to start work on this book. Prof. Lelgemann of TU Berlin is thanked for his encouragement and help. During this work, many valuable discussions have been held with many specialists. My grateful thanks go to Prof. Grafarend of the University Stuttgart, Prof. Tscherning of Copenhagen University, Dr. Peter Schwintzer of GFZ, Dr. Luisa Bastos of the Astronomical Observatory of University Porto, Dr. Oscar Colombo of Maryland University, Dr. Detlef Angermann of German Geodetic Research Institute Munich, Dr. Shengyuan Zhu of GFZ, Dr. Peiliang Xu of the University Kyoto, Prof. Guanyun Wang of IGG in Wuhan, Dr. Ludger Timmen of the University Hannover, Ms. Daniela Morujao of Coimbra University. Dr. Jürgen Neumeyer of GFZ and Dr. Heping Sun of IGG in Wuhan are thanked for their support. Dipl.-Ing. Horst Scholz of TU Berlin is thanked for redrawing a part of the graphics. I am also grateful to Dr. Engel of Springer-Verlag Heidelberg for his advice.

My wife Liping, son Jia and daughters Yuxi and Pan are thanked for their lovely support and understanding, as well as for their help on part of the text processing and graphing.

Guochang Xu
March 2003

(c) ketabton.com: The Digital Library

Contents

1 Introduction 1
1.1 A Key Note of GPS 2
1.2 A Brief Message About GLONASS 3
1.3 Basic Information of Galileo 4
1.4 A Combined Global Navigation Satellite System 5

2 Coordinate and Time Systems 7
2.1 Geocentric Earth-Fixed Coordinate Systems 7
2.2 Coordinate System Transformations 10
2.3 Local Coordinate System 11
2.4 Earth-Centred Inertial Coordinate System 13
2.5 Geocentric Ecliptic Inertial Coordinate System 17
2.6 Time Systems 17

3 Satellite Orbits 21
3.1 Keplerian Motion 21
3.1.1 Satellite Motion in the Orbital Plane 24
3.1.2 Keplerian Equation 27
3.1.3 State Vector of the Satellite 29
3.2 Disturbed Satellite Motion 31
3.3 GPS Broadcast Ephemerides 32
3.4 IGS Precise Ephemerides 34
3.5 GLONASS Ephemerides 35

4 GPS Observables 37
4.1 Code Pseudoranges 37
4.2 Carrier Phases 39
4.3 Doppler Measurements 41

5 Physical Influences of GPS Surveying 43
5.1 Ionospheric Effects 43
5.1.1 Code Delay and Phase Advance 43
5.1.2 Elimination of the Ionospheric Effects 45
5.1.3 Ionospheric Models 48
5.1.4 Mapping Functions 51

(c) ketabton.com: The Digital Library

5.2 Tropospheric Effects ... 55
5.2.1 Tropospheric Models ... 56
5.2.2 Mapping Functions and Parameterisation ... 59
5.3 Relativistic Effects ... 62
5.3.1 Special Relativity and General Relativity ... 62
5.3.2 Relativistic Effects on GPS ... 64
5.4 Earth Tide and Ocean Loading Tide Corrections ... 67
5.4.1 Earth Tide Displacements of the GPS Station ... 67
5.4.2 Simplified Model of the Earth Tide Displacements ... 68
5.4.3 Numerical Examples of the Earth Tide Effects ... 70
5.4.4 Ocean Loading Tide Displacement ... 72
5.4.5 Computation of the Ocean Loading Tide Displacement ... 75
5.4.6 Numerical Examples of Loading Tide Effects ... 75
5.5 Clock Errors ... 76
5.6 Multipath Effects ... 78
5.6.1 GPS-Altimetry, Signals Reflected from the Earth-Surface ... 79
5.6.2 Reflecting Point Positioning ... 80
5.6.3 Image Point and Reflecting Surface Determination ... 81
5.7 Anti-Spoofing and Selective Availability Effects ... 82
5.8 Antenna Phase Centre Offset and Variation ... 82
5.9 Instrumental Biases ... 85

6 GPS Observation Equations and Equivalence Properties ... 87
6.1 General Mathematical Models of GPS Observations ... 87
6.2 Linearisation of the Observational Model ... 89
6.3 Partial Derivatives of Observational Function ... 90
6.4 Linear Transformation and Covariance Propagation ... 94
6.5 Data Combinations ... 95
6.5.1 Ionosphere-Free Combinations ... 97
6.5.2 Geometry-Free Combinations ... 98
6.5.3 Standard Phase-Code Combination ... 100
6.5.4 Ionospheric Residuals ... 101
6.5.5 Differential Doppler and Doppler Integration ... 102
6.6 Data Differentiations ... 104
6.6.1 Single Differences ... 105
6.6.2 Double Differences ... 107
6.6.3 Triple Differences ... 110
6.7 Equivalence of the Uncombined and Combining Algorithms ... 111
6.7.1 Uncombined GPS Data Processing Algorithms ... 112
6.7.2 Combining Algorithms of GPS Data Processing ... 114
6.7.3 Secondary GPS Data Processing Algorithms ... 119
6.7.4 Summary ... 122
6.8 Equivalence of Undifferenced and Differencing Algorithms ... 122
6.8.1 Introduction ... 122
6.8.2 Formation of Equivalent Observation Equations ... 123
6.8.3 Equivalent Equations of Single Differences ... 125

(c) ketabton.com: The Digital Library

6.8.4 Equivalent Equations of Double Differences 128
6.8.5 Equivalent Equations of Triple Differences 130
6.8.6 Method of Dealing with the Reference Parameters 130
6.8.7 Summary of the Unified Equivalent Algorithm 131

7 Adjustment and Filtering Methods 133
7.1 Introduction 133
7.2 Least Squares Adjustment 133
7.2.1 Least Squares Adjustment with Sequential Observation Groups 135
7.3 Sequential Least Squares Adjustment 137
7.4 Conditional Least Squares Adjustment 138
7.4.1 Sequential Application of Conditional Least Squares Adjustment 140
7.5 Block-Wise Least Squares Adjustment 141
7.5.1 Sequential Solution of Block-Wise Least Squares Adjustment 143
7.5.2 Block-Wise Least Squares for Code-Phase Combination 145
7.6 Equivalently Eliminated Observation Equation System 146
7.6.1 Diagonalised Normal Equation and the Equivalent Observation Equation 148
7.7 Kalman Filter 150
7.7.1 Classic Kalman Filter 150
7.7.2 Kalman Filter – A General Form of Sequential Least Squares Adjustment 151
7.7.3 Robust Kalman Filter 152
7.7.4 Adaptively Robust Kalman Filtering 155
7.8 A Priori Constrained Least Squares Adjustment 159
7.8.1 A Priori Parameter Constraints 159
7.8.2 A Priori Datum 160
7.8.3 Quasi-Stable Datum 161
7.9 Summary 163

8 Cycle Slip Detection and Ambiguity Resolution 167
8.1 Cycle Slip Detection 167
8.2 Method of Dealing with Cycle Slips 168
8.3 A General Criterion of Integer Ambiguity Search 169
8.3.1 Introduction 169
8.3.2 Summary of Conditional Least Squares Adjustment 170
8.3.3 Float Solution 171
8.3.4 Integer Ambiguity Search in Ambiguity Domain 172
8.3.5 Integer Ambiguity Search in Coordinate and Ambiguity Domains 174
8.3.6 Properties of the General Criterion 175
8.3.7 An Equivalent Ambiguity Search Criterion and its Properties 176
8.3.8 Numerical Examples of the Equivalent Criterion 178
8.3.9 Conclusions and Comments 181
8.4 Ambiguity Function 182
8.4.1 Maximum Property of Ambiguity Function 183

(c) ketabton.com: The Digital Library

9 Parameterisation and Algorithms of GPS Data Processing 187
9.1 Parameterisation of the GPS Observation Model 187
9.1.1 Evidence of the Parameterisation Problem of the Undifferenced Observation Model 187
9.1.2 A Method of Uncorrelated Bias Parameterisation 189
9.1.3 Geometry-Free Illustration 195
9.1.4 Correlation Analysis in the Case of Phase-Code Combinations 195
9.1.5 Conclusions and Comments 197
9.2 Equivalence of the GPS Data Processing Algorithms 198
9.2.1 Equivalence Theorem of GPS Data Processing Algorithms 198
9.2.2 Optimal Baseline Network Forming and Data Condition 200
9.2.3 Algorithms Using Secondary GPS Observables 201
9.3 Non-Equivalent Algorithms 203
9.4 Standard Algorithms of GPS Data Processing 203
9.4.1 Preparation of GPS Data Processing 203
9.4.2 Single Point Positioning 204
9.4.3 Standard Un-Differential GPS Data Processing 209
9.4.4 Equivalent Method of GPS Data Processing 211
9.4.5 Relative Positioning 212
9.4.6 Velocity Determination 212
9.4.7 Kalman Filtering Using Velocity Information 215
9.5 Accuracy of the Observational Geometry 217

10 Applications of GPS Theory and Algorithms 219
10.1 Software Development 219
10.1.1 Functional Library 219
10.1.2 Data Platform 223
10.1.3 A Data Processing Core 225
10.2 Concept of Precise Kinematic Positioning and Flight-State Monitoring 226
10.2.1 Introduction 226
10.2.2 Concept of Precise Kinematic Positioning 229
10.2.3 Concept of Flight-State Monitoring 233
10.2.4 Results, Precision Estimation and Comparisons 235
10.2.5 Conclusions 240

11 Perturbed Orbit and its Determination 243
11.1 Perturbed Equation of Satellite Motion 243
11.1.1 Lagrangian Perturbed Equation of Satellite Motion 244
11.1.2 Gaussian Perturbed Equation of Satellite Motion 246
11.2 Perturbation Forces of Satellite Motion 249
11.2.1 Perturbation of the Earth's Gravitational Field 249
11.2.2 Perturbation of the Sun and the Moon as well as Planets 254
11.2.3 Earth Tide and Ocean Tide Perturbations 255
11.2.4 Solar Radiation Pressure 258
11.2.5 Atmospheric Drag 262
11.2.6 Additional Perturbations 265

(c) ketabton.com: The Digital Library

11.2.7 Order Estimations of Perturbations 267
11.2.8 Ephemerides of the Moon, the Sun and Planets 267
11.3 Analysis Solution of the $\overline{C}_{20}$ Perturbed Orbit 271
11.4 Orbit Correction 277
11.5 Principle of GPS Precise Orbit Determination 281
11.5.1 Algebra Solution of the Variation Equation 283
11.6 Numerical Integration and Interpolation Algorithms 284
11.6.1 Runge-Kutta Algorithms 284
11.6.2 Adams Algorithms 289
11.6.3 Cowell Algorithms 291
11.6.4 Mixed Algorithms and Discussions 293
11.6.5 Interpolation Algorithms 294
11.7 Orbit-Related Partial Derivatives 294

12 Discussions 305
12.1 Independent Parameterisation and A Priori Information 305
12.2 Equivalence of the GPS Data Processing Algorithms 307

Appendix 1
IAU 1980 Theory of Nutation 309

Appendix 2
Numerical Examples of the Diagonalisation of the Equations 311

References 317

Subject Index 337

(c) ketabton.com: The Digital Library

Abbreviations and Constants

Abbreviations

AF	Ambiguity Function
AS	Anti-Spoofing
AU	Astronomical Units
BDT	Barycentric Dynamic Time
C/A	Coarse Acquisition
CAS	Chinese Academy of Sciences
CIO	Conventional International Origin
CHAMP	Challenging Mini-satellite Payload
CRF	Conventional Reference Frame
CTS	Conventional Terrestrial System
DD	Double Difference
DGK	Deutsche Geodätische Kommission
DGPS	Differential GPS
DOP	Dilution of Precision
ECEF	Earth-Centred-Earth-Fixed (system)
ECI	Earth-Centred Inertial (system)
ECSF	Earth-Centred-Space-Fixed (system)
ESA	European Space Agency
EU	European Union
Galileo	Global Navigation Satellite System of EU
GAST	Greenwich Apparent Sidereal Time
GDOP	Geometric Dilution of Precision
GFZ	GeoForschungsZentrum Potsdam
GIS	Geographic Information System
GLONASS	Global Navigation Satellite System of Russia
GLOT	GLONASS time
GMST	Greenwich Mean Sidereal Time
GNSS	Global Navigation Satellite System
GPS	Global Positioning System
GPST	GPS Time
GRACE	Gravity Recovery and Climate Experiment
GRS	Geodetic Reference System
GST	Galileo system time
HDOP	Horizontal Dilution of Precision

(c) ketabton.com: The Digital Library

IAG	International Association of Geodesy
IAT	International Atomic Time
IAU	International Astronomical Union
IERS	International Earth Rotation Service
IGS	International GPS Geodynamics Service
INS	Inertial Navigation System
ION	Institute of Navigation
ITRF	IERS Terrestrial Reference Frame
IUGG	International Union for Geodesy and Geophysics
JD	Julian Date
JPL	Jet Propulsion Laboratory
KMS	National Survey and Cadastre (Denmark)
KSGsoft	Kinematic/Static GPS Software
LEO	Low Earth Orbit (satellite)
LS	Least Squares (adjustment)
LSAS	Least Squares Ambiguity Search (criterion)
MEO	Medium Earth Orbit (satellite)
MFGsoft	Multi-Functional GPS/Galileo Software
MIT	Massachusetts Institute of Technology
MJD	Modified Julian Date
NASA	National Aeronautics and Space Administration
NAVSTAR	Navigation System with Time and Ranging
NGS	National Geodetic Survey
OD	Orbits Determination
OTF	On-the-Fly
PC	Personal Computer
PDOP	Position Dilution of Precision
PRN	Pseudorandom Noise
PZ-90	Parameters of the Earth Year 1990
RINEX	Receiver Independent Exchange (format)
RMS	Root Mean Square
RTK	Real-Time Kinematic
SA	Selective Availability
SC	Semicircles
SD	Single Difference
SINEX	Software Independent Exchange (format)
SLR	Satellite Laser Ranging
SNR	Signal-to-Noise Ratio
SST	Satellite-Satellite Tracking
SV	Space Vehicle
TAI	International Atomic Time
TD	Triple Difference
TDB	Barycentric Dynamic Time
TDOP	Time Dilution of Precision
TDT	Terrestrial Dynamic Time
TEC	Total Electronic Content

(c) ketabton.com: The Digital Library

TJD	Time of Julian Date
TOPEX	(Ocean) Topography Experiment
TOW	Time of Week
TRANSIT	Time Ranging and Sequential
TT	Terrestrial Time
UT	Universal Time
UTC	Universal Time Coordinated
UTC_{SU}	Moscow time UTC
VDOP	Vertical Dilution of Precision
WGS	World Geodetic System
ZfV	Zeitschrift für Vermessungswesen

(c) ketabton.com: The Digital Library

Table of Constants

Symbol	Value	Unit	Explanation	cf.
a_e	6378137	m	Semimajor axis of WGS-84	§2.1
f_e	1 / 298.2572236		Flattening factor of WGS-84	§2.1
a_p	6378136	m	Semimajor axis of PZ-90	§2.1
f_p	1 / 298.2578393		Flattening factor of PZ-90	§2.1
a_{el}	6378136.54	m	Semimajor axis of ITRF-96	§2.1
f_{el}	1/298.25645		Flattening factor of ITRF-96	§2.1
ε	84381."412		Obliquity of the ecliptic at J2000.0	§2.4
JDGPS	2444244.5	JD	Julian Date of GPS standard epoch (1980 Jan. $6, 0^h$)	§2.6
JD2000.0	2451545.0	JD	Julian Date of 2000 January $1, 12^h$	§2.6
G	6.67259 e–11	$m^3\ s^{-2}\ kg^{-1}$	Constant of gravitation	§3.1
μ_e	3.986004418 e14	$m^3\ s^{-2}$	Geocentric gravitational constant	§3.1
ω_e	7.292115 e–5	rad s^{-1}	Nominal mean angular velocity of the Earth	§3.3
c	299792458	m s^{-1}	Speed of light	§4.1
μ_s	1.327124 e20	$m^3\ s^{-2}$	Heliocentric gravitational constant	§5.4
μ_m	$\mu_e(M_m / M_e)$	$m^3\ s^{-2}$	Gravitational constant of the Moon	§5.4
M_m / M_e	0.0123000345		Moon-Earth mass ratio	§5.4
h_2, h_3	0.6078, 0.292		Love number	§5.4
l_2	0.0847		Shida number	§5.4
f_0	10.23	MHz	Fundamental frequency of GPS	§8.5
f_1	$154\ f_0$	MHz	First carrier frequency of GPS	§8.5
λ_1	19.029	cm	Wavelength of f_1	§8.5
f_2	$120\ f_0$	MHz	Second carrier frequency of GPS	§8.5
λ_2	24.421	cm	Wavelength of f_2	§8.5
f_5	$115\ f_0$	MHz	Third carrier frequency of GPS	§8.5
λ_5	25.482	cm	Wavelength of f_5	§8.5
P_s	4.5605 e–6	N m^{-1}	Luminosity of the Sun	§11.2
a_s	1.0000002 AU	m	Semimajor axis of the orbit of the Sun	§11.2
AU	149597870691	m	Astronomical units	§11.2
a_m	384401000	m	Semimajor axis of the orbit of the Moon	§11.2
f_{g1}	1602	MHz	First carrier frequency of GLONASS	§1.2
Δf_{g1}	0.5625	MHz	First carrier frequency interval of GLONASS	§1.2
f_{g2}	1246	MHz	Second carrier frequency of GLONASS	§1.2
Δf_{g2}	0.4375	MHz	Second carrier frequency interval of GLONASS	§1.2

(c) ketabton.com: The Digital Library

Chapter 1

Introduction

GPS is a Global Positioning System based on satellite technology. The fundamental technique of GPS is to measure the ranges between the receiver and a few simultaneously observed satellites. The positions of the satellites are forecasted and broadcasted along with the GPS signal to the user. Through several known positions (of the satellites) and the measured distances between the receiver and the satellites, the position of the receiver can be determined. The position change, which can be also determined, is then the velocity of the receiver. The most important applications of the GPS are positioning and navigating.

Through the developments of a few decades, GPS is now even known by school children. GPS has been very widely applied in several areas, such as air, sea and land navigation, low earth orbit (LEO) satellite orbit determination, static and kinematic positioning, flight-state monitoring, as well as surveying, etc. GPS has become a necessity for daily life, industry, research and education.

If some one is jogging with a GPS watch and wants to know where he is located, what he needs to do is very simple; pressing a key will be enough. However, the principle of such an application is a complex one. It includes knowledge of electronics, orbital mechanics, atmosphere science, geodesy, relativity theory, mathematics, adjustment and filtering as well as software engineering. Many scientists and engineers have been devoted to making GPS theory easier to understand and its applications more precise.

Galileo is an EU Global Positioning System and GLONASS is a Russian one. The positioning and navigating principle is nearly the same compared with that of the US GPS system. The GPS theory and algorithms can be directly used for the Galileo and GLONASS systems with only a few exceptions. A global navigation satellite system of the future is a combined GNSS system by using the GPS, GLONASS and Galileo systems together.

In order to describe the distance measurement using a mathematical model, coordinate and time systems, orbital motion of the satellite and GPS observations have to be discussed (Chap. 2–4). The physical influences on GPS measurement such as ionospheric and tropospheric effects, etc. also have to be dealt with (Chap. 5). Then the linearised observation equations can be formed with various methods such as data combination and differentiation as well as the equivalent technique (Chap. 6). The equation system may be a full rank or a rank deficient one and may need to be solved in a post-processing or a quasi real time way, so the various adjustment and filtering methods shall be discussed (Chap. 7). For precise GPS applications, phase observations must be used; therefore, the ambiguity problem has to be dealt with (Chap. 8). And then the algorithms of parameterisation and the equivalence theorem as well as standard algorithms of GPS data processing can be discussed (Chap. 9). Sequentially, applications of the GPS theory and algorithms to GPS/Galileo software development are outlined, and

(c) ketabton.com: The Digital Library

a concept of precise kinematic positioning and flight-state monitoring from practical experience is given (Chap. 10). The theory of dynamic GPS applications for perturbed orbit determination has to be based on the above-discussed theory and can be described (Chap. 11). Discussions and comments are given at the last chapter. The contents and structure of this book are organised with such a logical sequence.

Contents of this book covered kinematic, static and dynamic GPS theory and algorithms. Most of the contents are refined theory, which has been applied to the independently developed scientific GPS software **KSGsoft** (**K**inematic and **S**tatic **G**PS **Soft**ware) and **MFGsoft** (**M**ulti-**F**unctional **G**PS/Galileo **Soft**ware) and which was obtained from extensive research on individual problems. Because of the strong research and application background, the theories are conformably described with complexity and self-confidence. A brief summary of the contents is given in the preface.

Numerous GPS books are frequently quoted and carefully studied. Some of them are warmly suggested for further reading, e.g., Bauer 1994; Hofmann-Wellenhof et al. 2001; King et al. 1987; Kleusberg and Teunissen (Eds.) 1996; Leick 1995; Liu et al. 1996; Parkinson and Spilker (Eds.) 1996; Remondi 1984; Seeber 1993; Strang and Borre 1997; Wang et al. 1988; Xu 1994; etc.

1.1 A Key Note of GPS

The Global Positioning System was designed and built, and is operated and maintained by the U.S. Department of Defence (c.f., e.g., Parkinson and Spilker 1996). The first GPS satellite was launched in 1978, and the system was fully operational in the mid-1990s. The GPS constellation consists of 24 satellites in six orbital planes with four satellites in each plane. The ascending nodes of the orbital planes are equally spaced by 60 degrees. The orbital planes are inclined 55 degrees. Each GPS satellite is in a nearly circular orbit with a semi-major axis of 26 578 km and a period of about twelve hours. The satellites continuously orient themselves to ensure that their solar panels stay pointed towards the Sun, and their antennas point toward the Earth. Each satellite carries four atomic clocks, is the size of a car and weighs about 1 000 kg. The long-term frequency stability of the clocks reaches better than a few parts of 10^{-13} over a day (cf. Scherrer 1985). The atomic clocks aboard the satellite produce the fundamental L-band frequency, 10.23 MHz.

The GPS satellites are monitored by five base stations. The main base station is in Colorado Springs, Colorado and the other four are located on Ascension Island (Atlantic Ocean), Diego Garcia (Indian Ocean), Kwajalein and Hawaii (both Pacific Ocean). All stations are equipped with precise cesium clocks and receivers to determine the broadcast ephemerides and to model the satellite clocks. Transmitted to the satellites are ephemerides and clock adjustments. The satellites in turn use these updates in the signals that they send to GPS receivers.

Each GPS satellite transmits data on three frequencies: L1 (1575.42 MHz), L2 (1227.60 MHz) and L5 (1176.45 MHz). The L1, L2 and L5 carrier frequencies are generated by multiplying the fundamental frequency by 154, 120 and 115, respectively. Pseudorandom noise (PRN) codes, along with satellite ephemerides, ionospheric model, and satellite clock corrections are superimposed onto the carrier frequencies L1, L2 and L5. The measured transmitting times of the signals that travel from the satellites to

(c) ketabton.com: The Digital Library

the receivers are used to compute the pseudoranges. The Course-Acquisition (C/A) code, sometimes called the Standard Positioning Service (SPS), is a pseudorandom noise code that is modulated onto the L1 carrier. The precision (P) code, sometimes called the Precise Positioning Service (PPS), is modulated onto the L1, L2 and L5 carriers allowing for the removal of the effects of the ionosphere.

The Global Positioning System (GPS) was conceived as a ranging system from known positions of satellites in space to unknown positions on land and sea, as well as in air and space. The orbits of the GPS satellites are available by broadcast or by the International Geodetic Service (IGS). IGS orbits are precise ephemerides after post-processing or quasi-real time processing. All GPS receivers have an almanac programmed into their computer, which tells them where each satellite is at any given moment. The almanac is a data file that contains information of orbits and clock corrections of all satellites. It is transmitted by a GPS satellite to a GPS receiver, where it facilitates rapid satellite vehicle acquisition within GPS receivers. The GPS receivers detect, decode and process the signals received from the satellites to create the data of code, phase and Doppler observables. The data may be available in real time or saved for downloading. The receiver internal software is usually used to process the real time data with the single point positioning method and to output the information to the user. Because of the limitation of the receiver software, precise positioning and navigating are usually carried out by an external computer with more powerful software. The basic contributions of the GPS are to tell the user where he is, how he moves, and what the timing is.

Applications for GPS already have become almost limitless since the GPS technology moved into the civilian sector. Understanding GPS has become a necessity.

1.2 A Brief Message About GLONASS

GLONASS is a Global Navigation Satellite System (GNSS) managed by the Russian Space Forces and the system is operated by the Coordination Scientific Information Center (KNITs) of the Ministry of Defense of the Russian Federation. The system is comparable to the American Global Positioning System (GPS), and both systems share the same principles of the data transmission and positioning methods. The first GLONASS satellite was launched into orbit in 1982. The system consists of 21 satellites in three orbital planes, with three on-orbit spares. The ascending nodes of three orbital planes are separated 120 degrees, and the satellites within the same orbit plane are equally spaced by 45 degrees. The arguments of the latitude of satellites in equivalent slots in two different orbital planes differ by 15 degrees. Each satellite operates in nearly circular orbits with a semi-major axis of 25 510 km. Each orbital plane has an inclination angle of 64.8 degrees, and each satellite completes an orbit in approximately 11 hours 16 minutes.

Cesium clocks are used on board the GLONASS satellites. The stability of the clocks reaches better than a few parts of 10^{-13} over a day. The satellites transmit coded signals in two frequencies located on two frequency bands, 1 602–1 615.5 MHz and 1 246–1 256.5 MHz, with a frequency interval of 0.5625 MHz and 0.4375 MHz, respectively. The antipodal satellites, which are separated by 180 degrees in the same orbit plane in argument of latitude, transmit on the same frequency. The signals can be

(c) ketabton.com: The Digital Library

received by users anywhere on the Earth's surface to identify their position and velocity in real time based on ranging measurements. Coordinate and time systems used in the GLONASS are different from that of the American GPS. And GLONASS satellites are distinguished by slightly different carrier frequencies instead of by different PRN codes. The ground control stations of the GLONASS are maintained only in the territory of the former Soviet Union due to the historical reasons. This lack of global coverage is not optimal for the monitoring of a global navigation satellite system.

GLONASS and GPS are not entirely compatible with each other; however, they are generally interoperable. Combining the GLONASS and GPS resources together, the GNSS user community will benefit not only with an increased accuracy, but also with a higher system integrity on a worldwide basis.

1.3 Basic Information of Galileo

Galileo is a Global Navigation Satellite System (GNSS) initiated by the European Union (EU) and the European Space Agency (ESA) for providing a highly accurate, guaranteed global positioning service under civilian control (cf., e.g., ESA homepage). As an independent navigation system, Galileo will meanwhile be interoperable with the two other global satellite navigation systems, GPS and GLONASS. A user will be able to position with the same receiver from any of the satellites in any combination. Galileo will guarantee availability of service with higher accuracy.

The first Galileo satellite, which has the size of $2.7 \times 1.2 \times 1.1$ m and weight of 650 kg, was launched in December 2005, and the system will be fully operational in 2010~2012. The Galileo constellation consists of 30 Medium Earth Orbit (MEO) satellites in three orbital planes with nine equally spaced operational satellites in each plane plus one inactive spare satellite. The ascending nodes of the orbital planes are equally spaced by 120 degrees. The orbital planes are inclined 56 degrees. Each Galileo satellite is in a nearly circular orbit with semi-major axis of 29 600 km (cf. ESA homepage) and a period of about 14 hours. The Galileo satellite rotates about its Earth-pointing axis so that the flat surface of the solar arrays always faces the Sun to collect maximum solar energy. The deployed solar arrays span 13 m. The antennas always point towards the Earth.

The Galileo satellite has four clocks, two of each type (passive maser and rubidium, stabilities: 0.45 ns and 1.8 ns over 12 hours, respectively). At any time, only one of each type is operating. The operating maser clock produces the reference frequency from which the navigation signal is generated. If the maser clock were to fail, the operating rubidium clock would take over instantaneously and the two reserve clocks would start up. The second maser clock would take the place of the rubidium clock after a few days when it is fully operational. The rubidium clock would then go on stand-by or reserve again. In this way, the Galileo satellite is guaranteed to generate a navigation signal at all times.

Galileo will provide ten navigation signals in the Right Hand Circular Polarization (RHCP) in the frequency ranges 1 164–1 215 MHz (E5a and E5b), 1 215–1 300 MHz (E6) and 1 559–1 592 MHz (E2-L1-E1) (cf. Hein et al. 2004). The interoperability and compatibility of Galileo and GPS is realized by having two common centre frequencies in E5a/L5 and L1 as well as adequate geodetic coordinate and time reference frames.

(c) ketabton.com: The Digital Library

1.4 A Combined Global Navigation Satellite System

The start of the Galileo system is a direct competition of the GPS and GLONASS systems. Without a doubt, it has a positive influence on the modernisation of the GPS system and the further development of the GLONASS system. Multiple navigation systems operating independently help increase the awareness and accuracy of the real time positioning and navigation. Undoubtedly, a global navigation satellite system of the future is a combined GNSS system which uses the GPS, GLONASS and Galileo systems together. A constellation of about 75 satellites of the three systems greatly increases the visibility of the satellites especially in critical areas such as urban canyons.

The times and coordinate systems used in the GPS, GLONAS and Galileo systems are different due to the system independency. The three time systems are all based on the UTC and the three coordinate systems are all Cartesian systems; therefore, their relationships can be determined and any system can be transformed from one to another. The origins of the GPS and GLONASS coordinates are meters apart from each other. The origins of GPS and Galileo coordinates have differences of a few centimetres. Several carrier frequencies are used in each system for the removal of the effects of the ionosphere. The frequency differences within the GLONASS system and between the GPS, GLONASS and Galileo systems are generally not a serious problem if the carrier phase observables are considered in a distance survey by multiplying the wavelength.

In the present edition of this book, the theory and algorithms of a global positioning system will be discussed in a more general aspect in order to take the differences of the GPS, GLONASS and Galileo systems into account.

(c) ketabton.com: The Digital Library

Chapter 2

Coordinate and Time Systems

GPS satellites are orbiting around the Earth with time. GPS surveys are made mostly on the Earth. To describe the GPS observation (distance) as a function of the GPS orbit (satellite position) and the measuring position (station location), suitable coordinate and time systems have to be defined.

2.1 Geocentric Earth-Fixed Coordinate Systems

It is convenient to use the Earth-Centred Earth-Fixed (ECEF) coordinate system to describe the location of a station on the Earth's surface. The ECEF coordinate system is a right-handed Cartesian system (x, y, z). Its origin and the Earth's centre of mass coincide, while its z-axis and the mean rotational axis of the Earth coincide; the x-axis is pointing to the mean Greenwich meridian, while the y-axis is directed to complete a right-handed system (cf., Fig. 2.1). In other words, the z-axis is pointing to a mean pole of the Earth's rotation. Such a mean pole, defined by international convention, is called the Conventional International Origin (CIO). Then the xy-plane is called mean equatorial plane, and the xz-plane is called mean zero-meridian.

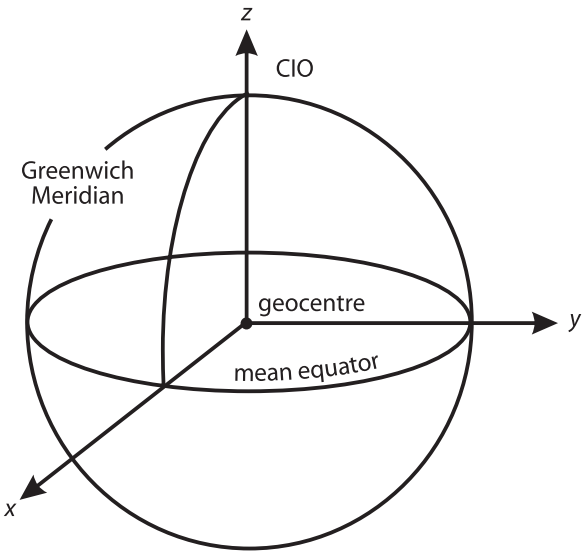

Fig. 2.1. Earth-Centred Earth-Fixed coordinates

(c) ketabton.com: The Digital Library

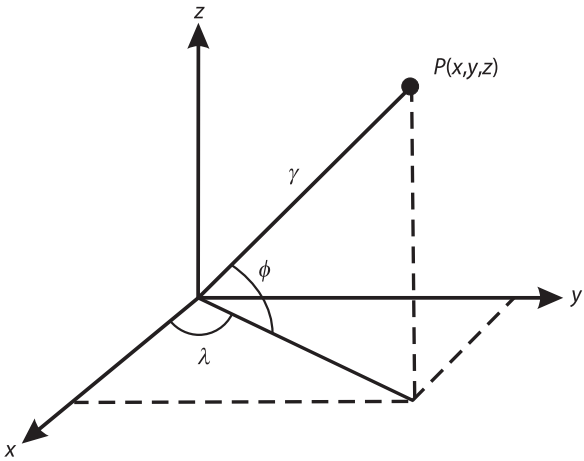

Fig. 2.2.
Cartesian and spherical coordinates

The ECEF coordinate system is also known as the Conventional Terrestrial System (CTS). The mean rotational axis and mean zero-meridian used here are necessary. The true rotational axis of the Earth changes its direction with respect to the Earth's body all the time. If such a pole would be used to define a coordinate system, then the coordinates of the station would also change all the time. Because the surveying is made in our true world, so it is obvious that the polar motion has to be taken into account and will be discussed later.

The ECEF coordinate system can, of course, be represented by a spherical coordinate system (r, ϕ, λ), where r is the radius of the point (x, y, z), ϕ and λ are the geocentric latitude and longitude, respectively (cf., Fig. 2.2). λ is counted eastward from the zero-meridian. The relationship between (x, y, z) and (r, ϕ, λ) is obvious:

$$\begin{pmatrix} x \\ y \\ z \end{pmatrix} = \begin{pmatrix} r\cos\phi\cos\lambda \\ r\cos\phi\sin\lambda \\ r\sin\phi \end{pmatrix}, \quad \text{or} \quad \begin{cases} r = \sqrt{x^2 + y^2 + z^2} \\ \tan\lambda = y / x \\ \tan\phi = z / \sqrt{x^2 + y^2} \end{cases}. \tag{2.1}$$

An ellipsoidal coordinate system (φ, λ, h) may be also defined based on the ECEF coordinates; however, geometrically, two additional parameters are needed to define the shape of the ellipsoid (cf., Fig. 2.3). φ, λ and h are geodetic latitude, longitude and height, respectively. The ellipsoidal surface is a rotational ellipse. The ellipsoidal system is also called the geodetic coordinate system. Geocentric longitude and geodetic longitude are identical. The two geometric parameters could be the semi-major radius (denote by a) and the semi-minor radius (denote by b) of the rotating ellipse, or the semi-major radius and the flattening (denote by f) of the ellipsoid. They are equivalent sets of parameters. The relationship between (x, y, z) and (φ, λ, h) is (cf., e.g., Torge 1991):

$$\begin{pmatrix} x \\ y \\ z \end{pmatrix} = \begin{pmatrix} (N+h)\cos\varphi\cos\lambda \\ (N+h)\cos\varphi\sin\lambda \\ (N(1-e^2)+h)\sin\varphi \end{pmatrix}, \tag{2.2}$$

or

(c) ketabton.com: The Digital Library

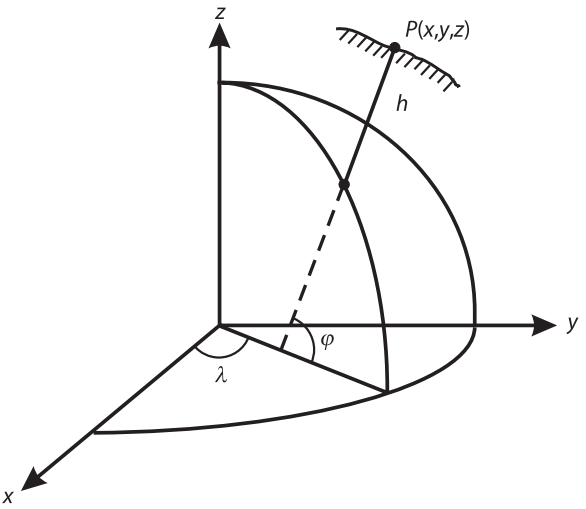

Fig. 2.3.
Ellipsoidal coordinate system

$$\begin{cases} \tan\varphi = \dfrac{z}{\sqrt{x^2+y^2}}\left(1-e^2\dfrac{N}{N+h}\right)^{-1} \\ \tan\lambda = y/x \\ h = \dfrac{\sqrt{x^2+y^2}}{\cos\varphi} - N \end{cases}, \tag{2.3}$$

where

$$N = \frac{a}{\sqrt{1-e^2\sin^2\varphi}}\ . \tag{2.4}$$

N is the radius of curvature in the prime vertical, and e is the first eccentricities. The geometric meaning of N is shown in Fig. 2.4. In Eq. 2.3, the φ and h have to be solved by iteration; however, the iteration process converges quickly, since $h \ll N$. The flattening and the first eccentricities are defined as:

$$f = \frac{a-b}{a}\ , \quad \text{and} \quad e = \frac{\sqrt{a^2-b^2}}{a}\ . \tag{2.5}$$

In cases where $\varphi = \pm 90°$ or h is very large, the iteration formulas of Eq. 2.3 could be instable. Alternatively, using (cf., Lelgemann 2002)

$$\operatorname{ctan}\varphi = \frac{\sqrt{x^2+y^2}}{z+\Delta z}\ ,$$

$$\Delta z = e^2 N\sin\varphi = \frac{ae^2\sin\varphi}{\sqrt{1-e^2\sin^2\varphi}}\ ,$$

(c) ketabton.com: The Digital Library

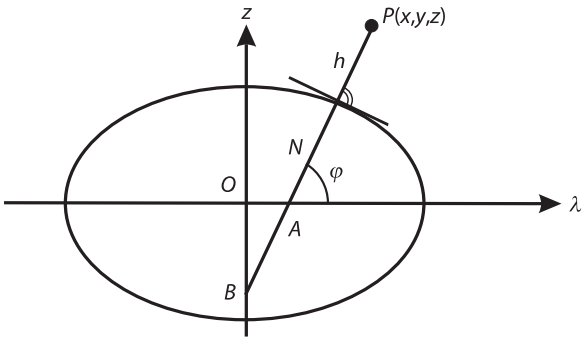

Fig. 2.4.
Radius of curvature in the prime vertical

may lead to a stably iterated result of φ. Δz and e^2N are the lengths of $\overline{OB}$ and $\overline{AB}$ (cf., Fig. 2.4) respectively. h can be obtained by using Δz, i.e.,

$$h = \sqrt{x^2 + y^2 + (z + \Delta z)^2} - N \ .$$

The two geometric parameters used in the World Geodetic System 1984 (WGS-84) are ($a = 6\,378\,137$ m, $f = 1 / 298.2572236$). In International Terrestrial Reference Frame 1996 (ITRF-96), the two parameters are ($a = 6\,378\,136.49$ m, $f = 1 / 298.25645$). ITRF uses the International Earth Rotation Service (IERS) Conventions (cf., McCarthy 1996). In PZ-90 (Parameters of the Earth Year 1990) coordinate system of GLONASS, the two parameters are ($a = 6\,378\,136$ m, $f = 1 / 298.2578393$).

The relation between the geocentric and geodetic latitude ϕ and φ may be given by (cf., Eqs. 2.1 and 2.3):

$$\tan\phi = \left(1 - e^2 \frac{N}{N + h}\right) \tan\varphi \ . \tag{2.6}$$

2.2 Coordinate System Transformations

Any Cartesian coordinate system can be transformed to another Cartesian coordinate system through three succeeded rotations if their origins are the same and if they are both right-handed or left-handed coordinate systems. These three rotational matrices are:

$$R_1(\alpha) = \begin{pmatrix} 1 & 0 & 0 \\ 0 & \cos\alpha & \sin\alpha \\ 0 & -\sin\alpha & \cos\alpha \end{pmatrix},$$

$$R_2(\alpha) = \begin{pmatrix} \cos\alpha & 0 & -\sin\alpha \\ 0 & 1 & 0 \\ \sin\alpha & 0 & \cos\alpha \end{pmatrix}, \tag{2.7}$$

$$R_3(\alpha) = \begin{pmatrix} \cos\alpha & \sin\alpha & 0 \\ -\sin\alpha & \cos\alpha & 0 \\ 0 & 0 & 1 \end{pmatrix},$$

(c) ketabton.com: The Digital Library

where α is the rotating angle, which has a positive sign for a counter-clockwise rotation as viewed from the positive axis to the origin. R_1, R_2, and R_3 are called the rotating matrix around the x, y, and z-axis, respectively. For any rotational matrix R, there are $R^{-1}(\alpha) = R^T(\alpha)$ and $R^{-1}(\alpha) = R(-\alpha)$; that is, the rotational matrix is an orthogonal one, where R^{-1} and R^T are the inverse and transpose of the matrix R.

For two Cartesian coordinate systems with different origins and different length units, the general transformation can be given in vector (matrix) form as

$$X_{\mathrm{n}} = X_0 + \mu R X_{\mathrm{old}} \quad , \quad \text{or} \tag{2.8}$$

$$\begin{pmatrix} x_{\mathrm{n}} \\ y_{\mathrm{n}} \\ z_{\mathrm{n}} \end{pmatrix} = \begin{pmatrix} x_0 \\ y_0 \\ z_0 \end{pmatrix} + \mu R \begin{pmatrix} x_{\mathrm{old}} \\ y_{\mathrm{old}} \\ z_{\mathrm{old}} \end{pmatrix} ,$$

where μ is the scale factor (or the ratio of the two length units), and R is a transformation matrix that can be formed by three suitably succeeded rotations. x_{n} and x_{old} denote the new and old coordinates, respectively; x_0 denotes the translation vector and is the coordinate vector of the origin of the old coordinate system in the new one.

If rotational angle α is very small, then one has $\sin\alpha \approx \alpha$ and $\cos\alpha \approx 0$. In such a case, the rotational matrix can be simplified. If the three rotational angles α_1, α_2, α_3 in R of Eq. 2.8 are very small, then R can be written as (cf., e.g., Lelgemann and Xu 1991):

$$R = \begin{pmatrix} 1 & \alpha_3 & -\alpha_2 \\ -\alpha_3 & 1 & \alpha_1 \\ \alpha_2 & -\alpha_1 & 1 \end{pmatrix} , \tag{2.9}$$

where α_1, α_2, α_3 are small rotating angles around the x, y and z-axis, respectively. Using the simplified R, the transformation 2.8 is called the Helmert transformation.

As an example, the transformation from WGS-84 to ITRF-90 is given by (McCarthy 1996):

$$\begin{pmatrix} x_{\text{ITRF-90}} \\ y_{\text{ITRF-90}} \\ z_{\text{ITRF-90}} \end{pmatrix} = \begin{pmatrix} 0.060 \\ -0.517 \\ -0.223 \end{pmatrix} + \mu \begin{pmatrix} 1 & -0.0070'' & -0.0003'' \\ 0.0070'' & 1 & -0.0183'' \\ 0.0003'' & 0.0183'' & 1 \end{pmatrix} \begin{pmatrix} x_{\text{WGS-84}} \\ y_{\text{WGS-84}} \\ z_{\text{WGS-84}} \end{pmatrix} ,$$

where $\mu = 0.999999989$, the translation vector has the unit of meter.

The transformations between the coordinate systems of GPS, GLONASS and Galileo can be generally represented by Eq. 2.8 with the scale factor $\mu = 1$ (i.e., the length units used in the three systems are the same). A formula of velocity transformations between different coordinate systems can be obtained by differentiating the Eq. 2.8 with respect to the time.

2.3 Local Coordinate System

The local left-handed Cartesian coordinate system (x', y', z') can be defined by placing the origin to the local point $P_1(x_1, y_1, z_1)$, whose z'-axis is pointed to the vertical, x'-axis is directed to the north, and y' is pointed to the east (cf., Fig. 2.5). The $x'y'$-plane is called the horizontal plane; the vertical is defined perpendicular to the ellipsoid.

(c) ketabton.com: The Digital Library

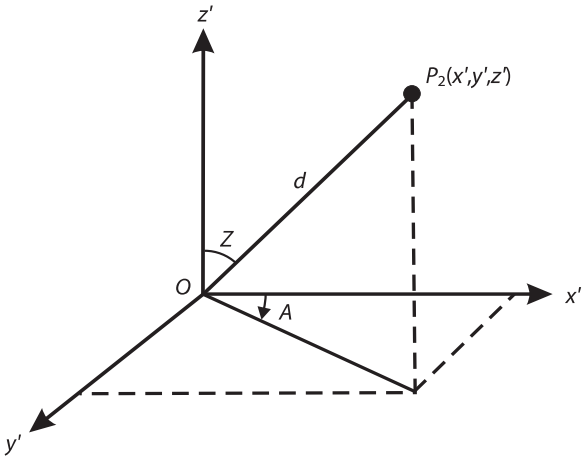

Fig. 2.5.
Astronomical coordinate system

Such a coordinate system is also called a local horizontal coordinate system. For any point P_2, whose coordinates in the global and local coordinate system are (x_2, y_2, z_2) and (x', y', z'), respectively, one has relations of

$$\begin{pmatrix} x' \\ y' \\ z' \end{pmatrix} = d \begin{pmatrix} \cos A \sin Z \\ \sin A \sin Z \\ \cos Z \end{pmatrix}, \quad \text{and} \quad \begin{pmatrix} d = \sqrt{x'^2 + y'^2 + z'^2} \\ \tan A = y' / x' \\ \cos Z = z' / d \end{pmatrix}, \tag{2.10}$$

where A is the azimuth, Z is the zenith distance and d is the radius of the P_2 in the local system. A is measured from the north clockwise; Z is the angle between the vertical and the radius d.

The local coordinate system (x', y', z') can indeed be obtained by two succeeded rotations of the global coordinate system (x, y, z) by $R_2(90° - \varphi)R_3(\lambda)$ and then by changing the x-axis to a right-handed system. In other words, the global system has to be rotated around the z-axis with angle λ, then around the y-axis with angle $90° - \varphi$, and then change the sign of the x-axis. The total transformation matrix R is then

$$R = \begin{pmatrix} -\sin\varphi\cos\lambda & -\sin\varphi\sin\lambda & \cos\varphi \\ -\sin\lambda & \cos\lambda & 0 \\ \cos\varphi\cos\lambda & \cos\varphi\sin\lambda & \sin\varphi \end{pmatrix}, \tag{2.11}$$

and there are:

$$X_{\text{local}} = RX_{\text{global}} \quad \text{and} \quad X_{\text{global}} = R^T X_{\text{local}}, \tag{2.12}$$

where X_{local} and X_{global} are the same vector represented in local and global coordinate systems. (φ, λ) are the geodetic latitude and longitude of the local point.

If the vertical direction is defined as the plump line of the gravitational field at the local point, then such a local coordinate system is called an astronomic horizontal system (its x'-axis is pointed to the north, left-handed system). The plump line of gravity g

(c) ketabton.com: The Digital Library

and the vertical line of the ellipsoid at the point p are generally not coinciding with each other; however, the difference is very small. The difference is omitted in GPS practice.

Combining Eqs. 2.10 and 2.12, the zenith angle and azimuth of a point P_2 (satellite) related to the station P_1 can be directly computed by using the global coordinates of the two points by

$$\cos Z = \frac{z'}{d} \quad \text{and} \quad \tan A = \frac{y'}{x'}, \tag{2.13}$$

where

$$\begin{aligned} d &= \sqrt{(x_2 - x_1)^2 + (y_2 - y_1)^2 + (z_2 - z_1)^2}\ , \\ x' &= -(x_2 - x_1)\sin\varphi\cos\lambda - (y_2 - y_1)\sin\varphi\sin\lambda + (z_2 - z_1)\cos\varphi\ , \\ y' &= -(x_2 - x_1)\sin\lambda + (y_2 - y_1)\cos\lambda \quad \text{and} \\ z' &= (x_2 - x_1)\cos\varphi\cos\lambda + (y_2 - y_1)\cos\varphi\sin\lambda + (z_2 - z_1)\sin\varphi\ . \end{aligned}$$

2.4 Earth-Centred Inertial Coordinate System

To describe the motion of the GPS satellites, an inertial coordinate system has to be defined. The motion of the satellites follows the Newtonian mechanics, and the Newtonian mechanics is valid and expressed in an inertial coordinate system. For reasons, the Conventional Celestial Reference Frame (CRF) is suitable for our purpose. The xy-plane of the CRF is the plane of the Earth's equator; the coordinates are celestial longitude, measured eastward along the equator from the vernal equinox, and celestial latitude. The vernal equinox is a crossover point of the ecliptic and the equator. So the right-handed Earth-centred inertial (ECI) system uses the Earth centre as the origin, CIO (Conventional International Origin) as the z-axis, and its x-axis is directed to the equinox of J2000.0 (Julian Date of 12^h 1st January 2000). Such a coordinate system is also called equatorial coordinates of date. Because of the motion (acceleration) of the Earth's centre, ECI is indeed a quasi-inertial system, and the general relativistic effects have to be taken into account in this system. The system moves around the Sun, however, without rotating with respect to the CIO. This system is also called the Earth-centred space-fixed (ECSF) coordinate system.

An excellent figure has been given by Torge (1991) to illustrate the motion of the Earth's pole with respect to the ecliptic pole (cf., Fig. 2.6). The Earth's flattening, combined with the obliquity of the ecliptic, results in a slow turning of the equator on the ecliptic due to the differential gravitational effect of the Moon and the Sun. The slow circular motion with a period of about 26 000 years is called precession, and the other quicker motion with periods from 14 days to 18.6 years is called nutation. Taking the precession and nutation into account, the Earth's mean pole (related to the mean equator) is transformed to the Earth's true pole (related to the true equator). The x-axis of the ECI is pointed to the vernal equinox of date.

The angle of the Earth's rotation from the equinox of date to the Greenwich meridian is called Greenwich Apparent Sidereal Time (GAST). Taking GAST into account (called the Earth's rotation), the ECI of date is transformed to the true equatorial co-

(c) ketabton.com: The Digital Library

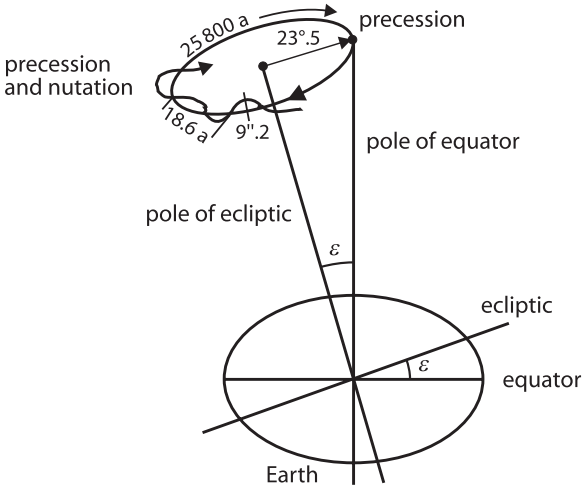

Fig. 2.6.
Precession and nutation

ordinate system. The difference between the true equatorial system and the ECEF system is the polar motion. So we have transformed the ECI system with a geometric way to the ECEF system. Such a transformation process can be written as

$$X_{\mathrm{ECEF}} = R_{\mathrm{M}} R_{\mathrm{S}} R_{\mathrm{N}} R_{\mathrm{P}} X_{\mathrm{ECI}} \ , \tag{2.14}$$

where R_{P} is the precession matrix, R_{N} is the nutation matrix, R_{S} is the Earth rotation matrix, R_{M} is the polar motion matrix, X is the coordinate vector, and indices ECEF and ECI denote the related coordinate systems.

Precession

The precession matrix consists of three succeeded rotational matrices, i.e., (cf., e.g., Hofman-Wellenhof et al. 1997; Leick 1995; McCarthy 1996)

$$\begin{aligned} R_{\mathrm{P}} &= R_3(-z) R_2(\theta) R_3(-\zeta) \\ &= \begin{pmatrix} \cos z \cos\theta \cos\zeta - \sin z \sin\zeta & -\cos z \cos\theta \sin\zeta - \sin z \cos\zeta & -\cos z \sin\theta \\ \sin z \cos\theta \cos\zeta + \cos z \sin\zeta & -\sin z \cos\theta \sin\zeta + \cos z \cos\zeta & -\sin z \sin\theta \\ \sin\theta \cos\zeta & -\sin\theta \sin\zeta & \cos\theta \end{pmatrix} , \end{aligned} \tag{2.15}$$

where z, θ, ζ are precession parameters and

$$\begin{aligned} z &= 2306.''2181\,T + 1.''09468\,T^2 + 0.''018203\,T^3 \ , \\ \theta &= 2004.''3109\,T - 0.''42665\,T^2 - 0.''041833\,T^3 \ \text{ and} \\ \zeta &= 2306.''2181\,T + 0.''30188\,T^2 + 0.''017998\,T^3 \ , \end{aligned} \tag{2.16}$$

where T is the measuring time in Julian centuries (36 525 days) counted from J2000.0 (cf., Sect. 2.6 time systems).

(c) ketabton.com: The Digital Library

Nutation

The nutation matrix consists of three succeeded rotational matrices, i.e., (cf., e.g., Hoffman-Wellenhof et al. 1997; Leick 1995; McCarthy 1996)

$$
\begin{aligned}
R_N &= R_1(-\varepsilon-\Delta\varepsilon)R_3(-\Delta\psi)R_1(\varepsilon) \\
&= \begin{pmatrix} \cos\Delta\psi & -\sin\Delta\psi\cos\varepsilon & -\sin\Delta\psi\sin\varepsilon \\ \sin\Delta\psi\cos\varepsilon_t & \cos\Delta\psi\cos\varepsilon_t\cos\varepsilon+\sin\varepsilon_t\sin\varepsilon & \cos\Delta\psi\cos\varepsilon_t\sin\varepsilon-\sin\varepsilon_t\cos\varepsilon \\ \sin\Delta\psi\sin\varepsilon_t & \cos\Delta\psi\sin\varepsilon_t\cos\varepsilon-\cos\varepsilon_t\sin\varepsilon & \cos\Delta\psi\sin\varepsilon_t\sin\varepsilon+\cos\varepsilon_t\cos\varepsilon \end{pmatrix} \\
&\approx \begin{pmatrix} 1 & -\Delta\psi\cos\varepsilon & -\Delta\psi\sin\varepsilon \\ \Delta\psi\cos\varepsilon_t & 1 & -\Delta\varepsilon \\ \Delta\psi\sin\varepsilon_t & \Delta\varepsilon & 1 \end{pmatrix},
\end{aligned} \tag{2.17}
$$

where ε is the mean obliquity of the ecliptic angle of date, $\Delta\psi$ and $\Delta\varepsilon$ are nutation angles in longitude and obliquity, $\varepsilon_t = \varepsilon + \Delta\varepsilon$, and

$$
\varepsilon = 84381.''448 - 46.''8150T - 0.''00059T^2 + 0.''001813T^3 \ . \tag{2.18}
$$

The approximation is made by letting $\cos\Delta\psi = 1$ and $\sin\Delta\psi = \Delta\psi$ for very small $\Delta\psi$. For precise purposes, the exact rotation matrix shall be used. The nutation parameters $\Delta\psi$ and $\Delta\varepsilon$ can be computed by using the International Astronomical Union (IAU) theory or IERS theory:

$$
\Delta\Psi = \sum_{i=1}^{106}(A_i + A_i' T)\sin\beta \ ,
$$

$$
\Delta\varepsilon = \sum_{i=1}^{106}(B_i + B_i' T)\cos\beta
$$

or

$$
\Delta\Psi = \sum_{i=1}^{263}(A_i + A_i' T)\sin\beta + A_i''\cos\beta \ ,
$$

$$
\Delta\varepsilon = \sum_{i=1}^{263}(B_i + B_i' T)\cos\beta + B_i''\cos\beta \ ,
$$

where argument

$$
\beta = N_{1i}l + N_{2i}l' + N_{3i}F + N_{4i}D + N_{5i}\Omega \ ,
$$

where l is the mean anomaly of the Moon, l' is the mean anomaly of the Sun, $F = L - \Omega$, D is the mean elongation of the Moon from the Sun, Ω is the mean longitude of the ascending node of the Moon, and L is the mean longitude of the Moon. The formulas of l, l', F, D, and Ω, are given in Sect. 11.2.8. The coefficient values of N_{1i}, N_{2i}, N_{3i}, N_{4i},

(c) ketabton.com: The Digital Library

N_{5i}, A_i, B_i, A_i', B_i', A_i'', and B_i'' can be found in, e.g., McCarthy (1996). The updated formulas and tables can be found in updated IERS conventions. For convenience, the coefficients of the IAU 1980 nutation model are given in Appendix 1.

Earth Rotation

The Earth rotation matrix can be represented as

$$R_S = R_3(\mathrm{GAST})\,, \tag{2.19}$$

where GAST is Greenwich Apparent Sidereal Time and

$$\mathrm{GAST} = \mathrm{GMST} + \Delta\Psi\cos\varepsilon + 0.''00264\sin\Omega + 0.''000063\sin 2\Omega\,, \tag{2.20}$$

where GMST is Greenwich Mean Sidereal Time. Ω is the mean longitude of the ascending node of the Moon; the second term on the right-hand side is the nutation of the equinox. Furthermore,

$$\mathrm{GMST} = \mathrm{GMST}_0 + \alpha\mathrm{UT1}\,, \tag{2.21}$$

$$\begin{aligned}\mathrm{GMST}_0 &= 6\times 3\,600.''0 + 41\times 60.''0 + 50.''54841\\ &\quad + 8\,640\,184\,.''812866\,T_0 + 0.''093104\,T_0^2 - 6.''2\times 10^{-6}T_0^3\,,\end{aligned}$$

$$\alpha = 1.0027379093\,50795 + 5.9006\times 10^{-11}T_0 - 5.9\times 10^{-15}T_0^2\,,$$

where GMST_0 is Greenwich Mean Sidereal Time at midnight on the day of interest. α is the rate of change. UT1 is the polar motion corrected Universal Time (cf., Sect. 2.6). T_0 is the measuring time in Julian centuries (36 525 days) counted from J2000.0 to 0^hUT1 of the measuring day. By computing GMST, UT1 is used (cf., Sect. 2.6).

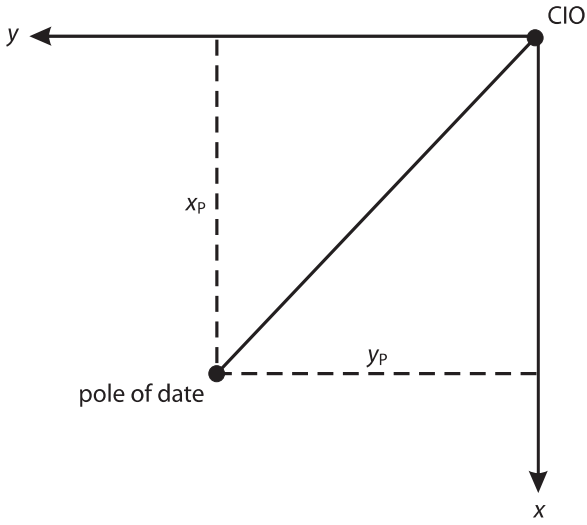

Fig. 2.7.
Polar motion

(c) ketabton.com: The Digital Library

Polar Motion

As shown in Fig. 2.7, the polar motion is defined as the angles between the pole of date and the CIO pole. The polar motion coordinate system is defined by *xy*-plane coordinates, whose *x*-axis is pointed to the south and is coincided to the mean Greenwich meridian, and whose *y*-axis is pointed to the west. x_p and y_p are the angles of the pole of date, so the rotation matrix of polar motion can be represented as

$$R_M = R_2(-x_p)R_1(-y_p) = \begin{pmatrix} \cos x_p & \sin x_p \sin y_p & \sin x_p \cos y_p \\ 0 & \cos y_p & -\sin y_p \\ -\sin x_p & \cos x_p \sin y_p & \cos x_p \cos y_p \end{pmatrix} \approx \begin{pmatrix} 1 & 0 & x_p \\ 0 & 1 & -y_p \\ -x_p & y_p & 1 \end{pmatrix} \tag{2.22}$$

The IERS determined x_p and y_p can be obtained from the home pages of IERS.

2.5 Geocentric Ecliptic Inertial Coordinate System

As discussed above, ECI used the CIO pole in the space as the *z*-axis (through consideration of the polar motion, nutation and precession). If the ecliptic pole is used as the *z*-axis, then an ecliptic coordinate system is defined, and it may be called the Earth Centred Ecliptic Inertial (ECEI) coordinate system. ECEI places the origin at the mass centre of the Earth, its *z*-axis is directed to ecliptic pole (or, *xy*-plane is the mean ecliptic), and its *x*-axis is pointed to the vernal equinox of date. The coordinate transformation between the ECI and ECEI systems can be represented as

$$X_{ECEI} = R_1(-\varepsilon)X_{ECI} \ ,$$

where ε is the ecliptic angle (mean obliquity) of the ecliptic plane related to the equatorial plane. The formula for ε is given in Sect. 2.4. Usually, coordinates of the Sun and the Moon as well as planets are given in the ECEI system.

2.6 Time Systems

Three time systems are used in satellite surveying. They are sidereal time, dynamic time and atomic time (cf., e.g., Hofman-Wellenhof et al. 1997; Leick 1995; McCarthy 1996; King et al. 1987).

Sidereal time is a measure of the Earth's rotation and is defined as the hour angle of the vernal equinox. If the measure is counted from the Greenwich meridian, the sidereal time is called Greenwich Sidereal Time. Universal Time (UT) is the Greenwich hour angle of the apparent Sun, which is orbiting uniformly in the equatorial

(c) ketabton.com: The Digital Library

plane. Because the angular velocity of the Earth's rotation is not a constant, sidereal time is not a uniformly-scaled time. The oscillation of UT is also partly caused by the polar motion of the Earth. The universal time corrected for the polar motion is denoted by UT1.

Dynamical time is a uniformly-scaled time used to describe the motion of bodies in a gravitational field. Barycentric Dynamic Time (TDB) is applied in an inertial coordinate system (its origin is located at the centre-of-mass (Barycentre)). Terrestrial Dynamic Time (TDT) is used in a quasi-inertial coordinate system (such as ECI). Because of the motion of the Earth around the Sun (or say, in the Sun's gravitational field), TDT will have a variation with respect to TDB. However, both the satellite and the Earth are subject to almost the same gravitational perturbations. TDT may be used for describing the satellite motion without taking into account the influence of the gravitational field of the Sun. TDT is also called Terrestrial Time (TT).

Atomic Time is a time system kept by atomic clocks such as International Atomic Time (TAI). It is a uniformly-scaled time used in the ECEF coordinate system. TDT is realised by TAI in practice with a constant offset (32.184 sec). Because of the slowing down of the Earth's rotation with respect to the Sun, Coordinated Universal Time (UTC) is introduced to keep the synchronisation of TAI to the solar day (by inserting the leap seconds). GPS Time (GPST) is also an atomic time.

The relationships between different time systems are given as follows:

$$\begin{aligned} \mathrm{TAI} &= \mathrm{GPST} + 19.0\,\mathrm{sec} \\ \mathrm{TAI} &= \mathrm{TDT} - 32.184\,\mathrm{sec} \\ \mathrm{TAI} &= \mathrm{UTC} + n\,\mathrm{sec} \\ \mathrm{UT1} &= \mathrm{UTC} + \mathrm{dUT1} \end{aligned} \quad , \tag{2.23}$$

where dUT1 can be obtained by IERS, (dUT1 < 0.7 sec, cf., Zhu et al. 1996), (dUT1 is also broadcasted with the navigation data), n is the number of leap seconds of date and is inserted into UTC on the 1st of January and 1st of July of the years. The actual n can be found in the IERS report.

Time argument T (Julian centuries) is used in the formulas given in Sect. 2.4. For convenience, T is denoted by TJD, and TJD can be computed from the civil date (Year, Month, Day, and Hour) as follows:

$$\mathrm{JD} = \mathrm{INT}(365.25Y) + \mathrm{INT}(30.6001(M+1)) + \mathrm{Day} + \mathrm{Hour}/24 + 1\,720\,981.5 \quad \text{and}$$

$$\mathrm{TJD} = \mathrm{JD}/36\,525\,, \tag{2.24}$$

where

$$Y = \mathrm{Year} - 1, \quad M = \mathrm{Month} + 12, \quad \text{if Month} \le 2\,,$$

$$Y = \mathrm{Year}, \quad M = \mathrm{Month}, \quad \text{if Month} > 2\,,$$

where JD is the Julian Date, Hour is the time of UT and INT denotes the integer part of a real number. The Julian Date counted from JD2000.0 is then JD2000 = JD – JD2000.0,

(c) ketabton.com: The Digital Library

where JD2000.0 is the Julian Date of 2000 January 1^{st} 12^{h} and has the value of 2 451 545.0 days. One Julian century is 36 525 days.

Inversely, the civil date (Year, Month, Day and Hour) can be computed from the Julian Date (JD) as follows:

$$b = \mathrm{INT}(\mathrm{JD} + 0.5) + 1537 ,$$

$$c = \mathrm{INT}((b - 122.1) / 365.25) ,$$

$$d = \mathrm{INT}(365.25c) ,$$

$$e = \mathrm{INT}((b - d) / 30.6001) ,$$

$$\mathrm{Hour} = \mathrm{JD} + 0.5 - \mathrm{INT}(\mathrm{JD} + 0.5) ,$$

$$\mathrm{Day} = b - d - \mathrm{INT}(30.6001e) ,$$

$$\mathrm{Month} = e - 1 - 12\mathrm{INT}(e / 14) \quad \text{and}$$

$$\mathrm{Year} = c - 4715 - \mathrm{INT}((7 + \mathrm{Month}) / 10) \quad , \tag{2.25}$$

where b, c, d, and e are auxiliary numbers.

Because the GPS standard epoch is defined as JD = 2 444 244.5 (1980 January 6, 0^{h}), GPS week and the day of week (denoted by Week and N) can be computed by

$$N = \mathrm{modulo}(\mathrm{INT}(\mathrm{JD} + 1.5), 7) \quad \text{and}$$

$$\mathrm{Week} = \mathrm{INT}((\mathrm{JD} - 2\,444\,244.5) / 7) , \tag{2.26}$$

where N is the day of week ($N = 0$ for Monday, $N = 1$ for Tuesday, and so on).

For saving digits and counting the date from midnight instead of noon, the Modified Julian Date (MJD) is defined as

$$\mathrm{MJD} = (\mathrm{JD} - 2\,400\,000.5) . \tag{2.27}$$

GLONASS time (GLOT) is defined by Moscow time $\mathrm{UTC_{SU}}$, which equals UTC plus three hours (corresponding to the offset of Moscow time to Greenwich time), theoretically. GLOT is permanently monitored and adjusted by the GLONASS Central Synchroniser (cf. Roßbach 2000). UTC and GLOT then has a simple relation

$$\mathrm{UTC} = \mathrm{GLOT} + \tau_c - 3h ,$$

where τ_c is the system time correction with respect to $\mathrm{UTC_{SU}}$, which is broadcasted by the GLONASS ephemerides and is less than one microsecond. Therefore there is approximately

$$\mathrm{GPST} = \mathrm{GLOT} + m - 3h ,$$

(c) ketabton.com: The Digital Library

where m is called a number of "leap seconds" between GPS and GLONASS (UTC) time and is given in the GLONASS ephemerides. m is indeed the leap seconds since GPS standard epoch (1980 January 6, 0^h).

Galileo system time (GST) will be maintained by a number of UTC laboratory clocks. GST and GPST are time systems of various UTC laboratories. After the offset of GST and GPST is made available to the user, the interoperability will be ensured.

(c) ketabton.com: The Digital Library

Chapter 3

Satellite Orbits

The principle of the GPS system is to measure the signal transmitting paths from the satellites to the receivers. Therefore, the satellite orbits are very important topics in GPS theory. In this chapter, the basic orbits theory is briefly described. For the GPS applications in orbits correction and orbits determination, the advanced orbits perturbation theory will be discussed in Chap. 11.

3.1 Keplerian Motion

The simplified satellite orbiting is called Keplerian motion, and the problem is called the two-bodies problem. The satellite is supposed to move in a central force field. The equation of satellite motion is described by Newton's second law of motion by

$$\vec{f} = m \cdot a = m \cdot \ddot{\vec{r}}\,, \tag{3.1}$$

where $\vec{f}$ is the attracting force, m is the mass of the satellite, a, or alternatively, $\ddot{\vec{r}}$ is the acceleration of the motion (second order differentiation of vector $\vec{r}$ with respect to the time), and according to Newton's law,

$$\vec{f} = -\frac{GMm}{r^2}\frac{\vec{r}}{r}\,, \tag{3.2}$$

where G is the universal gravitational constant, M is the mass of the Earth, r is the distance between the mass centre of the Earth and the mass centre of the satellite. The equation of satellite motion is then

$$\ddot{\vec{r}} = -\frac{\mu}{r^2}\frac{\vec{r}}{r}\,, \tag{3.3}$$

where μ (= GM) is called Earth's gravitational constant.

Equation 3.3 of satellite motion is valid only in an inertial coordinate system, so the ECSF coordinate system discussed in Chap. 2 will be used for describing the orbit of the satellite. The vector form of the equation of motion can be rewritten through three x, y and z components ($\vec{r} = (x, y, z)$) as

(c) ketabton.com: The Digital Library

$$\begin{aligned}\ddot{x} &= -\frac{\mu}{r^3}x \\ \ddot{y} &= -\frac{\mu}{r^3}y \\ \ddot{z} &= -\frac{\mu}{r^3}z\end{aligned} \quad . \tag{3.4}$$

Multiplying y, z to the first equation of 3.4, and x, z to the second, x, y to the third, and then forming differences of them, one gets

$$\begin{aligned}y\ddot{z} - z\ddot{y} &= 0 \\ z\ddot{x} - x\ddot{z} &= 0 \\ x\ddot{y} - y\ddot{x} &= 0\end{aligned} \quad , \tag{3.5}$$

or in vector form:

$$\vec{r} \times \ddot{\vec{r}} = 0 \, . \tag{3.6}$$

Equations 3.5 and 3.6 are equivalent to

$$\begin{aligned}\frac{\mathrm{d}(y\dot{z} - z\dot{y})}{\mathrm{d}t} &= 0 \\ \frac{\mathrm{d}(z\dot{x} - x\dot{z})}{\mathrm{d}t} &= 0 \\ \frac{\mathrm{d}(x\dot{y} - y\dot{x})}{\mathrm{d}t} &= 0\end{aligned} \quad , \tag{3.7}$$

$$\frac{\mathrm{d}(\vec{r} \times \dot{\vec{r}})}{\mathrm{d}t} = 0 \, . \tag{3.8}$$

Integrating Eqs. 3.7 and 3.8 lead to

$$\begin{aligned}y\dot{z} - z\dot{y} &= A \\ z\dot{x} - x\dot{z} &= B \\ x\dot{y} - y\dot{x} &= C\end{aligned} \quad , \tag{3.9}$$

$$\vec{r} \times \dot{\vec{r}} = \vec{h} = \begin{pmatrix} A \\ B \\ C \end{pmatrix} \quad , \tag{3.10}$$

where A, B, C are integration constants; they form the integration constant vector $\vec{h}$. That is:

$$h = \sqrt{A^2 + B^2 + C^2} = \left| \vec{r} \times \dot{\vec{r}} \right| \, . \tag{3.11}$$

The constant h is two times of the area that the radius vector sweeps during a unit time. This is indeed Kepler's second law. Then $h/2$ is called the area velocity of the radius of the satellite.

(c) ketabton.com: The Digital Library

Multiplying x, y and z to the three equations of 3.9 and adding them together, one has

$$Ax + By + Cz = 0 \ . \tag{3.12}$$

That is, the satellite motion fulfils the equation of a plane, and the origin of the coordinate system is in the plane. In other words, the satellite moves in a plane in the central force field of the Earth. The plane is called the orbital plane of the satellite.

The angle between the orbital plane and the equatorial plane is called inclination of the satellite (denoted by i, cf., Fig. 3.1). Alternatively, the inclination i is the angle between the vector $\vec{z} = (0, 0, 1)$ and $\vec{h} = (A, B, C)$, i.e.,

$$\cos i = \frac{\vec{z} \cdot \vec{h}}{|\vec{z}| \cdot |\vec{h}|} = \frac{C}{h} \ . \tag{3.13}$$

The orbital plane cuts the equator at two points. They are called ascending node N and descending node. (See the next section for details). Vector $\vec{s}$ denotes the vector from the Earth centre pointed to the ascending point. The angle between the ascending node and the x-axis (vernal equinox) is called the right ascension of the ascending node (denoted by Ω). Thus,

$$\vec{s} = \vec{z} \times \vec{h} \ ,$$

and

$$\cos \Omega = \frac{\vec{s} \cdot \vec{x}}{|\vec{s}| \cdot |\vec{x}|} = \frac{-B}{\sqrt{A^2 + B^2}} \ ,$$

$$\sin \Omega = \frac{\vec{s} \cdot \vec{y}}{|\vec{s}| \cdot |\vec{y}|} = \frac{A}{\sqrt{A^2 + B^2}} \ . \tag{3.14}$$

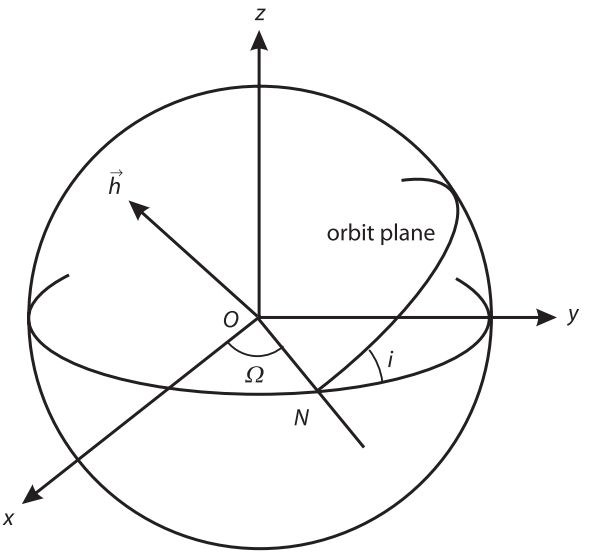

Fig. 3.1.
Orbital plane

(c) ketabton.com: The Digital Library

Parameters i and Ω uniquely defined the place of orbital plane and therefore are called orbital plane parameters. Ω, i and h are then selected as integration constants, which have significant geometric meanings of the satellite orbits.

3.1.1 Satellite Motion in the Orbital Plane

In the orbital plane, a two-dimensional rectangular coordinate system is given in Fig. 3.2. The coordinates can be represented in polar coordinate r and ϑ as

$$\begin{aligned} p &= r\cos\vartheta \\ q &= r\sin\vartheta \end{aligned} \quad . \tag{3.15}$$

The equation of motion in pq-coordinates is similar to the Eq. 3.4 as

$$\begin{aligned} \ddot{p} &= -\frac{\mu}{r^3}p \\ \ddot{q} &= -\frac{\mu}{r^3}q \end{aligned} \quad . \tag{3.16}$$

From Eq. 3.15, one has

$$\begin{aligned} \dot{p} &= \dot{r}\cos\vartheta - r\dot{\vartheta}\sin\vartheta \\ \dot{q} &= \dot{r}\sin\vartheta + r\dot{\vartheta}\cos\vartheta \\ \ddot{p} &= (\ddot{r} - r\dot{\vartheta}^2)\cos\vartheta - (r\ddot{\vartheta} + 2\dot{r}\dot{\vartheta})\sin\vartheta \\ \ddot{q} &= (\ddot{r} - r\dot{\vartheta}^2)\sin\vartheta + (r\ddot{\vartheta} + 2\dot{r}\dot{\vartheta})\cos\vartheta \end{aligned} \quad . \tag{3.17}$$

Substituting Eqs. 3.17 and 3.15 into Eq. 3.16, one gets

$$\begin{aligned} (\ddot{r} - r\dot{\vartheta}^2)\cos\vartheta - (r\ddot{\vartheta} + 2\dot{r}\dot{\vartheta})\sin\vartheta &= -\frac{\mu}{r^2}\cos\vartheta \\ (\ddot{r} - r\dot{\vartheta}^2)\sin\vartheta + (r\ddot{\vartheta} + 2\dot{r}\dot{\vartheta})\cos\vartheta &= -\frac{\mu}{r^2}\sin\vartheta \end{aligned} \quad . \tag{3.18}$$

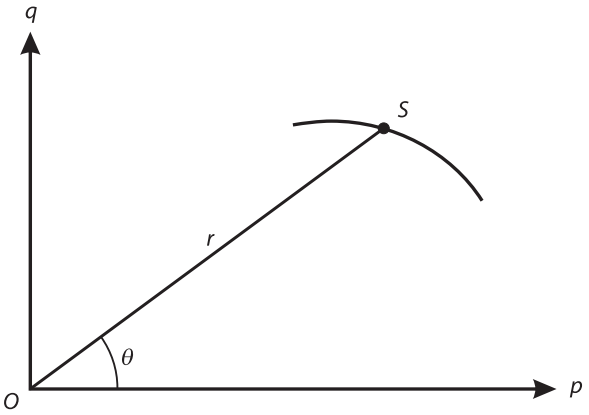

Fig. 3.2. Polar coordinates in the orbital plane

(c) ketabton.com: The Digital Library

The point from which the polar angle ϑ is measured is arbitrary. So setting ϑ as zero, the equation of motion is then

$$\begin{aligned} &\ddot{r} - r\dot{\vartheta}^2 = -\frac{\mu}{r^2} \\ &r\ddot{\vartheta} + 2\dot{r}\dot{\vartheta} = 0 \end{aligned} . \tag{3.19}$$

Multiplying r to the second equation of 3.19, it turns out to be

$$\frac{\mathrm{d}(r^2\dot{\vartheta})}{\mathrm{d}t} = 0 . \tag{3.20}$$

Because $r\dot{\vartheta}$ is the tangential velocity, $r^2\dot{\vartheta}$ is the two times of the area velocity of the radius of the satellite. Integrating Eq. 3.20 and comparing it with the discussion in Sect. 3.1, one has

$$r^2\dot{\vartheta} = h . \tag{3.21}$$

$h/2$ is the area velocity of the radius of the satellite.

For solving the first differential equation of 3.19, the equation has to be transformed into a differential equation of r with respect to variable f. Let

$$u = \frac{1}{r} , \tag{3.22}$$

then from Eq. 3.21, one gets

$$\frac{\mathrm{d}\vartheta}{\mathrm{d}t} = hu^2 \tag{3.23}$$

and

$$\begin{aligned} &\frac{\mathrm{d}r}{\mathrm{d}t} = \frac{\mathrm{d}r}{\mathrm{d}\vartheta}\frac{\mathrm{d}\vartheta}{\mathrm{d}t} = \frac{\mathrm{d}}{\mathrm{d}\vartheta}\left(\frac{1}{u}\right)hu^2 = -h\frac{\mathrm{d}u}{\mathrm{d}\vartheta} \\ &\frac{\mathrm{d}^2r}{\mathrm{d}t^2} = -h\frac{\mathrm{d}^2u}{\mathrm{d}\vartheta^2}\frac{\mathrm{d}\vartheta}{\mathrm{d}t} = -h^2u^2\frac{\mathrm{d}^2u}{\mathrm{d}\vartheta^2} \end{aligned} . \tag{3.24}$$

Substituting Eqs. 3.22 and 3.24 into the first of equation of 3.19, the equation of motion is then

$$\frac{\mathrm{d}^2u}{\mathrm{d}\vartheta^2} + u = \frac{\mu}{h^2} , \tag{3.25}$$

and its solution is

$$u = d_1\cos\vartheta + d_2\sin\vartheta + \frac{\mu}{h^2} ,$$

(c) ketabton.com: The Digital Library

where d_1 and d_2 are constants of integration. The above equation may be simplified as

$$u = \frac{\mu}{h^2}(1 + e\cos(\vartheta - \omega)) \ , \tag{3.26}$$

where

$$d_1 = \frac{\mu}{h^2} e\cos\omega \ , \quad d_2 = \frac{\mu}{h^2} e\sin\omega \ .$$

Thus the moving equation of satellite in the orbital plane is

$$r = \frac{h^2 / \mu}{1 + e\cos(\vartheta - \omega)} \ . \tag{3.27}$$

Comparing Eq. 3.27 with a standard polar equation of conic:

$$r = \frac{a(1 - e^2)}{1 - e\cos\varphi} \ , \tag{3.28}$$

orbit Eq. 3.27 is obviously a polar equation of conic section with the origin at one of the foci. Where parameter e is the eccentricity, for $e = 0$, $e < 1$, $e = 1$, $e > 1$, the conic is a circle, an ellipse, a parabola, and a hyperbola, respectively. For the satellite orbiting around the Earth, generally, $e < 1$. Thus the satellite orbit is an ellipse, and this is indeed the Kepler's first law. Parameter a is the semimajor axis of the ellipse, and

$$h^2 / \mu = a(1 - e^2) \ . \tag{3.29}$$

It is obvious that parameter a has more significant geometric sense than that of h, so a is preferred to be used. Parameters a and e define the size and shape of the ellipse and are called ellipse parameters. The ellipse cuts the equator at the ascending and descending nodes. Polar angle φ is counted from the apogee of the ellipse. This can be seen by let $\varphi = 0$, thus $r = a(1 + e)$. φ has a 180 degree difference with the angle $\vartheta - \omega$. Letting $f = \vartheta - \omega$, where f is called the true anomaly of the satellite counted from the perigee, then the orbit Eq. 3.27 can be written as

$$r = \frac{a(1 - e^2)}{1 + e\cos f} \ . \tag{3.30}$$

In the case of $f = 0$, i.e., the satellite is in the point of perigee, $\omega = \vartheta$, ϑ is the polar angle of the perigee counted from the p-axis. Supposing the p-axis is an axis in the equatorial plane and is pointed to the ascending node N, then ω is the angle of perigee counted from the ascending node (cf., Fig. 3.3) and is called the argument of perigee. The argument of perigee defines the axis direction of the ellipse related to the equatorial plane.

(c) ketabton.com: The Digital Library

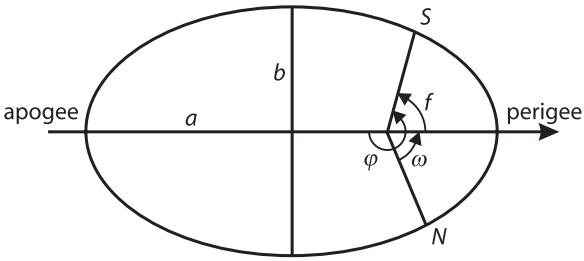

Fig. 3.3.
Ellipse of the satellite motion

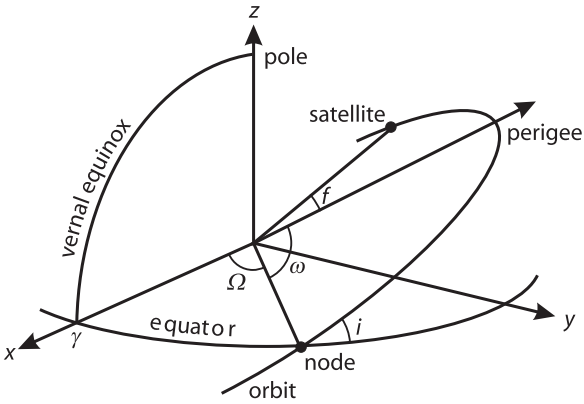

Fig. 3.4.
Orbital geometry

3.1.2 Keplerian Equation

Up to now, five integration constants have been derived. They are inclination angle i, right ascension of ascending node Ω, semimajor axis a, eccentricity e of the ellipse, and argument of perigee ω. Parameters i and Ω decide the place of the orbital plane, a and e decide the size and shape of the ellipse and ω decides the direction of the ellipse (cf., Fig. 3.4). To describe the satellite position in the ellipse, velocity of the motion has to be discussed.

The period T of the satellite motion is the area of ellipse divided by area velocity:

$$T = \frac{\pi ab}{\frac{1}{2}h} = \frac{2\pi ab}{\sqrt{\mu a(1-e^2)}} = 2\pi a^{3/2}\mu^{-1/2} \quad . \tag{3.31}$$

The average angular velocity n is then

$$n = \frac{2\pi}{T} = a^{-3/2}\mu^{1/2} \quad . \tag{3.32}$$

Equation 3.32 is the Kepler's third law. It is obvious that it is easier to describe the angular motion of the satellite under the average angular velocity n in the geometric centre of the ellipse (than in the geocentre). For simplifying the problem, an angle called

(c) ketabton.com: The Digital Library

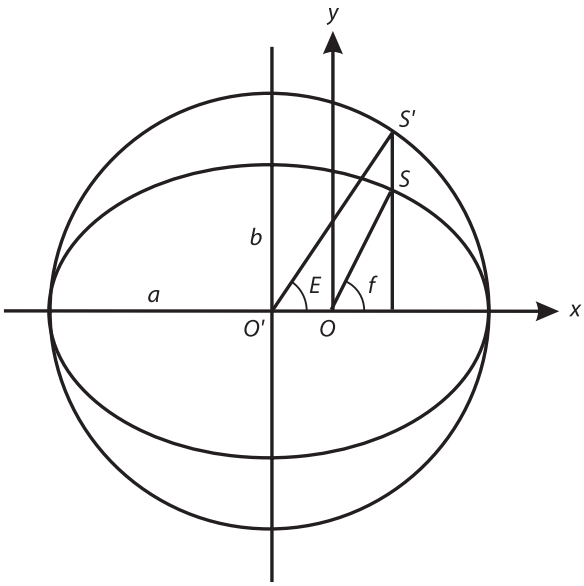

Fig. 3.5.
Mean anomaly of satellite

the eccentric anomaly is defined (denoted by E, cf., Fig. 3.5). S' is the vertical projection of the satellite S on the circle with a radius of a (semimajor axis of the ellipse). The distance between the geometric centre O' of the ellipse and the geocentre O is ae. Thus,

$$\begin{aligned} x &= r\cos f = a\cos E - ae \\ y &= r\sin f = b\sin E = a\sqrt{1-e^2}\,\sin E \end{aligned} \quad , \tag{3.33}$$

where the second equation can be obtained by substituting the first into the standard ellipse equation ($x^2/a^2 + y^2/b^2 = 1$) and omitting the small terms that contain e (for the satellite, generally, $e \ll 1$), where b is the semiminor axis of the ellipse. The orbit equation can then be represented by variable E as

$$r = a(1 - e\cos E) \quad . \tag{3.34}$$

The relation between true and eccentric anomalies can be derived by using Eqs. 3.33 and 3.34:

$$\tan\frac{f}{2} = \frac{\sin f}{1+\cos f} = \frac{\sin E}{1+\cos E}\frac{\sqrt{1-e^2}}{1-e} = \frac{\sqrt{1+e}}{\sqrt{1-e}}\tan\frac{E}{2} \quad . \tag{3.35}$$

If the xyz-coordinates are rotated so that the xy-plane coincides with the orbital plane, then the area velocity formulas of Eqs. 3.9 and 3.10 have only one component along the z-axis, i.e.,

$$x\dot{y} - y\dot{x} = h = \sqrt{\mu a(1-e^2)} \quad . \tag{3.36}$$

(c) ketabton.com: The Digital Library

From Eq. 3.33, one has

$$\begin{aligned} \dot{x} &= -a \sin E \frac{\mathrm{d}E}{\mathrm{d}t} \\ \dot{y} &= a\sqrt{1-e^2}\cos E \frac{\mathrm{d}E}{\mathrm{d}t} \end{aligned} \quad . \tag{3.37}$$

Substituting Eqs. 3.33 and 3.37 into Eq. 3.36 and taking Eq. 3.32 into account, a relation between E and t is obtained

$$(1-e\cos E)\mathrm{d}E = \sqrt{\mu}a^{-3/2}\mathrm{d}t = n\mathrm{d}t \ . \tag{3.38}$$

Suppose at the time t_p satellite is at the point perigee, i.e. $E(t_\mathrm{p}) = 0$, and at any time t, $E(t) = E$, then integration of Eq. 3.38 from 0 to E, namely from t_p to t is

$$E - e\sin E = M \ , \tag{3.39}$$

where

$$M = n(t - t_p) \ . \tag{3.40}$$

Equation 3.39 is the Keplerian equation. E is given as a function of M, namely t. Because of Eq. 3.34, the Keplerian equation indirectly assigns r as a function of t. M is called the mean anomaly. M describes the satellite as orbiting the Earth with a mean angular velocity n. t_p is called the perigee passage and is the sixth integration constant of the equation of satellite motion in a centre-force field.

Knowing M to compute E, the Keplerian Eq. 3.39 may be solved iteratively. Because of the small e, the convergence can be achieved very quickly.

Three anomalies (true anomaly f, eccentric anomaly E and mean anomaly M) are equivalent through the relations of Eqs. 3.35 and 3.39. They are functions of time t (including the perigee passage t_p), and they describe the position changes of the satellite with the time in the ECSF coordinates.

3.1.3 State Vector of the Satellite

Consider the orbital right-handed coordinate system: if the xy-plane is the orbital plane, the x-axis is pointing to the perigee, the z-axis is in the direction of vector $\vec{h}$, and the origin is in the geocentre, the position vector $\vec{q}$ of the satellite is then (cf., Eq. 3.33)

$$\vec{q} = \begin{pmatrix} a(\cos E - e) \\ a\sqrt{1-e^2}\sin E \\ 0 \end{pmatrix} = \begin{pmatrix} r\cos f \\ r\sin f \\ 0 \end{pmatrix} \ . \tag{3.41}$$

(c) ketabton.com: The Digital Library

Differentiating Eq. 3.41 with respect to time t and taking Eq. 3.38 into account, the velocity vector of the satellite is then

$$\dot{\vec{q}} = \begin{pmatrix} -\sin E \\ \sqrt{1-e^2}\cos E \\ 0 \end{pmatrix} \frac{na}{1-e\cos E} = \begin{pmatrix} -\sin f \\ e+\cos f \\ 0 \end{pmatrix} \frac{na}{\sqrt{1-e^2}} \ . \tag{3.42}$$

The second part of above equation can be derived from the relation between E and f. The state vector of the satellite in the orbital coordinate system can be rotated to the ECSF coordinate system by three succeeded rotations. First, a clockwise rotation around the 3rd-axis from the perigee to the node is given by (cf., Fig. 3.4)

$$R_3(-\omega) \ .$$

Next, a clockwise rotation around the 1st-axis with the angle of inclination i is given by

$$R_1(-i) \ .$$

Finally, a clockwise rotation around the 3rd-axis from the node to the vernal equinox is given by

$$R_3(-\Omega) \ .$$

So the state vector of the satellite in the ECSF coordinate system is then

$$\begin{pmatrix} \vec{r} \\ \dot{\vec{r}} \end{pmatrix} = R_3(-\Omega)R_1(-i)R_3(-\omega)\begin{pmatrix} \vec{q} \\ \dot{\vec{q}} \end{pmatrix} \ , \tag{3.43}$$

where

$$\vec{r} = \begin{pmatrix} x \\ y \\ z \end{pmatrix} \ , \quad \dot{\vec{r}} = \begin{pmatrix} \dot{x} \\ \dot{y} \\ \dot{z} \end{pmatrix} \ .$$

For given six Keplerian elements (Ω, i, ω, a, e, M_0) of t_0, where $M_0 = n(t_0 - t_p)$, the satellite state vector of time t can be computed, e.g., as follows:

1. Using Eq. 3.32 to compute the mean angular velocity n;
2. Using Eqs. 3.40, 3.39, 3.33 and 3.30 to compute the three anomalies M, E, f and r;
3. Using Eqs. 3.41 and 3.42 to compute the state vector $\vec{q}$ and $\dot{\vec{q}}$ in orbital coordinates;
4. Using Eq. 3.43 to rotate state vector $\vec{q}$ and $\dot{\vec{q}}$ to the ECSF coordinates.

Keplerian Elements can be given in practice at any time. For example, with t_0, where only f is a function of t_0, other parameters are constants. In this case, the related E and M can be computed by Eqs. 3.35 and 3.39, thus t_p can be computed by Eq. 3.40.

(c) ketabton.com: The Digital Library

From Eq. 3.42, one has

$$v^2 = \frac{a^2n^2}{(1-e\cos E)^2}[\sin^2 E + (1-e^2)\cos^2 E] = \frac{a^2n^2(1+e\cos E)}{1-e\cos E} \ . \tag{3.44}$$

Taking Eqs. 3.32 and 3.34 into account leads to

$$v^2 = \frac{\mu(1+e\cos E)}{r} = \frac{\mu(2-r/a)}{r} = \mu(\frac{2}{r} - \frac{1}{a}) \ , \tag{3.45}$$

where $v^2/2$ is the kinetic energy scaled by mass, μ/r is the potential energy, and a is the semimajor axis of the ellipse. This is the total energy conservative law of mechanics.

Rotate the vector $\vec{q}$ and $\dot{\vec{q}}$ in Eqs. 3.41 and 3.42 by $R_3(-\omega)$ and denote by $\vec{p}$ and $\dot{\vec{p}}$, i.e.:

$$\vec{p} = \begin{pmatrix} p_1 \\ p_2 \\ p_3 \end{pmatrix} = R_3(-\omega)\begin{pmatrix} r\cos f \\ r\sin f \\ 0 \end{pmatrix} = \begin{pmatrix} r\cos(\omega+f) \\ r\sin(\omega+f) \\ 0 \end{pmatrix} \ , \tag{3.46}$$

and

$$\dot{\vec{p}} = \begin{pmatrix} \dot{p}_1 \\ \dot{p}_2 \\ \dot{p}_3 \end{pmatrix} = R_3(-\omega)\begin{pmatrix} -\sin f \\ e+\cos f \\ 0 \end{pmatrix}\frac{na}{\sqrt{1-e^2}} = \begin{pmatrix} -\sin(\omega+f) - e\sin\omega \\ \cos(\omega+f) + e\cos\omega \\ 0 \end{pmatrix}\frac{na}{\sqrt{1-e^2}} \ . \tag{3.47}$$

The reverse problem of Eq. 3.43, i.e., for given rectangular satellite state vector $(\vec{r}, \dot{\vec{r}})^T$ to compute the Keplerian elements, can be carried out as follows. $\omega + f$ is called argument of latitude and denoted by u.

1. Using the given state vector to compute the modulus r and v ($r = |\vec{r}|$, $v = |\dot{\vec{r}}|$);
2. Using Eqs. 3.10 and 3.11 to compute vector $\vec{h}$ and its modulus h;
3. Using Eqs. 3.13 and 3.14 to compute inclination i and the right ascension of ascending node Ω;
4. Using Eqs. 3.45, 3.29 and 3.32 to compute semimajor axis a, eccentricity e and average angular velocity n;
5. Rotating $\vec{r}$ by $\vec{p} = R_1(i)R_3(\Omega)\vec{r}$ and then using Eq. 3.46 to compute $\omega + f$;
6. Rotating $\dot{\vec{r}}$ by $\dot{\vec{p}} = R_1(i)R_3(\Omega)\dot{\vec{r}}$ and then using Eq. 3.47 to compute ω and f;
7. Using Eqs. 3.33, 3.39 and 3.40 to compute E, M and t_p.

To transform the GPS state vector from the ECSF coordinate system to other coordinate systems, the formulas discussed in Chap. 2 can be used.

3.2 Disturbed Satellite Motion

Keplerian motion of the satellite is a motion under the assumption that the satellite is only attracted by the central force of the Earth. This is, of course, an approximation. The Earth cannot be considered a mass point or a homogenous sphere for a satellite problem. The total attracting force of the Earth can be considered the central force plus the non-central force. The latter one is called Earth's disturbing force, which has

(c) ketabton.com: The Digital Library

an order of 10^{-4} compared with the central force. The other attracting forces are simply called disturbing forces. They are the attracting forces of the Sun and the Moon, the Earth and ocean tide, as well as surface forces such as solar radiation pressure, atmospheric drag, etc. The satellite motion can then be considered a nominal motion (e.g., Keplerian motion) plus a disturbed motion.

If we further use the Keplerian elements to describe the disturbed motion of the satellite, all elements should be functions of time. Keplerian elements ($\Omega(t)$, $i(t)$, $\omega(t)$, $a(t)$, $e(t)$, $M(t)$) can be represented by $\sigma_j(t)$, $j = 1, \ldots, 6$, thus the polynomial approximations are

$$\sigma_j(t) = \sigma_j(t_0) + \left.\frac{\mathrm{d}\sigma_j(t)}{\mathrm{d}t}\right|_{t=t_0} (t - t_0) + \ldots \quad j = 1, \ldots, 6 \,. \tag{3.48}$$

In other words, the disturbed orbit can be further represented by Keplerian elements; however, all elements are time variables. If the initial elements and their changing rates are given, the instantaneous elements can be obtained. This principle is used in the broadcast ephemerides.

Detailed disturbing theory and orbit correction as well as orbit determination will be discussed in Chap. 11 later.

3.3 GPS Broadcast Ephemerides

GPS broadcast ephemerides are forecasted, predicted or extrapolated satellite orbits data which are transmitted from the satellite to the receiver in the navigation message. Because of the nature of the extrapolation, broadcast ephemerides do not have enough high qualities for precise applications. The predicted orbits are curve fitted to a set of relatively simple disturbed Keplerian elements and transmitted to the users.

The broadcast messages are

- SV-id : satellite number;
- t_c : reference epoch of the satellite clock;
- a_0, a_1, a_2: polynomial coefficients of the clock error;
- t_{oe} : reference epoch of the ephemerides;
- $\sqrt{a}$: square root of the semimajor axis of the orbital ellipse;
- e : numerical eccentricity of the ellipse;
- M_0 : mean anomaly at the reference epoch t_{oe};
- ω_0 : argument of perigee;
- i_0 : inclination of the orbital plane;
- Ω_0 : right ascension of ascending node;
- Δn : mean motion difference;
- $idot$: rate of inclination angle;
- $\dot{\Omega}$: rate of node's right ascension;
- C_{uc}, C_{us} : correction coefficients (of argument of latitude);
- C_{rc}, C_{rs} : correction coefficients (of geocentric distance);
- C_{ic}, C_{is} : correction coefficients (of inclination).

(c) ketabton.com: The Digital Library

The satellite position at epoch t can be computed as follows:

$$M = M_0 + \left(\sqrt{\frac{\mu}{a^3}} + \Delta n\right)(t - t_{oe}),$$

$$\Omega = \Omega_0 + \dot{\Omega}(t - t_{oe}),$$

$$\omega = \omega_0 + C_{uc}\cos(2u_0) + C_{us}\sin(2u_0),$$

$$r = r_0 + C_{rc}\cos(2u_0) + C_{rs}\sin(2u_0), \quad \text{and}$$

$$i = i_0 + C_{ic}\cos(2u_0) + C_{is}\sin(2u_0) + idot(t - t_{oe}), \tag{3.49}$$

where

$$E = M + e\sin E,$$

$$r_0 = a(1 - e\cos E),$$

$$f = 2\tan^{-1}\left(\frac{\sqrt{1+e}}{\sqrt{1-e}}\tan\frac{E}{2}\right), \quad \text{and}$$

$$u_0 = \omega_0 + f. \tag{3.50}$$

μ is the Earth's gravitational constant (which can be read from the IERS Conventions, cf., table of constants). The satellite position in the orbital plane coordinate system (the 1st-axis points to the ascending node, the 3rd-axis is vertical to the orbital plane, and the 2nd-axis completes a right-handed system) is then

$$\begin{pmatrix} x' \\ y' \\ z' \end{pmatrix} = \begin{pmatrix} r\cos u \\ r\sin u \\ 0 \end{pmatrix},$$

where $u = \omega + f$. The position vector can be rotated to the ECSF coordinate system by $R_3(-\Omega)R_1(-i)$ and then rotated to the ECEF coordinate system by $R_3(\Theta)$, where Θ is Greenwich Sidereal Time and

$$\Theta = \omega_e(t - t_{oe}) + \omega_e t_{oe}, \tag{3.51}$$

where ω_e is the angular velocity of the Earth (can be read from the IERS Conventions, cf., table of constants). The satellite position vector in the ECEF coordinate system is then

$$\begin{pmatrix} x \\ y \\ z \end{pmatrix}_{ECEF} = R_3(-\Omega + \Theta)R_1(-i)\begin{pmatrix} r\cos u \\ r\sin u \\ 0 \end{pmatrix}. \tag{3.52}$$

(c) ketabton.com: The Digital Library

The first equation of 3.50 is the Keplerian equation, which may be solved iteratively. It is notable that the time t above should be the signal transmitting time. $(t - t_{oe})$ should be the actual total time difference of the two time epochs and must account for the beginning and end of week crossovers (cf., Spilker 1996). That is, if the difference is greater (or less) than 302 400 sec, subtract (or add) 604 800 sec. The satellite clock error can be computed by (denoting k as the satellite's id)

$$\delta t_k = a_0 + a_1(t - t_c) + a_2(t - t_c)^2 \ . \tag{3.53}$$

Unit seconds are used for the time variable; the computed clock error has units of 10^{-6} sec.

3.4 IGS Precise Ephemerides

GPS satellite precise orbits are available through the International GPS Service (IGS) in the form of post-proceeded results. Such orbits data are called IGS precise ephemerides. They can be downloaded for free from several internet homepages (e.g., *www.gfz-potsdam.de*).

IGS data are given in the ECEF coordinate system. For all possible satellites, the position vectors are given in x, y, z three components (units: km), and the related clock errors are also given (units: 10^{-6} sec). The data are given in a suitable time interval (15 min).

To obtain the ephemerides of any interested epoch, a Lagrange polynomial is used to fit the given data and then to interpolate the data at the needed epoch. The general Lagrange polynomial is (e.g., Wang et al. 1979):

$$y(t) = \sum_{j=0}^{m} L_j(t) \cdot y(t_j) \ , \tag{3.54}$$

where

$$L_j(t) = \prod_{k=0}^{m} \frac{(t - t_k)}{(t_j - t_k)}, \quad k \neq j \ , \tag{3.55}$$

where symbol Π is a multiplying operator from $k = 0$ to $k = m$, m is the order of the polynomial, $y(t_j)$ are given data at the time t_j, $L_j(t)$ is called the base function of order m, and t is the time on which data will be interpolated. Generally speaking, t should be placed around the middle of the time duration (t_0, t_m) if possible. Therefore, m is usually selected as an odd number. For IGS orbit interpolation, a standard m is selected as 7 or 9 from experience.

For the equal distance Lagrange interpolation there is

$$\begin{aligned} t_k &= t_0 + k\Delta t \\ t - t_k &= t - t_0 - k\Delta t \ , \\ t_j - t_k &= (j - k)\Delta t \end{aligned}$$

(c) ketabton.com: The Digital Library

then

$$L_j(t) = \prod_{k=0}^{m} \frac{(t - t_0 - k\Delta t)}{(j-k)\Delta t}, \quad k \neq j \ , \tag{3.56}$$

where Δt is the data interval.

In order to deal with the broadcast ephemerides in a manner similar to IGS precise ephemerides, the broadcast orbit may be first computed and then transformed to an IGS like data for use.

The forecasted IGS ephemerides are now also available to download for free.

3.5 GLONASS Ephemerides

GLONASS broadcast ephemerides are forecasted, predicted or extrapolated satellite orbit data which are transmitted from the satellite to the receiver in the navigation message. The broadcast messages include the following: satellite number, reference epoch of the ephemerides, relative frequency offset, satellite clock offset, satellite position, satellite velocity, satellite acceleration, time system correction with respect to UTC_{SU}, the time difference between GLONASS time and GPS time, etc.

The satellite position and velocity at desired epoch t can be interpolated by using the Lagrange polynomial discussed in Sect. 3.4, or alternatively, by a five-order polynomial discussed in Sect. 5.4.2 where the position, velocity and acceleration data are used.

The precise GLONASS ephemerides are similarly available. The data has nearly the same format as that of GPS and includes the message of the time differences of the GLONASS time and GPS time.

(c) ketabton.com: The Digital Library

Chapter 4

GPS Observables

The basic GPS observables are code pseudoranges and carrier phases as well as Doppler measurements. The principle of the GPS measurements and their mathematical expressions are described.

4.1 Code Pseudoranges

The pseudorange is a measure of the distance between the satellite and the receiver's antenna. The distance is measured through measuring the GPS signal transmitting time from the satellite to the GPS receiver's antenna. Therefore, such a distance is referred to the distance between the satellite at the time of the GPS signal emission and the GPS antenna at the time of GPS signal reception. The transmitting time is measured through maximum correlation analysis of the receiver code and the GPS signal. The receiver code is derived from the clock used in the GPS receiver. The GPS signal is, of course, generated by the clock used in the GPS satellite. The measured pseudorange is different from the geometric distance between the satellite and the receiver's antenna because of the errors of the both clocks and the influences of the signal transmitting mediums. It is also notable that the path of the signal transmission differs slightly from the geometric path. The transmitting medium not only delays the transmitting of the signal, but also bends the transmitting path of the signal.

The GPS signal emission time of the satellite is denoted by t_e, and the GPS signal reception time of the receiver is denoted by t_r. In case of vacuum medium and error-free situation, the measured pseudorange is equal to the geometric distance and can be presented by

$$R_r^s(t_r, t_e) = (t_r - t_e)c \ , \tag{4.1}$$

where c denotes the speed of light, and subscript r and superscript s denote the receiver and satellite, respectively. On the left-hand side, t_r denotes the epoch at which the pseudorange is measured.

t_e and t_r are considered true emission time and reception time of the GPS signal. Taking both the satellite and receiver clock errors into account, the pseudorange can be represented as

$$R_r^s(t_r, t_e) = (t_r - t_e)c - (\delta t_r - \delta t_s)c \ , \tag{4.2}$$

where δt_r and δt_s denote the clock errors of the receiver and satellite, respectively. The GPS satellite clock error term δt_s is indeed known through GPS satellite orbit determination. The clock errors are usually modelled by polynomials of time. The constant term repre-

(c) ketabton.com: The Digital Library

sents the bias and the linear term the drift of the clocks. These coefficients are transmitted along with the navigation message to the users. More precisely, the satellite clock error corrections can be also obtained from all IGS data centres (cf., e.g., *www.gfz-potsdam.de*). They are determined along with the precise IGS orbits and have higher resolution in time.

The geometric distance of the first term on the right-hand side of Eq. 4.2 is given by

$$\rho_r^s(t_r,t_e) = \sqrt{(x_s - x_r)^2 + (y_s - y_r)^2 + (z_s - z_r)^2}\ , \tag{4.3}$$

where the satellite coordinate vector (x_s, y_s, z_s) is a vector function of the time t_e, and the receiver coordinate (x_r, y_r, z_r) is a function of the time t_r. Therefore, the geometric distance is indeed a function of two time variables. Furthermore, the emission time t_e is unknown in practice. Denoting the transmitting time as Δt, there is

$$\Delta t = t_r - t_e\,. \tag{4.4}$$

For illustrating the transmitting time computation, the geometric distance can be generally written as

$$\rho_r^s(t_r,t_e) = \rho_r^s(t_r,t_r - \Delta t)\,. \tag{4.5}$$

The transmitting time of the signal travelling from the GPS satellite to the receiver is about 0.07 sec. The geometric distance function on the right-hand side of Eq. 4.5 can be expanded into a Taylor series at the reception time t_r with respect to the transmitting time by

$$\rho_r^s(t_r,t_e) = \rho_r^s(t_r) + [\mathrm{d}\rho_r^s(t_r)/\mathrm{d}t]\Delta t\ , \tag{4.6}$$

where $\mathrm{d}\rho_r^s(t_r)/\mathrm{d}t$ denotes the time derivation of the radial distance between satellite and receiver. The second term on the right-hand side of Eq. 4.6 is called the transmitting time correction. It is notable that the coordinates of GPS antennas are usually given in the ECEF coordinate system. During the signal transmission, the receiver rotates with the Earth, therefore by computing the distance of Eq. 4.3, the so-called Earth rotation correction has to be considered.

Taking the ionospheric effects, tropospheric effects, Earth tide and loading tide effects, multipath and relativistic effects as well as remaining errors into account, the pseudorange model Eq. 4.2 can be completed by

$$R_r^s(t_r,t_e) = \rho_r^s(t_r,t_e) - (\delta t_r - \delta t_s)c + \delta_{ion} + \delta_{tro} + \delta_{tide} + \delta_{mul} + \delta_{rel} + \varepsilon\,. \tag{4.7}$$

Where the measured pseudorange is on the left-hand side, it equals to the geometric distance between the satellite at the emission time and the antenna at the reception time plus or minus several corrections. The clock error corrections are scaled by the velocity of light c. δ_{ion} and δ_{tro} denote the ionospheric and tropospheric effects of the station r. δ_{tide} denotes the Earth tide and ocean loading tide effects, δ_{mul} denotes the multipath effects, and δ_{rel} denotes the relativistic effects. The remaining errors are denoted by ε. For convenience, unit meter is used for all terms and instrumental biases are omitted here.

The height of the GPS satellite is about 20 200 km; thus, the GPS signal transmitting time is about 0.07 sec. The Earth rotates during the signal transition. The angular

(c) ketabton.com: The Digital Library

velocity of the Earth rotation is about 15 arcsec sec^{-1}. The related Earth rotation correction is about 1 arcsec (cf., Goad 1996). The effects of such a correction depend on the latitude of the station. At the equator, 1 arcsec rotation is equivalent to about 31 meters position displacement. The clock errors could be very big. There are examples where the negative pseudoranges are observed in practice.

The above-discussed pseudorange model is generally valid for both C/A code and P code. The precision of the pseudorange measurements depends on the electronic abilities. Generally speaking, it is no problem nowadays to measure with precision up to 1% of the chip length. Therefore, the C/A code has a precision of about 3 m, and the P code 30 cm. The mentioned corrections will be discussed later in detail.

4.2 Carrier Phases

The carrier phase is a measure of the phase of the received satellite signal relative to the receiver-generated carrier phase at the reception time. The measurement is made by shifting the receiver-generated phase to track the received phase. The number of full carrier waves between the receiver and the satellite cannot be accounted for at the initial signal acquisition. Therefore, measuring the carrier phase is to measure the fractional phase and to keep track of changes in the cycles. The carrier phase observable is indeed an accumulated carrier phase observation. The fractional carrier phase can be measured by electronics with precision better than 1% of the wavelength, which corresponds to millimetre precision. This is also the reason why the phase measurement is more precise than that of the code. A full carrier wave is called a cycle. The ambiguous integer number of cycles in the carrier phase measurement is called ambiguity. The initial measuring has correct fractional phase and an arbitrary integer counter setting at the start epoch. Such an arbitrary initial setting will be adjusted to the correct one by modelling with ambiguity parameters.

In the case of a vacuum medium and an error-free situation, the measured phase can be presented by

$$\Phi_{\mathrm{r}}^{\mathrm{s}}(t_{\mathrm{r}}) = \Phi_{\mathrm{r}}(t_{\mathrm{r}}) - \Phi^{\mathrm{s}}(t_{\mathrm{r}}) + N_{\mathrm{r}}^{\mathrm{s}} \ , \tag{4.8}$$

where subscript r and superscript s denote the receiver and satellite, respectively. t_{r} denotes the GPS signal reception time of the receiver. Φ_{r} denotes the phase of receiver's oscillator. Φ^{s} denotes the received signal phase of the satellite. $N_{\mathrm{r}}^{\mathrm{s}}$ is the ambiguity related to receiver r and satellite s.

There is an interesting property of the signal phase transmission, i.e., the received phase of the satellite signal at the reception time is exactly the same as the phase of the emitted satellite signal at the emission time (Remondi 1984; Leick 1995), i.e.:

$$\Phi^{\mathrm{s}}(t_{\mathrm{r}}) = \Phi_{\mathrm{e}}^{\mathrm{s}}(t_{\mathrm{r}} - \Delta t) \ , \tag{4.9}$$

where $\Phi_{\mathrm{e}}^{\mathrm{s}}$ denotes the satellite emitted phase and Δt is the GPS signal transmitting time. This can be represented by

$$\Delta t = \frac{\rho_{\mathrm{r}}^{\mathrm{s}}(t_{\mathrm{r}}, t_{\mathrm{e}})}{c} \ , \tag{4.10}$$

(c) ketabton.com: The Digital Library

where $\rho_r^s(t_r, t_e)$ is geometric distance between the satellite at the emission time t_e, and the GPS antenna at the reception time t_r, c is the speed of light. Then Eq. 4.8 can be written as:

$$\Phi_r^s(t_r) = \Phi_r(t_r) - \Phi_e^s(t_r - \Delta t) + N_r^s \ . \tag{4.11}$$

Suppose the initial time is zero and the received satellite signal and the reference carrier of the receiver have the nominal frequency f. Then one has

$$\Phi_r(t_r) = f t_r \quad \text{and} \tag{4.12}$$

$$\Phi_e^s(t_r - \Delta t) = f(t_r - \Delta t) \ . \tag{4.13}$$

Substituting Eqs. 4.10, 4.12 and 4.13 into Eq. 4.11 gives

$$\Phi_r^s(t_r) = \frac{\rho_r^s(t_r, t_e) f}{c} + N_r^s \, . \tag{4.14}$$

Taking both the satellite and receiver clock errors into account, the carrier phase can be represented as

$$\Phi_r^s(t_r) = \frac{\rho_r^s(t_r, t_e) f}{c} - f(\delta t_r - \delta t_s) + N_r^s \, , \tag{4.15}$$

where δt_r and δt_s denote the clock errors of the receiver and satellite, respectively. The frequency f and wavelength λ have the relation of

$$c = f\lambda \ . \tag{4.16}$$

Taking the ionospheric effects, tropospheric effects, Earth tide and loading tide effects, multipath and relativistic effects as well as remaining errors into account, the carrier phase model Eq. 4.15 can be completed by

$$\Phi_r^s(t_r) = \frac{\rho_r^s(t_r, t_e)}{\lambda} - f(\delta t_r - \delta t_s) + N_r^s - \frac{\delta_{ion}}{\lambda} + \frac{\delta_{tro}}{\lambda} + \frac{\delta_{tide}}{\lambda} + \frac{\delta_{mul}}{\lambda} + \frac{\delta_{rel}}{\lambda} + \frac{\varepsilon}{\lambda} \tag{4.17}$$

or

$$\lambda\Phi_r^s(t_r) = \rho_r^s(t_r, t_e) - (\delta t_r - \delta t_s)c + \lambda N_r^s - \delta_{ion} + \delta_{tro} + \delta_{tide} + \delta_{mul} + \delta_{rel} + \varepsilon \, , \tag{4.18}$$

where the measured phase on the left-hand side with a factor of λ equals the geometric distance between the satellite at the emission time and the antenna at the reception time plus or minus several corrections. The clock error corrections are scaled by the speed of light c. δ_{ion} and δ_{tro} denote the ionospheric and tropospheric effects of the station r. δ_{tide} denotes the Earth tide and ocean loading tide effects. The multipath and relativistic effects as well as remaining errors are denoted by δ_{mul}, δ_{rel}, ε respectively. Equation 4.18 is convenient to use, because all terms have units of length (meter). It is notable that the sign of the ionospheric term is negative, whereas in the pseudorange model it is positive (see Sect. 4.1). This will be discussed later in Sect. 5.1 in detail.

(c) ketabton.com: The Digital Library

During GPS signal tracking, the phase and the integer account are continuously modelled and frequently measured. In this way, the changing oscillator frequency is accounted for. Every time the phase is measured, the coefficients in the tracking loop model are updated (Remondi 1984) to ensure sufficient precision of measurement.

4.3 Doppler Measurements

The Doppler effect is a phenomenon of frequency shift of the electromagnetic signal caused by the relative motion of the emitter and receiver. Supposing the emitted signal has the nominal frequency f, the radial velocity of the satellite related to the receiver is

$$V_\rho = \vec{V} \cdot \vec{U}_\rho = \left|\vec{V}\right| \cos\alpha \ , \tag{4.19}$$

where $\vec{V}$ is the velocity vector of the satellite related to the receiver, $V = \left|\vec{V}\right|$, $\vec{U}_\rho$ is the identity vector in the direction from the receiver to the satellite, α is the projection angle of the vector $\vec{V}$ to $\vec{U}_\rho$ (see Fig. 4.1), index ρ is the distance from the receiver to satellite. Then the received signal has a frequency of

$$f_\mathrm{r} = f\left(1 + \frac{V_\rho}{c}\right)^{-1} \approx f\left(1 - \frac{V_\rho}{c}\right) , \tag{4.20}$$

where c is the speed of light. The Doppler frequency shift is then

$$f_\mathrm{d} = f - f_\mathrm{r} \approx f\frac{V_\rho}{c} = \frac{V_\rho}{\lambda} = \frac{\mathrm{d}\rho}{\lambda \mathrm{d}t} \ , \tag{4.21}$$

where $\lambda = (f/c)$ is the wavelength.

The Doppler count (or integrated Doppler) D is the historical observable of the TRANSIT satellite and is the integration of the frequency shift over a time interval (ca. 1 minute). If the time interval is selected small enough, the Doppler count is the same as the instantaneous frequency shift, or

$$D = \frac{\mathrm{d}\rho}{\lambda \mathrm{d}t} \ . \tag{4.22}$$

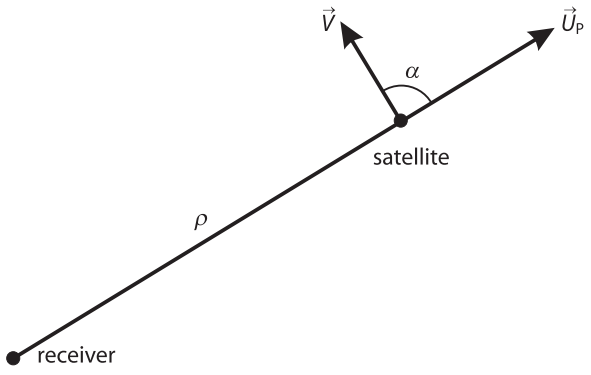

Fig. 4.1.
Doppler effects

(c) ketabton.com: The Digital Library

The approximately predicted Doppler frequency shift is required to get the satellite signal acquired. Prediction of D is a part of the GPS signal tracking process. The predicted D is used to predict the phase change first, and then the phase change is compared with the measured value to get the precise value of the Doppler frequency shift. The accumulated integer account of cycles is obtained through a polynomial fitting of a series of predicted phase changes and measured values (Remondi 1984). Therefore, the Doppler frequency shift is a by-product of the carrier phase measurements. However, the Doppler frequency shift is an independent observable and a measure of the instantaneous range rate.

Notice that in an error free environment, $\mathrm{d}\rho/(\lambda \mathrm{d}t)$ is the same as $\mathrm{d}\Phi/\mathrm{d}t$ and Φ is the phase measurement discussed in Sect. 4.2. Then the model of Eq. 4.22 can be obtained by differentiating the Eq. 4.17 with respect to the time t:

$$D = \frac{\mathrm{d}\rho_{\mathrm{r}}^{s}(t_{\mathrm{r}}, t_{\mathrm{e}})}{\lambda \mathrm{d}t} - f\frac{\mathrm{d}\beta}{\mathrm{d}t} + \delta_f + \varepsilon\,, \tag{4.23}$$

where β is the term of clock error ($\delta t_{\mathrm{r}} - \delta t_{\mathrm{s}}$), δ_f is the frequency correction of the relativistic effects and ε is error. Effects with low frequency properties such as ionosphere, troposphere, tide, and multipath effects are cancelled out.

(c) ketabton.com: The Digital Library

Chapter 5

Physical Influences of GPS Surveying

This chapter covers all physical influences of GPS observations, including ionospheric effects, tropospheric effects, relativistic effects, Earth tide and ocean loading tide effects, clock errors, antenna mass centre and phase centre corrections, multipath effects, anti-spoofing and historical selective availability, as well as instrumental biases. Theories, models and algorithms are discussed in detail.

5.1 Ionospheric Effects

The ionospheric effect is an important error source in GPS measuring. The amount of the ionospheric delay or advance of the GPS signal can vary from a few meters to more than twenty meters within one day. Generally, it is difficult to model the ionospheric effects due to complicated physical interactions among the geomagnetic field and solar activities. However, the ionosphere is a dispersive medium, i.e., the ionospheric effect is frequency dependent. Using this property, the GPS system is designed with several working frequencies, so that ionospheric effects can be measured or corrected.

5.1.1 Code Delay and Phase Advance

The phase velocity v_p of an electromagnetic wave with one frequency propagating in the space can be represented by

$$v_p = \lambda f, \tag{5.1}$$

where λ is the wavelength and f is the frequency; index p denotes phase. This formula is valid for both GPS L1 and L2 phase signals.

A modulated signal will propagate in the space with a velocity, which is called group velocity. Group velocity is different from phase velocity. The relationship between group velocity and phase velocity was found more than 100 years ago by Rayleigh (Seeber 1993):

$$v_g = v_p - \lambda \frac{dv_p}{d\lambda}, \tag{5.2}$$

where $dv_p / d\lambda$ is the differentiation of v_p with respect to wave length λ; index g denotes group. This group velocity is valid for GPS code measurements.

(c) ketabton.com: The Digital Library

From Eq. 5.1, one has the total differentiation

$$\mathrm{d}\lambda / \lambda = -\mathrm{d}f / f \ , \tag{5.3}$$

and Eq. 5.2 can be rewritten as

$$v_\mathrm{g} = v_\mathrm{p} + f(\mathrm{d}v_\mathrm{p} / \mathrm{d}f) \ . \tag{5.4}$$

If the electromagnetic wave is transmitted in vacuum space, the phase velocity and the group velocity are the same and are equal to the speed of light in a vacuum. In such a case, the medium is called a non-dispersive one; otherwise, the medium is called a dispersive one. Two factors n_p and n_g are introduced so that both

$$v_\mathrm{g} n_\mathrm{g} = c \quad \text{and} \tag{5.5}$$

$$v_\mathrm{p} n_\mathrm{p} = c \tag{5.6}$$

are valid. These two factors n_p and n_g are called refractive indices. Such a refractive index characterises how the medium delays or advances the signal propagating velocity from the speed of light in a vacuum.

Differentiation of v_p with respect to frequency f can then be obtained from Eq. 5.6 by

$$\frac{\mathrm{d}v_\mathrm{p}}{\mathrm{d}f} = -\frac{c}{n_\mathrm{p}^2}\left(\frac{\mathrm{d}n_\mathrm{p}}{\mathrm{d}f}\right). \tag{5.7}$$

Substituting the above three formulas into Eq. 5.4 yields

$$\frac{c}{n_\mathrm{g}} = \frac{1}{n_\mathrm{p}^2}\left(cn_\mathrm{p} - fc\frac{\mathrm{d}n_\mathrm{p}}{\mathrm{d}f}\right) \quad \text{or} \quad n_\mathrm{g} = \frac{n_\mathrm{p}^2}{n_\mathrm{p} - f\dfrac{\mathrm{d}n_p}{\mathrm{d}f}} \ . \tag{5.8}$$

Using the mathematical expansion

$$(1-x)^{-1} = 1 + x - x^2 - \ldots \qquad |x| < 1 \ , \tag{5.9}$$

Eq. 5.8 can be approximated to the first order by

$$n_\mathrm{g} = n_\mathrm{p} + f(\mathrm{d}n_\mathrm{p} / \mathrm{d}f) \ . \tag{5.10}$$

The phase refractive index can be represented by

$$n_\mathrm{p} = 1 + a_1 / f^2 + a_2 / f^3 + \ldots \ , \tag{5.11}$$

where coefficients a_1 and a_2 depend on the electronic density N_e and can be determined. Substituting Eq. 5.11 into Eq. 5.10 yields

$$n_\mathrm{g} = 1 - a_1 / f^2 - 2a_2 / f^3 \ . \tag{5.12}$$

(c) ketabton.com: The Digital Library

The change of the length of the signal transmitting path in the medium with refractivity n is

$$\Delta r = \int (n-1)\mathrm{d}s \ . \tag{5.13}$$

The integration is made along the signal transmitting path. Therefore, the ionospheric effects on the phase and code signal transmission can be represented as

$$\delta_\mathrm{p} = \int (n_\mathrm{p} - 1)\mathrm{d}s = \int \left(\frac{a_1}{f^2} + \frac{a_2}{f^3} \right) \mathrm{d}s \quad \text{and}$$

$$\delta_\mathrm{g} = \int (n_\mathrm{g} - 1)\mathrm{d}s = \int \left(-\frac{a_1}{f^2} - \frac{2a_2}{f^3} \right) \mathrm{d}s \ . \tag{5.14}$$

Omitting the second term on the right-hand side, one gets

$$\delta_\mathrm{p} = -\delta_\mathrm{g} = \int \left(\frac{a_1}{f^2} \right) \mathrm{d}s \ . \tag{5.15}$$

That is, the ionospheric effects on the phase and code measurements have the opposite signs and have approximately the same amount. The coefficient a_1 has been estimated by (cf. Seeber 1993)

$$a_1 = -40.3 N_\mathrm{e} \ , \tag{5.16}$$

where N_e is the electronic density.

The total electronic content (TEC) in the zenith direction can be defined as

$$\mathrm{TEC} = \int_{\text{zenith}} N_\mathrm{e} \mathrm{d}s \ , \tag{5.17}$$

which can be computed from special models. To combine the TEC in the zenith and in the signal transmitting path, a so-called slant factor or mapping function has to be introduced and will be discussed in Sect. 5.1.4 in detail.

The electronic density always has a positive value; therefore, δ_g has a positive value and δ_p negative. That is, the ionosphere delays the code signal transmission and advances the phase signal transmission.

5.1.2 Elimination of the Ionospheric Effects

Dual-Frequency Combination

The ionospheric effects on the phase (cf. Sect. 5.1.1) is rewritten as

$$\delta_\mathrm{p} = \frac{A_1}{f^2} \ , \quad \text{where} \quad A_1 = \int a_1 \mathrm{d}s \ . \tag{5.18}$$

(c) ketabton.com: The Digital Library

For the dual-frequency GPS phase observations, the ionospheric effects can be written as

$$\delta_{\mathrm{p}}(f_1) = \frac{A_1}{f_1^2} \quad \text{and} \tag{5.19}$$

$$\delta_{\mathrm{p}}(f_2) = \frac{A_1}{f_2^2} \,. \tag{5.20}$$

It is obvious that the following combination leads to an elimination of the ionospheric effects:

$$f_1^2 \delta_{\mathrm{p}}(f_1) - f_2^2 \delta_{\mathrm{p}}(f_2) = 0 \,. \tag{5.21}$$

In other words, through linear combination of the GPS phase observations, the ionospheric effects can be eliminated. The above discussion is valid for both the code and carrier phase measurements of dual-frequencies, i.e., there is

$$f_1^2 \delta_{\mathrm{g}}(f_1) - f_2^2 \delta_{\mathrm{g}}(f_2) = 0 \,. \tag{5.22}$$

It should be pointed out that such ionosphere-free combination is indeed a first order approximation because of the omission of the terms of the second order ionospheric effects of Eq. 5.14 in 5.15. Furthermore, the combinations of Eqs. 5.21 and 5.22 have to be standardised by dividing $f_1^2 - f_2^2$, so that the combined code and phase observations also have the sense that they are code and phase observables at a special frequency. The standard (first order) ionosphere-free phase and code combinations can be represented then as

$$\frac{f_1^2 \delta_{\mathrm{p}}(f_1) - f_2^2 \delta_{\mathrm{p}}(f_2)}{f_1^2 - f_2^2} = 0 \quad \text{and} \tag{5.23}$$

$$\frac{f_1^2 \delta_{\mathrm{g}}(f_1) - f_2^2 \delta_{\mathrm{g}}(f_2)}{f_1^2 - f_2^2} = 0 \,. \tag{5.24}$$

Formally the combined observations are observed at frequency

$$f = \frac{f_1^2 f_1 - f_2^2 f_2}{f_1^2 - f_2^2} \,, \tag{5.25}$$

which has the wavelength of $\lambda = c/f$, where c is the speed of light in a vacuum.

Triple-Frequency Combination

As mentioned above, a dual-frequency combination can only eliminate the first order ionospheric effects. It is obvious that a triple-frequency combination can eliminate the ionospheric effects up to the second order.

The ionospheric effects on the phase (cf. Sect. 5.1.1) are rewritten as

$$\delta_{\mathrm{p}} = \frac{A_1}{f^2} + \frac{A_2}{f^3} \,, \quad \text{where} \quad A_1 = \int a_1 \mathrm{d}s \,, \quad A_2 = \int a_2 \mathrm{d}s \,. \tag{5.26}$$

(c) ketabton.com: The Digital Library

For the triple-frequency GPS phase observations, the ionospheric effects can be written as

$$\delta_{\mathrm{p}}(f_1) = \frac{A_1}{f_1^2} + \frac{A_2}{f_1^3}\,, \tag{5.27}$$

$$\delta_{\mathrm{p}}(f_2) = \frac{A_1}{f_2^2} + \frac{A_2}{f_2^3} \quad \text{and} \tag{5.28}$$

$$\delta_{\mathrm{p}}(f_5) = \frac{A_1}{f_5^2} + \frac{A_2}{f_5^3}\,. \tag{5.29}$$

The first order ionosphere-free combinations can be formed as

$$f_1^2\delta_{\mathrm{p}}(f_1) - f_2^2\delta_{\mathrm{p}}(f_2) = \frac{A_2}{f_1} - \frac{A_2}{f_2} \quad \text{and} \tag{5.30}$$

$$f_1^2\delta_{\mathrm{p}}(f_1) - f_5^2\delta_{\mathrm{p}}(f_5) = \frac{A_2}{f_1} - \frac{A_2}{f_5} \quad \text{or} \tag{5.31}$$

$$\frac{f_1^2\delta_{\mathrm{p}}(f_1) - f_2^2\delta_{\mathrm{p}}(f_2)}{\dfrac{1}{f_1} - \dfrac{1}{f_2}} = A_2 \quad \text{and} \tag{5.32}$$

$$\frac{f_1^2\delta_{\mathrm{p}}(f_1) - f_5^2\delta_{\mathrm{p}}(f_5)}{\dfrac{1}{f_1} - \dfrac{1}{f_5}} = A_2\,. \tag{5.33}$$

Then the second order ionosphere-free combination can be formed by

$$\frac{(f_1^2\delta_{\mathrm{p}}(f_1) - f_2^2\delta_{\mathrm{p}}(f_2))(f_1 f_2)}{(f_2 - f_1)} - \frac{(f_1^2\delta_{\mathrm{p}}(f_1) - f_5^2\delta_{\mathrm{p}}(f_5))(f_1 f_5)}{(f_5 - f_1)} = 0 \tag{5.34}$$

or

$$B_1\delta_{\mathrm{p}}(f_1) + B_2\delta_{\mathrm{p}}(f_2) + B_5\delta_{\mathrm{p}}(f_5) = 0\,, \tag{5.35}$$

where

$$B_1 = f_1^3 f_1 \frac{(f_5 - f_2)}{(f_2 - f_1)(f_5 - f_1)}\,, \tag{5.36}$$

$$B_2 = -\frac{f_2^3 f_1}{f_2 - f_1} \quad \text{and} \tag{5.37}$$

$$B_5 = \frac{f_5^3 f_1}{f_5 - f_1}\,. \tag{5.38}$$

(c) ketabton.com: The Digital Library

A standardisation of the combination in Eq. 5.35 can be made through

$$\frac{B_1\delta_p(f_1) + B_2\delta_p(f_2) + B_5\delta_p(f_5)}{B_1 + B_2 + B_5} = 0 \quad \text{or} \tag{5.39}$$

$$C_1\delta_p(f_1) + C_2\delta_p(f_2) + C_5\delta_p(f_5) = 0\,, \tag{5.40}$$

where

$$C_1 = \frac{f_1^3(f_5 - f_2)}{C_4}\,, \tag{5.41}$$

$$C_2 = -\frac{f_2^3(f_5 - f_1)}{C_4}\,, \tag{5.42}$$

$$C_5 = \frac{f_5^3(f_2 - f_1)}{C_4} \quad \text{and} \tag{5.43}$$

$$C_4 = f_1^3(f_5 - f_2) - f_2^3(f_5 - f_1) + f_5^3(f_2 - f_1)\,. \tag{5.44}$$

The above discussion is also valid for the code measurements of triple-frequencies, i.e., there is

$$C_1\delta_g(f_1) + C_2\delta_g(f_2) + C_5\delta_g(f_5) = 0\,. \tag{5.45}$$

Phase-Code Combination

Recalling the discussion in Sect. 5.1.1 and limiting ourselves to the first order approximation, the ionospheric effects on the phase and code measurements have the opposite signs and have approximately the same amount, i.e.,

$$\delta_p = -\delta_g = A_1 / f^2\,, \quad \text{where} \quad A_1 = \int a_1 \mathrm{d}s\,. \tag{5.46}$$

Therefore, a straightforward method to eliminate the ionospheric effects is then to combine the phase and code observables at the same frequency f together, i.e.,

$$\delta_p(f) + \delta_g(f) = 0\,. \tag{5.47}$$

It is notable that such a combination has lower precision than that of the carrier phase and code measurements, respectively.

5.1.3 Ionospheric Models

The Broadcast Ionospheric Model

The GPS broadcast message includes the parameters of a predicted ionospheric model (Klobuchar 1996; Leick 1995). Using the model parameters, the ionospheric effects can be computed and corrected.

(c) ketabton.com: The Digital Library

The input parameters of the broadcast ionospheric model are the eight model coefficients of $\alpha_i, \beta_i, i = 1, 2, 3, 4$, geodetic latitude φ and longitude λ of the GPS antenna, GPS observing time T in seconds, as well as the azimuth A and elevation E of the observed satellite. All four angular arguments φ, λ, A and E have the units of semicircles (SC), and 1 SC equals 180 degrees. The formulas are given below:

$$F = 1 + 16(0.53 - E)^3 \ , \tag{5.48}$$

$$\Psi = \frac{0.0137}{E + 0.11} - 0.022 \, , \tag{5.49}$$

$$\varphi_i = \varphi + \Psi \cos A \ , \tag{5.50}$$

$$\varphi_i = \frac{0.416\varphi_i}{|\varphi_i|} \ , \quad \text{if} \quad |\varphi_i| > 0.416 \, , \tag{5.51}$$

$$\lambda_i = \lambda + \psi \frac{\sin A}{\cos \varphi_i} \, , \tag{5.52}$$

$$\phi = \varphi_i + 0.064 \cos(\lambda_i - 1.167) \ , \tag{5.53}$$

$$t = \lambda_i 43200 + T \ , \tag{5.54}$$

$$t = t - 86400 \ , \quad \text{if} \quad t \geq 86400 \ , \tag{5.55}$$

$$t = t + 86400 \ , \quad \text{if} \quad t < 0 \ , \tag{5.56}$$

$$P = \sum_{i=1}^{4} \beta_i \phi^i \ , \tag{5.57}$$

$$P = 72000 \ , \quad \text{if} \quad P < 72000 \ , \tag{5.58}$$

$$x = \frac{2\pi(t - 50400)}{P} \ , \tag{5.59}$$

$$Q = \sum_{i=1}^{4} \alpha_i \phi^i \ , \tag{5.60}$$

$$Q = 0 \ , \quad \text{if} \quad Q < 0 \ , \tag{5.61}$$

$$\delta_{\mathrm{g}}(f_1) = cF5 \times 10^{-9} \ , \quad \text{if} \quad |x| > 1.57 \quad \text{and} \tag{5.62}$$

$$\delta_{\mathrm{g}}(f_1) = cF\left(5 \times 10^{-9} + Q\left(1 - \frac{x^2}{2} + \frac{x^4}{4}\right)\right) , \quad \text{if} \quad |x| < 1.57 \, . \tag{5.63}$$

φ_i and λ_i are the geodetic latitude and longitude of the sub-ionospheric point. The ionospheric point is defined as the point on the sight of the satellite, which has the average ionospheric height (350 km), and the sub-ionospheric point is the projection

(c) ketabton.com: The Digital Library

point of the ionospheric point onto the Earth's surface, which has a height of 50 km, ϕ being the geomagnetic latitude of the sub-ionospheric point. ψ is the Earth's central angle between the GPS station and the ionospheric point. F is the slant factor or mapping function that maps the ionospheric effects of the zenith direction onto the signal transmitting path. The local time at the sub-ionospheric point is denoted by t. P and Q are the period and amplitude in seconds. The phase is denoted by x. c is the speed of light. Frequency of L1 is denoted by f_1.

The ionospheric group delay on the L2 frequency can be computed by

$$\delta_g(f_2) = \frac{f_1^2}{f_2^2}\delta_g(f_1)\,. \tag{5.64}$$

The phase advance has only an opposite sign if the phase has been scaled to have units of length. Dividing the length with the wavelength can transform the units of length to the units of cycle.

Figure 5.1 shows the ionospheric effects of the broadcasted ionospheric model of 9 September 2001. The ionospheric parameters are

$$(\alpha_i) = \begin{pmatrix}3073 & 1490 & -11920 & -11920\end{pmatrix}\times 10^{-11} \quad \text{and}$$

$$(\beta_i) = \begin{pmatrix}1372 & 1638 & -1966 & 3932\end{pmatrix}\times 10^{+2}\,.$$

Station coordinates are selected as ($\varphi = 45°$, $\lambda = 0°$). Computation has been carried out for a whole day of 24 hours in GPS time. The continuous line shows the ionospheric effects on a satellite that repeats its orbit every four hours and changes its elevation and azimuth regularly from (5°–85°–5°) and (30°–150°), respectively. The broken line shows the (zenith) ionospheric effects of a space fixed satellite in the zenith direction (elevation = 90°, azimuth = 180°). It shows the strong dependency of the ionospheric effects on the time and zenith angle of the satellite. In the zenith direction, the ionospheric effects remain constant (1.5 meter) before 9 o'clock and after 19 o'clock. Strong changes happen at the time of sunrise and sunset and the ionospheric noon (14:00). Depending on the elevation of the satellite, the ionospheric effects may be amplified up to three times.

The broadcast ionospheric model can remove the ionospheric delay more than 50% (Langly 1998).

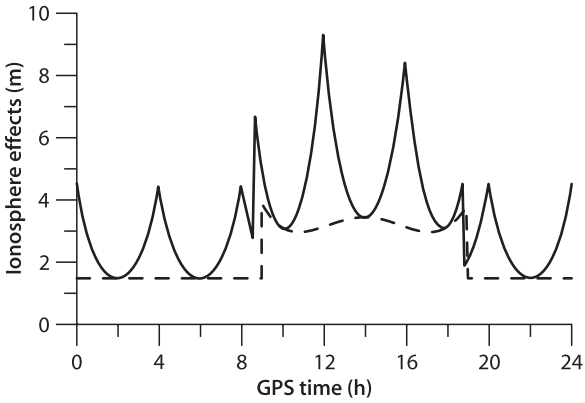

Fig. 5.1.
Broadcasted ionospheric model

(c) ketabton.com: The Digital Library

Dual-Frequency Ionosphere Measuring Model

In pseudorange measurement only the ionospheric effects depend on the working frequency. Therefore, a simple difference of the pseudoranges of the dual-frequencies can eliminate all other effects except the ionospheric effects and subsequently can be used for determining the ionospheric delay:

$$R_1 - R_2 = \delta_g(f_1) - \delta_g(f_2) = \left(1 - \frac{f_1^2}{f_2^2}\right)\delta_g(f_1) \quad \text{or} \tag{5.65}$$

$$\delta_g(f_1) = \frac{R_1 - R_2}{1 - \frac{f_1^2}{f_2^2}}, \tag{5.66}$$

where R_1 and R_2 are the L1 and L2 pseudoranges, and f_1 and f_2 are the frequencies of the L1 and L2 carriers. Here the random measurement error and un-modelled bias are omitted.

Similarly, the ionospheric effects can be determined by dual-frequency phase observables. Recall the phase observable model discussed in Sect. 4.2 where a simple differential combination of both phase pseudoranges can be formed as:

$$\begin{aligned}\lambda_1\Phi_1 - \lambda_2\Phi_2 &= \delta_p(f_1) - \delta_p(f_2) + \lambda_1 N_1 - \lambda_2 N_2 \\ &= \left(1 - \frac{f_1^2}{f_2^2}\right)\delta_p(f_1) + \lambda_1 N_1 - \lambda_2 N_2 ,\end{aligned} \tag{5.67}$$

or

$$\delta_p(f_1) = \frac{\lambda_1\Phi_1 - \lambda_2\Phi_2 - \lambda_1 N_1 + \lambda_2 N_2}{1 - \frac{f_1^2}{f_2^2}}, \tag{5.68}$$

where Φ_1 and Φ_2 are the L1 and L2 phase pseudoranges (in units of cycles), and N_1 and N_2 are the ambiguities of the L1 and L2 carriers. The random measurement error and un-modelled bias are omitted here. As long as the phase measurements are continuous (no cycle slips), the $\lambda_1 N_1 - \lambda_2 N_2$ remains a constant. Through a long term statistic comparison of Eqs. 5.66 and 5.68, the constant $\lambda_1 N_1 - \lambda_2 N_2$ can be approximately determined. The variation of the ionospheric effects can be determined very well by using this method.

5.1.4 Mapping Functions

As mentioned in Sect. 5.1.1, in order to combine the TEC in zenith direction and in the signal transmitting path, the slant factor or mapping function F is needed so that:

$$\mathrm{TEC}_\rho = \mathrm{TEC}_z F , \tag{5.69}$$

where indices ρ and z denote the path and zenith directions, respectively.

Generally, the ionosphere begins at a height of 50 km and ends at a height of about 750 km. It is therefore assumed that the ionosphere has an average height of 350 km (see Fig. 5.2). The sight line of the satellite crosses over the shell at the so-called iono-

(c) ketabton.com: The Digital Library

spheric point. The projection of the ionospheric point at a height of 50 km is called the sub-ionospheric point. The point at the sight line of the satellite at a height of 50 km is called the sub-ionospheric point in sight. The point at the sight line of the satellite at a height of 750 km is called the sup-ionospheric point in sight. These four points are denoted by P_{ip}, P_{sip}, P_{sips} and P_{supip} respectively.

Projection Mapping Function

Based on a single layer model, a homogeneous distribution of the free electrons is assumed (Fig. 5.2). This is equivalent to assuming all free electrons are concentrated in a shell of infinitesimal thickness at a height of 350 km. In such a case, the mapping function may be written as

$$F = \frac{1}{\cos z_{ip}}, \tag{5.70}$$

where z_{ip} is the satellite zenith angle at the ionospheric point. Using the sinus theorem, the relationship between the z_{ip} and zenith distance (z) of the satellite viewed from the receiver can be obtained by

$$\sin z_{ip} = \frac{r}{r + 350} \sin z, \tag{5.71}$$

where r is the mean radius of the Earth in km. Such a mapping function is called a single layer mapping function or projection mapping function. It is notable that Eq. 5.71 is exactly valid only for the spherical zenith angles.

Geometric Mapping Function

If a height-dependent homogeneous distribution of the free electrons is assumed, then the mapping function is a geometric one and is equivalent to

$$\mathrm{d}\rho = \mathrm{d}HF, \tag{5.72}$$

where $\mathrm{d}\rho$ and $\mathrm{d}H$ are the ionospheric path delay and zenith delay respectively.

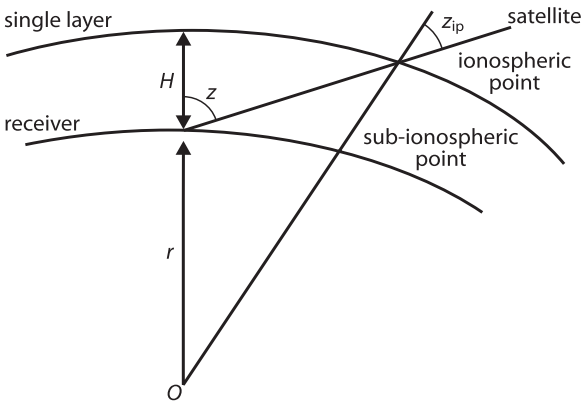

Fig. 5.2. Single-layer ionospheric model

(c) ketabton.com: The Digital Library

The zenith angle of the satellite at the sub-ionospheric point (in sight) P_{sips} is denoted by z_{sips} (Fig. 5.3). It can be computed by using the sinus theorem

$$\sin z_{sips} = \frac{r}{r+50}\sin z \ , \tag{5.73}$$

where z is the zenith angle of the satellite viewed from the receiver and r is the mean radius of the Earth in km. In the geometry, the spherical zenith angles are used here. The difference between the spherical zenith and geodetic zenith depends on the latitude of the station and the azimuth of the satellite. The maximum difference is the difference between geodetic latitude and geocentric latitude of the computing point; this is about $(e^2/2)\sin(2\varphi)$ (Torge 1991), where e^2 is the first numerical eccentricity (<0.0067) and φ is the geodetic latitude of the computing point. Therefore, the small angle difference can be omitted. Of course, for correctness the spherical zenith angle should be used here. It is the angle of the sight line to satellite with respect to the Earth centred radius vector of the station. Using the cosines theorem, one has

$$(r+50+H)^2 = (r+50)^2 + \rho^2 - 2(r+50)\rho\cos(180 - z_{sips}) \tag{5.74}$$

or

$$\rho^2 + 2(r+50)\cos(z_{sips})\rho + (r+50)^2 - (r+50+H)^2 = 0 \ , \tag{5.75}$$

where ρ and H are the lengths of lines from the sup-ionospheric point to the sub-ionospheric point in sight and sub-ionospheric point, respectively. The second order equation can be solved by

$$\rho = -(r+50)\cos(z_{sips}) \pm \sqrt{(r+50)^2\cos^2(z_{sips}) - (r+50)^2 + (r+50+H)^2} \tag{5.76}$$

or

$$\rho = -(r+50)\cos(z_{sips}) \pm \sqrt{(r+50+H)^2 - (r+50)^2\sin^2(z_{sips})} \ . \tag{5.77}$$

Because $\rho > 0$, Eq. 5.75 has a unique solution:

$$\rho = -(r+50)\cos(z_{sips}) + \sqrt{(r+50+H)^2 - (r+50)^2\sin^2(z_{sips})} \ . \tag{5.78}$$

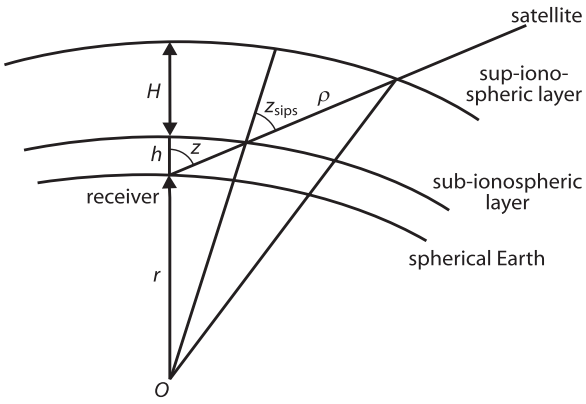

Fig. 5.3.
Spherical ionospheric model

(c) ketabton.com: The Digital Library

Comparing Eq. 5.72 with Eq. 5.78, one gets the geometric mapping function

$$F = -\frac{r+50}{H}\cos(z_{\text{sips}}) + \frac{\sqrt{(r+50+H)^2 - (r+50)^2\sin^2(z_{\text{sips}})}}{H}, \tag{5.79}$$

or approximately

$$F = -9.183\cos(z_{\text{sips}}) + 10.183\sqrt{1 - 0.81\sin^2(z_{\text{sips}})}\ , \tag{5.80}$$

where $r = 6\,378$ km and $H = 700$ km are used.

Above, the derived geometric mapping function of Eq. 5.79 is a spherical approximation if r is considered a constant.

Ellipsoidal Mapping Function

Taking the dependency of the radius r on the latitude φ into account, an ellipsoidal mapping function can be derived. According to Torge (1991),

$$r^2 = a^2\cos^2\beta + b^2\sin^2\beta \quad \text{and} \tag{5.81}$$

$$\tan\beta = \frac{b}{a}\tan\varphi\ ,$$

where r is the radius of the rotational ellipsoid, a and b are the semimajor axis and semiminor axis of the ellipsoid, and β is an angle that has the relation with geodetic latitude φ. Using the triangle formulae

$$2\cos^2\beta - 1 = 1 - 2\sin^2\beta = \frac{1-\tan^2\beta}{1+\tan^2\beta}\ , \tag{5.82}$$

Eq. 5.81 can be rewritten as

$$r^2 = \frac{a^2}{2}\left(\frac{1-\tan^2\beta}{1+\tan^2\beta} + 1\right) + \frac{b^2}{2}\left(1 - \frac{1-\tan^2\beta}{1+\tan^2\beta}\right), \quad \text{or} \tag{5.83}$$

$$r^2 = \frac{a^2}{2}\left(\frac{a^2 - b^2\tan^2\varphi}{a^2 + b^2\tan^2\varphi} + 1\right) + \frac{b^2}{2}\left(1 - \frac{a^2 - b^2\tan^2\varphi}{a^2 + b^2\tan^2\varphi}\right). \tag{5.84}$$

In an ellipsoid case, Eqs. 5.74 and 5.79 turn out to be

$$(r_s + 50 + H)^2 = (r_i + 50)^2 + \rho^2 - 2(r_i + 50)\rho\cos(180 - z_{\text{sips}}) \quad \text{and}$$

$$F = -\frac{r_{\text{i}} + 50}{H}\cos(z_{sips}) + \sqrt{(r_{\text{s}} + 50 + H)^2 - (r_{\text{i}} + 50)^2\sin^2(z_{\text{sips}})}\,/\,H\ , \tag{5.85}$$

where r_{s} and r_{i} denote the geocentric radius of the sub-ionospheric point and sub-ionospheric point in sight, respectively. They can be obtained by substituting the geodetic latitudes φ_{s} and φ_{i} of the related two positions into Eq. 5.84. The ellipsoidal mapping function is then Eq. 5.85.

(c) ketabton.com: The Digital Library

The mapping functions are needed if the ionospheric effects have to be determined. In Eq. 5.72, dρ may be considered to be an ionospheric path delay observed by GPS, and dH may be considered to be an ionospheric model, which is independent from the path zenith such as given in Eq. 5.27. The determined parameters have then the physical meanings of the total electron contents in the zenith direction.

5.2 Tropospheric Effects

Troposphere is the lower part of atmosphere over the Earth's surface. Unlike the ionosphere, the troposphere is a non-dispersive medium at GPS carrier frequencies. That is, the tropospheric effects on the GPS signal transmission are independent from the working frequency. The electromagnetic signals are affected by the neutral atoms and molecules in the troposphere. The effects are called tropospheric delay, or tropospheric refraction. Indeed, the word "tropospheric" used here is not an exact one; however, due to historical reasons, tropospheric effects are simply considered to be the effects of the atmosphere below the ionosphere. The amount of tropospheric delay in the zenith direction is about 2 m. It increases with the increase of the zenith angle of the sight line to the satellite. In the case of a lower satellite elevation of a few degrees, the tropospheric delay of the GPS signal can reach up to more than a few meters. Therefore, the tropospheric effect is an important error source in precise GPS applications.

Generally speaking, the tropospheric delay depends on temperature, pressure, humidity as well as the location of the GPS antenna. Analogous to the ionospheric path delay, the tropospheric path delay can be written as

$$\delta = \int (n-1)\mathrm{d}s\,, \tag{5.86}$$

where n is the refractive index of the troposphere, the integration is taken along the signal transmitting path, which could be simplified as the geometric path. Scaling of the refractive index anomaly (n – 1) is usually made by

$$N = 10^6(n-1)\ , \tag{5.87}$$

where N is called tropospheric refractivity. N can be separated into wet (about 10%) and dry (about 90%) parts:

$$N = N_\mathrm{w} + N_\mathrm{d}\ , \tag{5.88}$$

where indices w and d denote the wet and dry. They are caused by the water vapour and the dry atmosphere, respectively. Therefore Eq. 5.86 becomes

$$\delta = \delta_\mathrm{w} + \delta_\mathrm{d} = 10^{-6}\int N\mathrm{d}s\,, \tag{5.89}$$

where

$$\delta_\mathrm{w} = 10^{-6}\int N_\mathrm{w}\mathrm{d}s \quad \text{and} \tag{5.90}$$

(c) ketabton.com: The Digital Library

$$\delta_{\mathrm{d}} = 10^{-6} \int N_{\mathrm{d}} \mathrm{d}s \,. \tag{5.91}$$

If the integrations are made along the zenith direction, then the related mapping functions should be defined by

$$\delta_{\mathrm{w}} = \delta_{\mathrm{wz}} F_{\mathrm{w}} \,, \tag{5.92}$$

$$\delta_{\mathrm{d}} = \delta_{\mathrm{dz}} F_{\mathrm{d}} \quad \text{and} \tag{5.93}$$

$$\delta = \delta_{\mathrm{z}} F \,, \tag{5.94}$$

where index z denotes the tropospheric delays in the zenith direction, and F_{w} and F_{d} are mapping functions related to the wet and dry components. Analogous to the discussions made in Sect. 5.1.4, mapping functions are needed for determining the related delay models in the zenith direction. All empirical tropospheric path delay models have their own mapping functions.

5.2.1 Tropospheric Models

Modified Saastamoinen Model

The modified Saastamoinen tropospheric model (Saastamoinen 1972, 1973) for calculating the tropospheric path delay can be outlined as

$$\delta = \frac{0.002277}{\cos z}\left[P + \left(\frac{1255}{T} + 0.05\right)e - B\tan^2 z\right] + \delta R \,, \tag{5.95}$$

where z is the zenith angle of the satellite, T is the temperature at the station (in units of Kelvin (K)), P is the atmospheric pressure (in units of millibars (mb)), e is the partial pressure of water vapour (in mb). B and δR are the correction terms that depend on H and z, respectively. H is the height of the station. δ is the tropospheric path delay (in meters), and (cf. e.g. Wang et al. 1988)

$$e = R_{\mathrm{h}} \exp(-37.2465 + 0.213166T - 0.000256908T^2) \,, \tag{5.96}$$

where R_{h} is the relative humidity (in %) and exp() is the exponential function. B and δR can be interpolated from Table 5.1 and Table 5.2, respectively.

To transform the unit of the temperature T from K (Kelvin) to °C (Celsius) one may use:

$$T(\mathrm{K}) = T(\mathrm{Celsius}) + 273.16 \,. \tag{5.97}$$

In the model either measured values of pressure, temperature, and humidity or the values derived from a standard atmospheric model may be used. The height-dependent values of pressure, temperature and humidity may be obtained by the equations

$$P = P_0[1 - 0.000226(H - H_0)]^{5.225} \,, \tag{5.98}$$

(c) ketabton.com: The Digital Library

$$T = T_0 - 0.0065(H - H_0) \quad \text{and} \tag{5.99}$$

$$R_h = R_{h0} \exp[-0.0006396(H - H_0)] \ , \tag{5.100}$$

where P_0, T_0, and R_{h0} are called standard pressure, temperature, and humidity at the reference height H_0. It is obvious that the values are dependent on the geographic position of the station and time as well as the weather. Without the values of P_0, T_0 and R_{h0}, a direct correction using the model is not possible. In such a case, the tropospheric effects are usually estimated through the factor parameters of the mapping function, which will be discussed later. Additionally, the following values will be used as standard input:

$$H_0 = 0 \text{ m} \ , \tag{5.101}$$

$$P_0 = 1013.25 \text{ mbar} \ , \tag{5.102}$$

$$T_0 = 18 \text{ °Celsius} \quad \text{and} \tag{5.103}$$

$$R_{h0} = 50\% \ . \tag{5.104}$$

Table 5.1.
Function of $B(H)$

Height (km)	B (mbar)
0.0	1.156
0.5	1.079
1.0	1.006
1.5	0.938
2.0	0.874
2.5	0.813
3.0	0.757
4.0	0.654
5.0	0.563

Table 5.2. Function of $\delta R(H, z)$

Height (km)	z (degree)												
	60.00	66.00	70.00	73.00	75.00	76.00	77.00	78.00	78.50	79.00	79.50	79.75	80.00
0.0	0.003	0.006	0.012	0.020	0.031	0.039	0.050	0.065	0.075	0.087	0.102	0.111	0.121
0.5	0.003	0.006	0.011	0.018	0.028	0.035	0.045	0.059	0.068	0.079	0.093	0.101	0.110
1.0	0.002	0.005	0.010	0.017	0.025	0.032	0.041	0.054	0.062	0.072	0.085	0.092	0.100
1.5	0.002	0.005	0.009	0.015	0.023	0.029	0.037	0.049	0.056	0.065	0.077	0.083	0.091
2.0	0.002	0.004	0.008	0.013	0.021	0.026	0.033	0.044	0.051	0.059	0.070	0.076	0.083
3.0	0.002	0.003	0.006	0.011	0.017	0.021	0.027	0.036	0.042	0.049	0.058	0.063	0.068
4.0	0.001	0.003	0.005	0.009	0.014	0.017	0.022	0.030	0.034	0.040	0.047	0.052	0.056
5.0	0.001	0.002	0.004	0.007	0.011	0.014	0.018	0.024	0.028	0.033	0.039	0.043	0.047

(c) ketabton.com: The Digital Library

The original Saastamoinen tropospheric model has a constant value of B and $\delta R = 0$ in the modified model of Eq. 5.95. Three kinds of mapping functions are used in the modified model. The first one is obviously $1/\cos z$; this is the mapping function of the flat Earth model or single layer model. The second one is $\tan^2 z/\cos z$ (cf. Eq. 5.95). The third one is an implicit one, which is represented by the numerical Table 5.2.

Modified Hopfield Model

The modified Hopfield model (Hopfield 1969, 1970, 1972) for calculating the tropospheric path delay can be summarised as:

$$\delta = \delta_{\mathrm{d}} + \delta_{\mathrm{w}} \quad \text{and} \tag{5.105}$$

$$\delta_{\mathrm{i}} = 10^{-6} N_{\mathrm{i}} \sum_{k=1}^{9} \frac{f_{k,\mathrm{i}}}{k} r_{\mathrm{i}}^{k}, \quad \mathrm{i} = \mathrm{d}, \mathrm{w}\,. \tag{5.106}$$

Subscript i is used to identify the dry and wet components of the tropospheric delay, and

$$r_{\mathrm{i}} = \sqrt{(R_{\mathrm{E}} + h_{\mathrm{i}})^2 - R_{\mathrm{E}}^2 \sin^2 z} - R_{\mathrm{E}} \cos z\,, \tag{5.107}$$

$$f_{1,\mathrm{i}} = 1\,, \quad f_{2,\mathrm{i}} = 4a_{\mathrm{i}}\,,$$

$$f_{3,\mathrm{i}} = 6a_{\mathrm{i}}^2 + 4b_{\mathrm{i}}\,, \quad f_{4,\mathrm{i}} = 4a_i(a_{\mathrm{i}}^2 + 3b_{\mathrm{i}})\,,$$

$$f_{5,\mathrm{i}} = a_{\mathrm{i}}^4 + 12a_{\mathrm{i}}^2 b_{\mathrm{i}} + 6b_{\mathrm{i}}^2\,, \quad f_{6,\mathrm{i}} = 4a_{\mathrm{i}} b_{\mathrm{i}}(a_{\mathrm{i}}^2 + 3b_{\mathrm{i}})\,,$$

$$f_{7,\mathrm{i}} = b_{\mathrm{i}}^2(6a_{\mathrm{i}}^2 + 4b_{\mathrm{i}})\,, \quad f_{8,\mathrm{i}} = 4a_{\mathrm{i}} b_{\mathrm{i}}^3\,,$$

$$f_{9,\mathrm{i}} = b_{\mathrm{i}}^4\,,$$

$$a_{\mathrm{i}} = -\frac{\cos z}{h_{\mathrm{i}}}, \quad b_{\mathrm{i}} = -\frac{\sin^2 z}{2h_{\mathrm{i}} R_{\mathrm{E}}}\,,$$

$$h_{\mathrm{d}} = 40136 + 148.72(T - 273.16) \quad (\mathrm{m})\,,$$

$$h_{\mathrm{w}} = 11000 \quad (\mathrm{m})\,,$$

$$N_{\mathrm{d}} = \frac{77.64P}{T} \quad (\mathrm{K\,mb^{-1}})\,,$$

$$N_{\mathrm{w}} = -\frac{12.96e}{T} + \frac{371800e}{T^2} \quad \text{and}$$

$$R_E = 6378137\,\mathrm{m}\,, \tag{5.108}$$

(c) ketabton.com: The Digital Library

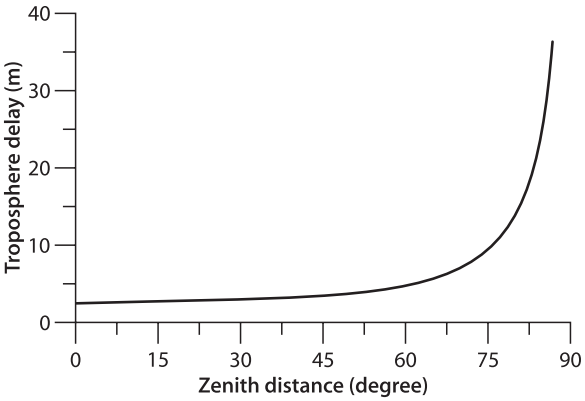

Fig. 5.4. Modified Hopfield tropospheric model (troposphere delay of GPS signal)

where z is the zenith angle of the satellite, T is the temperature at the station (in units of Kelvin (K)), P is the atmospheric pressure (in units of millibars (mb)), and e is the partial pressure of water vapour (in mb, c.f. Eq 5.96). R_E is the Earth's radius. δ is the tropospheric path delay (in meters).

In the model either measured values of pressure, temperature, and humidity or the values derived from a standard atmospheric model may be used. The height-dependent values of pressure, temperature and humidity may be obtained using Eqs. 5.98–5.104. As mentioned before, the tropospheric effects are usually estimated through suitable parameterisation, which will be discussed in the next section.

A graphic of the modified Hopfield model with standard input parameters is given in Fig. 5.4.

There are still many other models for computing the tropospheric delay, such as the Davis model (Davis and Herring 1984), original Hopfield and Saastamoinen models (cf. e.g. Hof-mann-Wellenhof et al. 1997), Niellis model and Yionoulis model (Zhu 2001). The differences between these models are generally very small for a zenith distance less than 75 degrees.

5.2.2 Mapping Functions and Parameterisation

In Sect. 5.1.4 the ionospheric mapping functions are discussed under the assumptions of symmetry of the sphere and rotating ellipsoid shapes of the ionosphere. For similar assumptions of the troposphere shapes, all mapping functions discussed in Sect. 5.1.4 can be directly used here for troposphere by changing the related values.

Projection Mapping Function

Because the troposphere has a maximal height of 50 km, the zenith angle of the satellite at the observation point may be simply used in the single layer mapping function:

$$F = \frac{1}{\cos z} \ . \tag{5.109}$$

(c) ketabton.com: The Digital Library

Geometric Mapping Function

It can be similarly derived as in Sect. 5.1.4 by:

$$F = -\frac{r}{H}\cos z + \frac{\sqrt{(r+H)^2 - r^2\sin^2 z}}{H}\,, \tag{5.110}$$

where $r = 6\,378$ km, $H = 50$ km may be used, and z is the spherical zenith distance of the satellite viewed from the station.

Due to the complexity of the troposphere, the so-called co-mapping function is needed. If a height-dependent homogeneous distribution of the troposphere is assumed, then the co-mapping function is a geometric one and is defined as

$$\mathrm{d}\rho = \mathrm{d}SF_{\mathrm{c}}\,, \tag{5.111}$$

where $\mathrm{d}\rho$ and $\mathrm{d}S$ are the tropospheric path delay and the delay mapped to the line from station to the sub-tropospheric point. In the case of zenith angle z equals zero, the $\mathrm{d}S$ is zero and co-mapping function is undefined. Index c in F_{c} is used to denote the co-mapping function. It is obvious that the projection co-mapping function is

$$F_{\mathrm{c}} = \frac{1}{\sin z}\,. \tag{5.112}$$

Geometric Co-Mapping Function

The zenith angle of the satellite at the sup-tropospheric point is denoted by z_{st} (Fig. 5.5). It can be computed by using the sinus theorem

$$\sin z = \frac{r}{r+50}\sin z_{\mathrm{st}}\,, \tag{5.113}$$

where z is the zenith angle of the satellite viewed from the receiver and r is the mean radius of the Earth in km. Using the cosines theorem, one has

$$S^2 = H^2 + \rho^2 - 2H\rho\cos z_{\mathrm{st}} \quad \text{or} \tag{5.114}$$

$$S = \sqrt{H^2 + \rho^2 - 2H\rho\cos z_{\mathrm{st}}}\,, \tag{5.115}$$

where ρ and S are the lengths of lines from the station to the sup-tropospheric point and sub-tropospheric point, respectively. Then the geometric co-mapping function is

$$F_{\mathrm{c}} = \frac{\rho}{\sqrt{H^2 + \rho^2 - 2H\rho\cos z_{\mathrm{st}}}}\,, \tag{5.116}$$

where

$$\rho = -r\cos z + \sqrt{(r+H)^2 - r^2\sin^2 z}\,, \tag{5.117}$$

(c) ketabton.com: The Digital Library

where $r = 6\,378$ km, $H = 50$ km may be used. Above, the derived geometric co-mapping function of Eq. 5.116 is a spherical approximation if r is considered a constant.

The mapping and co-mapping functions are necessary for two purposes: one is for the determination of a related tropospheric model; the other is for the determination of the tropospheric path delay effects on the GPS observations. Recall the definitions of $\mathrm{d}\rho = \mathrm{d}H \cdot F$ (cf. Eq. 5.72). Here, $\mathrm{d}H$ may be considered a tropospheric model that is independent from the zenith distance of the signal transmitting path, whereas $\mathrm{d}\rho$ represents observed tropospheric delays of path direction. With the observed $\mathrm{d}\rho$ and known mapping function F, the parameters of the model $\mathrm{d}H$ may be determined. Usually the model $\mathrm{d}H$ is a function of the temperature, pressure and humidity as seen in the models discussed in Sect. 5.2.1. For correction of the tropospheric effects on the GPS observations, one needs tropospheric models. However, the input parameters of the models are usually not measured together with the GPS measurements. The standard method of dealing with such a problem includes two steps. First, the standard temperature, pressure and humidity values for everywhere and any time will be used as input of the tropospheric model to compute the path delay $\mathrm{d}\rho$. Then, the computed $\mathrm{d}\rho$ should be amplified with a functional factor g and the g has to be determined by GPS data processing. The formulation of g is called parameterisation of the tropospheric path delay effects. Two factorisation methods are given here:

$$g_\rho \mathrm{d}\rho\,, \quad g_\mathrm{z}\frac{\mathrm{d}\rho}{F} + g_\mathrm{a}\frac{\mathrm{d}\rho}{F_\mathrm{c}}\,. \tag{5.118}$$

Physically, g_ρ, g_z and g_a are factors in path direction, zenith direction and in azimuth component, respectively. Mapping function F and co-mapping function F_c are used to map the computed $\mathrm{d}\rho$ to the desired directions.

A step function or a first order polynomial function

$$g = g(t) = g_i\,, \quad \text{if} \quad t_{i-1} \le t < t_i\,, \quad i = 1,\ldots,n \quad \text{or} \tag{5.119}$$

$$g = g(t) = g_{i-1} + (g_i - g_{i-1})\frac{(t - t_{i-1})}{\Delta t}\,, \quad \text{if} \quad t_{i-1} \le t < t_i\,, \quad i = 1,\ldots,n \tag{5.120}$$

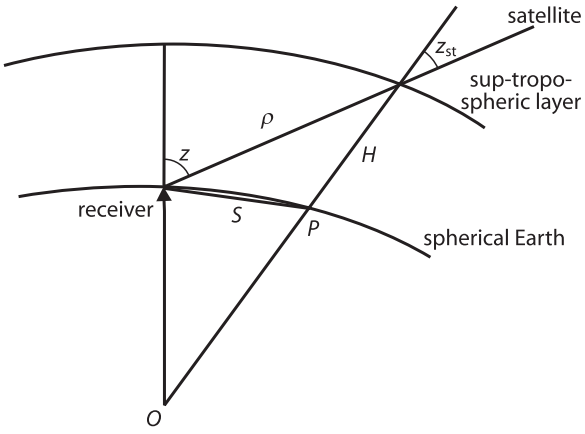

Fig. 5.5.
Spherical troposphere model

(c) ketabton.com: The Digital Library

may be used as path factor g_ρ. Where in Eqs. 5.119 and 5.120 $\Delta t = (t_e - t_0)/n$, t_0 and t_e are the beginning time and ending time of the GPS surveying, n is an integer that may be selected with a reasonable value, $t_i = t_0 + (i-1)\Delta t$, g_i are constant unknowns which shall be determined.

The azimuth dependency may be assumed as

$$g_a = g_1 \cos a + g_2 \sin a \ , \tag{5.121}$$

where a is the azimuth of the satellite at the station, g_1 and g_2 may be in turn a step function or a first order polynomial function given in Eqs. 5.119 and 5.120.

5.3 Relativistic Effects

5.3.1 Special Relativity and General Relativity

Einstein's special relativity is based on two postulates. The first one is called the principle of relativity, i.e., "No inertial system is preferred. The equations expressing the laws of physics have the same form in all inertial systems." The second one is called the principle of the constancy of the speed of light, i.e., "The speed of light is a universal constant independent of the state of motion of the source. Any light ray moves in the inertial system of coordinates with constant velocity, c, whether the ray is emitted by a stationary or by a moving source." Of course, the speed of light refers to velocity in a vacuum (Ashby and Spilker 1996).

Consider two inertial coordinate systems S' and S in Fig. 5.6, where the x'-axis and x-axis coincide. Two origins are placed at point A and B, respectively. Origin A of system S' moves with a constant velocity v along the x-axis toward B. The distance between A and B viewed in system S is Δx. The mirror surface is parallel to the x-axis and is faced to the x-axis. The perpendicular distance of the mirror to the x-axis is ΔL. Suppose a light flash is emitted from A and the reflected light is receipted at B by the moving system S'. Then the transmitting time of the light measured in system S is

$$\Delta t = \frac{2\sqrt{(\Delta L)^2 + (\Delta x/2)^2}}{c} \ . \tag{5.122}$$

According to our assumption, one gets $\Delta x = v\Delta t$. Substituting this into Eq. 5.122, Δt can be obtained by

$$\Delta t = \frac{2\Delta L/c}{\sqrt{1-(v/c)^2}} \ . \tag{5.123}$$

Because of Einstein's postulates, the speed of light, c, is the same in two systems. Therefore, $2\Delta L/c$ is the light flash transmitting time viewed in the moving system S', i.e., $\Delta t' = 2\Delta L/c$, and

$$\Delta t = \frac{\Delta t'}{\sqrt{1-(v/c)^2}} \ . \tag{5.124}$$

(c) ketabton.com: The Digital Library

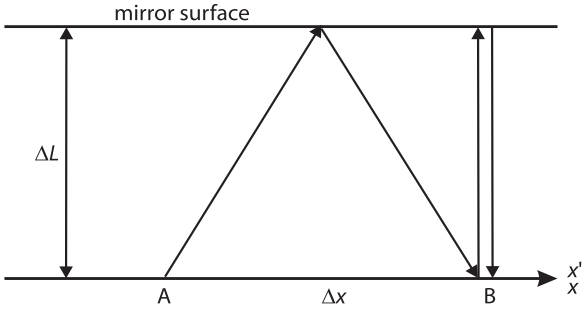

Fig. 5.6.
Light transmission viewed in two inertial frames

This indicates that the time interval viewed in the system at rest is shorter than the time interval viewed in the system, which is moving with velocity v.

Again, because of the constant c in the two systems, one may denote $\Delta s = c\Delta t$ and $\Delta s' = c\Delta t'$, where Δs and $\Delta s'$ are the lengths of the light transmitting paths viewed in the two systems. Multiplying c by Eq. 5.124 gets

$$\Delta s = \frac{\Delta s'}{\sqrt{1-(v/c)^2}} \ . \tag{5.125}$$

This indicates that the length viewed in the moving system is lengthened.

Consider the relation of $c = f\lambda$, where c is constant in both systems, λ is wavelength and f is the related frequency. Because the wavelength λ viewed in two systems is different, denoted by $\lambda = \Delta s$ and $\lambda' = \Delta s'$, the relationship of the frequencies f and f', which are viewed in two systems, can be obtained by dividing c into Eq. 5.125:

$$f = f'\sqrt{1-(v/c)^2} \ . \tag{5.126}$$

This indicates that the frequency f' viewed in the moving system is reduced to f when it is viewed by a resting system.

Using mathematical expansions

$$\frac{1}{\sqrt{1-(v/c)^2}} = 1+\frac{1}{2}\left(\frac{v}{c}\right)^2 \ldots \ , \tag{5.127}$$

$$\sqrt{1-(v/c)^2} = 1-\frac{1}{2}\left(\frac{v}{c}\right)^2 \ldots \ , \tag{5.128}$$

for Eqs. 5.124, 5.125 and 5.126, we have

$$\frac{\Delta t-\Delta t'}{\Delta t'} = \frac{\Delta s-\Delta s'}{\Delta s'} = -\frac{f-f'}{f'} = \frac{1}{2}\left(\frac{v}{c}\right)^2 \ . \tag{5.129}$$

This is the formula of the special relativity effects caused by a constant motion of a moving inertial coordinate system viewed from a resting inertial coordinate system.

(c) ketabton.com: The Digital Library

Einstein's general relativity incorporates gravitation by virtue of the principle of equivalence. The mathematics of the general relativity is extremely complex. However, for treatment of the relativistic effects on GPS, only a simplified and small fraction of the theory is required. Note that the right-hand side of Eq. 5.129 is indeed the point-mass (or unit mass) kinetic energy ($v^2/2$) scaled by the speed of light c (exactly $1/c^2$). That is, the special relativity effects may be interpreted as the effects caused by kinetic energy due to motion. The analogous effects may also be caused by potential energy ΔU due to the presence of the gravitation field U. Then

$$\frac{\Delta t - \Delta t'}{\Delta t'} = \frac{\Delta s - \Delta s'}{\Delta s'} = -\frac{f - f'}{f'} = \frac{\Delta U}{c^2} \tag{5.130}$$

represents the relativistic relations in the case of the presence of a gravitational field U. Thus the total relativistic effects may be formulated as

$$\frac{\Delta t - \Delta t'}{\Delta t'} = \frac{\Delta s - \Delta s'}{\Delta s'} = -\frac{f - f'}{f'} = \frac{1}{2}\left(\frac{v}{c}\right)^2 + \frac{\Delta U}{c^2} \quad . \tag{5.131}$$

The presence of a gravitational field indicates an acceleration of the frame S' with respect to the system S in rest.

The special relativity effects of rotation may be similarly discussed. Details can be found, e.g., in Ashby and Spilker (1996).

5.3.2 Relativistic Effects on GPS

The inertial coordinate system at rest, its origin located at the centre of the Earth, is taken as reference to view all GPS related activities. Because of the large motion velocities and near circular orbits of the GPS satellite, the non-negligible gravitational potential difference between the satellite and the users, as well as the rotation of the Earth, the relativistic effects have to be taken into account. For convenience, we may imagine that the whole GPS process is viewed in an inertial reference at a point where the gravitational potential is the same as that of the geoid of the Earth. Taking the Earth's rotational effects into account, the view point is equivalent to the point of the GPS user on the geoid of the rotating Earth.

Frequency Effects

The fundamental frequency f_0 of the GPS system is selected as 10.23 MHz. All clocks on the GPS satellites and GPS receivers operate based on this frequency. If all the GPS satellites are working simply on the frequency $f' = f_0$, then we will view a frequency f at our reference point, and f is not the same as f_0 due to relativistic effects. In order to be able to view the fundamental frequency $f = f_0$, the desired working frequency f' of the GPS satellites can be computed using Eq. 5.131 by

$$-\frac{f_0 - f'}{f'} = \frac{1}{2}\left(\frac{v}{c}\right)^2 + \frac{\Delta U}{c^2} \ , \tag{5.132}$$

(c) ketabton.com: The Digital Library

where v is the velocity of the satellite and ΔU is the difference of the Earth's gravitational potential between the satellite and the geoid. The difference between the setting frequency f' of satellite clock and the fundamental frequency f_0 is called the offset in the satellite clock frequency. Such an offset of the relativistic effects has been implemented in the satellite clock settings, and therefore users do not need to consider this effect. The offset can be computed by using the mean velocity of the satellite and $\Delta U = \mu / (R_E + H) - \mu / R_E$, where μ is the gravitational constant of the Earth, R_E is the Earth radius (ca. 6 370 km), and H is the height of the satellite above the Earth (ca. 20 200 km). The offset is approximately 0.00457 Hz; in other words, the satellite clock frequency is set to $f_0 - 4.57 \times 10^{-9}$ MHz.

For the receiver fixed on the earth's surface, the frequency of the clock in the receiver is also affected by the relativistic effects. The effects can be represented analogously by Eq. 5.132, where $\Delta U = 0$ and v is the velocity of the receiver due to the rotation of the Earth. Such effects are corrected by the software of the receiver.

Path Range Effects

The general relativity effects of the signal transmitting from the GPS satellite to the receiver can be represented by the Holdridge (1967) model:

$$\Delta\rho_{\text{rel}} = \frac{2\mu}{c^2} \ln \frac{\rho^j + \rho_i + \rho_i^j}{\rho^j + \rho_i - \rho_i^j} \ , \tag{5.133}$$

where ρ^j and ρ_i are the geocentric distances of the satellite j and station i, respectively, ρ_i^j is the distance between the satellite and the observing station, $\Delta\rho_{\text{rel}}$ has the units of meters and a maximum value of about 2 cm. It is notable that by computing the distance ρ_i^j, the effect of the rotation of the Earth during the signal transmission has to be taken into account (if it is done in the Earth's fixed system).

Earth's Rotational Effects

All corrections related to the rotation of the Earth are called Sagnac corrections. The geocentric vector of the GPS satellite is denoted by $\vec{r}_s$, the geocentric vector of the receiver by $\vec{r}_r$, and the velocity vector of the receiver by $\vec{v}_r$. These are the vectors during GPS signal emission. Suppose the transmitting time between the signal emission from satellite and signal reception of receiver is Δt. During the time of GPS signal transmission, the receiver has moved to position $\vec{r}_r + \vec{v}_r \Delta t$. Observing from the non-rotating frame, the distance of the signal transmission can be represented by

$$c\Delta t = \left| \vec{r}_r + \vec{v}_r \Delta t - \vec{r}_s \right| \ . \tag{5.134}$$

Therefore the transmitting path correction due to the rotation of the Earth can be presented as

$$\Delta\rho = \left| \vec{r}_r + \vec{v}_r \Delta t - \vec{r}_s \right| - \left| \vec{r}_r - \vec{r}_s \right| \ . \tag{5.135}$$

(c) ketabton.com: The Digital Library

This can be simplified as (Ashby and Spiler 1996)

$$\Delta\rho = \frac{(\vec{r}_\mathrm{r} - \vec{r}_\mathrm{s}) \cdot \vec{v}_\mathrm{r}}{c} . \tag{5.136}$$

The correction can reach up to 30 meters and must be taken into account.

If the signal transmitting time Δt has been solved through iteration of Eq. 5.134, then the Sagnac correction will automatically be taken into account.

This term of correction is also valid for the kinematic GPS receivers that are not fixed on the Earth's surface. The velocity vector in Eq. 5.136 is

$$\vec{v}_\mathrm{r} = \vec{\omega}_\mathrm{e} \times \vec{r}_\mathrm{r} + \vec{v}_\mathrm{k} \ , \tag{5.137}$$

where the first term on the right-hand side is the velocity vector of the receiver due to the Earth's rotation, and the second term $\vec{v}_\mathrm{k}$ is the kinematic velocity vector of the receiver related to the Earth's surface. A kinematic motion of 100 km h^{-1} related to the Earth's surface can cause additional Sagnac effects up to 2 meters.

The Sagnac correction also has to be taken into account for low-Earth orbit (LEO) satellites (e.g., TOPEX, CHAMP and GRACE), which are equipped with GPS receivers onboard for satellite-satellite tracking (SST).

Relativistic Effects due to the Orbit Eccentricity

The theoretical formula of the clock correction of the satellite can be written as (Ashby and Spilker 1996)

$$\Delta t_e = \frac{2}{c^2}\sqrt{\mu a}\, e \sin E + \text{const.} \ , \tag{5.138}$$

where a is the semimajor axis of the satellite orbit, e is the eccentricity of the orbit, E is the eccentric anomaly of the orbit, μ is the gravitational constant of the Earth, and Δt_e is the clock correction due to the eccentricity of the orbit. The second term on the right-hand side is a constant that cannot be separated from the clock offset. This total correction has already been taken into account in the GPS orbits determination and is broadcasted in the navigation message by the parameters of the clock error polynomial. Therefore, this term of correction only needs to be considered in the satellite orbits determination.

Using the relation of $e \sin E = (xv_x + yv_y + zv_z) / \sqrt{(\mu a)}$ (cf. Kaula 1966), the Eq. 5.138 can be presented by the position (x, y, z) and velocity (v_x, v_y, v_z) of the satellite.

General Relativity Acceleration of the Satellite

The IERS standard correction for the acceleration of the Earth satellite is (McCarthy 1996)

$$\Delta\vec{a} = \frac{\mu}{c^2 r^3}\left\{\left[4\frac{\mu}{r} - v^2\right]\vec{r} + 4(\vec{r}\cdot\vec{v})\vec{v}\right\} \ , \tag{5.139}$$

where c is the speed of light, μ is the gravitational constant of the Earth, $\vec{r}$, $\vec{v}$, and $\vec{a}$ are the geocentric satellite position, velocity and acceleration vectors, respectively.

(c) ketabton.com: The Digital Library

5.4
Earth Tide and Ocean Loading Tide Corrections

5.4.1
Earth Tide Displacements of the GPS Station

The Earth tide is a phenomenon of the deformation of the elastic body of the Earth caused by the gravitational attracting force of the Moon and the Sun. Such a deformation depends not only on the changing of the force, but also on the physical structure and motion of the Earth (Melchior 1978).

Generally, the Sun-Moon-Earth system may be separated into two two-body systems for discussing the effects of the Sun and the Moon on the Earth, respectively. For the Moon-Earth system, the mass centre can be found out according to the definition. It lies on a straight line between the centres of the Earth and the Moon, and has a distance to the centre of the Earth of about $0.73R_E$, where R_E is the radius of the Earth (Fig. 5.7). For the point-mass p (with unit mass) on the Earth, the tidal potential generated by the Moon can be derived as

$$W_p = \mu_m \left(\frac{1}{r'} - \frac{1}{r} - \frac{\rho}{r^2} \cos z \right) , \tag{5.140}$$

where r is the geocentric distance of the Moon, ρ is the geocentric distance of point p, μ_m is the gravitational constant of the Moon, z is the geocentric zenith angle of the Moon, and r' is the distance between the point p and the centre of the Moon. The $1/r'$ in Eq. 5.140 can be developed by Legendre polynomials, and then

$$W_p = \mu_m \sum_{n=2}^{\infty} \frac{\rho^n}{r^{n+1}} P_n(\cos z) , \tag{5.141}$$

where $P_n(\cos z)$ is the conventional Legendre polynomials of n degree. Applying the well-known formula of spherical astronomy (cf., e.g., Lambeck 1988),

$$\cos z = \sin\varphi \sin\delta + \cos\varphi \cos\delta \cos H , \tag{5.142}$$

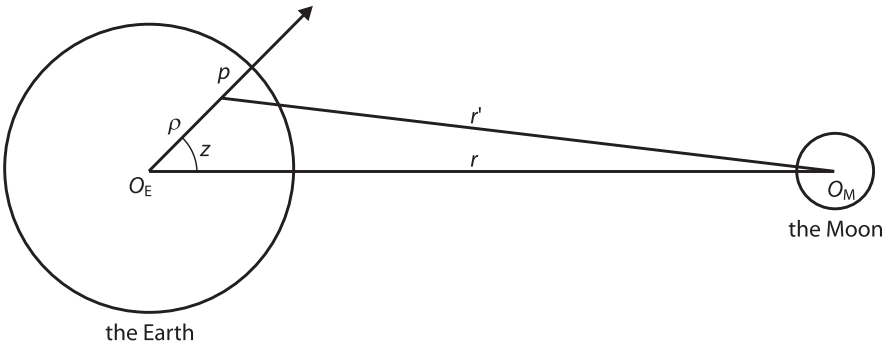

Fig. 5.7. The Earth-Moon system

(c) ketabton.com: The Digital Library

to Eq. 5.141 and using the addition theorem (cf., e.g., Lambeck 1988), Laplace's formula of the tidal potential can be obtained by

$$W_p = \mu_m \sum_{n=2}^{\infty} \frac{\rho^n}{r^{n+1}} [P_n(\sin\varphi) P_n(\sin\delta) + 2\sum_{k=1}^{n} \frac{(n-k)!}{(n+k)!} P_{nk}(\sin\varphi) P_{nk}(\sin\delta)\cos kH] , \quad (5.143)$$

where φ is the latitude of computing point p, δ and H are the declination and local hour angle of the Moon, and $P_{nk}(x)$ is the associated Legendre polynomials of degree n and order k. Laplace's formula shows the significant geometric and periodic characters of the tidal potential. Similar discussions can be made for the Earth-Sun system, and the related tidal potential can be obtained by substituting the gravitational constant of the Sun μ_s and geocentric distance of the Sun into Eq. 5.143. The total tidal potential is the summation of both potentials generated by the Moon and the Sun. The truncating order of the summation can be selected due to the precision requirement and the truncating errors can be estimated by considering μ_m, μ_s and the ratio R_E / r of the Moon and the Sun.

The tidal displacements resulting from the tidal potential are then

$$\Delta S_r = h \frac{W_p}{g} = \sum_{n=2}^{\infty} h_n \frac{W_p(n)}{g} , \quad (5.144)$$

$$\Delta S_\varphi = l \frac{\partial W_p}{g \partial \varphi} = \sum_{n=2}^{\infty} l_n \frac{\partial W_p(n)}{g \partial \varphi} \quad \text{and} \quad (5.145)$$

$$\Delta S_\lambda = l \frac{\partial W_p}{g \cos\varphi \partial \lambda} = \sum_{n=2}^{\infty} l_n \frac{\partial W_p(n)}{g \cos\varphi \partial \lambda} , \quad (5.146)$$

where $\Delta S_r, \Delta S_\varphi$ and ΔS_λ are the tidal displacements in the radial, north and east directions, respectively; h and l are the Love and Shida numbers (in more detailed words, h_n and l_n are the Love and Shida numbers of degree n); $W_p(n)$ is the tidal potential of degree n, $g \approx \mu / R_E^2$; μ is the gravitational constant of the Earth; and R_E is the radius of the Earth.

It is notable that the tidal potential includes a permanent (i.e., time independent) part. This part of the tide is now included in the geoid definition, which has already been accepted by IAG in 1983 (Poutanen et al. 1996). Therefore, such a term has to be carefully dealt with. Examples to move or to keep the permanent tidal term from the above formulas may be found in IERS standard (McCarthy 1996).

5.4.2 Simplified Model of the Earth Tide Displacements

The vector displacement of the station due to degree 2 of the tidal potential is (McCarthy 1996; Zhu et al. 1996)

$$\Delta\vec{\rho} = \sum_{j=1}^{2} \frac{\mu_j R_E^4}{\mu r_j^3} \left\{ h_2 \hat{\rho} \left[\frac{3}{2} (\hat{r}_j \cdot \hat{\rho})^2 - \frac{1}{2} \right] + 3 l_2 (\hat{r}_j \cdot \hat{\rho}) [\hat{r}_j - (\hat{r}_j \cdot \hat{\rho}) \hat{\rho}] \right\} , \quad (5.147)$$

where μ is the gravitational constant of the Earth, R_E is the equatorial radius of the Earth, $j = 1, 2$ are indices for the Moon and Sun, respectively, $\hat{r}_i$ and $\hat{\rho}$ are the geocentric iden-

(c) ketabton.com: The Digital Library

tity vectors of the Moon (or Sun) and station, r_j and ρ are the magnitude of the related geocentric vectors, and h_2 and l_2 are nominal degree 2 Love and Shida numbers (for an elastic Earth model, the nominal values are 0.6078 and 0.0847). In Eq. 5.147, the terms factorised by h_2 and l_2 are the radial and transverse components of the tidal displacement. Taking the latitude dependence into account, h_2 and l_2 shall have the forms of

$$h_2 = 0.6078 - 0.0006\frac{3\sin^2\varphi - 1}{2} \quad \text{and}$$

$$l_2 = 0.0847 + 0.0002\frac{3\sin^2\varphi - 1}{2}. \tag{5.148}$$

The vector displacement of the station due to degree 3 of the tidal potential is (McCarthy 1996)

$$\Delta\vec{\rho} = \frac{\mu_1 R_E^5}{\mu r_1^4} h_3 \hat{\rho}\left[\frac{5}{2}(\hat{r}_1\cdot\hat{\rho})^3 - \frac{3}{2}(\hat{r}_1\cdot\hat{\rho})\right], \tag{5.149}$$

where $h_3 = 0.292$. Here only the radial component of the Moon is considered.

As discussed in Sect. 5.4.1, there is a permanent part of the tidal deformation included in the degree 2 tidal potential. The projects of the permanent displacement into the radial and north directions are

$$-0.0603(3\sin^2\varphi - 1) \quad \text{and} \quad -0.0252\sin 2\varphi\ .$$

This must be removed from the computation of Eq. 5.147 according to the IERS standard. Generally, the tidal displacements computed using the model given above have accuracy on a mm level.

In GPS applications, the computing time is usually the GPS time, and the coordinates of the stations are given in the CTS system. However, the ephemerides of the Sun and Moon are given in the CIS coordinate system with time TDT. Therefore, time and coordinates have to be transformed to a unique time-coordinate system. The details of the time-coordinate system can be found in Chap. 2.

Usually the ephemerides of the Sun and the Moon are computed or forecasted every half day (12 hours). The ephemerides of the Sun and the Moon at a required epoch are interpolated from the data of the two adjacent epochs (t_1, t_2) by using a 5-order polynomial:

$$f(t) = a + b(t-t_1) + c(t-t_1)^2 + d(t-t_1)^3 + e(t-t_1)^4 + f(t-t_1)^5\ .$$

For data at two epochs, e.g.:

$$t_1 : x_1, y_1, z_1, \dot{x}_1, \dot{y}_1, \dot{z}_1, \ddot{x}_1, \ddot{y}_1, \ddot{z}_1 \quad \text{and}$$

$$t_2 : x_2, y_2, z_2, \dot{x}_2, \dot{y}_2, \dot{z}_2, \ddot{x}_2, \ddot{y}_2, \ddot{z}_2\ ,$$

where $\dot{x}$ and $\ddot{x}$ are the velocity and acceleration components related to x. Considering the formulas of $f(t)$, $\mathrm{d}f(t)/\mathrm{d}t$, $\mathrm{d}^2f(t)/\mathrm{d}t^2$ and letting $t = t_1$, one gets $a = x_1$, $b = \dot{x}_1$ and

(c) ketabton.com: The Digital Library

$c = \ddot{x}_1 / 2$. Letting $t = t_2$, coefficients of d, e, f can be derived theoretically, e.g., in the case of $t_2 - t_1 = 0.5$:

$$d = 80(x_2 - x_1) - 16\dot{x}_2 - 24\dot{x}_1 + \ddot{x}_2 - 3\ddot{x}_1 ,$$

$$e = -240(x_2 - x_1) + 56\dot{x}_2 + 64\dot{x}_1 - 4\ddot{x}_2 + 6\ddot{x}_1 ,$$

$$f = 192(x_2 - x_1) - 48\dot{x}_2 - 48\dot{x}_1 + 4\ddot{x}_2 - 4\ddot{x}_1 .$$

For y and z components, the formulas are similar. Such an interpolating algorithm is accurate enough for using the given half day ephemerides of the Sun and Moon to get the data at the required epoch. The computation of the ephemerides of the Sun and Moon will be discussed in Sect. 11.2.8.

5.4.3 Numerical Examples of the Earth Tide Effects

The Earth tide effects could reach up to 60 cm world-wide (Melchior 1978; Poutanen et al. 1996) and, e.g., 30 cm in Greenland (Xu and Knudsen 2000). The effect of the Earth tide on the GPS positioning is a well-known correction term, which has to be taken into account in many cases as soon as the Earth tide effect is greater than the accuracy requirement of GPS results. The tidal parameters (Love and Shida numbers) can be also determined through global GPS observations.

Only the GPS positioning, which is carried out on the air without fixed reference on the Earth, is free from the Earth tide effects. For the GPS relative positioning of a small regional area, the tidal effects may be neglected because of the small differences in the tidal displacements. In the relative airborne kinematic GPS positioning, the airborne antennas are free from Earth tide effects. However, the static references fixed on the Earth are not free from tidal effects. In this case, the tidal displacements are independent from the size of the applied area or lengths of the baselines and have to be taken into account.

Three examples are given to illustrate the tidal displacements (Xu and Knudsen 2000). The IERS standards are used as the principle of the Earth tide effect computation (McCarthy 1996).

Three stations in Greenland were selected for computation of a whole day (GPS time used) of tidal displacements on 31 December 1998. Coordinates were quite roughly selected for Narsarsuaq (60°, 315°), Scoresbysund (70°, 339°) and Thule (77°, 290°). Heights were selected as 50 meters. Results of the vertical components are illustrated as 2-D graphics with the 1st axis time in hours and the 2nd axis displacement in meters. Continuous, broken-dot, broken lines represent the results of the 1st, 2nd and 3rd stations, respectively (Fig. 5.8, units: meters). The tidal displacements of the three stations in Greenland have a maximum difference of about 15 cm. The size of the triangle of the three stations is about 2 000 km. The change of the tidal displacements in the vertical component is about 27 cm. That change could happen within the duration of 4 to 5 hours.

Two grid data of 0.2×0.3 degrees for Denmark ($54.0° \le \varphi \le 57.8°, 8° \le \lambda \le 12.9°$) and 1×1 degrees for Greenland ($59.5° \le \varphi \le 84°, 285° \le \lambda \le 350°$) with real topography height are used to compute vertical tidal displacements at time 1:00 and 1:45, respectively.

(c) ketabton.com: The Digital Library

The displacements are illustrated with contour lines (units: meters) plotted in Fig. 5.9 and Fig. 5.10 with the 1st axis longitude in degrees and the 2nd axis latitude in degrees. In Fig. 5.9 there is a tidal difference of 15 mm, which shows that within an 80 km distance or area in Denmark the tidal difference can reach up to 5 mm. Figure 5.10 shows that there is a vertical tidal difference of about 17 cm in Greenland.

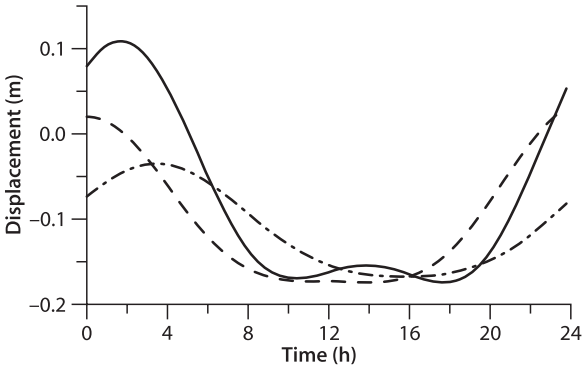

Fig. 5.8.
Earth tide displacements at three stations in Greenland (vertical component; date: Dec. 31, 1998)

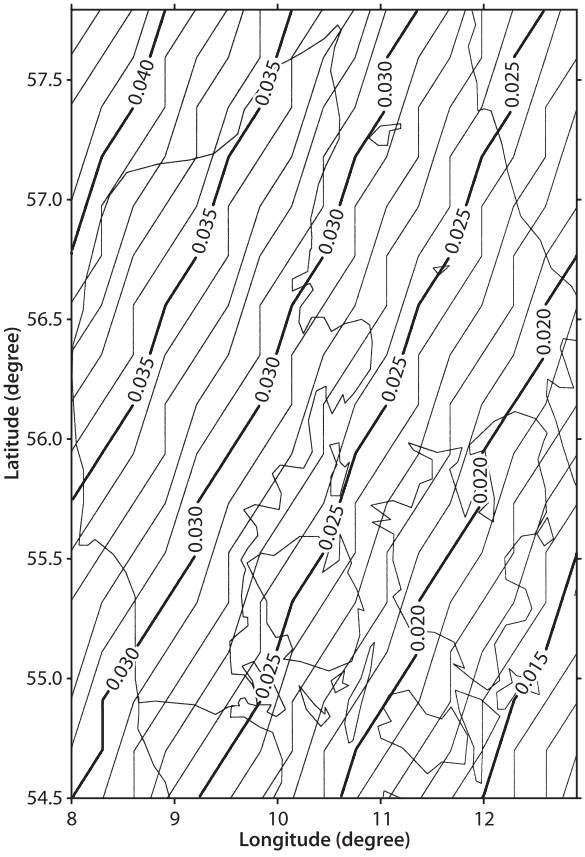

Fig. 5.9.
Earth tide displacement (in meters) in Denmark (Dec. 31, 1998; GPS time 1:00; height component)

(c) ketabton.com: The Digital Library

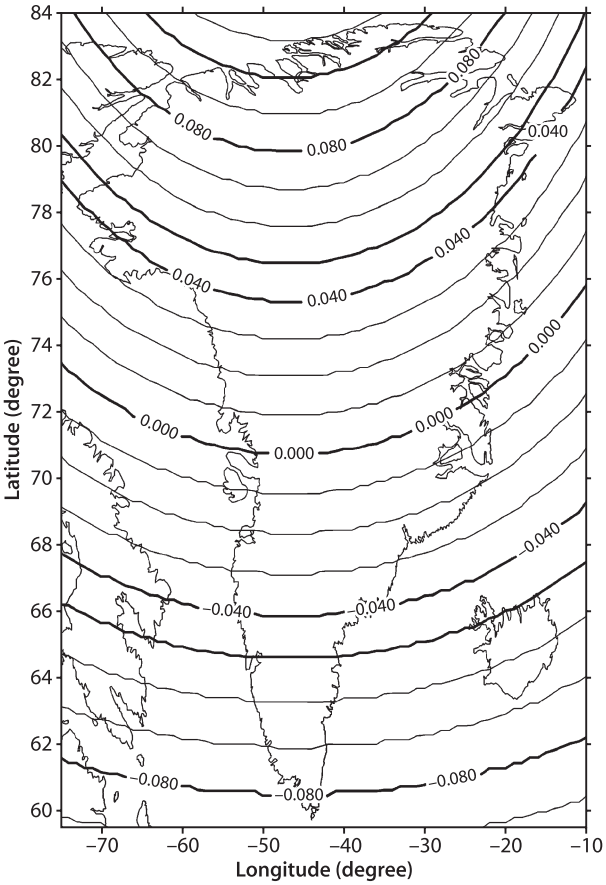

Fig. 5.10.
Earth tide displacement (in meters) in Greenland (Dec. 31, 1998; GPS time 1:45; height component)

These computations indicate that in differential GPS kinematic airborne (not touching the Earth) applications, a lack of the Earth tide correction could cause an accuracy of less than 30 cm in Denmark and Greenland. For the Earth-touched kinematic and static differential GPS applications, a lack of Earth tide correction would cause an accuracy of less than 2 cm in Denmark and 15 cm in Greenland.

It is worth mentioning that the average value of the Earth tide effects on a GPS station during 24 hours is generally not zero (it may be up to a few cm). This is because the Earth tide is an effect that includes many periodical components. This indicates that the Earth tide effects cannot be eliminated through daily averaging.

5.4.4
Ocean Loading Tide Displacement

The ocean tide is a time varying load on the Earth's surface. The displacement of the Earth's surface due to loading is called the ocean tide loading effect. Similar to the Earth tide, the loading Love numbers are introduced to describe the relationships of the loading potential and the loading displacement as

(c) ketabton.com: The Digital Library

$$\Delta S_{\mathrm{r}} = h' \frac{W_p}{g} = \sum_{n=0}^{\infty} h'_n \frac{W_{\mathrm{p}}(n)}{g} \quad , \tag{5.150}$$

$$\Delta S_{\varphi} = l' \frac{\partial W_{\mathrm{p}}}{g \partial \varphi} = \sum_{n=0}^{\infty} l'_n \frac{\partial W_{\mathrm{p}}(n)}{g \partial \varphi} \quad \text{and} \tag{5.151}$$

$$\Delta S_{\lambda} = l' \frac{\partial W_{\mathrm{p}}}{g \cos\varphi \partial \lambda} = \sum_{n=0}^{\infty} l'_n \frac{\partial W_{\mathrm{p}}(n)}{g \cos\varphi \partial \lambda} \quad , \tag{5.152}$$

where ΔS_{r}, ΔS_{φ} and ΔS_{λ} are the loading tide displacements in the radial, north and east directions, respectively, h' and l' are the loading Love numbers (in more detail, h'_n and l'_n are the loading Love numbers of degree n), $W_{\mathrm{p}}(n)$ is the loading potential of degree n, $g \approx \mu / R_{\mathrm{E}}^2$, μ is the gravitational constant of the Earth, and R_{E} is the radius of the Earth. It is notable that the zero degree loading Love number and 1 degree loading displacement exist and in the case of $n \to \infty, h'_n \to h_{\infty}, nl'_n \to l_{\infty}$. Loading Love numbers can be obtained from a theoretical model.

The loading displacement shall fulfil the elastic balance equation under the boundary condition of loading. This is called the Boussinesq boundary value problem. The response of the spherical Earth under the loading of a point-mass (or unit mass) is called the Green function. In other words, the Green function is the solution of the partial differential equation of the Boussinesq problem under a certain spherical boundary condition of a point-mass loading. For a related boundary condition, the related Green function can be derived. Farrell derived the following loading displacement Green functions (Farrel 1972):

$$u(k) = \frac{R h'_{\infty}}{2 M_{\mathrm{e}} \sin(k/2)} + \frac{R}{M_{\mathrm{e}}} \sum_{n=0}^{N} (h'_n - h'_{\infty}) P_n(\cos k) \quad \text{and} \tag{5.153}$$

$$v(k) = \frac{-R\cos(k/2)[1+2\sin(k/2)]}{2 M_{\mathrm{e}} \sin(k/2)[1+\sin(k/2)]} + \frac{R}{M_{\mathrm{e}}} \sum_{n=1}^{N} \frac{(nl'_n - l'_{\infty})}{n} \frac{\partial P_n(\cos k)}{\partial k} \quad , \tag{5.154}$$

where R is the radius of the Earth, M_{e} is the mass of the Earth, k is the geocentric zenith distance of the loading point (related to the computing point, see Fig. 5.11), $P_n(\cos k)$ is the Legendre function, and $u(k)$ and $v(k)$ are the radial and tangential loading displacement Green functions, respectively.

According to the definition of the Green function, the loading displacements of the ocean tide of the whole Earth can be obtained by multiplying the tidal mass to the Green function and integrating that over the whole ocean

$$u_{\mathrm{r}} = \iint_{\text{ocean}} \delta H u(k) \mathrm{d}\sigma \, , \tag{5.155}$$

$$u_{\varphi} = \iint_{\text{ocean}} \delta H v(k) \cos a \mathrm{d}\sigma \quad \text{and} \tag{5.156}$$

$$u_{\lambda} = \iint_{\text{ocean}} \delta H v(k) \sin a \mathrm{d}\sigma \, , \tag{5.157}$$

(c) ketabton.com: The Digital Library

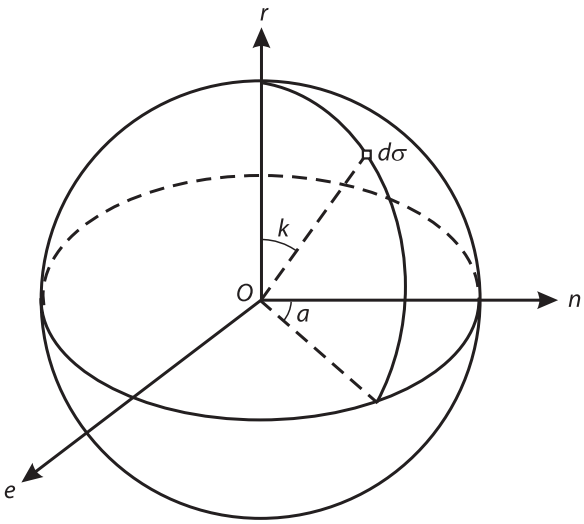

Fig. 5.11.
Ocean loading

where a is the azimuth of the integrating surface element $\mathrm{d}\sigma$, δ is the density of the oceanic water ($\delta \approx 1.03$), H is the height of ocean tide, and u_r, u_φ and u_λ are the loading displacements of radial, north and east components, respectively. It is obvious that an ocean tide model is needed here.

The Schwiderski global ocean tide model is one of the most used models, which has a resolution of $1° \times 1°$ and represents the tidal amplitude and phase (Schwiderski 1978, 1979, 1980, 1981a–c). The accuracy of the loading tide modelling depends on the accuracy of the loading response and ocean tide model. Because of the irregularity of coastlines and because the loading response is more dependent on the local variable properties of the lithosphere (Farrel 1972), modelling of the loading effects cannot be done very accurately.

Let

$$H = \sum_{i=1}^{I} H_i\,,\quad \oiint_{\text{ocean}} F\mathrm{d}\sigma = \sum_{n=1}^{N} F(n)\mathrm{d}\sigma_n\,,\quad \sum_{n=1}^{N} \mathrm{d}\sigma_n = \text{total surface of the ocean}\,,$$

where H_i is the ocean tide constituent with angular velocity ω_i, I is the truncating wave number, F is any to be integrated function, $F(n)$ and $\mathrm{d}\sigma_n$ are the functional value and the size of the n^{th} surface element, and N is the total elements number. If one changes the order sequence of the summations then Eqs. 5.155–5.157 turn out to be

$$u_r = \sum_{i=1}^{I}\sum_{n=1}^{N} \delta H_i u(k)\mathrm{d}\sigma_n\,, \tag{5.158}$$

$$u_\varphi = \sum_{i=1}^{I}\sum_{n=1}^{N} \delta H_i v(k)\cos a\mathrm{d}\sigma_n \quad \text{and} \tag{5.159}$$

$$u_\lambda = \sum_{i=1}^{I}\sum_{n=1}^{N} \delta H_i v(k)\sin a\mathrm{d}\sigma_n\,. \tag{5.160}$$

(c) ketabton.com: The Digital Library

In other words, the loading displacements can be represented by summations of displacements of the different wave of frequencies, and the amplitude and phase of the related wave are dependent on the computing position.

5.4.5 Computation of the Ocean Loading Tide Displacement

Computation of the loading displacement depends on which ocean tide model is used. Because of the strong dependence of the loading on the coast near tide, besides a global ocean tide model a modified model near the coastlines is added quite often to raise the precision of computation. Taking advantage of the fact that the amplitude and phase of the related wave depends only on the computing position, the computation can be greatly simplified. Generally, only 11 tidal constituents are taken into account. These are the semi-diurnal waves M_2, S_2, K_2 and N_2, the diurnal waves O_1, K_1, P_1 and Q_1, and the long-period waves M_f, M_m and M_{sa}. The loading displacement vector in IERS standard (McCarthy 1996) is

$$\Delta\rho_j = \sum_{i=1}^{11} f_i \cdot \mathrm{amp}_j(i) \cdot \cos[\arg(i,t) - \mathrm{phase}_j(i)] \quad \text{and} \tag{5.161}$$

$$\arg(i,t) = \omega_i t + \chi_i + u_i \ . \tag{5.162}$$

where $j = 1, 2, 3$ represent the displacement in radial, west and south directions, respectively, $\mathrm{amp}_j(i)$ and $\mathrm{phase}_j(i)$ are the amplitude and phase of the i^{th} wave related to the computing station of j^{th} component, $\arg(i, t)$ is the argument of i^{th} wave at the computing time t, ω_i is the angular velocity of the i^{th} wave, χ_i is the astronomical argument at time of 0 hour, and f_i and u_i depend on the longitude of the lunar node. ω_i, f_i and u_i can be found in Table 26 of Doodson (1928). The $\mathrm{amp}_j(i)$ and $\mathrm{phase}_j(i)$ are computed for a list of stations by Scherneck (McCarthy 1996). The coefficients and software are available by Scherneck.

5.4.6 Numerical Examples of Loading Tide Effects

Loading tide effects could reach up to 10 cm at some special coast regions (cf., e.g., Andersen 1994; Khan 1999). The loading displacements affect mostly only the GPS stations near the coast. The displacements at most continental stations are less than 1 cm. Loading correction has not been commonly considered in GPS data processing because the computation is more complicated, and modelling is less accurate. However, for precise applications, loading effects have to be taken into account. Using software, e.g., designed by Scherneck, the loading amplitude and phase of the significant waves can be obtained for static stations. The coefficients can be computed beforehand and used for even real time applications. Kinematic GPS receivers on the air are free of loading effects. Car-borne kinematic GPS applications are generally limited within regional areas, and the relative effects are generally very small. For exactness, the loading effects can be interpolated from that of the surrounding static stations.

(c) ketabton.com: The Digital Library

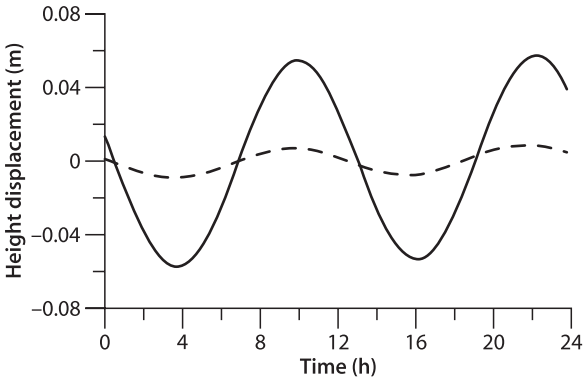

Fig. 5.12. Ocean loading tide effects of two GPS stations (height components)

An example is given to illustrate the loading tide displacements of a vertical component (Fig. 5.12). The AG95 model is used as the principle of the loading effects computation (Andersen 1994). Loading displacements of two stations are computed for a whole day (GPS time used) on the 18 March 1999. Coordinates are quite roughly selected for station Brst (48.3805°, 355.5034°) and IGS station Wtzr (49.1442°, 12.8789°). Results of the height components are illustrated as 2-D graphics with the 1st axis as time in hours and the 2nd axis displacement in meters. Continuous and broken lines represent the results of the 1st and 2nd stations, respectively. The loading displacements of the two stations have a maximum difference of about 6 cm.

This computation indicates that a lack of loading tide correction could cause an accuracy of a few centimetres for some applications. Even for differential applications, a lack of loading tide correction could cause an accuracy of less than 6 cm in the given example.

It is worth mentioning that the average value of the loading effects on a GPS station during 24 hours is generally very small. This indicates that the loading effects could be eliminated through daily averaging. In a static case, either loading correction or no loading correction may cause a difference of the standard deviation of the length of a baseline up to 0.5 cm (Khan 1999).

Analogue to the tropospheric model parameterisation, a loading parameter may be introduced for a static station near the coast due to less accuracy of the loading modelling. The parameter (e.g., a factor of the total loading vector) may be determined through GPS data processing.

5.5 Clock Errors

As discussed in Chap. 4 in the models of GPS observables, the clocks on the satellites and receivers play a very important role in precise GPS surveying. The influences of the clock errors on the GPS may be grouped into three types. One is factorised with the speed of light, *c*. Another is factorised with the speed of satellites. And the third is factorised with the working frequency.

The influence of the first type of clock error is obvious. For code measurements, one measures the transmitting time of the signal and multiplies the transmitting

(c) ketabton.com: The Digital Library

time with c to obtain the transmitting path length. A clock error of δt will cause a path length error of $c\delta t$. Similarly, a clock error of δt will cause a phase error of $c\delta t / \lambda$. Because of the factor c, a small clock error may cause a very large code and phase error. Therefore, high quality clocks have to be used on the satellites and receivers. Meanwhile, clock errors must be carefully modelled. A simple model may be expressed as

$$\delta t = b + dt + at^2 \ , \quad t_1 \le t \le t_2 \ , \tag{5.163}$$

where b is the bias, d is the drift and a is the acceleration of the related clock. Time interval (t_1, t_2) is the valid period of clock error polynomial. The length of the interval depends directly on the stability of the clock. Such a model describes that the clock has a small drift and acceleration, and the drift and acceleration as well as bias are stable ones. The interval may be estimated by using the drift and acceleration accordingly.

In the case of SA (selective availability, for details cf. Sect. 5.7), the frequency of the clock on the satellite is manipulated artificially. In other words, the scale of the clock on the satellite is not any more a constant; i.e., the clock is not any more stable. Therefore in such a case, the model of Eq. 5.163 is not good enough for use. An alternative model of the clock error of the satellite in the case of SA is

$$\delta t = b_i \ , \quad t = t_i \ . \tag{5.164}$$

That is, the clock bias has to be modelled for every measuring epoch. The clock error parameters have to be determined or equivalently eliminated every epoch.

The influence of the second type of clock error is more or less implicit. Recalling the code and phase models discussed in Chap. 4, there is a geometric distance between the satellite at the signal emission time and the receiver at the signal reception time. The position and velocity of the satellite are functions of time. Therefore, a clock error causes a computing error of the position of the satellite by $\vec{v}_s \delta t$, where $\vec{v}_s$ is the velocity vector of the satellite. These errors pass through the distance function and cause errors of the computed distance. Such an influence is implicitly presented in all the GPS observation models and cannot be eliminated through forming differences. However, the influence of the clock error is factorised by the velocity of the satellite (about 3 km s^{-1}), so an estimation of δt up to an accuracy of 10^{-6} would be enough to ensure the needed accuracy of the computed satellite position. Usually, such an estimation is made through the single point positioning of every station at the every epoch (details cf. the section of single point positioning in Sect. 9.42). Of course, we must also take the relativistic effects into account.

As discussed above, the clock error causes a phase error of $c\delta t / \lambda$; this is equivalent to a frequency error of $f\delta t$. It is obvious that this correction has to be taken into account in Doppler data processing.

Synchronisation of the clocks on the satellites and receivers is a basic prerequisite of a meaningful GPS measurement. Clock modeling leads automatically to the synchronisation of all clocks.

A recent study showed that the clock error parameters are linearly correlated with the ambiguity parameters (for details, see Sect. 9.1).

(c) ketabton.com: The Digital Library

5.6 Multipath Effects

Multipath is the phenomenon whereby a GPS signal arrives at a receiver's antenna via more than one different paths. Multipath propagation affects both pseudorange and carrier phase measurements. In GPS static and kinematic precise positioning, the multipath effect is an error source that has to be taken into account. Related studies have been carried out for many years to reduce or eliminate the multipath effects (cf., e.g., Braasch 1996; Langley 1998; Hofmann-Wellenhof et al. 1997).

Multipath is a very localised effect, which depends only on the local environment surrounding the antenna. As illustrated in Fig. 5.13, the receiver may receive both the direct transmitted signal and the reflected (indirect) signal. The indirect path is obviously dependent on the reflecting surface and the satellite position. The reflecting surface is usually a static one related to the receiver; however, the satellite moves with time. Therefore, the multipath effect is also a variable of time.

Consider the direct signal $s(t) = A\cos(\omega t + \varphi)$, where A is the amplitude, ω is the angular velocity and φ is the phase; then the indirect signal can be represented as $f \cdot s(t + \delta t)$, where f is a factor which has the physical meaning of reduced energy through reflection and δt is the time delay. The multipath effect is indeed the influence of the indirect signal on the observations of the receiver. Because different receiver deals with the signals with a different manner, multipath error is highly dependent upon the architecture of the receivers.

Theoretically (Braasch 1996; Langley 1998), the multipath effect may reach up to 15 meters for P-code measurements and 150 meters for C/A-code. Due to the chip length, P-code is much less sensitive to the indirect signal. Typically, multipath error of the carrier phase is on the order of a few cm.

GPS signals are right-handed circularly polarised (RHCP); therefore, conventional GPS antennas are designed as RHCP antennas. This property helps to reject the multipath signal because the reflected signal has changed its polarisation. The pure reflected signals received by the RHCP antenna usually have only 1/3 of the signal to noise ratio compared with that of the direct signals (Knudsen et al. 1999). This may also be used for detecting multipath effects. The simplest method to avoid the influence of the multipath effects is to set up the antenna far away from possible reflecting surfaces. Using only the carrier phase measurement is possibly the other method. (Code

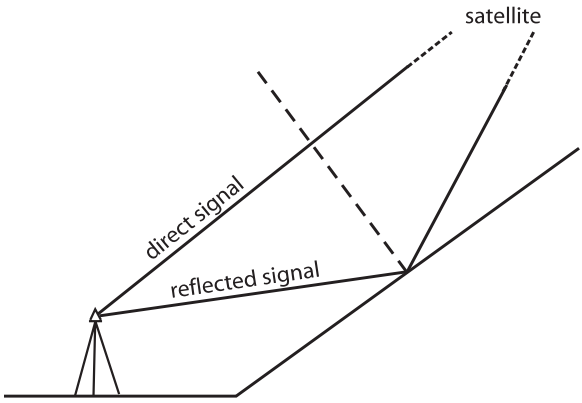

Fig. 5.13.
Geometry of multipath effects

(c) ketabton.com: The Digital Library

is usually used for clock error correction for the satellite coordinates computation; this would be accurate enough even if the multipath effects existed in code; for details, see the discussion in Sect. 5.5). In the case of code positioning, a phase smoothed code should be used. This can reduce the maximum multipath effects to a few cm.

An exact method to deal with the multipath effects is to detect the multipath using code-phase data, and then reject the related phase data or set the phase data to a lower weight for phase data processing. Recalling the models of the code and phase observables discussed in Sect. 4.1 and Sect. 4.2, a code-phase difference can be formed by using Eqs. 4.7 and 4.18 as

$$R_r^s(t_r,t_e) - \lambda\Phi_r^s(t_r) = 2\delta_{ion} + \lambda N_r^s + \delta_{mul} + \varepsilon\,, \tag{5.165}$$

where $R_r^s(t_r, t_e)$ and $\Phi_r^s(t_r)$ are the measured pseudorange and phase, λ is the wave length, t_e is the GPS signal emission time and t_r the signal reception time, δ_{ion} denotes the ionospheric effects of the station r, N_r^s is the integer ambiguity parameter, δ_{mul} is the multipath effect of code measurements, and ε is error of code measurements. The errors of phase and frequency as well as multipath in phase measurements are omitted here. Using the above formula, multipath effects in code measurements can be determined or detected. Because of the higher noise level of the code measurements, detection over a given period of time is reasonable so that the noise can be smoothed.

5.6.1 GPS-Altimetry, Signals Reflected from the Earth-Surface

The existence of multipath effects indicates that a GPS receiver can be used for receiving the reflected GPS signal. That is to say, through receiving the reflected GPS signal, GPS may be used for measuring the reflecting surface topography. Early in 1993, the European Space Agency's Manuel Martin-Neira first suggested using a GPS reflected signal as a signal source for measuring. The accidental acquisition of ocean-reflected GPS signals by an airborne receiver was reported by French engineers in 1994. Katzberg and Garrison (1996) discussed how the GPS signal reflected from the ocean can be used for the determination of ionospheric effects in satellite altimetry. Komjathy et al. (1999) used the GPS signal reflected from the ocean to determine the wave height, wind speed and direction. Knudsen et al. (1999) used a downward-pointing GPS antenna to receive the reflected GPS signal to see if it was possible to use it for determining the topography of the sea surface and ice sheet as well as snow covered land. CHAMP satellite has a downward-pointing GPS antenna on board for an experiment of GPS-altimetry.

Usually, profiles of footprints over the sea surface are measured from satellite altimetry or airborne altimetry; however, by using GPS-altimetry, every profile of footprints has a bandwidth, so that such GPS-altimetry can be used for covering the topography of the reflecting surface. The sea and ice sheet as well as snow covered land are good reflecting surfaces for the GPS signals (Knudsen et al. 1999).

The polarisation of the reflected signal changes after the reflection. A conventional GPS antenna is right-handed circularly polarised; therefore, for receiving the reflected GPS signals a left-handed circularly polarised antenna shall be used (Komjathy et al. 1999; Katzberg and Garrison 1996). Such an antenna has been designed and used in the experiments reported. The power of the reflected signal is then reduced insignificantly.

(c) ketabton.com: The Digital Library

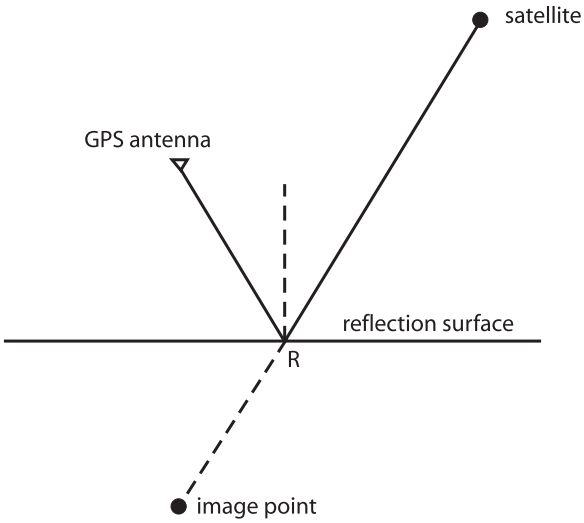

Fig. 5.14.
Geometry of the reflecting signal

5.6.2
Reflecting Point Positioning

The method to process the downward-pointing antenna measured GPS data is quite different from the known method to process the GPS data obtained by an upward-pointing antenna. As shown in Fig. 5.14, the GPS signal is transmitted from the satellite to the downward-pointing antenna through the reflecting point R (or more exactly, a small zone surrounding R, cf. Komjathy et al. 1999) of the reflecting surface. The satellite orbit is known. The position of the downward-pointing antenna can be determined by using the data received from an upward-looking antenna. So the purpose of the GPS-altimetry is to determine the unknown point R. The vertical line of the satellite and the antenna forms a plane. Such a plane will intersect with the Earth's surface and form a curved line. The reflecting point shall be on the line. Due to the principle of reflection, the angle of fall in and the angle of fall out must be equal. In other words, the elevations of the antenna and the satellite related to the reflecting surface at the reflecting point must be the same. Therefore, the reflecting point shall be generally a unique one if the reflecting surface is a fixed surface. Even in a static case, i.e., the GPS antenna does not move, the reflecting point R is a kinematic point because of the movement of the satellite. Different satellites have generally different reflecting points. These points are independent if one does not take the a priori knowledge of the reflecting surface into account.

For every observed satellite of every epoch there are three new coordinate unknowns. A straightforward solution is mathematically impossible. However, suppose the reflecting surface is a geoid or a known sea surface, for example, then the latitude and longitude of the reflecting point can be computed from the satellite position and the known antenna position. Then the left unknown is just one parameter of height. Suppose the reflecting surface is just needed to be determined up to, say, a resolution of two kilometres, then the height of every point located within the one km radius could be considered the same, and in such case the GPS altimetry problem is clearly solvable.

(c) ketabton.com: The Digital Library

The signal transmitting distance d can be described below:

$$d=\sqrt{(x_s-x_r)^2+(y_s-y_r)^2+(z_s-z_r)^2}+\sqrt{(x_k-x_r)^2+(y_k-y_r)^2+(z_k-z_r)^2}\ , \quad (5.166)$$

where indices s, r and k denote satellite, reflecting point and downward-pointing GPS antenna, respectively. Of course the transmitting time correction has to be taken into account. Cartesian coordinates x, y and z of the reflecting point can be represented by geodetic coordinates φ, λ and h. φ and λ of the reflecting point shall fulfil the following linear equation:

$$(\varphi-\varphi_k)=(\lambda-\lambda_k)\frac{\varphi_s-\varphi_k}{\lambda_s-\lambda_k}\ . \quad (5.167)$$

For any given φ between value φ_k and φ_s, a related λ can be obtained. Then the zero height reflecting point in Cartesian coordinates can be obtained. The zenith distances of the downward-pointing GPS antenna and the GPS satellite related to the reflecting point can be then computed respectively. By using the criteria that both zenith distances shall be the same, a best set of φ and λ can be found. Taking the known coordinates of the zero height reflecting point into account, there is just one parameter of height remaining as an unknown in the Eq. 5.166.

By reducing the resolution rate to every two epochs, i.e., suppose within every two epochs the height of the reflecting point remained the same, the problem including the receiver clock error and ambiguity can be solved with enough redundancies.

5.6.3 Image Point and Reflecting Surface Determination

An alternative method to determine the reflecting surface is proposed below.

The reflecting surface is considered a mirror and the downward-pointing antenna is an image point behind the mirror. If the reflecting surface is a plane, then the image point positioning can be done with the same method used in kinematic positioning of the upward-looking antenna. Usually, the longitude and latitude of the image point can be obtained from the results of the upward-looking antenna; therefore, the image point positioning problem has just one coordinate-unknown height and can be well determined. Now one has two heights, one is the height of the downward-pointing antenna; another is the height of the image point. The average value of these two heights is then the footprint height of the downward-pointing antenna on the reflecting surface. The longitude and latitude of the reflecting point can be determined by using the method discussed in Sect. 5.6.2; therefore in this way, the reflecting point can be determined.

However, the reflecting surface is usually not a plane; therefore, the above-discussed image point positioning result is a kind of average height. For convenience, we define the reflecting point, which has such an average height, as a nominal reflecting point. The distances between the nominal reflecting point and the satellite and downward-pointing antenna can be computed. Comparing the computed value with the true signal transmitting distance, the bias of heights of the real reflecting point and the nominal reflecting point can be determined. In such a way, the reflecting surface can be determined.

(c) ketabton.com: The Digital Library

5.7 Anti-Spoofing and Selective Availability Effects

Anti-Spoofing

The function of anti-spoofing (AS) of the GPS system is designed for an anti potential spoofer (or jammer). A spoofer generates a signal that mimics the GPS signal and attempts to cause the receiver to track the wrong signal. When the AS mode of operation is activated, the P code will be replaced with a secure Y code available only to authorised users, and the unauthorised receiver becomes a single L1 frequency receiver. AS had been tested frequently since 1 August 1992 and formally activated at 00:00 UT on 31 January 1994 and now is in continuous operation on all Block II and later satellites.

The broadcasted ionospheric model (in the navigation message) may be used to overcome the problem of absence of the dual-frequencies, which are originally implemented for eliminating the ionospheric effects. Of course, the method of using the ionospheric model cannot be as accurate as the method of using dual-frequencies data, and consequently the precision is degraded. Carrier phase smoothed C/A code may be used to replace the absence of the P code.

Selective Availability

Selective availability (SA) is a degradation of the GPS signal with the objective to deny full position and velocity accuracy to unauthorised users by dithering the satellite clock and manipulating the ephemerides. In case SA is on, the fundament frequency of the satellite clock is dithered, so that the GPS measurements are affected. The broadcast ephemerides are manipulated so that the computed orbit will have slow variations. Several levels of SA effects are possible. The SA is enabled on Block II and later satellites (Graas and Braasch 1996).

The authorised users may recover the un-degraded data and exploit the full system potential. For doing so they must possess a key that allows them to decrypt correction data transmitted in the navigation message (Georgiadou and Daucet 1990). For high-precision users, IGS precise orbit and forecast orbit data may be used. Using known positions (or monitor stations), the range corrections can be computed. Differential GPS may also eliminate at least a part of the SA effects.

SA has been switched off since May 2000.

5.8 Antenna Phase Centre Offset and Variation

Satellite Antenna Phase Centre Correction

The geometric distance between the satellite (at signal emission time) and the receiver (at signal reception time) is in fact the distance of the phase centres of the two antennas. However, the orbit data, which describes the position of the satellite, is usually referred to the mass centre of the satellite. Therefore, a phase centre correction (also called mass centre correction) has to be applied to the satellite coordinates in precise applications.

A satellite fixed coordinate system shall be set up for describing the antenna phase centre offset to the mass centre of the satellite. As shown in Fig. 5.15, the origin of the

(c) ketabton.com: The Digital Library

frame coincides with the mass centre of the satellite, the z-axis is parallel to the antenna pointing direction, the y-axis is parallel to the solar-panel axis, and the x-axis is selected to complete the right-handed frame. A solar vector is a vector from the satellite mass centre pointed to the Sun. During the motion of the satellite, the z-axis is always pointing to the Earth, and the y-axis (solar-panel axis) shall be kept perpendicular to the solar vector. In other words, the y-axis is always perpendicular to the plane, which is formed by the Sun, the Earth and satellite. The solar-panel can be rotated around its axis to keep the solar-panel perpendicular to the ray of the Sun for optimally collecting the solar energy. The solar angle β is defined as the angle between the z-axis and the solar identity vector $\vec{n}_{\text{sun}}$ (see Fig. 5.16). Denoting the identity vector of the satellite fixed frame as ($\vec{e}_x$ $\vec{e}_y$ $\vec{e}_z$), then the solar identity vector can be represented as

$$\vec{n}_{\text{sun}} = (\sin\beta \quad 0 \quad \cos\beta) \ . \tag{5.168}$$

β is needed for computation of the solar radiation pressure in orbit determination.

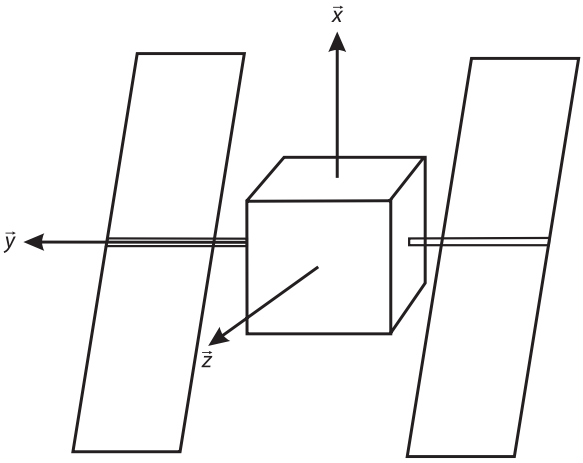

Fig. 5.15.
Satellite fixed coordinate system

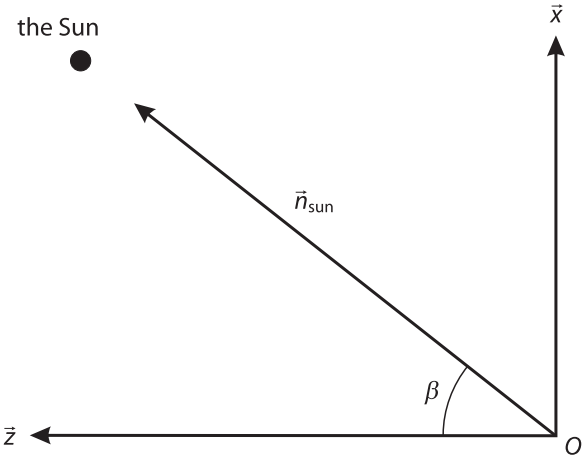

Fig. 5.16.
The Sun vector in satellite fixed frame

(c) ketabton.com: The Digital Library

Denoting $\vec{r}$ as the geocentric satellite vector and $\vec{r}_s$ as the geocentric solar vector (Fig. 5.17),

$$\vec{r} = \begin{pmatrix} X \\ Y \\ Z \end{pmatrix}, \qquad \vec{r}_s = \begin{pmatrix} X_{\text{sun}} \\ Y_{\text{sun}} \\ Z_{\text{sun}} \end{pmatrix}, \tag{5.169}$$

then in a geocentric coordinate system one has

$$\vec{e}_z = -\frac{\vec{r}}{|\vec{r}|}, \tag{5.170}$$

$$\vec{e}_y = \frac{\vec{e}_z \times \vec{n}_{\text{sun}}}{|\vec{e}_z \times \vec{n}_{\text{sun}}|}, \tag{5.171}$$

$$\vec{e}_x = \vec{e}_y \times \vec{e}_z, \tag{5.172}$$

$$\vec{n}_{\text{sun}} = \frac{\vec{r}_s - \vec{r}}{|\vec{r}_s - \vec{r}|} \quad \text{and} \tag{5.173}$$

$$\cos\beta = \vec{n}_{\text{sun}} \cdot \vec{e}_z, \tag{5.174}$$

or

$$\vec{e}_z = \frac{-1}{r}\begin{pmatrix} X \\ Y \\ Z \end{pmatrix}, \qquad r = \sqrt{X^2 + Y^2 + Z^2}, \tag{5.175}$$

$$\vec{n}_{\text{sun}} = \frac{1}{R}\begin{pmatrix} X_{\text{sun}} - X \\ Y_{\text{sun}} - Y \\ Z_{\text{sun}} - Z \end{pmatrix}, \tag{5.176}$$

$$\vec{e}_y = \frac{-1}{S}\begin{pmatrix} YZ_{\text{sun}} - Y_{\text{sun}}Z \\ ZX_{\text{sun}} - Z_{\text{sun}}X \\ XY_{\text{sun}} - X_{\text{sun}}Y \end{pmatrix} \quad \text{and} \tag{5.177}$$

$$\vec{e}_x = \frac{1}{S \cdot r}\begin{pmatrix} (ZX_{\text{sun}} - Z_{\text{sun}}X)Z - (XY_{\text{sun}} - X_{\text{sun}}Y)Y \\ (XY_{\text{sun}} - X_{\text{sun}}Y)X - (YZ_{\text{sun}} - Y_{\text{sun}}Z)Z \\ (YZ_{\text{sun}} - Y_{\text{sun}}Z)Y - (ZX_{\text{sun}} - Z_{\text{sun}}X)X \end{pmatrix}, \tag{5.178}$$

where

$$R = \sqrt{(X_{\text{sun}} - X)^2 + (Y_{\text{sun}} - Y)^2 + (Z_{\text{sun}} - Z)^2} \quad \text{and} \tag{5.179}$$

$$S = \sqrt{(YZ_{\text{sun}} - Y_{\text{sun}}Z)^2 + (ZX_{\text{sun}} - Z_{\text{sun}}X)^2 + (XY_{\text{sun}} - X_{\text{sun}}Y)^2}. \tag{5.180}$$

(c) ketabton.com: The Digital Library

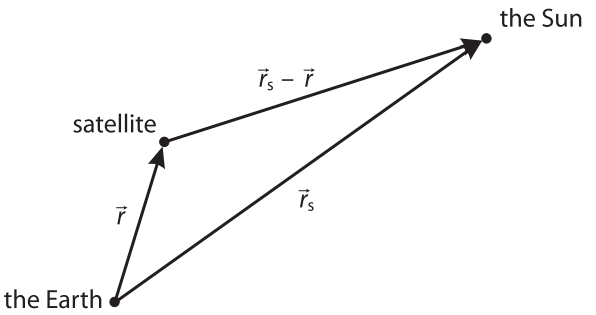

Fig. 5.17.
The Earth-Sun-satellite vectors

Table 5.3.
GPS satellite antenna phase centre offset

Satellites of	*x*	*y*	*z*
Block I	0.2100	0.0	0.8540
Block II/IIA	0.2794	0.0	1.0259
Block IIR	0.0000	0.0	1.2053

Suppose the satellite antenna phase centre in the satellite fixed frame is (x, y, z), then the offset vector in the geocentric frame can be obtained by substituting Eqs. 5.175, 5.177 and 5.178 into the following formula:

$$\vec{d} = x\vec{e}_x + y\vec{e}_y + z\vec{e}_z\,, \tag{5.181}$$

which may be added to the vector $\vec{r}$.

GPS satellite antenna phase centre offsets in the satellite fixed frame are given in Table 5.3.

The dependence of the phase centre on the signal direction and frequencies is not considered for the satellite here. A mis-orientation of the $\vec{e}_y$ ($\vec{e}_x$ too) of the satellite with respect to the Sun may cause errors in the geometrical phase centre correction. In the Earth's shadow (for up to 55 minutes), the mis-orientation becomes worse. The geometrical mis-orientation may be modelled and estimated.

Receiver Antenna Phase Centre Correction

In the case of receiver antenna phase centre correction, the dependence of the phase centre on the signal direction and frequencies has to be taken into account. Both the phase centre offset and variation should be modelled. Generally, the phase centre corrections can be obtained through careful calibration. Receiver antenna phase centre offset is also antenna type dependent. For a GPS network, antenna phase centre corrections are usually predetermined and listed in a table for use.

5.9 Instrumental Biases

Study of ionospheric effects by using GPS observations indicates the existence of the instrumental biases (cf., e.g., Yuan and Ou 1999). The biases are systematic errors, which are

(c) ketabton.com: The Digital Library

different from the frequency-to-frequency and from the code to phase measurements. However, they are constants for given frequency and given observable type as well as given instruments (receiver or GPS satellite). For code, phase and Doppler observable of receiver i, satellite j at working frequency k, instrumental biases can be modelled as

$$\begin{matrix} \delta I_{\mathrm{c}}(i,k) + \delta J_{\mathrm{c}}(j,k) \\ \delta I_{\mathrm{p}}(i,k) + \delta J_{\mathrm{p}}(j,k) \quad \text{and} \\ \delta I_{\mathrm{d}}(i,k) + \delta J_{\mathrm{d}}(j,k) \end{matrix} \tag{5.182}$$

respectively, where indices c, p and d denote the code, phase and Doppler observables. δI and δJ denote the instrumental biases of the GPS receiver and GPS satellite. The separation of the instrumental biases and the ambiguities are possible because the biases of the receiver and satellite are independent from each other, whereas the ambiguity parameters are dependent both on the receiver and the satellite. However, by modelling and solving the problem, the correlation between the parameters has to be carefully studied. Instrumental biases of one of the frequencies and one of the channels are linearly correlated with the clock biases. Without modelling of the instrumental biases, the biases may merge into the ambiguity parameters so that the integer property of the ambiguities may be destroyed.

(c) ketabton.com: The Digital Library

Chapter 6

GPS Observation Equations and Equivalence Properties

In this chapter, first the general mathematical model of GPS observation and its linearisation are discussed. All partial derivatives of the observational function are given in detail. These are necessary for forming GPS observation equations. Then, linear transformation and covariance propagation are outlined. In the data combinations section, all meaningful and useful data combinations are discussed, such as ionosphere-free, geometry-free, code-phase combinations, ionospheric residuals, as well as differential Doppler and Doppler integration. In the section of data differentiation, single, double and triple differences as well as their related observation equations and weight propagation are discussed. The parameters in the equations are greatly reduced through difference forming; however, the covariance derivations are tedious. In the last two sections, the equivalent properties between the uncombined and combining as well as undifferenced and differencing algorithms are discussed. A unified GPS data processing method is proposed in detail. The method is selectively equivalent to the zero-, single-, double-, triple-, and user-defined differential methods.

6.1 General Mathematical Models of GPS Observations

Recalling the discussions in Chap. 4, the GPS code pseudorange, carrier phase and Doppler observables are formulated as (cf. Eqs. 4.7, 4.18, 4.23):

$$R_i^k(t_r,t_e)=\rho_i^k(t_r,t_e)-(\delta t_r-\delta t_k)c+\delta_{ion}+\delta_{trop}+\delta_{tide}+\delta_{rel}+\varepsilon_c\,, \tag{6.1}$$

$$\lambda\Phi_i^k(t_r,t_e)=\rho_i^k(t_r,t_e)-(\delta t_r-\delta t_k)c+\lambda N_i^k-\delta_{ion}+\delta_{trop}+\delta_{tide}+\delta_{rel}+\varepsilon_p \text{ and} \tag{6.2}$$

$$D=\frac{\mathrm{d}\rho_i^k(t_r,t_e)}{\lambda\mathrm{d}t}-f\frac{\mathrm{d}(\delta t_r-\delta t_k)}{\mathrm{d}t}+\delta_{rel_f}+\varepsilon_d\,. \tag{6.3}$$

Where ionospheric effects can be approximated as (cf. Sect. 5.1.2, Eq. 5.26)

$$\delta_{ion}=\frac{A_1}{f^2}+\frac{A_2}{f^3}\ ,$$

and R is the observed pseudorange, Φ is the observed phase, D is Doppler measurement, t_e denotes the GPS signal emission time of the satellite k, t_r denotes the GPS signal reception time of the receiver i, c denotes the speed of light, subscript i and

(c) ketabton.com: The Digital Library

superscript k denote the receiver and satellite, and δt_r and δt_k denote the clock errors of the receiver and satellite at the time t_r and t_e, respectively. The terms δ_{ion}, δ_{trop}, δ_{tide}, and δ_{rel} denote the ionospheric, tropospheric, tidal and relativistic effects, respectively. Tidal effects include Earth tide and ocean loading tide effects. The multipath effect has been discussed in Sect. 5.6 and is omitted here. ε_c, ε_p and ε_d are the remaining errors, respectively. f is the frequency, wavelength is denoted by λ, A_1 and A_2 are ionospheric parameters, N_i^k is the ambiguity related to receiver i and satellite k, δ_{rel_f} is the frequency correction of the relativistic effects, the ρ_i^k is the geometric distance, and (cf. Eq. 4.6)

$$\rho_i^k(t_r, t_e) = \rho_i^k(t_r) + \frac{d\rho_i^k(t_r)}{dt}\Delta t \ , \tag{6.4}$$

where Δt denotes the signal transmitting time and $\Delta t = t_r - t_e$. $d\rho_i^k(t_r) / dt$ denotes the time derivation of the radial distance between the satellite and receiver at the time t_r. All terms in Eqs. 6.1 and 6.2 have units of length (meters).

Considering Eq. 6.4 in the ECEF coordinate system, the geometric distance is a function of station state vector $(x_i, y_i, z_i, \dot{x}_i, \dot{y}_i, \dot{z}_i)$ (denoted by X_i) and satellite state vector $(x_k, y_k, z_k, \dot{x}_k, \dot{y}_k, \dot{z}_k)$ (denoted by X_k). GPS observation Eqs. 6.1, 6.2 and 6.3 can then be generally presented as

$$O = F(X_i,\ X_k,\ \delta t_i,\ \delta t_k,\ \delta_{ion},\ \delta_{trop},\ \delta_{tide},\ \delta_{rel},\ N_i^k,\ \delta_{rel_f}) \ , \tag{6.5}$$

where O denotes observation and F denotes implicit function. In other words, the GPS observable is a function of state vectors of the station and satellite, and numbers of physical effects as well as ambiguity parameters. In principle, through GPS observations, the desired parameters of the function in Eq. 6.5 can be solved for. This is why nowadays GPS has been widely used for positioning and navigation (to determine the state vector of the station), for orbit determination (to determine the state vector of satellite), for timing (to synchronise clocks), for meteorological applications (i.e. troposphere profiling), and for ionospheric occultation (i.e. ionosphere sounding). In turn, the satellite orbit is a function of the gravitational field of the Earth and numbers of disturbing effects such as solar radiation pressure and atmospheric drags. GPS is now also used for gravity field mapping, as well as solar and Earth system study.

It is obvious that Eq. 6.5 is a non-linear one. The straightforward mathematical method to solve problem 6.5 is to search for the optimal solution by using some effective search algorithms. The so-called ambiguity function (AF, see Sect. 8.5 and Sect. 12.2) method is one of the examples. Generally speaking, solving a non-linear problem is much more complicated than first linearising the problem and then solving the linearised problem.

It is notable that the satellite state vector and the station state vector shall be represented in the same coordinate system; otherwise coordinate transformation discussed in Chap. 2 shall be made. Because the rotations are "distance keeping" transformations, the distances computed in two different coordinate systems must be the same. However, because of the Earth's rotation, the velocities expressed in the ECI and ECEF coordinate systems are not the same. Generally, the station coordinates and ionospheric effects as well as tropospheric effects are given and presented in the ECEF system. A satellite state vector may be given in both the ECSF system and the ECEF system. This depends on the need of the concerned applications.

(c) ketabton.com: The Digital Library

6.2 Linearisation of the Observational Model

The non-linear multivariable function F in Eq. 6.5 can be further generalised as

$$O = F(Y) = F(y_1, y_2, \ldots, y_n) \ , \tag{6.6}$$

where variable vector Y has n elements. The linearisation is accomplished by expanding the function in a Taylor series to the first order (linear term) as

$$O = F(Y^0) + \left.\frac{\partial F(Y)}{\partial Y}\right|_{Y^0} \cdot \mathrm{d}Y + \varepsilon(\mathrm{d}Y) \ , \tag{6.7}$$

where

$$\frac{\partial F(Y)}{\partial Y} = \left(\frac{\partial F}{\partial y_1} \quad \frac{\partial F}{\partial y_2} \quad \ldots \quad \frac{\partial F}{\partial y_n} \right), \quad \text{and} \quad \mathrm{d}Y = \left(Y - Y^0\right) = \begin{pmatrix} \mathrm{d}y_1 \\ \mathrm{d}y_2 \\ \vdots \\ \mathrm{d}y_n \end{pmatrix} ;$$

the symbol $|_{Y^0}$ means that the partial derivative $\partial F(Y)/\partial Y$ takes the value of $Y = Y^0$ and ε is the truncating error, which is a function of the second order partial derivative and $\mathrm{d}Y$. Y^0 is called the initial value vector. Equation 6.7 turns out then to be

$$O - C = \left(\frac{\partial F}{\partial y_1} \quad \frac{\partial F}{\partial y_2} \quad \cdots \quad \frac{\partial F}{\partial y_n} \right)_{Y^0} \cdot \begin{pmatrix} \mathrm{d}y_1 \\ \mathrm{d}y_2 \\ \vdots \\ \mathrm{d}y_n \end{pmatrix} + \varepsilon \ , \tag{6.8}$$

where $F(Y^0)$ is denoted by C (or say, the computed value). So GPS observation Eq. 6.6 is linearised as a linear equation (Eq. 6.8). Denoting the observational error and truncating error as v and $O - C$ as l, partial derivative $(\partial F/\partial y_j)|_{Y^0} = a_j$, then Eq. 6.8 can be written as

$$l_i = \begin{pmatrix} a_{i1} & a_{i2} & \ldots & a_{in} \end{pmatrix} \cdot \begin{pmatrix} \mathrm{d}y_1 \\ \mathrm{d}y_2 \\ \vdots \\ \mathrm{d}y_n \end{pmatrix} + v_i \ , \quad (i = 1, 2, \ldots, m) \ , \tag{6.9}$$

where l is also often called "observable" in adjustment or $O - C$ (observed minus computed), and j and i are indices of unknowns and the observations. Equation 6.9 is a linear error equation. A set of GPS observables then forms a linear error equation system:

(c) ketabton.com: The Digital Library

$$\begin{pmatrix} l_1 \\ l_2 \\ \vdots \\ l_m \end{pmatrix} = \begin{pmatrix} a_{11} & a_{12} & \dots & a_{1n} \\ a_{21} & a_{22} & \dots & a_{2n} \\ \vdots & \vdots & \vdots & \vdots \\ a_{m1} & a_{m2} & \dots & a_{mn} \end{pmatrix} \cdot \begin{pmatrix} \mathrm{d}y_1 \\ \mathrm{d}y_2 \\ \vdots \\ \mathrm{d}y_n \end{pmatrix} + \begin{pmatrix} v_1 \\ v_2 \\ \vdots \\ v_m \end{pmatrix},$$

or in matrix form (denotes dY by X)

$$L = AX + V, \tag{6.10}$$

where m is the observable number. A number of adjustment and filtering methods (cf. Chap. 7) can be applied for solving the GPS problem 6.10. The solved parameter vector is X (or dY). The original unknown vector Y can be obtained by adding dY to Y^0. V is the residual vector. Statistically, V shall be assumed to be a random vector, and is normally distributed with zero expectation and variance var(V). To characterise the different qualities and correlation situations of the observables, a so-called weight matrix P is introduced to Eq. 6.10. Supposing all observations are linearly independent or un-correlated, the covariance of observable vector L is

$$Q_{LL} = \mathrm{cov}(L) = \sigma^2 E \tag{6.11}$$

or

$$P = Q_{LL}^{-1} = \frac{1}{\sigma^2} E, \tag{6.12}$$

where E is an identity matrix of dimension $m \times m$, superscript $^{-1}$ is an inversion operator, and cov(L) is covariance of L.

Generally, only if the solved unknown vector dY is small enough, the linearisation process can be considered done well. Therefore, the initial vector Y^0 has to be carefully given. In case the initial vector is not well-known or not well-given, the linearisation process has to be iterated. In other words, the initial vector that is not well-known has to be modified by the solved vector dY, and the linearisation process has to be made again until dY converges. If $X = 0$, then $L = V$; therefore, the "observable" vector L is also called a residual vector sometimes. If the initial vector Y^0 is well-known or well-given, then the residual vector V can also be used as a criterion to judge the "goodness or badness" of the original observable vector. This property is used in robust Kalman filtering to adjust the weight of the observable (cf. Chap. 7).

6.3 Partial Derivatives of Observational Function

Partial Derivatives of Geometric Path Distance with Respect to the State Vector (x_i, y_i, z_i, $\dot{x}_i$, $\dot{y}_i$, $\dot{z}_i$) of the GPS Receiver

The signal transmitting path is described by (cf. Eqs. 4.3 and 4.6 in Chap. 4)

$$\rho_i^k(t_r, t_e) = \sqrt{(x_k(t_e) - x_i)^2 + (y_k(t_e) - y_i)^2 + (z_k(t_e) - z_i)^2}, \text{ and} \tag{6.13}$$

(c) ketabton.com: The Digital Library

$$\rho_i^k(t_r,t_e) \approx \rho_i^k(t_r,t_r) + \frac{d\rho_i^k(t_r,t_r)}{dt}\Delta t \ , \tag{6.14}$$

where index k denotes the satellite, and the satellite coordinates are related to the signal emission time t_e, i denotes the station, and the station coordinates are related to the signal reception time t_r, $\Delta t = t_e - t_r$. Then one has

$$\frac{d\rho_i^k(t_r,t_r)}{dt} = \frac{1}{\rho_i^k(t_r,t_r)} \times\left((x_k - x_i)(\dot{x}_k - \dot{x}_i) \ \ (y_k - y_i)(\dot{y}_k - \dot{y}_i) \ \ (z_k - z_i)(\dot{z}_k - \dot{z}_i)\right), \tag{6.15}$$

where the satellite state vector is related to the time t_r, and

$$\frac{\partial\rho_i^k(t_r,t_e)}{\partial(x_i,y_i,z_i)} = \frac{-1}{\rho_i^k(t_r,t_e)}\begin{pmatrix} x_k - x_i & y_k - y_i & z_k - z_i \end{pmatrix} , \tag{6.16}$$

$$\frac{\partial\rho_i^k(t_r,t_e)}{\partial(\dot{x}_i,\dot{y}_i,\dot{z}_i)} = \frac{-\Delta t}{\rho_i^k(t_r,t_r)}\begin{pmatrix} x_k - x_i & y_k - y_i & z_k - z_i \end{pmatrix} . \tag{6.17}$$

Partial Derivatives of Geometric Path Distance with Respect to the State Vector (x_k, y_k, z_k, $\dot{x}_k$, $\dot{y}_k$, $\dot{z}_k$) of the GPS Satellite

Similar to above, one has

$$\frac{\partial\rho_i^k(t_r,t_e)}{\partial(x_k,y_k,z_k)} = \frac{1}{\rho_i^k(t_r,t_e)}\begin{pmatrix} x_k - x_i & y_k - y_i & z_k - z_i \end{pmatrix} , \tag{6.18}$$

$$\frac{\partial\rho_i^k(t_r,t_e)}{\partial(\dot{x}_k,\dot{y}_k,\dot{z}_k)} = \frac{\Delta t}{\rho_i^k(t_r,t_r)}\begin{pmatrix} x_k - x_i & y_k - y_i & z_k - z_i \end{pmatrix} . \tag{6.19}$$

Partial Derivatives of the Doppler Observable with Respect to the Velocity Vector of the Station

The time differentiation of the geometric signal path distance can be derived as

$$\frac{d\rho_i^k(t_r,t_e)}{dt} = \frac{1}{\rho_i^k(t_r,t_e)} \ ; \tag{6.20}$$
$$((x_k(t_e)-x_i)(\dot{x}_k(t_e)-\dot{x}_i)+(y_k(t_e)-y_i)(\dot{y}_k(t_e)-\dot{y}_i)+(z_k(t_e)-z_i)(\dot{z}_k(t_e)-\dot{z}_i))$$

then one has

$$\frac{\partial(d\rho_i^k(t_r,t_e)/dt)}{\partial(\dot{x}_i,\dot{y}_i,\dot{z}_i)} = \frac{-1}{\rho_i^k(t_r,t_e)}\begin{pmatrix} x_k(t_e) - x_i & y_k(t_e) - y_i & z_k(t_e) - z_i \end{pmatrix} . \tag{6.21}$$

(c) ketabton.com: The Digital Library

Partial Derivatives of Clock Errors with Respect to the Clock Parameters

If the clock errors are modelled by Eq. 5.163 (cf. Sect. 5.5)

$$\delta t_i = b_i + d_i t + e_i t^2 , \quad \delta t_k = b_k + d_k t + e_k t^2 , \tag{6.22}$$

where i and k are the indices of the clock error parameters of the receiver and satellite, then one has

$$\frac{\partial \delta t_i}{\partial (b_i, d_i, e_i)} = \begin{pmatrix} 1 & t & t^2 \end{pmatrix} \quad \text{and}$$

$$\frac{\partial \delta t_k}{\partial (b_k, d_k, e_k)} = \begin{pmatrix} 1 & t & t^2 \end{pmatrix} . \tag{6.23}$$

If the clock errors are modelled by Eq. 5.164 (cf. Sect. 5.5)

$$\delta t_i = b_i , \quad \delta t_k = b_k , \tag{6.24}$$

then

$$\frac{\partial \delta t_i}{\partial b_i} = 1, \quad \frac{\partial \delta t_k}{\partial b_k} = 1 . \tag{6.25}$$

The above derivatives are valid for both the code and phase observable equations. For the Doppler observable, denote (cf. Eq. 6.3)

$$\delta_{\text{clock}} = f \frac{\mathrm{d}(\delta t_i - \delta t_k)}{\mathrm{d}t} , \tag{6.26}$$

then for the clock error model of Eq. 6.22 one has

$$\frac{\partial \delta_{\text{clock}}}{\partial (d_i, e_i)} = \begin{pmatrix} 1 & 2t \end{pmatrix} f \quad \text{and} \quad \frac{\partial \delta_{\text{clock}}}{\partial (d_k, e_k)} = -\begin{pmatrix} 1 & 2t \end{pmatrix} f . \tag{6.27}$$

Partial Derivatives of Tropospheric Effects with Respect to the Tropospheric Parameters

If the tropospheric effects can be modelled by (cf. Sect. 5.2)

$$\text{I:} \quad \delta_{\text{trop}} = f_{\text{p}} \mathrm{d}\rho \quad \text{and}$$

$$\text{II:} \quad \delta_{\text{trop}} = \frac{f_{\text{z}} \mathrm{d}\rho}{F} + \frac{f_{\text{a}} \mathrm{d}\rho}{F_{\text{c}}} , \tag{6.28}$$

where $\mathrm{d}\rho$ is the tropospheric effect computed by using the standard tropospheric model, $f_{\text{p}}, f_{\text{z}}, f_{\text{a}}$ are parameters of the tropospheric delay in path, zenith, azimuth di-

(c) ketabton.com: The Digital Library

rections, and F and F_c are the mapping and co-mapping functions discussed in Sect. 5.2. The derivatives with respect to the parameters f_p, f_z, f_a are then

$$\text{I:}\quad \frac{\partial \delta_{\text{trop}}}{\partial f_p} = \mathrm{d}\rho \quad \text{and}$$

$$\text{II:}\quad \frac{\partial \delta_{\text{trop}}}{\partial (f_z, f_a)} = \begin{pmatrix} \dfrac{\mathrm{d}\rho}{F} & \dfrac{\mathrm{d}\rho}{F_c} \end{pmatrix}. \tag{6.29}$$

Furthermore, if the tropospheric parameters are defined as a step function or first order polynomial (cf. Sect. 5.2) by

$$\text{I:}\quad f_p = f_z = f_j \quad \text{if} \quad t_{j-1} < t \le t_j, \quad j = 1, 2, \ldots, n \quad \text{and}$$

$$\text{II:}\quad f_p = f_z = f_{j-1} + (f_j - f_{j-1}) \frac{t - t_{j-1}}{\Delta t} \quad \text{if} \quad t_{j-1} < t \le t_j, \quad j = 1, 2, \ldots, n+1, \tag{6.30}$$

where $\Delta t = (t_n - t_0) / n$, t_0 and t_n are the beginning and the ending times of the GPS survey, and Δt is usually selected by two to four hours. Then one has

$$\text{I:}\quad \frac{\partial f_p}{\partial f_j} = \frac{\partial f_z}{\partial f_j} = 1 \quad \text{and}$$

$$\text{II:}\quad \frac{\partial f_p}{\partial (f_{j-1}, f_j)} = \frac{\partial f_z}{\partial (f_{j-1}, f_j)} = \begin{pmatrix} 1 + \dfrac{-t + t_{j-1}}{\Delta t} & \dfrac{t - t_{j-1}}{\Delta t} \end{pmatrix}. \tag{6.31}$$

The azimuth dependency may be assumed to be (cf. Eq. 5.121)

$$f_a = g_1 \cos a + g_2 \sin a\,, \tag{6.32}$$

where a is the azimuth, and g_1 and g_2 are called azimuth-dependent parameters. Then one gets

$$\frac{\partial f_a}{\partial (g_1, g_2)} = (\cos a \quad \sin a)\,. \tag{6.33}$$

If parameters g_1 and g_2 are also defined as step functions or first order polynomials like Eq. 6.30, the partial derivatives can be obtained in a similar manner to Eq. 6.31.

Partial Derivatives of the Phase Observable with Respect to the Ambiguity Parameters

Depending on which scale one prefers, there is

$$\frac{\partial \lambda N}{\partial \lambda N} = 1 \quad \text{or} \quad \frac{\partial \lambda N}{\partial N} = \lambda\,. \tag{6.34}$$

(c) ketabton.com: The Digital Library

Partial Derivatives of Tidal Effects with Respect to the Tidal Parameters

If the Earth tide model in Eqs. 5.147 and 5.149 are used, then the tidal effects can be generally written as

$$\delta_{\text{earth-tide}} = s_1 h_2 + s_2 l_2 + s_3 h_3 \ , \tag{6.35}$$

where s_1, s_2 and s_3 are the coefficient functions, which are given in Sect. 5.4.2 in detail, and h_2, h_3 and l_2 are the love numbers and Shida number, respectively. Then one has

$$\frac{\partial \delta_{\text{earth-tide}}}{\partial (h_2, l_2, h_3)} = \begin{pmatrix} s_1 & s_2 & s_3 \end{pmatrix} . \tag{6.36}$$

Ocean loading tide effects can be modelled as

$$\delta_{\text{loading-tide}} = f_{\text{load}} \begin{pmatrix} \mathrm{d}x_{\text{load}} & \mathrm{d}y_{\text{load}} & \mathrm{d}z_{\text{load}} \end{pmatrix} , \tag{6.37}$$

where f_{load} is the factor of the computed ocean loading effect vector $(\mathrm{d}x_{\text{load}} \ \ \mathrm{d}y_{\text{load}} \ \ \mathrm{d}z_{\text{load}})$. Then one has

$$\frac{\partial \delta_{\text{loading-tide}}}{\partial f_{\text{load}}} = \begin{pmatrix} \mathrm{d}x_{\text{load}} & \mathrm{d}y_{\text{load}} & \mathrm{d}z_{\text{load}} \end{pmatrix} . \tag{6.38}$$

6.4 Linear Transformation and Covariance Propagation

For any linear equation system

$$L = AX \quad \text{or} \tag{6.39}$$

$$\begin{pmatrix} l_1 \\ l_2 \\ \vdots \\ l_m \end{pmatrix} = \begin{pmatrix} a_{11} & a_{12} & \cdots & a_{1n} \\ a_{21} & a_{22} & \cdots & a_{2n} \\ \vdots & \vdots & \vdots & \vdots \\ a_{m1} & a_{m2} & \cdots & a_{mn} \end{pmatrix} \begin{pmatrix} x_1 \\ x_2 \\ \vdots \\ x_n \end{pmatrix} ,$$

a linear transformation can be defined as a multiplying operation of matrix T to Eq. 6.39, i.e.,

$$TL = TAX \quad \text{or} \tag{6.40}$$

$$\begin{pmatrix} t_{11} & t_{12} & \cdots & t_{1m} \\ t_{21} & t_{22} & \cdots & t_{2m} \\ \vdots & \vdots & \vdots & \vdots \\ t_{k1} & t_{k2} & \cdots & t_{km} \end{pmatrix} \begin{pmatrix} l_1 \\ l_2 \\ \vdots \\ l_m \end{pmatrix} = \begin{pmatrix} t_{11} & t_{12} & \cdots & t_{1m} \\ t_{21} & t_{22} & \cdots & t_{2m} \\ \vdots & \vdots & \vdots & \vdots \\ t_{k1} & t_{k2} & \cdots & t_{km} \end{pmatrix} \begin{pmatrix} a_{11} & a_{12} & \cdots & a_{1n} \\ a_{21} & a_{22} & \cdots & a_{2n} \\ \vdots & \vdots & \vdots & \vdots \\ a_{m1} & a_{m2} & \cdots & a_{mn} \end{pmatrix} \begin{pmatrix} x_1 \\ x_2 \\ \vdots \\ x_n \end{pmatrix} ,$$

(c) ketabton.com: The Digital Library

where T is called the linear transformation matrix and has a dimension of $k \times m$. An inverse transformation of T is denoted by T^{-1}. An invertible linear transformation does not change the property (and solutions) of the original linear equations. This may be verified by multiplying T^{-1} to Eq. 6.40. A non-invertible linear transformation is called a rank deficient (or not full rank) transformation.

The covariance matrix of L is denoted by cov(L) or Q_{LL} (cf. Sect. 6.2); then the covariance of the transformed L (i.e., TL) can be obtained by covariance propagation theorem by (cf., e.g., Koch 1988)

$$\mathrm{cov}(TL) = T\,\mathrm{cov}(L)T^T = TQ_{LL}T^T \quad , \tag{6.41}$$

where superscript T denotes the transpose of the transformation matrix.

If transformation matrix T is a vector (i.e., $k = 1$) and L is an inhomogeneous and independent observable vector (i.e., covariance matrix Q_{LL} is a diagonal matrix with elements of σ_j^2, where σ_j^2 is the variance (σ_j is called standard deviation) of the observable l_j), then Eqs. 6.40 and 6.41 can be written as

$$\begin{pmatrix} t_1 & t_2 & \dots & t_m \end{pmatrix} \begin{pmatrix} l_1 \\ l_2 \\ \vdots \\ l_m \end{pmatrix} = \begin{pmatrix} t_1 & t_2 & \dots & t_m \end{pmatrix} \begin{pmatrix} a_{11} & a_{12} & \dots & a_{1n} \\ a_{21} & a_{22} & \dots & a_{2n} \\ \vdots & \vdots & \vdots & \vdots \\ a_{m1} & a_{m2} & \dots & a_{mn} \end{pmatrix} \begin{pmatrix} x_1 \\ x_2 \\ \vdots \\ x_n \end{pmatrix} \quad \text{and}$$

$$\mathrm{cov}(TL) = \begin{pmatrix} t_1 & t_2 & \dots & t_m \end{pmatrix} \begin{pmatrix} \sigma_1^2 & 0 & \dots & 0 \\ 0 & \sigma_2^2 & \dots & 0 \\ \vdots & \vdots & \vdots & \vdots \\ 0 & 0 & \dots & \sigma_m^2 \end{pmatrix} \begin{pmatrix} t_1 \\ t_2 \\ \vdots \\ t_m \end{pmatrix} . \tag{6.42}$$

Denoting cov(TL) as σ_{TL}^2, one gets

$$\sigma_{TL}^2 = t_1^2\sigma_1^2 + t_2^2\sigma_2^2 + \ldots + t_m^2\sigma_m^2 = \sum_{j=1}^{m} t_j^2\sigma_j^2 \quad . \tag{6.43}$$

Equation 6.43 is called the error propagation theorem.

6.5 Data Combinations

Data combinations are methods of combining GPS data measured with the same receiver at the same station. Usually, observables are the code pseudoranges, carrier phases and Doppler at working frequencies such as C/A code, P_1 and P_2 code, L1 phase Φ_1 and L2 phase Φ_2, and Doppler D_1 and D_2. In the future, there will also be P_5 code, L5 phase Φ_5 and Doppler D_5. According to the observation equations of the observables, a suitable combination can be advantageous for understanding and solving GPS problems.

(c) ketabton.com: The Digital Library

For convenience, code, phase and Doppler observables are simplified and rewritten as (cf. Eqs. 6.1–6.3)

$$R_j = \rho - (\delta t_r - \delta t_k)c + \delta_{ion}(j) + \delta_{trop} + \delta_{tide} + \delta_{rel} + \varepsilon_c \,, \tag{6.44}$$

$$\lambda_j \Phi_j = \rho - (\delta t_r - \delta t_k)c + \lambda_j N_j - \delta_{ion}(j) + \delta_{trop} + \delta_{tide} + \delta_{rel} + \varepsilon_p \,, \tag{6.45}$$

$$D_j = \frac{d\rho}{\lambda_j dt} - f_j \frac{d(\delta t_r - \delta t_k)}{dt} + \varepsilon_d \quad \text{and} \tag{6.46}$$

$$\delta_{ion}(j) = \frac{A_1}{f_j^2} + \frac{A_2}{f_j^3} \,. \tag{6.47}$$

Where j is the index of frequency f, the means of the other symbols are the same as the notes of Eqs. 6.1–6.3. Equation 6.47 is an approximation for code.

A general code-code combination can be formed by $n_1R_1 + n_2R_2 + n_5R_5$, where n_1, n_2 and n_5 are arbitrary constants. However, in order to make such a combination that still has the sense of a code survey, a standardised combination has to be formed by

$$R = \frac{n_1R_1 + n_2R_2 + n_5R_5}{n_1 + n_2 + n_5} \,. \tag{6.48}$$

The newly-formed code R can then be interpreted as a weight-averaged code survey of R_1, R_2 and R_5. The mathematical model of the observable Eq. 6.44 is generally still valid for R. Denoting the standard deviation of code observable R_i as σ_{ci} (i = 1, 2, 5), the newly-formed code observation R has the standard deviation of

$$\sigma_c^2 = \frac{1}{(n_1 + n_2 + n_5)^2}(n_1^2\sigma_{c1}^2 + n_2^2\sigma_{c2}^2 + n_5^2\sigma_{c5}^2) \,.$$

Because of

$$\left|\frac{n_1 + n_2 + \ldots + n_m}{m}\right| \le \sqrt{\frac{n_1^2 + n_2^2 + \ldots + n_m^2}{m}} \,,$$

(cf., e.g., Wang et al. 1979; Bronstein and Semendjajew 1987), one has the property of

$$(n_1 + n_2 + \ldots + n_m)^2 \le m(n_1^2 + n_2^2 + \ldots + n_m^2) \,,$$

where m is the maximum index. Therefore in our case, one has

$$\sigma_c^2 \ge m \cdot \min\left\{\sigma_{c1}^2, \sigma_{c2}^2, \sigma_{c5}^2\right\} \,, \quad m = 2 \text{ or } 3$$

for combinations of two or three code observables.

A general phase-phase linear combination can be formed by

$$\Phi = n_1\Phi_1 + n_2\Phi_2 + n_5\Phi_5 \,, \tag{6.49}$$

(c) ketabton.com: The Digital Library

where the combined signal has the frequency and wavelength

$$f = n_1 f_1 + n_2 f_2 + n_5 f_5 \quad \text{and} \quad \lambda = \frac{c}{f}\,. \tag{6.50}$$

$\lambda\Phi$ means the measured distance (with ambiguity!) and can be presented alternatively as

$$\lambda\Phi = \frac{1}{f^2}\left(n_1 f_1 \lambda_1 \Phi_1 + n_2 f_2 \lambda_2 \Phi_2 + n_5 f_5 \lambda_5 \Phi_5\right). \tag{6.51}$$

Mathematical model of Eq. 6.45 is generally still valid for the newly-formed $\lambda\Phi$. Denoting the standard deviation of phase observable $\lambda_i \Phi_i$ as σ_i (i = 1, 2, 5), the newly-formed observation has a variance of

$$\sigma^2 = \frac{1}{f^2}(n_1^2 f_1^2 \sigma_1^2 + n_2^2 f_2^2 \sigma_2^2 + n_5^2 f_5^2 \sigma_5^2) \quad \text{and} \tag{6.52}$$

$$\sigma^2 \geq m \cdot \min\left\{\sigma_1^2, \sigma_2^2, \sigma_5^2\right\},$$

with m = 2 or 3 for combinations of two or three phases.

That is, the data combination will degrade the quality of the original data.

Linear combinations $\Phi_W = \Phi_1 - \Phi_2$ and $\Phi_X = 2\Phi_1 - \Phi_2$ are called wide-lane and x-lane combinations with wavelengths of about 86.2 cm and 15.5 cm. They reduce the first order ionospheric effects on frequency f_2 to 40% and 20%, respectively. $\Phi_N = \Phi_1 + \Phi_2$ is called a narrow-lane combination.

6.5.1 Ionosphere-Free Combinations

Due to Eqs. 6.44–6.47, phase-phase and code-code ionosphere-free combinations can be formed by (cf. Sect. 5.1)

$$\lambda\Phi = \frac{f_1^2 \lambda_1 \Phi_1 - f_2^2 \lambda_2 \Phi_2}{f_1^2 - f_2^2} = \lambda(f_1 \Phi_1 - f_2 \Phi_2) \quad \text{and} \tag{6.53}$$

$$R = \frac{f_1^2 R_1 - f_2^2 R_2}{f_1^2 - f_2^2}\,. \tag{6.54}$$

The related observation equations can be formed from Eqs. 6.44 and 6.45 as

$$R = \rho - (\delta t_r - \delta t_k)c + \delta_{trop} + \delta_{tide} + \delta_{rel} + \varepsilon_{cc} \quad \text{and} \tag{6.55}$$

$$\lambda\Phi = \rho - (\delta t_r - \delta t_k)c + \lambda N + \delta_{trop} + \delta_{tide} + \delta_{rel} + \varepsilon_{pc}\,, \tag{6.56}$$

where

$$N = f_1 N_1 - f_2 N_2\,, \quad \lambda = \frac{c}{f_1^2 - f_2^2}\,, \tag{6.57}$$

ε_{cc} and ε_{pc} denote the residuals after the combination of code and phase, respectively.

(c) ketabton.com: The Digital Library

The advantages of such ionosphere-free combinations are that the ionospheric effects have disappeared from the observation Eqs. 6.55 and 6.56 and the other terms of the equations have remained the same. However, the combined ambiguity is not an integer anymore, and the combined observables have higher standard deviations. Equations 6.55 and 6.56 are indeed first order ionosphere-free combinations.

Second order ionosphere-free combinations can be formed by (see Sect. 5.1.2 for details)

$$\lambda\Phi = C_1\lambda_1\Phi_1 + C_2\lambda_2\Phi_2 + C_5\lambda_5\Phi_5 \quad \text{and} \tag{6.58}$$

$$R = C_1R_1 + C_2R_2 + C_5R_5\,, \tag{6.59}$$

where

$$C_1 = \frac{f_1^3(f_5 - f_2)}{C_4}, \quad C_2 = \frac{-f_2^3(f_5 - f_1)}{C_4}\,,$$

$$C_5 = \frac{f_5^3(f_2 - f_1)}{C_4}, \quad C_4 = f_1^3(f_5 - f_2) - f_2^3(f_5 - f_1) + f_5^3(f_2 - f_1)\,,$$

$$\lambda = \frac{c}{C_4}, \quad N = C_4(C_1N_1 + C_2N_2 + C_5N_5)\,.$$

The related observation equations are the same as Eqs. 6.55 and 6.56, with λ and N given above.

6.5.2 Geometry-Free Combinations

Due to Eqs. 6.44–6.46, code-code, phase-phase and phase-code geometry-free combinations can be formed by

$$R_1 - R_2 = \delta_{\text{ion}}(1) - \delta_{\text{ion}}(2) + \Delta\varepsilon_{\text{c}} = \frac{A_1}{f_1^2} - \frac{A_1}{f_2^2} + \Delta\varepsilon_{\text{c}}\,, \tag{6.60}$$

$$\lambda_1\Phi_1 - \lambda_2\Phi_2 = \lambda_1N_1 - \lambda_2N_2 - \frac{A_1}{f_1^2} + \frac{A_1}{f_2^2} + \Delta\varepsilon_{\text{p}}\,, \tag{6.61}$$

$$\lambda_1D_1 - \lambda_2D_2 = \Delta\varepsilon_{\text{d}}\,, \tag{6.62}$$

$$\lambda_j\Phi_j - R_j = \lambda_jN_j - 2\delta_{\text{ion}}(j) + \Delta\varepsilon_{\text{pc}} \quad \text{and} \quad j{=}1,2,5\,, \tag{6.63}$$

where

$$\Delta\delta_{\text{ion}} = \delta_{\text{ion}}(1) - \delta_{\text{ion}}(2) = \frac{A_1}{f_1^2} - \frac{A_1}{f_2^2}\,. \tag{6.64}$$

(c) ketabton.com: The Digital Library

For an ionospheric model of the second order, one has approximately

$$\Delta\delta_{\text{ion}} = \delta_{\text{ion}}(1) - \delta_{\text{ion}}(2) = \frac{A_1}{f_1^2} - \frac{A_1}{f_2^2} + \frac{A_2}{f_1^3} - \frac{A_2}{f_2^3} \ .$$

The geometry-free code-code and phase-phase combinations cancel out all other terms in the observation equations except the ionospheric term and the ambiguity parameters. Recalling the discussions of Sect. 5.1, δ_{ion} is the ionospheric path delay and can be considered a mapping of the zenith delay δ_{ion}^z or $\delta_{\text{ion}} = \delta_{\text{ion}}^z F$, where F is the mapping function (cf. Sect. 5.1). So one has

$$\delta_{\text{ion}}(1) = \frac{A_1^z}{f_1^2} F = \frac{A_1}{f_1^2} \ , \tag{6.65}$$

where A_1 and A_1^z have the physical meaning of total electronic contents at the signal path direction and the zenith direction, respectively. A_1^z is then independent from the zenith angle of the satellite. If the variability of the electronic contents at the zenith direction is stable enough, A_1^z can be modelled by a step function or a first order polynomial with a reasonably short time interval Δt by

$$A_1^z = g_j \quad \text{if} \quad t_{j-1} < t \le t_j \ , \quad j = 1, 2, \ldots, n+1 \tag{6.66}$$

or

$$A_1^z = g_{j-1} + (g_j - g_{j-1}) \frac{t - t_{j-1}}{\Delta t} \quad \text{if} \quad t_{j-1} < t \le t_j , \quad j = 1, 2, \ldots, n+1 \ , \tag{6.67}$$

where $\Delta t = (t_n - t_0) / n$, and t_0 and t_n are the beginning and ending time of the GPS survey. Δt can be, e.g., selected by 30 minutes. g_j is the coefficient of the polynomial.

Geometry-free combinations of Eqs. 6.60, 6.61 and 6.63 (only for $j = 1$) can be considered a linear transformation of the original observable vector $L = (R_1 \ \ R_2 \ \ \lambda_1\Phi_1 \ \ \lambda_2\Phi_2)^T$ by

$$\begin{pmatrix} 1 & -1 & 0 & 0 \\ 0 & 0 & 1 & -1 \\ -1 & 0 & 1 & 0 \end{pmatrix} \cdot \begin{pmatrix} R_1 \\ R_2 \\ \lambda_1\Phi_1 \\ \lambda_2\Phi_2 \end{pmatrix} = \begin{pmatrix} 0 & 0 & g \\ \lambda_1 & -\lambda_2 & -g \\ \lambda_1 & 0 & d \end{pmatrix} \cdot \begin{pmatrix} N_1 \\ N_2 \\ A_1 \end{pmatrix} + \begin{pmatrix} \Delta\varepsilon_{\text{c}} \\ \Delta\varepsilon_{\text{p}} \\ \Delta\varepsilon_{\text{pc}} \end{pmatrix}, \tag{6.68}$$

where Eq. 6.65 is used and

$$g = \left(\frac{1}{f_1^2} - \frac{1}{f_2^2} \right), \quad d = -\frac{2}{f_1^2} \quad \text{and} \quad T = \begin{pmatrix} 1 & -1 & 0 & 0 \\ 0 & 0 & 1 & -1 \\ -1 & 0 & 1 & 0 \end{pmatrix}.$$

(c) ketabton.com: The Digital Library

Equation 6.68 is called an ambiguity-ionospheric equation. For any viewed GPS satellite, Eq. 6.68 is solvable. If the variance vector of the observable vector is

$$\left(\sigma_c^2 \quad \sigma_c^2 \quad \sigma_p^2 \quad \sigma_p^2\right)^T ,$$

then the covariance matrix of the original observable vector is (cf. Sect. 6.2)

$$Q_{LL} = \begin{pmatrix} \sigma_c^2 & 0 & 0 & 0 \\ 0 & \sigma_c^2 & 0 & 0 \\ 0 & 0 & \sigma_p^2 & 0 \\ 0 & 0 & 0 & \sigma_p^2 \end{pmatrix},$$

and the covariance matrix of the transformed observable vector (left side of Eq. 6.68) is (cf. Sect. 6.4)

$$\operatorname{cov}(TL) = TQ_{LL}T^T = \begin{pmatrix} 2\sigma_c^2 & 0 & -\sigma_c^2 \\ 0 & 2\sigma_p^2 & \sigma_p^2 \\ -\sigma_c^2 & \sigma_p^2 & \sigma_c^2+\sigma_p^2 \end{pmatrix},$$

$$P = (\operatorname{cov}(TL))^{-1} = \frac{1}{2}\begin{pmatrix} h+\sigma_c^{-2} & -h & 2h \\ -h & h+\sigma_p^{-2} & -2h \\ 2h & -2h & 4h \end{pmatrix}, \quad h = \frac{1}{\sigma_c^2+\sigma_p^2} . \tag{6.69}$$

Taking all the data measured at a station into account, the ambiguity and the ionospheric parameters (as a step function of the polynomial) can be solved by using Eq. 6.68 with the weight of Eq. 6.69. Taking the data station by station into account, all ambiguity and ionospheric parameters can be determined. The different weights of the code and phase measurements are considered exactly here. Due to the physical property of the ionosphere, all solved ionospheric parameters shall have the same sign. Even though the observation Eq. 6.68 is already a linear equation system, an initialisation is still helpful to avoid numbers from ambiguities that are too big. The broadcasting ionospheric model can be used for initialisation of the related ionospheric parameters.

A geometry-free combination of Eq. 6.62 can be used as a quality check of the Doppler data.

6.5.3 Standard Phase-Code Combination

Traditionally, phase and code combinations are used to compute the wide-lane ambiguity (cf. Sjoeberg 1999; Hofmann-Wellenhof et al. 1997). The formulas can be derived as follows. Dividing λ_j into Eq. 6.63 and forming the difference for $j = 1$ and $j = 2$, one gets

$$\Phi_w - \frac{R_1}{\lambda_1} + \frac{R_2}{\lambda_2} = N_w - \frac{2A_1}{c}\left(\frac{1}{f_1} - \frac{1}{f_2}\right), \tag{6.70}$$

(c) ketabton.com: The Digital Library

where $\Phi_W = \Phi_1 - \Phi_2$, $N_W = N_1 - N_2$, and they are called wide-lane observable and ambiguity; c is the velocity of light and A_1 is the ionospheric parameter. The error term is omitted here. Equation 6.60 can be rewritten as (by omitting the error term)

$$A_1 = (R_1 - R_2)\frac{f_1^2 f_2^2}{f_2^2 - f_1^2} \ , \tag{6.71}$$

and then one gets

$$\frac{A_1}{c}\left(\frac{1}{f_1} - \frac{1}{f_2}\right) = \left(\frac{R_1}{\lambda_1 f_1} - \frac{R_2}{\lambda_2 f_2}\right)\frac{f_1 f_2}{f_2 + f_1} = \frac{R_1}{\lambda_1}\frac{f_2}{(f_1 + f_2)} - \frac{R_2}{\lambda_2}\frac{f_1}{(f_1 + f_2)} \ . \tag{6.72}$$

Substituting Eq. 6.72 into 6.70 yields

$$N_w = \Phi_w - \frac{f_1 - f_2}{f_1 + f_2}\left(\frac{R_1}{\lambda_1} + \frac{R_2}{\lambda_2}\right) \ . \tag{6.73}$$

Equation 6.73 is the most popular formula for computing wide-lane ambiguities using phase and code observables. The un-differenced ambiguity N_1 can be derived as follows. Setting $\Phi_2 = \Phi_1 - \Phi_W$, $N_2 = N_1 - N_W$ into Eq. 6.61 and omitting the error term, one has

$$\lambda_1 N_1 - \lambda_2(N_1 - N_w) = \frac{A_1}{f_1^2} - \frac{A_1}{f_2^2} + \lambda_1\Phi_1 - \lambda_2(\Phi_1 - \Phi_w) \ ,$$

$$N_1 = \Phi_1 - (\Phi_w - N_w)\frac{f_1}{f_w} + \frac{A_1}{c}\frac{f_1 + f_2}{f_1 f_2} \quad \text{or}$$

$$N_1 = \Phi_1 - (\Phi_w - N_w)\frac{f_1}{f_w} - \frac{R_1}{\lambda_1}\frac{f_2}{f_w} + \frac{R_2}{\lambda_2}\frac{f_1}{f_w} \ , \tag{6.74}$$

where $f_w = f_1 - f_2$ is the wide-lane frequency.

Compared with the adjustment method derived in Sect. 6.5.2, it is obvious that the quality differences of the phase and code data are not considered by using Eqs. 6.73 and 6.74 for determining the ambiguity parameters. Therefore, the method proposed in Sect. 6.5.2 is suggested for use.

6.5.4 Ionospheric Residuals

Considering the GPS observables as a time series, the geometry-free combinations of Eqs. 6.60–6.64 can be rewritten as

$$R_1(t_j) - R_2(t_j) = \Delta\delta_{ion}(t_j) + \Delta\varepsilon_c \ , \tag{6.75}$$

$$\lambda_1\Phi_1(t_j) - \lambda_2\Phi_2(t_j) = \lambda_1 N_1 - \lambda_2 N_2 - \Delta\delta_{ion}(t_j) + \Delta\varepsilon_p \ \text{and} \tag{6.76}$$

$$\lambda_i\Phi_i(t_j) - R_i(t_j) = \lambda_i N_i - 2\delta_{ion}(i, t_j) + \Delta\varepsilon_{pc} \ , \quad i = 1,2,5 \ , \tag{6.77}$$

(c) ketabton.com: The Digital Library

where

$$\Delta\delta_{\text{ion}}(t_j)=\delta_{\text{ion}}(1,t_j)-\delta_{\text{ion}}(2,t_j)=\frac{A_1(t_j)}{f_1^2}-\frac{A_1(t_j)}{f_2^2}\ ,\quad j=1,2,\ldots,m\ . \tag{6.78}$$

The differences of the above observable combinations at the two succeeded epochs t_j and t_{j-1} can be formed:

$$\Delta_t R_1(t_j)-\Delta_t R_2(t_j)=\Delta_t\Delta\delta_{\text{ion}}(t_j)+\Delta_t\Delta\varepsilon_{\text{c}}\ , \tag{6.79}$$

$$\lambda_1\Delta_t\Phi_1(t_j)-\lambda_2\Delta_t\Phi_2(t_j)=\lambda_1\Delta_t N_1-\lambda_2\Delta_t N_2-\Delta_t\Delta\delta_{\text{ion}}(t_j)+\Delta_t\Delta\varepsilon_{\text{p}}\ \text{ and} \tag{6.80}$$

$$\lambda_i\Delta_t\Phi_i(t_j)-\Delta_t R_i(t_j)=\lambda_i\Delta_t N_i-2\Delta_t\delta_{\text{ion}}(i,t_j)+\Delta_t\Delta\varepsilon_{\text{pc}}\ ,\quad i=1,2,5\ , \tag{6.81}$$

where Δ_t is a time difference operator, for any time function $G(t)$, $\Delta_t G(t_j) = G(t_j) - G(t_{j-1})$ is valid.

Because the time differences of the ionospheric effects $\Delta_t\delta_{\text{ion}}$ and $\Delta_t\Delta\delta_{\text{ion}}$ are generally very small, they are called ionospheric residuals. In the case of no cycle slips, i.e., ambiguities N_1 and N_2 are constant, ΔN_1 and ΔN_2 equal zero. Equations 6.79–6.81 are called ionospheric residual combinations. The first combination of Eq. 6.79 can be used for a consistency check of two code measurements. Equations 6.80 and 6.81 can be used for a cycle slip check. Equation 6.81 is a phase-code combination, due to the lower accuracy of the code measurements; it can be used only to check for big cycle slips. Equation 6.80 is a phase-phase combination, and therefore it has higher sensibility related to the cycle slips. However, two special cycle slips ΔN_1 and ΔN_2 can lead to a very small combination of $\delta_1\Delta_t N_1 - \delta_2\Delta_t N_2$. Examples of the combinations can be found, e.g., in (Hofmann-Wellenhof et al. 1997). That is, even the ionospheric residual of Eq. 6.80 is very small; it may not guarantee that there are no cycle slips.

6.5.5 Differential Doppler and Doppler Integration

Differential Doppler

The numerical differentiation of the original observables given in Eqs. 6.44 and 6.45 at the two succeeded epochs t_j and t_{j-1} can be formed as

$$\frac{\Delta_t R_j}{\lambda_j\Delta t}=\frac{\Delta_t\rho}{\lambda_j\Delta t}-f_j\frac{\Delta_t(\delta t_{\text{r}}-\delta t_{\text{k}})}{\Delta t}+\frac{\Delta_t\varepsilon_c}{\lambda_j\Delta t}\ ,\quad j=1,2\ ,\ \text{ and} \tag{6.82}$$

$$\frac{\Delta_t\Phi_j}{\Delta t}=\frac{\Delta_t\rho}{\lambda_j\Delta t}-f_j\frac{\Delta_t(\delta t_{\text{r}}-\delta t_{\text{k}})}{\Delta t}+\frac{\Delta_t\varepsilon_p}{\lambda_j\Delta t}\ ,\quad j=1,2\ , \tag{6.83}$$

where $\Delta_t/\Delta t$ is a numerical differentiation operator and $\Delta t = t_j - t_{j-1}$.

The left-hand side of Eq. 6.83 is called differential Doppler. Ionospheric residuals are negligible and omitted here. The third terms of Eqs. 6.82 and 6.83 on the right-hand side are small residual errors. For convenience of comparison, the Doppler observable model of Eq. 6.46 is copied below:

(c) ketabton.com: The Digital Library

$$D_j = \frac{\mathrm{d}\rho}{\lambda_j \mathrm{d}t} - f_j \frac{\mathrm{d}(\delta t_\mathrm{r} - \delta t_\mathrm{k})}{\mathrm{d}t} + \varepsilon_\mathrm{d} \,. \tag{6.84}$$

It is obvious that Eqs. 6.83 and 6.84 are nearly the same. The only difference is that in Doppler Eq. 6.84 the observed Doppler is an instantaneous one and its model is presented by theoretical differentiation, whereas the term on the left-hand side of Eq. 6.83 is the numerically differenced Doppler (formed by phases) and its model is presented by numerical differentiation. Doppler measurement measures the instantaneous motion of the GPS antenna, whereas differential Doppler describes a kind of average velocity of the antenna during the two succeeded epochs. The velocity solution of Eq. 6.83 (denoted by $(\dot{x}\ \ \dot{y}\ \ \dot{z})^T$) can be used to predict the future kinematic position by

$$\begin{pmatrix} x_{j+1} \\ y_{j+1} \\ z_{j+1} \end{pmatrix} = \begin{pmatrix} x_j \\ y_j \\ z_j \end{pmatrix} + \begin{pmatrix} \dot{x}_j \\ \dot{y}_j \\ \dot{z}_j \end{pmatrix} \cdot \Delta t \ . \tag{6.85}$$

In other words, differential Doppler can be used as the system equation of a Kalman filter for kinematic positioning. The Kalman filter will be discussed in the next chapter. A Kalman filter using differential Doppler will be discussed in Sect. 9.8.

Doppler Integration

Integrating the instantaneous Doppler Eq. 6.84, one has

$$\lambda_j \int_{t_{j-1}}^{t_j} D_j \mathrm{d}t = \Delta_t \rho - \Delta_t (\delta t_\mathrm{r} - \delta t_\mathrm{k}) c + \varepsilon_\mathrm{d} \,.$$

Using the operator Δ_t to the un-differenced phase Eq. 6.45 and code Eq. 6.44, one gets

$$\lambda_j \Delta_t \Phi_j = \Delta_t \rho - \Delta_t (\delta t_\mathrm{r} - \delta t_k) c + \lambda_j \Delta_t N_j + \varepsilon_\mathrm{p} \quad \text{and}$$

$$\Delta_t R_j = \Delta_t \rho - \Delta_t (\delta t_\mathrm{r} - \delta t_k) c + \varepsilon_\mathrm{c} \,, \tag{6.86}$$

where the same symbols are used for the error terms (later too). Differencing the first equation of Eq. 6.86 with the integrated Doppler leads to

$$\lambda_j \Delta_t N_j = \lambda_j \Delta_t \Phi_j - \lambda_j \int_{t_{j-1}}^{t_j} D_j \mathrm{d}t + \varepsilon_1$$

or

$$\Delta_t N_j = \Delta_t \Phi_j - \int_{t_{j-1}}^{t_j} D_j \mathrm{d}t + \varepsilon_1 \ , \quad j = 1,2,5 \,. \tag{6.87}$$

(c) ketabton.com: The Digital Library

That is, the integrated Doppler can be used for cycle slip detection. Such a cycle slip detection method is very reasonable. Phase is measured by keeping track of the partial phase and accumulating the integer count. If any loss of lock of the signal happens during the time, the integer accumulating will be wrong, i.e., cycle slip happens. Therefore, an external instantaneous Doppler integration can be used as an alternative method of cycle slip detection. The integration can be made first by fitting the Doppler with a suitable order polynomial, and then integrating that within the time interval.

Code Smoothing

Comparing the two formulas of Eq. 6.86, one has

$$\Delta_t R_j = \lambda_j \Delta_t \Phi_j - \lambda_j \Delta_t N_j + \varepsilon_2 \quad \text{or}$$

$$\Delta_t R_j = \lambda_j \Delta_t \Phi_j + \varepsilon_3 \ . \tag{6.88}$$

Equation 6.88 can be used for smoothing the code survey by phase if there are no cycle slips.

Differential Phases

The first formula of Eq. 6.86 is the numerical difference of the phases at the two succeeded epochs t_j and t_{j-1}

$$\lambda_j \Delta_t \Phi_j = \Delta_t \rho - \Delta_t (\delta t_{\mathrm{r}} - \delta t_k) c + \lambda_j \Delta_t N_j + \varepsilon_{\mathrm{p}}, \quad j = 1,2 \ .$$

All other terms on the right-hand side are of low variation ones except the ambiguity term. Any cycle slips will lead to a sudden jump of the time difference of the phases. Therefore, the time differenced phase can be used as an alternative method of cycle slip detection.

6.6 Data Differentiations

Data differentiations are methods of combining GPS data (of the same type) measured at different stations. For the convenience of later discussions, tidal effects and relativistic effects are considered corrected before forming the differences. The original code, phase and Doppler observables as well as their standardised combinations can be rewritten as (cf. Eqs. 6.44–6.47)

$$R_i^k(j) = \rho_i^k - c\delta t_i + c\delta t_k + \delta_{\mathrm{ion}}(j) + \delta_{\mathrm{trop}} + \varepsilon_{\mathrm{c}} \ , \tag{6.89}$$

$$\lambda_j \Phi_i^k(j) = \rho_i^k - c\delta t_i + c\delta t_k + \lambda_j N_i^k(j) - \delta_{\mathrm{ion}}(j) + \delta_{\mathrm{trop}} + \varepsilon_{\mathrm{p}} \ , \tag{6.90}$$

$$\delta_{\mathrm{ion}}(j) = \frac{A_1}{f_j^2} + \frac{A_2}{f_j^3} \quad \text{and} \tag{6.91}$$

(c) ketabton.com: The Digital Library

$$D_i^k(j) = \frac{\mathrm{d}\rho_i^k}{\lambda_j \mathrm{d}t} - f_j \frac{\mathrm{d}(\delta t_i - \delta t_k)}{\mathrm{d}t} + \varepsilon_\mathrm{d} \ , \tag{6.92}$$

where j ($j = 1, 2, 5$) is the index of frequency f, subscript i is the index of station number and superscript k is the id number of satellite.

6.6.1 Single Differences

Single difference (SD) is the difference formed by data observed at two stations on the same satellite as

$$\mathrm{SD}_{i1,i2}^k(O) = O_{i2}^k - O_{i1}^k \ , \tag{6.93}$$

where O is the original observable, and $i1$ and $i2$ are two id number of the stations. Supposing the original observables have the same variance of σ^2, then the single difference observable has a variance of $2\sigma^2$. Considering Eqs. 6.89–6.92, one has

$$\mathrm{SD}_{i1,i2}^k(R(j)) = \rho_{i2}^k - \rho_{i1}^k - c\delta t_{i2} + c\delta t_{i1} + \mathrm{d}\delta_\mathrm{ion}(j) + \mathrm{d}\delta_\mathrm{trop} + \mathrm{d}\varepsilon_\mathrm{c} \ , \tag{6.94}$$

$$\begin{aligned}\mathrm{SD}_{i1,i2}^k(\lambda_j \Phi(j)) = {} & \rho_{i2}^k - \rho_{i1}^k - c\delta t_{i2} + c\delta t_{i1} + \lambda_j N_{i2}^k(j) - \lambda_j N_{i1}^k(j) \\ & - \mathrm{d}\delta_\mathrm{ion}(j) + \mathrm{d}\delta_\mathrm{trop} + \mathrm{d}\varepsilon_\mathrm{p}\end{aligned} \quad \text{and} \tag{6.95}$$

$$\mathrm{SD}_{i1,i2}^k(D(j)) = \frac{\dot{\rho}_{i2}^k - \dot{\rho}_{i1}^k}{\lambda_j} - f_j \frac{\mathrm{d}(\delta t_{i2} - \delta t_{i1})}{\mathrm{d}t} + \mathrm{d}\varepsilon_\mathrm{d} \ , \tag{6.96}$$

where $\dot{\rho}$ is the time differentiation of ρ, and $\mathrm{d}\delta_\mathrm{ion}(j)$ and $\mathrm{d}\delta_\mathrm{trop}$ are the differenced ionospheric and tropospheric effects at the two stations related to the satellite k, respectively.

The most important property of single differences is that the satellite clock error terms in the model are eliminated. However, it should be emphasised that the satellite clock error, which implicitly affects the computation of satellite position, still has to be carefully considered. Ionospheric and tropospheric effects are reduced through difference forming, especially for those stations that are not very far away from each other. Because of the identical mathematical models of the station clock errors and ambiguities, not all clock and ambiguity parameters can be resolved in the single difference equations of Eqs. 6.94–6.96.

For the original observable vector of station $i1$ and $i2$,

$$O = \begin{pmatrix} O_{i1}^{k1} & O_{i1}^{k2} & O_{i1}^{k3} & O_{i2}^{k1} & O_{i2}^{k2} & O_{i2}^{k3} \end{pmatrix}^T \ , \quad \mathrm{cov}(O) = \sigma^2 E \ ,$$

the single differences

$$\mathrm{SD}(O) = \begin{pmatrix} O_{i1,i2}^{k1} & O_{i1,i2}^{k2} & O_{i1,i2}^{k3} \end{pmatrix}^T \ ,$$

can be formed by a linear transformation

(c) ketabton.com: The Digital Library

$$\mathrm{SD}(O) = C \cdot O \quad \text{and}$$

$$C = \begin{pmatrix} -1 & 0 & 0 & 1 & 0 & 0 \\ 0 & -1 & 0 & 0 & 1 & 0 \\ 0 & 0 & -1 & 0 & 0 & 1 \end{pmatrix} = \begin{pmatrix} -E & E \end{pmatrix} . \tag{6.97}$$

Where common satellites $k1$, $k2$, $k3$ are observed, E is an identity matrix that has the size of the observed satellite number; in the above example the size is 3×3.

The covariance matrix of the single differences is then

$$\mathrm{cov}(\mathrm{SD}(O)) = C \cdot \mathrm{cov}(O) \cdot C^T = \sigma^2 C \cdot C^T = 2\sigma^2 E \ , \tag{6.98}$$

i.e., the weight matrix is

$$P = \frac{1}{2\sigma^2} E \ .$$

That is, the single differences are un-correlated observables in the case of a single baseline. C in Eq. 6.97 is a general form, so C is denoted by $C_s = (-E_{n\times n} \quad E_{n\times n})$, and n is the number of commonly viewed satellites.

Single differences can be formed for any baselines as long as the two stations have common satellites in sight. However, the baselines should be a set of "independent" ones. The most-used methods are to form the radial baselines or traverse baselines. Supposing the stations' id vector is ($i1$, $i2$, $i3$, …, $i(m-1)$, im) and the baseline between station $i1$ and $i2$ is denoted by ($i1$, $i2$), then the radial baselines could be formed, e.g., by ($i1$, $i2$), ($i1$, $i3$), …, ($i1$, im), and the traverse baselines could be formed, e.g., by ($i1$, $i2$), ($i2$, $i3$), …, ($i(m-1)$, im). Station $i1$ is called a reference station and is freely selectable. In some cases, a mixed radial and traverse baselines have to be formed such as, e.g., by ($i1$, $i2$), ($i1$, $i3$), ($i3$, $i4$), …, ($i3$, $i(m-1)$), ($i3$, im). Sometimes the baselines have to be formed by several groups, and therefore several references have to be selected. A method of forming an independent and optimal baseline network will be discussed Sects. 9.1 and 9.2.

In case three stations are used to measure the GPS data, the original observable vector of station $i1$, $i2$ and $i3$ is

$$O_i = \begin{pmatrix} O_i^{k1} & \cdots & O_i^{kn} \end{pmatrix}^T , \quad \mathrm{cov}(O_i) = \sigma^2 E_{n\times n} \ , \quad i = i1, i2, i3 \ ,$$

where n is the commonly observed satellite number. The single differences of the baseline (i, j) are

$$\mathrm{SD}_{i,j}(O) = \begin{pmatrix} O_{i,j}^{k1} & \cdots & O_{i,j}^{kn} \end{pmatrix}^T , \quad i,j = i1, i2, i3, \quad i \neq j \ .$$

If the baselines are formed in a radial way, i.e., baselines are formed as ($i1$, $i2$) and ($i1$, $i3$), then one has

$$\begin{pmatrix} \mathrm{SD}_{i1,i2}(O) \\ \mathrm{SD}_{i1,i3}(O) \end{pmatrix} = \begin{pmatrix} -E & E & 0 \\ -E & 0 & E \end{pmatrix} \begin{pmatrix} O_{i1} \\ O_{i2} \\ O_{i3} \end{pmatrix}$$

(c) ketabton.com: The Digital Library

$$\mathrm{cov(SD)} = \sigma^2 \begin{pmatrix} -E & E & 0 \\ -E & 0 & E \end{pmatrix} \begin{pmatrix} -E & -E \\ E & 0 \\ 0 & E \end{pmatrix} = \sigma^2 \begin{pmatrix} 2E & E \\ E & 2E \end{pmatrix} \quad \text{and} \tag{6.99}$$

$$P_s = [\mathrm{cov(SD)}]^{-1} = \frac{1}{3\sigma^2} \begin{pmatrix} 2E & -E \\ -E & 2E \end{pmatrix} .$$

If the baselines are formed in a traverse way, i.e., baselines are formed as ($i1$, $i2$) and ($i2$, $i3$), then one has

$$\begin{pmatrix} \mathrm{SD}_{i1,i2}(O) \\ \mathrm{SD}_{i2,i3}(O) \end{pmatrix} = \begin{pmatrix} -E & E & 0 \\ 0 & -E & E \end{pmatrix} \begin{pmatrix} O_{i1} \\ O_{i2} \\ O_{i3} \end{pmatrix} ,$$

$$\mathrm{cov(SD)} = \sigma^2 \begin{pmatrix} -E & E & 0 \\ 0 & -E & E \end{pmatrix} \begin{pmatrix} -E & 0 \\ E & -E \\ 0 & E \end{pmatrix} = \sigma^2 \begin{pmatrix} 2E & -E \\ -E & 2E \end{pmatrix} \quad \text{and}$$

$$P_s = [\mathrm{cov(SD)}]^{-1} = \frac{1}{3\sigma^2} \begin{pmatrix} 2E & E \\ E & 2E \end{pmatrix} .$$

It is obvious that the single differences are correlated if the station numbers are more than two. And the correlation depends on the ways the baselines are formed. Therefore, a general covariance formula of the single differences of a network is not possible to be derived. Furthermore, the commonly viewed satellite number n could be different from baseline to baseline, so the formulation of the covariance matrix could be more complicated.

A baseline-wise processing of the GPS data of a network by using single differences is equivalent to an omission of the correlation between the baselines.

6.6.2 Double Differences

Double differences are formed between two single differences related to two observed satellites as

$$\mathrm{DD}_{i1,i2}^{k1,k2}(O) = \mathrm{SD}_{i1,i2}^{k2}(O) - \mathrm{SD}_{i1,i2}^{k1}(O) \tag{6.100}$$

or

$$\mathrm{DD}_{i1,i2}^{k1,k2}(O) = (O_{i2}^{k2} - O_{i1}^{k2}) - (O_{i2}^{k1} - O_{i1}^{k1}) , \tag{6.101}$$

where $k1$ and $k2$ are the two id numbers of the satellites. Supposing the original observables have the same variance of σ^2, then the double differenced observables have a variance of $4\sigma^2$. Considering Eqs. 6.89–6.92, one has

(c) ketabton.com: The Digital Library

$$\mathrm{DD}_{i1,i2}^{k1,k2}(R(j)) = \rho_{i2}^{k2} - \rho_{i1}^{k2} - \rho_{i2}^{k1} + \rho_{i1}^{k1} + \mathrm{dd}\delta_{\mathrm{ion}}(j) + \mathrm{dd}\delta_{\mathrm{trop}} + \mathrm{dd}\varepsilon_{\mathrm{c}} \ , \tag{6.102}$$

$$\begin{aligned}\mathrm{DD}_{i1,i2}^{k1,k2}(\lambda_j \Phi(j)) = {} & \rho_{i2}^{k2} - \rho_{i1}^{k2} - \rho_{i2}^{k1} + \rho_{i1}^{k1} + \lambda_j (N_{i2}^{k2}(j) - N_{i1}^{k2}(j) \\ & - N_{i2}^{k1}(j) + N_{i1}^{k1}(j)) - \mathrm{dd}\delta_{\mathrm{ion}}(j) + \mathrm{dd}\delta_{\mathrm{trop}} + \mathrm{dd}\varepsilon_{\mathrm{p}}\end{aligned} \quad \text{and} \tag{6.103}$$

$$\mathrm{DD}_{i1,i2}^{k1,k2}(D(j)) = \frac{\dot{\rho}_{i2}^{k2} - \dot{\rho}_{i1}^{k2} - \dot{\rho}_{i2}^{k1} + \dot{\rho}_{i1}^{k1}}{\lambda_j} + \mathrm{dd}\varepsilon_{\mathrm{d}} \ , \tag{6.104}$$

where $\mathrm{dd}\delta_{\mathrm{ion}}(j)$ and $\mathrm{dd}\delta_{\mathrm{trop}}$ are the differenced ionospheric and tropospheric effects at the two stations related to the two satellites, respectively. For the ionosphere-free combined observables (denoted by $j = 4$ for distinguishing), the ionospheric error terms have vanished from above equations.

The most important property of the double differences is that the clock error terms in the equation (model) are completely eliminated. It should be emphasised that the clock error, which implicitly affects the computation of the position of the satellite, still has to be carefully considered. Ionospheric and tropospheric effects are reduced greatly through difference forming, especially for those stations that are not very far away from each other. Double differenced Doppler directly describes the geometry change. Double differenced ambiguities can be denoted by

$$N_{i1,i2}^{k1,k2}(j) = N_{i2}^{k2}(j) - N_{i1}^{k2}(j) - N_{i2}^{k1}(j) + N_{i1}^{k1}(j) \ . \tag{6.105}$$

The original ambiguities used in Eq. 6.103 are for convenience in case of reference satellite changing.

For the single difference observable vector

$$\mathrm{SD}(O) = \left(O_{i1,i2}^{k1} \quad O_{i1,i2}^{k2} \quad O_{i1,i2}^{k3}\right)^T \quad \text{and} \quad \mathrm{cov}(\mathrm{SD}(O)) = 2\sigma^2 E \ , \tag{6.106}$$

the double differences

$$\mathrm{DD}(O) = \left(O_{i1,i2}^{k1,k2} \quad O_{i1,i2}^{k1,k3}\right)^T \tag{6.107}$$

can be formed by a linear transformation

$$\mathrm{DD}(O) = C_{\mathrm{d}} \cdot \mathrm{SD}(O) \ , \tag{6.108}$$

$$C_{\mathrm{d}} = \begin{pmatrix} -1 & 1 & 0 \\ -1 & 0 & 1 \end{pmatrix} = \left(-I_m \quad E_{m \times m}\right) \ \ (\text{here } m = 2) \ , \tag{6.109}$$

where E is an identity matrix of size $m \times m$, I is a 1 vector of size m (all elements of the vector are 1), m is the number of formed double differences, and $m = n - 1$. The covariance matrix of the double differences is then

$$\mathrm{cov}(\mathrm{DD}(O)) = C_{\mathrm{d}} \cdot \mathrm{cov}(\mathrm{SD}(O)) \cdot C_{\mathrm{d}}^T = 2\sigma^2 C_{\mathrm{d}} \cdot C_{\mathrm{d}}^T = 2\sigma^2 \begin{pmatrix} 2 & 1 \\ 1 & 2 \end{pmatrix} . \tag{6.110}$$

(c) ketabton.com: The Digital Library

For single and double differences

$$\mathrm{SD}(O)=\left(O_{i1,i2}^{k1} \quad O_{i1,i2}^{k2} \quad O_{i1,i2}^{k3} \quad O_{i1,i2}^{k4}\right)^T, \quad \mathrm{cov}(\mathrm{SD}(O))=2\sigma^2 E \quad \text{and} \tag{6.111}$$

$$\mathrm{DD}(O)=\left(O_{i1,i2}^{k1,k2} \quad O_{i1,i2}^{k1,k3} \quad O_{i1,i2}^{k1,k4}\right)^T, \tag{6.112}$$

the linear transformation matrix C_d and the covariance matrix can be obtained by

$$C_\mathrm{d}=\begin{pmatrix}-1 & 1 & 0 & 0\\ -1 & 0 & 1 & 0\\ -1 & 0 & 0 & 1\end{pmatrix}=\begin{pmatrix}-I & E\end{pmatrix} \quad \text{and} \tag{6.113}$$

$$\mathrm{cov}(\mathrm{DD}(O))=C_\mathrm{d}\cdot\mathrm{cov}(\mathrm{SD}(O))\cdot C_\mathrm{d}^T=2\sigma^2 C_\mathrm{d}\cdot C_\mathrm{d}^T=2\sigma^2\begin{pmatrix}2 & 1 & 1\\ 1 & 2 & 1\\ 1 & 1 & 2\end{pmatrix}. \tag{6.114}$$

For the general case of

$$\mathrm{SD}(O)=\left(O_{i1,i2}^{k1} \quad O_{i1,i2}^{k2} \quad O_{i1,i2}^{k3} \quad \ldots \quad O_{i1,i2}^{kn}\right)^T, \quad \mathrm{cov}(\mathrm{SD}(O))=2\sigma^2 E, \text{ and}$$

$$\mathrm{DD}(O)=\left(O_{i1,i2}^{k1,k2} \quad O_{i1,i2}^{k1,k3} \quad \ldots \quad O_{i1,i2}^{k1,km}\right)^T, \tag{6.115}$$

it is obvious that the general transformation matrix C_d and the related covariance matrix can be represented as

$$C_\mathrm{d}=\left(-I_m \quad E_{m\times m}\right) \quad \text{and} \tag{6.116}$$

$$\mathrm{cov}(\mathrm{DD}(O))=C_\mathrm{d}\,\mathrm{cov}(\mathrm{SD}(O))C_\mathrm{d}^T=2\sigma^2 C_\mathrm{d}C_\mathrm{d}^T=2\sigma^2\left(I_{m\times m}+E_{m\times m}\right), \tag{6.117}$$

where $I_{\mathrm{m\times m}}$ is an $m\times m$ matrix whose elements are all 1, and the weight matrix has the form of

$$P=[\mathrm{cov}(\mathrm{DD}(O))]^{-1}=\frac{1}{2\sigma^2 n}\left(nE_{m\times m}-I_{m\times m}\right), \tag{6.118}$$

where $n = m + 1$. Equation 6.118 can be verified by an identity matrix test (i.e., $P\cdot\mathrm{cov}(\mathrm{DD}(O)) = E$).

In the case of three stations, supposing n common satellites ($k1, k2, \ldots, kn$) are viewed, then the single and double differences can be written as

$$\mathrm{SD}_{i,j}(O)=\left(O_{i,j}^{k1} \quad O_{i,j}^{k2} \quad O_{i,j}^{k3} \quad \ldots \quad O_{i,j}^{kn}\right)^T \quad \text{and}$$

$$\mathrm{DD}_{i,j}(O)=\left(O_{i,j}^{k1,k2} \quad O_{i,j}^{k1,k3} \quad \ldots \quad O_{i,j}^{k1,km}\right)^T \quad i,j=i1,i2,i3, \quad i\neq j. \tag{6.119}$$

(c) ketabton.com: The Digital Library

Then one has the transformation and covariance

$$\begin{pmatrix} \mathrm{DD}_{i1,i2}(O) \\ \mathrm{DD}_{i1,i3}(O) \end{pmatrix} = \begin{pmatrix} C_\mathrm{d} & 0 \\ 0 & C_\mathrm{d} \end{pmatrix} \begin{pmatrix} \mathrm{SD}_{i1,i2}(O) \\ \mathrm{SD}_{i1,i3}(O) \end{pmatrix} \quad \text{and}$$

$$\mathrm{cov}(\mathrm{DD}) = \begin{pmatrix} C_\mathrm{d} & 0 \\ 0 & C_\mathrm{d} \end{pmatrix} \mathrm{cov}(SD) \begin{pmatrix} C_\mathrm{d} & 0 \\ 0 & C_\mathrm{d} \end{pmatrix}^T = \sigma^2 \begin{pmatrix} 2E & -E \\ -E & 2E \end{pmatrix} (C_\mathrm{d} C_\mathrm{d}^T) .$$

Because of the dependency of the cov(SD) on the baselines forming, cov(DD) is also dependent on the baselines forming. A baseline-wise processing of a network GPS data using double differences is equivalent to an omission of the correlation between the baselines.

6.6.3 Triple Differences

Triple differences are formed between two double differences related to the same stations and satellites at the two adjacent epochs as

$$\mathrm{TD}_{i1,i2}^{k1,k2}(O(t1,t2)) = \mathrm{DD}_{i1,i2}^{k1,k2}(O(t2)) - \mathrm{DD}_{i1,i2}^{k1,k2}(O(t1))$$

or

$$\begin{aligned} \mathrm{TD}_{i1,i2}^{k1,k2}(O(t1,t2)) = {} & O_{i2}^{k2}(t2) - O_{i1}^{k2}(t2) - O_{i2}^{k1}(t2) + O_{i1}^{k1}(t2) \\ & - O_{i2}^{k2}(t1) + O_{i1}^{k2}(t1) + O_{i2}^{k1}(t1) - O_{i1}^{k1}(t1) \end{aligned} , \tag{6.120}$$

where $t1$ and $t2$ are two adjacent epochs. Supposing the original observables have the same variance of σ^2, then the triple differenced observables have a variance of $8\sigma^2$. Considering Eqs. 6.102–6.104, one has

$$\begin{aligned} \mathrm{TD}_{i1,i2}^{k1,k2}(R(j,t1,t2)) = {} & \rho_{i2}^{k2}(t2) - \rho_{i1}^{k2}(t2) - \rho_{i2}^{k1}(t2) + \rho_{i1}^{k1}(t2) - \rho_{i2}^{k2}(t1) \\ & + \rho_{i1}^{k2}(t1) + \rho_{i2}^{k1}(t1) - \rho_{i1}^{k1}(t1) + td\varepsilon_\mathrm{c} \end{aligned} , \tag{6.121}$$

$$\begin{aligned} \mathrm{TD}_{i1,i2}^{k1,k2}(\lambda_j \Phi(j,t1,t2)) = {} & \rho_{i2}^{k2}(t2) - \rho_{i1}^{k2}(t2) - \rho_{i2}^{k1}(t2) + \rho_{i1}^{k1}(t2) - \rho_{i2}^{k2}(t1) \\ & + \rho_{i1}^{k2}(t1) + \rho_{i2}^{k1}(t1) - \rho_{i1}^{k1}(t1) + \delta N + t\mathrm{d}\varepsilon_\mathrm{p} \end{aligned} \quad \text{and} \tag{6.122}$$

$$\begin{aligned} \mathrm{TD}_{i1,i2}^{k1,k2}(D(j,t1,t2)) = {} & \frac{\dot{\rho}_{i2}^{k2}(t2) - \dot{\rho}_{i1}^{k2}(t2) - \dot{\rho}_{i2}^{k1}(t2) + \dot{\rho}_{i1}^{k1}(t2)}{\lambda_j} \\ & - \frac{\dot{\rho}_{i2}^{k2}(t1) - \dot{\rho}_{i1}^{k2}(t1) - \dot{\rho}_{i2}^{k1}(t1) + \dot{\rho}_{i1}^{k1}(t1)}{\lambda_j} + t\mathrm{d}\varepsilon_\mathrm{d} \end{aligned} , \tag{6.123}$$

where

$$\delta N = \lambda_j (N_{i1,i2}^{k1,k2}(j,t2) - N_{i1,i2}^{k1,k2}(j,t1)) . \tag{6.124}$$

(c) ketabton.com: The Digital Library

Ionospheric and tropospheric effects are eliminated. If there are no cycle slips during the time, the term of Eq. 6.124 is zero. Therefore, triple differences of Eq. 6.122 can also be used as a check for the cycle slips. Through triple difference forming, the systematic cycle slip turns out to be an effect like an outlier.

The most important property of the triple differences is that only the geometric changing is left in the models. Triple differences of Doppler describe the acceleration of the position.

For double differences

$$\mathrm{DD}(O(t)) = \left(O_{i1,i2}^{k1,k2}(t) \quad O_{i1,i2}^{k1,k3}(t) \quad \ldots \quad O_{i1,i2}^{k1,km}(t)\right)^T , \tag{6.125}$$

one has

$$\mathrm{TD}(O(t1,t2)) = C_T \cdot \begin{pmatrix} \mathrm{DD}(O(t1)) \\ \mathrm{DD}(O(t2)) \end{pmatrix} , \tag{6.126}$$

where

$$C_T = \left(-E_{m\times m} \quad E_{m\times m}\right) . \tag{6.127}$$

Then the related covariance matrix can be represented as

$$\begin{aligned} \mathrm{cov}(\mathrm{TD}(O(t1,t2))) &= C_T \cdot \mathrm{cov}(\mathrm{DD}(O)) \cdot C_T^T \\ &= C_T \cdot C_{d2}\, \mathrm{cov}(\mathrm{SD}(O)) \cdot C_{\mathrm{d2}}^T C_T^T = 2\sigma^2 C_T C_{\mathrm{d2}} C_{\mathrm{d2}}^T C_T^T \end{aligned} , \tag{6.128}$$

where C_{d2} is the double difference transformation matrix of two epochs. Because double differences are independent epoch wise, C_{d2} is a diagonal matrix of C_{d}, i.e.,

$$C_{\mathrm{d2}} = \begin{pmatrix} C_{\mathrm{d}} & 0 \\ 0 & C_{\mathrm{d}} \end{pmatrix} . \tag{6.129}$$

It is notable that the triple differences formed by epochs ($t1$, $t2$) are correlated to the differences formed by epochs ($t0$, $t1$) and ($t1$, $t2$). Such a correlation makes a sequential processing of the triple difference data very complicated. Sequentially using the above covariance formula indicates an omission of the correlation related to the previous epoch and the next epoch.

Taking the correlation between the baselines into account, an exact correlation description of the triple differences of a GPS network turns out to be very complicated.

6.7 Equivalence of the Uncombined and Combining Algorithms

Uncombined and combining algorithms are standard GPS data processing methods, which can often be found in the literature (cf., e.g., Leick 2004, Hofmann-Wellenhof et al. 2001). Different combinations own different properties and are beneficial for dealing with the data and solving the problem in different cases (Hugentobler et al. 2001, Kouba and Heroux 2001, Zumberge et al. 1997). The equivalence between the undifferenced and differencing algorithms were proved, and a unified equivalent data pro-

(c) ketabton.com: The Digital Library

cessing method was proposed by Xu (2002, cf. Sect. 6.8). The question of whether the uncombined and combining algorithms are also equivalent is an interesting topic and will be addressed here in detail (cf. Xu et al. 2006a).

6.7.1 Uncombined GPS Data Processing Algorithms

Original GPS Observation Equations

The original GPS code pseudorange and carrier phase measurements represented in Eqs. 6.44 and 6.45 (cf. Sect. 6.5) can be simplified as

$$R_j = C_\rho + \delta_{\text{ion}}(j) \ , \tag{6.130}$$

$$\lambda_j \Phi_j = C_\rho + \lambda_j N_j - \delta_{\text{ion}}(j) \ , j = 1, 2 \tag{6.131}$$

where

$$C_\rho = \rho - (\delta t_{\text{r}} - \delta t_{\text{k}})\text{c} + \delta_{\text{trop}} + \delta_{\text{tide}} + \delta_{\text{rel}} + \varepsilon_i \ , \quad i = c, p \ , \tag{6.132}$$

$$\delta_{\text{ion}}(j) = \frac{A_1}{f_j^2} = \frac{A_1^z}{f_j^2} F = \frac{f_s^2 B_1}{f_j^2} = \frac{f_s^2 B_1^z}{f_j^2} F \ . \tag{6.133}$$

Where symbols have the same meanings as those of Eqs. 6.44–6.47. j is the index of the frequency f and wavelength λ. A_1 and A_1^z are the ionospheric parameters in the path and zenith directions; B_1 and B_1^z are scaled A_1 and A_1^z with f_s^2 for numerical reasons. c denotes the speed of light, index c denotes code. C_ρ is called geometry and N_j is the ambiguity. For simplicity, the residuals of the codes (and phases) are denoted with the same symbol ε_c (and ε_p) and have the same standard deviations of σ_c (and σ_p). Equations 6.130 and 6.131 can be written in a matrix form with weight matrix P as (Blewitt 1998)

$$\begin{pmatrix} R_1 \\ R_2 \\ \lambda_1\Phi_1 \\ \lambda_2\Phi_2 \end{pmatrix} = \begin{pmatrix} 0 & 0 & f_s^2/f_1^2 & 1 \\ 0 & 0 & f_s^2/f_2^2 & 1 \\ 1 & 0 & -f_s^2/f_1^2 & 1 \\ 0 & 1 & -f_s^2/f_2^2 & 1 \end{pmatrix} \begin{pmatrix} \lambda_1 N_1 \\ \lambda_2 N_2 \\ B_1 \\ C_\rho \end{pmatrix} \ , \ P = \begin{pmatrix} \sigma_c^2 & 0 & 0 & 0 \\ 0 & \sigma_c^2 & 0 & 0 \\ 0 & 0 & \sigma_p^2 & 0 \\ 0 & 0 & 0 & \sigma_p^2 \end{pmatrix}^{-1} \ . \tag{6.134}$$

Solutions of Uncombined Observation Equations

Equation 6.134 includes the observations of one satellite viewed by one receiver at one epoch. Alternatively, Eq. 6.134 can be considered a transformation between the observations and unknowns, and the transformation is a linear and invertible one. Denoting

$$a = \frac{f_1^2}{f_1^2 - f_2^2}, \quad b = \frac{-f_2^2}{f_1^2 - f_2^2}, \quad g = \frac{1}{f_1^2} - \frac{1}{f_2^2}, \quad q = g f_s^2 \ , \tag{6.135}$$

(c) ketabton.com: The Digital Library

then one has relations of

$$1-a=b,\quad \frac{1}{f_1^2 g}=b,\quad \frac{1}{f_2^2 g}=-a \tag{6.136}$$

and

$$\begin{pmatrix} 0 & 0 & f_s^2/f_1^2 & 1 \\ 0 & 0 & f_s^2/f_2^2 & 1 \\ 1 & 0 & -f_s^2/f_1^2 & 1 \\ 0 & 1 & -f_s^2/f_2^2 & 1 \end{pmatrix}^{-1} = \begin{pmatrix} 1-2a & -2b & 1 & 0 \\ -2a & 2a-1 & 0 & 1 \\ 1/q & -1/q & 0 & 0 \\ a & b & 0 & 0 \end{pmatrix} = T \ . \tag{6.137}$$

Where a and b are the coefficients of the ionosphere-free combinations of the observables of L1 and L2. The solution of Eq. 6.134 has a form of (by multiplying the transformation matrix T to Eq. 6.134)

$$\begin{pmatrix} \lambda_1 N_1 \\ \lambda_2 N_2 \\ B_1 \\ C_\rho \end{pmatrix} = \begin{pmatrix} 1-2a & -2b & 1 & 0 \\ -2a & 2a-1 & 0 & 1 \\ 1/q & -1/q & 0 & 0 \\ a & b & 0 & 0 \end{pmatrix} \begin{pmatrix} R_1 \\ R_2 \\ \lambda_1 \Phi_1 \\ \lambda_2 \Phi_2 \end{pmatrix} . \tag{6.138}$$

The related covariance matrix of the above solution vector is then

$$Q = \mathrm{cov}\begin{pmatrix} \lambda_1 N_1 \\ \lambda_2 N_2 \\ B_1 \\ C_\rho \end{pmatrix} = T \begin{pmatrix} \sigma_c^2 & 0 & 0 & 0 \\ 0 & \sigma_c^2 & 0 & 0 \\ 0 & 0 & \sigma_p^2 & 0 \\ 0 & 0 & 0 & \sigma_p^2 \end{pmatrix} T^T$$

$$= \begin{pmatrix} (1-2a)^2+4b^2+\frac{\sigma_p^2}{\sigma_c^2} & 4a^2-4ab-2a+2b & \frac{1-2a+2b}{q} & a-2a^2-2b^2 \\ 4a^2-4ab-2a+2b & 8a^2-4a+1+\frac{\sigma_p^2}{\sigma_c^2} & \frac{1-4a}{q} & -2a^2+2ab-b \\ \frac{1-2a+2b}{q} & \frac{1-4a}{q} & \frac{2}{q^2} & \frac{a-b}{q} \\ a-2a^2-2b^2 & -2a^2+2ab-b & \frac{a-b}{q} & a^2+b^2 \end{pmatrix} \sigma_c^2 \tag{6.139}$$

Equation 6.139 can be simplified by using the relation of $1-a=b$ and neglecting the terms of $(\sigma_p/\sigma_c)^2$ (because (σ_p/σ_c) is less than 0.01) as well as letting $f_s = f_1$ (so that $q = 1/b$). Taking the relationships of ratios of the frequencies into account ($f_1 = 154 f_0$ and $f_2 = 120 f_0$, f_0 is the fundamental frequency), one has approximately

(c) ketabton.com: The Digital Library

$$\operatorname{cov}\begin{pmatrix}\lambda_1 N_1\\ \lambda_2 N_2\\ B_1\\ C_\rho\end{pmatrix}=\begin{pmatrix}26.2971 & 33.4800 & 11.1028 & -15.1943\\ 33.4800 & 42.6629 & 14.1943 & -19.2857\\ 11.1028 & 14.1943 & 4.7786 & -6.3243\\ -15.1943 & -19.2857 & -6.3243 & 8.8700\end{pmatrix}\sigma_c^2 \ . \tag{6.140}$$

The precisions of the solutions will be further discussed in Sect. 6.7.3. The parameterisation of the GPS observation models is an important issue and can be found in Chap. 9 or (Blewitt 1998; Xu 2004), if interested.

6.7.2 Combining Algorithms of GPS Data Processing

Ionosphere-free Combinations

Letting transformation matrix

$$T_1=\begin{pmatrix}1 & -1 & 0 & 0\\ a & b & 0 & 0\\ 0 & 0 & a & b\\ 1/2 & 0 & 1/2 & 0\end{pmatrix}, \tag{6.141}$$

and applying the transform to the Eq. 6.134, one has

$$T_1\begin{pmatrix}R_1\\ R_2\\ \lambda_1\Phi_1\\ \lambda_2\Phi_2\end{pmatrix}=\begin{pmatrix}0 & 0 & q & 0\\ 0 & 0 & 0 & 1\\ a & b & 0 & 1\\ 1/2 & 0 & 0 & 1\end{pmatrix}\begin{pmatrix}\lambda_1 N_1\\ \lambda_2 N_2\\ B_1\\ C_\rho\end{pmatrix} . \tag{6.142}$$

The ionosphere parameter in Eq. 6.142 is free in the last three equations, which are traditionally called ionosphere-free combinations. To solve the ionosphere-free equations or the whole Eq. 6.142 will lead to the same results. Equation 6.142 has a unique solution vector of

$$\begin{pmatrix}\lambda_1 N_1\\ \lambda_2 N_2\\ B_1\\ C_\rho\end{pmatrix}=\begin{pmatrix}0 & -2 & 0 & 2\\ 0 & (2a-1)/b & 1/b & -2a/b\\ 1/q & 0 & 0 & 0\\ 0 & 1 & 0 & 0\end{pmatrix}T_1\begin{pmatrix}R_1\\ R_2\\ \lambda_1\Phi_1\\ \lambda_2\Phi_2\end{pmatrix}, \tag{6.143}$$

or (noticing $(1-a)=b$, cf., Eq. 6.136)

$$\begin{pmatrix}\lambda_1 N_1\\ \lambda_2 N_2\\ B_1\\ C_\rho\end{pmatrix}=\begin{pmatrix}1-2a & -2b & 1 & 0\\ -2a & 2a-1 & 0 & 1\\ 1/q & -1/q & 0 & 0\\ a & b & 0 & 0\end{pmatrix}\begin{pmatrix}R_1\\ R_2\\ \lambda_1\Phi_1\\ \lambda_2\Phi_2\end{pmatrix} . \tag{6.144}$$

(c) ketabton.com: The Digital Library

Equations 6.144 and 6.138 are identical. Therefore the covariance matrix of the solution vector on the left side of Eq. 6.144 is the same as that given in Eq. 6.139. This shows that the uncombined algorithms and the ionosphere-free combinations are equivalent in this discussed case.

Geometry-free Combinations

Letting transformation matrix

$$T_2 = \begin{pmatrix} a & b & 0 & 0 \\ 1 & -1 & 0 & 0 \\ 0 & 0 & 1 & -1 \\ -1 & 0 & 1 & 0 \end{pmatrix}, \tag{6.145}$$

and applying the transformation to Eq. 6.134, one has

$$T_2 \begin{pmatrix} R_1 \\ R_2 \\ \lambda_1 \Phi_1 \\ \lambda_2 \Phi_2 \end{pmatrix} = \begin{pmatrix} 0 & 0 & 0 & 1 \\ 0 & 0 & q & 0 \\ 1 & -1 & -q & 0 \\ 1 & 0 & -2f_s^2/f_1^2 & 0 \end{pmatrix} \begin{pmatrix} \lambda_1 N_1 \\ \lambda_2 N_2 \\ B_1 \\ C_\rho \end{pmatrix}. \tag{6.146}$$

The geometric component in Eq. 6.146 is free in the last three equations, which are traditionally called geometry-free combinations. The geometry-free equations must be solved or Eq. 6.146 will lead to the same results. Equation 6.146 has a unique solution vector of

$$\begin{pmatrix} \lambda_1 N_1 \\ \lambda_2 N_2 \\ B_1 \\ C_\rho \end{pmatrix} = \begin{pmatrix} 0 & 2/(f_1^2 g) & 0 & 1 \\ 0 & 2/(f_1^2 g) - 1 & -1 & 1 \\ 0 & 1/q & 0 & 0 \\ 1 & 0 & 0 & 0 \end{pmatrix} T_2 \begin{pmatrix} R_1 \\ R_2 \\ \lambda_1 \Phi_1 \\ \lambda_2 \Phi_2 \end{pmatrix}, \tag{6.147}$$

or (noticing $1/(f_1^2 g) = b$, cf., Eq. 6.136)

$$\begin{pmatrix} \lambda_1 N_1 \\ \lambda_2 N_2 \\ B_1 \\ C_\rho \end{pmatrix} = \begin{pmatrix} 2b-1 & -2b & 1 & 0 \\ 2b-2 & 1-2b & 0 & 1 \\ 1/q & -1/q & 0 & 0 \\ a & b & 0 & 0 \end{pmatrix} \begin{pmatrix} R_1 \\ R_2 \\ \lambda_1 \Phi_1 \\ \lambda_2 \Phi_2 \end{pmatrix}. \tag{6.148}$$

Taking the relations of Eq. 6.136 (i.e., $b = 1 - a$) into account, Eqs. 6.148 and 6.138 are identical. Therefore the covariance matrix of the solution vector on the left side of Eq. 6.148 is identical with Eq. 6.139. This shows that the uncombined algorithms and the geometry-free combinations are equivalent in this discussed case.

(c) ketabton.com: The Digital Library

Ionosphere-free and Geometry-free Combinations

Letting transformation matrix

$$T_3 = \begin{pmatrix} 1 & 0 & 0 & 0 \\ 0 & 1 & 0 & 0 \\ 0 & -1 & 1 & 0 \\ 0 & -1 & 0 & 1 \end{pmatrix}, \tag{6.149}$$

one then has

$$T_3T_1 = \begin{pmatrix} 1 & 0 & 0 & 0 \\ 0 & 1 & 0 & 0 \\ 0 & -1 & 1 & 0 \\ 0 & -1 & 0 & 1 \end{pmatrix} \begin{pmatrix} 1 & -1 & 0 & 0 \\ a & b & 0 & 0 \\ 0 & 0 & a & b \\ 1/2 & 0 & 1/2 & 0 \end{pmatrix} = \begin{pmatrix} 1 & -1 & 0 & 0 \\ a & b & 0 & 0 \\ -a & -b & a & b \\ 1/2-a & -b & 1/2 & 0 \end{pmatrix}. \tag{6.150}$$

Applying the transformation 6.150 to Eq. 6.134 or applying the transformation 6.149 to Eq. 6.142 leads to the same results, and one has

$$T_3T_1 \begin{pmatrix} R_1 \\ R_2 \\ \lambda_1\Phi_1 \\ \lambda_2\Phi_2 \end{pmatrix} = \begin{pmatrix} 0 & 0 & q & 0 \\ 0 & 0 & 0 & 1 \\ a & b & 0 & 0 \\ 1/2 & 0 & 0 & 0 \end{pmatrix} \begin{pmatrix} \lambda_1N_1 \\ \lambda_2N_2 \\ B_1 \\ C_\rho \end{pmatrix} \quad \text{or} \tag{6.151}$$

$$\begin{pmatrix} R_1 - R_2 \\ aR_1 + bR_2 \\ a\lambda_1\Phi_1 + b\lambda_2\Phi_2 - aR_1 - bR_2 \\ (\lambda_1\Phi_1 + R_1)/2 - aR_1 - bR_2 \end{pmatrix} = \begin{pmatrix} 0 & 0 & q & 0 \\ 0 & 0 & 0 & 1 \\ a & b & 0 & 0 \\ 1/2 & 0 & 0 & 0 \end{pmatrix} \begin{pmatrix} \lambda_1N_1 \\ \lambda_2N_2 \\ B_1 \\ C_\rho \end{pmatrix}. \tag{6.152}$$

The ionosphere and geometry are both free in the last two equations, which are called ionosphere-geometry-free combinations. Solving the ionosphere-free and geometry-free equations or directly solving Eq. 6.152 will lead to the same results. Eq. 6.152 has a unique solution vector of

$$\begin{pmatrix} \lambda_1N_1 \\ \lambda_2N_2 \\ B_1 \\ C_\rho \end{pmatrix} = \begin{pmatrix} 0 & 0 & 0 & 2 \\ 0 & 0 & 1/b & -2a/b \\ 1/q & 0 & 0 & 0 \\ 0 & 1 & 0 & 0 \end{pmatrix} T_3T_1 \begin{pmatrix} R_1 \\ R_2 \\ \lambda_1\Phi_1 \\ \lambda_2\Phi_2 \end{pmatrix}, \tag{6.153}$$

or (noticing $(1-a)/b = 1$, cf., Eq. 6.136)

$$\begin{pmatrix} \lambda_1N_1 \\ \lambda_2N_2 \\ B_1 \\ C_\rho \end{pmatrix} = \begin{pmatrix} 1-2a & -2b & 1 & 0 \\ -2a & 2a-1 & 0 & 1 \\ 1/q & -1/q & 0 & 0 \\ a & b & 0 & 0 \end{pmatrix} \begin{pmatrix} R_1 \\ R_2 \\ \lambda_1\Phi_1 \\ \lambda_2\Phi_2 \end{pmatrix}. \tag{6.154}$$

(c) ketabton.com: The Digital Library

Equations 6.154 and 6.138 are identical. This shows that the uncombined algorithms and the ionosphere-geometry-free combinations are equivalent in this discussed case.

Diagonal Combinations

Letting transformation matrix

$$T_4 = \begin{pmatrix} 1 & 0 & 0 & 0 \\ 0 & 1 & 0 & 0 \\ 0 & 0 & 1 & -2a \\ 0 & 0 & 0 & 1 \end{pmatrix}, \tag{6.155}$$

one has

$$T_4T_3T_1 = \begin{pmatrix} 1 & 0 & 0 & 0 \\ 0 & 1 & 0 & 0 \\ 0 & 0 & 1 & -2a \\ 0 & 0 & 0 & 1 \end{pmatrix} \begin{pmatrix} 1 & -1 & 0 & 0 \\ a & b & 0 & 0 \\ -a & -b & a & b \\ 1/2-a & -b & 1/2 & 0 \end{pmatrix} = \begin{pmatrix} 1 & -1 & 0 & 0 \\ a & b & 0 & 0 \\ -2ab & b(2a-1) & 0 & b \\ 1/2-a & -b & 1/2 & 0 \end{pmatrix}. \tag{6.156}$$

If applying the transformation 6.156 to Eq. 6.134 or applying the transformation 6.155 to Eq. 6.151, one has the same results of

$$T_4T_3T_1 \begin{pmatrix} R_1 \\ R_2 \\ \lambda_1\Phi_1 \\ \lambda_2\Phi_2 \end{pmatrix} = \begin{pmatrix} 0 & 0 & q & 0 \\ 0 & 0 & 0 & 1 \\ 0 & b & 0 & 0 \\ 1/2 & 0 & 0 & 0 \end{pmatrix} \begin{pmatrix} \lambda_1N_1 \\ \lambda_2N_2 \\ B_1 \\ C_\rho \end{pmatrix}. \tag{6.157}$$

In the above equation, the ionosphere and geometry as well as the ambiguities are diagonal to each other. Such combinations are called diagonal ones. The solution vector of Eq. 6.157 may be easily derived:

$$\begin{pmatrix} \lambda_1N_1 \\ \lambda_2N_2 \\ B_1 \\ C_\rho \end{pmatrix} = \begin{pmatrix} 0 & 0 & 0 & 2 \\ 0 & 0 & 1/b & 0 \\ 1/q & 0 & 0 & 0 \\ 0 & 1 & 0 & 0 \end{pmatrix} T_4T_3T_1 \begin{pmatrix} R_1 \\ R_2 \\ \lambda_1\Phi_1 \\ \lambda_2\Phi_2 \end{pmatrix} \tag{6.158}$$

or

$$\begin{pmatrix} \lambda_1N_1 \\ \lambda_2N_2 \\ B_1 \\ C_\rho \end{pmatrix} = \begin{pmatrix} 1-2a & -2b & 1 & 0 \\ -2a & 2a-1 & 0 & 1 \\ 1/q & -1/q & 0 & 0 \\ a & b & 0 & 0 \end{pmatrix} \begin{pmatrix} R_1 \\ R_2 \\ \lambda_1\Phi_1 \\ \lambda_2\Phi_2 \end{pmatrix}. \tag{6.159}$$

(c) ketabton.com: The Digital Library

Equations 6.159 and 6.138 are identical. This shows that the uncombined algorithms and the diagonal combinations are equivalent in the discussed case.

General Combinations

For arbitrary combinations, as soon as the transformation matrix is an invertible one, the transformed equations are equivalent to the original ones based on algebra theory. Both the solution vector and the variance-covariance matrix are identical. That is, no matter what kinds of combinations are used, neither different solutions nor different precisions of the solutions will be obtained. The different combinations lead to an easier dealing of the related special problems.

Wide- and Narrow-lane Combinations

Denoting

$$T_5 = \begin{pmatrix} 0 & 0 & 0 & 2 \\ 0 & 0 & 1/b & 0 \\ 1/q & 0 & 0 & 0 \\ 0 & 1 & 0 & 0 \end{pmatrix} \tag{6.160}$$

and letting transformation matrix

$$T_6 = \begin{pmatrix} \dfrac{1}{\lambda_1} & \dfrac{-1}{\lambda_2} & 0 & 0 \\ \dfrac{1}{\lambda_1} & \dfrac{1}{\lambda_2} & 0 & 0 \\ 0 & 0 & 1 & 0 \\ 0 & 0 & 0 & 1 \end{pmatrix}, \tag{6.161}$$

one may form the wide and narrow lanes (Petovello 2006) directly by multiplying Eq. 6.161 to Eq. 6.158 to obtain the related wide- and narrow-lane ambiguities

$$\begin{pmatrix} N_1 - N_2 \\ N_1 + N_2 \\ B_1 \\ C_\rho \end{pmatrix} = T_6 T_5 T_4 T_3 T_1 \begin{pmatrix} R_1 \\ R_2 \\ \lambda_1 \Phi_1 \\ \lambda_2 \Phi_2 \end{pmatrix}. \tag{6.162}$$

Indeed, there is $T_5 T_4 T_3 T_1 = T$. Because of the unique property of the solutions of different combinations, any direct combinations of the solutions must be equivalent to each other. None of the combinations will lead to better solutions or better precisions of the solutions. From this rigorous theoretical aspect, the traditional wide-lane ambiguity fixing technique may lead to a more effective search, but not a better solution and precision of the ambiguity.

(c) ketabton.com: The Digital Library

6.7.3
Secondary GPS Data Processing Algorithms

In the Case of More Satellites in View

Up to now, the discussions have been limited for the observations of one satellite viewed by one receiver at one epoch. The original observation equation is given in Eq. 6.134. The solution vector and its covariance matrix are given in Eqs. 6.138 and 6.139, respectively. The elements of the covariance matrix depend on the coefficients of Eq. 6.134, and the coefficients of the observation equation depend on the way of parameterisation. E.g., if instead of B_1, B_1^z is used, then Eq. 6.134 turns out to be

$$\begin{pmatrix} R_1(k) \\ R_2(k) \\ \lambda_1\Phi_1(k) \\ \lambda_2\Phi_2(k) \end{pmatrix} = \begin{pmatrix} 0 & 0 & F_k f_s^2/f_1^2 & 1 \\ 0 & 0 & F_k f_s^2/f_2^2 & 1 \\ 1 & 0 & -F_k f_s^2/f_1^2 & 1 \\ 0 & 1 & -F_k f_s^2/f_2^2 & 1 \end{pmatrix} \begin{pmatrix} \lambda_1 N_1(k) \\ \lambda_2 N_2(k) \\ B_1^z \\ C_\rho(k) \end{pmatrix}, \tag{6.163}$$

where k is the index of the satellite. Ionospheric mapping function F_k is dependent on the zenith distance of the satellite k. The solution vector of Eq. 6.163 is then similar to that of Eq. 6.138:

$$\begin{pmatrix} \lambda_1 N_1(k) \\ \lambda_2 N_2(k) \\ B_1^z \\ C_\rho(k) \end{pmatrix} = \begin{pmatrix} 1-2a & -2b & 1 & 0 \\ -2a & 2a-1 & 0 & 1 \\ 1/q_k & -1/q_k & 0 & 0 \\ a & b & 0 & 0 \end{pmatrix} \begin{pmatrix} R_1(k) \\ R_2(k) \\ \lambda_1\Phi_1(k) \\ \lambda_2\Phi_2(k) \end{pmatrix}, \quad Q(k), \tag{6.164}$$

where $q_k = qF_k$ and $Q(k)$ is the covariance matrix, which can be similarly derived and given by adding the index k to q in Q of Eq. 6.139. The terms on the right-hand side can be considered secondary "observations" of the unknowns on the left-hand side. If K satellites are viewed, one has the observation equations of one receiver

$$\begin{pmatrix} \lambda_1 N_1(1) \\ \lambda_2 N_2(1) \\ B_1^z \\ C_\rho(1) \\ \vdots \\ \lambda_1 N_1(K) \\ \lambda_2 N_2(K) \\ B_1^z \\ C_\rho(K) \end{pmatrix} = \begin{pmatrix} 1-2a & -2b & 1 & 0 & \cdots & 0 & 0 & 0 & 0 \\ -2a & 2a-1 & 0 & 1 & \cdots & 0 & 0 & 0 & 0 \\ 1/q_1 & -1/q_1 & 0 & 0 & \cdots & 0 & 0 & 0 & 0 \\ a & b & 0 & 0 & \cdots & 0 & 0 & 0 & 0 \\ \vdots & \vdots & \vdots & \vdots & \cdots & \vdots & \vdots & \vdots & \vdots \\ 0 & 0 & 0 & 0 & \cdots & 1-2a & -2b & 1 & 0 \\ 0 & 0 & 0 & 0 & \cdots & -2a & 2a-1 & 0 & 1 \\ 0 & 0 & 0 & 0 & \cdots & 1/q_K & -1/q_K & 0 & 0 \\ 0 & 0 & 0 & 0 & \cdots & a & b & 0 & 0 \end{pmatrix} \begin{pmatrix} R_1(1) \\ R_2(1) \\ \lambda_1\Phi_1(1) \\ \lambda_2\Phi_2(1) \\ \vdots \\ R_1(K) \\ R_2(K) \\ \lambda_1\Phi_1(K) \\ \lambda_2\Phi_2(K) \end{pmatrix}, \tag{6.165}$$

and variance matrix

(c) ketabton.com: The Digital Library

$$Q_K = \begin{pmatrix} Q(1) & \cdots\cdots & 0 \\ \vdots & :::::: & \vdots \\ 0 & \cdots\cdots & Q(K) \end{pmatrix}. \tag{6.166}$$

Multiplying a transformation matrix

$$T(K) = \begin{pmatrix} 1 & 0 & 0 & 0 & \cdots\cdots & 0 & 0 & 0 & 0 \\ 0 & 1 & 0 & 0 & \cdots\cdots & 0 & 0 & 0 & 0 \\ 0 & 0 & 1/K & 0 & \cdots\cdots & 0 & 0 & 1/K & 0 \\ 0 & 0 & 0 & 1 & \cdots\cdots & 0 & 0 & 0 & 0 \\ \vdots & \vdots & \vdots & \vdots & :::::: & \vdots & \vdots & \vdots & \vdots \\ 0 & 0 & 0 & 0 & \cdots\cdots & 1 & 0 & 0 & 0 \\ 0 & 0 & 0 & 0 & \cdots\cdots & 0 & 1 & 0 & 0 \\ 0 & 0 & 0 & 0 & \cdots\cdots & 0 & 0 & 0 & 1 \end{pmatrix} \tag{6.167}$$

to Eq. 6.165, one has the solutions of GPS observation equations of one station

$$\begin{pmatrix} \lambda_1 N_1(1) \\ \lambda_2 N_2(1) \\ B_1^z \\ C_\rho(1) \\ \vdots \\ \lambda_1 N_1(K) \\ \lambda_2 N_2(K) \\ C_\rho(K) \end{pmatrix} = T(K) \begin{pmatrix} 1-2a & -2b & 1 & 0 & \cdots\cdots & 0 & 0 & 0 & 0 \\ -2a & 2a-1 & 0 & 1 & \cdots\cdots & 0 & 0 & 0 & 0 \\ 1/q_1 & -1/q_1 & 0 & 0 & \cdots\cdots & 0 & 0 & 0 & 0 \\ a & b & 0 & 0 & \cdots\cdots & 0 & 0 & 0 & 0 \\ \vdots & \vdots & \vdots & \vdots & :::::: & \vdots & \vdots & \vdots & \vdots \\ 0 & 0 & 0 & 0 & \cdots\cdots & 1-2a & -2b & 1 & 0 \\ 0 & 0 & 0 & 0 & \cdots\cdots & -2a & 2a-1 & 0 & 1 \\ 0 & 0 & 0 & 0 & \cdots\cdots & 1/q_K & -1/q_K & 0 & 0 \\ 0 & 0 & 0 & 0 & \cdots\cdots & a & b & 0 & 0 \end{pmatrix} \begin{pmatrix} R_1(1) \\ R_2(1) \\ \lambda_1 \Phi_1(1) \\ \lambda_2 \Phi_2(1) \\ \vdots \\ R_1(K) \\ R_2(K) \\ \lambda_1 \Phi_1(K) \\ \lambda_2 \Phi_2(K) \end{pmatrix}, \tag{6.168}$$

and the related

$$Q = T(K) Q_K (T(K))^T \tag{6.169}$$

where mapping function is used to combine the K ionosphere parameters into one. Similar discussions can be made for the cases of using more receivers. The original observation vector and the so-called secondary "observation" vector are

$$\begin{pmatrix} R_1(k) \\ R_2(k) \\ \lambda_1 \Phi_1(k) \\ \lambda_2 \Phi_2(k) \end{pmatrix}, \quad \begin{pmatrix} \lambda_1 N_1(k) \\ \lambda_2 N_2(k) \\ B_1(k) \\ C_\rho(k) \end{pmatrix}. \tag{6.170}$$

Both vectors are equivalent as proved in Sect. 6.7.2 and they can be transformed uniquely from one to the other. Any further data processing can be considered process-

(c) ketabton.com: The Digital Library

ing based on the secondary "observations". The secondary "observations" own the equivalence property whether they are uncombined or combining ones. Therefore the equivalence property is valid for further data processing based on the secondary "observations".

GPS Data Processing Using Secondary "Observations"

A by-product of the above equivalence discussions is that the GPS data processing can be performed directly by using the so-called secondary observations. Besides the two ambiguity parameters (scaled with the wavelengths), the other two secondary observations are the electronic density in the observing path (scaled by square of f_1) and the geometry. The geometry includes the whole observation model except the ionosphere and ambiguity terms. For a time series of the secondary "observations", the electron density (or, for simplicity, "ionosphere") and the "geometry" are real time observations, whereas the "ambiguities" are constants in case no cycle-slip occurs (Langley 1998a, b). Sequential adjustment or filtering methods can be used to deal with the observation time series. It is notable that the secondary "observations" are correlated with each other (see the covariance matrix Eq. 6.139). However, the "ambiguities" are direct observations of the ambiguity parameters, and the "ionosphere" and "geometry" are modelled by Eqs. 6.132 and 6.133, respectively. The "ambiguity" observables are ionosphere-geometry-free. The "ionosphere" observable is geometry-free and ambiguity-free. The "geometry" observable is ionosphere-free. It is notable that some algorithms may be more effective; however, the results and the precisions of the solutions are equivalent no matter which algorithms are used. It should be emphasized that all the above discussions are based on the observation Model 6.134. The problem concerning the parameterisation of the GPS observation model will not affect the conclusions of the discussions and will be further discussed in Chap. 9.

Precision Analysis

If the sequential time series of the original observations are considered time independent as they traditionally have been, then the secondary "observations" and their precisions are also independent time series. From Eq. 6.140, the standard deviations of the L1 and L2 ambiguities are approximately $5.1281\sigma_c$ and $6.5317\sigma_c$. The standard deviation of ionosphere and geometry "observations" are about $2.1860\sigma_c$ and $2.9783\sigma_c$, respectively. That is, the precisions of the "observed" ambiguities are worse than that of the others at one epoch. If the standard deviation of the P code is about 1 decimetre (phase smoothed), then the precisions of the ambiguities determined by one epoch are worse than 0.5 meters. However, an average filter of m epoch data will raise the precisions by a factor of sqrt(m) (square root of m). After 100 or 10000 epochs, the ambiguities are able to be determined with precisions of about 5 cm or 5 mm. "Ionosphere" data are observed with better precisions. However, due to the high dynamic of the electron movements, ionosphere effects may not be easily smoothed to raise the precision. The "Geometry" model is the most complicated one compared with the others, and discussions can be found from numerous publications for static, kinematic and dynamic applications (cf., e.g., ION proceedings, Chap. 10).

(c) ketabton.com: The Digital Library

6.7.4 Summary

The equivalence properties between uncombined and combining algorithms are proved theoretically by algebraic linear transformations. The solution vector and the related covariance matrix are identical no matter which algorithms are used. Different combinations can lead to a more effective and easier dealing with the data. The so-called ionosphere-geometry-free and diagonal combinations are derived, which own better properties than that of the traditional combinations. A data processing algorithm using the uniquely transformed secondary "observations" is outlined and used to prove the equivalence. Because of the unique property of the solutions of different combinations, any direct combinations of the solutions must be equivalent to each other. None of the combinations will lead to better solutions or better precisions of the solutions than that of the others. From this aspect, the traditional wide-lane ambiguity fixing technique may lead to a more effective search of ambiguity, but it will not lead to a better solution and precision of the ambiguity.

6.8 Equivalence of Undifferenced and Differencing Algorithms

In Sect. 6.6 the single, double and triple differences as well as their related observation equations are discussed. The number of unknown parameters in the equations is greatly reduced through difference forming; however, the covariance derivations are tedious, especially for a GPS network.

In this section, a unified GPS data processing method based on equivalently eliminated equations is proposed and the equivalence between undifferenced and differencing algorithms is proved. The theoretic background of the method is given. By selecting the eliminated unknown vector as a vector of zero, a vector of satellite clock error, a vector of all clock error, a vector of clock and ambiguity parameters, or a vector of user-defined unknowns, the selectively eliminated equivalent observation equations can be formed, respectively. The equations are equivalent to the zero-, single-, double-, triple-, or user-defined differencing equations. The advantage of such a method is that the different GPS data processing methods are unified to a unique one, whereas the observational vector remains the original one and the weight matrix keeps the un-correlated diagonal form. In other words, by using this equivalent method, one may selectively reduce the unknown number; however, one does not have to deal with the complicated correlation problem. Several special cases of single-, double-, and triple-difference are discussed in detail to illustrate the theory. The reference-related parameters are dealt with using the a priori datum method.

6.8.1 Introduction

In GPS data processing practice, the commonly used methods are so-called zero-difference (un-differential), single-difference, double-difference and triple-differ-

(c) ketabton.com: The Digital Library

ence methods (Bauer 1994; Hofmann-Wellenhof et al. 1997; King et al. 1987; Leick 1995; Remondi 1984; Seeber 1993; Strang and Borre 1997; Wang et al. 1988). It is well-known that the observation equations of the differencing methods can be obtained by carrying out a related linear transformation to the original equations. As soon as the weight matrix is similarly transformed according to the law of covariance propagation, all methods are equivalent, theoretically. A theoretical proof of the equivalence between the un-differential and differential methods can be found in Schaffrin and Grafarend (1986). A comparison of the advantages and disadvantages of the un-differential and differential methods can be found, e.g., in de Jong (1998). The advantage of the differential methods is that the unknown parameters are fewer so that the whole problem to be solved becomes smaller. The disadvantage of the differential methods is that there is a correlation problem, which appears in cases of multiple baselines of single-difference and all double difference as well as triple difference. The correlation problem is often complicated and not easy to be dealt with exactly (compared with the un-correlated problem). The advantages and disadvantages reach a balance. If one wants to deal with a reduced problem (cancellation of many unknowns), then one has to deal with the correlation problem. As an alternative, we use the equivalent observation equation approach to unify the un-differential and differential methods, while keeping all the advantages of the un-differential and differential methods.

In the next sections, the theoretical basis of the equivalently eliminated equations will be given based on the derivation of Zhou (1985). Several detailed cases are then discussed to illustrate the theory. The reference-related parameters are dealt with using the a priori datum method. A summary of the selectively eliminated equivalent GPS data processing method is outlined at the end.

6.8.2 Formation of Equivalent Observation Equations

For the convenience of later discussion, the method to form an equivalently eliminated equation system is outlined here. The theory is given in Sect. 7.6 in detail. In practice, sometimes only one group of unknowns is of interest; it is better to eliminate the other group of unknowns (called nuisance parameters), for example, because of their size. In this case, using the so-called equivalently eliminated observation equation system could be very beneficial (Wang et al. 1988; Xu and Qian 1986; Zhou 1985). The nuisance parameters can be eliminated directly from the observation equations instead of from the normal equations.

The linearised observation equation system can be represented using the matrix:

$$V = L - \begin{pmatrix} A & B \end{pmatrix} \begin{pmatrix} \mathrm{X}_1 \\ \mathrm{X}_2 \end{pmatrix} \quad \text{and} \quad P\,, \tag{6.171}$$

where L is an observation vector of dimension n, A and B are coefficient matrices of dimension $n \times (s - r)$ and $n \times r$, X_1 and X_2 are unknown vectors of dimension $s - r$ and r, V is residual error, s is the total number of unknowns, and P is the weight matrix of dimension $n \times n$.

(c) ketabton.com: The Digital Library

The related least squares normal equation can be formed then as:

$$\begin{pmatrix} A & B \end{pmatrix}^T P \begin{pmatrix} A & B \end{pmatrix} \begin{pmatrix} X_1 \\ X_2 \end{pmatrix} = \begin{pmatrix} A & B \end{pmatrix}^T PL \quad \text{or} \tag{6.172}$$

$$M_{11}X_1 + M_{12}X_2 = B_1 \quad \text{and} \tag{6.173}$$

$$M_{21}X_1 + M_{22}X_2 = B_2 \ , \tag{6.174}$$

where

$$B_1 = A^T PL \ , \quad B_2 = B^T PL \quad \text{and}$$

$$\begin{pmatrix} A^T PA & A^T PB \\ B^T PA & B^T PB \end{pmatrix} = \begin{pmatrix} M_{11} & M_{12} \\ M_{21} & M_{22} \end{pmatrix} . \tag{6.175}$$

After eliminating the unknown vector X_1, the eliminated equivalent normal equation system is then

$$M_2 X_2 = R_2 \ , \tag{6.176}$$

where

$$M_2 = -M_{21}M_{11}^{-1}M_{12} + M_{22} = B^T PB - B^T PA\, M_{11}^{-1} A^T PB \quad \text{and} \tag{6.177}$$

$$R_2 = B_2 - M_{21}M_{11}^{-1}B_1 \ . \tag{6.178}$$

The related equivalent observation equation of Eq. 6.176 is then (cf. Sect. 7.6; Xu and Qian 1986; Zhou 1985)

$$U = L - (E - J)BX_2 \ , \quad P \ , \tag{6.179}$$

where

$$J = AM_{11}^{-1}A^T P \ . \tag{6.180}$$

E is an identity matrix of size n, L and P are the original observation vector and weight matrix, and U is the residual vector, which has the same property as V in Eq. 6.171. The advantage of using Eq. 6.179 is that the unknown vector X_1 has been eliminated; however, L vector and P matrix remain the same as the originals.

Similarly, the X_2 eliminated equivalent equation system is:

$$U_1 = L - (E - K)AX_1 \quad \text{and} \quad P \ , \tag{6.181}$$

where

$$K = BM_{22}^{-1}B^T P \ , \quad M_{22} = B^T PB \ ,$$

and U_1 is the residual vector (which has the same property as V).

We have separated the observation Eq. 6.171 into two equations, Eqs. 6.179 and 6.181; each equation contains only one of the unknown vectors. Each unknown vec-

(c) ketabton.com: The Digital Library

tor can be solved independently and separately. Equations 6.179 and 6.181 are called equivalent observation equations of Eq. 6.171.

The equivalence property of Eqs. 6.171 and 6.179 is valid under three implicit assumptions. The first one is that the identical observation vector is used. The second is that the parameterisation of X_2 is identical. The third is that X_1 could be eliminated. Otherwise, the equivalence does not hold.

6.8.3 Equivalent Equations of Single Differences

In this section, the equivalent equations are formed to eliminate the satellite clock errors from the original zero-difference equations first, then the equivalency of the single differences (in two cases) related to the original zero-difference equations is proved.

Single differences cancel all the satellite clock errors out of the observation equations. This can also be achieved by forming equivalent equations where satellite clock errors are eliminated. Considering Eq. 6.171 the original observation equation and X_1 the vector of satellite clock errors, the equivalent equations of single differences can be formed as outlined in Sect. 6.8.2.

Suppose n common satellites ($k1, k2, \ldots, kn$) are observed at station $i1$ and $i2$. The original observation equation can then be written as

$$\begin{pmatrix} V_{i1} \\ V_{i2} \end{pmatrix} = \begin{pmatrix} L_{i1} \\ L_{i2} \end{pmatrix} - \begin{pmatrix} E & B_{i1} \\ E & B_{i2} \end{pmatrix} \cdot \begin{pmatrix} X_1 \\ X_2 \end{pmatrix} \quad \text{and} \quad P = \frac{1}{\sigma^2} \begin{pmatrix} E & 0 \\ 0 & E \end{pmatrix}, \tag{6.182}$$

where X_1 is the vector of satellite clock errors and X_2 is the vector of other unknowns. For simplicity, clock errors are scaled by the speed of light c and directly used as unknowns; then the X_1-related coefficient matrix is an identity matrix, E.

Comparing Eq. 6.182 with Eq. 6.171, one has (cf. Sect. 6.8.2)

$$A = \begin{pmatrix} E \\ E \end{pmatrix}, \quad B = \begin{pmatrix} B_{i1} \\ B_{i2} \end{pmatrix}, \quad L = \begin{pmatrix} L_{i1} \\ L_{i2} \end{pmatrix} \quad \text{and} \quad V = \begin{pmatrix} V_{i1} \\ V_{i2} \end{pmatrix},$$

and

$$M_{11} = \begin{pmatrix} E & E \end{pmatrix} \frac{1}{\sigma^2} \begin{pmatrix} E & 0 \\ 0 & E \end{pmatrix} \begin{pmatrix} E \\ E \end{pmatrix} = \frac{2}{\sigma^2} E,$$

$$J = \begin{pmatrix} E \\ E \end{pmatrix} \frac{\sigma^2}{2} E \begin{pmatrix} E & E \end{pmatrix} P = \frac{1}{2} \begin{pmatrix} E & E \\ E & E \end{pmatrix},$$

$$E_{2n \times 2n} - J = \frac{1}{2} \begin{pmatrix} E & -E \\ -E & E \end{pmatrix} \quad \text{and}$$

$$(E_{2n \times 2n} - J) B = \frac{1}{2} \begin{pmatrix} B_{i1} - B_{i2} \\ B_{i2} - B_{i1} \end{pmatrix}.$$

(c) ketabton.com: The Digital Library

So the equivalently eliminated equation system of Eq. 6.182 is

$$\begin{pmatrix} U_{i1} \\ U_{i2} \end{pmatrix} = \begin{pmatrix} L_{i1} \\ L_{i2} \end{pmatrix} - \frac{1}{2}\begin{pmatrix} B_{i1} - B_{i2} \\ B_{i2} - B_{i1} \end{pmatrix} \cdot X_2 , \quad P = \frac{1}{\sigma^2}\begin{pmatrix} E & 0 \\ 0 & E \end{pmatrix} , \tag{6.183}$$

where the satellite clock error vector X_1 is eliminated, and the observable vector and weight matrix are unchanged.

Denoting $B_s = B_{i2} - B_{i1}$, the least squares normal equation of Eq. 6.183 can then be formed as (cf. Chap. 7) (suppose Eq. 6.183 is solvable)

$$\frac{1}{2}\begin{pmatrix} -B_s^T & B_s^T \end{pmatrix} \cdot P \cdot \begin{pmatrix} -B_s \\ B_s \end{pmatrix} \cdot X_2 = \begin{pmatrix} -B_s^T & B_s^T \end{pmatrix} \cdot P \cdot \begin{pmatrix} L_{i1} \\ L_{i2} \end{pmatrix} \quad \text{or}$$

$$B_s^T B_s \cdot X_2 = B_s^T (L_{i2} - L_{i1}) . \tag{6.184}$$

Alternatively, a single difference equation can be obtained by multiplying Eq. 6.182 with a transformation matrix C_s

$$C_s = \begin{pmatrix} -E & E \end{pmatrix} ,$$

giving

$$C_s \cdot \begin{pmatrix} V_{i1} \\ V_{i2} \end{pmatrix} = C_s \cdot \begin{pmatrix} L_{i1} \\ L_{i2} \end{pmatrix} - C_s \cdot \begin{pmatrix} E & B_{i1} \\ E & B_{i2} \end{pmatrix} \cdot \begin{pmatrix} X_1 \\ X_2 \end{pmatrix} \quad \text{or}$$

$$V_{i2} - V_{i1} = (L_{i2} - L_{i1}) - (B_{i2} - B_{i1}) X_2 \tag{6.185}$$

and

$$\text{cov}(\text{SD}(O)) = C_s \sigma^2 \begin{pmatrix} E & 0 \\ 0 & E \end{pmatrix} C_s^T = 2\sigma^2 E \quad \text{and} \quad P_s = \frac{1}{2\sigma^2} E , \tag{6.186}$$

where P_s is the weight matrix of single differences, and cov(SD(O)) is the covariance of the single differences (SD) observational vector (O). Supposing Eq. 6.185 is solvable, the least squares normal equation system of Eq. 6.185 is then

$$(B_{i2} - B_{i1})^T (B_{i2} - B_{i1}) X_2 = (B_{i2} - B_{i1})^T (L_{i2} - L_{i1}) . \tag{6.187}$$

It is obvious that Eqs. 6.187 and 6.184 are identical. Therefore in the case of two stations, the single difference Eq. 6.185 is equivalent to the equivalently eliminated Eq. 6.183 and consequently equivalent to the original zero-difference equation.

Suppose n common satellites ($k1$, $k2$, …, kn) are observed at station $i1$, $i2$ and $i3$. The original observation equation can then be written as

$$\begin{pmatrix} V_{i1} \\ V_{i2} \\ V_{i3} \end{pmatrix} = \begin{pmatrix} L_{i1} \\ L_{i2} \\ L_{i3} \end{pmatrix} - \begin{pmatrix} E & B_{i1} \\ E & B_{i2} \\ E & B_{i3} \end{pmatrix} \cdot \begin{pmatrix} X_1 \\ X_2 \end{pmatrix} \quad \text{and} \quad P = \frac{1}{\sigma^2}\begin{pmatrix} E & 0 & 0 \\ 0 & E & 0 \\ 0 & 0 & E \end{pmatrix} . \tag{6.188}$$

(c) ketabton.com: The Digital Library

Comparing Eq. 6.188 with Eq. 6.171, one has (cf. Sect. 6.8.2)

$$A=\begin{pmatrix}E\\E\\E\end{pmatrix},\quad B=\begin{pmatrix}B_{i1}\\B_{i2}\\B_{i3}\end{pmatrix},\quad L=\begin{pmatrix}L_{i1}\\L_{i2}\\L_{i3}\end{pmatrix}\quad\text{and}\quad V=\begin{pmatrix}V_{i1}\\V_{i2}\\V_{i3}\end{pmatrix},$$

and

$$M_{11}=A^TPA=\frac{3}{\sigma^2}E\ ,$$

$$J=A\frac{\sigma^2}{3}EA^TP=\frac{1}{3}\begin{pmatrix}E&E&E\\E&E&E\\E&E&E\end{pmatrix},$$

$$E_{3n\times 3n}-J=\frac{1}{3}\begin{pmatrix}2E&-E&-E\\-E&2E&-E\\-E&-E&2E\end{pmatrix}\quad\text{and}$$

$$(E_{3n\times 3n}-J)B=\frac{1}{3}\begin{pmatrix}2B_{i1}-B_{i2}-B_{i3}\\-B_{i1}+2B_{i2}-B_{i3}\\-B_{i1}-B_{i2}+2B_{i3}\end{pmatrix}.$$

So the equivalently eliminated equation system of Eq. 6.188 is

$$\begin{pmatrix}U_{i1}\\U_{i2}\\U_{i3}\end{pmatrix}=\begin{pmatrix}L_{i1}\\L_{i2}\\L_{i3}\end{pmatrix}-\frac{1}{3}\begin{pmatrix}2B_{i1}-B_{i2}-B_{i3}\\-B_{i1}+2B_{i2}-B_{i3}\\-B_{i1}-B_{i2}+2B_{i3}\end{pmatrix}\cdot X_2\ ,\qquad P=\frac{1}{\sigma^2}\begin{pmatrix}E&0&0\\0&E&0\\0&0&E\end{pmatrix},\tag{6.189}$$

and the related least squares normal equation can be formed as

$$\frac{1}{3}\begin{pmatrix}2B_{i1}-B_{i2}-B_{i3}\\-B_{i1}+2B_{i2}-B_{i3}\\-B_{i1}-B_{i2}+2B_{i3}\end{pmatrix}^T\begin{pmatrix}2B_{i1}-B_{i2}-B_{i3}\\-B_{i1}+2B_{i2}-B_{i3}\\-B_{i1}-B_{i2}+2B_{i3}\end{pmatrix}X_2=\begin{pmatrix}2B_{i1}-B_{i2}-B_{i3}\\-B_{i1}+2B_{i2}-B_{i3}\\-B_{i1}-B_{i2}+2B_{i3}\end{pmatrix}^T\begin{pmatrix}L_{i1}\\L_{i2}\\L_{i3}\end{pmatrix}.\tag{6.190}$$

Alternatively, for the Eq. system 6.188, single differences can be formed using transformation (cf. Sect. 6.6.1):

$$C_s=\begin{pmatrix}-E&E&0\\0&-E&E\end{pmatrix}$$

and

$$P_s=[\mathrm{cov(SD)}]^{-1}=\frac{1}{3\sigma^2}\begin{pmatrix}2E&E\\E&2E\end{pmatrix}.$$

(c) ketabton.com: The Digital Library

The correlation problem appears in the case of single differences of multiple baselines. The related observation equations and the least squares normal equation can be written as

$$\begin{pmatrix} V_{i2}-V_{i1} \\ V_{i3}-V_{i2} \end{pmatrix} = \begin{pmatrix} L_{i2}-L_{i1} \\ L_{i3}-L_{i2} \end{pmatrix} - \begin{pmatrix} B_{i2}-B_{i1} \\ B_{i3}-B_{i2} \end{pmatrix} X_2 \ , \quad P_s \quad \text{and} \tag{6.191}$$

$$\begin{pmatrix} B_{i2}-B_{i1} \\ B_{i3}-B_{i2} \end{pmatrix}^T \begin{pmatrix} 2E & E \\ E & 2E \end{pmatrix} \begin{pmatrix} B_{i2}-B_{i1} \\ B_{i3}-B_{i2} \end{pmatrix} X_2 = \begin{pmatrix} B_{i2}-B_{i1} \\ B_{i3}-B_{i2} \end{pmatrix}^T \begin{pmatrix} 2E & E \\ E & 2E \end{pmatrix} \begin{pmatrix} L_{i2}-L_{i1} \\ L_{i3}-L_{i2} \end{pmatrix} . \tag{6.192}$$

Equations 6.190 and 6.192 are identical. This may be proved by expanding both equations and comparing the results. Again, this shows that the equivalently eliminated equations are equivalent to the single difference equations, however, without the need to deal with the correlation problem.

6.8.4 Equivalent Equations of Double Differences

Double differences cancel all the clock errors out of the observation equations. This can also be achieved by forming equivalent equations where all clock errors are eliminated. Considering Eq. 6.171 the original observation equation and X_1 the vector of all clock errors, the equivalent equation of double differences can be formed as outlined in Sect. 6.8.2.

In the case of two stations, supposing n common satellites ($k1, k2, \ldots, kn$) are observed at station $i1$ and $i2$, the equivalent single difference observation equation is then Eq. 6.183. Denoting $B_{s1} = B_{i2} - B_{i1}$, the station clock error parameter as $\delta t_{i1} - \delta t_{i2}$ (cf. Eqs. 6.89–6.92), and assigning the coefficients of the first column to the station clock errors, i.e., $B_{s1} = (I_{n\times 1}\ B_s)$, Eq. 6.183 turns out to be

$$\begin{pmatrix} U_{i1} \\ U_{i2} \end{pmatrix} = \begin{pmatrix} L_{i1} \\ L_{i2} \end{pmatrix} - \frac{1}{2} \begin{pmatrix} -I_{n\times 1} & -B_s \\ I_{n\times 1} & B_s \end{pmatrix} \begin{pmatrix} X_c \\ X_3 \end{pmatrix} \quad \text{and} \quad P = \frac{1}{\sigma^2} \begin{pmatrix} E & 0 \\ 0 & E \end{pmatrix} , \tag{6.193}$$

where X_c is the station clock error vector, X_3 is the other unknown vector, B_s is the X_3-related coefficient matrix, $I_{n\times 1}$ is a 1 matrix (where all elements are 1), and clock errors are scaled by the speed of light.

Comparing Eq. 6.193 with Eq. 6.171, one has (cf. Sect. 6.8.2)

$$A = \frac{1}{2} \begin{pmatrix} -I_{n\times 1} \\ I_{n\times 1} \end{pmatrix}, \quad B = \frac{1}{2} \begin{pmatrix} -B_s \\ B_s \end{pmatrix}, \quad L = \begin{pmatrix} L_{i1} \\ L_{i2} \end{pmatrix} \quad \text{and} \quad V = \begin{pmatrix} U_{i1} \\ U_{i2} \end{pmatrix} ,$$

and

$$M_{11} = \frac{1}{4} \begin{pmatrix} -I_{n\times 1}^T & I_{n\times 1}^T \end{pmatrix} \frac{1}{\sigma^2} \begin{pmatrix} E & 0 \\ 0 & E \end{pmatrix} \begin{pmatrix} -I_{n\times 1} \\ I_{n\times 1} \end{pmatrix} = \frac{n}{2\sigma^2} ,$$

$$J = \begin{pmatrix} -I_{n\times 1} \\ I_{n\times 1} \end{pmatrix} \frac{\sigma^2}{2n} \begin{pmatrix} -I_{n\times 1}^T & I_{n\times 1}^T \end{pmatrix} \cdot P = \frac{1}{2n} \begin{pmatrix} I_{n\times n} & -I_{n\times n} \\ -I_{n\times n} & I_{n\times n} \end{pmatrix} \quad \text{and}$$

(c) ketabton.com: The Digital Library

$$(E_{2n\times 2n}-J)\frac{1}{2}\begin{pmatrix}-B_s\\ B_s\end{pmatrix}=\frac{1}{2}\begin{pmatrix}-E_{n\times n}+\frac{1}{n}I_{n\times n}\\ E_{n\times n}-\frac{1}{n}I_{n\times n}\end{pmatrix}B_s\ .$$

So the equivalently eliminated equation system of Eq. 6.193 is

$$\begin{pmatrix}U_{i1}\\ U_{i2}\end{pmatrix}=\begin{pmatrix}L_{i1}\\ L_{i2}\end{pmatrix}-\frac{1}{2}\begin{pmatrix}-E_{n\times n}+\frac{1}{n}I_{n\times n}\\ E_{n\times n}-\frac{1}{n}I_{n\times n}\end{pmatrix}B_sX_3 \quad \text{and} \quad P=\frac{1}{\sigma^2}\begin{pmatrix}E & 0\\ 0 & E\end{pmatrix}, \tag{6.194}$$

where the receiver clock error vector X_c is eliminated, observable vector and weight matrix are unchanged. The normal equation has a simple form of

$$B_s^T\left(E_{n\times n}-\frac{1}{n}I_{n\times n}\right)B_sX_3=B_s^T\left(E_{n\times n}-\frac{1}{n}I_{n\times n}\right)(L_{i2}-L_{i1})\ . \tag{6.195}$$

Alternatively, the traditional single difference observation Eqs. 6.185 and 6.186 can be rewritten as

$$V_{i2}-V_{i1}=(L_{i2}-L_{i1})-\begin{pmatrix}I_{n\times 1} & B_s\end{pmatrix}\begin{pmatrix}X_c\\ X_3\end{pmatrix} \quad \text{or}$$

$$\begin{pmatrix}V_{i2}^1-V_{i1}^1\\ V_{i2}^k-V_{i1}^k\end{pmatrix}=\begin{pmatrix}L_{i2}^1-L_{i1}^1\\ L_{i2}^k-L_{i1}^k\end{pmatrix}-\begin{pmatrix}1 & B_s^1\\ I_{m\times 1} & B_s^k\end{pmatrix}\begin{pmatrix}X_c\\ X_3\end{pmatrix} \tag{6.196}$$

and

$$\text{cov}(\text{SD}(O))=C_s\sigma^2\begin{pmatrix}E & 0\\ 0 & E\end{pmatrix}C_s^T=2\sigma^2E \quad \text{and} \quad P_s=\frac{1}{2\sigma^2}E\ ,$$

where $m = n - 1$, and the superscript 1 and k denote the first row and remaining rows of the matrices (or columns in case of vectors). The double difference transformation matrix and covariance are (cf. Sect. 6.6.2, Eqs. 6.116–6.118)

$$C_d=\begin{pmatrix}-I_{m\times 1} & E_{m\times m}\end{pmatrix},$$

$$\text{cov}(\text{DD}(O))=C_d\,\text{cov}(\text{SD}(O))C_d^T=2\sigma^2C_dC_d^T=2\sigma^2\left(I_{m\times m}+E_{m\times m}\right) \quad \text{and}$$

$$P_d=[\text{cov}(\text{DD}(O))]^{-1}=\frac{1}{2\sigma^2n}\left(nE_{m\times m}-I_{m\times m}\right)\ .$$

The double difference observation equation and related normal equation are

$$C_d\begin{pmatrix}V_{i2}^1-V_{i1}^1\\ V_{i2}^k-V_{i1}^k\end{pmatrix}=C_d\begin{pmatrix}L_{i2}^1-L_{i1}^1\\ L_{i2}^k-L_{i1}^k\end{pmatrix}-C_d\begin{pmatrix}1 & B_s^1\\ I_{m\times 1} & B_s^k\end{pmatrix}\begin{pmatrix}X_c\\ X_3\end{pmatrix}$$

(c) ketabton.com: The Digital Library

or

$$C_{\mathrm{d}}\begin{pmatrix} V_{i2}^{1}-V_{i1}^{1} \\ V_{i2}^{k}-V_{i1}^{k} \end{pmatrix}=C_{\mathrm{d}}\begin{pmatrix} L_{i2}^{1}-L_{i1}^{1} \\ L_{i2}^{k}-L_{i1}^{k} \end{pmatrix}-C_{\mathrm{d}}\begin{pmatrix} B_{\mathrm{s}}^{1} \\ B_{\mathrm{s}}^{k} \end{pmatrix}X_3 \ ,$$

i.e.,

$$C_{\mathrm{d}}(V_{i2}-V_{i1})=C_{\mathrm{d}}(L_{i2}-L_{i1})-C_{\mathrm{d}}B_{\mathrm{s}}X_3 \tag{6.197}$$

and

$$B_{\mathrm{s}}^{T}C_{\mathrm{d}}^{T}P_{\mathrm{d}}C_{\mathrm{d}}B_{\mathrm{s}}X_3=B_{\mathrm{s}}^{T}C_{\mathrm{d}}^{T}P_{\mathrm{d}}C_{\mathrm{d}}(L_{i2}-L_{i1}) \ , \tag{6.198}$$

where

$$C_{\mathrm{d}}^{T}P_{\mathrm{d}}C_{\mathrm{d}}=\frac{1}{2\sigma^2 n}\left(-I_{m\times 1}\quad E_{m\times m}\right)^{T}\left(nE_{m\times m}-I_{m\times m}\right)\left(-I_{m\times 1}\quad E_{m\times m}\right) \ , \tag{6.199}$$

$$\left(-I_{m\times 1}\quad E_{m\times m}\right)^{T}\left(nE_{m\times m}-I_{m\times m}\right)=\left(-I_{m\times 1}\quad nE_{m\times m}-I_{m\times m}\right)^{T}\quad\text{and} \tag{6.200}$$

$$\left(-I_{m\times 1}\quad nE_{m\times m}-I_{m\times m}\right)^{T}\left(-I_{m\times 1}\quad E_{m\times m}\right)=nE_{n\times n}-I_{n\times n} \ . \tag{6.201}$$

The above three equations can be proved readily. Substituting Eqs. 6.199–6.201 into Eq. 6.198, then Eq. 6.198 turns out to be the same as Eq. 6.195. So the equivalency between the double difference equation and the directly formed equivalent Eq. 6.193 is proved.

6.8.5 Equivalent Equations of Triple Differences

Triple differences cancel all the clock errors and ambiguities out of the observation equations. This can also be achieved by forming equivalent equations where all clock errors and ambiguities are eliminated. Considering Eq. 6.171 the original observation equation and X_1 the parameter vector of all clock errors and ambiguities, then the equivalent equations of triple differences can be formed as outlined in Sect. 6.8.2.

It is well-known that traditional triple differences are correlated between adjacent epochs and between baselines. In the case of sequential (epoch by epoch) data processing of triple differences, the correlation problem is difficult to be dealt with. However, using the equivalently eliminated equations, the weight matrix remains diagonal. The GPS observables remain the original ones.

6.8.6 Method of Dealing with the Reference Parameters

In differential GPS data processing, the reference-related parameters are usually considered known and are fixed (or not adjusted). This may be realised by the a priori datum method (for details cf. Sect. 7.8.2). Here we just outline the basic principle.

(c) ketabton.com: The Digital Library

The equivalent observation Eq. system 6.179 can be rewritten as

$$U = L - \begin{pmatrix} D_1 & D_2 \end{pmatrix} \begin{pmatrix} X_{21} \\ X_{22} \end{pmatrix} \quad \text{and} \quad P, \tag{6.202}$$

where

$$D = \begin{pmatrix} D_1 & D_2 \end{pmatrix} \quad \text{and} \quad X_2 = \begin{pmatrix} X_{21} \\ X_{22} \end{pmatrix}.$$

Suppose there are a priori constraints of (cf. e.g. Zhou et al. 1997)

$$W = \overline{X}_{22} - X_{22} \quad \text{and} \quad P_2, \tag{6.203}$$

where $\overline{X}_{22}$ is the "directly observed" parameter sub-vector, P_2 is the weight matrix with respect to the parameter sub-vector X_{22}, and W is a residual vector, which has the same property as U. Usually, $\overline{X}_{22}$ is "observed" independently, so P_2 is a diagonal matrix. If X_{22} is a sub-vector of station coordinates, then the constraint of Eq. 6.203 is called a datum constraint. (This is also the reason why the name a priori datum is used). We consider here X_{22} a vector of reference-related parameters (such as clock errors and ambiguities of the reference satellite and reference station). Generally, the a priori weight matrix P_2 is given by covariance matrix Q_W and

$$P_2 = Q_W^{-1} \ . \tag{6.204}$$

In practice, the sub-vector $\overline{X}_{22}$ is usually a zero vector; this can be achieved through careful initialisation by forming observation Eq. 6.171.

The least squares normal equation of the a priori datum problem of Eqs. 6.202 and 6.203 can be formed (cf. Sect. 7.8.2). Compared with the normal equation of Eq. 6.202, the only difference between the two normal equations is that the a priori weight matrix P_2 has been added to the normal matrix. This indicates that the a priori datum problem can be dealt with simply by adding P_2 to the normal equation of observation Eq. 6.202.

If some diagonal components of the weight matrix P_2 is set to zero, then the related parameters (in X_{22}) are free parameters (or free datum) of the adjustment problem (without a priori constraints). Otherwise, parameters with a priori constraints are called a priori datum. Large weight indicates strong constraint and small weight indicates soft constraint. The strongest constraint is to keep the datum fixed. The reference-related datum (coordinates and clock errors as well as ambiguities) can be fixed by applying the strongest constraints to the related parameters, i.e., by adding the strongest constraints to the datum-related diagonal elements of the normal matrix.

6.8.7 Summary of the Unified Equivalent Algorithm

For any linearised zero-difference GPS observation Eq. system 6.171

$$V = L - \begin{pmatrix} A & B \end{pmatrix} \begin{pmatrix} X_1 \\ X_2 \end{pmatrix} \quad \text{and} \quad P, \tag{6.205}$$

(c) ketabton.com: The Digital Library

the X_1 eliminated equivalent GPS observation equation system is then Eq. 6.179:

$$U = L - (E - J)BX_2 \quad \text{and} \quad P, \tag{6.206}$$

where

$$J = AM_{11}^{-1}A^T P, \quad M_{11} = A^T PA,$$

E is an identity matrix, L is original observational vector, P is original weight matrix, and U is residual vector, which has the same property as V.

Similarly, the X_2 eliminated equivalent equation system is Eq. 6.181

$$U_1 = L - (E - K)AX_1 \quad \text{and} \quad P, \tag{6.207}$$

where

$$K = BM_{22}^{-1}B^T P, \quad M_{22} = B^T PB,$$

and U_1 is the residual vector (which has the same property as V).

Fixing the values of sub-vector X_{22} (of X_2) can be realised by adding the strongest constraints to the X_{22}-related diagonal elements of the normal matrix formed by Eq. 6.206. Alternatively, we may apply the strongest constraints directly to the normal equation formed by Eq. 6.205 first. In this way, the reference-related parameters (clock errors, ambiguities, coordinates, etc.) are fixed. And then we may form the equivalently eliminated observation Eq. 6.206. In this way, the relative and differential GPS data processing can be realised by using Eq. 6.206 after selecting the to be eliminated X_1.

The GPS data processing algorithm using Eq. 6.206 is then a selectively eliminated equivalent method. Selecting X_1 in Eq. 6.205 as a zero vector, then the algorithm is identical to the zero-difference method. Selecting X_1 in Eq. 6.205 as the satellite clock error vector, the vector of all clock errors, the clock error and ambiguity vector, and any user-defined vector, then the algorithm is equivalent to the single-difference method, double-difference method, triple-difference method, and user-defined eliminating method, respectively. The eliminated unknown X_1 can be solved separately if desired.

The advantages of this method are (compared with un-differential and differential methods):

- The un-differential and differential GPS data processing can be dealt with in an equivalent and unified way. The data processing scenarios can be selected by a switch and used in a combinative way;
- The eliminated parameters can be also solved separately with the same algorithm;
- The weight matrix remains the original diagonal one;
- The original observations are used; no differencing is required.

It is obvious that the described algorithm meanwhile has all the advantages of all un-differential and differential GPS data processing methods.

(c) ketabton.com: The Digital Library

Chapter 7

Adjustment and Filtering Methods

7.1 Introduction

Most useful and necessary adjustment and filtering algorithms for static and kinematic as well as dynamic GPS data processing are outlined in this chapter. The necessary estimators are derived. The relationships between the presented methods are also discussed in detail.

The adjustment algorithms discussed here include least squares adjustment, sequential application of least squares adjustment via accumulation, sequential least squares adjustment, conditional least squares adjustment, a sequential application of conditional least squares adjustment, block-wise least squares adjustment, a sequential application of block-wise least squares adjustment, a special application of block-wise least squares adjustment for code-phase combination, an equivalent algorithm to form the eliminated observation equation system and the algorithm to diagonalise the normal equation and equivalent observation equation.

The filtering algorithms discussed here include the classic Kalman filter, the sequential least squares adjustment method as a special case of Kalman filtering, the robust Kalman filter, and the adaptively robust Kalman filter.

A priori constrained adjustment and filtering are discussed for solving the rank deficient problems. After a general discussion on the a priori parameter constraints, a special case of the so-called a priori datum method is given. A quasi-stable datum method is also discussed.

A summary is given at the end of this chapter. The applications of the discussed methods in GPS data processing are outlined.

7.2 Least Squares Adjustment

The principle of least squares adjustment can be summarised as below (Gotthardt 1978; Cui et al. 1982):

1. The linearised observation equation system can be represented by:

$$V = L - AX \ , \quad P \tag{7.1}$$

where
L : observation vector of dimension m,
A : coefficient matrix of dimension $m \times n$,
X : unknown parameter vector of dimension n,
V : residual vector of dimension m,

(c) ketabton.com: The Digital Library

n : number of unknowns,
m: number of observations, and
P : symmetric and definite weight matrix of dimension $m \times m$.

2. The least squares criterion for solving the observation equations is well-known as

$$V^T PV = \min , \tag{7.2}$$

where V^T is the transpose of the related vector V.

3. To solve X and compute V, a function F is set as

$$F = V^T PV . \tag{7.3}$$

The function F reaches minimum value if the partial differentiation of F with respect to X equals zero, i.e.,

$$\frac{\partial F}{\partial X} = 2V^T P(-A) = 0$$

or

$$A^T PV = 0 , \tag{7.4}$$

where
A^T: transpose matrix of A.

4. Multiplying $A^T P$ with Eq. 7.1, one has

$$A^T PAX - A^T PL = -A^T PV . \tag{7.5}$$

Setting Eq. 7.4 into 7.5, one has:

$$A^T PAX - A^T PL = 0 . \tag{7.6}$$

5. For simplification, let $M = A^T PA$, $Q = M^{-1}$, where superscript $^{-1}$ is an inverse operator, and M is usually called a normal matrix. The least squares solution of Eq. 7.1 is then

$$X = Q(A^T PL) . \tag{7.7}$$

6. The precision of the i^{th} element of the estimated parameter is

$$p[i] = m_0 \sqrt{Q[i][i]} , \tag{7.8}$$

where i is the element index of a vector or a matrix, m_0 is the so-called standard deviation (or sigma), $p[i]$ is the i^{th} element of the precision vector, $Q[i][i]$ is the i^{th} diagonal element of the cofactor matrix Q, and

$$m_0 = \text{sqrt}(V^T PV / (m-n)), \quad \text{if} \quad (m > n) . \tag{7.9}$$

(c) ketabton.com: The Digital Library

7. For convenience of sequential computation, V^TPV can be calculated by using

$$V^TPV = L^TPL - (A^TPL)^TX\,. \tag{7.10}$$

This can be obtained by substituting Eq. 7.1 into V^TPV and considering Eq. 7.4. Up to now the complete formulas of least squares adjustment have been derived.

7.2.1 Least Squares Adjustment with Sequential Observation Groups

Suppose one has two sequential observation equation systems:

$$V_1 = L_1 - A_1X \tag{7.11}$$

and

$$V_2 = L_2 - A_2X\,, \tag{7.12}$$

with weight matrices P_1 and P_2. These two equation systems are un-correlated or independent and have the common unknown vector X. The combined problem can be represented as

$$\begin{pmatrix}V_1\\V_2\end{pmatrix} = \begin{pmatrix}L_1\\L_2\end{pmatrix} - \begin{pmatrix}A_1\\A_2\end{pmatrix}X \quad \text{and} \quad P = \begin{pmatrix}P_1 & 0\\0 & P_2\end{pmatrix}. \tag{7.13}$$

The least squares normal equation can be formed then as:

$$\begin{pmatrix}A_1^T & A_2^T\end{pmatrix}\begin{pmatrix}P_1 & 0\\0 & P_2\end{pmatrix}\begin{pmatrix}A_1\\A_2\end{pmatrix}X = \begin{pmatrix}A_1^T & A_2^T\end{pmatrix}\begin{pmatrix}P_1 & 0\\0 & P_2\end{pmatrix}\begin{pmatrix}L_1\\L_2\end{pmatrix}$$

or

$$(A_1^TP_1A_1 + A_2^TP_2A_2)X = (A_1^TP_1L_1 + A_2^TP_2L_2)\,. \tag{7.14}$$

This is indeed the accumulation of the two least squares normal equations formed from Eqs. 7.11 and 7.12, respectively:

$$(A_1^TP_1A_1)X = A_1^TP_1L_1 \tag{7.15}$$

and

$$(A_2^TP_2A_2)X = A_2^TP_2L_2\,. \tag{7.16}$$

The solution is then

$$X = (A_1^TP_1A_1 + A_2^TP_2A_2)^{-1}(A_1^TP_1L_1 + A_2^TP_2L_2)\,. \tag{7.17}$$

(c) ketabton.com: The Digital Library

The precision of the i^{th} element of the estimated parameter is

$$p[i] = m_0 \sqrt{Q[i][i]}\,, \tag{7.18}$$

where

$$m_0 = \sqrt{\frac{V^T PV}{m-n}}, \quad \text{if} \quad (m > n)\,, \tag{7.19}$$

and

$$Q = (A_1^T P_1 A_1 + A_2^T P_2 A_2)^{-1}\,, \tag{7.20}$$

where m is the number of total observations and n is the number of unknowns. And $V^T PV$ can be calculated by using

$$\begin{aligned} V^T PV &= V_1^T P_1 V_1 + V_2^T P_2 V_2 \\ &= L_1^T P_1 L_1 + L_2^T P_2 L_2 - (A_1^T P_1 L_1)^T X - (A_2^T P_2 L_2)^T X\,. \\ &= (L_1^T P_1 L_1 + L_2^T P_2 L_2) - (A_1^T P_1 L_1 + A_2^T P_2 L_2)^T X \end{aligned} \tag{7.21}$$

Equation 7.17 indicates that the sequential least squares problem can be solved by simply accumulating the normal equations of the observation equations. The weighted squares residuals can also be computed by accumulating the individual quadratic forms of the residuals using Eq. 7.21.

For further sequential and independent observation equation systems,

$$V_1 = L_1 - A_1 X\,, \quad P_1\,, \tag{7.22}$$

$$V_2 = L_2 - A_2 X\,, \quad P_2\,, \tag{7.23}$$

$$\cdots$$

$$V_i = L_i - A_i X\,, \quad P_i\,, \tag{7.24}$$

the solution can be similarly derived as:

$$X = (A_1^T P_1 A_1 + A_2^T P_2 A_2 + \ldots + A_i^T P_i A_i)^{-1} (A_1^T P_1 L_1 + A_2^T P_2 L_2 + \ldots + A_i^T P_i L_i) \tag{7.25}$$

and

$$V^T PV = (L_1^T P_1 L_1 + L_2^T P_2 L_2 + \ldots + L_i^T P_i L_i) - (A_1^T P_1 L_1 + A_2^T P_2 L_2 + \ldots + A_i^T P_i L_i)^T X\,. \tag{7.26}$$

It is obvious that if the solution is needed for every epoch, then the accumulated equation system has to be solved at each epoch. The accumulations always have to be made with the sequential normal equations. Of course, the solutions can be computed after a defined epoch or at the last epoch. This could be very useful if the solution of the problem is unstable at the beginning.

(c) ketabton.com: The Digital Library

7.3 Sequential Least Squares Adjustment

Recalling the discussions in Sect. 7.2, one has sequential observation equation systems

$$V_1 = L_1 - A_1 X\,, \quad P_1 \quad \text{and} \tag{7.27}$$

$$V_2 = L_2 - A_2 X\,, \quad P_2\,. \tag{7.28}$$

These two equation systems are un-correlated. The sequential problem can be then solved by accumulating the individual normal equations as discussed in Sect. 7.2:

$$(A_1^T P_1 A_1 + A_2^T P_2 A_2) X = (A_1^T P_1 L_1 + A_2^T P_2 L_2) \quad \text{or} \tag{7.29}$$

$$X = (A_1^T P_1 A_1 + A_2^T P_2 A_2)^{-1} (A_1^T P_1 L_1 + A_2^T P_2 L_2)\,. \tag{7.30}$$

And $V^T PV$ can be calculated by using

$$V^T PV = (L_1^T P_1 L_1 + L_2^T P_2 L_2) - (A_1^T P_1 L_1 + A_2^T P_2 L_2)^T X\,. \tag{7.31}$$

If Eq. 7.27 is solvable, then the least squares solution can be represented as

$$X = (A_1^T P_1 A_1)^{-1} (A_1^T P_1 L_1) \quad \text{and} \tag{7.32}$$

$$V^T PV = L_1^T P_1 L_1 - (A_1^T P_1 L_1)^T X\,. \tag{7.33}$$

For convenience, the estimated vector of X by using the first group of observations is denoted by X_1 and the quadratic form of the residuals by $(V^T PV)_1$ as well as $Q_1 = (A_1^T P_1 A_1)^{-1}$.

Using the formula (Cui et al. 1982; Gotthardt 1978)

$$(D + ACB)^{-1} = D^{-1} - D^{-1} AKB\, D^{-1}\,, \tag{7.34}$$

where A and B are any matrices, C and D are matrices that can be inversed and

$$K = (C^{-1} + BD^{-1} A)^{-1}\,, \tag{7.35}$$

the inversion of the accumulated normal matrix can be represented as Q:

$$\begin{aligned} Q &= (A_1^T P_1 A_1 + A_2^T P_2 A_2)^{-1} \\ &= (A_1^T P_1 A_1)^{-1} - (A_1^T P_1 A_1)^{-1} A_2^T K A_2 (A_1^T P_1 A_1)^{-1} \\ &= Q_1 - Q_1 A_2^T K A_2 Q_1 \\ &= (E - Q_1 A_2^T K A_2) Q_1 \end{aligned} \quad \text{and} \tag{7.36}$$

$$K = (P_2^{-1} + A_2 Q_1 A_2^T)^{-1}\,, \tag{7.37}$$

(c) ketabton.com: The Digital Library

where E is an identity matrix. The total term in the parenthesis on the right-hand side of Eq. 7.36 can be interpreted as a modifying factor for Q_1 matrix; in other words, due to the sequential Eq. 7.28, the Q matrix can be computed by multiplying a factor to the Q_1 matrix. So sequential least squares solution of Eqs. 7.27 and 7.28 can be obtained:

$$\begin{aligned} X &= (Q_1 - Q_1 A_2^T K A_2 Q_1)(A_1^T P_1 L_1 + A_2^T P_2 L_2) \\ &= (E - Q_1 A_2^T K A_2) X_1 + Q(A_2^T P_2 L_2) \end{aligned} . \tag{7.38}$$

Mathematically, the solutions of the sequential problem of Eqs. 7.27 and 7.28 that are solved by using accumulation of the least squares method as discussed in Sect. 7.2.1 or using sequential adjustment as discussed above shall be the same. However, in practice, accuracy of the computation is always limited by the effective digits of the computer being used. Such a limit on the effective digits causes an inaccuracy of numerical computation. And this inaccuracy will be accumulated and propagated in further computing processes. By comparing the results obtained with the above-mentioned methods, it is noticed that the sequential method will give a drift in the results. The drift increases with time and is generally not negligible after a long time interval.

7.4 Conditional Least Squares Adjustment

The principle of least squares adjustment with condition equations can be summarised as below (Gotthardt 1978; Cui et al. 1982):

1. The linearised observation equation system can be represented by Eq. 7.1 (cf. Sect. 7.2).
2. The corresponding condition equation system can be written as

$$CX - W = 0 , \tag{7.39}$$

   where
   C : coefficient matrix of dimension $r \times n$,
   W : constant vector of dimension r, and
   r : number of conditions.
3. The least squares criterion for solving the observation equations with condition equations is well-known as

$$V^T P V = \min , \tag{7.40}$$

   where V^T is the transpose of the related vector V.
4. To solve X and compute V, a function F can be formed as

$$F = V^T P V + 2K^T (CX - W) , \tag{7.41}$$

   where K is a gain vector (of dimension r) to be determined.

(c) ketabton.com: The Digital Library

The function F reaches minimum value if the partial differentiation of F with respect to X equals zero, i.e.,

$$\frac{\partial F}{\partial X} = 2V^T P(-A) + 2K^T C = 0\,;$$

then one has

$$-A^T PV + C^T K = 0 \tag{7.42}$$

or

$$A^T PAX + C^T K - A^T PL = 0\,, \tag{7.43}$$

where A^T, C^T are transpose matrices of A and C, respectively.

5. Combining Eqs. 7.43 and 7.39 together, one has

$$A^T PAX + C^T K - A^T PL = 0 \quad \text{and} \tag{7.44}$$

$$CX - W = 0\,. \tag{7.45}$$

6. For simplification, let $M = A^{\mathrm{T}}PA$, $W_1 = A^{\mathrm{T}}PL$, $Q = M^{-1}$, where superscript $^{-1}$ is an inverse operator. The solutions of Eqs. 7.44 and 7.45 are then

$$K = (CQC^T)^{-1}(CQW_1 - W)\,, \tag{7.46}$$

$$X = -Q(C^T K - W_1)$$

or

$$\begin{aligned} X &= (A^T PA)^{-1}(A^T PL) - (A^T PA)^{-1}C^T K \\ &= (A^T PA)^{-1}(A^T PL - C^T K) \end{aligned}\,. \tag{7.47}$$

7. The precisions of the solutions are then

$$p[i] = m_0\sqrt{Q_{\mathrm{c}}[i][i]}\,, \tag{7.48}$$

where i is the element index of a vector or a matrix, m_0 is the so-called standard deviation (or sigma), $p[i]$ is the i^{th} element of the precision vector, $Q_{\mathrm{c}}[i][i]$ is the i^{th} diagonal element of the quadratic matrix Q_{c}, and

$$Q_{\mathrm{c}} = Q - QC^T Q_2 CQ\,, \tag{7.49}$$

$$Q_2 = (CQC^T)^{-1} \quad \text{and} \tag{7.50}$$

$$m_0 = \sqrt{\frac{V^T PV}{m - n + r}}\,, \quad \text{if} \quad (m > n - r)\,. \tag{7.51}$$

(c) ketabton.com: The Digital Library

8. For convenience of sequential computation, $V^{\mathrm{T}}PV$ can be calculated by using

$$V^T PV = L^T PL - (A^T PL)^T X - W^T K \,. \tag{7.52}$$

This can be obtained by substituting Eq. 7.1 into V^TPV and using the relations of Eqs. 7.39 and 7.42.

Up to now the complete formulas of conditional least squares adjustment have been derived.

7.4.1 Sequential Application of Conditional Least Squares Adjustment

Recalling the least squares adjustment discussed in Sect. 7.2, the linearised observation equation system

$$V = L - AX \,, \quad P \tag{7.53}$$

has the solution

$$X = (A^T PA)^{-1}(A^T PL) \,. \tag{7.54}$$

The precisions of the solutions can be obtained by

$$p[i] = m_0 \sqrt{Q[i][i]} \,, \tag{7.55}$$

where

$$m_0 = \sqrt{\frac{V^T PV}{m-n}} \,, \quad \text{if} \quad (m > n) \,, \tag{7.56}$$

and V^TPV can be calculated by using

$$V^T PV = L^T PL - (A^T PL)^T X \,. \tag{7.57}$$

For convenience, the least squares solution vector is denoted by X_0 and weighted residuals square by $(V^TPV)_0$.

Similarly, in the conditional least squares adjustment discussed in Sect. 7.4, the linearised observation equation system and conditional equations read

$$V = L - AX \quad \text{and} \tag{7.58}$$

$$CX - W = 0 \,; \tag{7.59}$$

the solution follows

$$X = (A^T PA)^{-1}(A^T PL - C^T K) \,, \tag{7.60}$$

(c) ketabton.com: The Digital Library

where K is the gain, and

$$K = (CQC^T)^{-1}(CQW_1 - W)\,. \tag{7.61}$$

The precision vector of the solution vector can be obtained by using Eqs. 7.48–7.52. Using the notations obtained in least squares solution, one has

$$X = X_0 - QC^T K \quad \text{and} \tag{7.62}$$

$$V^T PV = (V^T PV)_0 + (A^T PL)^T QC^T K - W^T K\,. \tag{7.63}$$

Equation 7.62 indicates that the conditional least squares problem can be solved first without the conditions, and then through the gain K to compute a modification's term. The change of the solution is caused by the conditions. For computing the weighted squares of the residuals, Eq. 7.63 can be used (by adding two modification's terms to the weighted squares of residuals of the least squares solution). This property is very important for many practical applications such as ambiguity fixing or coordinates fixing. For example, after the least squares solution and fixing the ambiguity values, one needs to compute the ambiguity fixed solution. Of course, one can put the fixed ambiguities as known parameters and go back to solve the problem once again. However, using the above formulas, one can use the fixed ambiguities as conditions to compute the gain and the modification's terms to get the ambiguity fixed solution directly. Similarly, this property can be also used for solutions with some fixed station coordinates.

7.5 Block-Wise Least Squares Adjustment

The principle of block-wise least squares adjustment can be summarised as below (Gotthardt 1978; Cui et al. 1982):

1. The linearised observation equation system can be represented by Eq. 7.1 (cf. Sect. 7.2).
2. The unknown vector X and observable vector L is rewritten as two sub-vectors:

$$\begin{pmatrix} V_1 \\ V_2 \end{pmatrix} = \begin{pmatrix} L_1 \\ L_2 \end{pmatrix} - \begin{pmatrix} A_{11} & A_{12} \\ A_{21} & A_{22} \end{pmatrix} \begin{pmatrix} X_1 \\ X_2 \end{pmatrix} \quad \text{and} \quad P = \begin{pmatrix} P_1 & 0 \\ 0 & P_2 \end{pmatrix}. \tag{7.64}$$

The least squares normal equation can then be formed as:

$$\begin{pmatrix} A_{11} & A_{12} \\ A_{21} & A_{22} \end{pmatrix}^T \begin{pmatrix} P_1 & 0 \\ 0 & P_2 \end{pmatrix} \begin{pmatrix} A_{11} & A_{12} \\ A_{21} & A_{22} \end{pmatrix} \begin{pmatrix} X_1 \\ X_2 \end{pmatrix} = \begin{pmatrix} A_{11} & A_{12} \\ A_{21} & A_{22} \end{pmatrix}^T \begin{pmatrix} P_1 & 0 \\ 0 & P_2 \end{pmatrix} \begin{pmatrix} L_1 \\ L_2 \end{pmatrix}. \tag{7.65}$$

The normal equation can be denoted by

$$\begin{pmatrix} M_{11} & M_{12} \\ M_{21} & M_{22} \end{pmatrix} \begin{pmatrix} X_1 \\ X_2 \end{pmatrix} = \begin{pmatrix} B_1 \\ B_2 \end{pmatrix} \quad \text{or} \tag{7.66}$$

(c) ketabton.com: The Digital Library

$$M_{11}X_1 + M_{12}X_2 = B_1 \quad \text{and} \tag{7.67}$$

$$M_{21}X_1 + M_{22}X_2 = B_2\,, \tag{7.68}$$

where

$$M_{11} = A_{11}^T P_1 A_{11} + A_{21}^T P_2 A_{21}\,, \tag{7.69}$$

$$M_{12} = M_{21}^T = A_{11}^T P_1 A_{12} + A_{21}^T P_2 A_{22}\,, \tag{7.70}$$

$$M_{22} = A_{12}^T P_1 A_{12} + A_{22}^T P_2 A_{22}\,, \tag{7.71}$$

$$B_1 = A_{11}^T P_1 L_1 + A_{21}^T P_2 L_2 \quad \text{and} \tag{7.72}$$

$$B_2 = A_{12}^T P_1 L_1 + A_{22}^T P_2 L_2\,. \tag{7.73}$$

3. Normal Eqs. 7.67 and 7.68 can be solved as follows: from Eq. 7.67, one has

$$X_1 = M_{11}^{-1}(B_1 - M_{12}X_2)\,. \tag{7.74}$$

Substituting X_1 into Eq. 7.68, one gets a normal equation related to the second block of unknowns:

$$M_2 X_2 = R_2\,, \tag{7.75}$$

where

$$M_2 = M_{22} - M_{21}M_{11}^{-1}M_{12} \quad \text{and} \tag{7.76}$$

$$R_2 = B_2 - M_{21}M_{11}^{-1}B_1\,. \tag{7.77}$$

The solution of Eq. 7.75 is then:

$$X_2 = M_2^{-1}R_2\,. \tag{7.78}$$

From Eqs. 7.78 and 7.74, the block-wise least squares solution of Eqs. 7.1 and 7.64 can be computed. For estimating the precision of the solved vector, one has (see discussion in Sect. 7.2):

$$p[i] = m_0\sqrt{Q[i][i]} \tag{7.79}$$

where

$$m_0 = \sqrt{\frac{V^T PV}{m-n}}\,, \quad \text{if} \quad (m > n)\,. \tag{7.80}$$

Q is the inversion of the total normal matrix M. m is the number of total observations, and n is the number of unknowns.

(c) ketabton.com: The Digital Library

Furthermore,

$$Q=\begin{pmatrix} M_{11} & M_{12} \\ M_{21} & M_{22} \end{pmatrix}^{-1} = \begin{pmatrix} Q_{11} & Q_{12} \\ Q_{21} & Q_{22} \end{pmatrix} \quad \text{is denoted,} \tag{7.81}$$

where (Gotthardt 1978; Cui et al. 1982)

$$Q_{11}=(M_{11}-M_{12}M_{22}^{-1}M_{21})^{-1}\,, \tag{7.82}$$

$$Q_{22}=(M_{22}-M_{21}M_{11}^{-1}M_{12})^{-1}\,, \tag{7.83}$$

$$Q_{12}=M_{11}^{-1}(-M_{12}Q_{22})\,, \quad \text{and} \tag{7.84}$$

$$Q_{21}=M_{22}^{-1}(-M_{21}Q_{11})\,. \tag{7.85}$$

And V^TPV can be calculated by using

$$V^TPV=L^TPL-(A^TPL)^TX\,. \tag{7.86}$$

One finds very important applications in GPS data processing by separating the unknowns into two groups, which will be discussed in the next sub-section.

7.5.1 Sequential Solution of Block-Wise Least Squares Adjustment

Suppose one has two sequential observation equation systems

$$V_{t1}=L_{t1}-A_{t1}Y_{t1} \quad \text{and} \tag{7.87}$$

$$V_{t2}=L_{t2}-A_{t2}Y_{t2}\,, \tag{7.88}$$

with weight matrices P_{t1} and P_{t2}. The unknown vector Y can be separated into two sub-vectors, one is sequential dependent, and another is time independent. Let us assume

$$Y_{t1}=\begin{pmatrix} X_{t1} \\ X_2 \end{pmatrix} \quad \text{and} \quad Y_{t2}=\begin{pmatrix} X_{t2} \\ X_2 \end{pmatrix}, \tag{7.89}$$

where X_2 is the common unknown vector, and X_{t1} and X_{t2} are sequential (time) independent unknowns (i.e., they are different from each other).

Equations 7.87 and 7.88 can be solved separately by using the block-wise least squares method as follows (cf. Sect. 7.5):

$$X_{t1}=(M_{11})_{t1}^{-1}(B_1-M_{12}X_2)_{t1}\,, \tag{7.90}$$

$$(M_2)_{t1}X_2=(R_2)_{t1} \quad \text{and} \tag{7.91}$$

$$X_2=(M_2)_{t1}^{-1}(R_2)_{t1}\,, \tag{7.92}$$

(c) ketabton.com: The Digital Library

and

$$X_{t2} = (M_{11})_{t2}^{-1}(B_1 - M_{12}X_2)_{t2}\,, \tag{7.93}$$

$$(M_2)_{t2}X_2 = (R_2)_{t2} \quad \text{and} \tag{7.94}$$

$$X_2 = (M_2)_{t2}^{-1}(R_2)_{t2}\,, \tag{7.95}$$

where indices $t1$ and $t2$ outside of the parenthesis indicate that the matrices and vectors are related to Eqs. 7.87 and 7.88, respectively.

The combined solution of Eqs. 7.87 and 7.88 then can be derived as:

$$X_{t1} = (M_{11})_{t1}^{-1}((B_1)_{t1} - (M_{12})_{t1}(X_2)_{ta})\,, \tag{7.96}$$

$$X_{t2} = (M_{11})_{t2}^{-1}((B_1)_{t2} - (M_{12})_{t2}(X_2)_{ta})\,, \tag{7.97}$$

$$((M_2)_{t1} + (M_2)_{t2})(X_2)_{ta} = (R_2)_{t1} + (R_2)_{t2} \quad \text{and} \tag{7.98}$$

$$(X_2)_{ta} = ((M_2)_{t1} + (M_2)_{t2})^{-1}((R_2)_{t1} + (R_2)_{t2})\,, \tag{7.99}$$

where index ta means that the solution is related to all equations. The normal equations related to the common unknowns are accumulated and solved for. The solved common unknowns are used for computing sequentially different unknowns.

In the case of many sequential observations, a combined solution could be difficult or even impossible because of the large number of unknowns and the requirement of the computing capacities. Therefore, a sequential solution could be a good alternative. For the sequential observation equations

$$V_{t1} = L_{t1} - A_{t1}Y_{t1}\,, \quad P_{t1}\,, \tag{7.100}$$

…

$$V_{ti} = L_{ti} - A_{ti}Y_{ti}\,, \quad P_{ti}\,, \tag{7.101}$$

the sequential solutions are

$$X_{t1} = (M_{11})_{t1}^{-1}(B_1 - M_{12}X_2)_{t1}\,, \tag{7.102}$$

$$(M_2)_{t1}X_2 = (R_2)_{t1}\,, \tag{7.103}$$

$$X_2 = (M_2)_{t1}^{-1}(R_2)_{t1}\,, \tag{7.104}$$

…

$$X_{ti} = (M_{11})_{ti}^{-1}((B_1)_{ti} - (M_{12})_{ti}X_2)\,, \tag{7.105}$$

$$((M_2)_{t1} + \ldots + (M_2)_{ti})X_2 = (R_2)_{t1} + \ldots + (R_2)_{ti} \quad \text{and} \tag{7.106}$$

$$X_2 = ((M_2)_{t1} + \ldots + (M_2)_{ti})^{-1}((R_2)_{t1} + \ldots + (R_2)_{ti})\,. \tag{7.107}$$

(c) ketabton.com: The Digital Library

It is notable that the sequential solution of the second unknown sub-vector X_2 is exactly the same as the combined solution at the last step. The only difference between the combined solution and the sequential solution is that the X_2 used are different. In the sequential solution, only the up-to-date X_2 is used. Therefore at end of the sequential solution (Eq. 7.107), the last obtained X_2 has to be sub-stituted into all X_{tj} computing formulas, where $j < i$. This can be done in two ways. The first way is to remember all formulas for computing X_{tj}, after X_2 is obtained from Eq. 7.107, using X_2 to compute X_{tj}. The second way is to go back to the beginning after the X_2 is obtained, and use X_2 as the known vector to solve X_{tj} once again. In these ways, the combined sequential observation equations can be solved exactly in a sequential way.

7.5.2 Block-Wise Least Squares for Code-Phase Combination

Recalling the block-wise observation equations discussed in Sect. 7.5, one has

$$\begin{pmatrix} V_1 \\ V_2 \end{pmatrix} = \begin{pmatrix} L_1 \\ L_2 \end{pmatrix} - \begin{pmatrix} A_{11} & A_{12} \\ A_{21} & A_{22} \end{pmatrix} \begin{pmatrix} X_1 \\ X_2 \end{pmatrix} \quad \text{and} \quad P = \begin{pmatrix} P_1 & 0 \\ 0 & P_2 \end{pmatrix}. \tag{7.108}$$

Such an observation equation can be used for solving the problem of codephase combination. Supposing L_1 and L_2 are phase and code observation vectors, respectively, and they have the same dimensions, then X_2 is a sub-vector that only exists in phase observational equations. Then one has $A_{22} = 0$, and $A_{11} = A_{21}$, as well as $P_1 = w_p P_0$, $P_2 = w_c P_0$, where P_0 is the weight matrix, and w_p and w_c are weight factors of phase and code observables. In order to keep the coefficient matrices $A_{11} = A_{21}$, the observable vectors L_1 and L_2 have to be carefully scaled. Equation 7.108 can be rewritten as:

$$\begin{pmatrix} V_1 \\ V_2 \end{pmatrix} = \begin{pmatrix} L_1 \\ L_2 \end{pmatrix} - \begin{pmatrix} A_{11} & A_{12} \\ A_{11} & 0 \end{pmatrix} \begin{pmatrix} X_1 \\ X_2 \end{pmatrix} \quad \text{and} \quad P = \begin{pmatrix} w_p P_0 & 0 \\ 0 & w_c P_0 \end{pmatrix}. \tag{7.109}$$

The least squares normal equation can be formed then as:

$$\begin{aligned} &\begin{pmatrix} A_{11} & A_{12} \\ A_{11} & 0 \end{pmatrix}^T \begin{pmatrix} w_p P_0 & 0 \\ 0 & w_c P_0 \end{pmatrix} \begin{pmatrix} A_{11} & A_{12} \\ A_{11} & 0 \end{pmatrix} \begin{pmatrix} X_1 \\ X_2 \end{pmatrix} \\ &= \begin{pmatrix} A_{11} & A_{12} \\ A_{11} & 0 \end{pmatrix}^T \begin{pmatrix} w_p P_0 & 0 \\ 0 & w_c P_0 \end{pmatrix} \begin{pmatrix} L_1 \\ L_2 \end{pmatrix}. \end{aligned} \tag{7.110}$$

The normal equation can be denoted by

$$\begin{pmatrix} M_{11} & M_{12} \\ M_{21} & M_{22} \end{pmatrix} \begin{pmatrix} X_1 \\ X_2 \end{pmatrix} = \begin{pmatrix} B_1 \\ B_2 \end{pmatrix} \tag{7.111}$$

where

$$M_{11} = (w_p + w_c) A_{11}^T P_0 A_{11}, \tag{7.112}$$

(c) ketabton.com: The Digital Library

$$M_{12} = M_{21}^T = w_p A_{11}^T P_0 A_{12}\,, \tag{7.113}$$

$$M_{22} = w_p A_{12}^T P_0 A_{12}\,, \tag{7.114}$$

$$B_1 = A_{11}^T P_0 (w_p L_1 + w_c L_2) \quad \text{and} \tag{7.115}$$

$$B_2 = w_p A_{12}^T P_0 L_1\,. \tag{7.116}$$

Normal equation 7.111 can be solved using the general formulas derived in Sect. 7.2 and Sect. 7.5.

7.6 Equivalently Eliminated Observation Equation System

In least squares adjustment, the unknowns can be divided into two groups and then solved in a block-wise manner as discussed in Sect. 7.5. In practice, sometimes only one group of unknowns is of interest, and it is better to eliminate the other group of unknowns (called nuisance parameters) because of its size, for example. In this case, using the so-called equivalently eliminated observation equation system could be very beneficial (Wang et al. 1988; Xu and Qian 1986; Zhou 1985). The nuisance parameters can be eliminated directly from the observation equations instead of from the normal equations.

The linearised observation equation system can be represented by

$$V = L - \begin{pmatrix} A & B \end{pmatrix} \begin{pmatrix} X_1 \\ X_2 \end{pmatrix}, \quad P\,, \tag{7.117}$$

where

L : observational vector of dimension m,
A, B : coefficient matrices of dimension $m \times (n - r)$ and $m \times r$,
X_1, X_2 : unknown vectors of dimension $n - r$ and r,
V : residual vector of dimension m,
n : number of total unknowns,
m : number of observations, and
P : symmetric and definite weight matrix, of dimension $m \times m$.

The least squares normal equation can then be formed by

$$\begin{pmatrix} M_{11} & M_{12} \\ M_{21} & M_{22} \end{pmatrix} \begin{pmatrix} X_1 \\ X_2 \end{pmatrix} = \begin{pmatrix} B_1 \\ B_2 \end{pmatrix}. \tag{7.118}$$

where

$$\begin{pmatrix} M_{11} & M_{12} \\ M_{21} & M_{22} \end{pmatrix} = \begin{pmatrix} A^T PA & A^T PB \\ B^T PA & B^T PB \end{pmatrix}, \tag{7.119}$$

where

$$B_1 = A^T PL\,, \quad B_2 = B^T PL\,. \tag{7.120}$$

(c) ketabton.com: The Digital Library

The elimination matrix

$$\begin{pmatrix} E & 0 \\ -Z & E \end{pmatrix} \quad \text{is formed,} \tag{7.121}$$

where E is the identity matrix, 0 is a zero matrix, and $Z = M_{21}M_{11}^{-1}$. M_{11}^{-1} is the inversion of M_{11}. Multiplying the elimination matrix Eq. 7.121 to the normal Eq. 7.118 one has

$$\begin{pmatrix} E & 0 \\ -Z & E \end{pmatrix}\begin{pmatrix} M_{11} & M_{12} \\ M_{21} & M_{22} \end{pmatrix}\begin{pmatrix} X_1 \\ X_2 \end{pmatrix}=\begin{pmatrix} E & 0 \\ -Z & E \end{pmatrix}\begin{pmatrix} B_1 \\ B_2 \end{pmatrix}, \quad \text{or}$$

$$\begin{pmatrix} M_{11} & M_{12} \\ 0 & M_2 \end{pmatrix}\begin{pmatrix} X_1 \\ X_2 \end{pmatrix}=\begin{pmatrix} B_1 \\ R_2 \end{pmatrix} \tag{7.122}$$

where

$$\begin{aligned} M_2 &= -M_{21}M_{11}^{-1}M_{12} + M_{22} \\ &= B^T PB - B^T PAM_{11}^{-1}A^T PB = B^T P(E - AM_{11}^{-1}A^T P)B\,. \end{aligned} \tag{7.123}$$

$$R_2 = B_2 - M_{21}M_{11}^{-1}B_1 = B^T P(E - AM_{11}^{-1}A^T P)L\,. \tag{7.124}$$

If one is only interested in the unknown vector X_2, one just needs to solve the second equation of 7.122. The solution is identical to that of solving whole Eq. 7.122. The above eliminating process is similar with the Gauss-Jordan algorithm, which has often been used for the inversion of the normal matrix (or for solving linear equation system). Indeed, the second equation of 7.122 is identical to Eq. 7.75 derived in the block-wise least squares adjustment (cf. Sect. 7.5).

Letting

$$J = AM_{11}^{-1}A^T P\,, \tag{7.125}$$

one has properties of

$$J^2 = (AM_{11}^{-1}A^T P)(AM_{11}^{-1}A^T P) = AM_{11}^{-1}A^T P\,AM_{11}^{-1}A^T P = AM_{11}^{-1}A^T P = J\,,$$

$$(E-J)(E-J) = E^2 - 2EJ + J^2 = E - 2J + J = E - J \quad \text{and}$$

$$\left[P(E-J)\right]^T = (E-J^T)P = P - (AM_{11}^{-1}A^T P)^T P = P - PAM_{11}^{-1}A^T P = P(E-J)\,,$$

i.e., matrices J and $(E - J)$ are idempotent and $(E - J)^T P$ is symmetric, or

$$J^2 = J\,, \quad (E-J)^2 = E - J \quad \text{and} \quad (E-J)^T P = P(E-J)\,. \tag{7.126}$$

Using the above derived properties, M_2 in Eq. 7.123 and R_2 in Eq. 7.124 can be re-written as

$$M_2 = B^T P(E-J)B = B^T P(E-J)(E-J)B = B^T (E-J)^T P(E-J)B \quad \text{and} \tag{7.127}$$

$$R_2 = B^T P(E-J)L = B^T (E-J)^T PL\,. \tag{7.128}$$

(c) ketabton.com: The Digital Library

Denoting

$$D_2 = (E - J)B\,, \tag{7.129}$$

then the eliminated normal equation (the secons equation of 7.122) can be rewritten as

$$B^T(E-J)^T P(E-J)BX_2 = B^T(E-J)^T PL \quad \text{or} \tag{7.130}$$

$$D_2^T P D_2 X_2 = D_2^T PL\,. \tag{7.131}$$

This is the least squares normal equation of the following linear observation equation:

$$U_2 = L - D_2 X_2\,, \quad P \quad \text{or} \tag{7.132}$$

$$U_2 = L - (E-J)BX_2\,, \quad P\,, \tag{7.133}$$

where L and P are the original observational vector and weight matrix, and U_2 is the residual vector, which has the same property as V in Eq. 7.117.

The advantage of using Eq. 7.133 is that the unknown vector X_1 has been eliminated; however, L vector and P matrix remain the same as the originals. Applications of this theory can be found in Sect. 6.8, 8.3 and 9.2.

7.6.1 Diagonalised Normal Equation and the Equivalent Observation Equation

In least squares adjustment, the unknowns can be divided into two groups. One group of unknowns can be eliminated by matrix partitioning to obtain an equivalently eliminated normal equation system of the other group of unknowns. Using the elimination process twice for the two groups of unknowns respectively, the normal equation can be diagonalised. The algorithm can be outlined as follows.

A linearised observation equation and the normal equations can be represented by Eqs. 7.117 and 7.118. From the first equation of 7.118, one has

$$X_1 = M_{11}^{-1}(B_1 - M_{12}X_2)\,. \tag{7.134}$$

Setting X_1 into the second equation of 7.118, one gets an equivalently eliminated normal equation of X_2:

$$M_2 X_2 = R_2\,, \tag{7.135}$$

where

$$\begin{aligned} M_2 &= M_{22} - M_{21}M_{11}^{-1}M_{12} \\ R_2 &= B_2 - M_{21}M_{11}^{-1}B_1 \end{aligned}\,. \tag{7.136}$$

Similarly, from the second equation of 7.118, one has

$$X_2 = M_{22}^{-1}(B_2 - M_{21}X_1)\,. \tag{7.137}$$

(c) ketabton.com: The Digital Library

Setting X_2 into the first equation of 7.118, one gets an equivalently eliminated normal equation of X_1:

$$M_1 X_1 = R_1 , \tag{7.138}$$

where

$$\begin{aligned} M_1 &= M_{11} - M_{12} M_{22}^{-1} M_{21} \\ R_1 &= B_1 - M_{12} M_{22}^{-1} B_2 \end{aligned} . \tag{7.139}$$

Combining Eqs. 7.138 and 7.135 together, one has

$$\begin{pmatrix} M_1 & 0 \\ 0 & M_2 \end{pmatrix} \begin{pmatrix} X_1 \\ X_2 \end{pmatrix} = \begin{pmatrix} R_1 \\ R_2 \end{pmatrix}, \tag{7.140}$$

where (cf., e.g., Cui et al. 1982; Gotthardt 1978)

$$\begin{aligned} Q_{11} &= M_1^{-1}, & Q_{22} &= M_2^{-1} \\ Q_{12} &= -M_{11}^{-1}(M_{12} Q_{22}), & Q_{21} &= -M_{22}^{-1}(M_{21} Q_{11}) \end{aligned} . \tag{7.141}$$

It is obvious that Eqs. 7.118 and 7.140 are two equivalent normal equations. The solutions of the both equations are identical. Equation 7.140 is a diagonalised normal equation related to X_1 and X_2. The process of forming Eq. 7.140 from Eq. 7.118 is called the diagonalisation process of a normal equation.

As discussed in Sect. 7.6, the equivalently eliminated observation equation of the second equation of 7.140 is Eq. 7.133. Similarly, if denote

$$I = B M_{22}^{-1} B^T P \quad \text{and}$$

$$D_1 = (E - I) A ,$$

then the equivalently eliminated observation equation of the first normal equation of Eq. 7.140 has a form of

$$U_1 = L - (E - I) A X_1 , \quad P .$$

Where U_1 is a residual vector which has the same property as V in Eq. 7.117. L and P are the original observational vector and weight matrix.

Above equation and Eq. 7.133 can be written together as

$$\begin{pmatrix} U_1 \\ U_2 \end{pmatrix} = \begin{pmatrix} L \\ L \end{pmatrix} - \begin{pmatrix} D_1 & 0 \\ 0 & D_2 \end{pmatrix} \begin{pmatrix} X_1 \\ X_2 \end{pmatrix}, \quad \begin{pmatrix} P & 0 \\ 0 & P \end{pmatrix} . \tag{7.142}$$

Equation 7.142 is derived from the normal Eq. 7.140; therefore, it is true inversely, i.e., Eq. 7.140 is the least squares normal equation of the observation Eq. 7.142. Equations 7.118 and 7.140 are normal equations of the observation Eqs. 7.117 and 7.142. So Eq. 7.142 is an equivalent observation equation of Eq. 7.117. Equations 7.140 and 7.142 are called diagonalised equations of 7.118 and 7.117, respectively.

(c) ketabton.com: The Digital Library

7.7 Kalman Filter

7.7.1 Classic Kalman Filter

The principle of the classical Kalman filter can be summarised as below (Yang et al. 1999):

The linearised observation equation system can be represented by

$$V_i = L_i - A_i X_i \quad P_i \,, \tag{7.143}$$

where
L : observational vector of dimension m,
A : coefficient matrix of dimension $m \times n$,
X : unknown vector of dimension n,
V : residual vector of dimension m,
n : number of unknowns,
m : number of observations,
i : sequential index, $i = 1, 2, 3, \ldots$, and
P_i : weight matrix of index i.

Suppose system equations are known and can be presented as

$$U_i = X_i - F_{i,i-1} X_{i-1} \,, \quad i = 2, 3, \ldots \,, \tag{7.144}$$

where
F : transition matrix of dimension $n \times n$, and
U : residual vector of dimension n.

U and V are un-correlated and have zero expectations. Using the covariance propagation law, one has from Eq. 7.144

$$Q(X_i) = F_{i,i-1} Q(X_{i-1}) (F_{i,i-1})^T + Q_U \,. \tag{7.145}$$

The normal Eq. 7.143 can be formed as

$$M_i X_i = B_i \,. \tag{7.146}$$

For the initial step or epoch, i.e., $i = 1$, Eq. 7.146 has the solution under the least squares principle

$$\tilde{X}_i = Q_i B_i \,, \quad \text{where} \quad Q_i = M_i^{-1} \,, \tag{7.147}$$

and here one will assume

$$\tilde{Q}_i = Q_i \,, \tag{7.148}$$

(c) ketabton.com: The Digital Library

where $\tilde{X}_i$ and $\tilde{Q}_i$ are called estimated values. Using the estimated values and transition matrix, one can predict the unknown values and covariance matrix of the next epoch (say $i = 2$):

$$\underline{X}_i = F_{i,i-1}\tilde{X}_{i-1} \quad \text{and} \tag{7.149}$$

$$\underline{Q}_i = F_{i,i-1}\tilde{Q}_{i-1}(F_{i,i-1})^T + Q_U\,, \tag{7.150}$$

where $\underline{X}_i$ and $\underline{Q}_i$ are called predicted values (vector and matrix). Then estimated values of this epoch can be calculated by

$$\tilde{X}_i = \underline{X}_i + K(L_i - A_i\underline{X}_i)\,, \tag{7.151}$$

$$\tilde{Q}_i = (E - KA_i)\underline{Q}_i \quad \text{and} \tag{7.152}$$

$$K = \underline{Q}_i A_i^T (A_i \underline{Q}_i A_i^T + Q_V)^{-1}\,, \tag{7.153}$$

where K is the gain matrix.

For the next sequential step i, the predicted values have to be computed by using Eqs. 7.149 and 7.150, and the estimated values can be computed by using Eqs. 7.151 and 7.152. Such an iterative process is called Kalman filtering.

In classical Kalman filtering, it is assumed that for the problem of Eq. 7.143 there exists a system transition matrix $F_{i,i-1}$ in Eq. 7.144 and the cofactor Q_U. Therefore, the estimated values in the Kalman filter process are dependent on $F_{i,i-1}$ and Q_U. The transition matrix shall be based on strengthened physical models, and the cofactor shall be well-known or reasonably given. If the system description is accurate enough, of course Kalman filtering will lead to a more precise solution. However, if the system is not sufficiently well-known, the results of Kalman filter will sometimes not converge to the true values (divergence). Furthermore, a kinematic process is generally difficult to be precisely represented by theoretical system equations. However, for a dynamic process (like on-board GPS for satellite to satellite tracking or orbit determination) the system equation can be well-formulated (by an orbital equation of motion). Another problem of Kalman filtering is the strong dependency of the given initial values. Many studies have been made in this area to overcome the above-mentioned shortages.

7.7.2
Kalman Filter – A General Form of Sequential Least Squares Adjustment

The sequential Least Squares problem is a special case of the classic Kalman filter. If one lets

$$F_{i,i-1} = E\,, \tag{7.154}$$

then the system Eq. 7.144 in Sect. 7.7.1 turns out to be

$$X_i = X_{i-1}, \quad U = 0 \quad \text{and} \quad Q_U = 0\,. \tag{7.155}$$

(c) ketabton.com: The Digital Library

The Kalman filter process is then as follows, for the initial step or epoch, i.e., $i = 1$, Eq. 7.27 in Sect. 7.3 has the solution under the least squares principle:

$$\tilde{X}_i = Q_i B_i\,, \quad Q_i = M_i^{-1}\,, \tag{7.156}$$

with

$$\tilde{Q}_i = Q_i\,, \tag{7.157}$$

where $\tilde{X}_i$ and $\tilde{Q}_i$ are called estimated values. The predicted unknown values and covariance matrix of the next epoch (say $i = 2$) of Eqs. 7.149 and 7.150 in Sect. 7.7.1 are then

$$\underline{X}_i = \tilde{X}_{i-1} \quad \text{and} \tag{7.158}$$

$$\underline{Q}_i = \tilde{Q}_{i-1}\,. \tag{7.159}$$

The estimated values of Eqs. 7.151, 7.152 and 7.153 in Sect. 7.7.1 can be simplified as

$$\tilde{X}_i = \tilde{X}_{i-1} + G(L_i - A_i\tilde{X}_{i-1})\,, \tag{7.160}$$

$$\tilde{Q}_i = (E - GA_i)\tilde{Q}_{i-1} \quad \text{and} \tag{7.161}$$

$$G = \tilde{Q}_{i-1}A_i^T(A_i\tilde{Q}_{i-1}A_i^T + Q_V)^{-1}\,, \tag{7.162}$$

where G denotes the gain matrix. If one notices that $Q_V = (P_i)^{-1}$ and applies the formula of Bennet (Cui et al. 1982; Koch 1986), one has:

$$\tilde{Q}_{i-1}A_i^T(A_i\tilde{Q}_{i-1}A_i^T + Q_V)^{-1} = \tilde{Q}_{i-1}A_i^T P_i\,. \tag{7.163}$$

Equation 7.160 can then be rewritten as

$$\begin{aligned}\tilde{X}_i &= (E - GA_i)\tilde{X}_{i-1} + GL_i \\ &= (E - GA_i)\tilde{X}_{i-1} + \tilde{Q}_i A_i^T P_i L_i\end{aligned}\,. \tag{7.164}$$

Comparing the derived Eqs. 7.161 and 7.164 with the Eqs. 7.36 and 7.38 derived in Sect. 7.3, one can easily find out that they are identical. Therefore, the sequential least squares adjustment is a special case of Kalman filtering.

7.7.3 Robust Kalman Filter

The classical Kalman filter is suitable for real time applications. The key problem of Kalman filtering is the divergence caused by the inexact descriptions of system equations and its statistic properties, as well as the divergence caused by data with inhomogeneous precisions.

Efforts have been made to modify the performance of Kalman filtering. In the classical Kalman filter, the weight matrix P of the observables is a static one, i.e., P is as-

(c) ketabton.com: The Digital Library

sumed to be a definite matrix. Taking the residuals of Kalman filtering into account, one may adjust the weight P of the observables accordingly. Such a process is called a robust Kalman filter (Koch and Yang 1998; Yang 1999).

Usually the observations are either accepted or rejected in least squares adjustment and the classical Kalman filter. In other words, the weight is either set as one (accepted) or zero (rejected). In the robust Kalman filter, a continuous weight between one and zero is introduced.

Originally one has $P = (Q_V)^{-1}$, the adjusted P is denoted by $\bar{P}$; then the Eq. 7.153 in the classical Kalman filter can be rewritten as

$$K = \underline{Q}_i A_i^T (A_i \underline{Q}_i A_i^T + \bar{P}_i^{-1})^{-1} . \tag{7.165}$$

In the case of independent observations, P_i is a diagonal matrix. Taking the residuals into account, P_i may be adjusted as (Huber 1964; Yang et al. 2000)

$$\bar{P}_i(k) = \begin{cases} P_i(k) & \text{if } |V_i(k)/\sigma_i| \le c \\ P_i(k)\dfrac{c}{|V_i(k)/\sigma_i|} & \text{if } |V_i(k)/\sigma_i| > c \end{cases}, \tag{7.166}$$

where $V_i(k)$ is the k^{th} element of the vector V, $P_i(k)$ is the diagonal element of matrix P_i, and c is a constant, which is usually chosen as 1.3~2.0 (Yang et al. 2000). V_i is the residual of the observation L_i, σ_i is the standard deviation of the i^{th} epoch, and $P_i = 1/\sigma_i$. In this way, the weight of the observation L_i is adjusted due to the related residual.

If the observations are correlated with each other, the weight matrix may be given by (Yang et al. 2000)

$$\bar{P}_{kj} = \begin{cases} P_{kj} & \text{if } |V_i(k)/\sigma_i| \le c \text{ and } |V_i(j)/\sigma_i| \le c \\ P_{kj}\dfrac{c}{\max\{|V_i(k)/\sigma_i|, |V_i(j)/\sigma_i|\}} & \text{if } |V_i(k)/\sigma_i| > c \text{ or } |V_i(j)/\sigma_i| > c \end{cases}. \tag{7.167}$$

It is obvious that an adjusted weight matrix can better reflect the different data quality and can better fit the reality of the observations.

Usually the outlier will be rejected if the absolute value of the residual is greater than $e\sigma_i$, i.e., $|V_i| > e\sigma_i$, where e is a constant, e may be selected as 3~4, σ_i is the standard deviation, and i is the iterative calculation index. That is, $\bar{P}_i = 0$ if $|V_i/\sigma_i| \ge e$. Setting $|V_i/\sigma_i| = e$ into Eq. 7.166 one gets $\bar{P}_i = (c/e)P_i$. In other words, the weight definitions of Eqs. 7.166 and 7.167 are not continuous at point e. A modification of Eq. 7.166 can be made by defining

$$\bar{P}_i(k) = \begin{cases} p_i(k) & \text{if } |V_i(k)/\sigma_i| \le c \\ y_1 P_i(k) & \text{if } c < |V_i(k)/\sigma_i| \le d \\ y_2 P_i(k) & \text{if } d < |V_i(k)/\sigma_i| \le e \\ 0 & \text{if } |V_i(k)/\sigma_i| > e \end{cases}, \tag{7.168}$$

(c) ketabton.com: The Digital Library

where

$$y_1 = 1 - \frac{1-b}{(d-c)^2}\left(\left|\frac{V_i(k)}{\sigma_i}\right| - c\right)^2 \quad \text{and} \tag{7.169}$$

$$y_2 = \frac{b}{(e-d)^2}\left(e - \left|\frac{V_i(k)}{\sigma_i}\right|\right)^2, \tag{7.170}$$

where b is the value of y_1 if $\left|V_i(k)/\sigma_i\right| = d$. c, d, e are constants, and $0 < c < d < e$. For simplification, if one lets $b = (e-d)/(e-c)$, then one has $1 - b = (d-c)/(e-c)$. One may let $d = (e+c)/2$ for further simplification and have

$$y_1 = 1 - \frac{2}{(e-c)^2}\left(\left|\frac{V_i(k)}{\sigma_i}\right| - c\right)^2 \quad \text{and}$$

$$y_2 = \frac{2}{(e-c)^2}\left(e - \left|\frac{V_i(k)}{\sigma_i}\right|\right)^2.$$

By selecting $c = 1$, $e = 3$, and using the above assumptions, the weight functions of Eqs. 7.166 and 7.168 are shown in Fig. 7.1 with broken and continuous lines. It is obvious that Eq. 7.168 is a more reasonable weight function, which may make the Kalman filter more robust.

Discussions can be made similarly for correlated case. Denoting $\left|V_i(k)/\sigma_i\right|$ as $v(k)$, a modification of Eq. 7.167 can be rewritten as

$$\overline{P}_i(k,j) = \begin{cases} p_i(k,j) \\ z_1 P_i(k,j) \\ z_2 P_i(k,j) \\ 0 \end{cases}, \quad \text{if} \quad \begin{cases} \max\{v(k), v(j)\} \le c \\ c < \max\{v(k), v(j)\} \le d \\ d < \max\{v(k), v(j)\} \le e \\ \max\{v(k), v(j)\} > e \end{cases}, \tag{7.171}$$

where

$$z_1 = 1 - \frac{1-b}{(d-c)^2}(\max\{v(k), v(j)\} - c)^2 \quad \text{and} \tag{7.172}$$

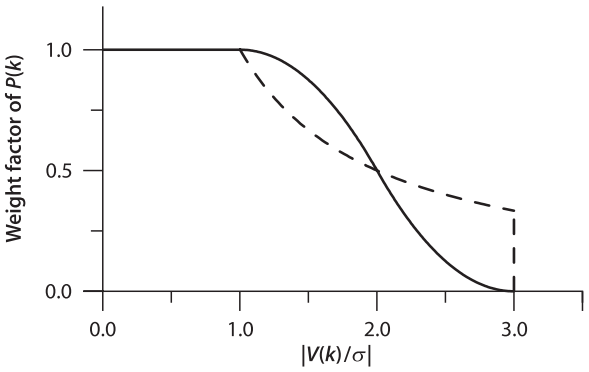

Fig. 7.1.
Weight functions

(c) ketabton.com: The Digital Library

$$z_2 = \frac{b}{(e-d)^2}(e - \max\{v(k), v(j)\})^2 , \tag{7.173}$$

where b is the value of z_1 if $\max\{v(k), v(j)\} = d$. For simplification, if one lets $b = (e - d) / (e - c)$, then one has $1 - b = (d - c) / (e - c)$. Further if one lets $d = (e - c) / 2$, then one has

$$z_1 = 1 - \frac{2}{(e-c)^2}(\max\{v(k), v(j)\} - c)^2 \quad \text{and}$$

$$z_2 = \frac{2}{(e-c)^2}(e - \max\{v(k), v(j)\})^2 .$$

7.7.4 Adaptively Robust Kalman Filtering

The reliability of the linear filtering results, however, will degrade when the noise of the kinematic model is not accurately modelled in filtering or the measurement noises at any measurement epoch are not normally distributed. A new adaptively robust filtering proposed by (Yang et al. 2001) based on the robust M (Maximum likelihood type) estimation is introduced in this section. It consists in weighting the influence of the updated parameters in accordance with the magnitude of discrepancy between the updated parameters and the robust estimates obtained from the kinematic measurements and in weighting individual measurement at each discrete epoch. The new procedure is different from functional model error compensation; it changes the covariance matrix or equivalently changes the weight matrix of the predicted parameters to cover the model errors. A general estimator for an adaptively robust filter is presented, which includes the estimators of the classical Kalman filter, adaptive Kalman filter, robust filter, sequential least squares (LS) adjustment and robust sequential adjustment. The procedure can not only resist the influence of outlying kinematic model errors, but also control the effects of measurement outliers. In addition to the robustising properties, feasibility in implementation of the new filter is achieved through the equivalent weights of the measurements and the predicted state parameters.

Applications of the Kalman filter in dynamic or kinematic positioning have sometimes encountered difficulties, which have been referred to as divergences. These divergences can often be traced to three factors: (*1*) insufficient accuracy in modelling the dynamics or kinematics (functional model errors of the state equations); (*2*) insufficient accuracy in modelling the observations (functional model errors of observation equations); and (*3*) insufficient accuracy in modelling the distributions or the priori covariance matrices of the measurements and the updated parameters (stochastic model errors).

The current basic procedure for the quality control of a Kalman filter consists of:

- Functional model compensation for model errors by introducing uncertain parameters into the state and/or the observation equations. Any model error term can be introduced into the models arbitrarily. One could then augment the state (Jazwinski 1970, p. 308). A similar approach is developed by Schaffrin (1991, p. 32–34). He partitions the state vector into h groups, each being affected by a common scale error. Then, $h \times 1$ vectors of scale parameters are introduced into the models. This kind of

(c) ketabton.com: The Digital Library

approach may, of course, lead to a high-dimensional state vector which, in turn, greatly increases the filter computational load (Jazwinski 1970, p. 305).

- Stochastic model compensation by introducing a variance-covariance matrix of the model errors. In taking this approach to prevent divergence, one has to determine what covariance matrix to add. A reasonable covariance matrix may compensate for the model errors. An ineffective covariance matrix, however, adds to the model divergence. For instance, when the model is accurate in some dynamic or kinematic periods, an unsuitable increasing of the covariance matrix of model error will degrade the state estimators. An effective covariance matrix for model errors can only be determined by trial and error.
- The DIA procedure – detection, identification and adaptation (Teunissen 1990). It uses a recursive testing procedure to eliminate outliers. In the detection step, one looks for unspecified model errors. In the identification step, one tries to find the cause of the model error and its most likely starting time. After a model error has been detected and identified, the bias in the state estimate caused by the model error has to be eliminated as well. This model recovery from errors is called adaptation (Salzmanm 1995). The identification of the model, however, is quite difficult, especially when the measurements are not accurate enough to detect the unspecified model errors.
- The sequential least squares procedure. A quite different procedure that has been frequently used for kinematic positioning does not use the dynamic model information at all but determines discrete positions at the measurement epochs (Cannon et al. 1986). In this case, no assumption on a dynamic model is made, only the measurements at the discrete epoch are employed to estimate the state parameters. The model error, therefore, does not affect the estimates of new state parameters. Usually, this method is presented as a sequential least squares algorithm (Schwarz et al. 1989). The current limitation of this approach is that it wastes the good information of the state model when the model accurately describes the dynamic process in cases.
- Adaptive Kalman filtering. An innovation-based adaptive Kalman filter for an integrated INS/GPS has been developed by Mohamed and Schwarz (1999), based on the maximum likelihood criterion by proper choice of the filter weight. Another adaptive Kalman filter algorithm to directly estimate the variance and covariance components for the measurements is studied by Wang et al. (1999). Both of the algorithms need to collect the residuals of the measurements or the update series to calculate the state variance-covariance matrices.
- A robust filter based on the min-max robust theory. The deviation of observation error distribution from the Gaussian one may also seriously degrade the performance of Kalman filtering. Thus, there appears to be considerable motivation for considering filters which are robustised to perform fairly well in non-Gaussian environments. Facing this problem, Masreliez and Martin (1997) applied the influence function of the min-max robust theory to replace the score function of the classical Kalman filter. The basic disadvantages associated with this kind of robust filter are that the estimator requires the unknown contaminating distribution to be symmetrical, and it cannot work as well as the standard Kalman filter does in Gaussian noise.
- A robust filter based on M estimation theory (Huber 1964) and Bayesian statistics. To resist the bad influences of both state model errors and measurement outliers, a robust M-M filter has been developed (Yang 1991, 1997; Zhou et al. 1997, p. 299) by which the measurement outliers are controlled by robust equivalent weights of the measurements,

(c) ketabton.com: The Digital Library

and the model errors are resisted by the equivalent weights of the update parameters according to the divergence of the predicted parameters and the estimated ones. Furthermore, a robust filter for rank deficient observation models has been developed by Koch and Yang (1998), by using Bayesian statistics and by applying the robust M estimate.

All the methods described above depend on the knowledge of the dynamic model errors, with which the functional or stochastic models for compensation for the model errors and the equivalent weights for the robust filter are constructed. In practical applications, it is very difficult to predict the error distribution or the error type of the updated parameters or the dynamic model errors; thus, it is very difficult to construct functional and stochastic models. Furthermore, when a moving vehicle has accelerated from zero or decelerated to a stop, the acceleration profile is discontinuous. If this discontinuity falls between two measurement epochs, the dynamics cannot be accurately modelled or predicted by state equations; in this case, the predicted information from the dynamic model should not be referred too much. Thus the filter procedure should weaken the effects of the updated parameters. In addition, if the updated parameter vector is contaminated by a model error, then it is usually distorted in its entirety. Thus, we do not need to consider the error influence of the individual element of the updated parameter vector like the robust M-M filter does. An adaptive filter is suitable in this case to balance the dynamic model information and the measurements.

1. *General Estimator of Adaptively Robust Filtering*

An adaptively robust filter is constructed as (cf. Yang et al. 2001)

$$\tilde{X}_i = (A_i^T \overline{P}_i A_i + \alpha P_{\underline{X}_i})^{-1} (A_i^T \overline{P}_i L_i + \alpha P_{\underline{X}_i} \underline{X}_i) \quad \text{and} \tag{7.174}$$

$$Q_{\tilde{X}_i} = (A_i^T \overline{P}_i A_i + \alpha P_{\underline{X}_i})^{-1} \sigma_0^2 , \tag{7.175}$$

where $\overline{P}_i$ is the equivalent weight matrix of the observational vector, $P_{\underline{X}_i}$ is the weight matrix of the predicted vector $\underline{X}_i$, $Q_{\tilde{X}_i}$ is the covariance matrix of the estimated state vector, σ_0^2 is a scale factor, and α is an adaptive factor which can be chosen as

$$\alpha = \begin{cases} 1 & \left|\Delta\tilde{X}_i\right| \le c_0 \\ \dfrac{c_0}{\left|\Delta\tilde{X}_i\right|}\left(\dfrac{c_1 - \left|\Delta\tilde{X}_i\right|}{c_1 - c_0}\right)^2 & c_0 < \left|\Delta\tilde{X}_i\right| \le c_1 \\ 0 & \left|\Delta\tilde{X}_i\right| > c_1 \end{cases} , \tag{7.176}$$

where c_0 and c_1 are constants that are experienced valued as $c_0 = 1.0 \sim 1.5$, $c_1 = 3.0 \sim 4.5$,

$$\Delta\tilde{X}_i = \frac{\left\|\hat{X}_i - \underline{\hat{X}}_i\right\|}{\sqrt{tr\{Q_{\underline{\hat{X}}_i}\}}} , \tag{7.177}$$

and $\hat{X}_i$ is a robust estimate of state vector (state position), which is only evaluated by new measurements at epoch i, and the raw velocity observations are not included in it. $\underline{\hat{X}}_i$ is a predicted position from Eq. 7.149 in which the a priori velocity components

(c) ketabton.com: The Digital Library

are not included. The change of the position expressed by Eq. 7.177 can also reflect the stability of the velocity (cf. Yang et al. 2001).

Expression 7.174 is a general estimator of an adaptively robust filter. In the case of $\alpha \neq 0$, Eq. 7.174 is changed into, by using the matrix identities (Koch 1988, p. 40)

$$\tilde{X}_i = \underline{X}_i + Q_{\underline{X}_i} A_i^T (A_i Q_{\underline{X}_i} A_i^T + \alpha Q_V)^{-1} (L_i - A_i \underline{X}_i) . \tag{7.178}$$

2. *Special Estimators*

The adaptive factor α changes between 0~1, which balances the contribution of the new measurements and the updated parameters to the new estimates of state parameters.

Case 1: If $\alpha = 0$ and $\overline{P}_i = P_i$, then

$$\tilde{X}_i = (A_i^T P_i A_i)^{-1} A_i^T P_i L_i , \tag{7.179}$$

which is an LS estimator by using only the new measurements at epoch i. This estimator is suitable in the case where the measurements are not contaminated by outliers and the updated parameters are biased so much that $\Delta\tilde{X}_i$ in Eq. 7.177 is larger than c_1 (rejecting point), and the information of updated parameters is forgotten completely.

Case 2: If $\alpha = 1$ and $\overline{P}_i = P_i$, then

$$\tilde{X}_i = (A_i^T P_i A_i + P_{\underline{X}_i})^{-1} (A_i^T P_i L_i + P_{\underline{X}_i} \underline{X}_i) , \tag{7.180}$$

which is a general estimator of the classical Kalman filter.

Case 3: If α is determined by Eq. 7.177 and $\overline{P}_i = P_i$, then

$$\tilde{X}_i = (A_i^T P_i A_i + \alpha P_{\underline{X}_i})^{-1} (A_i^T P_i L_i + \alpha P_{\underline{X}_i} \underline{X}_i) , \tag{7.181}$$

which is an adaptive LS estimator of the Kalman filter. It balances the contribution of the updated parameters and the measurements. The only difference between Eqs. 7.174 and 7.181 is the weight matrix of L_i. The former uses the equivalent weights and the latter uses the original weights of L_i.

Case 4: If $\alpha = 0$, then we obtain

$$\tilde{X}_i = (A_i^T \overline{P}_i A_i)^{-1} A_i^T \overline{P}_i L_i , \tag{7.182}$$

which is a robust estimator by using only the new measurements at epoch i.

Case 5: If $\alpha = 1$, then

$$\tilde{X}_i = (A_i^T \overline{P}_i A_i + P_{\underline{X}_i})^{-1} (A_i^T \overline{P}_i L_i + P_{\underline{X}_i} \underline{X}_i) , \tag{7.183}$$

which is an M-LS filter estimator (Yang 1997).

(c) ketabton.com: The Digital Library

Further Development of the Theory

The adaptive factor α is considered a diagonal matrix by Ou (2004) and grouped by the physical meanings of the parameters by Yang (2004). Since then, several progresses have been made (cf. Yang and Cui 2006; Yang and Gao 2005, 2006; Yang et al. 2006).

7.8 A Priori Constrained Least Squares Adjustment

Up to now in this chapter, several adjustment and filtering methods have been discussed. All of them are methods suitable for full rank linear equation problems. A full rank quadratic matrix means such a matrix can be inversed to obtain its inversion. A rank deficient linear equation system is sometimes called an over-parameterised problem. Except for the conditional least squares adjustment method, all other methods discussed above cannot be directly used for solving a rank deficient problem. The conditional least squares adjustment method with extra conditions can make the problem solvable. The conditions, of course, should be well-formulated mathematically and well-reasoned physically. In other words, the conditions are considered as exactly known. In practice, quite often, the conditions are known with certain a priori precisions. Adjustment, which uses such a priori information as constraints, is called a priori constrained adjustment, which will be discussed in this section.

7.8.1 A Priori Parameter Constraints

1. A linearised observation equation system can be represented by

$$V = L - AX\,, \quad P_L\,, \tag{7.184}$$

   where P_L is the symmetric and definite weight matrix of dimension $m \times m$.
2. The corresponding a priori condition equation system can be written as:

$$U = W - BX\,, \quad P_W\,, \tag{7.185}$$

   where
   B : coefficient matrix of dimension $r \times n$,
   W : constant vector of dimension r,
   U : residual vector of dimension r,
   P_W : a priori (symmetric and definite) weight matrix of dimension $r \times r$, and
   r : number of condition equations; $r < n$.
3. One may interpret the constraints of Eq. 7.185 as additional pseudo-observations or as fictitious observations. This leads to the total observation equations:

$$\begin{pmatrix} V \\ U \end{pmatrix} = \begin{pmatrix} L \\ W \end{pmatrix} - \begin{pmatrix} A \\ B \end{pmatrix} X\,, \quad P = \begin{pmatrix} P_L & 0 \\ 0 & P_W \end{pmatrix}. \tag{7.186}$$

(c) ketabton.com: The Digital Library

Then the least squares normal equations are well-known as (see, e.g., Sect. 7.2.1):

$$\begin{pmatrix} A^T & B^T \end{pmatrix}\begin{pmatrix} P_L & 0 \\ 0 & P_W \end{pmatrix}\begin{pmatrix} A \\ B \end{pmatrix} X = \begin{pmatrix} A^T & B^T \end{pmatrix}\begin{pmatrix} P_L & 0 \\ 0 & P_W \end{pmatrix}\begin{pmatrix} L \\ W \end{pmatrix} \quad \text{or}$$

$$(A^T P_L A + B^T P_W B)X = (A^T P_L L + B^T P_W W)\,. \tag{7.187}$$

For convenience, a factor k (here $k = 1$) is introduced in Eq. 7.187:

$$(A^T P_L A + kB^T P_W B)X = (A^T P_L L + kB^T P_W W)\,. \tag{7.188}$$

Equation 7.188 shows that the a priori information constraints can be added to the original least squares normal equations. In other words, the a priori information can be used for solving the rank deficient problem and making the normal matrix possible to be inversed. Of course, these a priori information constraints should be reasonable and realistic ones; otherwise the solutions could be disturbed by worse a priori constraints. In case of $k = 0$, the normal Eq. 7.188 turns to be the original one and will give the free solution (without any a priori constraints).

The solution of the a priori constrained least squares solution is then

$$X = (A^T P_L A + kB^T P_W B)^{-1}(A^T P_L L + kB^T P_W W)\,, \tag{7.189}$$

where $k = 1$. Generally, the a priori weight matrix is given by covariance matrix Q_W and

$$P_W = Q_W^{-1}\,. \tag{7.190}$$

The a priori constraints only cause two additional terms in both sides of the normal equations; therefore, all the above discussed adjustment and filtering methods can be directly used for solving the a priori constrained problem.

7.8.2 A Priori Datum

Suppose the B matrix in the a priori constraints of Eq. 7.185 is an identity matrix, and the parameter vector W is just a coordinate sub-vector of the total parameter vector. Then it turns out to be a special case called a priori datum. The observation equations and a priori constraints may be rewritten as

$$V = L - \begin{pmatrix} A_1 & A_2 \end{pmatrix}\begin{pmatrix} X_1 \\ X_2 \end{pmatrix}, \quad P_L \quad \text{and} \tag{7.191}$$

$$U = \overline{X}_2 - X_2\,, \quad P_2\,, \tag{7.192}$$

where $\overline{X}_2$ is the "observed" parameter sub-vector, P_2 is the weight matrix with respect to the parameter sub-vector X_2 and is generally a diagonal matrix, and U is a residual vector that has the same property as V. Usually, $\overline{X}_2$ is "observed" independently, so P_2 is a diagonal matrix. If X_2 is a sub-vector of station coordinates, then the constraint of

(c) ketabton.com: The Digital Library

Eq. 7.192 is called the datum constraint. (This is also the reason why the name a priori datum is used).

The least squares normal equation of problems 7.191 and 7.192 can be formed then (similar to what discussed in Sect. 7.8.1) as

$$\begin{pmatrix} M_{11} & M_{12} \\ M_{21} & M_{22} \end{pmatrix} \begin{pmatrix} X_1 \\ X_2 \end{pmatrix} = \begin{pmatrix} B_1 \\ B_2 \end{pmatrix} \quad \text{or} \tag{7.193}$$

$$M_{11}X_1 + M_{12}X_2 = B_1 \quad \text{and} \tag{7.194}$$

$$M_{21}X_1 + M_{22}X_2 = B_2 \,, \tag{7.195}$$

where

$$M_{11} = A_1^T P_L A_1 \,, \tag{7.196}$$

$$M_{12} = M_{21}^T = A_1^T P_L A_2 \,, \tag{7.197}$$

$$M_{22} = A_2^T P_L A_2 + P_2 \,, \tag{7.198}$$

$$B_1 = A_1^T P_L L \quad \text{and} \tag{7.199}$$

$$B_2 = A_2^T P_L L + P_2 \overline{X}_2 \,. \tag{7.200}$$

The least squares principle used here is

$$V^T P_L V + U^T P_2 U = \min \,. \tag{7.201}$$

The normal Eq. 7.193 can be also derived by differentiating Eq. 7.201 with respect to X, and then letting it equal zero and taking Eq. 7.192 into account. In practice, the sub-vector $\overline{X}_2$ is usually a zero vector; this can be achieved through careful initialisation by forming the observation Eq. 7.191. Comparing the normal equation system of the a priori datum problem of Eqs. 7.191 and 7.192 with the normal equation of Eq. 7.191, the only difference is that the a priori weight matrix P_2 has been added to M_{22}. This indicates that the a priori datum problem can be dealt with simply by adding P_2 to the normal equation of the observation Eq. 7.191.

If some diagonal components of the weight matrix P_2 are set to zero, then the related parameters (X_2) are free parameters (or free datum) of the adjustment problem (without a priori constraints). Otherwise, parameters with a priori constraints are called a priori datum. Large weight indicates strong constraint and small weight indicates soft constraint. The strongest constraint is to keep the datum fixed.

7.8.3 Quasi-Stable Datum

The quasi-stable datum method was proposed by Zhou (Zhou et al. 1997). The basic idea is that the network is a dynamic one, i.e., most parameters are changing all the

(c) ketabton.com: The Digital Library

time. However, a few points are relatively stable, or their geometric centre is relatively stable. All the assumptions and observation equations are the same as in Sect. 7.8.2:

$$V = L - \begin{pmatrix} A_1 & A_2 \end{pmatrix} \begin{pmatrix} X_1 \\ X_2 \end{pmatrix}, \quad P_L \quad \text{and} \tag{7.202}$$

$$U = \overline{X}_2 - X_2 , \quad P_2 . \tag{7.203}$$

The least squares principles for the quasi-stable datum are

$$V^T P_L V = \min \quad \text{and} \tag{7.204}$$

$$U^T P_2 U = \min . \tag{7.205}$$

Equation 7.204 is the same as the original least squares principle. From Eq. 7.204, one has the normal equation

$$\begin{pmatrix} M_{11} & M_{12} \\ M_{21} & M_{22} \end{pmatrix} \begin{pmatrix} X_1 \\ X_2 \end{pmatrix} = \begin{pmatrix} B_1 \\ B_2 \end{pmatrix}, \tag{7.206}$$

where

$$M_{11} = A_1^T P_L A_1 ,$$

$$M_{12} = M_{21}^T = A_1^T P_L A_2 ,$$

$$M_{22} = A_2^T P_L A_2 ,$$

$$B_1 = A_1^T P_L L \quad \text{and}$$

$$B_2 = A_2^T P_L L . \tag{7.207}$$

Even if Eq. 7.206 is a rank deficient equation, one may first solve Eq. 7.206 to get an explicit expression for X_2. Recalling the discussion in Sect. 7.5, one gets a normal equation related to X_2:

$$M_2 X_2 = R_2 , \tag{7.208}$$

where

$$M_2 = M_{22} - M_{21} M_{11}^{-1} M_{12} \quad \text{and}$$

$$R_2 = B_2 - M_{21} M_{11}^{-1} B_1^T . \tag{7.209}$$

The new condition can be considered by forming

$$F = U^T P_2 U + 2K^T (M_2 X_2 - R_2)$$

(c) ketabton.com: The Digital Library

and

$$\frac{\partial F}{\partial X} = 2U^T P_2 + 2K^T M_2 = 0 .$$

Considering the symmetry of M_2, we have

$$U = -P_2^{-1} M_2 K . \tag{7.210}$$

Substituting Eq. 7.210 into 7.203, one gets

$$X_2 = \overline{X}_2 + P_2^{-1} M_2 K \tag{7.211}$$

or

$$M_2 X_2 = M_2 \overline{X}_2 + M_2 P_2^{-1} M_2 K . \tag{7.212}$$

Substituting Eq. 7.208 into 7.212, one has

$$K = (M_2 P_2^{-1} M_2)^{-1} (M_2 \overline{X}_2 - R_2) . \tag{7.213}$$

Thus,

$$X_2 = \overline{X}_2 + P_2^{-1} M_2 K , \tag{7.214}$$

$$X_1 = M_{11}^{-1} (A_1^T P_L L - M_{12} X_2) \quad \text{and} \tag{7.215}$$

$$m_0 = \sqrt{\frac{V^T P_L V}{n - r}} , \tag{7.216}$$

where m_0 is the standard deviation, n is the number of observations, and r is the summation of the both ranks of the matrices A_1 and A_2.

7.9 Summary

In this chapter, the most applicable and necessary algorithms for static and kinematic as well as dynamic GPS data processing are outlined.

Least squares adjustment is the most basic adjustment method. It starts by establishing observation equations and forming normal equations; then it solves the unknowns. It is a suitable method for static GPS data processing. The sequential application of least squares adjustment by accumulating the sequential normal equations makes applications of least squares adjustment more effective. Normal equations can be formed epoch-wise and then accumulated. This method can be used not only for solving the problem at the end, but also for obtaining epoch-wise solutions. It is suitable for static GPS data processing. The equivalent sequential least squares adjustment, which can be read from different publications, is also derived. This is an epoch-wise solving method and therefore is generally not suitable for static GPS data processing. Xu (author) and

(c) ketabton.com: The Digital Library

Morujao (Coimbra University, Portugal) have independently pointed out that by applying such an algorithm, the obtained results compared with that which was obtained by the accumulating method will have differences. The differences increase with time and are generally not negligible. Therefore by using this method, the numerical process has to be carefully examined to avoid the accumulation of numerical errors.

The conditional least squares adjustment is needed if there are some constraints that have to be taken into account. The commonly used least squares ambiguity search criterion is derived from this principle (cf. Sect. 8.3.4). The general criterion of integer ambiguity search is also based on this theory (cf. Sect. 8.3.5). The typical application of this method in GPS data processing is taking into account the known distance of multiple kinematic antennas. The sequential application of conditional least squares adjustment is discussed because of practical needs. The problem may be solved first without conditions, and then the conditions may be applied afterward. The constraints such as the known distances of multiple antennas fixed on an aircraft have to be considered for every epoch.

Block-wise least squares adjustment is discussed for separating the unknowns into two groups. For example, one group is time dependent parameters such as kinematic coordinates, and the other is the group of time independent parameters such as ambiguities. The sequential application of block-wise least squares adjustment makes it possible to give up some unknowns (say, out of date unknowns, such as past coordinates) and keep the information related to the common unknowns during the processing process. This method avoids the problem that may be caused by rapid enlarging of the number of unknowns. There are two ways to keep the solution equivalent with a solution that is not sequential. One is to use the time independent unknowns at the end of data processing as known, and then go back to process the data once again. The other is to remember all sequential normal equations until the best solution of the time independent unknowns are obtained, and then the coordinates can be recomputed. A special application of block-wise least squares adjustment is discussed for a code-phase combination model. Of course, the two observables have to be suitably scaled and weighted.

The equivalently eliminated observation equation system is discussed for eliminating some nuisance parameters. This method is nearly the same as block-wise least squares adjustment if one carefully compares the normal equations of the second group of unknowns (see Sect. 7.5) and the eliminated normal equations (see Sect. 7.6). However, the most important point is that the equivalently eliminated observation equations have been derived here. Instead of solving the original problem, one may directly solve the equivalently eliminated observation equations, where the unknowns are greatly reduced, whereas the observation vector and weight matrix remain the originals (i.e., the problem remains un-correlated). The precision estimation can also be made more easily by using the formulas derived in least squares adjustment. The derivation of such an equivalent observation equation was made first by Zhou (1985) and applied in GPS theory by Xu (2002). The unified GPS data processing method is derived by using this principle (cf. Sect. 6.8). Based on the derivation of the equivalent equation, a diagonaliation algorithm of the normal equation and the observation equation are discussed. The diagonalisation algorithm can be used for separating one adjustment problem into two sub-problems.

(c) ketabton.com: The Digital Library

The classic Kalman filter is discussed. It is suitable for real time applications. A key problem of the classic Kalman filter is the divergence caused by the inexact description of system equations and its statistic properties as well as the inhomogeneous quality of the data. Furthermore, the solutions could be strongly dependent on the given initial values. The sequential least squares adjustment method as a special case of Kalman filtering is outlined.

Efforts have been made to modify the performance of classic Kalman filtering. In the classic Kalman filter, the weight matrix P of observables is a static one, i.e., P is assumed to be a definitive defined matrix. Taking the residuals of Kalman filtering into account, one may adjust the weight P of the observables accordingly; such a process is called robust Kalman filtering (Koch and Yang 1998). This principle can be also used for controlling the outliers of observations (Yang 1999). Such an idea indeed can be also used in all of the adjustment methods. Usually the weight of an observation is either one (be accepted) or zero (be rejected). In robust Kalman filtering, a continuous weight between one and zero is defined and introduced. A modified weight function is also discussed and given for use. Generally speaking, the robust weighting method may modify the convergence process of the filtering procedure.

As soon as the system is defined, the Kalman filter also obtains remembering abilities. However, if the system makes a discontinuous change (for example, aircraft from static begins to run), the Kalman filter should be able to forget a part of the updated parameters. Adding such ability to the robust Kalman filter is called an adaptively robust Kalman filter (Yang et al. 2001) and is discussed in detail.

A priori constrained least squares adjustment is discussed in Sect. 7.8 for solving the rank deficient problems. A general discussion on the a priori parameter constraints is given. This method makes it possible to form the observation equations in a general way, and then a priori information can be added to keep some references fixed, such as the clock error of the reference satellite and the coordinates of the reference station. As a special case of the a priori parameter constraints, a so-called a priori datum method is discussed. The advantage of this method is that the a priori constraints just change the normal equation by adding a term (the a priori weight matrix), so that all discussed least squares adjustment and filtering methods can be directly used for solving the rank deficient problems. Linear conditions related to the coordinate parameters can be introduced by using this method. A quasi-stable datum method is also discussed. From the point of view of the dynamic Earth, all stations are not fixed stations. The quasi-stable datum method takes such dynamic behaviour of the stations into account.

(c) ketabton.com: The Digital Library

Chapter 8

Cycle Slip Detection and Ambiguity Resolution

In phase measurement there is an ambiguity problem. If the signal happens with a loss of lock, the phase measurement has to be initiated again. This phenomenon is called cycle slips, i.e., the cycle counting has a new beginning because of an interruption of signal. The consequence of the cycle slips is that the adjacent carrier phase observable jumps by an integer number of cycles, and in the related observation model the ambiguity parameter should be a new one. Correct cycle slip detection becomes a guarantee for a correct ambiguity parameterisation. After the discussion of cycle slip detection, emphasis given to the integer ambiguity resolution problem includes the criteria of the integer ambiguity search. The historical ambiguity function method is also outlined and discussed.

8.1 Cycle Slip Detection

Recalling the discussions made in Sect. 6.5, several methods of cycle slip detection can be summarised as follows.

1. Phase-Code Comparison

Using the first equation of 6.88

$$\Delta_t R_j = \lambda_j \Delta_t \Phi_j - \lambda_j \Delta_t N_j + \varepsilon \,, \tag{8.1}$$

cycle slips of the phase observable in working frequency j can be detected. Δ_t, R_j, Φ_j, N_j, λ_j, ε, and j are the time difference operator, code range, phase, ambiguity, wavelength, residual, and index of the frequency, respectively. In the case of no cycle slips, the time difference of the ambiguity should be zero, i.e. $\Delta_t N_j = 0$. Because the noise level of the code range is much higher than that of the phase, this method can only be used for big cycle slip detection.

2. Phase-Phase Ionospheric Residual

Using Eq. 6.80

$$\lambda_1 \Delta_t \Phi_1(t_j) - \lambda_2 \Delta_t \Phi_2(t_j) = \lambda_1 \Delta_t N_1 - \lambda_2 \Delta_t N_2 - \Delta_t \Delta\delta_{\text{ion}}(t_j) + \Delta_t \Delta\varepsilon_{\text{p}} \,, \tag{8.2}$$

cycle slips of the two phase observables in frequency 1 and 2 can be detected. $\Delta_t \Delta\delta_{\text{ion}}(t_j)$ is the so-called ionospheric residual. Generally speaking, the computed ionospheric

(c) ketabton.com: The Digital Library

residual of the two adjacent epochs should be very small. Any unusual change of the ionospheric residual may indicate cycle slips in one or two phases. However, two special cycle slips, ΔN_1 and ΔN_2, can lead also to a very small combination of $\lambda_1 \Delta_t N_1 - \lambda_2 \Delta_t N_2$. Examples of such combinations can be found, e.g., in (Hofmann-Wellenhof et al. 1997). Therefore, a big ionospheric residual indicates the cycle slips, whereas a small ionospheric residual does not guarantee that there are no cycle slips. Another shortcoming of this method is that the ionospheric residual itself provides no possibility to check in which phase the cycle slips happen.

3. Doppler Integration

Using Eq. 6.87

$$\Delta_t N_j = \Delta_t \Phi_j - \int_{t_{j-1}}^{t_j} D_j \mathrm{d}t + \varepsilon, \quad j = 1, 2, 5, \tag{8.3}$$

cycle slips of the phase observable in working frequency j can be detected. D_j is the Doppler observable of frequency j. Recalling the discussions made in Chap. 4, the phase is measured by keeping track of the partial phase and accumulating the integer count. If there is any loss of lock of the signal during this time, the integer accumulation will be wrong, i.e., cycle slip happens. Therefore, an external instantaneous Doppler integration is a good choice for cycle slip detection. The integration can be made first by fitting the Doppler data with a polynomial of suitable order, and then integrating that within the desired time interval. Polynomial fitting and numerical integration methods can be found in Sect. 11.5.2 and 3.4.

4. Differential Phases (of Time)

Using the first equation of 6.86

$$\lambda_j \Delta_t \Phi_j = \Delta_t \rho - \Delta_t (\delta t_\mathrm{r} - \delta t_\mathrm{e}) c + \lambda_j \Delta_t N_j + \varepsilon_\mathrm{p}, \quad j = 1,2, \tag{8.4}$$

cycle slips can be detected. Except for the ambiguity term, all other terms on the right side are of low variation ones. Any cycle slips will lead to a sudden jump of the time difference of the phases. The differenced data may be fitted with polynomials, and the polynomials can be used for interpolating or extrapolating the data at the checking epoch; the computed and differenced data then can be compared to decide if there are any cycle slips.

8.2 Method of Dealing with Cycle Slips

As soon as the cycle slips have been detected, there are two ways to deal with them. One is to repair the cycle slips, the other is to set a new ambiguity unknown parameter in the GPS observation equations. To repair the cycle slips, the cycle slips have to be known exactly. Any incorrect reparation will affect all observations later. Setting a new unknown ambiguity parameter after a cycle slip is a more secure method. It seems that in this

(c) ketabton.com: The Digital Library

way there will be more unknowns in the observation equations. However, there exists a condition between the former ambiguity parameter $N(1)$ and the new one $N(2)$, i.e.,

$$N(1,i,j,k) = N(2,i,j,k) + I(i,j,k)\,, \tag{8.5}$$

where I is an integer constant and i, j and k are indices of the receiver, satellite, and observing frequency, respectively. For any solution of $N(1)$ and $N(2)$ with good qualities, the integer constant should be able to be easily distinguished. If $I = 0$, then no cycle slips have really happened.

If instrumental biases have not been modelled, the biases may destroy the integer property of the original ambiguity parameters. However, in such a case, the double differenced ambiguities are still integers.

8.3 A General Criterion of Integer Ambiguity Search

An integer ambiguity search method based on conditional adjustment theory is proposed in this section. By taking the coordinate and ambiguity residuals into account, a general criterion for ambiguity searching is derived. The search can be carried out in both ambiguity and coordinate domains. The optimality and uniqueness properties of the general criterion are also discussed. A numerical explanation of the general criterion is outlined. An equivalent criterion of the general criterion is derived based on a diagonalised normal equation. It shows that the commonly used least squares ambiguity search (LSAS) criterion is just one of the terms of the equivalent general criterion. Numerical examples are given to illustrate the two components of the equivalent criterion.

8.3.1 Introduction

It is well-known that the ambiguity resolution is a key problem that has to be solved in GPS precise positioning. Some well-derived ambiguity fixing and searching algorithms have been published during the last ten years. There are four types of methods that are categorized. The first type includes Remondi's static initialisation approach (cf., e.g., Remondi 1984; Wang et al. 1988; Hofmann-Wellenhof et al. 1997), which requires a static survey time to solve the ambiguity unknowns even after a complete loss of lock. Normally, the results are good enough to take a round up ambiguity fixing. The second type includes the so-called phase-code combined methods (cf., e.g., Goad and Remondi 1984; Han and Rizos 1997; Sjoeberg 1999); the phase and code have to be used in the derivation as if they have the same precision, and in the case of anti-spoofing (AS), the C/A code has to be used. A search process is still needed in this case. The third type is the so-called ambiguity function method (Remondi 1984; Han and Rizos 1997); its search domain is a geometric one. The fourth type includes approaches; their search domain is only in domain of ambiguity, including some optimal algorithms to reduce the search area and to accelerate the search process (cf., e.g., Euler and Landau 1992; Teunissen 1995; Cannon et al. 1997; Han and Rizos 1997). Because of the statistic character of validation criteria, sometimes no valid result is obtained at the end of the search processes. Gehlich and Lelgemann (1997) separated the ambiguities from the other parameters; this is similar to the equivalent method (cf. Sect. 6.7).

(c) ketabton.com: The Digital Library

The effort to develop KSGsoft (**K**inematic/**S**tatic **GPS** **Soft**ware) at the GeoForschungs-Zentrum (GFZ) in Potsdam began at the beginning of 1994 due to the requirement of kinematic GPS positioning in aerogravimetry applications (Xu et al. 1998). An optimal ambiguity resolution method is needed in order to implement it into the software; however, selecting the published algorithms has turned out to be a difficult task. This has led to the independent development of this so-called integer ambiguity search method. It turns out to be a very promising algorithm. Using this general criterion, an optimal solution vector can be searched for and found out. The searched result is the optimal one under the least squares principle and integer ambiguity property.

In the following sections, a brief summary of the conditional adjustment is given for the convenience of discussion. Then the ambiguity searches in the ambiguity domain, and both ambiguity and coordinate domains are discussed. Properties of the general criterion are discussed. An equivalent criterion of the general criterion is derived. Numerical examples, conclusions and comments are given.

8.3.2 Summary of Conditional Least Squares Adjustment

The principle of least squares adjustment with condition equations can be summarised as below (for details cf. Sect. 7.4; Gotthardt 1978; Cui et al. 1982):

1. The linearised observation equation system can be represented by

$$V = L - AX\,, \quad P \tag{8.6}$$

where L is the observation vector of dimension m, A is the coefficient matrix of dimension $m \times n$, X is the unknown vector of dimension n, V is the residual vector of dimension m, n and m are numbers of unknowns and observations, and P is the symmetric and quadratic weight matrix of dimension $m \times m$.

2. The condition equation system can be written as

$$CX - W = 0\,, \tag{8.7}$$

where C is the coefficient matrix of dimension $r \times n$, W is the constant vector of dimension r, and r is the number of conditions.

3. The least squares criterion for solving the observation equations with condition equations is well-known as

$$V^T PV = \min\,, \tag{8.8}$$

where V^T is the transpose of the related vector V.

4. The solution of the conditional problem in Eqs. 8.6 and 8.7 under the least squares principle of Eq. 8.8 is then

$$\begin{aligned} X_c &= (A^T PA)^{-1}(A^T PL) - (A^T PA)^{-1} C^T K \\ &= (A^T PA)^{-1}(A^T PL - C^T K) \end{aligned} \tag{8.9}$$

(c) ketabton.com: The Digital Library

and

$$K = (CQC^T)^{-1}(CQW_1 - W)\,, \tag{8.10}$$

where A^T and C^T are the transpose matrices of A and C, superscript $^{-1}$ is an inversion operator, $Q = (A^TPA)^{-1}$, K is a gain vector (of dimension r), index c is used to denote the variables related to the conditional solution, and $W_1 = A^TPL$.

5. The precisions of the solutions are then

$$p[i] = s_{\mathrm{d}}\sqrt{Q_{\mathrm{c}}[i][i]}\,, \tag{8.11}$$

where i is the element index of a vector or a matrix, s_{d} is the standard deviation (or sigma) of unit weight, $p[i]$ is the i^{th} element of the precision vector, $Q_{\mathrm{c}}[i][i]$ is the i^{th} diagonal element of the quadratic matrix Q_{c}, and

$$Q_{\mathrm{c}} = Q - QC^TQ_2CQ\,, \tag{8.12}$$

$$Q_2 = (CQC^T)^{-1}\,, \tag{8.13}$$

$$s_{\mathrm{d}} = \sqrt{\frac{(V^TPV)_{\mathrm{c}}}{m-n+r}}\,, \quad \text{if} \quad (m > n-r)\,. \tag{8.14}$$

6. For recursive convenience, $(V^TPV)_{\mathrm{c}}$ can be calculated by using

$$(V^TPV)_{\mathrm{c}} = L^TPL - (A^TPL)^TX_{\mathrm{c}} - W^TK\,. \tag{8.15}$$

Above are the complete formulas of conditional least squares adjustment. The application of such an algorithm for the purpose of integer ambiguity search will be further discussed in later sections.

8.3.3 Float Solution

GPS observation equation can be represented with Eq. 8.6. Considering the case without condition (Eq. 8.7), i.e., $C = 0$ and $W = 0$, the least squares solution of Eq. 8.6 is

$$X_0 = Q(A^TPL) = QW_1\,, \tag{8.16}$$

and

$$(V^TPV)_0 = L^TPL - (A^TPL)^TX_0\,, \tag{8.17}$$

$$s_{\mathrm{d}} = \sqrt{\frac{(V^TPV)_0}{m-n}}\,, \quad \text{if} \quad (m > n) \quad \text{and} \tag{8.18}$$

$$p[i] = s_{\mathrm{d}}\sqrt{Q[i][i]}\,, \tag{8.19}$$

(c) ketabton.com: The Digital Library

where index 0 is used for convenience to denote the variables related to the least squares solution without conditions. X_0 is the complete unknown vector including coordinates and ambiguities and is called a float solution later on. Solution X_0 is the optimal one under the least squares principle. However, because of the observation and model errors as well as method limitations, float solution X_0 may not be exactly the right one, e.g., the ambiguity parameters are real numbers and do not fit to the integer property. Therefore, one sometimes needs to search for a solution, say X, which not only fulfils some special conditions, but also meanwhile keeps the deviation of the solution as small as possible (minimum). This can be represented by

$$V_x^T P V_x = \min\,, \tag{8.20}$$

or equivalently by a symmetric quadratic form of (cf. also Eq. 8.35 derived later)

$$(X_0 - X)^T Q^{-1} (X_0 - X) = \min\,. \tag{8.21}$$

In Eq. 8.20, V_x is the residual vector in the case of solution X. For simplification, let:

$$X = \begin{pmatrix} Y \\ N \end{pmatrix}, \quad Q = \begin{pmatrix} Q_{11} & Q_{12} \\ Q_{21} & Q_{22} \end{pmatrix}, \quad W_1 = A^T P L = \begin{pmatrix} W_{11} \\ W_{12} \end{pmatrix},$$

$$M = A^T P A = \begin{pmatrix} M_{11} & M_{12} \\ M_{21} & M_{22} \end{pmatrix}, \quad M = Q^{-1}\,, \tag{8.22}$$

where Y is the coordinate vector, N is the ambiguity vector (generally, a real vector). The float solution is denoted by

$$X_0 = \begin{pmatrix} Y_0 \\ N_0 \end{pmatrix} = \begin{pmatrix} Q_{11}W_{11} + Q_{12}W_{12} \\ Q_{21}W_{11} + Q_{22}W_{12} \end{pmatrix},$$

where X_0 is the solution of Eq. 8.6 without Condition 8.7.

8.3.4 Integer Ambiguity Search in Ambiguity Domain

To use the conditional adjustment algorithm for integer ambiguity searching in the ambiguity domain, the condition shall be selected as $N = W$; here W of course is an integer vector. Generally, letting $C = (0, E)$, then Condition 8.7 turns out to be:

$$N = W\,. \tag{8.23}$$

Using the definitions of C and Q, one has

$$CQ = \begin{pmatrix} Q_{21} & Q_{22} \end{pmatrix} \quad \text{and}$$

$$CQC^T = Q_{22}\,.$$

(c) ketabton.com: The Digital Library

The gain K_N can be computed by using Eq. 8.10:

$$K_N = Q_{22}^{-1}(CQW_1 - W) = Q_{22}^{-1}(N_0 - W)\,. \tag{8.24}$$

So under Condition 8.23, the conditional least squares solution in Eq. 8.9 can be written as

$$X_c = \begin{pmatrix} Y_c \\ N_c \end{pmatrix} = \begin{pmatrix} Q_{11} & Q_{12} \\ Q_{21} & Q_{22} \end{pmatrix} \begin{pmatrix} W_{11} \\ W_{12} - K_N \end{pmatrix} = \begin{pmatrix} Y_0 \\ N_0 \end{pmatrix} - \begin{pmatrix} Q_{12} \\ Q_{22} \end{pmatrix} K_N\,. \tag{8.25}$$

Simplifying Eq. 8.25, one gets:

$$Y_c = Y_0 - Q_{12}K_N \tag{8.26}$$

and

$$N_c = N_0 - Q_{22}K_N = N_0 - Q_{22}Q_{22}^{-1}(N_0 - W) = W\,. \tag{8.27}$$

The precision computing formulas under Condition 8.23 can be derived as below:

$$Q_c = Q - QC^T Q_{22}^{-1} CQ = \begin{pmatrix} Q_{11} - Q_{12}Q_{22}^{-1}Q_{21} & 0 \\ 0 & 0 \end{pmatrix} \quad \text{and} \tag{8.28}$$

$$\begin{aligned} (V^T PV)_c &= L^T PL - (A^T PL)^T X_c - W^T K_N \\ &= L^T PL - (A^T PL)^T X_0 + (A^T PL)^T \begin{pmatrix} Q_{12} \\ Q_{22} \end{pmatrix} K_N - W^T K_N \\ &= (V^T PV)_0 + \begin{pmatrix} W_1^T & W_2^T \end{pmatrix} \begin{pmatrix} Q_{12} \\ Q_{22} \end{pmatrix} K_N - W^T K_N \\ &= (V^T PV)_0 + (N_0 - W)^T K_N \\ &= (V^T PV)_0 + (N_0 - W)^T Q_{22}^{-1}(N_0 - W) \end{aligned}\,, \tag{8.29}$$

where $(V^TPV)_0$ is the value obtained without Condition 8.23. The second term on the right side of the last line in Eq. 8.29 is the often-used least squares ambiguity search (LSAS) criterion for an integer ambiguity search in the ambiguity domain, which can be expressed as

$$\delta(\mathrm{d}N) = (N_0 - N)^T Q_{22}^{-1}(N_0 - N)\,. \tag{8.30}$$

It indicates that any ambiguity fixing will cause an enlargement of the standard deviation. However, one may also notice that here only the enlargement of the standard deviation caused by ambiguity parameter changing has been considered. Furthermore, the Condition 8.23 does not really exist. Ambiguities are integers, however, they are unknowns. The formula to compute the accuracy vector of the ambiguity does not exist too, because the ambiguity condition is considered exactly known in conditional adjustment.

(c) ketabton.com: The Digital Library

8.3.5 Integer Ambiguity Search in Coordinate and Ambiguity Domains

In order to see the enlargement of the standard deviation caused by the fixed solution, the condition shall be selected as $X = W$; here, W consists of two sub-vectors (coordinate and ambiguity parameter related sub-vectors). And only the ambiguity parameter related sub-vector is an integer one. Letting $C = E$, Condition 8.7 is then:

$$X = W \,. \tag{8.31}$$

One has

$$CQ = CQC^T = Q \,.$$

Denote $X_0 = QW_1$; here X_0 is the solution of Eq. 8.6 without Condition 8.31. The gain K can be computed by using Eq. 8.10:

$$K = Q^{-1}(CQW_1 - W) = Q^{-1}(X_0 - W) \,. \tag{8.32}$$

So under Condition 8.31, the conditional least squares solution in Eq. 8.9 can be written as

$$X_c = X_0 - QK = X_0 - QQ^{-1}(X_0 - W) = W \,. \tag{8.33}$$

Precision computing formulas under Condition 8.31 can be derived as below:

$$\begin{aligned} &Q_c = 0 \,, \\ &(V^T PV)_c = L^T PL - (A^T PL)^T X_c - W^T K \\ &\qquad = L^T PL - (A^T PL)^T X_0 + (A^T PL)^T (X_0 - X_c) - W^T K \\ &\qquad = (V^T PV)_0 + W_1^T QK - W^T K \\ &\qquad = (V^T PV)_0 + (X_0 - W)^T K \\ &\qquad = (V^T PV)_0 + (X_0 - W)^T Q^{-1}(X_0 - W) \end{aligned} \,, \tag{8.34}$$

where $(V^T PV)_0$ is the value obtained without Condition 8.31.

Condition 8.31 will force the observation Eq. 8.6 to take the condition W as the solution and will take the zero value as the precision of the conditional solution (i.e., the precision is undefined). The reason for this is that the condition is considered exactly known in conditional adjustment. The second term on the right side of Eq. 8.34 is denoted as

$$\delta = (X_0 - X)^T Q^{-1}(X_0 - X) \,. \tag{8.35}$$

This term in Eq. 8.34 indicates that any solution vector X, which is different from the float solution vector X_0, will enlarge the weighted squares residuals. It is well-known that the float solution is the optimal solution under the least squares principle. Therefore, statistically, the optimal solution X shall be that X which takes the minimum value

(c) ketabton.com: The Digital Library

of δ in Eq. 8.35. Mathematically speaking, Eq. 8.35 is the "distance" between vector X and X_0 in the solution space (of dimension n). If one considers $n = 3$ and Q^{-1} to be a diagonal matrix, then δ is the geometric distance of point X and X_0 in a cubic space. So Eq. 8.35 can be used as a general criterion to express the nearness of the two vectors. By using criterion of Eq. 8.35, one may search for solution X in the area being searched so that the value of δ reaches the minimum. Under such a criterion, the deviation of the result vector X related to the float vector X_0 is homogenously considered.

Furthermore, Condition 8.31 is considered exactly known in conditional adjustment. However, in integer ambiguity searching, we just know the ambiguities are integers, but their values are indeed not known, or say, they are known with uncertainty (precision) within an area around the float solution. So the best solution shall be searched for. For computing the precision of the searched X, the formulas of least squares adjustment shall be further used, and meanwhile the enlarged residuals shall be taken into account by

$$p[i] = s_{\mathrm{d}} \sqrt{Q[\mathrm{i}][\mathrm{i}]}\,,$$

$$s_{\mathrm{d}} = \sqrt{\frac{(V^T PV)_{\mathrm{c}}}{m-n}}\,, \quad \text{if} \quad (m > n) \quad \text{and}$$

$$(V^T PV)_{\mathrm{c}} = (V^T PV)_0 + \delta\,. \tag{8.36}$$

In other words, the original Q matrix and $(V^T PV)_0$ of the least squares problem in Eq. 8.6 are further used. The δ has the function of enlarging the standard deviation. The precision computing formulas have nothing to do with the conditions. Searching for a minimum δ leads to a minimum of standard deviation s_{d} and therefore the best precision values.

Equation 8.35 is called the general criterion of an integer ambiguity search, which may be used for searching for the optimal solution in the ambiguity domain, or both coordinate and ambiguity domains. In most cases, the search will be started from the ambiguity domain. An integer vector N can be selected in the searching area, then the related coordinate vector Y can be computed using the consistent relation of Y and N (cf. Eqs. 8.26 and 8.24). The optimal solution searched shall be that X which leads Eq. 8.35 to a minimum value.

In the case of searching in the ambiguity domain, X consists of the selected sub-vector of N_{c} in Eq. 8.27 and the computed coordinate sub-vector Y_{c} in Eq. 8.26, i.e.,

$$W = \begin{pmatrix} Y_{\mathrm{c}} \\ N_{\mathrm{c}} \end{pmatrix}\,. \tag{8.37}$$

8.3.6 Properties of the General Criterion

1. Equivalence of the Two Searching Scenarios

It should be emphasised that the same searching criterion of Eq. 8.35 and the same formulas of precision estimation in Eq. 8.36 are used in the two integer ambiguity search scenarios. And the same normal equation of 8.6 is used to compute the Y_{c} using the selected N_{c} if necessary. The two searching processes indeed deal with the same problem, just as different ways of searching are used.

(c) ketabton.com: The Digital Library

Suppose by searching in the ambiguity domain, the vector $X = (Y_c \quad N_c)^T$ is found so that δ reaches the minimum, where N_c is the selected integer sub-vector and Y_c is the computed one. And in the case of searching in both coordinate and ambiguity domains, a candidate vector $X = (Y \quad N)^T$ is selected so that δ reaches the minimum, where N is the selected integer sub-vector and Y is the selected coordinate vector. Because of the optimality and uniqueness properties of the vector X in Eq. 8.35 (please refer to 2, which is discussed next), here the selected $(Y \quad N)^T$ must be equal to $(Y_c \quad N_c)^T$. So the theoretical equivalency of the two searching processes is confirmed.

2. Optimality and Uniqueness Properties

The float solution X_0 is the optimal and unique solution of Eq. 8.6 under the principle of least squares. A minimum of δ in Eq. 8.35 will lead to a minimum of $(V^TPV)_c$ in Eq. 8.36. Therefore using criterion of Eq. 8.35 analogously, the searched vector X is the optimal solution of Eq. 8.6 under the least squares principle and integer ambiguity properties. The uniqueness property is obvious. If X_1 and X_2 are such that $\delta(X_1) = \delta(X_2) = \min$ or $\delta(X_1) - \delta(X_2) = 0$, then by using Eq. 8.35, one may assume that X_1 must be equal to X_2.

3. Geometric Explanation of the General Criterion

Geometrically, $\delta = (X_0 - X)^T(Q)^{-1}(X_0 - X)$ is the "distance" between the vector X and float vector X_0. The distance contributed to enlarge the standard deviation s_d (cf. Eq. 8.36). Ambiguity searching is then the search for the solution vector, which owns the integer ambiguity property and has the minimum distance to the float solution vector.

8.3.7 An Equivalent Ambiguity Search Criterion and its Properties

Suppose undifferenced GPS observation equation and related LS normal equation are

$$V = L - \begin{pmatrix} A_1 & A_2 \end{pmatrix} \begin{pmatrix} X_1 \\ X_2 \end{pmatrix}, \quad P \tag{8.38}$$

$$\begin{pmatrix} M_{11} & M_{12} \\ M_{21} & M_{22} \end{pmatrix} \begin{pmatrix} X_1 \\ X_2 \end{pmatrix} = \begin{pmatrix} W_1 \\ W_2 \end{pmatrix}, \tag{8.39}$$

where

$$\begin{pmatrix} A_1^T PA_1 & A_1^T PA_2 \\ A_2^T PA_1 & A_2^T PA_2 \end{pmatrix} = \begin{pmatrix} M_{11} & M_{12} \\ M_{21} & M_{22} \end{pmatrix} = M, \quad M^{-1} = Q = \begin{pmatrix} Q_{11} & Q_{12} \\ Q_{21} & Q_{22} \end{pmatrix}, \tag{8.40}$$

$$W_1 = A_1^T PL \quad \text{and} \quad W_2 = A_2^T PL\,.$$

Where all symbols have the same meanings as that of Eqs. 7.117 and 7.118. Equation 8.39 can be diagonalised as (cf. Sect. 7.6.1)

(c) ketabton.com: The Digital Library

$$\begin{pmatrix} M_1 & 0 \\ 0 & M_2 \end{pmatrix}\begin{pmatrix} X_1 \\ X_2 \end{pmatrix}=\begin{pmatrix} B_1 \\ B_2 \end{pmatrix}, \tag{8.41}$$

where

$$\begin{aligned} &Q_{11}=M_1^{-1}, && Q_{22}=M_2^{-1} \\ &Q_{12}=-M_{11}^{-1}(M_{12}Q_{22}), && Q_{21}=-M_{22}^{-1}(M_{21}Q_{11}) \end{aligned}. \tag{8.42}$$

The related equivalent observation equation of the diagonal normal Eq. 8.41 can be written (cf. Sect. 7.6.1)

$$\begin{pmatrix} U_1 \\ U_2 \end{pmatrix}=\begin{pmatrix} L \\ L \end{pmatrix}-\begin{pmatrix} D_1 & 0 \\ 0 & D_2 \end{pmatrix}\begin{pmatrix} X_1 \\ X_2 \end{pmatrix}, \quad \begin{pmatrix} P & 0 \\ 0 & P \end{pmatrix}, \tag{8.43}$$

where all symbols have the same meanings as that of Eqs. 7.140 and 7.142.

Suppose GPS observation equation is Eq. 8.38 and the related least squares normal equation is Eq. 8.39, where $X_2 = N$ (N is the ambiguity sub-vector) and $X_1 = Y$ (Y is the other unknown sub-vector). The general criterion is (cf. Eq. 8.35)

$$\delta(\mathrm{d}X)=(X_0-X)^T Q^{-1}(X_0-X), \tag{8.44}$$

where $X = (Y \quad N)^T$, $X_0 = (Y_0 \quad N_0)^T$, $\mathrm{d}X = X_0 - X$ and index 0 denotes the float solution. The search process in the ambiguity domain is a process to find out a solution X (which includes N in the searching area and the computed Y) so that the value of $\delta(\mathrm{d}X)$ reaches the minimum. The optimality property of this criterion is obvious.

For the equivalent observation Eq. 8.43, the related least squares normal equation is Eq. 8.41. The related equivalent general criterion is then (putting the diagonal cofactor of Eq. 8.41 into Eq. 8.44 and taking Eqs. 8.40 and 8.42 into account)

$$\begin{aligned} \delta_1(\mathrm{d}X)&=(Y_0-Y)^T Q_{11}^{-1}(Y_0-Y)+(N_0-N)^T Q_{22}^{-1}(N_0-N) \\ &=\delta(\mathrm{d}Y)+\delta(\mathrm{d}N) \end{aligned} \tag{8.45}$$

where index 1 is used to distinguish criterion of Eq. 8.45 from Eq. 8.44. The observation equations 8.38 and 8.43 are equivalent, and the related normal Eqs. 8.39 and 8.41 are also equivalent. Therefore, the Criterion 8.45 is called an equivalent criterion of the general Criterion 8.44.

Furthermore, Y and N shall be consistent to each other because they are presented in the same normal Eqs. 8.39 and 8.41. Using condition $W = N$ and notation of Eq. 8.42, one has from Eqs. 8.26 and 8.24

$$Y_0-Y=Q_{12}Q_{22}^{-1}(N_0-N). \tag{8.46}$$

Putting Eq. 8.46 into Eq. 8.45, one has

$$\delta_1(\mathrm{d}X)=(N_0-N)^T[Q_{22}^{-1}(E+Q_{21}Q_{11}^{-1}Q_{12}Q_{22}^{-1})](N_0-N). \tag{8.47}$$

It is notable that the second term $\delta(\mathrm{d}N)$ of the equivalent criterion Eq. 8.45 is exactly the same as the commonly used least squares ambiguity search (LSAS) criterion of Eq. 8.30 (cf., e.g., Teunissen 1995; Leick 1995; Hofmann-Wellenhof et al. 1997; Euler and Landau

(c) ketabton.com: The Digital Library

1992; Han and Rizos 1997). Through Eq. 8.47 one may clearly see the differences between the criteria of Eqs. 8.30 and 8.45. When the results searched using Eq. 8.30 are different from that of using Eq. 8.45, the results from the search using Eq. 8.30 shall be only sub-optimal ones due to the optimality and uniqueness property of Eq. 8.45. The first term on the right side of Eq. 8.45 signifies an enlarging of the residuals due to the coordinate change caused by ambiguity fixing (cf. Sect. 8.3.3). The second term on the right side of Eq. 8.45 signifies an enlarging of the residuals due to the ambiguity change caused by ambiguity fixing (cf. Sect. 8.3.4). Equation 8.45 takes both effects into account.

1. Optimality and Uniqueness Properties of the Equivalent Criterion

The float solution X_0 is the optimal and unique solution of Eq. 7.117 under the least squares principle. Criterion Eq. 8.45 is equivalent to criterion Eq. 8.44. A X leads to the minimum of $\delta_1(\mathrm{d}X)$ in Eq. 8.45, which will lead to the minimum of $\delta(\mathrm{d}X)$ in Eq. 8.44 and consequentially the minimum of $(V^TPV)_c$ in Eq. 8.36; therefore using criterion of Eq. 8.45, analogously, the searched vector X is the optimal solution of Eq. 8.38 under the least squares principle and integer ambiguity properties. The uniqueness property is obvious. If one has X_1 and X_2 so that $\delta_1(\mathrm{d}X_1) = \delta_2(\mathrm{d}X_2) = \text{min.}$, or $\delta_1(\mathrm{d}X_1) - \delta_1(\mathrm{d}X_2) = 0$, then by using Eq. 8.45, one may assume that X_1 must be equal to X_2.

It is notable that Eqs. 8.44 and 8.45 are equivalent for use in searching; however, they are neither the same nor equal. For computing the precision, δ in Eq. 8.36 has to be computed using Eq. 8.44.

8.3.8 Numerical Examples of the Equivalent Criterion

Several numerical examples are given here to illustrate the behaviour of the two terms of the criterion. The first and second terms on the right-hand side of Eq. 8.45 are denoted as $\delta(\mathrm{d}Y)$ and $\delta(\mathrm{d}N)$, respectively. $\delta_1(\mathrm{d}X) = \delta(\mathrm{d}Y) + \delta(\mathrm{d}N)$ is the equivalent criterion of the general criterion and is denoted as $\delta(\text{total})$. The term $\delta(\mathrm{d}N)$ is the LSAS criterion. Of course, the search is made in the ambiguity domain. The search area is determined by the precision vector of the float solution. All possible candidates are tested one by one, and the related $\delta_1(\mathrm{d}X)$ are compared with each other to find out the minimum.

In the first example, precise orbits and dual frequency GPS data of 15 April 1999 at station Brst (N 48.3805°, E 355.5034°) and Hers (N 50.8673°, E 0.3363°) are used. The session length is 4 hours. The total search candidate number is 1 020. Results of the two delta components are illustrated as 2-D graphics with the 1st axis of search number and the 2nd axis of delta in Fig. 8.1. The red and blue lines represent $\delta(\mathrm{d}Y)$ and $\delta(\mathrm{d}N)$, respectively. $\delta(\mathrm{d}Y)$ reaches the minimum at the search No. 237, and $\delta(\mathrm{d}N)$ at 769. $\delta(\text{total})$ is plotted in Fig. 8.2, and it shows that the general criterion reaches the minimum at the search No. 493. For more detail, a part of the results are listed in Table 8.1.

$\delta(\mathrm{d}N)$ reaches the second minimum at search No. 771. This example shows that the minimum of $\delta(\mathrm{d}N)$ may not lead to the minimum of total delta, because the related $\delta(\mathrm{d}Y)$ is large. If the delta ratio criterion is used in this case, the LSAS method will reject the found minimum and explain that no significant ambiguity fixing can be made. However, because of the uniqueness principle of the general criterion, the search reaches the total minimum uniquely.

(c) ketabton.com: The Digital Library

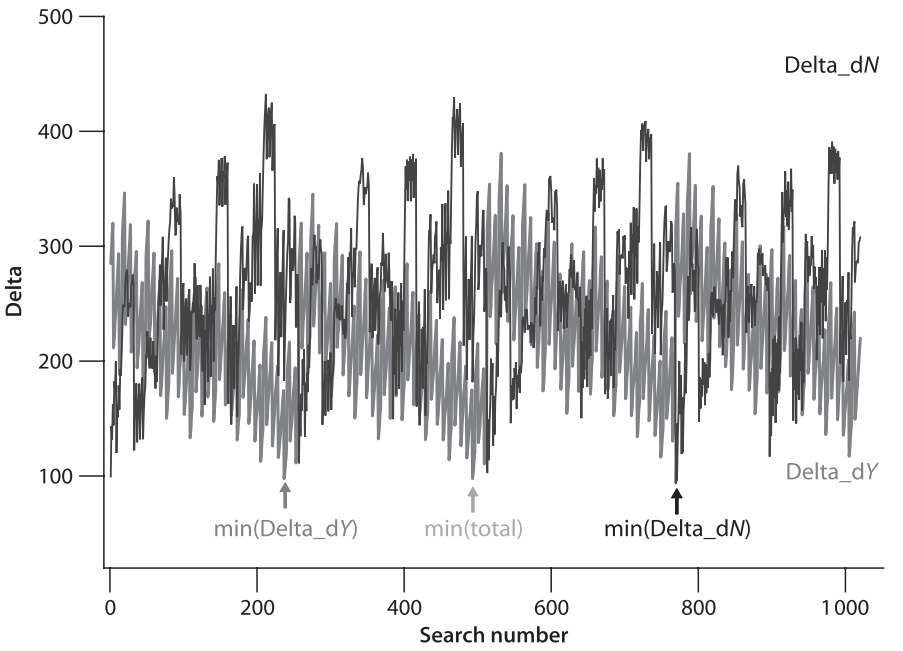

Fig. 8.1. Two components of the equivalent ambiguity search criterion

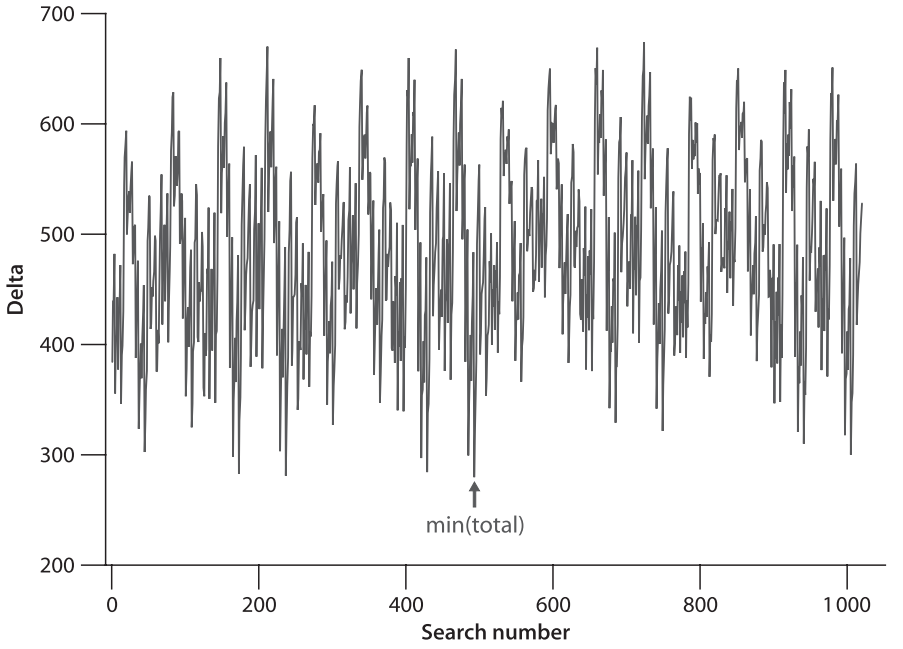

Fig. 8.2. Equivalent ambiguity search criterion

(c) ketabton.com: The Digital Library

The second example is very similar to the first one. The delta values of the search process are plotted in Fig. 8.3, where $\delta(\mathrm{d}Y)$ is much smaller than $\delta(\mathrm{d}N)$. $\delta(\mathrm{d}N)$ reaches the minimum at the search No. 5 and $\delta(\mathrm{d}Y)$ at 171. δ(total) reaches the minimum at the search No. 129. The total 11 ambiguity parameters are fixed and listed in Table 8.2. Two ambiguity fixings have just one cycle difference at the 6th ambiguity parameter. The related coordinate solutions after the ambiguity fixings are listed in Table 8.3. The coordinate differences at component x and z are about 5 mm. Even the results are very similar; however, two criteria do give different results.

In the third example, real GPS data of 3 October 1997 at station Faim (N 38.5295°, E 331.3711°) and Flor (N 39.4493°, E 328.8715°) are used. The delta values of the search process are listed in Table 8.4. Both $\delta(\mathrm{d}N)$ and δ(total) reach the minimum at the search No. 5. This indicates that the LSAS criterion may sometimes reach the same result as that of the equivalent criterion being used.

Table 8.1. Delta values of searching process

Search No.	$\delta(\mathrm{d}N)$	$\delta(\mathrm{d}Y)$	δ(total)
237	183.0937	97.8046	280.8984
493	181.7359	97.9494	279.6853
769	93.3593	315.2760	408.6353
771	96.0678	343.5736	439.6414

Table 8.2. Two kinds of ambiguity fixing due to two criteria

Ambiguity No.	1	2	3	4	5	6	7	8	9	10	11
LSAS fixing	0	0	1	0	0	0	–1	0	0	–1	–1
General fixing	0	0	1	0	0	–1	–1	0	0	–1	–1

Table 8.3. Ambiguity fixed coordinate solutions (in meters)

Coordinates	x	y	z
LSAS fixing	0.2140	–0.0449	0.1078
General fixing	0.2213	–0.0465	0.1127

Table 8.4. Deltas of the ambiguity search process

Search No.	$\delta(\mathrm{d}N)$	$\delta(\mathrm{d}Y)$	δ(total)
1	248.5681	129.0555	377.6236
2	702.6925	58.9271	761.6195
3	889.5496	107.9330	997.4825
4	452.1952	42.3226	494.5178
5	186.7937	112.3030	299.0967
6	739.0487	55.9744	795.0231
7	931.4125	89.9074	1021.3199
8	592.1887	38.0969	630.2856

(c) ketabton.com: The Digital Library

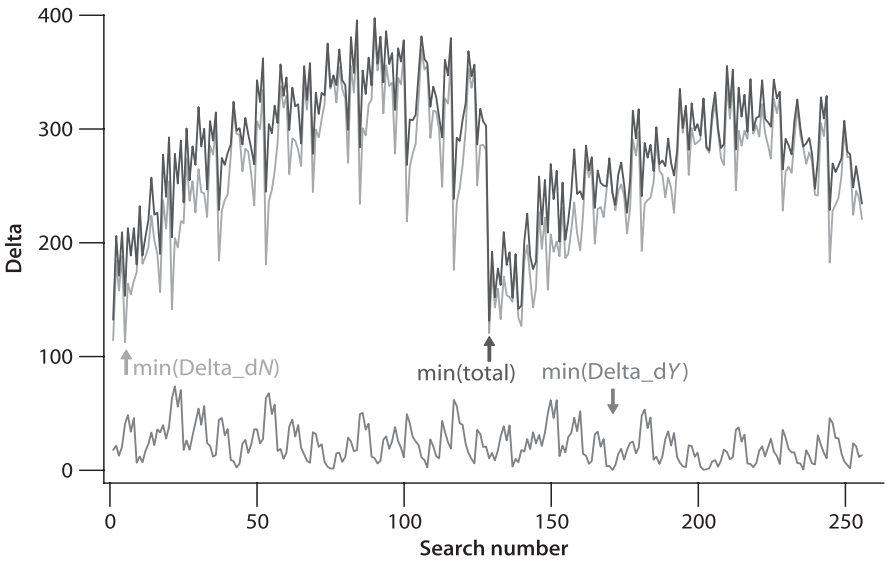

Fig. 8.3. Example of equivalent ambiguity search criterion

8.3.9 Conclusions and Comments

1. Conclusions

A general criterion and its equivalent criterion of integer ambiguity searching are proposed in this section. Using these two criteria, the searched result is optimal and unique under the least squares minimum principle and under the condition of integer ambiguities. The general criterion has a clear geometrical explanation. The theoretical relationship between the equivalent criterion and the commonly used least squares ambiguity search (LSAS) criterion is obvious. It shows that the LSAS criterion is just one of the terms of the equivalent criterion of the general criterion (this does not take into account the residual enlarging effect caused by coordinate change due to ambiguity fixing). Numerical examples show that a minimum $\delta(\mathrm{d}N)$ may have a relatively large $\delta(\mathrm{d}Y)$, and therefore a minimum $\delta(\mathrm{d}N)$ may not guarantee a minimum $\delta(\mathrm{total})$. For an optimal search, the equivalent criterion or the general criterion shall be used.

2. Comments

The float solution is the optimal solution of the GPS problem under the least squares minimum principle. Using the equivalent general criterion, the searched solution is the optimal solution under the least squares minimum principle and under the condition of integer ambiguities. However, the ambiguity-searching criterion is just a statistic criterion. Statistic correctness does not guarantee correctness in all applications. Ambiguity fixing only makes sense when the GPS observables are good enough and the data processing models are accurate enough.

(c) ketabton.com: The Digital Library

8.4 Ambiguity Function

It is well-known that in GPS precise positioning, ambiguity resolution is one of the key problems that has to be solved. Some well-derived ambiguity fixing and searching algorithms have been published in the past. One of these methods is the ambiguity function (AF) method, which can be found in many standard publications (Remondi 1984; Wang et al. 1988; Han and Rizos 1995; Hofmann-Wellenhof et al. 1997).

The principle of the ambiguity function method is to use the single-differenced phase observation

$$\Phi_j(t_k) = \frac{1}{\lambda}\rho_j(t_k) + N_j - \gamma(t_k), \tag{8.48}$$

to form an exponential complex function

$$e^{i2\pi[\Phi_j(t_k)-\rho_j(t_k)/\lambda]} = e^{i2\pi[N_j-\gamma(t_k)]} \quad \text{or} \tag{8.49}$$

$$e^{i2\pi[\Phi_j(t_k)-\rho_j(t_k)/\lambda]} = e^{-i2\pi\gamma(t_k)}, \tag{8.50}$$

where Φ is the phase observable, ρ is the geometric distance of the signal transmitting path, λ is the wavelength, index j denotes the observed satellite, t_k is the k^{th} observational time, N is ambiguity, γ is the model of the receiver clock errors, and i is the imaginary unit. All terms in Eq. 8.48 have the units of cycles and are single-differenced terms. Property

$$e^{i2\pi N_j} = 1$$

is used in order to get Eq. 8.50.

Making a summation over all satellites and then taking the modulus operation, one has

$$\left|\sum_{j=1}^{n_j} e^{i2\pi[\Phi_j(t_k)-\rho_j(t_k)/\lambda]}\right| = n_j(k), \tag{8.51}$$

where property

$$\left|e^{-i2\pi\gamma(t_k)}\right| = 1$$

is used, n_j is the satellite number and $n_j(k)$ is the observed satellite number at epoch k.

Making a summation of Eq. 8.51 over all the observed time epochs, one has

$$\sum_{k=1}^{n_k}\left|\sum_{j=1}^{n_j} e^{i2\pi[\Phi_j(t_k)-\rho_j(t_k)/\lambda]}\right| = \sum_{k=1}^{n_k} n_j(k), \tag{8.52}$$

where n_k is the total epochs number. The left side of Eq. 8.52 is called the ambiguity function, where unknowns are the coordinates of the remote station. The values of the ambiguity function have to be computed for all candidates of coordinates, and the optimum solution is found if the function reaches the maximum, i.e.,

(c) ketabton.com: The Digital Library

$$\sum_{k=1}^{n_k} \left| \sum_{j=1}^{n_j} \mathrm{e}^{i2\pi[\Phi_j(t_k)-\rho_j(t_k)/\lambda]} \right| \Rightarrow \text{maximum} . \tag{8.53}$$

The search area can be determined by the standard deviations (σ) of the initial coordinates (e.g., a cube with side lengths of 3σ or a sphere with a radius of 3σ). The AF method is indeed an ambiguity free method. The ambiguity can be computed using the optimal coordinate solution of Eq. 8.53.

Further discussion on the AF method is given in the next sub-section.

8.4.1 Maximum Property of Ambiguity Function

The ambiguity function is discussed in Sect. 8.4. Here a numerical study of the maximum property of the ambiguity function (AF) is given. It seems that the maximum value of the AF trends to be reached at the boundary of any given search area. Numerical examples are given to illustrate the conclusion. However, a theoretical proof has still not been found up to now; even the author tried to find one, but failed.

Numerical Examples

Several numerical examples are given here to illustrate the behaviours of the ambiguity function criterion. The GPS data of the EU AGMASCO project (cf., e.g., Xu et al. 1997) are used. Data are combined with the data of IGS network and solved for precise coordinates as references. The station Faim (N 38.5295°, E 331.3711°) is used as the reference and Flor (N 39.4493°, E 328.8715°) is used as the remote station. The baseline length is about 240 km. The data length is about four hours of 3 October, 1997. KSGsoft (Xu et al. 1998) is used for computing a static solution of the coordinates of Flor. The differences of the KSGsoft solution and IGS solution are (0.26, 1.93, 1.37) cm in the global Cartesian coordinate system. Related standard deviations of the KSGsoft solution are (0.04, 0.04, 0.02) cm. The differences are caused partly by the different data lengths. This assures a good standard for the software being used.

The search step is selected as 1 mm. Tropospheric and ionospheric effects are corrected. In the first example, three hours of data are used. The search area is a 3-D cube with side lengths of ±(0.7, 0.7, 0.4) cm in (x, y, z). Results show that the AF maximum is reached at point (–0.7, 0.7, 0.4) cm, which is on the boundary of the area being searched.

A search process (with a search area of ±7 mm and one hour of data) is illustrated in 2-D graphics with the 1st axis containing search numbers and the 2nd axis containing AF values in Fig. 8.4. The graphic looks like a 3-D AF projection of the cubic searching area (the picture could be quite different in other examples). Figure 8.4 clearly shows the boundary maximum effect of the AF criterion. Expanding the searched area (and, of course, its boundary), the maximum is reached on the new boundary (of the new cubic surface).

Alternatively, the search may be made on a spherical surface with an expanding radius. The results of such an example are illustrated in Fig. 8.5, where only radii of 1, 2, …, 10 mm are given. As the radius expands, the AF maximum becomes greater and is always reached over the spherical surface with the maximum radius.

(c) ketabton.com: The Digital Library

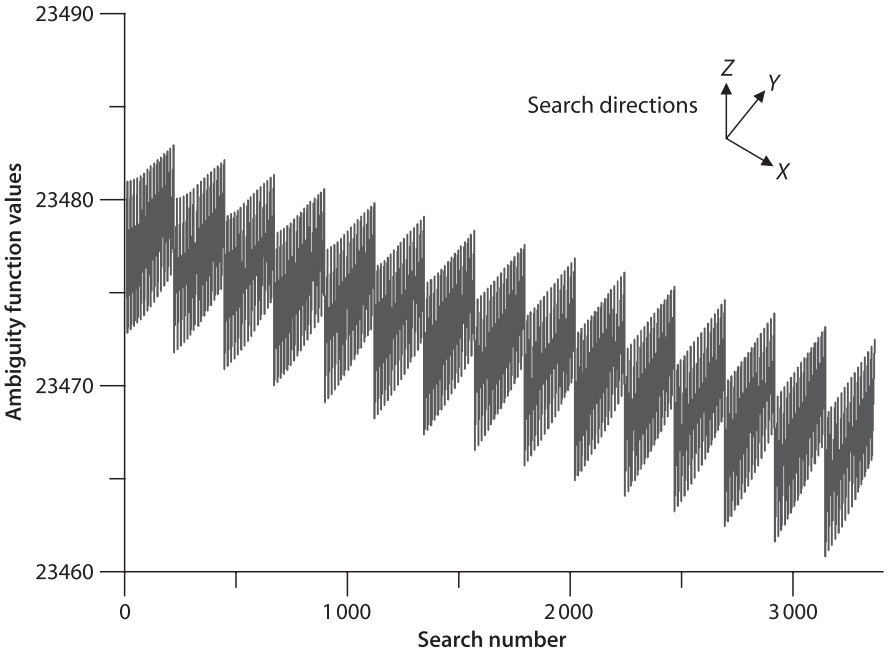

Fig. 8.4. 3-D coordinate search using ambiguity function

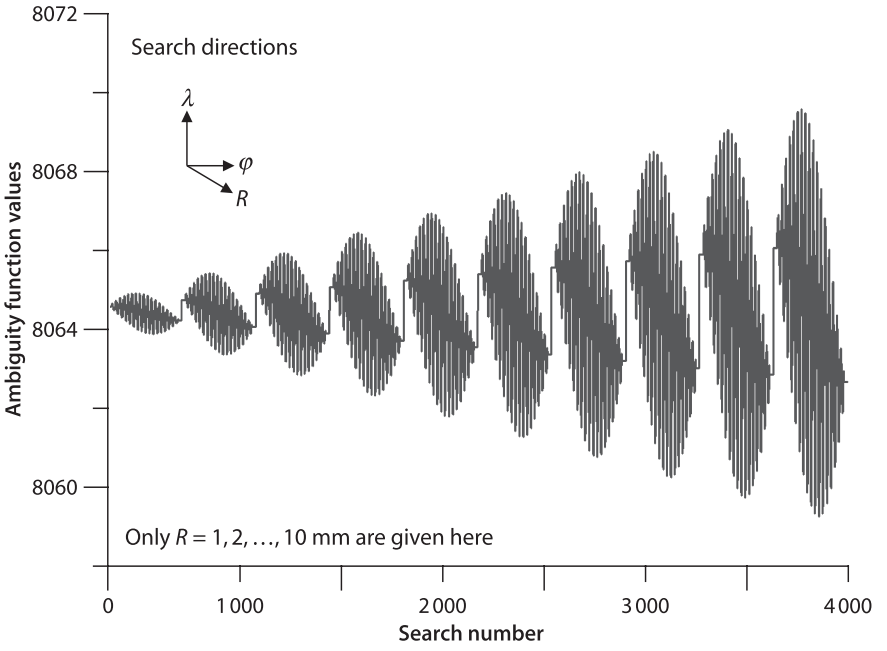

Fig. 8.5. Spherical coordinate search using ambiguity function

(c) ketabton.com: The Digital Library

Theoretical Indications

The AF Eq. 8.53 is rewritten as

$$\sum_{k=1}^{n_k} G(t_k) \Rightarrow \max , \tag{8.54}$$

$$G(t_k) = |S_k|, \quad S_k = \sum_{j=1}^{n_j} \mathrm{e}^{i2\pi \cdot v_j(t_k)} , \tag{8.55}$$

$$v_j(t_k) = \Phi_j(t_k) - \rho_j(t_k)/\lambda , \quad Y \in \Omega \quad \text{and} \tag{8.56}$$

$$\mathrm{e}^{i2\pi \cdot v_j(t_k)} = \cos(2\pi v_j(t_k)) + i \sin(2\pi v_j(t_k)) , \tag{8.57}$$

where Y is the coordinate vector, Ω is to be the searched coordinate area and is a closed area (i.e., it includes the boundary Γ), $v_j(t_k)$ are the residuals of GPS observation equations (a continuous function of Y), S_k is a complex function of Y, and $G(t_k)$ is the modulus of S_k.

If the GPS data sampling intervals are sufficiently close and the numerical integration error is negligible (cf. Xu 1992), then one has

$$\frac{1}{n_k} \sum_{k=1}^{n_k} G(t_k) = \frac{1}{T} \int_{t_1}^{t_e} G(t) \cdot \mathrm{d}t , \tag{8.58}$$

where $T = t_e - t_1$, $t_e = t(n_k)$, and t_1 and t_e are the beginning and end time of the observations. According to the *middle value theorem* of the integration (cf., e.g., Bronstain and Semendjajew 1987; Wang et al. 1979) (such a theorem can be found in all integration related books), one has a time point ξ ($t_1 < \xi < t_e$) so that

$$\frac{1}{T} \int_{t_1}^{t_e} G(t) \cdot \mathrm{d}t = G(\xi) , \tag{8.59}$$

i.e., the AF can be represented by a unique $G(t)$ at time ξ (the constant factor is omitted here). Equation 8.54 turns out to be

$$G(\xi) \Rightarrow \max . \tag{8.60}$$

Because of the definition of AF, $G(\xi)$ is a modulus of a complex function.

In complex function analysis theory, there is a so-called maximum theorem (cf., e.g., Bronstain and Semendjajew 1987; Wang et al. 1979), i.e.:

Maximum Modulus Theorem: if complex function $f(z)$ is analytic within a limited area Z and is continuous over the closed Z, then modulus $|f(z)|$ reaches the maximum on the boundary Γ of Z.

However, such a theorem cannot be directly used for Eq. 8.60 because the theorem is valid only for the analytic complex function defined over a complex plane, whereas function $G(\xi)$ is a complicated three-dimensional complex function.

Maybe the interested reader will consider this in detail and find out a theoretical proof.

(c) ketabton.com: The Digital Library

Chapter 9

Parameterisation and Algorithms of GPS Data Processing

The parameterisation problems of the bias parameters in the GPS observation model are outlined in the Sect. 12.1 of the first edition of this book. The problems are then mostly solved and the theory will be addressed here in detail (cf. Xu 2004; Xu et al. 2006b). The equivalence properties of the algorithms of GPS data processing are described. The standard algorithms are outlined.

9.1 Parameterisation of the GPS Observation Model

The commonly used GPS data processing methods are the so-called uncombined and combining, undifferenced and differencing algorithms (e.g., Hofmann-Wellenhof et al. 2001; Leick 2004; Remondi 1984; Seeber 1993; Strang and Borre 1997; Blewitt 1998). The observation equations of the combining and differencing methods can be obtained by carrying out linear transformations of the original (uncombined and undifferenced) equations. As soon as the weight matrix is similarly transformed according to the law of variance-covariance propagation, all methods are theoretically equivalent. The equivalences of combining and differencing algorithms are discussed in Sects. 6.7 and 6.8, respectively. The equivalence of the combining methods is an exact one, whereas the equivalence of the differencing algorithms is slightly different (Xu 2004, cf. Sect. 9.2). The parameters are implicitly expressed in the discussions; therefore, the parameterisation problems of the equivalent methods have not been discussed in detail. At that time, this topic was considered one of the remaining GPS theoretical problems (Xu 2003, p 279–280, Wells et al. 1987, p 34), and it will be discussed in the next subsection.

Three pieces of evidence of the parameterisation problem of the undifferenced GPS observation model are given first. Then the theoretical analysis and numerical derivation are made to show how to parameterise the bias effects of the undifferenced GPS observation model independently. A geometry-free illustration and a correlation analysis in the case of a phase-code combination are discussed. At the end, conclusions and comments are given.

9.1.1 Evidence of the Parameterisation Problem of the Undifferenced Observation Model

Evidence from Undifferenced and Differencing Algorithms

Suppose the undifferenced GPS observation equation and the related LS normal equation are

(c) ketabton.com: The Digital Library

$$V = L - \begin{pmatrix} A_1 & A_2 \end{pmatrix} \begin{pmatrix} X_1 \\ X_2 \end{pmatrix}, \quad P \tag{9.1}$$

$$\begin{pmatrix} M_{11} & M_{12} \\ M_{21} & M_{22} \end{pmatrix} \begin{pmatrix} X_1 \\ X_2 \end{pmatrix} = \begin{pmatrix} W_1 \\ W_2 \end{pmatrix}, \tag{9.2}$$

where all symbols have the same meanings as that of Eqs. 7.117 and 7.118. Equation 9.2 can be diagonalised as (cf. Sect. 7.6.1)

$$\begin{pmatrix} M_1 & 0 \\ 0 & M_2 \end{pmatrix} \begin{pmatrix} X_1 \\ X_2 \end{pmatrix} = \begin{pmatrix} B_1 \\ B_2 \end{pmatrix}. \tag{9.3}$$

The related equivalent observation equation of the diagonal normal Eq. 9.3 can be written (cf. Sect. 7.6.1)

$$\begin{pmatrix} U_1 \\ U_2 \end{pmatrix} = \begin{pmatrix} L \\ L \end{pmatrix} - \begin{pmatrix} D_1 & 0 \\ 0 & D_2 \end{pmatrix} \begin{pmatrix} X_1 \\ X_2 \end{pmatrix}, \quad \begin{pmatrix} P & 0 \\ 0 & P \end{pmatrix}, \tag{9.4}$$

where all symbols have the same meanings as that of Eqs. 7.142 and 7.140. If X_1 is the vector containing all clock errors, then the second equation of Eq. 9.3 is the equivalent double differencing GPS normal equation. It is well known that in a double differencing algorithm, the ambiguity sub-vector contained in X_2 must be the double differencing ambiguities; otherwise, the problem will be generally singular. It is notable that X_2 is identical with that of in the original undifferenced observation Eq. 9.1. Therefore, the ambiguity sub-vector contained in X_2 (in Eq. 9.1) must be a set of double differencing ambiguities (or an equivalent set of ambiguities). This is the first piece of evidence (or indication) of the singularity of the undifferenced GPS observation model in which the undifferenced ambiguities are used.

Evidence from Uncombined and Combining Algorithms

Suppose the original GPS observation equation of one viewed satellite is (cf. Eq. 6.134)

$$\begin{pmatrix} R_1 \\ R_2 \\ \lambda_1 \Phi_1 \\ \lambda_2 \Phi_2 \end{pmatrix} = \begin{pmatrix} 0 & 0 & f_s^2/f_1^2 & 1 \\ 0 & 0 & f_s^2/f_2^2 & 1 \\ 1 & 0 & -f_s^2/f_1^2 & 1 \\ 0 & 1 & -f_s^2/f_2^2 & 1 \end{pmatrix} \begin{pmatrix} \lambda_1 N_1 \\ \lambda_2 N_2 \\ B_1 \\ C_\rho \end{pmatrix}, \quad P; \tag{9.5}$$

then the uncombined or combining algorithms have the same solution of (cf. Eq. 6.138)

$$\begin{pmatrix} \lambda_1 N_1 \\ \lambda_2 N_2 \\ B_1 \\ C_\rho \end{pmatrix} = \begin{pmatrix} 1-2a & -2b & 1 & 0 \\ -2a & 2a-1 & 0 & 1 \\ 1/q & -1/q & 0 & 0 \\ a & b & 0 & 0 \end{pmatrix} \begin{pmatrix} R_1 \\ R_2 \\ \lambda_1 \Phi_1 \\ \lambda_2 \Phi_2 \end{pmatrix}, \tag{9.6}$$

(c) ketabton.com: The Digital Library

where all symbols have the same meanings as that of Eqs. 6.134 and 6.138. Then one notices that the ionosphere (B_1) and geometry (C_ρ) are functions of the codes (R_1 and R_2) and are independent from phases (Φ_1 and Φ_2) in Eq. 9.6. In other words, the phase observables do not have any contribution to the ionosphere and geometry. And this is not possible. Such an illogical conclusion is caused by the parameterisation of the ambiguities given in the observation model of Eq. 9.5. If one takes the first evidence discussed above into account and defines that for each station one of the satellites in view must be selected as reference and the related ambiguity has to be merged into the clock parameter, then the phases do have contributions to ionosphere and geometry. One notices again that the parameterisation is a very important topic and has to be discussed more specifically. An improper parameterisation of the observation model will lead to incorrect conclusions through the derivation from the model.

Evidence from Practice

Without using a priori information, a straightforward programming of the GPS data processing using an undifferenced algorithm leads to no results (i.e., the normal equation is singular, cf. Xu 2004). Therefore an exact parameterisation description is necessary and will be discussed in the next section.

9.1.2 A Method of Uncorrelated Bias Parameterisation

We restrict ourselves here to discuss the parameterisation problem of the bias parameters (or constant effects, i.e., the clock errors and ambiguities) only.

Recall the discussions of the equivalence of undifferenced and differencing algorithms in Sect. 6.8. The equivalence property is valid under three conditions: observation vector L used in Eq. 9.1 is identical; parameterisation of X_2 is identical; and X_1 is able to be eliminated (cf. Sect. 6.8).

The first condition is necessary for the exactness of the equivalence because of the fact that through forming differences, the unpaired data will be cancelled out in the differencing.

The second condition states that the parameterisation of the undifferenced and differencing model should be the same. This may be interpreted as the following: the rank of the undifferenced and differencing equations should be the same if the differencing is formed by a full rank linear transformation. If only the differencing equations are taken into account, then the rank of the undifferenced model should equal the rank of the differencing model plus the number of eliminated independent parameters.

It is well known that one of the clock error parameters is linearly correlated with the others. This may be seen in the proof of the equivalence property of the double differences, where the two receiver clock errors of the baseline may not be separated from each other and have to be transformed to one parameter and then eliminated (Xu 2002, Sect. 6.8). This indicates that if in the undifferenced model all clock errors are modelled, the problem will be singular (i.e. rank defect). Indeed, Wells et al. (1987) noticed that the equivalence is valid if measures are taken to avoid rank defect in the bias parameterisation. Which clock error has to be kept fixed is arbitrary. Because of

(c) ketabton.com: The Digital Library

the different qualities of the satellite and receiver clocks, a good choice is to fix a satellite clock error (the clock is called a reference clock). In practice, the clock error is an unknown; therefore, there is no way to keep that fixed except to fix it to zero. In such a case, the meaning of the other bias parameters will be changed and may represent the relative errors between the other biases.

The third condition is important to ensure a full-ranked parameterisation of the parameter vector X_1, which is going to be eliminated.

The undifferenced Eq. 9.1 is solvable if the parameters X_1 and X_2 are not over-parameterised. In the case of single differences, X_1 includes satellite clock errors and is able to be eliminated. Therefore, to guarantee that the undifferenced model Eq. 9.1 is not singular, X_2 in Eq. 9.1 must be not over-parameterised. In the case of double differences, X_1 includes all clock errors except the reference one. Here we notice that the second observation equation of 9.1 is equivalent to the double differencing observation equation and the second equation of 9.2 is the related normal equation. In a traditional double differencing observation equation, the ambiguity parameters are represented by double differencing ambiguities. Recall that for the equivalence property, the number (or rank) of ambiguity parameters in X_2 that are not linearly correlated must be equal to the number of the double differencing ambiguities. In the case of triple differences, X_1 includes all clock errors and ambiguities. The fact that X_1 should able to be eliminated leads again to the conclusion that the ambiguities should be linearly independent.

The two equivalent linear equations should have the same rank. Therefore, if all clock errors except the reference one are modelled, the number of independent undifferenced ambiguity parameters should be equal to the number of double differencing ambiguities. According to the definition of the double differencing ambiguity, one has for one baseline

$$\begin{aligned}
N_{i1,i2}^{k1,k2} &= N_{i2}^{k2} - N_{i1}^{k2} - N_{i2}^{k1} + N_{i1}^{k1} \\
N_{i1,i2}^{k1,k3} &= N_{i2}^{k3} - N_{i1}^{k3} - N_{i2}^{k1} + N_{i1}^{k1} \\
N_{i1,i2}^{k1,k4} &= N_{i2}^{k4} - N_{i1}^{k4} - N_{i2}^{k1} + N_{i1}^{k1} \\
&\cdots \\
N_{i1,i2}^{k1,kn} &= N_{i2}^{kn} - N_{i1}^{kn} - N_{i2}^{k1} + N_{i1}^{k1}
\end{aligned} \tag{9.7}$$

where $i1$ and $i2$ are station indices, kj is the j^{th} satellite's identification, n is the common observed satellite number and is a function of the baseline, and N is ambiguity. Then there are $n-1$ double differencing ambiguities and $2n$ undifferenced ambiguities. Taking the connection of the baselines into account, there are $n-1$ double differencing ambiguities and n new undifferenced ambiguities for any further baseline. If $i1$ is defined as the reference station of the whole network and $k1$ as the reference satellite of station $i2$, then undifferenced ambiguities of the reference station cannot be separated from the others (i.e., they are linearly correlated with the others). The undifferenced ambiguity of the reference satellite of station $i2$ cannot be separated from the others (i.e., it is linearly correlated with the others). That is, the ambiguities of the reference station cannot be determined, and the ambiguities of the reference

(c) ketabton.com: The Digital Library

satellites of non-reference stations cannot be determined. Either they should not be modelled or they should be kept fixed. A straightforward parameterisation of all undifferenced ambiguities will lead to rank defect, and the problem will be singular and not able to be solved.

Therefore, using the equivalence properties of the equivalent equation of GPS data processing, we come to the conclusion that the ambiguities of the reference station and ambiguities of the reference satellite of every station are linearly correlated with the other ambiguities and clock error parameters. However, a general method of parameterisation should be independent of the selection of the references (station and satellite). Therefore, we use a two-baseline network to further our analysis. The original observation equation can be written as follows:

$$\begin{aligned}
L_{i1}^{k1} &= \ldots \delta_{i1} + \delta_{k1} + N_{i1}^{k1} + \ldots \\
L_{i1}^{k2} &= \ldots \delta_{i1} + \delta_{k2} + N_{i1}^{k2} + \ldots \\
L_{i1}^{k3} &= \ldots \delta_{i1} + \delta_{k3} + N_{i1}^{k3} + \ldots \\
L_{i1}^{k4} &= \ldots \delta_{i1} + \delta_{k4} + N_{i1}^{k4} + \ldots \\
L_{i1}^{k5} &= \ldots \delta_{i1} + \delta_{k5} + N_{i1}^{k5} + \ldots \\
L_{i1}^{k6} &= \ldots \delta_{i1} + \delta_{k6} + N_{i1}^{k6} + \ldots
\end{aligned} \tag{9.8}$$

$$\begin{aligned}
L_{i2}^{k1} &= \ldots \delta_{i2} + \delta_{k1} + N_{i2}^{k1} + \ldots \\
L_{i2}^{k2} &= \ldots \delta_{i2} + \delta_{k2} + N_{i2}^{k2} + \ldots \\
L_{i2}^{k3} &= \ldots \delta_{i2} + \delta_{k3} + N_{i2}^{k3} + \ldots \\
L_{i2}^{k4} &= \ldots \delta_{i2} + \delta_{k4} + N_{i2}^{k4} + \ldots \\
L_{i2}^{k5} &= \ldots \delta_{i2} + \delta_{k5} + N_{i2}^{k5} + \ldots \\
L_{i2}^{k7} &= \ldots \delta_{i2} + \delta_{k7} + N_{i2}^{k7} + \ldots
\end{aligned} \tag{9.9}$$

$$\begin{aligned}
L_{i3}^{k2} &= \ldots \delta_{i3} + \delta_{k2} + N_{i3}^{k2} + \ldots \\
L_{i3}^{k3} &= \ldots \delta_{i3} + \delta_{k3} + N_{i3}^{k3} + \ldots \\
L_{i3}^{k4} &= \ldots \delta_{i3} + \delta_{k4} + N_{i3}^{k4} + \ldots \\
L_{i3}^{k5} &= \ldots \delta_{i3} + \delta_{k5} + N_{i3}^{k5} + \ldots \\
L_{i3}^{k6} &= \ldots \delta_{i3} + \delta_{k6} + N_{i3}^{k6} + \ldots \\
L_{i3}^{k7} &= \ldots \delta_{i3} + \delta_{k7} + N_{i3}^{k7} + \ldots
\end{aligned} \tag{9.10}$$

where only the bias terms are listed and L and δ represent observable and clock error, respectively. Observation equations of station $i1$, $i2$ and $i3$ are Eqs. 9.8, 9.9 and 9.10. Define that the baseline 1, 2 are formed by station $i1$ and $i2$, as well as $i2$ and $i3$, respectively. Select $i1$ as the reference station and then keep the related ambiguities fixed (set to zero for simplification). For convenience of later discussion,

(c) ketabton.com: The Digital Library

select δ_{i1} as the reference clock (set to zero, too) and select $k1$, $k2$ as reference satellites of the station $i2$, i3 (set the related ambiguities to zero), respectively. Then Eqs. 9.8–9.10 become

$$\begin{aligned}
L_{i1}^{k1} &= \ldots\delta_{k1} + \ldots \\
L_{i1}^{k2} &= \ldots\delta_{k2} + \ldots \\
L_{i1}^{k3} &= \ldots\delta_{k3} + \ldots \\
L_{i1}^{k4} &= \ldots\delta_{k4} + \ldots \\
L_{i1}^{k5} &= \ldots\delta_{k5} + \ldots \\
L_{i1}^{k6} &= \ldots\delta_{k6} + \ldots
\end{aligned} \tag{9.11}$$

$$\begin{aligned}
L_{i2}^{k1} &= \ldots\delta_{i2} + \delta_{k1} + \ldots \\
L_{i2}^{k2} &= \ldots\delta_{i2} + \delta_{k2} + N_{i2}^{k2} + \ldots \\
L_{i2}^{k3} &= \ldots\delta_{i2} + \delta_{k3} + N_{i2}^{k3} + \ldots \\
L_{i2}^{k4} &= \ldots\delta_{i2} + \delta_{k4} + N_{i2}^{k4} + \ldots \\
L_{i2}^{k5} &= \ldots\delta_{i2} + \delta_{k5} + N_{i2}^{k5} + \ldots \\
L_{i2}^{k7} &= \ldots\delta_{i2} + \delta_{k7} + N_{i2}^{k7} + \ldots
\end{aligned} \tag{9.12}$$

$$\begin{aligned}
L_{i3}^{k2} &= \ldots\delta_{i3} + \delta_{k2} + \ldots \\
L_{i3}^{k3} &= \ldots\delta_{i3} + \delta_{k3} + N_{i3}^{k3} + \ldots \\
L_{i3}^{k4} &= \ldots\delta_{i3} + \delta_{k4} + N_{i3}^{k4} + \ldots \\
L_{i3}^{k5} &= \ldots\delta_{i3} + \delta_{k5} + N_{i3}^{k5} + \ldots \\
L_{i3}^{k6} &= \ldots\delta_{i3} + \delta_{k6} + N_{i3}^{k6} + \ldots \\
L_{i3}^{k7} &= \ldots\delta_{i3} + \delta_{k7} + N_{i3}^{k7} + \ldots
\end{aligned} \tag{9.13}$$

Differences can be formed through linear operations. The total operation is a full rank linear transformation, which does not change the least squares solution of the original equations. Single differences can be formed by the following (Eq. 9.11 remains unchanged and therefore will not be listed again):

$$\begin{aligned}
L_{i2}^{k1} - L_{i1}^{k1} &= \ldots\delta_{i2} + \ldots \\
L_{i2}^{k2} - L_{i1}^{k2} &= \ldots\delta_{i2} + N_{i2}^{k2} + \ldots \\
L_{i2}^{k3} - L_{i1}^{k3} &= \ldots\delta_{i2} + N_{i2}^{k3} + \ldots \\
L_{i2}^{k4} - L_{i1}^{k4} &= \ldots\delta_{i2} + N_{i2}^{k4} + \ldots \\
L_{i2}^{k5} - L_{i1}^{k5} &= \ldots\delta_{i2} + N_{i2}^{k5} + \ldots \\
L_{i2}^{k7} &= \ldots\delta_{i2} + \delta_{k7} + N_{i2}^{k7} + \ldots
\end{aligned} \tag{9.14}$$

(c) ketabton.com: The Digital Library

$$
\begin{aligned}
L_{i3}^{k2} - L_{i2}^{k2} &= \ldots \delta_{i3} - \delta_{i2} - N_{i2}^{k2} + \ldots \\
L_{i3}^{k3} - L_{i2}^{k3} &= \ldots \delta_{i3} - \delta_{i2} + N_{i3}^{k3} - N_{i2}^{k3} + \ldots \\
L_{i3}^{k4} - L_{i2}^{k4} &= \ldots \delta_{i3} - \delta_{i2} + N_{i3}^{k4} - N_{i2}^{k4} + \ldots \\
L_{i3}^{k5} - L_{i2}^{k5} &= \ldots \delta_{i3} - \delta_{i2} + N_{i3}^{k5} - N_{i2}^{k5} + \ldots \\
L_{i3}^{k6} &= \ldots \delta_{i3} + \delta_{k6} + N_{i3}^{k6} + \ldots \\
L_{i3}^{k7} - L_{i2}^{k7} &= \ldots \delta_{i3} - \delta_{i2} + N_{i3}^{k7} - N_{i2}^{k7} + \ldots
\end{aligned}
\tag{9.15}
$$

where two observations are unpaired due to the baseline definitions. Double differences can be formed by

$$
\begin{aligned}
L_{i2}^{k1} - L_{i1}^{k1} &= \ldots \delta_{i2} + \ldots \\
L_{i2}^{k2} - L_{i1}^{k2} - L_{i2}^{k1} + L_{i1}^{k1} &= \ldots N_{i2}^{k2} + \ldots \\
L_{i2}^{k3} - L_{i1}^{k3} - L_{i2}^{k1} + L_{i1}^{k1} &= \ldots N_{i2}^{k3} + \ldots \\
L_{i2}^{k4} - L_{i1}^{k4} - L_{i2}^{k1} + L_{i1}^{k1} &= \ldots N_{i2}^{k4} + \ldots \\
L_{i2}^{k5} - L_{i1}^{k5} - L_{i2}^{k1} + L_{i1}^{k1} &= \ldots N_{i2}^{k5} + \ldots \\
L_{i2}^{k7} - L_{i2}^{k1} + L_{i1}^{k1} &= \ldots \delta_{k7} + N_{i2}^{k7} + \ldots
\end{aligned}
\tag{9.16}
$$

$$
\begin{aligned}
L_{i3}^{k2} - L_{i2}^{k2} &= \ldots \delta_{i3} - \delta_{i2} - N_{i2}^{k2} + \ldots \\
L_{i3}^{k3} - L_{i2}^{k3} - L_{i3}^{k2} + L_{i2}^{k2} &= \ldots N_{i3}^{k3} - N_{i2}^{k3} + N_{i2}^{k2} + \ldots \\
L_{i3}^{k4} - L_{i2}^{k4} - L_{i3}^{k2} + L_{i2}^{k2} &= \ldots N_{i3}^{k4} - N_{i2}^{k4} + N_{i2}^{k2} + \ldots \\
L_{i3}^{k5} - L_{i2}^{k5} - L_{i3}^{k2} + L_{i2}^{k2} &= \ldots N_{i3}^{k5} - N_{i2}^{k5} + N_{i2}^{k2} + \ldots \\
L_{i3}^{k6} &= \ldots \delta_{i3} + \delta_{k6} + N_{i3}^{k6} + \ldots \\
L_{i3}^{k7} - L_{i2}^{k7} - L_{i3}^{k2} + L_{i2}^{k2} &= \ldots N_{i3}^{k7} - N_{i2}^{k7} + N_{i2}^{k2} + \ldots
\end{aligned}
\tag{9.17}
$$

Using Eqs. 9.16 and 9.11, Eq. 9.17 can be further modified to

$$
\begin{aligned}
&L_{i3}^{k2} - L_{i2}^{k2} + (L_{i2}^{k1} - L_{i1}^{k1}) + (L_{i2}^{k2} - L_{i1}^{k2} - L_{i2}^{k1} + L_{i1}^{k1}) = \ldots \delta_{i3} + \ldots \\
&L_{i3}^{k3} - L_{i2}^{k3} - L_{i3}^{k2} + L_{i2}^{k2} + (L_{i2}^{k3} - L_{i1}^{k3} - L_{i2}^{k1} + L_{i1}^{k1}) - (L_{i2}^{k2} - L_{i1}^{k2} - L_{i2}^{k1} + L_{i1}^{k1}) \\
&\quad = \ldots N_{i3}^{k3} + \ldots \\
&L_{i3}^{k4} - L_{i2}^{k4} - L_{i3}^{k2} + L_{i2}^{k2} + (L_{i2}^{k4} - L_{i1}^{k4} - L_{i2}^{k1} + L_{i1}^{k1}) - (L_{i2}^{k2} - L_{i1}^{k2} - L_{i2}^{k1} + L_{i1}^{k1}) \\
&\quad = \ldots N_{i3}^{k4} + \ldots \\
&L_{i3}^{k5} - L_{i2}^{k5} - L_{i3}^{k2} + L_{i2}^{k2} + (L_{i2}^{k5} - L_{i1}^{k5} - L_{i2}^{k1} + L_{i1}^{k1}) - (L_{i2}^{k2} - L_{i1}^{k2} - L_{i2}^{k1} + L_{i1}^{k1}) \\
&\quad = \ldots N_{i3}^{k5} + \ldots \\
&L_{i3}^{k6} - L_{i1}^{k6} = \ldots \delta_{i3} + N_{i3}^{k6} + \ldots \\
&L_{i3}^{k7} - L_{i2}^{k7} - L_{i3}^{k2} + L_{i2}^{k2} + (L_{i2}^{k7} - L_{i2}^{k1} + L_{i1}^{k1}) - (L_{i2}^{k2} - L_{i1}^{k2} - L_{i2}^{k1} + L_{i1}^{k1}) \\
&\quad = \ldots - \delta_{k7} + N_{i3}^{k7} + \ldots
\end{aligned}
\tag{9.18}
$$

(c) ketabton.com: The Digital Library

or

$$
\begin{aligned}
L_{i3}^{k2} - L_{i1}^{k2} &= \ldots \delta_{i3} + \ldots \\
L_{i3}^{k3} - L_{i1}^{k3} - L_{i3}^{k2} + L_{i1}^{k2} &= \ldots N_{i3}^{k3} + \ldots \\
L_{i3}^{k4} - L_{i1}^{k4} - L_{i3}^{k2} + L_{i1}^{k2} &= \ldots N_{i3}^{k4} + \ldots \\
L_{i3}^{k5} - L_{i1}^{k5} - L_{i3}^{k2} + L_{i1}^{k2} &= \ldots N_{i3}^{k5} + \ldots \\
L_{i3}^{k6} - L_{i1}^{k6} - L_{i3}^{k2} + L_{i1}^{k2} &= \ldots N_{i3}^{k6} + \ldots \\
L_{i3}^{k7} - \quad L_{i3}^{k2} + L_{i1}^{k2} &= \ldots - \delta_{k7} + N_{i3}^{k7} + \ldots
\end{aligned}
\tag{9.19}
$$

From the last equation of Eqs. 9.16 and 9.19, it is obvious that the clock error and the ambiguities of satellite *k*7, which is not observed by the reference station, are linearly correlated. Keeping one of the ambiguities of the satellite *k*7 at station *i*2 or *i*3 is necessary and equivalent. Therefore, for any satellite that is not observed by the reference station, one of the related ambiguities should be kept fixed (station selection is arbitrary). In other words, one of the ambiguities of all satellites has to be kept fixed. In this way, every transformed equation includes only one bias parameter and the bias parameters are linearly independent (regular). Furthermore, the differencing cannot be formed for the unpaired observations of every baseline. However, in the case of an undifferenced adjustment, the situation would be different. We notice that the equation for *k*6 in Eq. 9.18 can be transformed to a double differencing one in Eq. 9.19. If more data is used in the undifferenced algorithm than in the differencing method, the number of undifferenced ambiguity parameters will be larger than that of the double differencing ones. Therefore, we have to drive the so-called data condition to guarantee that the data are able to be differenced, or equivalently, we have to extend the way of double differencing forming so that the differencing will be not limited by special baseline design. Both will be discussed in Sect. 9.2.

The meanings of the parameters are changed by independent parameterisation, and they can be read from Eqs. 9.11–9.13. The clock errors of the satellites observed by the reference station include the errors of receiver clock and ambiguities. The receiver clock errors include the error of ambiguity of the reference satellite of the same station. Due to the inseparable property of the bias parameters, the clock error parameters no longer represent pure clock errors, and the ambiguities represent no longer pure physical ambiguity. Theoretically speaking, the synchronisation applications of GPS may not be realised using the carrier-phase observations. Furthermore, Eq. 9.19 shows that the undifferenced ambiguities of *i*3 have the meaning of double differencing ambiguities of the station *i*3 and *i*1 in this case.

Up to now, we have discussed the correlation problem of the bias parameters and found a method of how to parameterise the GPS observations regularly to avoid the problem of rank defect. Of course, many other ways to parameterise the GPS observation model can be similarly derived. However, the parameter sets should be equivalent to each other and can be transformed from one set to another uniquely as long as the same data is used.

(c) ketabton.com: The Digital Library

9.1.3 Geometry-Free Illustration

The reason why the reference parameters have to be fixed lies in the nature of range measurements, which cannot provide information of the datum origin (cf., e.g., Wells et al. 1987, p 9). Suppose d is the direct measurement of clock errors of satellite k and receiver i, i.e. $d_i^k = \delta_i + \delta_k$, no matter how many observations were made and how the indices were changed, one parameter (i.e. reference clock) is inseparable from the others and has to be fixed. Suppose h is the direct measurement of ambiguity N and clock errors of satellite k and receiver i, i.e., $h_i^k = \delta_i + \delta_k + N_i^k$, the number of over-parameterised biases is exactly the number of total observed satellites and used receivers. This ensures again that our parameterisation method to fix the reference clock and one ambiguity of every satellite as well as one ambiguity of the reference satellite of every non-reference station is reasonable. The case of combination of d and h (as code and phase observations) will be discussed in the next section.

9.1.4 Correlation Analysis in the Case of Phase-Code Combinations

A phase-code combined observation equation can be written by (cf. Sect. 7.5.2)

$$\begin{pmatrix} V_1 \\ V_2 \end{pmatrix} = \begin{pmatrix} L_1 \\ L_2 \end{pmatrix} - \begin{pmatrix} A_{11} & A_{12} \\ A_{11} & 0 \end{pmatrix} \begin{pmatrix} X_1 \\ X_2 \end{pmatrix} \quad \text{and} \quad P = \begin{pmatrix} w_p P_0 & 0 \\ 0 & w_c P_0 \end{pmatrix}, \tag{9.20}$$

where L_1 and L_2 are the observational vectors of phase (scaled in length) and code, respectively; V_1 and V_2 are related residual vectors; X_2 and X_1 are unknown vectors of ambiguity and others; A_{12} and A_{11} are related coefficient matrices; P_0 is a symmetric and definite weight matrix; and w_p and w_c are weight factors of the phase and code observations.

The phase, code and phase-code normal equations can be formed respectively by

$$\begin{pmatrix} N_{11} & N_{12} \\ N_{21} & N_{22} \end{pmatrix} \begin{pmatrix} X_1 \\ X_2 \end{pmatrix} = \begin{pmatrix} R_1 \\ R_2 \end{pmatrix},$$

$$N_{11} X_1 = R_c, \quad \text{and}$$

$$\begin{pmatrix} M_{11} & M_{12} \\ M_{21} & M_{22} \end{pmatrix} \begin{pmatrix} X_1 \\ X_2 \end{pmatrix} = \begin{pmatrix} B_1 \\ B_2 \end{pmatrix}, \tag{9.21}$$

where

$$M_{11} = (w_p + w_c) A_{11}^T P_0 A_{11} = (w_p + w_c) N_{11},$$

$$M_{12} = M_{21}^T = w_p A_{11}^T P_0 A_{12} = w_p N_{12},$$

$$M_{22} = w_p A_{12}^T P_0 A_{12} = w_p N_{22}, \tag{9.22}$$

(c) ketabton.com: The Digital Library

$$B_1 = A_{11}^T P_0 (w_p L_1 + w_c L_2) = w_p R_1 + w_c R_c \,, \quad \text{and}$$

$$B_2 = w_p A_{12}^T P_0 L_1 = w_p R_2 \,.$$

The covariance matrix Q is denoted

$$Q = \begin{pmatrix} M_{11} & M_{12} \\ M_{21} & M_{22} \end{pmatrix}^{-1} = \begin{pmatrix} Q_{11} & Q_{12} \\ Q_{21} & Q_{22} \end{pmatrix}, \tag{9.23}$$

where (Gotthardt 1978; Cui et al. 1982)

$$\begin{aligned} Q_{11} &= (M_{11} - M_{12} M_{22}^{-1} M_{21})^{-1}, \\ Q_{22} &= (M_{22} - M_{21} M_{11}^{-1} M_{12})^{-1}, \\ Q_{12} &= M_{11}^{-1}(-M_{12} Q_{22}) \quad \text{and} \\ Q_{21} &= M_{22}^{-1}(-M_{21} Q_{11}) \,. \end{aligned} \tag{9.24}$$

i.e.,

$$\begin{aligned} Q_{11} &= ((w_p + w_c) N_{11} - w_p N_{12} N_{22}^{-1} N_{21})^{-1}, \\ Q_{22} &= (w_p N_{22} - w_p^2 (w_p + w_c)^{-1} N_{21} N_{11}^{-1} N_{12})^{-1} \quad \text{and} \\ Q_{21} &= -N_{22}^{-1} N_{21} ((w_p + w_c) N_{11} - w_p N_{12} N_{22}^{-1} N_{21})^{-1} . \end{aligned} \tag{9.25}$$

Thus the correlation coefficient C_{ij} is a function of w_p and w_c, i.e.,

$$C_{ij} = f(w_p, w_c) \,, \tag{9.26}$$

where indices i and j are the indices of unknown parameters in X_1 and X_2. For $w_c = 0$ (only phase is used, X_1 and X_2 are partly linear correlated) and $w_c = w_p$ (X_1 and X_2 are uncorrelated), there exists indices ij, so that

$$C_{ij} = f(w_p, w_c = 0) = 1 \quad \text{and} \quad C_{ij} = f(w_p, w_c = w_p) = 0 \,. \tag{9.27}$$

In other words, there exists indices i and j, the related unknowns are correlated if $w_c = 0$ and uncorrelated if $w_c = w_p$. In the case of a phase-code combination, $w_c = 0.01 w_p$ can be selected, and one has

$$C_{ij} = f(w_p, w_c = 0.01 w_p) \,, \tag{9.28}$$

whose value should be very close to 1 (strong correlated) in the discussed case. Equations 9.26, 9.27 and 9.28 indicate that for the correlated unknown pair ij, the correlation situation may not change much by combining the code to the phase because of

(c) ketabton.com: The Digital Library

the lower weight of the code related to the phase. A numerical test confirmed this conclusion (Xu 2004).

9.1.5 Conclusions and Comments

In this section, the singularity problem of the undifferenced GPS data processing is pointed out and an independent parameterisation method is proposed for bias parameters of the GPS observation model. The method is implemented into software, and the results confirm the correctness of the theory and algorithm. Conclusions can be summarised by

1. Bias parameterisation of undifferenced GPS phase observations with all clock errors except the reference one, and all undifferenced ambiguities are linearly correlated. The linear equation system of undifferenced GPS is then singular and cannot be solved theoretically;
2. A linear independent bias parameterisation can be reached by fixing the reference clock of the reference station, fixing one of the ambiguities of every satellite of arbitrary station (called reference station of every satellite), and fixing the ambiguities of the reference satellite of every non-reference station. The selections of the references are arbitrary; however, the selections are not allowed to be duplicated;
3. The linear independent ambiguity parameter set is equivalent to the parameter set of double differencing ambiguities, and they can be transformed from one to another uniquely if the same data is used;
4. The physical meanings of the bias parameters are varied depending on the way of parameterisation. Due to the inseparable property of the bias parameters, the synchronisation applications of GPS may not be realised using the carrier-phase observations;
5. The phase-code combination does not change the correlation relation between the correlated biases significantly.

Due to the facts regarding the use of the undifferenced algorithm, it is worthy to give some comments:

1. In the undifferenced algorithm, the observation equation is a rank defect one if the over-parameterisation problem has not been taken into account. The numerical inexactness introduced by eliminating the clock error parameters and the use of a priori information of some other parameters are the reason why the singular problem is solvable in practice so far;
2. Using the undifferenced and differencing methods, solutions of the common parameters must be the same if the undifferenced GPS data modelling is really an equivalent one and not over-parameterised;
3. A singular undifferenced parameterisation may become regular by introducing conditions or by fixing some of the parameters through introducing a priori information.

(c) ketabton.com: The Digital Library

9.2 Equivalence of the GPS Data Processing Algorithms

The equivalence theorem, an optimal method for forming an independent baseline network and a data condition as well as the equivalent algorithms using secondary observables are discussed in this section (cf. Xu et al. 2006c).

9.2.1 Equivalence Theorem of GPS Data Processing Algorithms

In Sect. 6.7 the equivalence properties of uncombined and combining algorithms of GPS data processing are given. Whether uncombined or combining algorithms are used, the results obtained are identical and the precisions of the solutions are identical, too. It is notable that the parameterisation is very important. The solutions depend on the parameterisation. For convenience, the original GPS observation equation and the solution are listed as (cf. Sect. 6.7)

$$\begin{pmatrix} R_1 \\ R_2 \\ \lambda_1\Phi_1 \\ \lambda_2\Phi_2 \end{pmatrix} = \begin{pmatrix} 0 & 0 & f_s^2/f_1^2 & 1 \\ 0 & 0 & f_s^2/f_2^2 & 1 \\ 1 & 0 & -f_s^2/f_1^2 & 1 \\ 0 & 1 & -f_s^2/f_2^2 & 1 \end{pmatrix} \begin{pmatrix} \lambda_1 N_1 \\ \lambda_2 N_2 \\ B_1 \\ C_\rho \end{pmatrix}, \quad P = \begin{pmatrix} \sigma_c^2 & 0 & 0 & 0 \\ 0 & \sigma_c^2 & 0 & 0 \\ 0 & 0 & \sigma_p^2 & 0 \\ 0 & 0 & 0 & \sigma_p^2 \end{pmatrix}^{-1}, \tag{9.29}$$

and

$$\begin{pmatrix} \lambda_1 N_1 \\ \lambda_2 N_2 \\ B_1 \\ C_\rho \end{pmatrix} = \begin{pmatrix} 1-2a & -2b & 1 & 0 \\ -2a & 2a-1 & 0 & 1 \\ 1/q & -1/q & 0 & 0 \\ a & b & 0 & 0 \end{pmatrix} \begin{pmatrix} R_1 \\ R_2 \\ \lambda_1\Phi_1 \\ \lambda_2\Phi_2 \end{pmatrix}, \tag{9.30}$$

where the meanings of the symbols are the same as that of Eqs. 6.134 and 6.138.

In Sect. 6.8, the equivalence properties of undifferenced and differencing algorithms of GPS data processing are given. Whether undifferenced or differencing algorithms are used, the results obtained are identical and the precisions of the solutions are equivalent. It is notable that the equivalence here is slightly different from the equivalence in combining algorithms. To distinguish them, we call the equivalence in differencing case a soft equivalence. The soft equivalence is valid under three so-called conditions. The first is a data condition, which guarantees that the data used in undifferenced or differencing algorithms are the same. The data condition will be discussed in the next section. The second is a parameterisation condition, i.e., the parameterisation must be the same. The third is the elimination condition, i.e., the parameter set to be eliminated should be able to be eliminated. (Implicitly, the parameter set of the problem should be a regular one). Because of the process of elimination, the cofactor matrices of the undifferenced and differencing equations are different. If the cofactor of an undifferenced normal equation has the form of

(c) ketabton.com: The Digital Library

$$\begin{pmatrix} M_{11} & M_{12} \\ M_{21} & M_{22} \end{pmatrix}^{-1} = Q = \begin{pmatrix} Q_{11} & Q_{12} \\ Q_{21} & Q_{22} \end{pmatrix}, \tag{9.31}$$

then we call the diagonal part of the cofactor

$$Q_e = \begin{pmatrix} M_1 & 0 \\ 0 & M_2 \end{pmatrix}^{-1} = \begin{pmatrix} Q_{11} & 0 \\ 0 & Q_{22} \end{pmatrix} \tag{9.32}$$

an equivalent cofactor. The equivalent cofactor has the same diagonal element blocks as the original cofactor matrix Q and guarantees that the precision relation between the unknowns remains the same. The soft equivalence is defined as follows: the solutions are identical and the covariance matrices are equivalent. Such a definition is implicitly used in the traditional block-wise least squares adjustment. It is notable that the parameterisation is very important and the rank of the normal equation of the undifferenced observation equation must be equal to the rank of the normal equation of the differencing observation equation plus the number of the eliminated independent parameters. For convenience, the original GPS observation equation and the equivalent differencing equation can be generally written as (cf. Eqs. 9.1 and 9.4)

$$V = L - \begin{pmatrix} A_1 & A_2 \end{pmatrix} \begin{pmatrix} X_1 \\ X_2 \end{pmatrix}, \quad P \tag{9.33}$$

$$\begin{pmatrix} U_1 \\ U_2 \end{pmatrix} = \begin{pmatrix} L \\ L \end{pmatrix} - \begin{pmatrix} D_1 & 0 \\ 0 & D_2 \end{pmatrix} \begin{pmatrix} X_1 \\ X_2 \end{pmatrix}, \quad \begin{pmatrix} P & 0 \\ 0 & P \end{pmatrix}. \tag{9.34}$$

In Sect. 9.1 the way to parameterise the GPS observables independently is proposed. A correct and reasonable parameterisation is the key to a correct conclusion by combining and differencing derivations. An example is given in Sect. 6.7 where an illogical conclusion is derived due to the inexact parameterisation.

For any GPS survey with a definitive space-time configuration, observed GPS data can be parameterised (or modelled) in a suitable way and listed together in a form of linear equations for processing. Combining and differencing are two linear transformations. Because the uncombined and combining data (or equations) are equivalent, differencing the uncombined or combining equations is (soft) equivalent. Inversely, the combining operator is an invertible transformation; making or not making the combination operation on the equivalent undifferenced or differencing equations (Eqs. 9.33 and 9.34) is equivalent. That is, the mixtures of the combining and differencing algorithms are also equivalent to the original undifferenced and uncombined algorithms. The equivalence properties can be summarised in a theorem as follows.

Equivalence Theorem of GPS Data Processing Algorithms

Under the three so-called equivalence conditions and the definition of the so-called soft equivalence, for any GPS survey with definitive space-time configuration, GPS data processing algorithms – uncombined and combining algorithms, undifferenced and differencing algorithms, as well as their mixtures – are at least soft equivalent. That is, the results obtained by using any algorithm or any mixture of the algorithms are identical. The diagonal elements of the covariance matrix are identical. The ratios of the

(c) ketabton.com: The Digital Library

precisions of the solutions are identical. None of the algorithms are preferred in view of the results and precisions. Suitable algorithms or mixtures of the algorithms will be specifically advantageous for special kinds of data dealings.

The implicit condition of this theorem is that the parameterisation must be the same and regular. The parameterisation depends on different configurations of the GPS surveys and strategies of the GPS data processing. The theorem says that if the data used are the same and the model is parameterised identically and regularly, then the results must be identical and the precision should be equivalent. This is a guiding principle for the GPS data processing practice.

9.2.2
Optimal Baseline Network Forming and Data Condition

It is well known that for a network with n stations there are n-1 independent baselines. An independent baseline network can be stated in words: all stations are connected through these baselines, and the shortest way from one station to any other stations is unique. Generally speaking, a shorter baseline leads to a better common view of the satellites. Therefore, the baseline should be formed so that the length of the baseline falls as short as possible. For a network, an optimal choice should be that the summation of weighted lengths of all independent baselines should be minimal. This is a specific mathematic problem called a minimum spanning tree (cf., e.g., Wang et al. 1977).

Algorithms exist to solve this minimum spanning tree problem with software. Therefore, we will just show an example here. An IGS network with ca. 100 stations and the related optimal and independent baseline tree is shown in Fig. 9.1. The average length of the baselines is ca. 1 300 km. The maximum distance is ca. 3 700 km.

In the traditional double differencing model, the unpaired GPS observations of every designed baseline have to be omitted because of the requirement of differencing (in the example of Sect. 9.1.2, two observations of $k6$ will be omitted. However, if the differencing is not limited by baseline design, no observations have to be cancelled

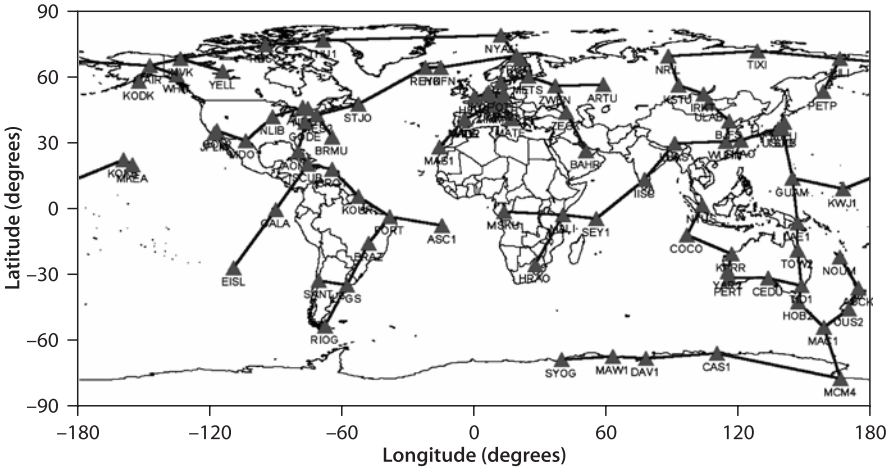

Fig. 9.1. Independent and Optimal IGS GPS Baseline Network (100 stations)

(c) ketabton.com: The Digital Library

out). Therefore, an optimal means of double differencing should be based on an optimal baseline design to form the differencing first, then, without limitation of the baseline design, to check for the unpaired observations in order to form possible differencing. This measure is useful for raising the rate of data used by the differencing method. An example of an IGS network with 47 stations and one day's observations has shown (Xu 2004) that 87.9% of all data is used in difference forming based on the optimal baseline design, whereas 99.1% of all data is used in the extended method of difference forming without limitation of the baseline design. That is, the original data may be nearly 100% used for such a means of double differencing.

In the undifferenced model, in order to be able to eliminate the clock error parameters, it is sufficient that every satellite is observed at least at two stations (for eliminating the satellite clock errors) and at every station there is a satellite combined with one of the other satellites that are commonly viewed by at least one of the other stations (for eliminating the receiver clock errors). The condition ensures that extended double differencing can be formed from the data. The data has to be cancelled out if the condition is not fulfilled or the ambiguities including in the related data have to be kept fixed.

For convenience, we state the data condition as follows.

Data Condition: All satellites must be observed at least twice (for forming single differences) and one satellite combined with one of the other satellites should be commonly viewed by at least one of the other stations (for forming double differences).

It is notable that the data condition above is valid for single and double differencing. For triple differencing and user defined differencing the data condition may be similarly defined. The data condition is one of the conditions of the equivalence of the undifferenced and differencing algorithms. The data condition is derived from the difference forming; however, it is suggested to use it also in undifferenced methods to reduce the singular data. The optimal baseline network forming is beneficial for differencing methods to raise the rate of used data.

9.2.3 Algorithms Using Secondary GPS Observables

As stated in Sects. 6.7 and 9.2, the uncombined and combining algorithms are equivalent. A method of GPS data processing using secondary data is outlined in Sect. 6.7.3. However, a concrete parameterisation of the observation model is only possible after the method of independent parameterisation is discussed in Sect. 9.1. The data processing using secondary observables leads to equivalent results of any combining algorithms. Therefore the concrete parameterisation of the GPS observation model has to be specifically discussed again. The observation model of m satellites viewed at one station is (cf. Eqs. 6.134 and 9.5)

$$\begin{pmatrix} R_1(k) \\ R_2(k) \\ \lambda_1\Phi_1(k) \\ \lambda_2\Phi_2(k) \end{pmatrix} = \begin{pmatrix} 0 & 0 & f_s^2/f_1^2 & 1 \\ 0 & 0 & f_s^2/f_2^2 & 1 \\ 1 & 0 & -f_s^2/f_1^2 & 1 \\ 0 & 1 & -f_s^2/f_2^2 & 1 \end{pmatrix} \begin{pmatrix} \lambda_1 N_1(k) \\ \lambda_2 N_2(k) \\ B_1(k) \\ C_\rho(k) \end{pmatrix}, \quad k = 1, \ldots, m\,, \tag{9.35}$$

(c) ketabton.com: The Digital Library

where the relation

$$B_1^z = \frac{1}{m}\sum_{k=1}^{m} B_1(k)/F_k \tag{9.36}$$

can be used to map the ionospheric parameters in the path directions to the parameter in the zenith direction. The meanings of the symbols are the same as stated in Sect. 6.7. Solutions of Eq. 9.35 are (similar to Eq. 9.6)

$$\begin{pmatrix} \lambda_1 N_1(k) \\ \lambda_2 N_2(k) \\ B_1(k) \\ C_\rho(k) \end{pmatrix} = \begin{pmatrix} 1-2a & -2b & 1 & 0 \\ -2a & 2a-1 & 0 & 1 \\ 1/q & -1/q & 0 & 0 \\ a & b & 0 & 0 \end{pmatrix} \begin{pmatrix} R_1(k) \\ R_2(k) \\ \lambda_1 \Phi_1(k) \\ \lambda_2 \Phi_2(k) \end{pmatrix}, \quad Q(k), k = 1, \ldots, m, \tag{9.37}$$

where the covariance matrix $Q(k)$ can be obtained by variance-covariance propagation law. The vector on the left side of Eq. 9.37 is called the secondary observation vector. In the case where K satellites are viewed, the traditional combinations of the observation model and the related secondary solutions are the same as the Eqs. 9.35 and 9.37, where the $m = K$. However, taking the parameterisation method into account, at least one satellite has to be selected as reference and the related ambiguities cannot be modelled. If one were to suppose that the satellite of index K is the reference one, then the first $m = K-1$ observation equations are the same as Eq. 9.35. The satellite K-related observation equations can be written as

$$\begin{pmatrix} R_1(k) \\ R_2(k) \\ \lambda_1 \Phi_1(k) \\ \lambda_2 \Phi_2(k) \end{pmatrix} = \begin{pmatrix} 0 & 0 & f_s^2/f_1^2 & 1 \\ 0 & 0 & f_s^2/f_2^2 & 1 \\ 0 & 0 & -f_s^2/f_1^2 & 1 \\ 0 & 0 & -f_s^2/f_2^2 & 1 \end{pmatrix} \begin{pmatrix} \lambda_1 N_1(k) \\ \lambda_2 N_2(k) \\ B_1(k) \\ C_\rho(k) \end{pmatrix}, \quad k = K, \tag{9.38}$$

where the ambiguities are not modelled and the constant effects will be absorbed by the clock parameters. Solutions of Eq. 9.38 are

$$\begin{pmatrix} \lambda_1 N_1(k) \\ \lambda_2 N_2(k) \\ B_1(k) \\ C_\rho(k) \end{pmatrix} = \frac{1}{2} \begin{pmatrix} 0 & 0 & 0 & 0 \\ 0 & 0 & 0 & 0 \\ 1/q & -1/q & -1/q & 1/q \\ 1/2 & 1/2 & 1/2 & 1/2 \end{pmatrix} \begin{pmatrix} R_1(k) \\ R_2(k) \\ \lambda_1 \Phi_1(k) \\ \lambda_2 \Phi_2(k) \end{pmatrix}, \quad Q(K). \tag{9.39}$$

It is notable that the solutions of the traditional combinations are Eq. 9.37 with m=K, whereas for the combinations with independent bias parameterisation, the solutions are the combinations of the Eq. 9.37 with $m = K-1$ and Eq. 9.39. It is obvious that the two solutions are different. Because the traditional observation model used is an inexact one, the solutions of the traditional combinations are also inexact. The bias effects (of ambiguities) that are not modelled are merged into the clock bias param-

(c) ketabton.com: The Digital Library

eters. Due to the fact that the bias effects cannot be absorbed into the non-bias parameters, only the clock error parameters will be different in the results and the clock errors will have different meanings. Further, the ionosphere-free and geometry-free combinations are correct under the independent parameterisation.

It shows that through exact parameterisation, the combinations are not any more independent from satellite to satellite. For surveys with multiple stations, through correct parameterisation the combinations will be not any more independent from station to station. Therefore, traditional combinations will lead to incorrect results because of the inexact parameterisation.

The so-called secondary observables on the left-hand side of Eqs. 9.37 and 9.39 can be further processed. The original observables can be uniquely transformed to secondary observables. The secondary observables are equivalent and direct measurements of the ambiguities and ionosphere as well as geometry. Any further GPS data processing can be based on the secondary observables (cf. Sect. 6.7).

9.3 Non-Equivalent Algorithms

As stated in the equivalence theorem of GPS algorithms, the equivalence properties are valid for GPS surveys with definitive space-time configuration. As long as the measures are the same and the parameterisation is identical and regular, the GPS data processing algorithms are equivalent. It is notable that if the surveys and the parameterisation are different, then the algorithms are not equivalent to each other. For example, algorithms of single point positioning and multi-points positioning, algorithms of orbit-fixed and orbit co-determined positioning, algorithms of static and kinematic as well as dynamic applications, etc., are non-equivalent algorithms.

9.4 Standard Algorithms of GPS Data Processing

9.4.1 Preparation of GPS Data Processing

Preparation of GPS data processing can be carried out either in a pre-processing process or in the main data processing process. It depends on the strategy and the purpose of the data processing. Only in the case of data post-processing (i.e., data are available before the processing) is pre-processing possible. In the case of data quasi real time or real time processing, usually data are only available up to the instantaneous epoch. Data availability also causes different strategies of the data processing.

Data preparation may include raw GPS data decoding. ASCII code data are usually given in RINEX format (Gurthner 1994). Even in the unified format, different decoders may work a little bit differently from one another. This has to be noted only if one is going to process the data decoded by using different decoders. Usually, most GPS data processing software has its own internal input data format. Transforming the data from the RINEX format (maybe also from multiple stations) into the internal input data format should be no principle problem.

(c) ketabton.com: The Digital Library

Cycle slip detection is one of the most important works in data preparation. Marks are given for further use in the data where the cycle slips are detected. There are two types of cycle slips; one is repairable, and another is not repairable. Non-repairable cycle slips have to be modelled by new ambiguity unknowns. Repairing and setting new unknowns are equivalent if the repair is made correctly and the new unknown is well-solved. By real time data processing, such a process has to be done in the main data processing process.

Orbit data are also needed. Depending on the purposes of the data processing, broadcast navigation data, IGS precise orbits and IGS predicted orbits can be used where the satellite clock error model is also included. In broadcast data, there is also an ionospheric model available. Even for the GPS precise orbit determination, initial orbits are still needed.

Further preparations depend on the organisation and purpose of the data processing. Generally speaking, standard tropospheric models are needed for use (cf. Sect. 5.2). An ionospheric model (from broadcast) can be used as an initial model (cf. Sect. 5.1) if the non-ionosphere-free combination is used. An ionospheric model can be also obtained from the ambiguity-ionospheric equations (see discussions in Sect. 6.5.2). Earth tide and ocean loading tide as well as relativistic effects have to be computed for use (cf. Sect. 5.4).

In the case of orbit determination and/or geopotential determination, an initial geopotential model is needed. The initial models of the solar radiation and air drag have to be computed. All corrections can be computed in real time or in advance and then listed in tables for use. Coordinate transformations between the ECEF system and the ECSF system are also needed.

9.4.2 Single Point Positioning

Single point positioning is a sub-process of GPS data processing, which is needed in almost all GPS data processing. Station coordinates and receiver clock error are determined with such a sub-process. Depending on the accuracy requirement, single point positioning can be done with single frequency code or phase data, dual-frequency code or phase data, and combined code-phase data. Generally speaking, single point positioning has a lower accuracy than that of relative positioning, where systematic errors are reduced (through keeping the reference fixed). However, the receiver clock bias determined by single point positioning is accurate enough to correct the second type of clock error influence (the influence scaled by the velocity of the satellite, cf. Sect. 5.5).

Code Data Single Point Positioning

The GPS code pseudorange model is (cf. Sect. 6.1):

$$R_i^k(t_r,t_e)=\rho_i^k(t_r,t_e)-(\delta t_r-\delta t_k)c+\delta_{ion}+\delta_{trop}+\delta_{tide}+\delta_{rel}+\varepsilon\ , \tag{9.40}$$

where R is the observed pseudorange, t_e denotes the GPS signal emission time of the satellite k, t_r denotes the GPS signal reception time of the receiver i, c is the speed of light, subscript i and superscript k denote the receiver and satellite, and δt_r and δt_k are

(c) ketabton.com: The Digital Library

the clock errors of the receiver and satellite at the times t_r and t_e, respectively. The terms δ_{ion}, δ_{trop}, δ_{tide} and δ_{rel} denote the ionospheric, tropospheric, tidal, and relativistic effects, respectively. The multipath effect is omitted here. The remaining error is denoted as ε. ρ_i^k is the geometric distance. The computed value (denoted as C) of the pseudorange is

$$C = \rho_i^k(t_r, t_e) + \delta t_k c + \delta_{ion} + \delta_{trop} + \delta_{tide} + \delta_{rel}\,, \tag{9.41}$$

where the clock error of the satellites can be interpolated from the IGS orbit data or broadcast navigation message, models of other effects can be found in Chap. 5, and the initial value of receiver clock error is assumed to be zero. It should be emphasised that the earth rotation correction has to be taken into account by the geometric distance computation no matter if it is done in the Earth or space fixed coordinate systems (cf. Sect. 5.3.2).

The linearised observation Eq. 9.40 is then (cf. Sects. 6.2 and 6.3)

$$l_k = \frac{-1}{\rho_i^k(t_r, t_e)} \begin{pmatrix} x_k - x_{i0} & y_k - y_{i0} & z_k - z_{i0} \end{pmatrix} \begin{pmatrix} \Delta x \\ \Delta y \\ \Delta z \end{pmatrix} - \Delta t + v_k\,, \tag{9.42}$$

where l_k is the so-called $O - C$ (observed minus computed pseudorange), v_k is the residual, vector $(\Delta x \;\; \Delta y \;\; \Delta z)^T$ is the difference between the coordinate vector $(x_i \;\; y_i \;\; z_i)^T$ and the initial coordinate vector $(x_{i0} \;\; y_{i0} \;\; z_{i0})^T$, Δt is the receiver clock error in length (i.e. $\Delta t = \delta t_r c$), and the initial coordinate vector is used for computing the geometric distance. Equation 9.42 can be written in a more general form as

$$l_k = \begin{pmatrix} a_{k1} & a_{k2} & a_{k3} & -1 \end{pmatrix} \begin{pmatrix} \Delta x \\ \Delta y \\ \Delta z \\ \Delta t \end{pmatrix} + v_k\,, \tag{9.43}$$

where a_{kj} is the related coefficient given in Eq. 9.42. Putting all of the equations from all observed satellites together, we find the single point positioning equation system has a general form of

$$L = AX + V\,, \quad P\,, \tag{9.44}$$

where L is called the observation vector, X is the unknown vector, A is the coefficient matrix, V is the residual vector, and P is the weight matrix of the observation vector. The least squares solution of observational Eq. 9.44 is then (cf. Sect. 7.2)

$$X = (A^T P A)^{-1} A^T P L\,. \tag{9.45}$$

The formulas for computing the precision vector of the solved X can be found in Sect. 7.2. It is notable that the coefficients of the equation are computed using the initial coordinate vector, and the initial coordinate vector is usually not (exactly) known; therefore, an iterative process has to be carried out to solve the single point positioning problem. For the given initial vector, a modified one can be obtained by solving the

(c) ketabton.com: The Digital Library

above problem; the modified initial vector can be used in turn as the initial vector to form the equations, and the problem can be solved again until the process converges. Because there are four unknowns in the single point positioning equation, at least four observables are needed to make the problem solvable. In other words, as soon as four or more satellites are observed, single point positioning is always possible.

For static reference stations, as soon as the coordinates are known with sufficient accuracy, the unknown vector $(\Delta x \quad \Delta y \quad \Delta z)^T$ can be considered zero. Then the Eq. 9.43 turns out to be

$$l_k = -\Delta t + v_k \,, \tag{9.46}$$

and the receiver clock error can be computed directly by

$$\Delta t = \frac{-1}{K} \sum_{k=1}^{K} l_k \,, \tag{9.47}$$

where K is the total number of observed satellites at this epoch. Equation 9.47 can be used to compute the receiver clock error of the static reference.

Dual Codes Ionosphere-Free Single Point Positioning

The above-mentioned single point positioning (using single frequency code data) is accurate enough for correcting the second type of clock error influence (the influence scaled by the velocity of the satellite). For more precise single point positioning, dual-frequency code data can be used to form the ionosphere-free combinations (cf. Sect. 6.5). Assuming that for frequencies 1 and 2, the single point positioning equation of Eq. 9.44 can be formed as

$$L_1 = AX + V_1 \,, \quad P_1 \,, \tag{9.48}$$

$$L_2 = AX + V_2 \,, \quad P_2 \,,$$

then the ionosphere-free combination can be formed by (cf. Sect. 6.5.1)

$$\frac{f_1^2}{f_1^2 - f_2^2} L_1 - \frac{f_2^2}{f_1^2 - f_2^2} L_2 = AX + V \,, \quad P \,, \tag{9.49}$$

where

$$P = Q^{-1}, \quad Q = \left(\frac{f_1^2}{f_1^2 - f_2^2} \right)^2 P_1^{-1} + \left(\frac{f_2^2}{f_1^2 - f_2^2} \right)^2 P_2^{-1} \,,$$

and V is the residual vector. Because the ionospheric effects have been cancelled out of Eq. 9.49, the ionospheric model can be also omitted by computing L_1 and L_2 in Eq. 9.48. The solution of Eq. 9.49 is then the solution of the dual codes ionosphere-free single point positioning problem.

(c) ketabton.com: The Digital Library

Phase Single Point Positioning

GPS carrier phase model is (cf. Sect. 6.1)

$$\lambda\Phi_i^k(t_r,t_e)=\rho_i^k(t_r,t_e)-(\delta t_r-\delta t_k)c+\lambda N_i^k-\delta_{ion}+\delta_{trop}+\delta_{tide}+\delta_{rel}+\varepsilon\,, \tag{9.50}$$

where $\lambda\Phi$ is the observed phase in length, Φ is the phase in cycle, wave length is denoted as λ, and N_i^k is the ambiguity related to receiver i and satellite k, except for the ambiguity term and the sign difference of the term of ionospheric effect; other terms are the same as that of the pseudorange discussed at the beginning of this section.

The computed value (denoted as C) of phase is

$$C=\rho_i^k(t_r,t_e)+\delta t_k c+\lambda N_{i0}^k-\delta_{ion}+\delta_{trop}+\delta_{tide}+\delta_{rel}\,, \tag{9.51}$$

where N_{i0}^k is the initial ambiguity parameter related to the receiver i and satellite k. Scaling the ambiguity parameter in length and denoting

$$\Delta N_i^k=\lambda N_i^k-\lambda N_{i0}^k\,, \tag{9.52}$$

the phase single point positioning equation is (very similar to Eq. 9.43)

$$l_k=\begin{pmatrix}a_{k1} & a_{k2} & a_{k3} & -1\end{pmatrix}\begin{pmatrix}\Delta x\\ \Delta y\\ \Delta z\\ \Delta t\end{pmatrix}+\Delta N_i^k+v_k\,. \tag{9.53}$$

Putting all equations related to all observed satellites together, the single point positioning equation system has a general form of

$$L=AX+EN+V\,,\quad P\,, \tag{9.54}$$

where L is called the observation vector, X is the unknown vector of coordinates and clock error, A is the X related coefficient matrix, E is an identity matrix of order K, K is the number of observed satellites, N is the unknown vector of ambiguity parameters ΔN_i^k, V is the residual vector, and P is the weight matrix. If K satellites are observed, then there are K ambiguity parameters, three coordinate parameters and one clock parameter, so that the phase single point positioning problem is not solvable at the first few epochs. Using the ambiguity parameters obtained from the ambiguity-ionospheric equations (cf. Sect. 6.5) as the initial ambiguity values, N is then zero (can be cancelled), and Eq. 9.54 has the same form as that of Eq. 9.44. In this way, the equation system of single frequency phase point positioning can be formed and solved every epoch. Even the codes are used in the ambiguity-ionospheric equations, ambiguity parameters can be obtained with high accuracy through a reasonable weight and instrumental bias model (cf. Sects. 6.7 and 9.2).

(c) ketabton.com: The Digital Library

Dual Phases Ionosphere-Free Single Point Positioning

The single point positioning equation of the dual phase observables for frequencies 1 and 2 can be formed as

$$L_1 = AX + EN_1 + V_1\,, \quad P_1 \quad \text{and} \tag{9.55}$$

$$L_2 = AX + EN_2 + V_2\,, \quad P_2\,.$$

Then the ionosphere-free combinations can be formed by (cf. Sect. 6.5.1)

$$\frac{f_1^2}{f_1^2 - f_2^2} L_1 - \frac{f_2^2}{f_1^2 - f_2^2} L_2 = AX + EN_c + V\,, \quad P\,, \tag{9.56}$$

where

$$N_c = \frac{f_1^2}{f_1^2 - f_2^2} N_1 - \frac{f_2^2}{f_1^2 - f_2^2} N_2 \quad \text{and} \tag{9.57}$$

$$P = Q^{-1}, \quad Q = \left(\frac{f_1^2}{f_1^2 - f_2^2}\right)^2 P_1^{-1} + \left(\frac{f_2^2}{f_1^2 - f_2^2}\right)^2 P_2^{-1}\,. \tag{9.58}$$

V is the residual vector, and index c is used to denote the ionosphere-free combinations. Equation 9.56 is the dual phases ionosphere-free single point positioning equation system. The solution of Eq. 9.56 is then the solution of the dual phases ionosphere-free single point positioning problem.

Phase-Code Combined Single Point Positioning

Phase and code ionosphere-free single point positioning Eqs. 9.56 and 9.49 can be written in more compact forms as

$$L_p = A_{11} X_1 + A_{12} N + V_p\,, \quad P_p \quad \text{and} \tag{9.59}$$

$$L_c = A_{11} X_1 + V_c\,, \quad P_c\,,$$

where index p and c denote the phase and code related variables, X_1 is the vector of the coordinate and receiver clock error, N is the ambiguity vector, P is the weight matrix, and V is the residual vector. To guarantee the same coefficient matrix A_{11} for both the phase and code observation equations, data of commonly observed satellites have to be used.

Usually the code single point positioning problem (second equation system of Eq. 9.59) is always solvable (as soon as more than four satellites are observed). And the ambiguity parameter number is equal to the number of phase observables. Therefore, the phase-code combined single point positioning problem in Eq. 9.59 is usually solvable at every epoch.

Block-wise least squares adjustment for solving the phase-code combined problem has been discussed in Sect. 7.5.2. The algorithm can be used directly to solve the combined Eq. 9.59.

(c) ketabton.com: The Digital Library

9.4.3 Standard Un-Differential GPS Data Processing

In single point positioning, un-differenced GPS data are used. Usually, only four unknowns are solved for, as discussed in Sect. 9.4.2. Single point positioning has also a speciality of epoch-wise solution. Based on the algorithms of single point positioning, standard static un-differential GPS data processing should take more unknown models and more station data into account. In a kinematic case, because of the movement of the receiver, coordinates of the receiver are time variables; therefore, model parameters are usually pre-determined or determined with another algorithm in order to reduce the number of the unknowns.

The GPS code pseudorange and carrier phase are modelled as (cf. Sect. 6.1, Eqs. 6.1 and 6.2, or Eqs. 9.40 and 9.50)

$$R_i^k(t_r,t_e)=\rho_i^k(t_r,t_e)-(\delta t_r-\delta t_k)c+\delta_{ion}+\delta_{trop}+\delta_{tide}+\delta_{rel}+\varepsilon_c \quad \text{and} \tag{9.60}$$

$$\lambda\Phi_i^k(t_r,t_e)=\rho_i^k(t_r,t_e)-(\delta t_r-\delta t_k)c+\lambda N_i^k-\delta_{ion}+\delta_{trop}+\delta_{tide}+\delta_{rel}+\varepsilon_p\,. \tag{9.61}$$

Except for the ambiguity parameter and the sign of the ionospheric effect term, the other terms on the right sides of Eqs. 9.60 and 9.61 are the same.

For any standard data combinations (cf. Sect. 6.5 for details) as given in Eqs. 6.48 and 6.51, the above models of Eqs. 9.60 and 9.61 are still valid. Of course, on the left sides of Eqs. 9.60 and 9.61 the combined pseudorange and combined phase (scaled by wavelength) are used, and on the right side the ambiguity and ionospheric effect are combined ones respectively. Exactly, for combinations of

$$R=\frac{n_1R_1+n_2R_2}{n_1+n_2}\,, \tag{9.62}$$

$$\Phi=n_1\Phi_1+n_2\Phi_2\,, \quad \text{or} \tag{9.63}$$

$$\lambda\Phi=\frac{1}{f}(n_1f_1\lambda_1\Phi_1+n_2f_2\lambda_2\Phi_2)\,, \tag{9.64}$$

where the combined signal has the frequency and wavelength

$$f=n_1f_1+n_2f_2\,, \quad \text{and} \quad \lambda=c/f\,, \tag{9.65}$$

the combined ambiguity and ionospheric effects are

$$N_{com}=n_1N_1+n_2N_2\,, \tag{9.66}$$

$$\delta_{ion_comc}=\frac{n_1\delta_{ion1}+n_2\delta_{ion2}}{n_1+n_2} \quad \text{and}$$

$$\delta_{ion_comp}=\frac{-1}{f}(nn_{1f_1}\delta_{ion1}+n_2f_2\delta_{ion2})\,, \tag{9.67}$$

(c) ketabton.com: The Digital Library

where n_1 and n_2 are the selected real constants, indices 1 and 2 are referred to frequencies 1 and 2, and indices comc and comp denote the code and phase combined terms.

The computed pseudorange and phase range are

$$C_c = \rho_i^k(t_r,t_e) - (\delta t_r - \delta t_k)c + \delta^0_{ion_comc} + \delta^0_{trop} + \delta^0_{tide} + \delta_{rel} \quad \text{and} \tag{9.68}$$

$$C_p = \rho_i^k(t_r,t_e) - (\delta t_r - \delta t_k)c + \lambda N^k_{i0_com} - \delta^0_{ion_comp} + \delta^0_{trop} + \delta^0_{tide} + \delta_{rel}\,, \tag{9.69}$$

where superscript 0 denotes the initial values of individual models, indices c and p denote the terms related to the code and phase measurements, and index com denotes the combined terms. In the case of ionosphere-free combinations, the ionospheric effect terms will vanish. Otherwise, we should assume that the ionospheric effects are known by the given model or by the ambiguity-ionospheric equations.

The linearisation of GPS observation equations is generally discussed in Sect. 6.2, and the related partial derivatives are given in Sect. 6.3. Equations 9.62 and 9.64 can be linearised as

$$L_c = A_{11}X_{coor} + A_{12}X_{clock} + A_{13}X_{trop} + A_{14}X_{tide} + V_c\,, \quad P_c \quad \text{and}$$

$$L_p = A_{11}X_{coor} + A_{12}X_{clock} + A_{13}X_{trop} + A_{14}X_{tide} + A_{15}N + V_p\,, \quad P_p\,, \tag{9.70}$$

where X_{coor} is the coordinate vector, X_{clock} is clock error vector, indices trop and tide are used to denote the related unknown vectors, N is the ambiguity vector, P is the weight matrix, V is the residual vector, and A is the related coefficient matrix. The data of commonly observed satellites have to be used to guarantee the common coefficient matrices A for both phase and code observation equations.

To process the data of more stations, Eq. 9.70 shall be formed station by station and then combine them together. It is notable that some of the parameters are common ones for all stations, such as satellite clock errors and love numbers of the earth tide. In the case of orbit determination (cf. Chap. 11 for details), the orbit parameters and force model parameters are also common ones. The total observation equations of the un-differential GPS can then be written symbolically as

$$L_c = A_1X_1 + A_4X_4 + V_c\,, \quad P_c \quad \text{and} \tag{9.71}$$

$$L_p = A_1X_1 + A_4X_4 + A_5X_5 + V_p\,, \quad P_p\,,$$

where X_1 is a sub-vector of the common variables of the both equations, X_4 is the other variable vector of the both equations, and X_5 is the ambiguity vector. Adding $0X_5$ to the first equation and denoting $X_2 = [X_4\,X_5]^T$, Eq. 9.71 can be further simplified as

$$L_c = A_1X_1 + A_2X_2 + V_c\,, \quad P_c \quad \text{and} \tag{9.72}$$

$$L_p = A_1X_1 + A_3X_2 + V_p\,, \quad P_p\,.$$

Equation 9.72 can be considered an epoch-wise formed observation equation or observation equation of all observed epochs. Most adjustment algorithms discussed in Chap. 7 can be used directly to solve the above equation system.

(c) ketabton.com: The Digital Library

9.4.4
Equivalent Method of GPS Data Processing

As already discussed in Sect. 6.8, the equivalently eliminated equations of Eq. 9.72 can be formed as (cf. Sect. 6.8 and 7.6 for details)

$$U_c = L_c - (E - J_c)A_2X_2\,, \quad P_c \quad \text{and} \tag{9.73}$$

$$U_p = L_p - (E - J_p)A_3X_2\,, \quad P_p\,,$$

where

$$J_c = A_1M_{11c}^{-1}A_1^TP_c\,, \tag{9.74}$$

$$J_p = A_1M_{11p}^{-1}A_1^TP_p\,,$$

$$M_{11c} = A_1^TP_cA_1\,, \quad \text{and}$$

$$M_{11p} = A_1^TP_pA_1\,.$$

E is an identity matrix of size J, L and P are the original observation vector and weight matrix, and U is the residual vector, which has the same statistic property as V in Eq. 9.72. As soon as the X_1 in Eq. 9.72 is able to be eliminated, the equivalent Eq. 9.73 can be formed whether Eq. 9.72 is an epoch-wise equation or an all epoch equation.

Equation 9.73 is the zero-difference (un-differential) GPS observation equation system if the variable vector X_1 in Eq. 9.72 is considered a zero vector.

Equation 9.73 is the equivalent single-difference GPS observation equation system if the variable vector X_1 in Eq. 9.72 is considered an unknown vector of satellite clock errors.

Equation 9.73 is the equivalent double-difference GPS observation equation system if the variable vector X_1 in Eq. 9.72 is considered an unknown vector of satellite and receiver clock errors.

The second equation of 9.73 is the equivalent triple-difference GPS observation equation system if the variable vector X_1 in the second equation of 9.72 is considered an unknown vector of all clock errors and ambiguities.

The un-differential and differential GPS data processing can be dealt with in an equivalent and unified way. The advantages of this method are:

1. The weight remains the original one, so one does not have to deal with the correlation problem;
2. The original data are used, so one does not need to form the differences;
3. The un-differential and differential GPS data processing can be easily selected by a switch or can be used in a combined way, so that the number of unknowns (i.e., matrix size) of the whole adjustment and filtering problem can be greatly reduced.

The combinative way of using the equivalent method can be realised as follows. First, equivalent triple differences are used to determine the unknowns other than the

(c) ketabton.com: The Digital Library

clock error and ambiguity parameters. Taking these parameters as known, the observation Eq. system 9.72 can be reduced so that only the clock error and ambiguity parameters are included. Then second, equivalent double differences are used to determine the ambiguity vector. Again, taking the ambiguity vector as known, Eq. 9.72 can be further reduced so that only the clock error parameters are included. Then third, equivalent single differences are used to determine the receiver clock errors. At the end, Eq. 9.72 can be reduced so that only satellite clock errors are included in the equations, and they can be determined. The last two steps can be also done together in one step.

By the way, the ambiguity parameters are usually dealt with in an un-differential form for all methods, so that the problems caused by changing the reference satellite in a double difference case can be avoided. This is especially important for kinematic GPS applications.

9.4.5 Relative Positioning

Relative positioning is traditionally carried out with differential positioning. The key point of relative positioning is to keep the coordinates of the reference station fixed. In other words, the initial coordinate values of the reference station are considered true values so that the related unknowns are either not necessary to be adjusted or equal to zero. Therefore, the following two ways outline how relative positioning can be done. (*1*) Cancelling the reference coordinate unknowns out of Eq. 9.72; (*2*) The a priori datum method discussed in Sect. 7.8.2 and 6.8.6 is used to keep the coordinates fixed on the initial values. Both methods are equivalent. The a priori datum method (cf. Sect. 7.8.2 and 6.8.6) can be also used to keep some of the un-differential ambiguity parameters and clock parameters fixed. Keeping the reference coordinates fixed in relative positioning may lead to a better determination of the other parameters in the reference-related equations, and therefore may lead to an indirect reduction of the residuals.

9.4.6 Velocity Determination

Single Point Velocity Determination

Analogous to the single point positioning discussed in Sect. 9.4.2, single point velocity determination can be carried out by using Doppler data. The GPS Doppler observation is modelled as (cf. Eq. 6.46)

$$D = \frac{\mathrm{d}\rho_i^k(t_\mathrm{r}, t_\mathrm{e})}{\lambda \mathrm{d}t} - f\frac{\mathrm{d}(\delta t_\mathrm{r} - \delta t_\mathrm{k})}{\mathrm{d}t} + \delta_{\mathrm{rel}_f} + \varepsilon\,, \tag{9.75}$$

where D is the observed Doppler measurement, t_e denotes the GPS signal emission time of the satellite k, t_r denotes the GPS signal reception time of the receiver i, subscript i and superscript k denote receiver and satellite, and δt_r and δt_k denote the clock errors of the receiver and satellite at the time t_r and t_e, respectively. The remaining error

(c) ketabton.com: The Digital Library

is denoted as ε, f is the frequency, wavelength is denoted as λ, $\delta_{\text{rel_}f}$ is the frequency correction of the relativistic effects, ρ_i^k is the geometric distance, and $\mathrm{d}\rho_i^k/\mathrm{d}t$ denotes the time derivation of the radial distance between satellite and receiver at the time t_r.

The computed value (denoted as C) of Doppler is

$$C = \frac{\mathrm{d}\rho_i^k(t_r, t_e)}{\lambda \mathrm{d}t} + f\frac{\mathrm{d}(\delta t_k)}{\mathrm{d}t} + \delta_{\text{rel_}f}\,, \tag{9.76}$$

where the first term on the right-hand side can be computed by using Eqs. 6.14 and 6.15.

The time derivative of the satellite clock error and the satellite position as well as velocity can be computed from the IGS orbit data or broadcast navigation message; the relativistic effect on frequency can be found in Chap. 5. It is obvious that the initial position of the receiver is also needed for computing Eq. 9.76. Initial velocity of the receiver is assumed zero. It should be emphasised that the earth rotation correction has to be taken into account by the geometric distance computation (cf. Sect. 5.3.2).

The linearised observation Eq. 9.76 is then (cf. Sects. 6.2 and 6.3 as well as partial derivative Eq. 6.20)

$$l_k = \frac{-1}{\lambda\rho_i^k(t_r, t_e)}\begin{pmatrix} x_k - x_i & y_k - y_i & z_k - z_i \end{pmatrix}\begin{pmatrix} \dot{x}_i \\ \dot{y}_i \\ \dot{z}_i \end{pmatrix} - \Delta D + v_k\,, \tag{9.77}$$

where l_k is the $O - C$ (observed minus computed Doppler), v_k is the residual, the receiver's velocity vector is $(\dot{x}_i \;\; \dot{y}_i \;\; \dot{z}_i)^T$, $(x \;\; y \;\; z)^T$ is the coordinate vector with index k for satellite and i for receiver. ΔD is the receiver clock drift in cycle/second (i.e., $\Delta D = f(\mathrm{d}\rho t_r/\mathrm{d}t)$. Equation 9.77 can be written in a more general form as

$$l_k = \begin{pmatrix} a_{k1} & a_{k2} & a_{k3} & -1 \end{pmatrix}\begin{pmatrix} \dot{x} \\ \dot{y} \\ \dot{z} \\ \Delta D \end{pmatrix} + v_k\,, \tag{9.78}$$

where a_{kj} is the related coefficient given in Eq. 9.77. If one puts all of the equations that are related to all of the observed satellites together, the equation system of single point velocity determination has a general form of

$$L = AX + V\,, \quad P\,, \tag{9.79}$$

where L is called the observation vector, X is the unknown velocity vector including clock drift, A is the coefficient matrix, V is the residual vector, and P is the weight matrix of observation vector. The least squares solution of observation Eq. 9.79 is then (cf. Sect. 7.2)

$$X = (A^T P A)^{-1} A^T P L\,. \tag{9.80}$$

(c) ketabton.com: The Digital Library

The formulas for computing the precision vector of the solved X can be found in Sect. 7.2. It is notable that the coefficients of the equation are computed using the initial velocity vector, and the initial velocity vector is usually not known; therefore, an iterative process has to be carried out to solve the single point velocity determining problem. For the given initial velocity vector, a modified one can be obtained by solving the problem; the modified initial velocity vector can be used in turn to form the equation and solve it again until the process converges. Such an iterative process is needed if the kinematic motion is very fast. Because there are four unknowns in the single velocity determining equation, at least four observables are needed to make the problem solvable; in other words, when four or more satellites are observed, it is always possible to determine the single point velocity.

For static stations, the unknown velocity vector $(\dot{x}\ \ \dot{y}\ \ \dot{z})^T$ can be considered the zero one. Then the Eq. 9.77 turns out to be

$$l_k = -\Delta D + v_k \,, \tag{9.81}$$

and the receiver frequency error can be computed directly by

$$\Delta D = \frac{-1}{K} \sum_{k=1}^{K} l_k \,, \tag{9.82}$$

where K is the total number of observed satellites. Equation 9.82 can be used to compute the frequency drift of the static reference receiver. The frequency drift of kinematic receiver can be also computed by static initialisation.

Differential Doppler Data Processing

A more general model of Doppler data processing takes the satellite clock frequency bias (clock drift) into account:

$$l_k = \begin{pmatrix} a_{k1} & a_{k2} & a_{k3} & -1 \end{pmatrix} \begin{pmatrix} \dot{x} \\ \dot{y} \\ \dot{z} \\ \Delta D_i \end{pmatrix} + \Delta D_k + v_k \,, \tag{9.83}$$

where index i and k denote the receiver and satellite, and ΔD is the related frequency bias. For the satellite frequency bias, the initial value from the IGS data or navigation data can be used. If one puts together all of the equations related to all observed satellites of all of the stations, Eq. 9.83 has a general form of

$$L_D = A_1 X_1 + A_2 X_2 + V_D \,,\ P_D \,. \tag{9.84}$$

where X_1 is a sub-vector of the common variables, X_2 is the vector of the other variable, and A is the related coefficient matrix. The equivalently eliminated equations of Eq. 9.84 can be formed as (cf. Sect. 6.8 for details)

$$U_D = L_D - (E - J_D) A_2 X_2 \,,\ P_D \,, \tag{9.85}$$

(c) ketabton.com: The Digital Library

where

$$J_D = A_1 M_{11D}^{-1} A_1^T P_D \quad \text{and} \tag{9.86}$$

$$M_{11D} = A_1^T P_D A_1 .$$

E is an identity matrix of size J_D, L and P are the original observation vector and weight matrix, and U is the residual vector, which has the same property as V in Eq. 9.84.

Equation 9.85 is the equivalent single-difference GPS Doppler observation equation if the variable vector X_1 in Eq. 9.84 is considered a vector of satellite clock frequency bias.

Equation 9.85 is the equivalent double-difference GPS Doppler observation equation if the variable vector X_1 in Eq. 9.84 is considered a vector of the satellite and receiver clock frequency bias.

Relative Velocity Determination

Relative velocity determining is usually carried out with a differential method. The key point of relative velocity determination is to keep the velocity of the reference station as fixed, or zero. Therefore, relative velocity determination can be done the following two ways: (*1*) Cancel the reference velocity unknowns out of the Eq. 9.84; (*2*) Use the method of a priori datum discussed in Sect. 7.8.2 to keep the reference velocity fixed on the initial values.

9.4.7 Kalman Filtering Using Velocity Information

As already discussed in Sect. 6.5.5, velocity information from the differential Doppler can be used to describe the system that is needed in Kalman filtering. Whether the receiver is moving or resting, the differential Doppler includes information about the motion state of the receiver. Therefore, using velocity information as a system description should be better than any empirical model.

The principle of Kalman filtering using velocity information can be outlined as follows (cf. also Sect. 7.7):

For the initial (or predicted) vector $\bar{Z}$, the normal equation of the phase observation equation can be formed by

$$M_z Z = B_z , \quad Z = \begin{pmatrix} X \\ N \end{pmatrix}, \tag{9.87}$$

where M_z is the normal matrix, and B_z is the vector on the right side of the equation. These are formed by using initial vector $\bar{Z}$; Z includes sub-vector X (coordinates) and N (ambiguities). The estimated solution of Eq. 9.87 is then

$$\tilde{Z} = \tilde{Q}_z B_z , \quad \tilde{Q}_z = M_z^{-1} . \tag{9.88}$$

The normal equation of the differential Doppler observation equation (cf. Eq. 9.85, only the velocity vector is unknown) can be formed by

(c) ketabton.com: The Digital Library

$$M_{\dot{X}}\dot{X} = B_{\dot{X}}\,, \tag{9.89}$$

where $\dot{X}$ is the velocity vector of the receiver; it is also used as an index to denote the related normal matrix and vector on the right side of the equation. The solution of Eq. 9.89 is then

$$\dot{X} = Q_{\dot{X}}B_{\dot{X}}\,, \quad Q_{\dot{X}} = M_{\dot{X}}^{-1}\,. \tag{9.90}$$

Thus for the next epoch, denoted as k, the predicted vector turns out to be

$$\overline{Z}(k) = \tilde{Z}(k-1) + \dot{Z}(k-1)\cdot\Delta t\,, \tag{9.91}$$

where Δt is the time interval of the epoch $k-1$ and k, and

$$\dot{Z}(k-1) = \begin{pmatrix} \dot{X}(k-1) \\ 0 \end{pmatrix}. \tag{9.92}$$

Equation 9.91 indicates that the differential Doppler has to be used in Eq. 9.90 as observations, because the velocity is considered an average one here. The related covariance matrix of the predicted vector is then

$$\overline{Q}_z(k) = \tilde{Q}_z(k-1) + (\Delta t)^2 \begin{pmatrix} Q_{\dot{X}} & 0 \\ 0 & 0 \end{pmatrix}. \tag{9.93}$$

The weight matrix is

$$\overline{P}_z(k) = \overline{Q}_z^{-1}(k)\,. \tag{9.94}$$

The normal Eq. 9.87 of epoch k is

$$M_z(k)Z(k) = B_z(k)\,, \tag{9.95}$$

and the Kalman filter solution of Eq. 9.95 is then

$$\tilde{Z}(k) = \tilde{Q}_z(k)B_z(k), \quad \tilde{Q}_z(k) = (M_z(k) + \overline{P}_z(k))^{-1}\,. \tag{9.96}$$

It is notable that the normal equation 9.95 must be computed using the predicted vector $\overline{Z}(k)$ of Eq. 9.91.

Repeating the steps from Eqs. 9.89 to 9.96 for the further epoch is a process of Kalman filtering using velocity information. The algorithm outlined above is suitable both for the kinematic and static data processing. This is true especially for static data processing, because the station has not been exactly assumed as fixed (as described by Eq. 9.89); such an algorithm will modify the property of the strong dependency on the initial value of the Kalman filter. The forming of normal Eq. 9.89 is an iterative process (cf. Sect. 9.4.6), i.e., the velocity information has to be used for forming the equation. Equation 9.89 represents a realistic system description.

(c) ketabton.com: The Digital Library

9.5 Accuracy of the Observational Geometry

Recalling the discussions made in the adjustment of Chap. 7, the precision vector of the solved vector is usually represented as (cf., e.g., Eq. 7.8)

$$p[i] = m_0\sqrt{\mathrm{Q[i][i]}} \quad \text{and} \tag{9.97}$$

$$m_0 = \sqrt{\frac{V^T PV}{m-n}}, \quad \text{if} \quad (m>n).$$

where i is the element index, m_0 is the so-called standard deviation (or sigma), $p[i]$ is the i^{th} element of the precision vector, $Q[i][i]$ is the i^{th} diagonal element of the quadratic matrix Q (the inverse of the normal matrix), V is the residual vector, superscript T is the transpose of the vector, P is the weight matrix, n is the unknown number, and m is the observation number.

Equation 9.97 is used to describe the precision of the individual parameter of the unknown vector X. The parameters can be usually classified into several groups according to their physical properties, e.g., position unknowns and clock unknowns; in turn the position unknowns can be classified by stations, and the clock errors can be classified by satellites and receivers, etc. To describe the precision of a group of unknowns, a so-called mean-squares-root precision can be defined as

$$p_{jJ} = \sqrt{\frac{1}{n}\sum_{i=j}^{J} p[i]^2}, \tag{9.98}$$

where j is the first index and J is the last index of the parameters of the discussed group, and n is the total parameter number of the group. Of course, here we assume the parameters are ordered in groups. Putting Eq. 9.97 into above, one has

$$p_{jJ} = \frac{m_0}{\sqrt{n}}\mathrm{DOP}, \quad \mathrm{DOP} = \sqrt{\sum_{i=j}^{J} Q[i][i]}, \tag{9.99}$$

where DOP is the shortening of the Dilution of Precision factor. So we see that the DOP factor is a very important factor to describe the precision of a group of parameters that are the same kind. Supposing in the unknown vector $X[i]$, $i = 1, 2, 3$ are coordinate x, y, z of a receiver, and $i = 4$ is the receiver clock error, then the Position DOP (PDOP) is defined by $j = 1$, $J = 3$ in Eq. 9.99, and the Time DOP (TDOP) is defined by $j = J = 4$ in Eq. 9.99. The Geometric DOP (GDOP) is defined by $j = 1$, $J = 4$ in Eq. 9.99 (cf. Hofmann-Wellenhof et al. 1997). For the case of multiple stations, the definition can be similarly extended.

The PDOP is a factor, which indicates the factor of precision of the position. Quite often, one would prefer to express the position precision in a local coordinate system,

(c) ketabton.com: The Digital Library

i.e., in horizontal and vertical components. Recalling the relation between the global and local coordinates (cf. Sect. 2.3), there are

$$X_{\text{local}} = RX_{\text{global}}\,, \quad \text{and} \quad X_{\text{global}} = R^T X_{\text{local}}\,, \tag{9.100}$$

where X_{local} and X_{global} are identical vectors represented in local and global coordinate systems. R is the rotation matrix given in Eq. 2.11. According to the covariance propagation theorem, one has then

$$Q_{\text{local}} = RQ_{\text{global}}R^T\,, \quad \text{and} \quad Q_{\text{global}} = R^T Q_{\text{local}}R\,, \tag{9.101}$$

where Q_{global} is the sub-matrix of Q, which is related to the coordinates part. Supposing in the unknown vector $X_{\text{local}}[i]$, $i = 1, 2, 3$ are coordinates of horizontal x, y, and vertical z of a receiver, then the Horizontal Dilution of Precision (HDOP) and Vertical Dilution of Precision (VDOP) are defined as

$$\text{HDOP} = \sqrt{\sum_{i=1}^{2} Q_{\text{local}}[i][i]}\,, \quad \text{and} \quad \text{VDOP} = \sqrt{\sum_{i=3}^{3} Q_{\text{local}}[i][i]}\,. \tag{9.102}$$

For many stations, the definition can be similarly given.

(c) ketabton.com: The Digital Library

Applications of GPS Theory and Algorithms

Software development using GPS theory and algorithms is discussed in this chapter. A concept of precise kinematic positioning and flight-state monitoring of an airborne remote sensing system is presented.

10.1 Software Development

GPS/Galileo software consists generally of three basic components: a functional library, a data platform, and a data processing core. The functional library provides all possibly needed physical models, algorithms and tools for use. The data platform prepared all possibly needed data for use and performing the preparation in a time loop. The data processing core forms the observation equations, accumulates them within the time loop and solves the problem if desired. Software can be developed using the theory and algorithms outlined in this reference and handbook.

10.1.1 Functional Library

A functional library consists of physical models, algorithms and tools. For convenience, the functions are listed below with the references referring to the contents described in this book (cf. Figs. 10.1–10.3).

Physical Models

1. Tropospheric models for correcting or determining the tropospheric effects (cf. Sect. 5.2);
2. Ionospheric model for correcting the ionospheric effects (cf. Sect. 5.1);
3. Relativity models for correcting the relativistic effects (cf. Sect. 5.3);
4. Earth tide model for the correction of the tidal displacements of the Earth-fixed stations (cf. Sect. 5.4);
5. Ocean loading tide model for computing corrections of the ocean loading displacements especially for the stations near the coast (cf. Sect. 5.4);
6. Satellite mass centre model for transformation between the mass centre and receiver antenna centre of the GPS satellite (cf. Sect. 5.8);
7. Solar radiation model for orbit determination (cf. Sect. 11.2.4);
8. Atmospheric drag model for LEO orbit determination (cf. Sect. 11.2.5);

(c) ketabton.com: The Digital Library

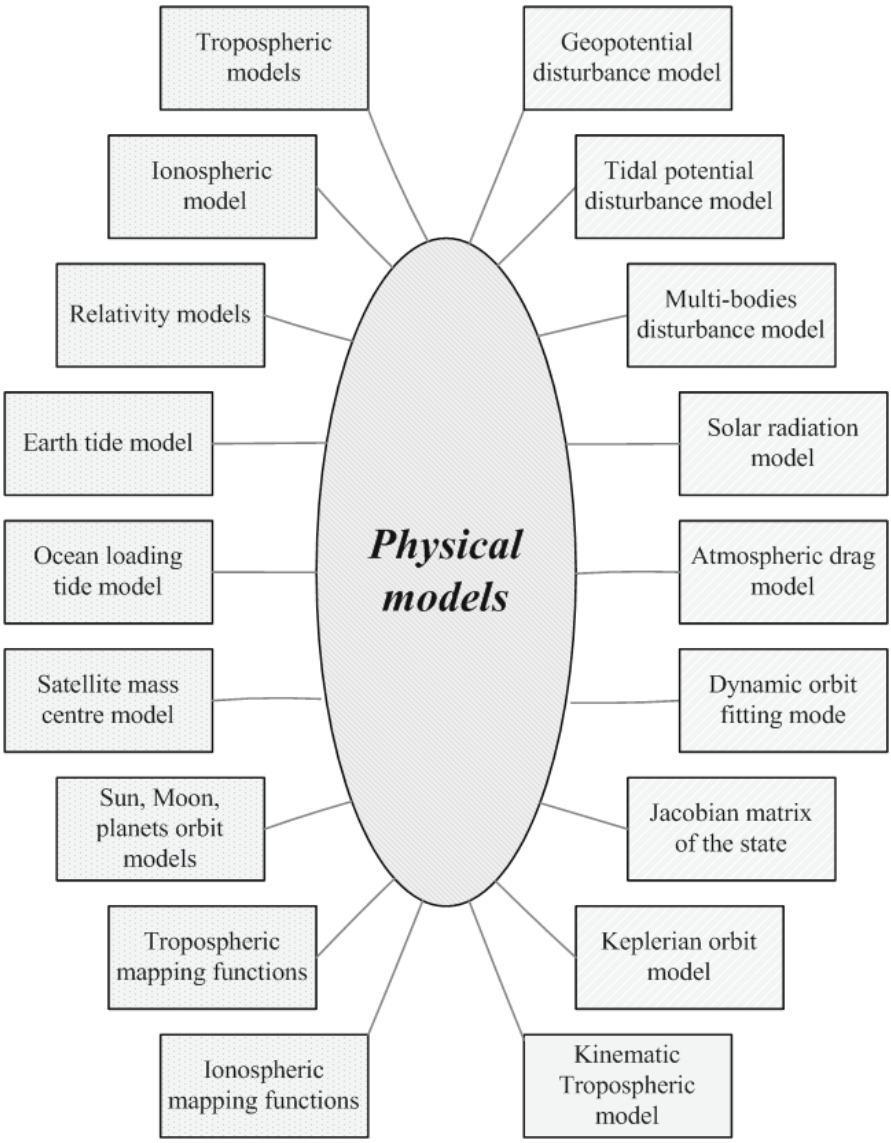

Fig. 10.1. Physical models

9. Geopotential disturbance model for dynamic orbit determination and LEO satellite geopotential determination (cf. Sect. 11.2.1);
10. Tidal potential disturbance model for precise dynamic orbit determination and LEO satellite geopotential determination (cf. Sect. 11.2.3);
11. Multi-body disturbance models for the correction of the perturbations (cf. Sect. 11.2.2);
12. Dynamic orbit fitting model for orbit correction in a regional network (cf. Sect. 11.4);

(c) ketabton.com: The Digital Library

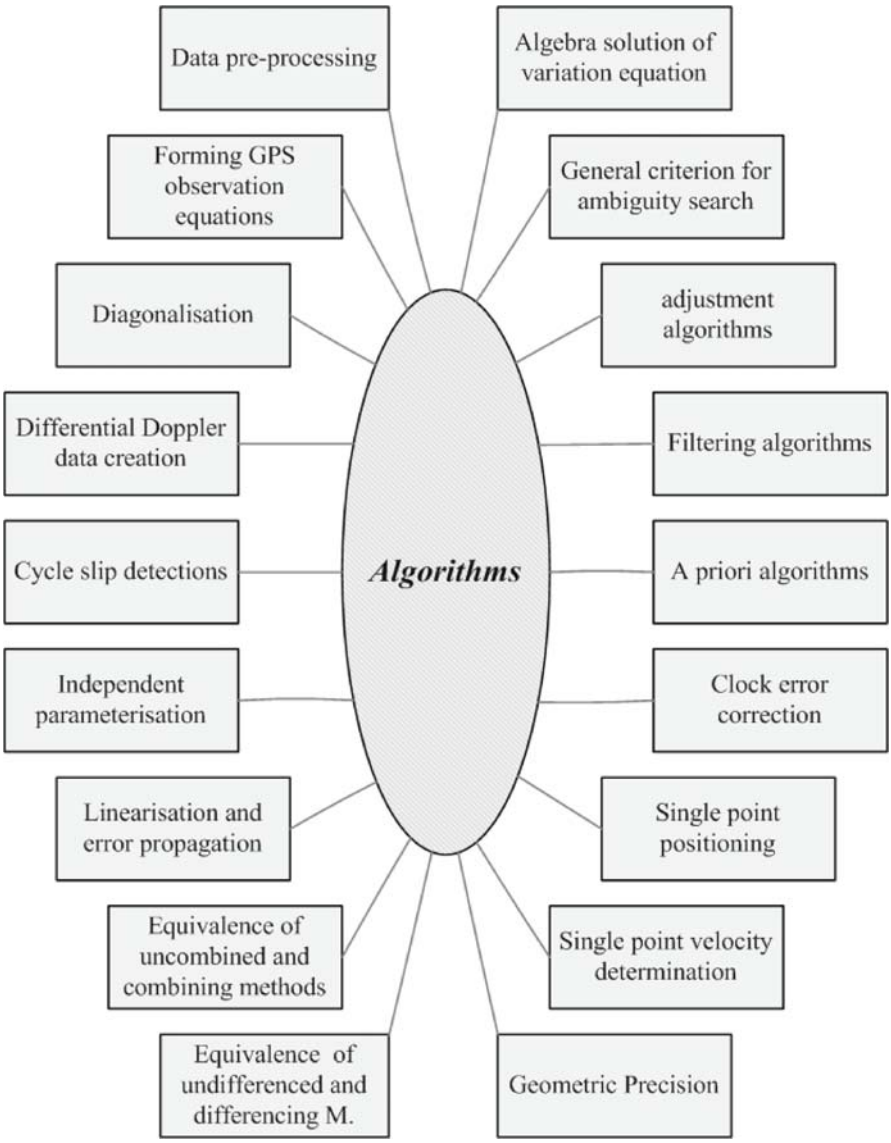

Fig. 10.2. Algorithms

13. Sun, Moon, and planet orbit models for computing the ephemerides of the Sun, Moon and planets, the multi-body disturbance and the Earth tide effects (cf. Sects. 11.2.8, 11.2.2 and 5.4);
14. Tropospheric mapping functions (cf. Sect. 5.2);
15. Ionospheric mapping functions (cf. Sect. 5.1);
16. Tropospheric model for kinematic receiver (cf. Sect. 10.2.2);
17. Keplerian orbit model (cf. Sect. 3.1.3);

(c) ketabton.com: The Digital Library

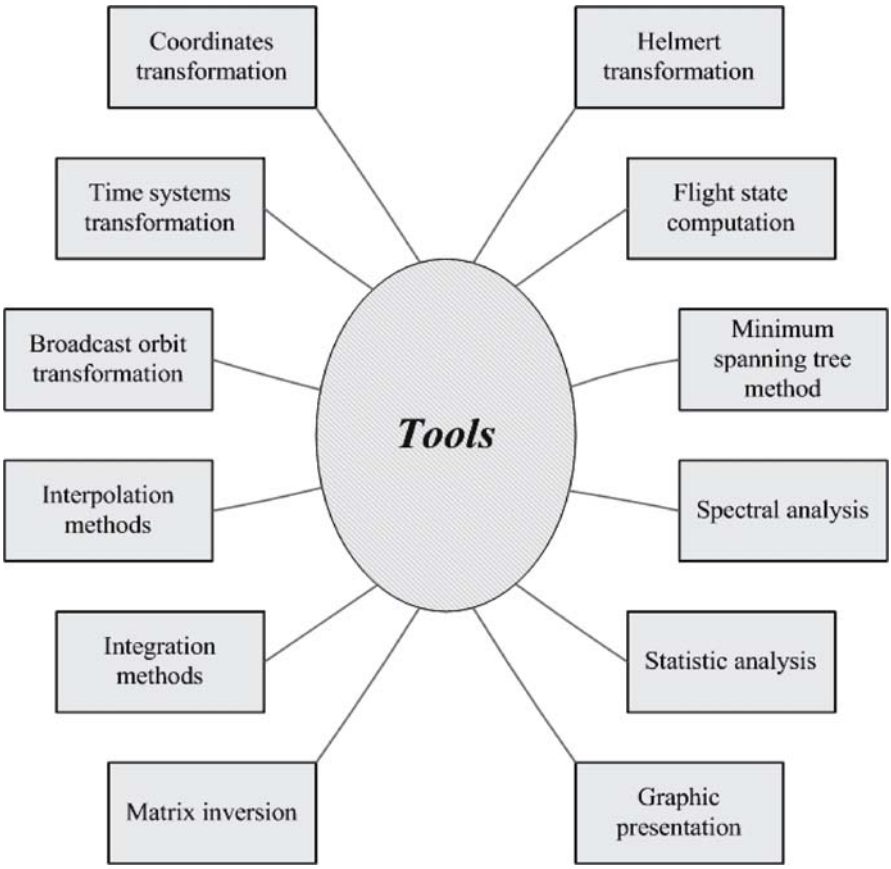

Fig. 10.3. Tools

18. Jacobian matrices of the Keplerian elements and the state vector of the satellite (cf. Sects. 3.1.1, 3.1.2, 3.1.3, 11.3 and 11.7).

Algorithms

1. Data pre-processing (cf. Sect. 9.4.1);
2. Forming GPS observation equations (cf. Sects. 4.1, 4.2, 4.3 and 6.1);
3. Differential Doppler data creation if necessary (cf. Sect. 6.5.5);
4. Cycle slip detections (cf. Sect. 8.1);
5. Independent parameterisation algorithms (cf. Sect. 9.1);
6. Linearisation and covariance propagation (cf. Sects. 6.3, 6.4, 11.5 and 11.7);
7. Equivalent algorithms of uncombined and combining methods (cf. Sects. 6.5, 6.7 and 9.2);
8. Equivalent algorithms of undifferenced and differencing algorithms (cf. Sects. 6.6, 6.8, 7.6 and 9.2);
9. Diagonalisation algorithm (cf. Sects. 7.6.1 and 9.1);

(c) ketabton.com: The Digital Library

10. Algebraic solution of the variation equation (cf. Sect. 11.5.1);
11. Ambiguity search using general and equivalent criteria (cf. Sect. 8.3);
12. Classical adjustment tools (Least Squares adjustment (LSA), sequential LSA, conditional LSA, block-wise LSA, and equivalent algorithms, cf. Sects. 7.1–7.5);
13. Filtering algorithms (Kalman filter, robust Kalman filter, and adaptive robust Kalman filter, cf. Sects. 7.7.1, 7.7.2 and 7.7.3);
14. A priori constrained LSA (cf. Sects. 7.8.1 and 7.8.2);
15. Clock error corrections (cf. Sect. 5.5);
16. Single point positioning (cf. Sect. 9.4.2);
17. Single point velocity determination (cf. Sect. 9.4.6);
18. Accuracy of the observational geometry (cf. Sect. 9.5).

Tools

1. Coordinate transformation tools (cf. Sects. 2.1, 2.3, 2.4 and 2.5);
2. Time system transformation functions (cf. Sect. 2.6);
3. Broadcast orbit transformation in IGS format (cf. Sect. 3.3);
4. Interpolation tools (cf. Sects. 3.4, 5.4.2 and 11.6.5);
5. Integration methods (cf. Sects. 11.6.1, 11.6.2, 11.6.3 and 11.6.4);
6. Matrix inverse functions (Gauss-Jordan and Cholesky algorithms)
7. Helmert transformation (cf. Sect. 2.2);
8. Flight state computation (cf. Sect. 10.2.3);
9. Minimum spanning tree method for forming optimal baseline network (cf. Sect. 9.2);
10. Spectral analysis methods (cf. Xu 1992);
11. Statistic analysis (cf. Sects. 6.4 and 7.2);
12. Graphic representation.

10.1.2 Data Platform

A data platform consists of three parts: the common part, the sequential time loop part, and the summary part. For convenience, the functions are listed below with the references referring to the contents described in this book (cf. Fig. 10.4).

Common Part

1. Program start;
2. Read input parameter file for controlling the run of the software (an example of the definition of the input parameter file, cf., e.g., Xu 2004);
3. Read all possible data files necessary for the run of the software (e.g., satellite information file, station information file, geopotential data file, ocean loading coefficients, GPS orbit data file, polar motion data file, etc.);
4. Read or create the Sun-Moon-planet orbit data;
5. Compute Earth/ocean loading tide displacements;
6. GPS satellite orbit data transformation if necessary;
7. Data pre-processing if possible;
8. Optimal baseline network construction and initialisations.

(c) ketabton.com: The Digital Library

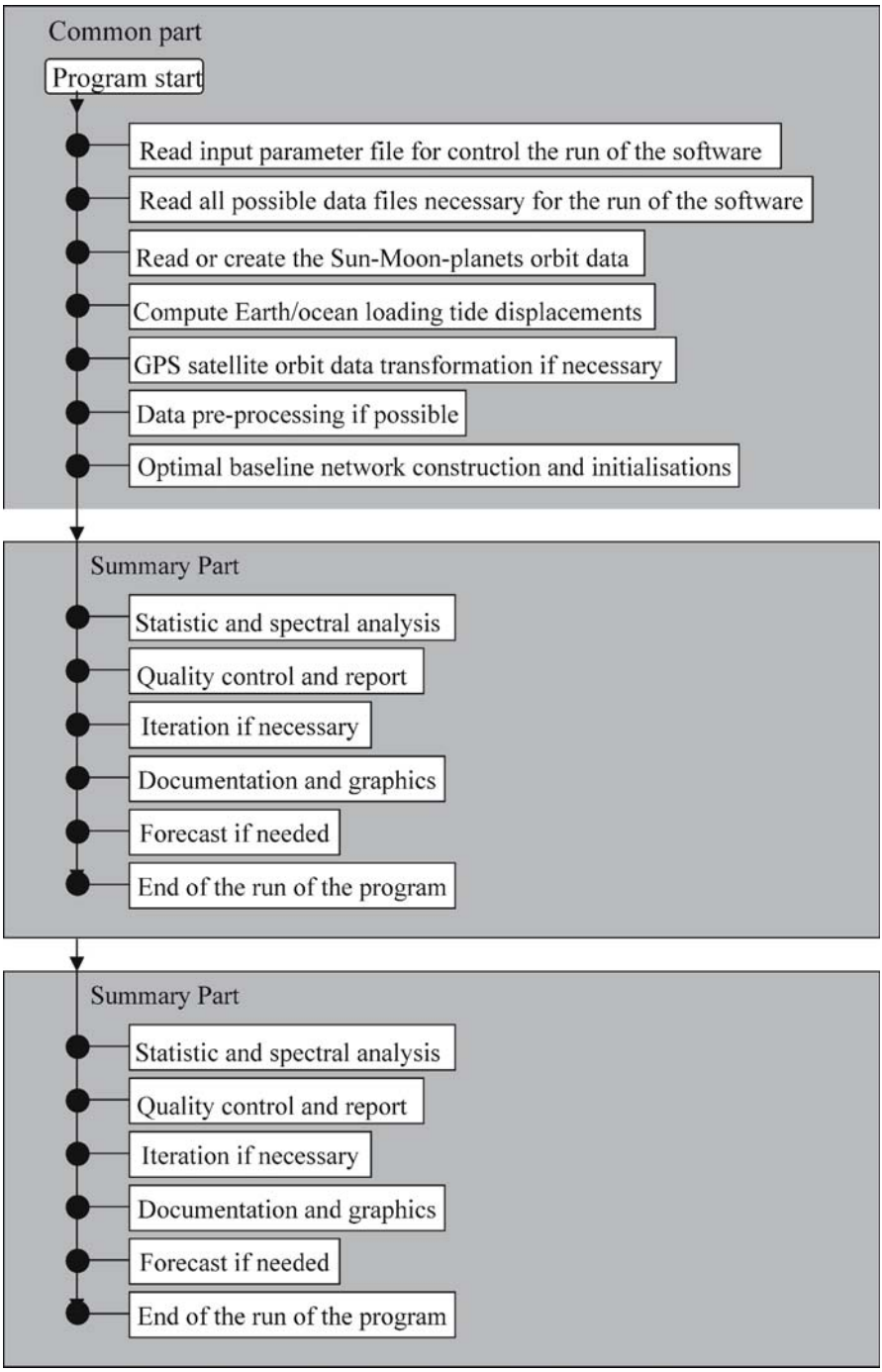

Fig. 10.4. Program common part, sequential time loop part, summary part

(c) ketabton.com: The Digital Library

Sequential Time Loop Part

1. Sequential time loop start;
2. Get the needed data for use at the related epoch (e.g., initial coordinates of the receivers, etc.);
3. Compute all possible parameters and model values for use at the related epoch (e.g., transformation matrices, interpolated orbit data, values of correcting models, etc.);
4. Read the GPS observation data and transform to a suitable form for use;
5. Single point positioning (e.g., for the second type of clock error correction);
6. Single point velocity determination (velocity belongs to the state vector of the station);
7. Data processing core (cf. Sect. 10.1.3);
8. End of the sequential time loop.

Summary Part

1. Statistic analysis and spectral analysis of the results;
2. Quality control and report;
3. Iteration if necessary;
4. Documentation and graphic representation;
5. Forecast if needed;
6. End of the run of the program.

10.1.3 A Data Processing Core

A data processing core is a collection of GPS data processing algorithms controlled by switches. Based on the above functional library and data platform, to realise a specific function of GPS software turns out to be a relatively simple job – one just needs to construct the function and add it to the data processing core. A multifunctional data processing core is a collection of individual functions and can be switched from one to the other through input parameters. Therefore, a data processing core is a list of specific program functions with switches. A specific function can be called a sub-core, which is dependent on the specific purposes of the data processing. Indeed the single point positioning and velocity determination functions are two functions of the data processing core. A list of the possible functions of a multifunctional data processing core and a structure of a sub-core are given below as examples.

Functions of a Multi-Functional Data Processing Core

1. Single point state vector determination for static and kinematic as well as dynamic applications;
2. Relative positioning for static and kinematic applications;
3. Ionosphere and atmosphere soundings;
4. Regional tectonic monitoring with orbit corrections;
5. Global network positioning and GPS orbit determination;
6. LEO orbit determination and geopotential determination.

(c) ketabton.com: The Digital Library

Structure of a Sub-Core

1. Computing the computed observables using the orbit and station data as well as the values of the physical models (may be used for system simulation);
2. Computing the coefficients of linearised observation equations;
3. In the case of dynamic applications, solving the variance equations for forming the orbit related observation equations;
4. Forming the normal equations;
5. Accumulation of the normal equations;
6. Solving the problem if desired.

10.2 Concept of Precise Kinematic Positioning and Flight-State Monitoring

A concept of precise kinematic positioning and flight-state monitoring of an airborne remote sensing system is presented here, based on the practical experiences from the EU project AGMASCO. Within the project, about two months of kinematic GPS flight data and static reference data have been collected in Europe over four campaigns during three years. An independently developed GPS software package and several commercial GPS software packages have been used for data processing. In this chapter, the methods of creating the tropospheric model for the aircraft trajectory and the use of static ambiguity results as conditions in the kinematic positioning are discussed. These concepts are implemented in the kinematic/static GPS software KSGsoft, and they have demonstrated excellent performance (cf. Xu 2000).

10.2.1 Introduction

The EU (European Union) project AGMASCO (**A**irborne **G**eoid **Ma**pping **S**ystem for **C**oastal **O**ceanography), in which five European institutions participated, has collected about two months of multiple static and airborne kinematic GPS data for the purpose of kinematic positioning and flight state monitoring of an airborne remote sensing system. The remote sensing system includes an aerogravimeter, accelerometer, radar and laser altimeter, INS and datalogger. During the project, four flight campaigns were performed in Europe (Fig. 10.5). They were the test campaign in Braunschweig in June 1996 (Fig. 10.6), the Skagerrak campaign in September 1996 (Fig. 10.7), the Fram Strait campaign in July 1997 (Fig. 10.8) and the Azores campaign in October 1997 (Fig. 10.9). Two to three kinematic GPS antennas were mounted on the fuselage, the back and the wing of the aircraft, and at least three GPS receivers were used as static reference receivers.

The above-mentioned remote sensing system has two very important objectives: to measure the gravity acceleration of the Earth and to determine the sea surface topography. Because the aerogravimeter (or accelerometer) and the altimeter are firmly attached to the aircraft, kinematic positioning and flight-state monitoring using GPS plays a key role for determining the flight acceleration, velocity and position, as well as orientation of the aircraft. The high sensitivity of the sensors requires high quality aircraft positioning and flight-state monitoring. Therefore, new strate-

(c) ketabton.com: The Digital Library

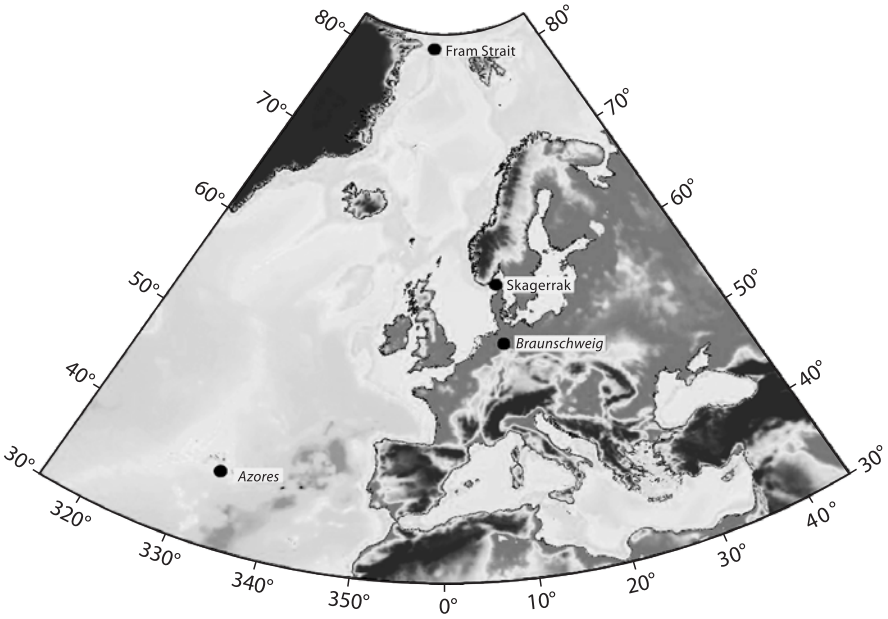

Fig. 10.5. Measured areas of the four flight campaigns

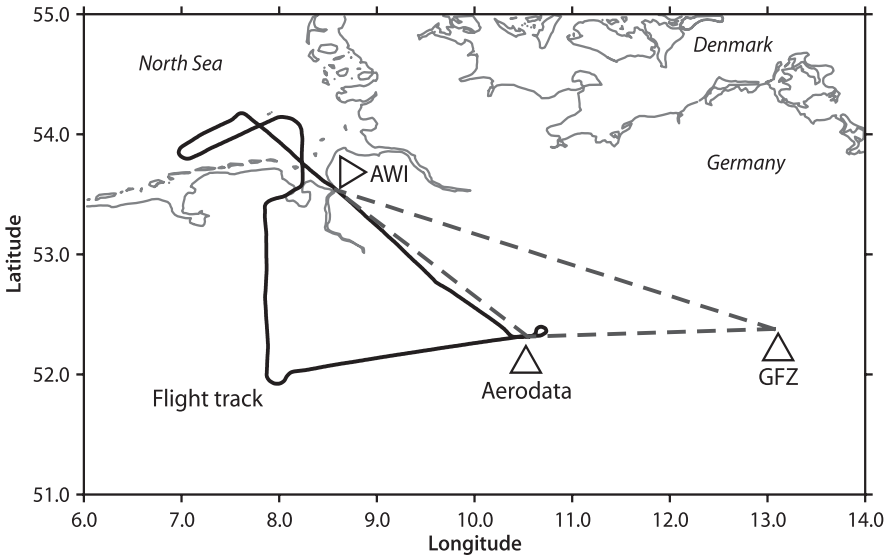

Fig. 10.6. Flights in the Braunschweig campaign (June 1996)

gies and methods have been studied, developed, tested and implemented for GPS data processing.

(c) ketabton.com: The Digital Library

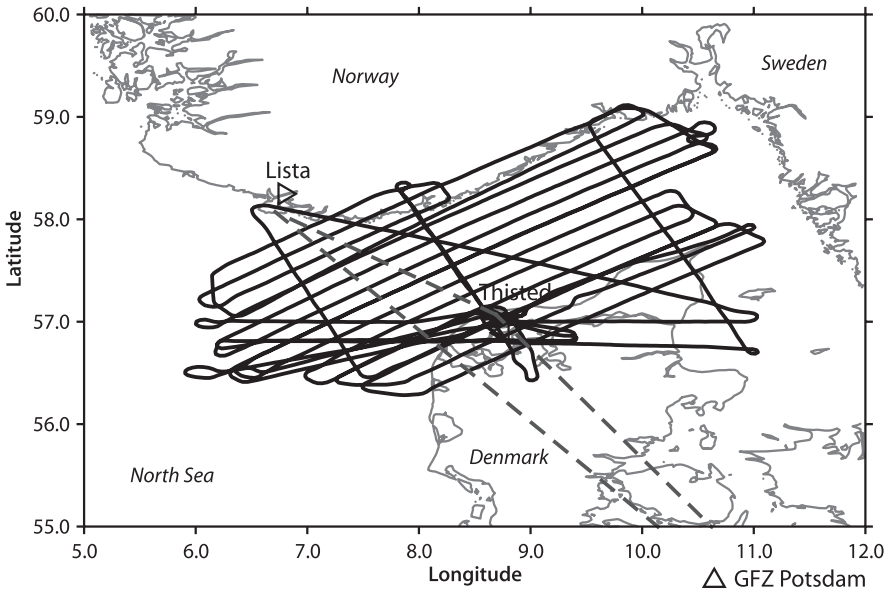

Fig. 10.7. Flights in the Skagerrak campaign (September 1996)

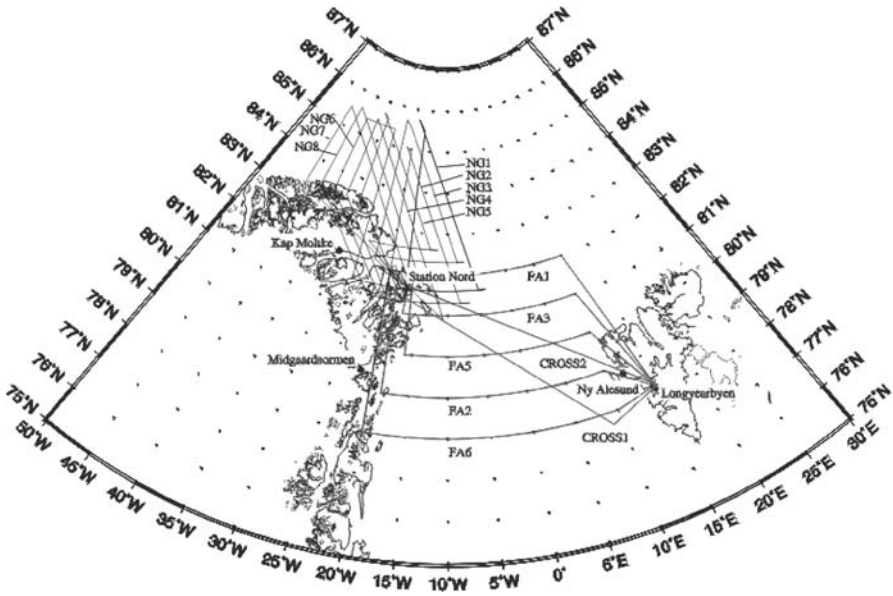

Fig. 10.8. Flights in the Fram Strait campaign (July 1997)

The adopted concept of precise kinematic positioning and flight-state monitoring are discussed in Sects. 10.2.2 and 10.2.3, respectively.

(c) ketabton.com: The Digital Library

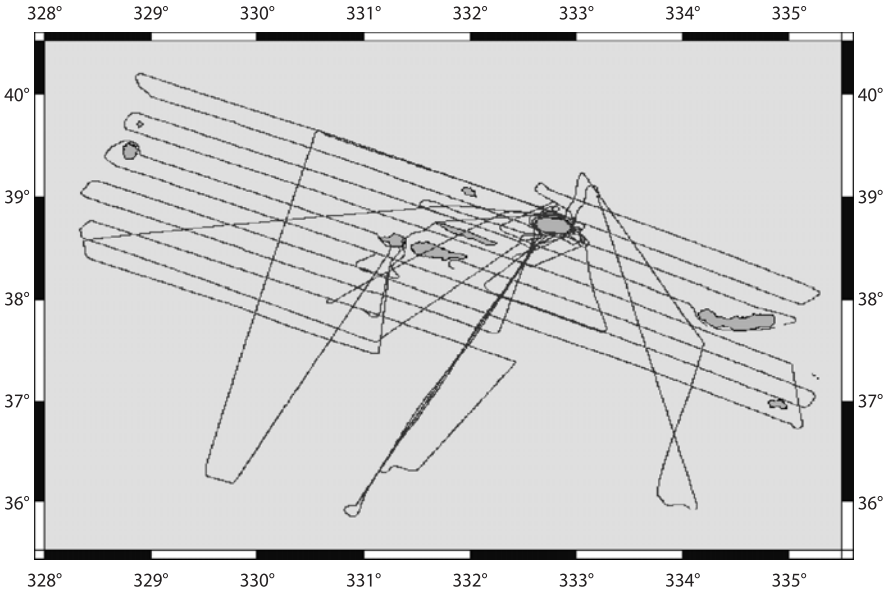

Fig. 10.9. Flights in the Azores campaign (October 1997)

10.2.2 Concept of Precise Kinematic Positioning

A vast literature exists on the topic of precise kinematic positioning (see, e.g., Goad and Remondi 1984; Wang et al. 1988; Schwarz et al. 1989; Cannon et al. 1997; Hofmann-Wellenhof et al. 1997). Based on AGMASCO practice, a modified concept has been developed and applied to data processing.

10.2.2.1 *Combining the Static References with IGS Station*

It is well-known that differential GPS positioning results depend on the accuracy of the reference station(s). However, it is not quite clear how strong this dependency is, or in the other words, how accurate the reference coordinates should be determined for use in kinematic differential positioning. During AGMASCO data processing, it was noticed that the accuracy of the reference coordinates is very important. A bias in the reference station coordinates will cause not only a bias in the kinematic flight path, but also a significant linear trend. Such a liner trend depends on the flight direction and the location of the reference receiver(s). Therefore, in precise kinematic positioning, the coordinates of the static reference station should be carefully determined by, for example, connecting these stations to the nearby IGS stations. A detailed study of the relationship between the accuracy of the reference station coordinate and the quality of kinematic and static positioning has been carried out by Jensen (1999).

(c) ketabton.com: The Digital Library

10.2.2.2
Earth Tide and Loading Tide Corrections

A detailed study of the Earth tide effects on GPS kinematic/static positioning is given in Xu and Knudsen (2000). For airborne kinematic differential GPS positioning, Earth tide effects on the static reference station need to be corrected for. Such tidal effects could reach up to 30 cm in Denmark and Greenland, and 60 cm at other locations in the world. Tidal effects could induce a "drift" over a few hours of measurement duration. For ground-based kinematic and static differential GPS positioning with baseline lengths less than 80 km, the impact of the Earth tide effects could reach more than 5 mm. In precise application of GPS positioning, both in kinematic and static cases, the Earth tide effects have to therefore be taken into account even for a relatively small local GPS network.

Ocean loading tide effects could also reach up to a few cm in magnitude, in special cases (Ramatschi 1998). Generally, ocean loading tide effects should be considered at the cm level in coastal areas, so that these effects have to be corrected for GPS data processing. However, unlike the Earth tide, ocean loading tide effects can only be modelled by ocean tide models at about 60% to 90% (Ramatschi 1998). Therefore, simply using a model to correct for the effects is not enough, and a detailed study of ocean loading tide effects is necessary for precise positioning. It is, however, possible to use GPS for determining the parameters of the local ocean loading tide effects (Khan 1999).

10.2.2.3
Multiple Static References for Kinematic Positioning

In differential GPS kinematic positioning, usually there is only one static reference used. It is obvious that if multiple static references are used, the reference station dependent errors, such as those due to the troposphere and ionosphere as well as ocean loading tide effects, could be reduced and the geometric stability could be strengthened. For simplicity, only the case of using two static reference receivers will be discussed here. In Fig. 10.10, 1 and 2 denote the static reference receivers, and k denotes the kinematic object. Suppose the two static stations are placed close by and both have the same GPS satellites in view. Using one static reference receiver for kinematic positioning, one has unknown vector $(X_k \quad N_{1k})$, where X is the coordinate sub-vector and N is the ambiguity sub-vector. Using two static references, one has unknown

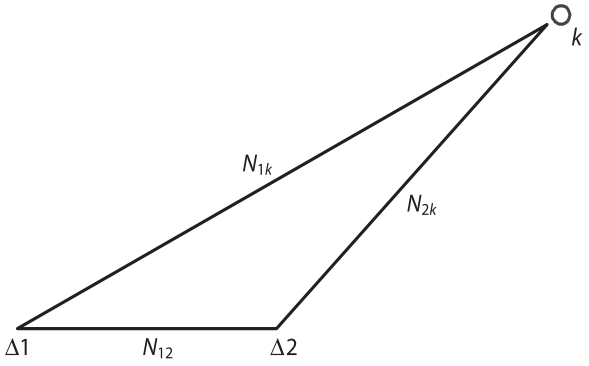

Fig. 10.10.
Multiple static references for kinematic positioning

(c) ketabton.com: The Digital Library

vector ($X_k \;\; N_{1k} \;\; N_{2k}$), because the unknown coordinate sub-vector X is the same. The number of elements of the sub-vector N compared with that of X is very small in the kinematic case. Therefore, by using multiple static reference receivers for kinematic positioning, the total number of observations is increased, but the total number of unknowns remains almost the same; hence the results will be modified.

Furthermore, according to the definition of double differenced ambiguities, one has

$$N_{1k} = N_1^j - N_k^j - N_1^J + N_k^J \,, \tag{10.1}$$

$$N_{2k} = N_2^j - N_k^j - N_2^J + N_k^J \tag{10.2}$$

and

$$N_{12} = N_1^j - N_2^j - N_1^J + N_2^J \,, \tag{10.3}$$

where N on the right sides is un-differenced ambiguity, indices j and J denote satellites, 1 and 2 denote the static stations, and k denotes the kinematic station. Then one gets

$$N_{1k} - N_{2k} = N_{12} \,, \tag{10.4}$$

where N_{12} is the double difference ambiguity vector of the static baseline, which can be obtained from the static solution. Using relation Eq. 10.4, N_{2k} can be represented by $(N_{1k} - N_{12})$. Thus, using two static references for kinematic positioning, one has nearly doubled the number of observables, yet the unknowns remain the same, if in addition the static results are used. (Usually static measuring can be made over a longer time, and hence the static results can be obtained precisely).

In the case of a single difference, one has

$$N_{1k} = N_1^j - N_k^j \,, \tag{10.5}$$

$$N_{2k} = N_2^j - N_k^j \,, \tag{10.6}$$

and

$$N_{12} = N_1^j - N_2^j \,, \tag{10.7}$$

where N on the right sides is un-differenced ambiguity, index j denotes the satellite, 1, 2 denote the static stations, and k denotes the kinematic station. Then one gets the same relation as in the case of double difference:

$$N_{1k} - N_{2k} = N_{12} \,. \tag{10.8}$$

For un-differenced data processing, ambiguity vectors are $(N_1^j \;\; N_k^j)$ and $(N_2^j \;\; N_k^j)$ in kinematic data processing using a single reference. $(N_1^j \;\; N_2^j)$ is the ambiguity vector in static data processing. No matter how one deals with the reference-related ambiguities, the common part of ambiguities obtained from static data processing can be used in kinematic data processing.

(c) ketabton.com: The Digital Library

Using multiple static reference receivers and introducing the ambiguities from the static solution as conditions, the accuracy of the kinematic positioning can be increased significantly. An example showing the differences in the height of the front antenna determined using multiple reference receivers, with and without using the static ambiguity condition, is given in Fig. 10.14 (the ambiguity float solutions are used). The average and standard deviation of the differences are 27.07 and 4.34 cm, respectively. These results clearly indicate that the multiple static conditions have modified the results. A change of ambiguity not only caused a bias in the position solution, but also a high frequency variation. The base-base separation is about 200 km, and the length of the kinematic path is about 400 km (cf. Fig. 10.9).

For three or more static references receivers, similar arguments and improved results can be presented.

10.2.2.4
Introducing Height Information as a Condition

Even after using multiple static reference receivers and the static conditions, the ambiguities in kinematic positioning can still be wrong. In such a case, there could be a bias and a variation in the kinematic trajectory (see Sect. 10.2.4.2 and Fig. 10.14). Therefore, introducing the height information of the aircraft at the start and/or resting point into the data processing is a great help, especially in the airborne altimetry applications. The bias of the results obtained by using different software can then be eliminated.

10.2.2.5
Creation of a Kinematic Tropospheric Model

Using the multiple static reference receivers, the parameters of the tropospheric model can be determined. Using these parameters, the tropospheric model parameters for the kinematic receiver can be interpolated. Such a model, however, generally is only suitable for the footprint point of the kinematic platform. Therefore, the vertical gradient of temperature and the exponential changes of pressure and humidity (Syndergaard 1999) are introduced into the standard model to create a tropospheric model for the kinematic station in the air. This is, of course, not an ideal model; however, it is a very reasonable one.

10.2.2.6
Higher Order Ionospheric Effect Correction

For long distance kinematic positioning, the ionosphere-free combination has to be used to eliminate the ionospheric effects. It is well-known that the ionosphere-free combination is indeed only a first order approximation (Klobuchar 1996). The second order ionospheric effects are about 0.1% of that of the first order (Syndergaard 1999). Therefore the residual ionospheric effects can reach the level of a few cm. This has to be taken into account by using some form of modelling of the total ionospheric effects.

(c) ketabton.com: The Digital Library

10.2.2.7
A General Method of Integer Ambiguity Fixing

An integer ambiguity search method based on the conditional adjustment theory was proposed in Sect. 8.3. This method has been implemented in the GPS software KSGsoft (Kinematic/Static GPS Software), developed in GFZ Potsdam (Xu et al. 1998), and used extensively for real data processing in the EU project AGMASCO (Xu et al. 1997). The search can be carried out in the coordinate domain, ambiguity domain or both domains. Most other least squares ambiguity search methods (Euler and Landau 1992; Teunissen 1995; Merbart 1995; Han and Rizos 1995, 1997) are special cases of this algorithm, if only the ambiguity search domain is selected and without considering the uncertainty of the coordinates caused by ambiguity fixing. By taking the coordinate and ambiguity residuals into account, a general criterion for ambiguity searching is proposed to ensure an optimal search result. Detailed formulas are derived and their usage can be found in Sect. 8.3. The theoretical relationship between the general criterion and the least squares ambiguity search criterion is also derived and illustrated by numerical examples in Sect. 8.3.

10.2.3
Concept of Flight-State Monitoring

For flight-state monitoring of an aircraft, it is necessary that several GPS antennas have to be used. The relative positions between the multiple antennas should be determined. Using, as an example, the method presented in Sect. 10.2.2, the position and velocity of one of the kinematic antennas can be determined. Using this point as a reference, the related position differences of other antennas can be determined. Because the distances between the multiple antennas are only a few meters, the atmospheric and ionospheric effects are nearly identical, and therefore only the single frequency L1 observations are needed for relative positioning. In addition, due to the short ranges, such relative positioning can be performed with high accuracy.

Early stage tests of multiple kinematic GPS antennas mounted on a platform were made for checking purposes, using the known baseline length. Typically, such checks indicate that the distance has a systematic bias if the distance is computed from the two positions and these two positions are determined separately. However, a combined solution of multiple kinematic positioning does not overcome the distance bias problem completely because of inaccuracies in the ambiguity solution. Therefore, for precise flight-state monitoring, it is necessary to introduce the known distances between the antennas fixed on the aircraft as additional constraints in the data processing.

The distance condition can be represented as

$$\rho = \sqrt{(\Delta X)^2 + (\Delta Y)^2 + (\Delta Z)^2}\ , \tag{10.9}$$

where ΔX, ΔY and ΔZ are the coordinate differences between two antennas, and ρ is the distance. Because of the short distances, the linearisation of the condition cannot be done precisely in the initial step, and therefore an iterative process has to be used. The conditions can be used in a conditional adjustment, or the conditions can be used for eliminating unknowns. Both methods are equivalent.

(c) ketabton.com: The Digital Library

Flight-state is usually represented by so-called "state angles" (heading, pitch, and roll). They are rotation angles between the body and the local horizontal coordinate frames of the aircraft. The axes of the local horizontal frame are selected as follows: the x^b axis points out the nose, the y^b axis points to the right parallel to the wing, and the z^b axis points out the belly to form a right-handed coordinate system, where b denotes the body frame. The body frame can be rotated to be aligned to the local horizontal frame in a positive, right-handed sense, which is outlined in three steps. First, the body frame is rotated about the local vertical downward axis z by angle ψ (heading). Then the body frame is rotated about the new y^b axis by angle θ (pitch). Finally, the body frame is rotated about the new x^b axis by angle ϕ (roll). In the local horizontal coordinate system, the heading is the azimuth of axis x^b of the body frame, the pitch is the elevation of axis x^b of the aircraft and the roll is the elevation of axis y^b of the aircraft. Note that the directions of the axis x^b and the velocity vector of aircraft are usually not the same. Through kinematic positioning, the three flight state monitoring angles can be computed (Cohen 1996).

Suppose three kinematic GPS antennas are mounted on the aircraft at the front, the back and the right wing (denoted as f, b, w), so that the y components of the coordinates of front and back antennas in the body frame are zero, i.e., $y_f^b = y_b^b = 0$, and x, z components of the coordinates of the wing antenna in the body frame are zero, i.e., $x_w^b = z_w^b = 0$. Then the coordinates of three antennas in body fixed frame are $P_f(x_f^b, 0, z_f^b)$, $P_b(x_b^b, 0, z_b^b)$, and $P_w(0, y_w^b, 0)$. Because the antennas are mounted as above supposed and because the flight-state is computed by the positions of three antennas, there are pitch and roll correction angles that can be computed from the three coordinates by

$$\tan(\theta_0) = \frac{z_f^b - z_b^b}{x_f^b - x_b^b} \quad \text{and} \tag{10.10}$$

$$\tan(\phi_0) = -\frac{z_0}{y_w^b}, \tag{10.11}$$

where

$$z_0 = z_f^b - x_f^b \tan(\theta_0). \tag{10.12}$$

Through kinematic positioning and coordinate transformation, one has the coordinates of the three points in the local horizontal frame $P_f(x_f, y_f, z_f)$, $P_b(x_b, y_b, z_b)$, and $P_w(x_w, y_w, z_w)$. Then the three flight-state monitoring angles can be computed by

$$\tan(\psi) = \frac{y_f - y_b}{x_f - x_b}, \tag{10.13}$$

$$\tan(\theta - \theta_0) = \frac{z_f - z_b}{S}, \tag{10.14}$$

$$S = \sqrt{(x_f - x_b)^2 + (y_f - y_b)^2}, \tag{10.15}$$

$$\tan(\phi - \phi_0) = \frac{z_w - z_0}{s} \quad \text{and} \tag{10.16}$$

$$s = \sqrt{(x_w - x_0)^2 + (y_w - y_0)^2}, \tag{10.17}$$

(c) ketabton.com: The Digital Library

where √ is the squares root operator and

$$x_0 = x_f - (x_f - x_b)K\,, \tag{10.18}$$

$$y_0 = y_f - (y_f - y_b)K\,, \tag{10.19}$$

$$z_0 = z_f - (z_f - z_b)K \quad \text{and} \tag{10.20}$$

$$K = \frac{x_f^b}{x_f^b - x_b^b}\,. \tag{10.21}$$

Comparisons of numerical GPS flight-state monitoring results are made with the results of INS. It is possible to use GPS to determine the heading with an accuracy up to 0.1 degree, and pitch and roll up to 0.2 degree. In this case, the distances between the three antennas were 5.224 m, 5.510 m and 4.798 m.

10.2.4 Results, Precision Estimation and Comparisons

Examples demonstrating the above-mentioned methods are given through kinematic/static processing a set of kinematic/static GPS data collected on the 3 October 1997 at the islands of Portugal in the Atlantic Ocean within the Azores campaign. Two reference stations (Faim and Flor) served as static references and have a distance of about 239.4 km. Three antennas are fixed at the front, the back and the wing of the aircraft for determining the flight-state. The distances between the baselines of front-back, front-wing, and back-wing are 5.224, 5.510, and 4.798 meters, respectively. The flight time is about 4 hours. The length of the area is about 400 km (Fig. 10.11). The height of the flight is about 400 meters (Fig. 10.12).

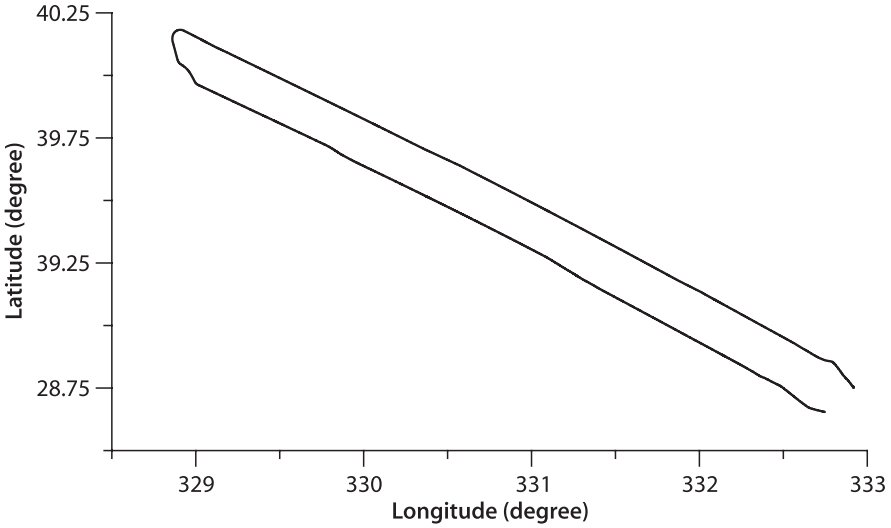

Fig. 10.11. One flight trace determined by kinematic GPS

(c) ketabton.com: The Digital Library

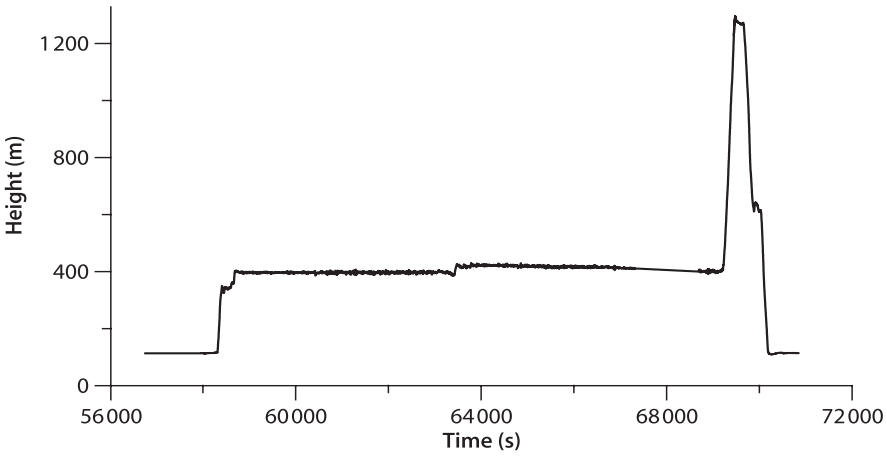

Fig. 10.12. Height profile of one flight determined by kinematic GPS

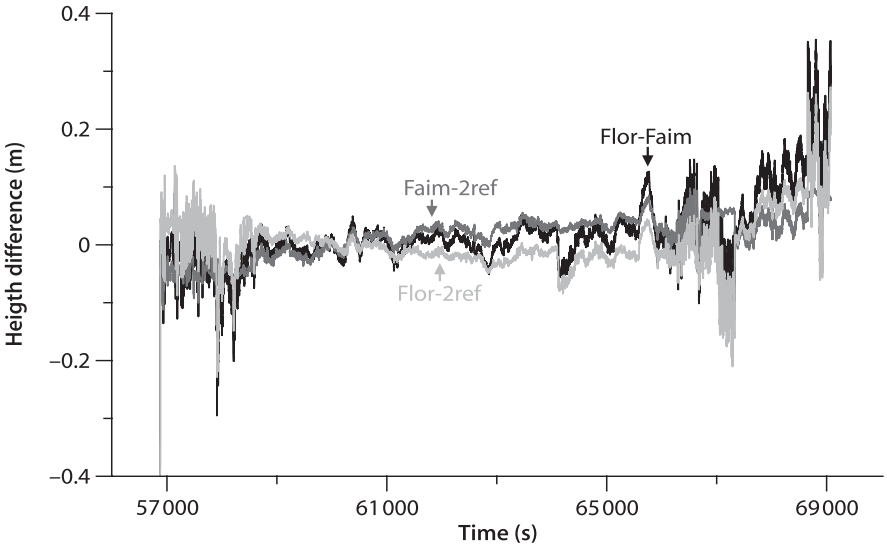

Fig. 10.13. Height differences caused by static references

10.2.4.1 *Multiple Static References for Kinematic Positioning*

The flight trajectory determined by using multiple references is a kind of weighted average path of the trajectories determined by using a single reference separately. The heights of the front antenna are determined by using a single reference and multiple references, respectively. The height differences of Flor-Faim, Flor-2ref, and Faim-2ref are given in Fig. 10.13 with dark, light, and medium grey lines. Where Flor-Faim means the height differences between the results obtained by using Flor and Faim as a static reference sepa-

(c) ketabton.com: The Digital Library

rately, 2ref means two references are used. The statistics of the differences are given in Table 10.1 (units: cm). It shows that the multiple references helped to stabilise the results.

10.2.4.2 *Ambiguity of Multiple Static References as a Condition for Kinematic Positioning*

In the case of multiple static references, a static solution between the static references can be made for obtaining the static ambiguity vector. Such a vector usually can be obtained with excellent quality. By introducing such results as conditions for kinematic positioning, the accuracy of the position solution can be modified. The differences of the heights of the front antenna determined by using multiple references with and without using static ambiguities as conditions are given in Fig. 10.14. The average and standard deviation of the differences are 27.07 and 4.34 cm, respectively. These have shown that the multiple static conditions have helped to modify the results. A change of ambiguity not only caused a bias, but also a variation in the results.

Using multiple static references and introducing the static ambiguities as conditions, accuracy of the kinematic positioning can rise significantly. However, the airborne altimetry results have shown that the GPS height solution still has a bias. Therefore, airport height information is introduced as a condition for modifying ambiguity resolution and eliminating the height bias of the GPS solution. To introduce tropospheric parameters for the aircraft, statically determined parameters and the vertical temperature gradient have been used.

Table 10.1. Statistics of the differences of the heights determined

Height differences	Average	Deviation
Flor-2ref	1.62	3.52
Faim-2ref	–0.27	4.76
Flor-Faim	1.89	6.27

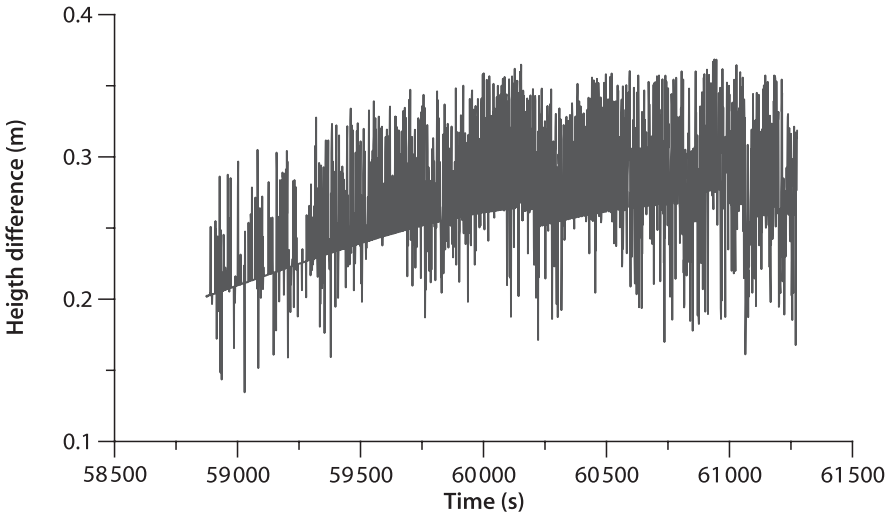

Fig. 10.14. Height differences caused by static references

(c) ketabton.com: The Digital Library

10.2.4.3
Multiple Kinematic GPS for Flight-State Monitoring and its Comparison with INS

GPS determined heading, pitch and roll are given in Fig. 10.15 and 10.16 (with dark and light lines), respectively. Comparisons are made with the results of INS. The differences of the flight-state angles determined by GPS and INS are given in Fig. 10.17. The differences of the heading, pitch and roll are represented with dark, medium and

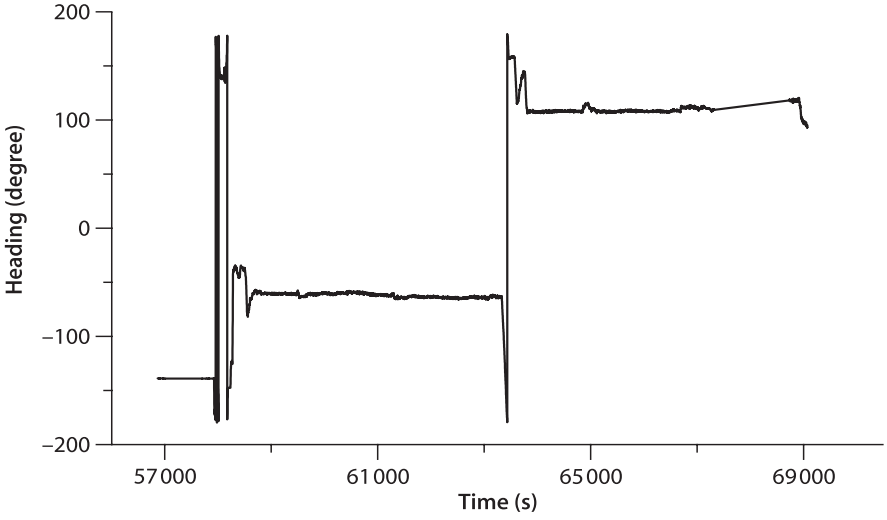

Fig. 10.15. Heading determined by GPS

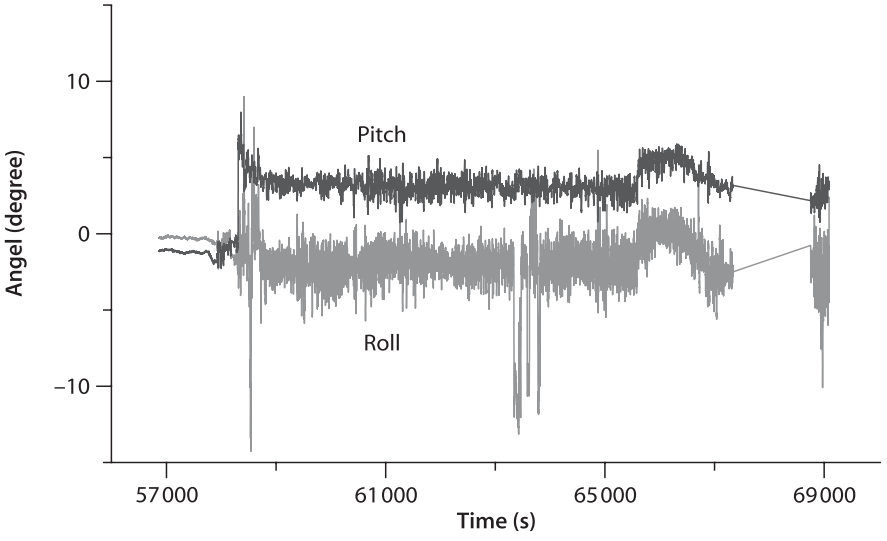

Fig. 10.16. Pitch and roll determined by GPS

(c) ketabton.com: The Digital Library

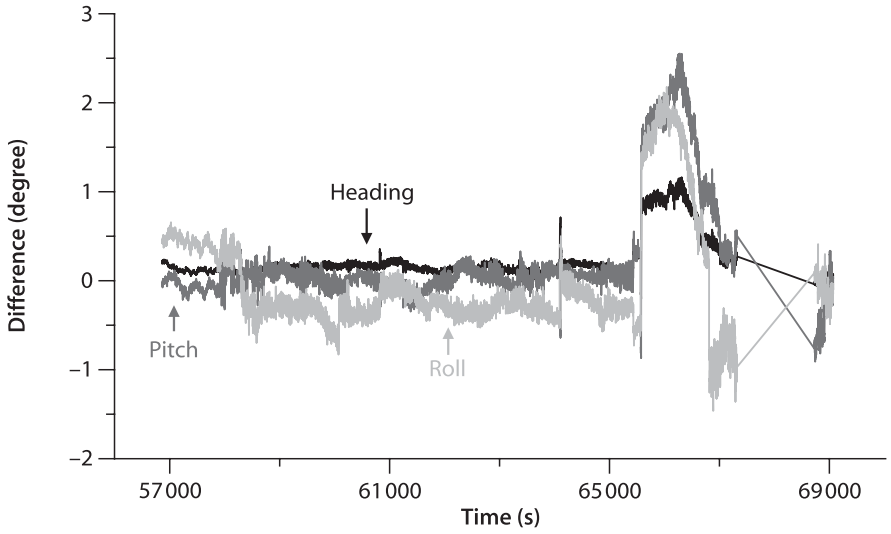

Fig. 10.17. Differences of flight state determined by GPS and INS

Table 10.2.
Statistics of the differences of the flight-state angles determined by GPS and INS

Differences of	Average	Deviation
Heading	0.230	0.238
Pitch	0.233	0.596
Roll	–0.249	0.612

light grey lines, respectively. The statistics of differences of the heading, pitch and roll are given in Table 10.2 (units: degrees). The larger deviations of the pitch and roll are due to larger uncertainties of the height components determined by GPS. Considering the large deviation around epoch 66 000 and the data gap in INS around epoch 68 000, it is possible to use GPS to determine the heading with accuracy up to 0.1 degree and pitch and roll up to 0.2 degree.

10.2.4.4 *Static GPS Data Kinematic Processing*

Static GPS data kinematic processing is one of the methods used to check the reliability of the GPS software working in a kinematic module. Such static data kinematic processing has been used for studying Earth tide effects (Xu and Knudsen 2000) and ocean loading tide effects. Faim has been used as a reference, and the position of Flor has been solved with static and kinematic modules. The static height of Flor is 98.257 m. The kinematic height average is 98.272 m, and its standard deviation is 3.8 cm. This indicates that kinematic data processing can reach an accuracy of about 4 cm with a baseline length of about 240 km. It seems that the results are very good; however, the kinematic height graphic (see Fig. 10.18) shows a clear ambiguity problem in kinematic data processing. As soon as a satellite goes up or down, a jump will occur in the solution trajectory.

(c) ketabton.com: The Digital Library

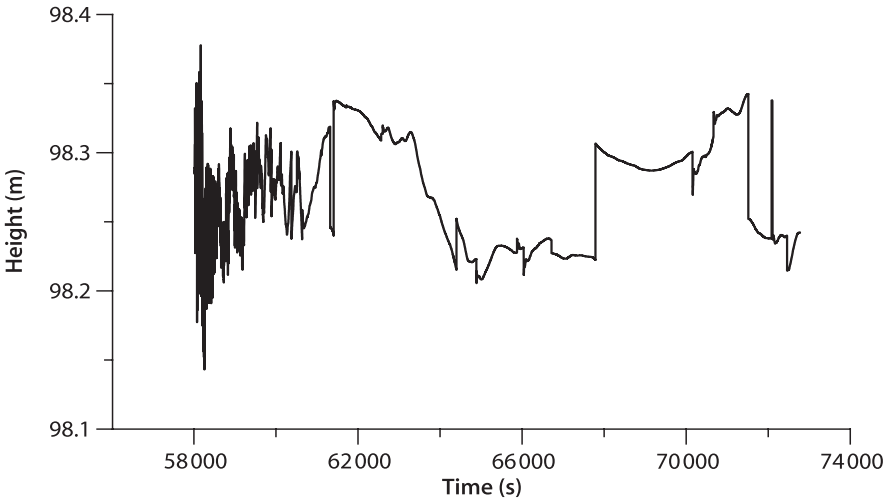

Fig. 10.18. Height changes by static data kinematic processing

Table 10.3.
Statistics of the differences of the velocity

Velocity difference	d*Vs*	d*Ve*	d*Vh*
Average	0.03	–0.01	–0.06
Deviation	0.27	0.17	0.53

10.2.4.5 *Doppler Velocity Comparisons*

Previous study (Xu et al. 1997) has shown that the velocity solution derived from Doppler measurements has a very high accuracy. It seems that the velocity solutions are independent from the static references. A statistic analysis of the differences of the velocity solved by using a different static reference (Flor or Faim) is given in Table 10.3 (units: cm s^{-1}), which confirms again the previous conclusion. The nominal flight velocity is about 80 m s^{-1} in horizontal. In the vertical component, the maximum velocity is about 5 m s^{-1}.

10.2.5 Conclusions

GPS research during the AGMASCO project has concluded that GPS is able to be used for airborne kinematic positioning and flight-state monitoring to fulfil the needs of navigating a remote sensing system for applications in aerogravimetry and oceanography.

A methodology has been proposed for precise kinematic GPS positioning that addresses the following issues:

- Using IGS stations to obtain precise reference coordinates, and introducing Earth tide and ocean loading tide corrections;

(c) ketabton.com: The Digital Library

- Introducing multiple static reference receivers, and using static ambiguity solution as conditions;
- Introducing the initial height information as a condition, and introducing the tropospheric model to the aircraft kinematic GPS receivers; and
- Modelling the higher order ionospheric effects, and using the general method of ambiguity searching in coordinate and ambiguity domains.

For flight-state monitoring, the kinematic reference and data of the single frequency L1 are used. Known distances between the multiple kinematic antennas are used as additional constraints.

Results have shown adequate performance of this methodology.

(c) ketabton.com: The Digital Library

Perturbed Orbit and its Determination

Satellites are attracted not only by the central force of the Earth, but also by the non-central force of the Earth, the attracting forces of the Sun and the Moon, and the drag force of the atmosphere. They are also affected by solar radiation pressure, Earth and ocean tides, general relativity effects (cf. Chap. 5) as well as coordinate perturbations. Equations of satellite motion have to be represented by perturbed equations. In this chapter, after discussions of the perturbed equations of motion and the attracting forces, for convenience of the Earth tide and ocean loading tide computations, the ephemerides of the Sun and the Moon are described. Orbit correction is discussed based on an analysis solution of the $\overline{C}_{20}$ perturbation. Emphasis is given to the precise orbit determination, which includes the principle of orbit determination, algebraic solution of the variation equation, numerical integration and interpolation algorithms as well as the related partial derivatives.

11.1 Perturbed Equation of Satellite Motion

The perturbed equation of motion of the satellite is described by Newton's second law in an inertial Cartesian coordinate system as

$$m\ddot{\vec{r}} = \vec{f}\,, \tag{11.1}$$

where $\vec{f}$ is the summated force vector acting on the satellite, and $\vec{r}$ is the radius vector of the satellite with mass m. $\ddot{\vec{r}}$ is the acceleration. Equation 11.1 is a second-order differential equation. For convenience, it can be written as two first-order differential equations as

$$\begin{aligned} \frac{\mathrm{d}\vec{r}}{\mathrm{d}t} &= \dot{\vec{r}} \\ \frac{\mathrm{d}\dot{\vec{r}}}{\mathrm{d}t} &= \frac{1}{m}\vec{f} \end{aligned}. \tag{11.2}$$

Denoting the state vector of the satellite as

$$\vec{X} = \begin{pmatrix} \vec{r} \\ \dot{\vec{r}} \end{pmatrix}, \tag{11.3}$$

then Eq. 11.2 can be written as

$$\dot{\vec{X}} = \vec{F}\,, \tag{11.4}$$

(c) ketabton.com: The Digital Library

where

$$\vec{F}=\begin{pmatrix}\dot{\vec{r}}\\ \vec{f}/m\end{pmatrix}. \tag{11.5}$$

Equation 11.4 is called the state equation of the satellite motion. Integrating Eq. 11.4 from t_0 to t, one has

$$\vec{X}(t)=\vec{X}(t_0)+\int_{t_0}^{t}\vec{F}\mathrm{d}t\ , \tag{11.6}$$

where $\vec{X}(t)$ is the instantaneous state vector of the satellite, $\vec{X}(t_0)$ is the initial state vector at time t_0, and $\vec{F}$ is a function of the state vector $\vec{X}(t)$ and time t. Denoting the initial state vector as $\vec{X}_0$, then the perturbed satellite orbit problem turns out to be a problem of solving the differential state equation under the initial condition as

$$\begin{cases}\dot{\vec{X}}(t)=\vec{F}\\ \vec{X}(t_0)=\vec{X}_0\end{cases}. \tag{11.7}$$

11.1.1 Lagrangian Perturbed Equation of Satellite Motion

If the force $\vec{f}$ includes only the conservative forces, then there is a potential function V so that

$$\frac{\vec{f}}{m}=\mathrm{grad}V=\left(\frac{\partial V}{\partial x}\ \frac{\partial V}{\partial y}\ \frac{\partial V}{\partial z}\right)=\left(\frac{\partial V}{\partial r}\ \frac{\partial V}{\partial \varphi}\ \frac{\partial V}{\partial \lambda}\right), \tag{11.8}$$

where (x, y, z) and (r, φ, λ) are Cartesian coordinates and spherical coordinates, respectively. Denotin R as the disturbance potential, V_0 as the potential of the centred force $\vec{f}_0$, then

$$R=V-V_0\ ,\qquad \frac{\vec{f}-\vec{f}_0}{m}=\mathrm{grad}R\ . \tag{11.9}$$

The perturbed Eq. 11.2 of satellite motion in Cartesian coordinates is then

$$\begin{aligned}
&\frac{\mathrm{d}x}{\mathrm{d}t}=\dot{x}\\
&\frac{\mathrm{d}y}{\mathrm{d}t}=\dot{y}\\
&\frac{\mathrm{d}z}{\mathrm{d}t}=\dot{z}\\
&\frac{\mathrm{d}\dot{x}}{\mathrm{d}t}=-\frac{\mu}{r^3}x+\frac{\partial R}{\partial x}\\
&\frac{\mathrm{d}\dot{y}}{\mathrm{d}t}=-\frac{\mu}{r^3}y+\frac{\partial R}{\partial y}\\
&\frac{\mathrm{d}\dot{z}}{\mathrm{d}t}=-\frac{\mu}{r^3}z+\frac{\partial R}{\partial z}
\end{aligned}\ , \tag{11.10}$$

where μ is the gravitational constant of the Earth. The state vector $(\vec{r}, \dot{\vec{r}})$ of the satellite corresponds to an instantaneous Keplerian ellipse $(a, e, \omega, i, \Omega, M)$. Using the relationships be-

(c) ketabton.com: The Digital Library

tween the two sets of parameters (cf. Chap. 3), the perturbed equation of motion 11.10 can be transformed into a so-called Lagrangian perturbed equation system (cf., e.g., Kaula 1966)

$$\begin{aligned}
\frac{\mathrm{d}a}{\mathrm{d}t} &= \frac{2}{na}\frac{\partial R}{\partial M} \\
\frac{\mathrm{d}e}{\mathrm{d}t} &= \frac{1-e^2}{na^2e}\frac{\partial R}{\partial M} - \frac{\sqrt{1-e^2}}{na^2e}\frac{\partial R}{\partial \omega} \\
\frac{\mathrm{d}\omega}{\mathrm{d}t} &= \frac{\sqrt{1-e^2}}{na^2e}\frac{\partial R}{\partial e} - \frac{\cos i}{na^2\sqrt{1-e^2}\sin i}\frac{\partial R}{\partial i} \\
\frac{\mathrm{d}i}{\mathrm{d}t} &= \frac{1}{na^2\sqrt{1-e^2}\sin i}\left(\cos i\frac{\partial R}{\partial \omega} - \frac{\partial R}{\partial \Omega}\right) \\
\frac{\mathrm{d}\Omega}{\mathrm{d}t} &= \frac{1}{na^2\sqrt{1-e^2}\sin i}\frac{\partial R}{\partial i} \\
\frac{\mathrm{d}M}{\mathrm{d}t} &= n - \frac{2}{na}\frac{\partial R}{\partial a} - \frac{1-e^2}{na^2e}\frac{\partial R}{\partial e}
\end{aligned} \quad . \tag{11.11}$$

Based on the above equation system, Kaula derived the first order perturbed analysis solution (cf. Kaula 1966). In the case of a small e ($e \ll 1$), the orbit is nearly circular, so that the perigee and the related Keplerian elements f and ω are not defined (this is not to be confused with the force vector $\vec{f}$ and true anomaly f). To overcome this problem, let $u = f + \omega$, and a parameter set of (a, i, Ω, ξ, η, λ) is used to describe the motion of the satellite, where

$$\begin{aligned}
\xi &= e\cos\omega \\
\eta &= -e\sin\omega \\
\lambda &= M + \omega
\end{aligned} \quad . \tag{11.12}$$

Thus, one has

$$\begin{aligned}
\frac{\mathrm{d}\xi}{\mathrm{d}t} &= \frac{\xi}{e}\frac{\mathrm{d}e}{\mathrm{d}t} + \eta\frac{\mathrm{d}\omega}{\mathrm{d}t} \\
\frac{\mathrm{d}\eta}{\mathrm{d}t} &= \frac{\eta}{e}\frac{\mathrm{d}e}{\mathrm{d}t} - \xi\frac{\mathrm{d}\omega}{\mathrm{d}t} \\
\frac{\mathrm{d}\lambda}{\mathrm{d}t} &= \frac{\mathrm{d}M}{\mathrm{d}t} + \frac{\mathrm{d}\omega}{\mathrm{d}t}
\end{aligned} \tag{11.13}$$

and

$$\begin{aligned}
\frac{\partial R}{\partial \omega} &= \frac{\partial R}{\partial(\xi,\eta,\lambda)}\frac{\partial(\xi,\eta,\lambda)}{\partial \omega} = \frac{\partial R}{\partial(\xi,\eta,\lambda)}(\eta,-\xi,1)^T = \eta\frac{\partial R}{\partial \xi} - \xi\frac{\partial R}{\partial \eta} + \frac{\partial R}{\partial \lambda} \\
\frac{\partial R}{\partial e} &= \frac{\partial R}{\partial(\xi,\eta,\lambda)}\frac{\partial(\xi,\eta,\lambda)}{\partial e} = \frac{\partial R}{\partial(\xi,\eta,\lambda)}\left(\frac{\xi}{e},\frac{\eta}{e},0\right)^T = \frac{\xi}{e}\frac{\partial R}{\partial \xi} + \frac{\eta}{e}\frac{\partial R}{\partial \eta} \\
\frac{\partial R}{\partial M} &= \frac{\partial R}{\partial(\xi,\eta,\lambda)}\frac{\partial(\xi,\eta,\lambda)}{\partial M} = \frac{\partial R}{\partial(\xi,\eta,\lambda)}(0,0,1)^T = \frac{\partial R}{\partial \lambda}
\end{aligned} \quad . \tag{11.14}$$

(c) ketabton.com: The Digital Library

Substituting Eq. 11.14 into Eq. 11.11 and then substituting the 2nd, 3rd and 6th equations into Eq. 11.13, one has

$$\begin{aligned}
\frac{\mathrm{d}a}{\mathrm{d}t} &= \frac{2}{na}\frac{\partial R}{\partial \lambda} \\
\frac{\mathrm{d}i}{\mathrm{d}t} &= \frac{1}{na^2\sqrt{1-e^2}\sin i}\left[\cos i\left(\eta\frac{\partial R}{\partial \xi}-\xi\frac{\partial R}{\partial \eta}+\frac{\partial R}{\partial \lambda}\right)-\frac{\partial R}{\partial \Omega}\right] \\
\frac{\mathrm{d}\Omega}{\mathrm{d}t} &= \frac{1}{na^2\sqrt{1-e^2}\sin i}\frac{\partial R}{\partial i} \\
\frac{\mathrm{d}\xi}{\mathrm{d}t} &= \frac{\sqrt{1-e^2}}{na^2}\frac{\partial R}{\partial \eta}-\eta\frac{\cos i}{na^2\sqrt{1-e^2}\sin i}\frac{\partial R}{\partial i}+\xi\frac{1-e^2-\sqrt{1-e^2}}{na^2e^2}\frac{\partial R}{\partial \lambda} \\
\frac{\mathrm{d}\eta}{\mathrm{d}t} &= -\frac{\sqrt{1-e^2}}{na^2}\frac{\partial R}{\partial \xi}+\xi\frac{\cos i}{na^2\sqrt{1-e^2}\sin i}\frac{\partial R}{\partial i}+\eta\frac{1-e^2-\sqrt{1-e^2}}{na^2e^2}\frac{\partial R}{\partial \lambda} \\
\frac{\mathrm{d}\lambda}{\mathrm{d}t} &= n-\frac{2}{na}\frac{\partial R}{\partial a}-\frac{\cos i}{na^2\sqrt{1-e^2}\sin i}\frac{\partial R}{\partial i}-\frac{1-e^2-\sqrt{1-e^2}}{na^2e^2}\left(\xi\frac{\partial R}{\partial \xi}+\eta\frac{\partial R}{\partial \eta}\right)
\end{aligned} \quad . \tag{11.15}$$

The new variables of Eq. 11.12 do not have clear geometric meanings. An alternative is to use the Hill variables (cf., e.g., Cui 1990).

11.1.2 Gaussian Perturbed Equation of Satellite Motion

Considering the non-conservative disturbance forces such as solar radiation and air drag, no potential functions exist for use; therefore, the Lagrangian perturbed equation of motion cannot be directly used in such a case. The equation of motion perturbed by non-conservative disturbance force has to be derived.

Considering any force vector $\vec{f} = (f_x \;\; f_y \;\; f_z)^T$ in ECSF coordinate system, one has

$$\begin{pmatrix} f_x \\ f_y \\ f_z \end{pmatrix} = R_3(-\Omega)R_1(-i)R_3(-u)\begin{pmatrix} f_r \\ f_\alpha \\ f_h \end{pmatrix}, \tag{11.16}$$

where $(f_r \;\; f_\alpha \;\; f_h)^T$ is a force vector with three orthogonal components in an orbital plane coordinate system, the first two components are in the orbital plane, f_r is the radial force component, f_α is the force component perpendicular to f_r and pointed in the direction of satellite motion, and f_h completes a right-handed system. For convenience, the force vector may also be represented by tangential, central components in the orbital plane (f_t, f_c) as well as f_h (cf. Fig. 11.1). It is obvious that

$$\begin{pmatrix} f_r \\ f_\alpha \\ f_h \end{pmatrix} = R_3(-\beta)\begin{pmatrix} f_t \\ f_c \\ f_h \end{pmatrix}, \tag{11.17}$$

where

(c) ketabton.com: The Digital Library

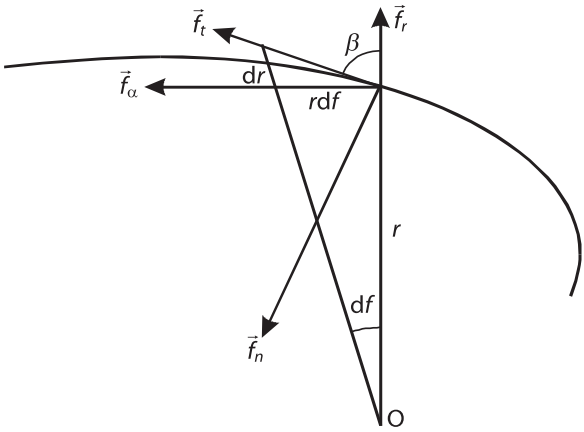

Fig. 11.1.
Relation of radial and tangential forces

$$\tan\beta = r\frac{\mathrm{d}f}{\mathrm{d}r} = \frac{a(1-e^2)}{1+e\cos f}\frac{\mathrm{d}f}{\frac{a(1-e^2)}{(1+e\cos f)^2}e\sin f\mathrm{d}f} = \frac{1+e\cos f}{e\sin f} \quad \text{or} \tag{11.18}$$

$$\begin{aligned}\sin\beta &= \frac{1+e\cos f}{\sqrt{1+2e\cos f+e^2}}\\ \cos\beta &= \frac{e\sin f}{\sqrt{1+2e\cos f+e^2}}\end{aligned}\quad . \tag{11.19}$$

In order to replace the partial derivatives $\partial R/\partial\sigma$ by force components, the relationships between them have to be derived, where σ is a symbol for all Keplerian elements. Using the regulation of partial derivatives, one has

$$\begin{aligned}\frac{\partial R}{\partial\sigma} &= \frac{\partial R}{\partial\vec{r}}\cdot\frac{\partial\vec{r}}{\partial\sigma} = \vec{f}\cdot\left(\frac{\partial r}{\partial\sigma}\vec{e}_r + r\frac{\partial\vec{e}_r}{\partial\sigma}\right)\\ &= R_3(-\Omega)R_1(-i)R_3(-u)\begin{pmatrix}f_r\\ f_\alpha\\ f_h\end{pmatrix}\cdot\left(\frac{\partial r}{\partial\sigma}\vec{e}_r + r\frac{\partial\vec{e}_r}{\partial\sigma}\right),\end{aligned} \tag{11.20}$$

where $\vec{e}_r$ is the radial identity vector of the satellite, the dot is the vector dot product, and

$$\begin{aligned}\vec{e}_r &= \begin{pmatrix}\varepsilon_1\\ \varepsilon_2\\ \varepsilon_3\end{pmatrix} = R_3(-\Omega)R_1(-i)R_3(-u)\begin{pmatrix}1\\ 0\\ 0\end{pmatrix} = \begin{pmatrix}\cos\Omega\cos u-\sin\Omega\cos i\sin u\\ \sin\Omega\cos u+\cos\Omega\cos i\sin u\\ \sin i\sin u\end{pmatrix}\\ \frac{\partial\vec{e}_r}{\partial\sigma} &= \begin{pmatrix}\sin\Omega\sin i\sin u\dfrac{\partial i}{\partial\sigma}-\varepsilon_2\dfrac{\partial\Omega}{\partial\sigma}-(\cos\Omega\sin u+\sin\Omega\cos i\cos u)\dfrac{\partial u}{\partial\sigma}\\ -\cos\Omega\sin i\sin u\dfrac{\partial i}{\partial\sigma}+\varepsilon_1\dfrac{\partial\Omega}{\partial\sigma}-(\sin\Omega\sin u-\cos\Omega\cos i\cos u)\dfrac{\partial u}{\partial\sigma}\\ \cos i\sin u\dfrac{\partial i}{\partial\sigma}+\sin i\cos u\dfrac{\partial u}{\partial\sigma}\end{pmatrix}.\end{aligned} \tag{11.21}$$

(c) ketabton.com: The Digital Library

Substituting Eq. 11.21 into Eq. 11.20 and simplifying it, one has

$$\frac{\partial R}{\partial \sigma}=\frac{\partial r}{\partial \sigma}f_r+r\left(\cos i\frac{\partial \Omega}{\partial \sigma}+\frac{\partial u}{\partial \sigma}\right)f_\alpha+r\left(\sin u\frac{\partial i}{\partial \sigma}-\sin i\cos u\frac{\partial \Omega}{\partial \sigma}\right)f_h\,. \tag{11.22}$$

For deriving the partial derivatives of r and u $(=f+\omega)$ with respect to the six Keplerian elements, the following basic relations (cf. Chap. 3) are used

$$\begin{aligned}
&r=\frac{a(1-e^2)}{1+e\cos f}=a(1-e\cos E)\\
&r\cos f=a(\cos E-e)\\
&r\sin f=a\sqrt{1-e^2}\sin E\\
&\tan\frac{f}{2}=\sqrt{\frac{1+e}{1-e}}\tan\frac{E}{2}\\
&E-e\sin E=M
\end{aligned}\quad , \tag{11.23}$$

where E is a function of (e, M), f is a function of (e, E), i.e., (e, M), r is a function of (a, e, M), and u is a function of (ω, f), i.e., (ω, e, M). Thus,

$$\begin{aligned}
&\frac{\partial E}{\partial(e,M)}=\left(\frac{a}{r}\sin E,\frac{a}{r}\right)\\
&\frac{\partial f}{\partial(e,M)}=\left(\frac{2+e\cos f}{1-e^2}\sin f,\left(\frac{a}{r}\right)^2\sqrt{1-e^2}\right)\\
&\frac{\partial r}{\partial M}=ae\sin E\frac{\partial E}{\partial M}=\frac{a^2e}{r}\sin E=\frac{ae}{\sqrt{1-e^2}}\sin f\\
&\frac{\partial r}{\partial(a,e,i,\Omega,\omega)}=\left(\frac{r}{a},-a\cos f,\ 0,0,0\right)\\
&\frac{\partial u}{\partial e}=\frac{\partial u}{\partial f}\frac{\partial f}{\partial e}=\frac{2+e\cos f}{1-e^2}\sin f\\
&\frac{\partial u}{\partial M}=\frac{\partial u}{\partial f}\frac{\partial f}{\partial M}=\left(\frac{a}{r}\right)^2\sqrt{1-e^2}\\
&\frac{\partial u}{\partial(a,i,\Omega,\omega)}=(0,\ 0,\ 0,\ 1)
\end{aligned}\quad . \tag{11.24}$$

Substituting Eq. 11.24 into Eq. 11.22, one has

$$\begin{aligned}
&\frac{\partial R}{\partial a}=\frac{r}{a}f_r\\
&\frac{\partial R}{\partial e}=-a\cos f\cdot f_r+\frac{r\sin f}{1-e^2}(2+e\cos f)\cdot f_\alpha\\
&\frac{\partial R}{\partial i}=r\sin u\cdot f_h
\end{aligned}$$

(c) ketabton.com: The Digital Library

$$\begin{aligned}
\frac{\partial R}{\partial \Omega} &= i\cos i \cdot f_\alpha - r\sin i\cos u \cdot f_h \\
\frac{\partial R}{\partial \omega} &= r \cdot f_\alpha \\
\frac{\partial R}{\partial M} &= \frac{ae}{\sqrt{1-e^2}}\sin f \cdot f_r + \frac{a(1+e\cos f)}{\sqrt{1-e^2}} \cdot f_\alpha
\end{aligned} \quad . \tag{11.25}$$

Putting Eq. 11.25 into Lagrangian perturbed equations of motion 11.11, the so-called Gaussian perturbed equations of motion are then

$$\begin{aligned}
\frac{\mathrm{d}a}{\mathrm{d}t} &= \frac{2}{n\sqrt{1-e^2}}\left[e\cos f \cdot f_r + (1+e\cos f)\cdot f_\alpha\right] \\
\frac{\mathrm{d}e}{\mathrm{d}t} &= \frac{\sqrt{1-e^2}}{na}\left[\sin f \cdot f_r + (\cos E + \cos f)\cdot f_\alpha\right] \\
\frac{\mathrm{d}i}{\mathrm{d}t} &= \frac{(1-e\cos E)\cos u}{na\sqrt{1-e^2}} \cdot f_h \\
\frac{\mathrm{d}\Omega}{\mathrm{d}t} &= \frac{(1-e\cos E)\sin u}{na\sqrt{1-e^2}\sin i} \cdot f_h \\
\frac{\mathrm{d}\omega}{\mathrm{d}t} &= \frac{\sqrt{1-e^2}}{nae}\left[-\cos f \cdot f_r + \frac{2+e\cos f}{1+e\cos f}\sin f \cdot f_\alpha\right] - \cos i\frac{\mathrm{d}\Omega}{\mathrm{d}t} \\
\frac{\mathrm{d}M}{\mathrm{d}t} &= n - \frac{1-e^2}{nae}\left[-\left(\cos f - \frac{2e}{1+e\cos f}\right)\cdot f_\alpha + \frac{2+e\cos f}{1+e\cos f}\sin f \cdot f_\alpha\right]
\end{aligned} \quad . \tag{11.26}$$

The force components of (f_r, f_α, f_h) are used. Using Eq. 11.17, the Gaussian perturbed equations of motion can be represented by a disturbed force vector of (f_t, f_c, f_h).

11.2 Perturbation Forces of Satellite Motion

Perturbation forces of satellite motion will be discussed in this section. They are the gravitational forces of the Earth, the attracting forces of the Sun, the Moon and the planets, the drag force of the atmosphere, solar radiation pressure, Earth and ocean tides, as well as coordinate perturbations.

11.2.1 Perturbation of the Earth's Gravitational Field

After a brief review of the Earth's gravitational field, the perturbation force of the Earth will be outlined here.

(c) ketabton.com: The Digital Library

11.2.1.1 *The Earth's Gravitational Field*

The complete real solution of the Laplace equation is called potential function V of the Earth. In spherical coordinates, V can be expressed by (Moritz 1980; Sigl 1989):

$$V = \sum_{lmi} \frac{1}{r^{l+1}} V_{lmi} = \sum_{l=0}^{\infty} \sum_{m=0}^{l} \frac{1}{r^{l+1}} P_{lm}(\sin\varphi)[C_{lm}\cos m\lambda + S_{lm}\sin m\lambda] , \tag{11.27}$$

where r is the radius, φ is the latitude, and λ is the longitude measured eastward (counter-clockwise looking toward the origin from the positive end of the z-axis). One can, of course, use the co-latitude ϑ (or polar distance) instead of the latitude φ ($\sin\varphi = \cos\vartheta$). The subscript i in the first term denotes the $\cos m\lambda$ or $\sin m\lambda$ term. $P_{lm}(\sin\varphi)$ is the so-called associated Legendre function, V_{lmi} denotes surface spherical harmonics, C_{lm}, S_{lm} are coefficients of the spherical functions, and

$$P_{lm}(\sin\varphi) = \cos^m\varphi \sum_{t=0}^{k} T_{lmt} \sin^{l-m-2t}\varphi , \tag{11.28}$$

where k is the integer part of $(l - m)/2$, and

$$T_{lmt} = \frac{(-1)^t (2l-2t)!}{2^l t!(l-t)!(l-m-2t)!} . \tag{11.29}$$

An important property of surface spherical harmonics V_{lmi} is that they are orthogonal ones. Namely for the integration over the surface of a sphere there is (Heiskanen and Moritz 1967; Kaula 1966):

$$\int_{\text{sphere}} V_{LMI} V_{lmi} \mathrm{d}\sigma = 0 , \quad \text{if} \quad L \neq l \quad \text{or} \quad M \neq m \quad \text{or} \quad I \neq i . \tag{11.30}$$

The integral of the square of V_{lmi} for $C_{lm} = 1$ or $S_{lm} = 1$ is

$$\int_{\text{sphere}} V^2{}_{lmi} \mathrm{d}\sigma = \left[\frac{(l+m)!}{(l-m)!(2l+1)(2-\delta_{0m})}\right] 4\pi , \tag{11.31}$$

where the Kronecker delta δ_{0m} is equal to 1 for $m = 0$ and 0 for $m \neq 0$.

The normalised Legendre functions can be defined and denoted by

$$\overline{P}_{lm}(x) = P_{lm}(x)\left[\frac{(l-m)!(2l+1)(2-\delta_{0m})}{(l+m)!}\right]^{1/2} , \tag{11.32}$$

where $x = \sin\varphi = \cos\vartheta$. Recurrence formulae can be easily derived (Wenzel 1985):

$$\overline{P}_{(l+1)(l+1)}(x) = \overline{P}_{ll}(x)\left[\frac{(2l+3)}{(l+1)(2-\delta_{0l})}\right]^{1/2} (1-x^2)^{1/2} ,$$

$$\overline{P}_{(l+1)l}(x) = \overline{P}_{ll}(x)\left[2l+3\right]^{1/2} x \quad l \geq 1 ,$$

(c) ketabton.com: The Digital Library

$$\bar{P}_{(l+1)m}(x)=\bar{P}_{lm}(x)\left[\frac{(2l+1)(2l+3)}{(l+m+1)(l-m+1)}\right]^{1/2}x - \bar{P}_{(l-1)m}(x)\left[\frac{(l+m)(l-m)(2l+3)}{(l+m+1)(l-m+1)(2l-1)}\right]^{1/2}, \quad \text{and}$$

$$\bar{P}_{00}(x)=1, \quad \bar{P}_{10}(x)=\sqrt{3}\,x, \quad \bar{P}_{11}(x)=\sqrt{3(1-x^2)}\,. \tag{11.33}$$

Since the first term of V (i.e., $l=0$) is represented by GM/r, the fully normalised geopotential function is taken as follows (Torge 1989; Rapp 1986):

$$V(r,\varphi,\lambda)=\frac{GM}{r}\left[1+\sum_{l=2}^{\infty}\sum_{m=0}^{l}\left(\frac{a}{r}\right)^{l}\bar{P}_{lm}(\sin\varphi)[\bar{C}_{lm}\cos m\lambda+\bar{S}_{lm}\sin m\lambda]\right], \tag{11.34}$$

where GM is the geocentric gravitational constant, $\bar{C}_{lm}, \bar{S}_{lm}$ are normalised coefficients and a is the mean equatorial radius of the Earth. The first term of V is the potential of the central force of the Earth. The perturbation potential of the Earth is then (denoting $GM=\mu$)

$$R_{\text{geo}}(r,\varphi,\lambda)=\frac{\mu}{r}\sum_{l=2}^{\infty}\sum_{m=0}^{l}\left(\frac{a}{r}\right)^{l}\bar{P}_{lm}(\sin\varphi)\left[\bar{C}_{lm}\cos m\lambda+\bar{S}_{lm}\sin m\lambda\right]. \tag{11.35}$$

For any initial external potential of the Earth

$$U(r,\varphi,\lambda)=\frac{\mu}{r}\left[1+\sum_{l=2}^{L}\sum_{m=0}^{l}\left(\frac{a}{r}\right)^{l}\bar{P}_{lm}(\sin\varphi)\left[\bar{C}^{N}_{lm}\cos m\lambda+\bar{S}^{N}_{lm}\sin m\lambda\right]\right], \tag{11.36}$$

the disturbing potential T is then

$$T=V-U=\frac{\mu}{r}\left[\sum_{l=2}^{\infty}\sum_{m=0}^{l}\left(\frac{a}{r}\right)^{l}\bar{P}_{lm}(\sin\varphi)[\Delta\bar{C}_{lm}\cos m\lambda+\Delta\bar{S}_{lm}\sin m\lambda]\right], \tag{11.37}$$

where $\bar{C}^{N}_{lm}, \bar{S}^{N}_{lm}$ are known normalised coefficients of the disturbing potential and

$$\bar{C}_{lm}=\Delta\bar{C}_{lm}-\bar{C}^{N}_{lm}, \quad \bar{S}_{lm}=\Delta\bar{S}_{lm}-\bar{S}^{N}_{lm}, \quad (l\le L)\,. \tag{11.38}$$

11.2.1.2 *Perturbation Force of the Earth's Gravitational Field*

Denoting (x', y', z') as three orthogonal Cartesian coordinates in ECEF system, then the force vector is

$$\vec{f}_{\text{ECEF}}=\begin{pmatrix}\frac{\partial V}{\partial x'}\\ \frac{\partial V}{\partial y'}\\ \frac{\partial V}{\partial z'}\end{pmatrix}=\begin{pmatrix}\frac{\partial V}{\partial(r,\varphi,\lambda)}\frac{\partial(r,\varphi,\lambda)}{\partial x'}\\ \frac{\partial V}{\partial(r,\varphi,\lambda)}\frac{\partial(r,\varphi,\lambda)}{\partial y'}\\ \frac{\partial V}{\partial(r,\varphi,\lambda)}\frac{\partial(r,\varphi,\lambda)}{\partial z'}\end{pmatrix}=\left(\frac{\partial V}{\partial(r,\varphi,\lambda)}\frac{\partial(r,\varphi,\lambda)}{\partial(x',y',z')}\right)^{T}. \tag{11.39}$$

(c) ketabton.com: The Digital Library

From the relation between the Cartesian and spherical coordinates

$$\begin{pmatrix} x' \\ y' \\ z' \end{pmatrix} = \begin{pmatrix} r\cos\varphi\cos\lambda \\ r\cos\varphi\sin\lambda \\ r\sin\varphi \end{pmatrix}, \quad \begin{pmatrix} r = \sqrt{x'^2 + y'^2 + z'^2} \\ \varphi = \tan^{-1}\dfrac{z'}{\sqrt{x'^2 + y'^2}} \\ \lambda = \tan^{-1}\dfrac{y'}{x'} \end{pmatrix}, \quad \text{one has} \tag{11.40}$$

$$\frac{\partial(r,\varphi,\lambda)}{\partial(x',y',z')} = \begin{pmatrix} \cos\varphi\cos\lambda & \cos\varphi\sin\lambda & \sin\varphi \\ -\dfrac{1}{r}\sin\varphi\cos\lambda & -\dfrac{1}{r}\sin\varphi\sin\lambda & \dfrac{1}{r}\cos\varphi \\ -\dfrac{1}{r\cos\varphi}\sin\lambda & \dfrac{1}{r\cos\varphi}\cos\lambda & 0 \end{pmatrix}. \tag{11.41}$$

For differentiations of the associated Legendre function, from the Eq. 11.33, one has similar recurrence formulae:

$$\frac{\mathrm{d}\bar{P}_{00}(\sin\varphi)}{\mathrm{d}\varphi} = 0\,, \tag{11.42}$$

$$\frac{\mathrm{d}\bar{P}_{10}(\sin\varphi)}{\mathrm{d}\varphi} = \sqrt{3}\cos\varphi\,,$$

$$\frac{\mathrm{d}\bar{P}_{11}(\sin\varphi)}{\mathrm{d}\varphi} = -\sqrt{3}\sin\varphi\,,$$

$$\frac{\mathrm{d}\bar{P}_{(l+1)(l+1)}(\sin\varphi)}{\mathrm{d}\varphi} = -q\sin\varphi\bar{P}_{ll}(\sin\varphi) + q\cos\varphi\frac{\mathrm{d}\bar{P}_{ll}(\sin\varphi)}{\mathrm{d}\varphi}\,,$$

$$q = \sqrt{\frac{2l+3}{2l+2}}, \quad l \geq 1\,,$$

$$\frac{\mathrm{d}\bar{P}_{(l+1)l}(\sin\varphi)}{\mathrm{d}\varphi} = g\cos\varphi\bar{P}_{ll}(\sin\varphi) + g\sin\varphi\frac{\mathrm{d}\bar{P}_{ll}(\sin\varphi)}{\mathrm{d}\varphi}\,, \quad l \geq 1\,,$$

$$g = \sqrt{2l+3}\,,$$

$$\frac{\mathrm{d}\bar{P}_{(l+1)m}(\sin\varphi)}{\mathrm{d}\varphi} = h\cos\varphi\bar{P}_{lm}(\sin\varphi) + h\sin\varphi\frac{\mathrm{d}\bar{P}_{lm}(\sin\varphi)}{\mathrm{d}\varphi} - k\frac{\mathrm{d}\bar{P}_{(l-1)m}(\sin\varphi)}{\mathrm{d}\varphi}\,,$$

$$h = \sqrt{\frac{(2l+1)(2l+3)}{(l+m+1)(l-m+1)}}\,,$$

$$k = \sqrt{\frac{(l+m)(l-m)(2l+3)}{(l+m+1)(l-m+1)(2l-1)}} \quad \text{and}$$

(c) ketabton.com: The Digital Library

$$\frac{\mathrm{d}^2\overline{P}_{00}(\sin\varphi)}{\mathrm{d}\varphi^2}=0\,, \tag{11.43}$$

$$\frac{\mathrm{d}^2\overline{P}_{10}(\sin\varphi)}{\mathrm{d}\varphi^2}=-\sqrt{3}\sin\varphi\,,$$

$$\frac{\mathrm{d}^2\overline{P}_{11}(\sin\varphi)}{\mathrm{d}\varphi^2}=-\sqrt{3}\cos\varphi\,,$$

$$\frac{\mathrm{d}^2\overline{P}_{(l+1)(l+1)}(\sin\varphi)}{\mathrm{d}\varphi^2}=-q\cos\varphi\overline{P}_{ll}(\sin\varphi)-2q\sin\varphi\frac{\mathrm{d}\overline{P}_{ll}(\sin\varphi)}{\mathrm{d}\varphi}+q\cos\varphi\frac{\mathrm{d}^2\overline{P}_{ll}(\sin\varphi)}{\mathrm{d}\varphi^2}\,,$$

$$\frac{\mathrm{d}^2\overline{P}_{(l+1)l}(\sin\varphi)}{\mathrm{d}\varphi^2}=-g\sin\varphi\overline{P}_{ll}(\sin\varphi)+2g\cos\varphi\frac{\mathrm{d}\overline{P}_{ll}(\sin\varphi)}{\mathrm{d}\varphi}+g\sin\varphi\frac{\mathrm{d}^2\overline{P}_{ll}(\sin\varphi)}{\mathrm{d}\varphi^2}\,,$$

$l\geq 1$,

$$\frac{\mathrm{d}^2\overline{P}_{(l+1)m}(\sin\varphi)}{\mathrm{d}\varphi^2}=-h\sin\varphi\overline{P}_{lm}(\sin\varphi)+2h\cos\varphi\frac{\mathrm{d}\overline{P}_{lm}(\sin\varphi)}{\mathrm{d}\varphi}$$
$$+h\sin\varphi\frac{\mathrm{d}^2\overline{P}_{lm}(\sin\varphi)}{\mathrm{d}\varphi^2}-k\frac{\mathrm{d}^2\overline{P}_{(l-1)m}(\sin\varphi)}{\mathrm{d}\varphi^2}$$

The partial derivatives of the potential function with respect to the spherical coordinates are

$$\frac{\partial V}{\partial r}=-\frac{\mu}{r^2}\left[1+\sum_{l=2}^{\infty}\sum_{m=0}^{l}(l+1)\left(\frac{a}{r}\right)^l\overline{P}_{lm}(\sin\varphi)\left[\overline{C}_{lm}\cos m\lambda+\overline{S}_{lm}\sin m\lambda\right]\right]$$

$$\frac{\partial V}{\partial\varphi}=\frac{\mu}{r}\sum_{l=2}^{\infty}\sum_{m=0}^{l}\left(\frac{a}{r}\right)^l\frac{\mathrm{d}\overline{P}_{lm}(\sin\varphi)}{\mathrm{d}\varphi}\left[\overline{C}_{lm}\cos m\lambda+\overline{S}_{lm}\sin m\lambda\right]\,. \tag{11.44}$$

$$\frac{\partial V}{\partial\lambda}=\frac{\mu}{r}\sum_{l=2}^{\infty}\sum_{m=0}^{l}m\left(\frac{a}{r}\right)^l\overline{P}_{lm}(\sin\varphi)\left[-\overline{C}_{lm}\sin m\lambda+\overline{S}_{lm}\cos m\lambda\right]$$

Using the transformation formula of Eq. 2.14, the perturbation force of the Earth's gravitational field in the ECSF system is then

$$\vec{f}_{\mathrm{ECSF}}=R_{\mathrm{P}}^{-1}R_{\mathrm{N}}^{-1}R_{\mathrm{S}}^{-1}R_{\mathrm{M}}^{-1}\vec{f}_{\mathrm{ECEF}}\,. \tag{11.45}$$

The computation process of disturbance force of the Earth's gravitational field in the ECSF coordinate system may be carried out by

1. Using Eq. 2.14 to transform the satellite coordinates in the ECSF system to the ECEF system;
2. Using Eq. 11.40 to compute the spherical coordinates of the satellite in the ECEF system;
3. Using Eq. 11.39 to compute the force vector in the ECEF system;
4. Using Eq. 11.45 to transform the force vector to the ECSF system.

(c) ketabton.com: The Digital Library

11.2.2
Perturbation of the Sun and the Moon as well as Planets

The equations of motion of two point-masses M and m under their mutual action can be given by

$$M\ddot{\vec{r}}_M = GMm\frac{\vec{r}_{Mm}}{r_{Mm}^3} \quad \text{and} \quad m\ddot{\vec{r}}_m = GMm\frac{\vec{r}_{mM}}{r_{mM}^3}, \tag{11.46}$$

where r is the length of the vector $\vec{r}$, index Mm means the vector is pointing from point-mass M to m, and single index M or m means the vector is pointing to point-mass M or m. Introducing additional point-masses $m(j)$, $j = 1, 2, \ldots$, the attractions of $m(j)$ on M and m can be given as equations similar to Eq. 11.46, and the total attractions may be obtained by summations

$$\begin{aligned} M\ddot{\vec{r}}_M &= GMm\frac{\vec{r}_{Mm}}{r_{Mm}^3} + \sum_j GMm(j)\frac{\vec{r}_{Mm(j)}}{r_{Mm(j)}^3} \\ m\ddot{\vec{r}}_m &= GMm\frac{\vec{r}_{mM}}{r_{mM}^3} + \sum_j Gmm(j)\frac{\vec{r}_{mm(j)}}{r_{mm(j)}^3} \end{aligned}. \tag{11.47}$$

By dividing the above two equations with $-M$ and m, respectively, then adding them together, one has

$$\ddot{\vec{r}}_m - \ddot{\vec{r}}_M = -G(M+m)\frac{\vec{r}_{Mm}}{r_{mM}^3} + \sum_j Gm(j)\left[\frac{\vec{r}_{mm(j)}}{r_{mm(j)}^3} - \frac{\vec{r}_{Mm(j)}}{r_{Mm(j)}^3}\right]. \tag{11.48}$$

Letting $\vec{r} = \vec{r}_m - \vec{r}_M$, i.e., using the point-mass M as the origin, substituting $\vec{r}_{mm(j)} = -(\vec{r}_m - \vec{r}_{m(j)})$ in the right side of Eq. 11.48 and omitting the mass m (mass of satellite), one has

$$\ddot{\vec{r}} = -GM\frac{\vec{r}}{r^3} - \sum_j Gm(j)\left[\frac{\vec{r} - \vec{r}_{m(j)}}{\left|\vec{r} - \vec{r}_{m(j)}\right|^3} + \frac{\vec{r}_{m(j)}}{r_{m(j)}^3}\right]. \tag{11.49}$$

It is obvious that the first term on the right side is the central force of the Earth; therefore, the disturbance forces of multiple point-masses acting on the satellite are then

$$\vec{f}_m = -m\sum_j Gm(j)\left[\frac{\vec{r} - \vec{r}_{m(j)}}{\left|\vec{r} - \vec{r}_{m(j)}\right|^3} + \frac{\vec{r}_{m(j)}}{r_{m(j)}^3}\right], \tag{11.50}$$

where $Gm(j)$ are the gravitational constants of the Sun and the Moon as well as the planets.

(c) ketabton.com: The Digital Library

11.2.3
Earth Tide and Ocean Tide Perturbations

As discussed in Sect. 5.4, the tidal potential generated by the Moon and the Sun can be written as

$$W_P = \sum_{j=1}^{2} \mu_j \sum_{n=2}^{\infty} \frac{\rho^n}{r_j^{n+1}} P_n(\cos z_j)$$

or

$$W_P = \sum_{j=1}^{2} \mu_j \sum_{n=2}^{\infty} \frac{\rho^n}{r_j^{n+1}} \left[\begin{array}{l} P_n(\sin\varphi) P_n(\sin\delta_j) \\ +2\sum_{k=1}^{n} \frac{(n-k)!}{(n+k)!} P_{nk}(\sin\varphi) P_{nk}(\sin\delta_j) \cos k h_j \end{array} \right], \tag{11.51}$$

where j is the index of the Moon ($j = 1$) and the Sun ($j = 2$), μ_j is the gravitational constant of body j, ρ is the geocentric distance of the Earth's surface (set as a_e), r_j is the geocentric distance of the body j, $P_n(x)$ and $P_{nk}(x)$ are the Legendre function and associated Legendre function, z_j is the zenith distance of the body j, δ_j and h_j are the declination and local hour angle of body j, $h_j = H_j - \lambda$, and H_j is the hour angle of j. The tidal deformation of the Earth caused by the tidal potential can be considered a tidal deformation potential acting on the satellite by Dirichlet's theorem (Melchior 1978; Dow 1988):

$$\delta V = \sum_{j=1}^{2} \mu_j \sum_{n=2}^{\infty} k_n \left(\frac{\rho}{r} \right)^{n+1} \frac{\rho^n}{r_j^{n+1}} P_n(\cos z_j)$$

or

$$\delta V = \sum_{j=1}^{2} \mu_j \sum_{n=2}^{N} k_n \frac{a_e^{2n+1}}{r^{n+1} r_j^{n+1}} \left[\begin{array}{l} P_n(\sin\varphi) P_n(\sin\delta_j) \\ +2\sum_{k=1}^{n} \frac{(n-k)!}{(n+k)!} P_{nk}(\sin\varphi) P_{nk}(\sin\delta_j) \cos k h_j \end{array} \right], \tag{11.52}$$

where k_n is the Love number, (r, φ, λ) is the spherical coordinate of the satellite in the ECEF system, and N is the truncating number. The recurrence formulas of the Legendre function are (cf., e.g., Xu 1992)

$$\begin{array}{l} (n+1) P_{n+1}(x) = (2n+1) x P_n(x) - n P_{n-1}(x) \\ (1-x^2) \frac{\mathrm{d}P_n(x)}{\mathrm{d}x} = n P_{n-1}(x) - n x P_n(x) \\ P_0(x) = 1 \quad P_1(x) = x \end{array} . \tag{11.53}$$

The disturbing force vector of the tidal potential in the ECEF coordinate system is then

(c) ketabton.com: The Digital Library

$$\vec{f}_{\mathrm{ECEF}} = \begin{pmatrix} \dfrac{\partial \delta V}{\partial x'} \\ \dfrac{\partial \delta V}{\partial y'} \\ \dfrac{\partial \delta V}{\partial z'} \end{pmatrix} = \begin{pmatrix} \dfrac{\partial \delta V}{\partial (r,\varphi,\lambda)} \dfrac{\partial (r,\varphi,\lambda)}{\partial x'} \\ \dfrac{\partial \delta V}{\partial (r,\varphi,\lambda)} \dfrac{\partial (r,\varphi,\lambda)}{\partial y'} \\ \dfrac{\partial \delta V}{\partial (r,\varphi,\lambda)} \dfrac{\partial (r,\varphi,\lambda)}{\partial z'} \end{pmatrix} = \left(\dfrac{\partial \delta V}{\partial (r,\varphi,\lambda)} \dfrac{\partial (r,\varphi,\lambda)}{\partial (x',y',z')} \right)^T , \tag{11.54}$$

where

$$\frac{\partial \delta V}{\partial r} = \sum_{j=1}^{2} \mu_j \sum_{n=2}^{N} -k_n \frac{(n+1) a_e^{2n+1}}{r^{n+2} r_j^{n+1}} \left[\begin{array}{l} P_n(\sin\varphi) P_n(\sin\delta_j) \\ +2 \sum_{k=1}^{n} \dfrac{(n-k)!}{(n+k)!} P_{nk}(\sin\varphi) P_{nk}(\sin\delta_j) \cos kh_j \end{array} \right] ,$$

$$\frac{\partial \delta V}{\partial \varphi} = \sum_{j=1}^{2} \mu_j \sum_{n=2}^{N} k_n \frac{a_e^{2n+1}}{r^{n+1} r_j^{n+1}} \left[\begin{array}{l} \dfrac{n}{\cos\varphi} (P_{n-1}(\sin\varphi) - \sin\varphi P_n(\sin\varphi)) P_n(\sin\delta_j) \\ +2 \sum_{k=1}^{n} \dfrac{(n-k)!}{(n+k)!} (P_{n(k+1)}(\sin\varphi) - k \tan\varphi P_{nk}(\sin\varphi)) \\ \qquad \cdot P_{nk}(\sin\delta_j) \cos kh_j \end{array} \right]$$

and

$$\frac{\partial \delta V}{\partial \lambda} = \sum_{j=1}^{2} \mu_j \sum_{n=2}^{N} k_n \frac{a_e^{2n+1}}{r^{n+1} r_j^{n+1}} \left[2 \sum_{k=1}^{n} \frac{(n-k)!}{(n+k)!} k P_{nk}(\sin\varphi) P_{nk}(\sin\delta_j) \sin kh_j \right] . \tag{11.55}$$

Other partial derivatives in Eq. 11.54 have been given in Sect. 11.2.1. The transformation of the force vector from the ECEF to the ECSF coordinate system can be done by Eq. 11.45.

As discussed in Sect. 5.4, the ocean tidal potential generated by tide element $\sigma H \mathrm{d}s$ can be written as

$$\frac{G \sigma H \mathrm{d}s}{r'} \quad \text{or} \quad G \sigma H \mathrm{d}s \sum_{n=0}^{\infty} \frac{a_e^n}{r^{n+1}} P_n(\cos z) , \tag{11.56}$$

where H is the ocean tide height of the area ds, G is the gravitational constant, σ is the water density, r' is the distance between the satellite and the water element ds, r is the geocentric distance of the satellite, z is the zenith distance of the ds, and a_e is the radius of the Earth. Using the spherical triangle

$$\cos z = \sin\varphi \sin\varphi_s + \cos\varphi \cos\varphi_s \cos(\lambda_s - \lambda) ,$$

where (φ_s, λ_s) is the spherical coordinate of ds and (r, φ, λ) is the spherical coordinate of satellite in the ECEF system, Eq. 11.56 turns out to be (denoted by Q)

(c) ketabton.com: The Digital Library

$$Q = G\sigma H \mathrm{d}s \sum_{n=0}^{\infty} \frac{a_e^n}{r^{n+1}} \left[\begin{array}{l} P_n(\sin\varphi) P_n(\sin\varphi_s) + (2-\delta_{0n}) \\ \cdot \sum_{k=0}^{n} \frac{(n-k)!}{(n+k)!} P_{nk}(\sin\varphi) P_{nk}(\sin\varphi_s) \cos k(\lambda_s - \lambda) \end{array} \right] . \tag{11.57}$$

The direct ocean tide potential is then the integration of $Q/\mathrm{d}s$ over the ocean (denotes by O), including the potential of the deformation of the ocean loading. The ocean tide potential is then

$$\delta V_1 = \iint_O G\sigma H \sum_{n=0}^{\infty} (1+k_n') \frac{a_e^n}{r^{n+1}} \left[\begin{array}{l} P_n(\sin\varphi) P_n(\sin\varphi_s) + (2-\delta_{0n}) \\ \cdot \sum_{k=0}^{n} \frac{(n-k)!}{(n+k)!} P_{nk}(\sin\varphi) P_{nk}(\sin\varphi_s) \cos k(\lambda_s - \lambda) \end{array} \right] \mathrm{d}s , \tag{11.58}$$

where k_n' is the ocean loading Love number. Equation 11.58 does not include the potential changing due to the loading deformation over the continents, which may give a non negligible contribution to the orbit motion of the satellite (cf. Knudsen et al. 2000). Recalling the discussion in Sect. 5.4, the loading deformation generated by the ocean tide can be represented as

$$u_r(\varphi,\lambda) = \iint_{\text{ocean}} \sigma H u(z) \mathrm{d}s \quad \text{and}$$

$$u(z) = \frac{a_e h_\infty'}{2M \sin(z/2)} + \frac{a_e}{M} \sum_{n=0}^{N} (h_n' - h_\infty') P_n(\cos z) , \tag{11.59}$$

where a_e is the radius of the Earth, M is the mass of the Earth, z is the geocentric zenith distance of the loading point (related to the computing point, see Fig. 5.11), $P_n(\cos z)$ is the Legendre function, $u(z)$ is the radial loading displacement Green function, h_n' is the loading Love number of order n, and u_r is the radial loading deformation. Substituting u_r for H in Eq. 11.57 and integrating $Q/\mathrm{d}s$ over the continents (denoted by C), the potential of the loading deformation is then

$$\delta V_2 = \iint_C G\sigma_e u_r \sum_{n=0}^{\infty} \frac{a_e^n}{r^{n+1}} \left[\begin{array}{l} P_n(\sin\varphi) P_n(\sin\varphi_s) + (2-\delta_{0n}) \\ \cdot \sum_{k=0}^{n} \frac{(n-k)!}{(n+k)!} P_{nk}(\sin\varphi) P_{nk}(\sin\varphi_s) \cos k(\lambda_s - \lambda) \end{array} \right] \mathrm{d}s , \tag{11.60}$$

where σ_e is the density of the mass $u_r \mathrm{d}s$ on the Earth's surface. The total ocean tide potential disturbance is the summation of Eqs. 11.58 and 11.60. Similar to above, the disturbing force can be derived and transformed to the ECSF system. There are

$$\vec{f}_{\text{ECEF}} = \begin{pmatrix} \frac{\partial(\delta V_1 + \delta V_2)}{\partial x'} \\ \frac{\partial(\delta V_1 + \delta V_2)}{\partial y'} \\ \frac{\partial(\delta V_1 + \delta V_2)}{\partial z'} \end{pmatrix} = \left(\frac{\partial(\delta V_1 + \delta V_2)}{\partial(r,\varphi,\lambda)} \frac{\partial(r,\varphi,\lambda)}{\partial(x',y',z')} \right)^T , \tag{11.61}$$

(c) ketabton.com: The Digital Library

where

$$\frac{\partial \delta V_1}{\partial r}=\iint_O G\sigma H\sum_{n=0}^{\infty}(1+k_n')\frac{-(n+1)a_e^n}{r^{n+2}}\left[\begin{array}{l}P_n(\sin\varphi)P_n(\sin\varphi_s)+(2-\delta_{0n})\\ \times\sum_{k=0}^{n}\frac{(n-k)!}{(n+k)!}P_{nk}(\sin\varphi)P_{nk}(\sin\varphi_s)\cos k(\lambda_s-\lambda)\end{array}\right]\mathrm{d}s\,,$$

$$\frac{\partial \delta V_1}{\partial \varphi}=\iint_O G\sigma H\sum_{n=0}^{\infty}(1+k_n')\frac{a_e^n}{r^{n+1}}\left[\begin{array}{l}\frac{\mathrm{d}P_n(\sin\varphi)}{\mathrm{d}\varphi}P_n(\sin\varphi_s)+(2-\delta_{0n})\\ \times\sum_{k=0}^{n}\frac{(n-k)!}{(n+k)!}\frac{\mathrm{d}P_{nk}(\sin\varphi)}{\mathrm{d}\varphi}P_{nk}(\sin\varphi_s)\cos k(\lambda_s-\lambda)\end{array}\right]\mathrm{d}s\,,$$

$$\frac{\partial \delta V_1}{\partial \lambda}=\iint_O G\sigma H\sum_{n=0}^{\infty}(1+k_n')\frac{a_e^n}{r^{n+1}}\left[\begin{array}{l}(2-\delta_{0n})\\ \times\sum_{k=0}^{n}\frac{(n-k)!}{(n+k)!}P_{nk}(\sin\varphi)P_{nk}(\sin\varphi_s)k\sin k(\lambda_s-\lambda)\end{array}\right]\mathrm{d}s\,,$$

$$\frac{\partial \delta V_2}{\partial r}=\iint_C G\sigma_e u_r\sum_{n=0}^{\infty}\frac{-(n+1)a_e^n}{r^{n+2}}\left[\begin{array}{l}P_n(\sin\varphi)P_n(\sin\varphi_s)+(2-\delta_{0n})\\ \times\sum_{k=0}^{n}\frac{(n-k)!}{(n+k)!}P_{nk}(\sin\varphi)P_{nk}(\sin\varphi_s)\cos k(\lambda_s-\lambda)\end{array}\right]\mathrm{d}s\,,$$

$$\frac{\partial \delta V_2}{\partial \varphi}=\iint_C G\sigma_e u_r\sum_{n=0}^{\infty}\frac{a_e^n}{r^{n+1}}\left[\begin{array}{l}\frac{\mathrm{d}P_n(\sin\varphi)}{\mathrm{d}\varphi}P_n(\sin\varphi_s)+(2-\delta_{0n})\\ \times\sum_{k=0}^{n}\frac{(n-k)!}{(n+k)!}\frac{\mathrm{d}P_{nk}(\sin\varphi)}{\mathrm{d}\varphi}P_{nk}(\sin\varphi_s)\cos k(\lambda_s-\lambda)\end{array}\right]\mathrm{d}s$$

and

$$\frac{\partial \delta V_2}{\partial \lambda}=\iint_C G\sigma_e u_r\sum_{n=0}^{\infty}\frac{a_e^n}{r^{n+1}}\left[\begin{array}{l}(2-\delta_{0n})\\ \times\sum_{k=0}^{n}\frac{(n-k)!}{(n+k)!}P_{nk}(\sin\varphi)P_{nk}(\sin\varphi_s)k\sin k(\lambda_s-\lambda)\end{array}\right]\mathrm{d}s\,. \quad (11.62)$$

11.2.4 Solar Radiation Pressure

Solar radiation pressure is force acting on the satellite's surface caused by the sunlight. The radiation force can be represented as (cf., e.g., Seeber 1993)

$$\vec{f}_{\mathrm{solar}}=m\gamma P_s C_r r_{\mathrm{sun}}^2\frac{S}{m}\frac{\vec{r}-\vec{r}_{\mathrm{sun}}}{\left|\vec{r}-\vec{r}_{\mathrm{sun}}\right|^3}\,, \quad (11.63)$$

where γ is the shadow factor, P_s is the luminosity of the Sun, C_r is the surface reflectivity, r_{sun} is the geocentric distance of the Sun, (S/m) is the surface to mass ratio of the satel-

(c) ketabton.com: The Digital Library

lite, and $\vec{r}$ and $\vec{r}_{sun}$ are the geocentric vector of the satellite and the Sun. Usually, P_s has the value of 4.5605×10^{-6} Newton / meter, C_r has values from 1 to 2, 1 is for the complete absorption of the sunlight, and for aluminium, $C_r = 1.95$.

The shadow factor is defined as

$$\gamma = 1 - \frac{A_{ss}}{A_s}, \tag{11.64}$$

where A_s is the sight surface of the Sun viewed from the satellite, and A_{ss} is the shadowed sight surface of the Sun. The sunlight may be shadowed by the Earth and the Moon. For convenience, we will discuss both parameters that are only in the satellite-Earth-Sun system (cf. Fig. 11.2). It is obvious that the half sight angles of the Earth and the Moon as well as the Sun viewed from the satellite are

$$\begin{aligned} \alpha_e &= \sin^{-1}\left(\frac{a_e}{|\vec{r}|}\right) \\ \alpha_m &= \sin^{-1}\left(\frac{a_m}{|\vec{r}_m - \vec{r}|}\right), \\ \alpha_s &= \sin^{-1}\left(\frac{a_s}{|\vec{r}_s - \vec{r}|}\right) \end{aligned} \tag{11.65}$$

where a_e, a_s and a_m are semimajor radii of the Earth, Sun and Moon, respectively; $a_m = 0.272493 a_e$, and $a_s = 959.63\pi/(3\,600 \times 180)$ (AU). For the GPS satellite, $\alpha_s < 0.3°$, $\alpha_e \approx 16.5°$ and $\alpha_m \approx \alpha_s \pm 0.03°$. Furthermore, $A_s = \alpha_s^2 \pi$ and $A_m = \alpha_m^2 \pi$. The angles between the centre of the Earth and the Sun, as well as the centre of the Moon and the Sun are

$$\begin{aligned} \beta_{es} &= \cos^{-1}\left(\frac{-\vec{r} \cdot (\vec{r}_s - \vec{r})}{r|\vec{r}_s - \vec{r}|}\right) \\ \beta_{ms} &= \cos^{-1}\left(\frac{(\vec{r}_m - \vec{r}) \cdot (\vec{r}_s - \vec{r})}{|\vec{r}_m - \vec{r}| \cdot |\vec{r}_s - \vec{r}|}\right) \end{aligned}, \tag{11.66}$$

where the vectors with indices s and m are the geocentric vectors of the Sun and Moon, respectively. The vector without an index is the geocentric vector of the satellite, and $r = |\vec{r}|$. If $\beta_{es} \geq \alpha_e + \alpha_s$, then the satellite is not in the shadow of the Earth (i.e., $A_{ss} = 0$). If $\beta_{es} \geq \alpha_e - \alpha_s$,

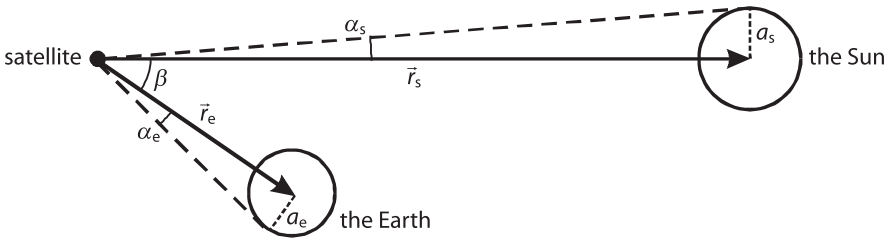

Fig. 11.2. Satellite-Earth-Sun system

(c) ketabton.com: The Digital Library

then the Sun is not in view of the satellite (i.e. $A_{ss} = A_s$). If $\alpha_e - \alpha_s < \beta_{es} < \alpha_e + \alpha_s$, then the sunlight is partly shadowed by the Earth. The formula of the shadowed surface can be derived as follows (cf. Fig. 11.3). The two circles with radius α_e and α_s cut each other at point p and q, line $\overline{pq}$ is called a chord (denoted by 2a), the chord-related central angle at origin o_s is denoted by ϕ_1, the surface area between the chord and the arc of the circle α_s on the right side of the chord is denoted by A_1. Line $\overline{pq}$ cuts $\overline{O_sO_e}$ at point g, while $\overline{O_sg}$ and $\overline{gO_e}$ are denoted by b and b_1. Then one has

$$
\begin{aligned}
a^2 &= \alpha_s^2 - b^2, \quad b_1 = \frac{\alpha_e^2 + \beta_{es}^2 - \alpha_s^2}{2\beta_{es}} \\
b &= \begin{cases} \beta_{es} - b_1 & \text{if} \quad b_1 \le \alpha_e \\ b_1 - \beta_{es} & \text{if} \quad b_1 > \alpha_e \end{cases} \\
\phi_1 &= \begin{cases} 2\cos^{-1}\left(\dfrac{b}{\alpha_s}\right) & \text{if} \quad b_1 \le \alpha_e \\ 2\pi - 2\cos^{-1}\left(\dfrac{b}{\alpha_s}\right) & \text{if} \quad b_1 > \alpha_e \end{cases} \\
A_1 &= \begin{cases} \dfrac{1}{2}\phi_1\alpha_s^2 - ab & \text{if} \quad b_1 \le \alpha_e \\ \dfrac{1}{2}\phi_1\alpha_s^2 + ab & \text{if} \quad b_1 > \alpha_e \end{cases}
\end{aligned}
\qquad (11.67)
$$

Similarly, the chord-related central angle at origin o_e is denoted by ϕ_2, while the surface area between the chord and the arc of the circle α_e on the left side of chord is denoted by A_2. Then one has

$$
\phi_2 = 2\cos^{-1}\left(\frac{b_1}{\alpha_e}\right), \quad A_2 = \frac{1}{2}\phi_2\alpha_e^2 - ab_1 \qquad (11.68)
$$

and

$$
\gamma = 1 - \frac{A_1 + A_2}{\alpha_s^2\pi} \,. \qquad (11.69)
$$

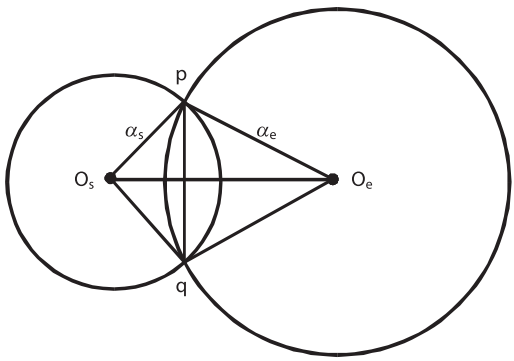

Fig. 11.3.
Shadowed surface area

(c) ketabton.com: The Digital Library

A similar discussion can be made for the Moon. If $\beta_{ms} \geq \alpha_m + \alpha_s$, then the satellite is not in the shadow of the Moon, i.e., $A_{ss} = 0$. If $\beta_{ms} \geq \alpha_m - \alpha_s$, then the full shadow has occurred, i.e., $A_{ss} = \min(A_s, A_m)$. If $|\alpha_m - \alpha_s| < \beta_{ms} < \alpha_m + \alpha_s$, then the sunlight is partially shadowed by the Moon. The formula of the shadowed surface can be similarly derived by changing the index *e* to *m* in Eqs. 11.67 and 11.68. Because of the small sight angle of the Moon viewed from the satellite, the shadowed time will be very short if it happens. By GPS satellite dynamic orbit determination (e.g., in IGS orbit determination), only the data that have the γ value of 0 or 1 are used.

Because of the complex shape of the satellite, the use of constant reflectivity and homogenous luminosity of the Sun, as well as the existence of indirect solar radiation (reflected from the Earth's surface), the model of Eq. 11.63 discussed above is not accurate enough for precise purposes and will be used as a first order approximation. A further model for the adjustment to fit solar radiation effects is needed.

The force vector is pointed from the Sun to the satellite. The satellite fixed coordinate system is introduced in Sect. 5.8 (cf. Sect. 5.8 for details). The solar radiation force vector in the ECSF system is then

$$\begin{aligned} \vec{f}_{\text{solar}} &= m\gamma P_s C_r \frac{S}{m} \frac{r_{\text{sun}}^2}{\left|\vec{r} - \vec{r}_{\text{sun}}\right|^2} \vec{n}_{\text{sun}} \\ &= m\gamma P_s C_r \frac{S}{m} \frac{r_{\text{sun}}^2}{\left|\vec{r} - \vec{r}_{\text{sun}}\right|^2} \left(\sin\beta \cdot \vec{e}_x + \cos\beta \cdot \vec{e}_z\right) , \end{aligned} \tag{11.70}$$

where

$$\vec{e}_z = -\frac{\vec{r}}{|\vec{r}|}, \quad \vec{e}_y = \frac{\vec{e}_z \times \vec{n}_{\text{sun}}}{|\vec{e}_z \times \vec{n}_{\text{sun}}|}, \quad \vec{e}_x = \vec{e}_y \times \vec{e}_z \quad \text{and} \quad \vec{n}_{\text{sun}} = \frac{\vec{r} - \vec{r}_{\text{sun}}}{|\vec{r} - \vec{r}_{\text{sun}}|} . \tag{11.71}$$

Further formulas of Eq. 11.71 can be found in Sect. 5.8. Taking the remaining error of the radiation pressure into account, the solar radiation force model can be represented as (cf. Fliegel et al. 1992; Beutler et al. 1994)

$$\vec{f}_{\text{solar-force}} = \vec{f}_{\text{solar}} + \begin{pmatrix} a_{11} & a_{12} & a_{13} \\ a_{21} & a_{22} & a_{23} \\ a_{31} & a_{32} & a_{33} \end{pmatrix} \begin{pmatrix} 1 \\ \cos u \\ \sin u \end{pmatrix} . \tag{11.72}$$

That is, 9 parameters are used to model the solar radiation force error for every satellite.

An alternative adjustment model of solar radiation is given by introducing a so-called disturbance coordinate system and will be outlined below (cf. Xu 2004).

Disturbance Coordinate System and Radiation Error Model

The solar radiation force vector is pointed from the Sun to the satellite. If the shadow factor is computed exactly, the luminosity of the Sun is a constant, and the surface reflectivity of the satellite is a constant, then the length of the solar force vector can be considered as a constant, because

(c) ketabton.com: The Digital Library

$$\frac{r_{sun}^2}{(r_{sun}+r)^2} \le \frac{r_{\text{sun}}^2}{\left|\vec{r}-\vec{r}_{\text{sun}}\right|^2} \le \frac{r_{sun}^2}{(r_{sun}-r)^2}\,, \tag{11.73}$$

and

$$\frac{r_{\text{sun}}^2}{(r_{\text{sun}}\pm r)^2} = \left(\frac{r_{\text{sun}}}{r_{\text{sun}}\pm r}\right)^2 \approx \left(1\mp\frac{r}{r_{\text{sun}}}\pm\ldots\right)^2 \approx 1\mp\frac{2r}{r_{\text{sun}}} \approx 1\mp 3\times 10^{-5}\,.$$

Any bias error in P_s, C_r and (S/m) may cause a model error of $\alpha\vec{f}_{\text{solar}}$, where α is a parameter. So the $\alpha\vec{f}_{\text{solar}}$ can be considered a main error model of the solar radiation. Because the ratio of the geocentric distances of the satellite and the Sun is so small, the direction and distance changes of the Sun-satellite vector are negligible. With the motion of the Sun, the solar radiation force vector changes its direction with the time in the ECSF (Earth-Centred-Space-Fixed) coordinate system ca. 1 degree per day. Such an effect can only be considered a small drift, not a periodical change for the orbit determination. To model such an effect in the ECSF, system one needs three bias parameters in three coordinate axes and three drift terms instead of a few periodical parameters. It is obvious that to model such an effect in the direction of $\vec{n}$, just one parameter α is needed. Therefore, it is very advantageous to define a so-called disturbance coordinate system as follows: the origin is the geo-centre, and the three axes are defined by $\vec{r}$ (radial vector of the satellite), $\vec{n}$ (the Sun-satellite identity vector) and $\vec{p}$(the atmospheric drag identity vector). These three axes are always in the main disturbance directions of the indirect solar radiation (reflected from the Earth's surface), direct solar radiation and atmospheric drag, respectively. This coordinate system is not a Cartesian one and the axes are not orthogonal to each other. The parameters in individual axes are mainly used to model the related disturbance effects, and meanwhile to absorb the remained error of other un-modelled effects.

In the so-called disturbance coordinate system, the solar radiation pressure error model can be represented alternatively by (cf. Xu 2004)

$$\alpha\vec{f}_{\text{solar}} = \begin{pmatrix} a_1 & b_1 \\ a_2 & b_2 \\ a_3 & b_3 \end{pmatrix}\begin{pmatrix} 1 \\ t \end{pmatrix}, \tag{11.74}$$

where b-terms are very small.

11.2.5 Atmospheric Drag

Atmospheric drag is the disturbance force acting on the satellite's surface caused by the air. Air drag force can be represented as (cf., e.g., Seeber 1993; Liu and Zhao 1979)

$$\vec{f}_{\text{drag}} = -m\frac{1}{2}\left(\frac{C_{\text{d}}S}{m}\right)\sigma\left|\dot{\vec{r}}-\dot{\vec{r}}_{\text{air}}\right|\left(\dot{\vec{r}}-\dot{\vec{r}}_{\text{air}}\right), \tag{11.75}$$

where S is the cross section (or effective area) of the satellite, C_{d} is the drag factor, m is the mass of the satellite, $\dot{\vec{r}}$ and $\dot{\vec{r}}_{\text{air}}$ are the geocentric velocity vectors of the satellite and

(c) ketabton.com: The Digital Library

the atmosphere, and σ is the density of the atmosphere. Usually, S has a value of 1 / 4 of the outer surface area of the satellite, and C_d has labour values of 2.2 ±0.2. The velocity vector of the atmosphere can be modelled by

$$\dot{\vec{r}}_{\text{air}} = k\vec{\omega}\times\vec{r} = k\omega\begin{pmatrix} -y \\ x \\ 0 \end{pmatrix}, \tag{11.76}$$

where $\bar{\omega}$ is the angular velocity vector of the Earth's rotation, and $\omega = |\bar{\omega}|$, k is the atmospheric rotation factor. For the lower layer of the atmosphere, $k = 1$, i.e., the lower layer of the atmosphere is considered rotating with the Earth. For the higher layer, $k = 1.2$, because the higher ionosphere is accelerated by the Earth's magnetic field.

Gravity balanced atmospheric density model has the exponential form of (cf. Liu and Zhao 1979)

$$\sigma = \sigma_0(1+q)\exp\left(-\frac{r-\rho}{H}\right), \tag{11.77}$$

where σ_0 is the atmospheric density at the reference point ρ, q is the daily change factor of the density, r is the geocentric distance of the satellite, and H is the density-height scale factor. For the spherical and rotating ellipsoidal layer atmospheric models, one has

$$\rho = a_e + h_i \tag{11.78}$$

and

$$\rho = (a_e + h_i)\sqrt{1-e^2}\sqrt{\frac{1+\tan^2\varphi}{1+\tan^2\varphi - e^2}}, \tag{11.79}$$

respectively. Where a_e is the semimajor radius of the Earth, h_i ($i = 1, 2, \ldots$) is a set of numbers, φ is the geocentric latitude of the satellite, and e is the eccentricity of the ellipsoid. Equations 11.78 and 11.79 are sphere with radius $a_e + h_i$ and rotating ellipsoid with semimajor axis $a_e + h_i$. Equation 11.79 can be derived from the relation of $\tan\varphi$ and the ellipsoid equation

$$\begin{aligned} z^2 &= (x^2+y^2)\tan^2\varphi \\ x^2+y^2+z^2\frac{1}{1-e^2} &= (a_e+h_i)^2 \end{aligned}.$$

A reference of atmospheric densities can be read from Table 11.1, which is given by Cappellari (1976) (cf. Seeber 1993)

The density-height scale H between every two layers can be then computed from the above values. It is notable that the air density may change its value up to a factor of 10 due to the radiation of the Sun. The density of the atmosphere at a defined point reaches its maximum value at 14^h local time and its minimum at 3.5^h. The most sig-

(c) ketabton.com: The Digital Library

nificant period of change is the daily change and is represented by the daily changing factor as

$$q = \frac{f-1}{f+1}\cos\psi\,, \tag{11.80}$$

where f is the ratio of the maximum density and the minimum density, and ψ is the angle between the satellite vector $\vec{r}$ and the daily maximum density direction $\vec{r}_{\mathrm{m}}$. The f may have the value of 3 and

$$\cos\psi = \frac{\vec{r}\cdot\vec{r}_{\mathrm{m}}}{|\vec{r}|\cdot|\vec{r}_{\mathrm{m}}|}\,, \tag{11.81}$$

where

$$\begin{pmatrix} x \\ y \\ z \end{pmatrix}_{\mathrm{sun}} = \begin{pmatrix} r\cos\delta\cos\alpha \\ r\cos\delta\sin\alpha \\ r\sin\delta \end{pmatrix}, \quad \begin{pmatrix} r = \sqrt{x^2+y^2+z^2} \\ \delta = \tan^{-1}\dfrac{z}{\sqrt{x^2+y^2}} \\ \alpha = \tan^{-1}\dfrac{y}{x} \end{pmatrix}, \tag{11.82}$$

$$\vec{r}_{\mathrm{m}} = \begin{pmatrix} x \\ y \\ z \end{pmatrix}_{\mathrm{m}} = \begin{pmatrix} r\cos\delta\cos(\alpha+\pi/6) \\ r\cos\delta\sin(\alpha+\pi/6) \\ r\sin\delta \end{pmatrix}$$

where (α, δ) are the coordinates (right ascension, latitude) of the Sun in the ECSF coordinate system.

Taking the remaining error of the atmospheric drag into account, the air drag force model can be represented as

$$\vec{f}_{\mathrm{air-drag}} = \vec{f}_{\mathrm{drag}} + (1+q)\Delta\vec{f}_{\mathrm{drag}}\,. \tag{11.83}$$

Table 11.1. Reference of atmospheric densities

h_i (km)	$\sigma_0(i)$ (g km^{-3})
100	497 400
200	255 – 316
300	17 – 35
400	2.2 – 7.5
500	0.4 – 2.0
600	0.08 – 0.64
700	0.02 – 0.22
800	0.07 – 0.01
900	0.003 – 0.04
1 000	0.001 – 0.02

(c) ketabton.com: The Digital Library

Where the force error vector is denoted by $\Delta\vec{f}_{\text{drag}}$ and the time variation part of atmospheric density is considered in parameter q.

Error Model in Disturbance Coordinate System

In the atmospheric drag model Eq.11.75, the velocity vector of the atmosphere is always perpendicular to the z-axis of the ECSF coordinates and the satellite velocity vector is always in the tangential direction of the orbit. The variation of the term $|\dot{\vec{r}} - \dot{\vec{r}}_{\text{air}}|$ (denoted by g) is dominated by the direction changes of the velocity vectors of the satellite and the atmosphere. Any bias error in S (effective area of the satellite), C_{d} (drag factor) and σ (density of the atmosphere) may cause a model error of $\mu\vec{f}_{\text{drag}}$, where μ is a parameter. So the $\mu\vec{f}_{\text{drag}}$ can be considered a main error model of the un-modelled atmospheric drag. To simplify our discussion, we consider the velocities of the satellite and atmosphere are constants, and call the satellite positions with max(z) and –max(z) the highest and lowest points, respectively. With the satellite at the lowest point, the two velocity vectors are in the same direction and therefore the g reaches the minimum. At the ascending node, the two vectors have the maximum angle of inclination i and the g reaches the maximum. Then g reaches the minimum again at the highest point and reaches the maximum again at the descending node, and at the end reaches the minimum at the lowest point. It is obvious that, besides the constant part, g has a dominant periodical component of cos2f and sin2f where f is the true anomaly of the satellite.

In the so-called disturbance coordinate system the atmospheric drag error model can be represented alternatively by (cf. Xu 2004)

$$\mu\vec{f}_{drag} = \left[a + b\varphi(2\omega)\cos(2f) + c\varphi(3\omega)\cos(3f) + d\varphi(\omega)\cos f\right]\vec{p}\,, \tag{11.84}$$

where

$$\varphi(k\omega) = \begin{cases} \sin k\omega & if\ \cos k\omega = 0 \\ \dfrac{1}{\cos k\omega} & if\ \cos k\omega \neq 0 \end{cases}, \quad k = 1, 2, 3 \tag{11.85}$$

where ω is the angle of perigee and f is the true anomaly of the satellite; a, b, c and d are model parameters to be determined. According to the simulation, a-term and b-term are the most significant terms. The amount of d is just about 1% of the amount of c, and the amount of c is about 1% of that of b.

11.2.6 Additional Perturbations

As mentioned above, the disturbed equation of motion of the satellite is valid only in an inertial coordinate system, or ECSF system. Therefore, the state vector and force vectors as well as the disturbing potential function have also to be represented in the ECSF system. As seen above, for some reason, the state vector and the force vectors as well as the disturbing potential function R are sometimes given in the ECEF system and then transformed to the ECSF system by (cf. Sect. 11.2.4)

(c) ketabton.com: The Digital Library

$$\begin{aligned}
\vec{X}_{\mathrm{ECSF}} &= R_{\mathrm{t}} \cdot \vec{X}_{\mathrm{ECEF}} \\
\vec{f}_{\mathrm{ECSF}} &= R_{\mathrm{t}} \cdot \vec{f}_{\mathrm{ECEF}} \\
R_{\mathrm{ECSF}} &= R(R_{\mathrm{t}}^{-1} X_{\mathrm{ECSF}}) \quad \text{for} \quad R(X_{\mathrm{ECEF}})
\end{aligned} \quad , \tag{11.86}$$

where R_{t} is the transformation matrix in general. Variable transformation is further denoted by $X_{\mathrm{ECSF}} = R_{\mathrm{t}} X_{\mathrm{ECEF}}$. We have also seen that sometimes the state vectors (of the satellite, the Sun, the Moon) in the ECSF system have to be transformed to the ECEF system for use, and then the result vectors will be transformed back to the ECSF system again. However, due to the complication of transformation R_{t}^{-1}, quite often a simplified R_{s}^{-1} is used. (cf. in later discussions, for example to represent the disturbing potential function using Keplerian elements, only the Earth rotation is considered). Thus,

$$R_{\mathrm{ECSF}} = \{R(R_{\mathrm{t}}^{-1} X_{\mathrm{ECSF}}) - R(R_{\mathrm{s}}^{-1} X_{\mathrm{ECSF}})\} + R(R_{\mathrm{s}}^{-1} X_{\mathrm{ECSF}}) \,, \tag{11.87}$$

where the first term on the right side is the correction because of the approximation using the second term. The transformations of Eqs. 11.86 and 11.87 are exact operations, and their differentiation with respect to time t and the partial derivatives with respect to variable X_{ECSF} are then

$$\begin{aligned}
\frac{\mathrm{d}\vec{X}_{\mathrm{ECSF}}}{\mathrm{d}t} &= \frac{\mathrm{d}R_{\mathrm{t}}}{\mathrm{d}t} \vec{X}_{\mathrm{ECEF}} + R_{\mathrm{t}} \frac{\mathrm{d}\vec{X}_{\mathrm{ECEF}}}{\mathrm{d}t} \\
\frac{\mathrm{d}\vec{f}_{\mathrm{ECSF}}}{\mathrm{d}t} &= \frac{\mathrm{d}R_{\mathrm{t}}}{\mathrm{d}t} \vec{f}_{\mathrm{ECEF}} + R_{\mathrm{t}} \frac{\mathrm{d}\vec{f}_{\mathrm{ECEF}}}{\mathrm{d}t} \\
\frac{\partial R_{\mathrm{ECSF}}}{\partial X_{\mathrm{ECSF}}} &= \frac{\partial \left[R(R_{\mathrm{t}}^{-1} X_{\mathrm{ECSF}}) - R(R_{\mathrm{s}}^{-1} X_{\mathrm{ECSF}}) \right]}{\partial X_{\mathrm{ECSF}}} + \frac{\partial R(R_{\mathrm{s}}^{-1} X_{\mathrm{ECSF}})}{\partial X_{\mathrm{ECSF}}}
\end{aligned} \quad . \tag{11.88}$$

That is, the time differentiations of the state vector and force vectors cannot be transformed directly like in Eq. 11.86. In other words, if the state vector and force vectors are not directly given in the ECSF system, they are not allowed to be differentiated as usual afterward. An approximated and transformed perturbing potential function will introduce an error. The first term on the right-hand side of Eq. 11.88 signifies additional perturbations, or coordinate perturbations. The order of such perturbations can be estimated by the first term on the right-hand side. If the relationship between two coordinate systems changes with time or the transformation has not been made exactly, such perturbations will occur. Recalling

$$R = R_{\mathrm{P}}^{-1} R_{\mathrm{N}}^{-1} R_{\mathrm{S}}^{-1} R_{\mathrm{M}}^{-1}$$

and their definitions (cf. Chap. 2), one has

$$\begin{aligned}
\frac{\mathrm{d}R}{\mathrm{d}t} = {} & R_{\mathrm{P}}^{-1} R_{\mathrm{N}}^{-1} R_{\mathrm{S}}^{-1} \frac{\mathrm{d}R_{\mathrm{M}}^{-1}}{\mathrm{d}t} + R_{\mathrm{P}}^{-1} R_{\mathrm{N}}^{-1} \frac{\mathrm{d}R_{\mathrm{S}}^{-1}}{\mathrm{d}t} R_{\mathrm{M}}^{-1} \\
& + R_{\mathrm{P}}^{-1} \frac{\mathrm{d}R_{\mathrm{N}}^{-1}}{\mathrm{d}t} R_{\mathrm{S}}^{-1} R_{\mathrm{M}}^{-1} + \frac{\mathrm{d}R_{\mathrm{P}}^{-1}}{\mathrm{d}t} R_{\mathrm{N}}^{-1} R_{\mathrm{S}}^{-1} R_{\mathrm{M}}^{-1}
\end{aligned} \,, \tag{11.89}$$

(c) ketabton.com: The Digital Library

Where

$$\frac{\mathrm{d}R_{\mathrm{M}}^{-1}}{\mathrm{d}t}=\begin{pmatrix}0 & 0 & -\dot{x}_p\\ 0 & 0 & \dot{y}_p\\ \dot{x}_p & -\dot{y}_p & 0\end{pmatrix},\qquad \frac{\mathrm{d}R_{\mathrm{S}}^{-1}}{\mathrm{d}t}=\frac{\mathrm{d}R_3(\mathrm{GAST})}{\mathrm{d}t}$$

$$\begin{aligned}\frac{\mathrm{d}R_{\mathrm{N}}^{-1}}{\mathrm{d}t}&=\frac{\mathrm{d}R_1(-\varepsilon)}{\mathrm{d}t}R_3(\Delta\psi)R_1(\varepsilon+\Delta\varepsilon)+R_1(-\varepsilon)\frac{\mathrm{d}R_3(\Delta\psi)}{\mathrm{d}t}R_1(\varepsilon+\Delta\varepsilon)\\ &\quad+R_1(-\varepsilon)R_3(\Delta\psi)\frac{\mathrm{d}R_1(\varepsilon+\Delta\varepsilon)}{\mathrm{d}t}\end{aligned}\quad , \quad (11.90)$$

$$\frac{\mathrm{d}R_{\mathrm{P}}^{-1}}{\mathrm{d}t}=\frac{\mathrm{d}R_3(\zeta)}{\mathrm{d}t}R_2(-\theta)R_3(z)+R_3(\zeta)\frac{\mathrm{d}R_2(-\theta)}{\mathrm{d}t}R_3(z)+R_3(\zeta)R_2(-\theta)\frac{\mathrm{d}R_3(z)}{\mathrm{d}t}$$

where all elements are defined and given in Chap. 2, $(\dot{x}_{\mathrm{p}}, \dot{y}_{\mathrm{p}})$ is the polar motion rate of time, and

$$\begin{aligned}\frac{\mathrm{d}R_1(\alpha)}{\mathrm{d}t}&=\begin{pmatrix}0 & 0 & 0\\ 0 & -\sin\alpha & \cos\alpha\\ 0 & -\cos\alpha & -\sin\alpha\end{pmatrix}\frac{\mathrm{d}\alpha}{\mathrm{d}t}\\ \frac{\mathrm{d}R_2(\alpha)}{\mathrm{d}t}&=\begin{pmatrix}-\sin\alpha & 0 & -\cos\alpha\\ 0 & 0 & 0\\ \cos\alpha & 0 & -\sin\alpha\end{pmatrix}\frac{\mathrm{d}\alpha}{\mathrm{d}t}.\\ \frac{\mathrm{d}R_1(\alpha)}{\mathrm{d}t}&=\begin{pmatrix}-\sin\alpha & \cos\alpha & 0\\ -\cos\alpha & -\sin\alpha & 0\\ 0 & 0 & 0\end{pmatrix}\frac{\mathrm{d}\alpha}{\mathrm{d}t}\end{aligned}\quad (11.91)$$

Further formulas may be easily derived.

11.2.7 Order Estimations of Perturbations

Perturbation forces that are scaled by the mass of the satellite are the accelerations. The accelerations caused by the discussed forces have been estimated for the GPS satellite by several authors and are summarised in Table 11.2.

If the coordinate system is used without taking precession and nutation into account, additional perturbation acceleration can reach up to 3×10^{-10}. Additional acceleration of gravitational potential can reach up to 1×10^{-9} (cf. Liu and Zhao 1979).

11.2.8 Ephemerides of the Moon, the Sun and Planets

The ephemerides of the Sun and the Moon are used above for the computation of shadow functions of the Sun and Moon (solar radiation pressure), the tidal disturbance forces, and tidal and loading deformations (cf. Sect. 5.8). The computation of the ephemerides of the Sun and the Moon can be simplified by considering the orbit of the Sun (indeed it is the Earth!) and the Moon as Keplerian motion. Consider the orbital right-handed coordinate

(c) ketabton.com: The Digital Library

Table 11.2.
Accelerations ($m\,s^{-2}$) caused by forces (cf. Seeber 1993; Kang 1998)

Acceleration	$m\,s^{-2}$
Central force acceleration	0.56
Gravitational C_2 acceleration	5×10^{-5}
Other gravitational acceleration	3×10^{-7}
The Moon's central force acceleration	5×10^{-6}
The Sun's central force acceleration	2×10^{-6}
Planets' central force acceleration	3×10^{-10}
The Earth's tidal acceleration	2×10^{-9}
The Ocean's tidal acceleration	5×10^{-10}
Solar pressure acceleration	1×10^{-7}
Atmospheric drag acceleration (Topex)	4×10^{-10}
General relativity acceleration	3×10^{-10}

system, the origin in the geocentre, the *xy*-plane as the orbital plane, the *x*-axis pointing to the perigee, and the *z*-axis pointing in the direction of $\vec{q}\times\dot{\vec{q}}$, where $\vec{q}$ and $\dot{\vec{q}}$ are the position and velocity vectors of the Sun or the Moon. The two vectors are (cf. Eqs. 3.41, 3.42)

$$\vec{q}=\begin{pmatrix} a(\cos E-e)\\ a\sqrt{1-e^2}\,\sin E\\ 0\end{pmatrix}=\begin{pmatrix} q\cos f\\ q\sin f\\ 0\end{pmatrix},\quad \dot{\vec{q}}=\begin{pmatrix} -\sin f\\ e+\cos f\\ 0\end{pmatrix}\frac{na}{\sqrt{1-e^2}}, \tag{11.92}$$

where

$$q=\frac{a(1-e^2)}{1+e\cos f}. \tag{11.93}$$

The position and velocity vectors of the Sun or the Moon in the ECEI and ECSF coordinate systems are then (cf. Sect. 2.5 and Eq. 3.43)

$$\begin{aligned}\begin{pmatrix}\vec{p}\\ \dot{\vec{p}}\end{pmatrix}&=R_3(-\Omega)R_1(-i)R_3(-\omega)\begin{pmatrix}\vec{q}\\ \dot{\vec{q}}\end{pmatrix}\\ \begin{pmatrix}\vec{r}\\ \dot{\vec{r}}\end{pmatrix}&=R_1(-\varepsilon)\begin{pmatrix}\vec{p}\\ \dot{\vec{p}}\end{pmatrix}\end{aligned}, \tag{11.94}$$

where a and i are the semimajor axis of the orbit and the inclination angle of the orbital plane of the Moon or the Sun in the ecliptic coordinate system (ECEI). Ω is the ecliptic right ascension of the ascending node, e is the eccentricity of the ellipse, ω is the argument of perigee, f is the true anomaly of the Moon or the Sun, and ε is the mean obliquity (the formula is given in Sect. 2.4). Because the Sun moves along the ecliptic and the ascending node is defined as the equinox, parameters i and Ω are zero. True anomaly f, eccentric anomaly E and mean anomaly M are given by the Keplerian equation and the following formulas

$$\begin{aligned}&E-e\sin E=M\\ &q\cos f=a\cos E-ae\\ &q\sin f=b\sin E=a\sqrt{1-e^2}\,\sin E\end{aligned}. \tag{11.95}$$

(c) ketabton.com: The Digital Library

For the Moon, eccentricity $e_m = 0.05490$, inclination $i_m = 5.°145396$ and semimajor axis $a_m = 384\,401$ km. For the Sun, eccentricity $e_s = 0.016709114 - 0.000042052T - 0.000000126T^2$ and semimajor axis $a_s = 1.0000002$ AU. AU signifies the astronomical units (AU = $1.49597870691 \times 10^8$ km). The fundamental arguments are given in the IERS Conventions (cf. McCarthy 1996) as follows:

$$
\begin{aligned}
l &= 134.^\circ 96340251 + 1717915923.''2178T + 31.''8792T^2 + 0.''051635T^3 - 0.''00024470T^4 \\
l' &= 357.^\circ 52910918 + 129596581.''0481T - 0.''5532T^2 + 0.''000136T^3 - 0.''00001149T^4 \\
F &= 93.^\circ 27209062 + 1739527262.''8478T - 12.''7512T^2 - 0.''001037T^3 + 0.''00000417T^4 \\
D &= 297.^\circ 85019547 + 1602961601.''2090T - 6.''3706T^2 + 0.''006593T^3 - 0.''00003169T^4 \\
\Omega &= 125.^\circ 04455501 - 6962890.''2665T + 7.''4722T^2 + 0.''007702T^3 - 0.''00005939T^4
\end{aligned}
\tag{11.96}
$$

where l and l' are the mean anomalies of the Moon and the Sun, respectively. D is the mean elongation of the Moon from the Sun. Ω is the mean longitude of the ascending node of the Moon. $F = L - \Omega$, L is the mean longitude of the Moon (or L_{moon}), and T is the Julian centuries measured from epoch J2000.0. Formulas of Eq. 11.96 are the arguments used to compute the nutation. Mean angular velocities n of the Sun and Moon are the coefficients of the linear terms of l and l' (units: second / century), respectively.

For computation of the ephemerides of the Sun, l' is set as M in Eq. 11.95, so that E and f of the Sun can be computed. Using $D = L_{moon} - L_{sun} = F + \Omega - L_{sun}$, the mean longitude L_{sun} can be computed. ω can be computed by relation $L_{sun} = \omega + f$.

For computation of the ephemerides of the Moon, l is set as M in Eq. 11.95, so that E and f of the Moon can be computed. ω can be computed by using the spherical triangle formula:

$$
\tan(\omega + f) = \tan F / \cos i_m \,, \tag{11.97}
$$

where angles u ($= \omega + f$) and F are in the same compartment.

Substituting the above values of the Moon and the Sun into Eqs. 11.92–11.94 respectively, ephemerides of the Moon and the Sun are obtained in the ECSF coordinate system. For more precise computation of the ephemerides of the Moon, several corrections have to be considered (cf. Meeus 1992; Montenbruck 1989). Equivalently, a correction dF can be added to F, and the change of du in Eq. 11.97 can be considered df and added to f, where dF has the form of (units: seconds)

$$
\begin{aligned}
\mathrm{d}F = {} & 22640\sin l + 769\sin(2l) + 36\sin(3l) - 125\sin D + 2370\sin(2D) - 668\sin l' \\
& - 412\sin(2F) + 212\sin(2D - 2l) + 4586\sin(2D - l) + 192\sin(2D + l) \\
& + 165\sin(2D - l') + 206\sin(2D - l - l') - 110\sin(l + l') + 148\sin(l - l')
\end{aligned} \,.
$$

The orbits of the planets are given in the Sun-centred ecliptic coordinate system by six Keplerian elements. They are the mean longitude (L) of the planet, the semimajor axis (a, units: AU) of the orbit of the planet, the eccentricity (e) of the orbit, the

(c) ketabton.com: The Digital Library

inclination (i) of the orbit to the ecliptic plane, the argument (ω) of the perihelion, and the longitude (Ω) of the ascending node. The orbital elements are expressed as a polynomial function of the instant of time T (Julian centuries) for planet Mercury, Venus, Mars, Jupiter, and Saturn as follows (cf. Meeus 1992):

$$\begin{pmatrix} L \\ a \\ e \\ i \\ \omega \\ \Omega \end{pmatrix}_{\text{Mercury}} = \begin{pmatrix} 252.250906 & 149474.0722491 & 0.00030397 & -0.00000002 \\ 0.38709831 & 0 & 0 & 0 \\ 0.20563175 & 0.000020406 & -0.0000000284 & -0.0000000002 \\ 7.0049860 & 0.0018215 & -0,00001809 & 0.000000053 \\ 29.1252260 & 0.3702885 & 0.00012002 & -0.000000155 \\ 48.3308930 & 1.1861890 & 0.00017587 & 0.000000211 \end{pmatrix} \begin{pmatrix} 1 \\ T \\ T^2 \\ T^3 \end{pmatrix},$$

$$\begin{pmatrix} L \\ a \\ e \\ i \\ \omega \\ \Omega \end{pmatrix}_{\text{Venus}} = \begin{pmatrix} 181.979801 & 58519.2130302 & 0.00031060 & 0.000000015 \\ 0.72332982 & 0 & 0 & 0 \\ 0.00677118 & -0.000047766 & 0.0000000975 & 0.00000000044 \\ 3.3946620 & 0.00100370 & -0,00000088 & -0.000000007 \\ 54.883787 & 0.50109980 & -0.00148002 & -0.000005235 \\ 76.6799200 & 0.90111900 & 0.00040665 & -0.00000008 \end{pmatrix} \begin{pmatrix} 1 \\ T \\ T^2 \\ T^3 \end{pmatrix},$$

$$\begin{pmatrix} L \\ a \\ e \\ i \\ \omega \\ \Omega \end{pmatrix}_{\text{Mars}} = \begin{pmatrix} 355.4332750 & 19141.6964746 & 0.00031097 & 0.000000015 \\ 1.523679342 & 0 & 0 & 0 \\ 0.09340062 & 0.000090483 & -0.0000000806 & -0.00000000035 \\ 1.8497260 & -0.0006010 & 0.00012760 & -0.000000006 \\ 286.502141 & 1.0689408 & 0.00011910 & -0.000002007 \\ 49.558093 & 0.7720923 & 0.00001605 & 0.000002325 \end{pmatrix} \begin{pmatrix} 1 \\ T \\ T^2 \\ T^3 \end{pmatrix},$$

$$\begin{pmatrix} L \\ a \\ e \\ i \\ \omega \\ \Omega \end{pmatrix}_{\text{Jupiter}} = \begin{pmatrix} 34.351484 & 3036.3027889 & 0.00022374 & 0.000000025 \\ 5.202603191 & 0.0000001913 & 0 & 0 \\ 0.04849485 & 0.000163244 & -0.0000004719 & -0.00000000197 \\ 1.303270 & -0.00549660 & 0.00000465 & -0.000000004 \\ 273.866868 & 0.5917118 & 0.00063010 & -0.000005138 \\ 100.464441 & 1.0209550 & 0.00040117 & 0.000000569 \end{pmatrix} \begin{pmatrix} 1 \\ T \\ T^2 \\ T^3 \end{pmatrix}$$

and

$$\begin{pmatrix} L \\ a \\ e \\ i \\ \omega \\ \Omega \end{pmatrix}_{\text{Saturn}} = \begin{pmatrix} 50.0774710 & 1223.5110141 & 0.00051952 & -0.000000003 \\ 9.554909596 & -0.0000021389 & 0 & 0 \\ 0.05550862 & -0.000346818 & -0.0000006456 & 0.00000000338 \\ 2.488878 & -0.0037363 & -0.00001516 & 0.000000089 \\ 339.391263 & 1.0866715 & 0.00095824 & 0.000007279 \\ 113.665524 & 0.8770979 & -0.00012067 & -0.00000238 \end{pmatrix} \begin{pmatrix} 1 \\ T \\ T^2 \\ T^3 \end{pmatrix},$$

(c) ketabton.com: The Digital Library

Table 11.3. Gravitational constants of the Sun, the Moon and planets

Object	Gravitational constant ($m^3 s^{-2}$)
Sun	1.3271240000000E+20
Moon	4.9027993000000E+12
Earth	3.9860044180000E+14
Mercury	2.2032070000000E+13
Venus	3.2485850000000E+14
Mars	4.2828300000000E+13
Jupiter	1.2671270000000E+17
Saturn	3.7940610000000E+16

where except for the semimajor axis a and eccentricity e, all other elements have units of degrees. $F = L - \Omega$, and f and E can be computed by using Eqs. 11.97 and 11.95. Mean angular velocities n of the planets are the coefficients of the linear term of L (units: degree / century). The coordinate vector of the planet can then be computed by using Eqs. 11.92–11.94. The results are in the Sun-centred equatorial coordinate system. The results have to be transformed to the ECSF coordinate system by a translation

$$\begin{pmatrix} \vec{r} \\ \dot{\vec{r}} \end{pmatrix}_{\mathrm{ECSF}} = \begin{pmatrix} \vec{r} \\ \dot{\vec{r}} \end{pmatrix}_{\mathrm{sun}} + \begin{pmatrix} \vec{r} \\ \dot{\vec{r}} \end{pmatrix}_{\mathrm{SCES}}, \tag{11.98}$$

where vectors with an index of sun and SCEF are geocentric position and velocity vectors of the Sun and the planet in the Sun-centred equatorial system.

Gravitational constants of the Sun, the Moon and planets are given in Table 11.3.

11.3 Analysis Solution of the $\bar{C}_{20}$ Perturbed Orbit

The geopotential term of $\overline{C}_{20}$ is a zonal term. Compared with other geopotential terms, $\overline{C}_{20}$ has a value that is at least 100 times larger. According to the order estimation discussed in Sect. 11.2.7, $\overline{C}_{20}$ term perturbation is one of the most significant disturbing factors. $\overline{C}_{20}$ disturbance is a perturbation of first order. The analysis solution of the $\overline{C}_{20}$ perturbation will give a clear insight of the orbit disturbance. The related perturbing potential is (cf. Sect. 11.2.1.1)

$$R_2 = \frac{\mu a_e^2}{r^3} \overline{C}_{20} \overline{P}_{20}(\sin\varphi)$$

or

$$R_2 = \frac{b}{r^3}(3\sin^2\varphi - 1), \tag{11.99}$$

where

$$b = \frac{\sqrt{5}\mu a_e^2}{2} \overline{C}_{20}.$$

(c) ketabton.com: The Digital Library

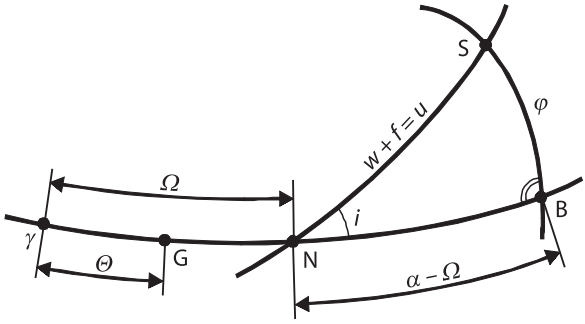

Fig. 11.4.
Orbit-equator-meridian triangle

The variables (r, φ, λ) of the geopotential disturbance function in the ECEF system are transformed into orbital elements in the ECSF system by using the following relations (cf. Fig. 11.4, cf. Kaula 1966):

$$\begin{aligned}
&\sin\varphi = \sin i \sin u \\
&\lambda = \alpha - \Theta = \Omega - \Theta + (\alpha - \Omega) \\
&\cos(\alpha - \Omega) = \frac{\cos u}{\cos\varphi} \\
&\sin(\alpha - \Omega) = \frac{\sin u \cos i}{\cos\varphi}
\end{aligned} \quad . \tag{11.100}$$

Where α is the right ascension of the satellite, $u = \omega + f$, Θ is the Greenwich Sidereal Time, and other parameters are Keplerian elements. It is obvious that such a coordinate transformation only takes the Earth's rotation into account; this will cause a coordinate perturbation (cf. Sect. 11.2.6). But such an effect can be neglected by the first order solution. Substituting the first formula of Eq. 11.100 into Eq. 11.99 and taking the triangle formula (for reducing the order) into account, one has

$$R_2 = \frac{b}{r^3}\left[\frac{3}{2}\sin^2 i(1-\cos 2u) - 1\right], \tag{11.101}$$

where

$$r = \frac{a(1-e^2)}{1+e\cos f}, \tag{11.102}$$

where Ω has not appeared in the zonal disturbance. Taking the partial derivatives of f with respect to (M, e) and r with respect to (a, M, e) into account (cf. Sect. 11.1), the derivatives of R_2 with respect to Keplerian elements are then

$$\frac{\partial R_2}{\partial a} = \frac{\partial R_2}{\partial r}\frac{\partial r}{\partial a} = \frac{-3}{a}R_2, \quad \frac{\partial R_2}{\partial \Omega} = 0,$$

$$\frac{\partial R_2}{\partial i} = \frac{b}{r^3}\left[\frac{3}{2}\sin 2i(1-\cos 2u)\right],$$

(c) ketabton.com: The Digital Library

$$\frac{\partial R_2}{\partial \omega}=\frac{b}{r^3}\left[3\sin^2 i\sin 2u\frac{\partial u}{\partial \omega}\right]=\frac{3b}{r^3}\sin^2 i\sin 2u\,,$$

$$\frac{\partial R_2}{\partial e}=\frac{-3R_2}{r}\frac{\partial r}{\partial e}+\frac{b}{r^3}\left[3\sin^2 i\sin 2u\frac{\partial u}{\partial e}\right]$$
$$=\frac{3a\cos f}{r}R_2+\frac{b}{r^3}\left[3\sin^2 i\sin 2u\frac{2+e\cos f}{1-e^2}\sin f\right] \quad \text{and}$$

$$\frac{\partial R_2}{\partial M}=\frac{-3R_2}{r}\frac{\partial r}{\partial M}+\frac{b}{r^3}\left[3\sin^2 i\sin 2u\frac{\partial u}{\partial M}\right]$$
$$=\frac{-3ae\sin f}{r\sqrt{1-e^2}}R_2+\frac{b}{r^3}\left[3\sin^2 i\sin 2u\left(\frac{a}{r}\right)^2\sqrt{1-e^2}\right]. \tag{11.103}$$

Substituting the above derivatives and R_2 into the equation of motion 11.103, one has

$$\frac{\mathrm{d}a}{\mathrm{d}t}=\frac{6b\sqrt{1-e^2}}{na^4}\left\{\frac{-e}{(1-e^2)}\frac{a^4}{r^4}\sin f\left[\frac{3}{2}\sin^2 i(1-\cos 2u)-1\right]+\frac{a^5}{r^5}\left[\sin^2 i\sin 2u\right]\right\},$$

$$\frac{\mathrm{d}e}{\mathrm{d}t}=\frac{3b(1-e^2)^{3/2}}{na^5e}\left\{\frac{-e}{(1-e^2)}\frac{a^4}{r^4}\sin f\left[\frac{3}{2}\sin^2 i(1-\cos 2u)-1\right]+\frac{a^5}{r^5}\left[\sin^2 i\sin 2u\right]\right\}$$
$$-\frac{3b\sqrt{1-e^2}}{na^5e}\frac{a^3}{r^3}\sin^2 i\sin 2u\,,$$

$$\frac{\mathrm{d}\omega}{\mathrm{d}t}=\frac{3b\sqrt{1-e^2}}{na^5e}\left\{\frac{a^4}{r^4}\cos f\left[\frac{3}{2}\sin^2 i(1-\cos 2u)-1\right]+\frac{a^3}{r^3}\left[\sin^2 i\sin 2u\frac{2+e\cos f}{1-e^2}\sin f\right]\right\}$$
$$-\frac{3b}{na^5\sqrt{1-e^2}}\frac{a^3}{r^3}\left[\cos^2 i(1-\cos 2u)\right],$$

$$\frac{\mathrm{d}i}{\mathrm{d}t}=\frac{3b}{2na^5\sqrt{1-e^2}}\frac{a^3}{r^3}\sin 2i\sin 2u\,,$$

$$\frac{\mathrm{d}\Omega}{\mathrm{d}t}=\frac{3b}{na^5\sqrt{1-e^2}}\frac{a^3}{r^3}\left[\cos i(1-\cos 2u)\right] \quad \text{and}$$

$$\frac{\mathrm{d}M}{\mathrm{d}t}=n+\frac{6b}{na^5}\frac{a^3}{r^3}\left[\frac{3}{2}\sin^2 i(1-\cos 2u)-1\right]$$
$$-\frac{3b(1-e^2)}{na^5e}\left\{\begin{array}{l}\left[\frac{a^4}{r^4}\cos f\left[\frac{3}{2}\sin^2 i(1-\cos 2u)-1\right]\right.\\ \left.+\frac{a^3}{r^3}\left[\sin^2 i\sin 2u\frac{2+e\cos f}{1-e^2}\sin f\right]\right]\end{array}\right. . \tag{11.104}$$

(c) ketabton.com: The Digital Library

For convenience the right-hand side of the above equations will be separated into three parts:

$$\frac{\mathrm{d}\sigma_i}{\mathrm{d}t}=\left(\frac{\mathrm{d}\sigma_i}{\mathrm{d}t}\right)_0+\left(\frac{\mathrm{d}\sigma_i}{\mathrm{d}t}\right)_\omega+\left(\frac{\mathrm{d}\sigma_i}{\mathrm{d}t}\right)_f \quad \text{or} \tag{11.105}$$

$$\frac{\mathrm{d}\sigma_i}{\mathrm{d}t}=\dot{\sigma}_{i0}+\left(\frac{\mathrm{d}\sigma_i}{\mathrm{d}t}\right)_\omega+\left(\frac{\mathrm{d}\sigma_i}{\mathrm{d}t}-\dot{\sigma}_{i0}-\dot{\sigma}_{i\omega}\right), \tag{11.106}$$

where the first term (denoted by $\dot{\sigma}_{i0}$) on the right-hand side includes all terms that are only functions of (a, i, e), the second term includes all terms of ω (without f) (denoted by $\dot{\sigma}_{i\omega}$), and the third term includes all terms of f. They are denoted by the sub-index of 0, ω and f, respectively. Equation 11.106 is needed for later integral variable transformation. The second terms on the right-hand side of the above two equations are the same. It is notable that the r is a function of f. The solution of the R_2 perturbed orbit is the integration of the above equations between initial epoch t_0 and any instantaneous epoch t. The three terms on the right side can be integrated with the integral variable of t, ω, and f respectively. The integral variable dt can be changed to df by

$$\mathrm{d}t=\frac{\partial t}{\partial f}\mathrm{d}f=\frac{1}{\dfrac{\partial f}{\partial M}\dfrac{\partial M}{\partial t}}\mathrm{d}f=\left(\frac{r}{a}\right)^2\frac{1}{\sqrt{1-e^2}}\frac{1}{n}\mathrm{d}f\,. \tag{11.107}$$

All terms of ω are presented in the terms of $\sin 2u$ and $\cos 2u$. Omitting the terms of $\sin 2u$ and $\cos 2u$ in Eq. 11.104, the remaining terms of f are included in the following functions:

$$\left(\frac{a}{r}\right)^3,\quad \left(\frac{a}{r}\right)^4\sin f \quad \text{and} \quad \left(\frac{a}{r}\right)^4\cos f\,, \tag{11.108}$$

where

$$\frac{a}{r}=\frac{1+e\cos f}{1-e^2},\quad \left(\frac{a}{r}\right)^2=\frac{1+0.5e^2+2e\cos f+0.5e^2\cos 2f}{(1-e^2)^2}\,,$$

$$\left(\frac{a}{r}\right)^3=\frac{1+1.5e^2+(3e+0.75e^3)\cos f+1.5e^2\cos 2f+0.25e^3\cos 3f}{(1-e^2)^3}\,,$$

$$\left(\frac{a}{r}\right)^4=\frac{1}{(1-e^2)^4}\left[\begin{array}{l}\left(1+3e^2+\dfrac{3}{8}e^4\right)+(4e+3e^3)\cos f\\ +(3e^2+0.5e^4)\cos 2f+e^3\cos 3f+\dfrac{1}{8}e^4\cos 4f\end{array}\right],$$

$$\left(\frac{a}{r}\right)^4\sin f=\frac{1}{(1-e^2)^4}\left[\begin{array}{l}\left(1+1.5e^2+\dfrac{1}{8}e^4\right)\sin f+(2e+e^3)\sin 2f\\ +\left(1.5e^2+\dfrac{3}{16}e^4\right)\sin 3f+0.5e^3\sin 4f+\dfrac{1}{16}e^4\sin 5f\end{array}\right],$$

(c) ketabton.com: The Digital Library

$$\left(\frac{a}{r}\right)^4 \cos f = \frac{1}{(1-e^2)^4}\begin{bmatrix} (2e+1.5e^3)+\left(1+4.5e^2+\frac{5}{8}e^4\right)\cos f \\ +(2e+2e^3)\cos 2f+\left(1.5e^2+\frac{5}{16}e^4\right)\cos 3f \\ +0.5e^3\cos 4f+\frac{1}{16}e^4\cos 5f \end{bmatrix}, \tag{11.109}$$

and

$$\begin{aligned} \sin jf \sin mf &= -0.5\left[\cos(j+m)f-\cos(j-m)f\right] \\ \cos jf \cos mf &= 0.5\left[\cos(j+m)f+\cos(j-m)f\right] \\ \sin jf \cos mf &= 0.5\left[\sin(j+m)f+\sin(j-m)f\right] \end{aligned} . \tag{11.110}$$

Then the first term (long term perturbation) in Eq. 11.106 is

$$\begin{aligned} \left(\frac{\mathrm{d}a}{\mathrm{d}t}\right)_0 &= \left(\frac{\mathrm{d}e}{\mathrm{d}t}\right)_0 = \left(\frac{\mathrm{d}i}{\mathrm{d}t}\right)_0 = 0 \\ \left(\frac{\mathrm{d}\omega}{\mathrm{d}t}\right)_0 &= \frac{3b}{na^5(1-e^2)^{3.5}}\left(4\sin^2 i-3+\frac{15}{4}e^2\sin^2 i-3e^2\right) \\ \left(\frac{\mathrm{d}\Omega}{\mathrm{d}t}\right)_0 &= \frac{3b}{2na^5}\cos i\frac{(2+3e^2)}{(1-e^2)^{3.5}} \\ \left(\frac{\mathrm{d}M}{\mathrm{d}t}\right)_0 &= n+\frac{9b}{2na^5}\left(\frac{3}{2}\sin^2 i-1\right)\frac{e^2}{(1-e^2)^3} \end{aligned} . \tag{11.111}$$

Due to the slow changing property of the variable ω, the integral variable changing between t and ω can be approximated by

$$\mathrm{d}t = \left(\frac{\mathrm{d}\omega}{\mathrm{d}t}\right)_0^{-1}\mathrm{d}\omega\,. \tag{11.112}$$

The second term (long period perturbation) in Eq. 11.106 exists only in $\sin 2u$ and $\cos 2u$ related terms. All $\sin 2u$ and $\cos 2u$ terms are factorised by the following functions:

$$\left(\frac{a}{r}\right)^3,\quad \left(\frac{a}{r}\right)^5,\quad \left(\frac{a}{r}\right)^4\sin f,\quad \left(\frac{a}{r}\right)^4\cos f \quad \text{and} \quad \left(\frac{a}{r}\right)^3\frac{2+e\cos f}{1-e^2}\sin f\,, \tag{11.113}$$

Where

$$\left(\frac{a}{r}\right)^5 = \frac{1}{(1-e^2)^5}\begin{bmatrix} \left(1+5e^2+1\frac{7}{8}e^4\right)+\left(5e+7.5e^3+\frac{5}{8}e^5\right)\cos f \\ +(5e^2+2.5e^4)\cos 2f+\left(2.5e^3+\frac{5}{16}e^5\right)\cos 3f \\ +\frac{5}{8}e^4\cos 4f+\frac{1}{16}e^5\cos 5f \end{bmatrix} \quad \text{and}$$

(c) ketabton.com: The Digital Library

$$\left(\frac{a}{r}\right)^3 \frac{2+e\cos f}{1-e^2}\sin f = \frac{1}{(1-e^2)^4}\begin{bmatrix}\left(2+2.25e^2+\frac{1}{8}e^4\right)\sin f\\ +(3.5e+0.25e^3)\sin 2f\\ +\left(2.5e^2+\frac{3}{16}e^4\right)\sin 3f\\ +\frac{5}{8}e^3\sin 4f+\frac{1}{16}e^4\sin 5f\end{bmatrix}. \tag{11.114}$$

From properties of Eq. 11.110 and

$$\begin{aligned}\sin 2u &= \sin 2\omega\cos 2f+\cos 2\omega\sin 2f\\ \cos 2u &= \cos 2\omega\cos 2f-\sin 2\omega\sin 2f\end{aligned}', \tag{11.115}$$

it is obvious that all ω terms (without f) may be created only by multiplying $\sin 2u$ and $\cos 2u$ by $\sin 2f$ and $\cos 2f$ in Eq. 11.113. In other words, only $\sin^2 2f$ and $\cos^2 2f$ will lead to a constant of 0.5. Therefore when seeking the ω terms (without f), just $\sin 2f$ and $\cos 2f$ related terms in Eq. 11.113 have to be taken into account. Thus,

$$\left(\frac{da}{dt}\right)_\omega = \frac{3be^2(2+e^2)}{na^4(1-e^2)^{4.5}}\sin^2 i\sin 2\omega\,,$$

$$\left(\frac{de}{dt}\right)_\omega = \frac{3be(1+5e^2)}{4na^5(1-e^2)^{3.5}}\sin^2 i\sin 2\omega\,,$$

$$\left(\frac{d\omega}{dt}\right)_\omega = \frac{3b}{4na^5(1-e^2)^{3.5}}\left((1-5.5e^2)\sin^2 i+3e^2\cos^2 i\right)\cos 2\omega\,,$$

$$\left(\frac{di}{dt}\right)_\omega = \frac{9be^2}{8na^5(1-e^2)^{3.5}}\sin 2i\sin 2\omega\,,$$

$$\left(\frac{d\Omega}{dt}\right)_\omega = \frac{-9be^2}{4na^5(1-e^2)^{3.5}}\cos i\cos 2\omega \quad \text{and}$$

$$\left(\frac{dM}{dt}\right)_\omega = -\frac{3b(2+7e^2)}{8na^5(1-e^2)^3}\sin^2 i\cos 2\omega\,. \tag{11.116}$$

The third term of Eq. 11.106 includes all terms of f and can be denoted and represented by

$$\left(\frac{d\sigma_i}{dt}\right)_f = \left(\frac{d\sigma_i}{dt}-\dot\sigma_{i0}-\dot\sigma_{i\omega}\right) = \sum_{m=1}^{m(i)}\left(A'''_{im}\cos mf+B'''_{im}\sin mf\right), \tag{11.117}$$

where $m(i)$ is the upper limit of the summation, $m(i) = (7, 7, 7, 5, 5, 7)$ for the related Keplerian elements, A'''_{im}, B'''_{im} are coefficients as well as functions of (a, e, i, ω) and can be derived from Eqs. 11.104, 11.111 and 11.116. Through integral variable transformation (cf. Eq. 11.107), one has

(c) ketabton.com: The Digital Library

$$\left(\frac{\mathrm{d}\sigma_i}{\mathrm{d}t}\right)_f \left(\frac{r}{a}\right)^2 \frac{1}{\sqrt{1-e^2}}\frac{1}{n} = \sum_{m=1}^{m(i)-2} \left(A''_{im}\cos mf + B''_{im}\sin mf\right), \tag{11.118}$$

where the upper limit of the summation is reduced by 2. A''_{im}, B''_{im} are transformed coefficients. It is notable that in Eq. 11.118 the constant term ($m = 0$) doesn't exist because of the property of the short periodic term perturbations.

For the integral area of (t_0, t), related areas for ω and f are (ω_0, ω) and (f_0, f) respectively. For any f there is an integer k, so that $k2\pi + f_0 \le f \le (k+1)2\pi + f_0$. Using the periodic property, the integration of the terms of Eq. 11.118 over the area of (f_0, $f_0 + 2k\pi$) is zero; therefore, Eq. 11.118 just needs to be integrated over the area of ($f_0 + 2k\pi$, f). Denoting the coefficients of $\sin 2\omega$ and $\cos 2\omega$ in Eq. 11.116 as

$$\left(\frac{\mathrm{d}\sigma_i}{\mathrm{d}t}\right)_{\omega s} \quad \text{and} \quad \left(\frac{\mathrm{d}\sigma_i}{\mathrm{d}t}\right)_{\omega c},$$

the total integration of Eq. 11.106 is then

$$\int_{t_0}^{t} \mathrm{d}\sigma_i = \int_{t_0}^{t} \dot{\sigma}_{i0}\mathrm{d}t + \int_{\omega_0}^{\omega} \left(\frac{\mathrm{d}\sigma_i}{\mathrm{d}t}\right)_{\omega} \left(\frac{\mathrm{d}\omega}{\mathrm{d}t}\right)_0^{-1} \mathrm{d}\omega + \int_{k2\pi+f_0}^{f} \left(\frac{\mathrm{d}\sigma_i}{\mathrm{d}t}\right)_f \left(\frac{r}{a}\right)^2 \frac{1}{\sqrt{1-e^2}}\frac{1}{n}\mathrm{d}f \tag{11.119}$$

or

$$\begin{aligned}\sigma_i(t) &= \sigma_i(t_0) + \dot{\sigma}_{i0}(t-t_0) \\ &+ \frac{1}{2}\left(\frac{\mathrm{d}\omega}{\mathrm{d}t}\right)_0^{-1}\left[\left(\frac{\mathrm{d}\sigma_i}{\mathrm{d}t}\right)_{\omega c}(\sin 2\omega - \sin 2\omega_0) - \left(\frac{\mathrm{d}\sigma_i}{\mathrm{d}t}\right)_{\omega s}(\cos 2\omega - \cos 2\omega_0)\right] \\ &+ \sum_{m=1}^{m(i)-2}\frac{1}{m}\left[A''_{im}(\sin mf - \sin mf_0) - B''_{im}(\cos mf - \cos mf_0)\right]\end{aligned} \tag{11.120}$$

That is, the $\overline{C}_{20}$ term perturbation of the orbit has a linear term (long-term perturbation), a long periodic term (with argument of ω), and a short period term (with argument of f). The instantaneous Keplerian elements are equal to the initial elements plus the perturbations.

Such a $\overline{C}_{20}$ disturbed orbit solution provides an indication of a general model of the perturbed orbit, which will be used as a basis for orbit correction purposes and will be discussed in the next section.

11.4 Orbit Correction

When the orbit errors of GPS satellites become not negligible for special GPS applications, a process of orbit correction is the first option. Generally, orbit correction is applied to the regional or very long baseline of GPS precise positioning. Even IGS precise GPS orbits are not homogenously precise, because they are dependent on the distribution of the IGS reference stations and the length of the data used. The orbit correction

(c) ketabton.com: The Digital Library

is an adjustment or filtering process in which, besides the station position, the orbit errors are also modelled, determined, and corrected based on a known orbit.

Keplerian elements also describe the orbit geometry for instantaneous time. Orbit errors can be considered geometric element errors of the orbit in general. Recalling above discussions of the $\overline{C}_{20}$ perturbed orbit solution, a general orbit model can be written as

$$\sigma_j(t) = \sigma_{jc}(t) + \dot{\sigma}_{j0}(t-t_0) + A_{j\omega}\cos 2\omega + B_{j\omega}\sin 2\omega + \sum_{m=1}^{m(j)} \left[A'_{jm}\cos mf + B'_{jm}\sin mf \right] , \tag{11.121}$$

where $\sigma_j(t)$, $\sigma_{jc}(t)$, $\dot{\sigma}_{i0}$ are true orbit element at time t, computed element at t, element rate with respect to the initial epoch t_0, A_{ji}, B_{ji}, A'_{jm}, B'_{jm} are the coefficients of the long and short periodic perturbations respectively, and $m(j)$ is the truncating integer of index m related to the j^{th} Keplerian element. ω and f are Keplerian elements. Generally speaking, the coefficients of A'_{jm}, B'_{jm} are also functions of ω, and ω can be considered in the short periodic term as a constant. Therefore Eq. 11.121 is equivalent to

$$\sigma_j(t) = \sigma_{jc}(t) + \dot{\sigma}_{j0}(t-t_0) + A_{j\omega}\cos 2\omega + B_{j\omega}\sin 2\omega + \sum_{m=1}^{m(j)} \left[A_{jm}\cos mu + B_{jm}\sin mu \right] , \tag{11.122}$$

where $u = \omega + f$. The order of the polynomial term can be risen to 2, further terms of ω may also be added, and $m(j)$ is selectable. The selection of the number of the order depends on the need and the situation of orbit errors.

In the GPS observation equations (cf. Chap. 6), the orbit state vector is presented in the range or range rate functions. It depends on the use of the GPS observables. We denote the range and range rate function generally as ρ ; their partial derivatives with respect to the orbit state vector are given in Sect. 6.3 and have the forms of

$$\frac{\partial \rho}{\partial \vec{r}} \quad \text{and} \quad \frac{\partial \rho}{\partial \dot{\vec{r}}} ,$$

where the satellite state vector is $(\vec{r}, \dot{\vec{r}})$. The relations between $(\vec{r}, \dot{\vec{r}})$ and Keplerian elements σ_j are discussed in Sect. 3.1. Also, the relations between σ_j and the parameters of the orbit correction model are given in Eq. 11.122. Therefore, the orbit correction parts in the GPS observation equations are then

$$\frac{\partial \rho}{\partial \vec{r}} \frac{\partial \vec{r}}{\partial \vec{\sigma}} \frac{\partial \vec{\sigma}}{\partial \vec{y}} \Delta \vec{y}^T + \frac{\partial \rho}{\partial \dot{\vec{r}}} \frac{\partial \dot{\vec{r}}}{\partial \vec{\sigma}} \frac{\partial \vec{\sigma}}{\partial \vec{y}} \Delta \vec{y}^T , \tag{11.123}$$

where $\vec{y}$, $\Delta\vec{y}$ are the parameter vector in model 11.122 and the parameter correction vector of the model, and $\vec{\sigma}$ is the vector of Keplerian elements. If the initial parameter vector is selected as zero, then $\vec{y} = \Delta\vec{y}$. It is obvious that

$$\vec{y} = \left(\dot{\sigma}_{j0}, A_{j\omega}, B_{j\omega}, A_{jm}, B_{jm} \right) \tag{11.124}$$

(c) ketabton.com: The Digital Library

and

$$\frac{\partial \sigma_j}{\partial(\dot{\sigma}_{j0}, A_{j\omega}, B_{j\omega}, A_{jm}, B_{jm})} = \left((t-t_0), \cos 2\omega, \sin 2\omega, \cos mu, \sin mu\right). \tag{11.125}$$

Here parameters A_{jm}, B_{jm} represent symbolically the unknowns of all m. For the convenience of presenting the partial derivatives of the state vector with respect to the Keplerian elements, the Keplerian element vector is reordered as

$$\vec{\sigma} = \left(\Omega, i, \omega, a, e, M\right). \tag{11.126}$$

This does not affect Eq. 11.125, because the right-hand side of the equation has nothing to do with index j. According to the formulas in Sect. 3.1.3 (Eqs. 3.41–3.43)

$$\begin{pmatrix} \vec{r} \\ \dot{\vec{r}} \end{pmatrix} = R_3(-\Omega) R_1(-i) R_3(-\omega) \begin{pmatrix} \vec{q} \\ \dot{\vec{q}} \end{pmatrix}, \tag{11.127}$$

where

$$\vec{q} = \begin{pmatrix} a(\cos E - e) \\ a\sqrt{1-e^2}\sin E \\ 0 \end{pmatrix} = \begin{pmatrix} r\cos f \\ r\sin f \\ 0 \end{pmatrix} \quad \text{and} \tag{11.128}$$

$$\dot{\vec{q}} = \begin{pmatrix} -\sin E \\ \sqrt{1-e^2}\cos E \\ 0 \end{pmatrix} \frac{na}{1-e\cos E} = \begin{pmatrix} -\sin f \\ e+\cos f \\ 0 \end{pmatrix} \frac{na}{\sqrt{1-e^2}}, \tag{11.129}$$

one has

$$\frac{\partial \vec{r}}{\partial(\Omega, i, \omega)} = \frac{\partial R}{\partial(\Omega, i, \omega)} \vec{q} \quad \text{and} \quad \frac{\partial \dot{\vec{r}}}{\partial(\Omega, i, \omega)} = \frac{\partial R}{\partial(\Omega, i, \omega)} \dot{\vec{q}}, \tag{11.130}$$

where $(\vec{q}, \dot{\vec{q}})$ are position and velocity vectors of the satellite in the orbital plane coordinate system, and

$$R = R_3(-\Omega) R_1(-i) R_3(-\omega) \quad \text{and} \tag{11.131}$$

$$\frac{\partial R}{\partial(\Omega, i, \omega)} = \left(\frac{\partial R_3(-\Omega)}{\partial \Omega} R_1(-i) R_3(-\omega), R_3(-\Omega) \frac{\partial R_1(-i)}{\partial i} R_3(-\omega), R_3(-\Omega) R_1(-i) \frac{\partial R_3(-\omega)}{\partial \omega} \right),$$

where

$$\frac{\partial R_1(-i)}{\partial i} = \begin{pmatrix} 0 & 0 & 0 \\ 0 & -\sin i & -\cos i \\ 0 & \cos i & -\sin i \end{pmatrix},$$

(c) ketabton.com: The Digital Library

$$\frac{\partial R_3(-\Omega)}{\partial \Omega} = \begin{pmatrix} -\sin\Omega & -\cos\Omega & 0 \\ \cos\Omega & -\sin\Omega & 0 \\ 0 & 0 & 0 \end{pmatrix} \quad \text{and}$$

$$\frac{\partial R_3(-\omega)}{\partial \omega} = \begin{pmatrix} -\sin\omega & -\cos\omega & 0 \\ \cos\omega & -\sin\omega & 0 \\ 0 & 0 & 0 \end{pmatrix}.$$

For the Keplerian elements in the orbital plane (a, e, M), one has

$$\frac{\partial \vec{r}}{\partial(a,e,M)} = R\frac{\partial \vec{q}}{\partial(a,e,M)} \quad \text{and} \quad \frac{\partial \dot{\vec{r}}}{\partial(a,e,M)} = R\frac{\partial \dot{\vec{q}}}{\partial(a,e,M)}, \tag{11.132}$$

where

$$\frac{\partial \vec{q}}{\partial(a,e,M)} = \begin{pmatrix} \cos E - e & \dfrac{-a\sin^2 E}{1-e\cos E} - a & \dfrac{-a\sin E}{1-e\cos E} \\ \sqrt{1-e^2}\sin E & a\sqrt{1-e^2}\left(\dfrac{\sin 2E}{2(1-e\cos E)} - \dfrac{e\sin E}{1-e^2}\right) & \dfrac{a\sqrt{1-e^2}\cos E}{1-e\cos E} \\ 0 & 0 & 0 \end{pmatrix}$$

and

$$\frac{\partial \dot{\vec{q}}}{\partial(a,e,M)} = \begin{pmatrix} \dfrac{n\sin E}{2(1-e\cos E)} & \dfrac{na\sin E(e-2\cos E+e\cos^2 E)}{(1-e\cos E)^3} & \dfrac{na(e-\cos E)}{(1-e\cos E)^3} \\ \dfrac{-n\sqrt{1-e^2}\cos E}{2(1-e\cos E)} & \dfrac{na\left[1+e^2-2e\cos E+\sin^2 E(e\cos E-2)\right]}{\sqrt{1-e^2}(1-e\cos E)^3} & \dfrac{-na\sqrt{1-e^2}\sin E}{(1-e\cos E)^3} \\ 0 & 0 & 0 \end{pmatrix}.$$

The partial derivatives formulas given in Sect. 11.1 and the relation in Eq. 3.32 between n and a (mean angular velocity and semimajor axis of the satellite) given in Chap. 3 are used, i.e.

$$\frac{\partial E}{\partial(e,M)} = \left(\frac{a}{r}\sin E, \frac{a}{r}\right) \quad \text{and}$$

$$n^2 = \mu/a^3.$$

(c) ketabton.com: The Digital Library

11.5 Principle of GPS Precise Orbit Determination

Recalling the discussions made in Sect. 11.1, the perturbed orbit of the satellite is the solution (or integration)

$$\vec{X}(t)=\vec{X}(t_0)+\int_{t_0}^{t}\vec{F}\mathrm{d}t\ , \tag{11.133}$$

which can be obtained by integrating the differential state equation under the initial condition

$$\begin{cases}\dot{\vec{X}}(t)=\vec{F}\\ \vec{X}(t_0)=\vec{X}_0\end{cases}, \tag{11.134}$$

where $\vec{X}(t)$ is the instantaneous state vector of the satellite, $\vec{X}(t_0)$ is the initial state vector at time t_0 (denoted by $\vec{X}_0$), $\vec{F}$ is a function of the state vector $\vec{X}(t)$ and time t, and

$$\vec{X}=\begin{pmatrix}\vec{r}\\ \dot{\vec{r}}\end{pmatrix}\ \text{ and }\ \vec{F}=\begin{pmatrix}\dot{\vec{r}}\\ \vec{f}/m\end{pmatrix},$$

where $\vec{f}$ is the summated force vector of all possible force vectors acting on the satellite, m is the mass of satellite, and $\vec{r}$, $\dot{\vec{r}}$ are the position and velocity vectors of the satellite.

If the initial state vector and the force vectors are precisely known, then the precise orbits can be computed through the integration in Eq. 11.133. Expanding the integration time t into the future, the so-called forecasted orbits can be obtained. Therefore, suitable numerical integration algorithms are needed (see next section).

In practice, the precise initiate state vector and force models have to be determined, which are related to the approximate initial state vector and force models. These can be realised through suitable parameterisation of the models in the GPS observation equations and then the parameters can be solved by adjustment or filtering.

We denote the range and range rate function generally by ρ; their partial derivatives with respect to the orbit state vector are given in Sect. 6.3 and have the forms of

$$\frac{\partial\rho}{\partial\vec{r}},\ \frac{\partial\rho}{\partial\dot{\vec{r}}},\quad\text{or}\quad\frac{\partial\rho}{\partial\vec{X}}\ .$$

Therefore, the orbit parameter related parts in the linearised GPS observation equation are then

$$\frac{\partial\rho}{\partial(\vec{r},\dot{\vec{r}})}\frac{\partial(\vec{r},\dot{\vec{r}})}{\partial\vec{y}}\Delta\vec{y}^{T},\quad\text{or}\quad\frac{\partial\rho}{\partial\vec{X}}\frac{\partial\vec{X}}{\partial\vec{y}}\Delta\vec{y}^{T}\ , \tag{11.135}$$

where

$$\vec{y}=\left(\vec{X}_0,\vec{Y}\right),\quad\Delta\vec{y}^{T}=\left(\Delta\vec{X}_0,\Delta\vec{Y}\right)^{T},\quad\frac{\partial\vec{X}}{\partial\vec{y}}=\frac{\partial\vec{X}}{\partial(\vec{X}_0,\vec{Y})}\ .$$

(c) ketabton.com: The Digital Library

$\vec{X}$, $\vec{Y}$ are the state vector of satellite and the parameter vector of the force models, and index 0 denotes the related initial vectors of time t_0. $\bar{y}$ is the total unknown vector of the orbit determination problem, the related correction vector is $\Delta\bar{y} = \bar{y} - \bar{y}_0$, and $\Delta\vec{X}_0$ is the correction vector of the initial state vector. The partial derivatives of $\vec{X}$ with respect to $\bar{y}$ is called transition matrix which has the dimension of $6\times(6+n)$, where n is the dimension of vector $\vec{Y}$. The partial derivatives of the equation of motion of the satellite (cf., Eq. 11.134) with respect to the vector $\bar{y}$ are

$$\frac{\partial\dot{\vec{X}}(t)}{\partial\bar{y}} = \frac{\partial\vec{F}}{\partial\bar{y}} = \frac{\partial\vec{F}}{\partial\vec{X}}\frac{\partial\vec{X}}{\partial\bar{y}} + \left(\frac{\partial\vec{F}}{\partial\bar{y}}\right)^{*}, \tag{11.136}$$

where the superscript * denotes the partial derivatives of $\vec{F}$ with respect to the explicit parameter vector $\bar{y}$ in $\vec{F}$, and

$$D(t) = \left(\frac{\partial\vec{F}}{\partial\vec{X}}\right) = \begin{pmatrix} 0_{3\times3} & E_{3\times3} \\ \frac{1}{m}\frac{\partial\vec{f}}{\partial\vec{r}} & \frac{1}{m}\frac{\partial\vec{f}}{\partial\dot{\vec{r}}} \end{pmatrix} = \begin{pmatrix} 0_{3\times3} & E_{3\times3} \\ A(t) & B(t) \end{pmatrix},$$

$$C(t) = \left(\frac{\partial\vec{F}}{\partial\bar{y}}\right)^{*} = \begin{pmatrix} 0_{3\times6} & 0_{3\times n} \\ 0_{3\times6} & \frac{1}{m}\frac{\partial\vec{f}}{\partial\vec{Y}} \end{pmatrix} = \begin{pmatrix} 0_{3\times(6+n)} \\ G(t) \end{pmatrix}, \tag{11.137}$$

where E is an identity matrix; the partial derivatives will be discussed and derived in a later section in detail. It is notable that the force parameters are not functions of t. Therefore the order of the differentiations can be exchanged. Denoting transition matrix by $\Phi(t, t_0)$, then Eq. 11.136 turns out to be

$$\frac{\mathrm{d}\Phi(t,t_0)}{\mathrm{d}t} = D(t)\Phi(t,t_0) + C(t)\,. \tag{11.138}$$

Equation 11.138 is called differential equation of the transition matrix or variational equation (cf., e.g., Montenbruck and Gill 2000). Denoting

$$\Phi(t,t_0) = \begin{pmatrix} \Psi(t,t_0) \\ \dot{\Psi}(t,t_0) \end{pmatrix}, \tag{11.139}$$

an alternate expression of Eq. 11.138 can be obtained by substituting Eqs. 11.139 and 11.137 into Eq. 11.138

$$\frac{\mathrm{d}^2\Psi(t,t_0)}{\mathrm{d}t^2} = A(t)\Psi(t,t_0) + B(t)\frac{\mathrm{d}\Psi(t,t_0)}{\mathrm{d}t} + G(t)\,. \tag{11.140}$$

The initial value matrix is (initial state vector does not depend on force parameters):

$$\Phi(t_0,t_0) = \begin{pmatrix} E_{6\times6} & 0_{6\times n} \end{pmatrix}. \tag{11.141}$$

That is, in the GPS observation equation, the transition matrix has to be obtained by solving initial value problem of the variation equation 11.138 or 11.140. The problem is solved by integration traditionally.

(c) ketabton.com: The Digital Library

11.5.1 Algebra Solution of the Variation Equation

The variation equation can also be solved by numerical differentiation.

Equation 11.140 is a matrix differential equation system of size $3\times(6+n)$. Because $A(t)$ and $B(t)$ are 3×3 matrices, the differential equations are independent from column to column. That is, we need just to discuss the solution of the equation of a column. For column j, the Eqs. 11.140 and 11.141 are

$$\frac{\mathrm{d}^2\Psi_{ij}(t)}{\mathrm{d}t^2}=\sum_{k=1}^{3}\left(A_{ik}(t)\Psi_{kj}(t)+B_{ik}(t)\frac{\mathrm{d}\,\Psi_{kj}(t)}{\mathrm{d}t}\right)+G_{ij}(t),\quad i=1,2,3\,, \tag{11.142}$$

$$\begin{pmatrix}\Psi_{ij}(t_0)\\ \dot{\Psi}_{ij}(t_0)\end{pmatrix}=\begin{pmatrix}\delta_{ij}\\ \delta_{(i+3)j}\end{pmatrix},\quad i=1,2,3,\qquad \delta_{kj}=\begin{cases}1 & \text{if } k=j\\ 0 & \text{if } k\neq j\end{cases},$$

where index ij denotes the related element of the matrix. For time interval $[t_0, t]$ and differentiation step $h=(t-t_0)/m$, one has $t_n=t_0+nh$, $n=1,\ldots,m$ and

$$\left.\frac{\mathrm{d}^2\Psi_{ij}(t)}{\mathrm{d}t^2}\right|_{t=t_n}=\frac{\Psi_{ij}(t_{n+1})-2\Psi_{ij}(t_n)+\Psi_{ij}(t_{n-1})}{h^2},\quad i=1,2,3\,,$$

$$\left.\frac{\mathrm{d}\mathrm{d}\,\Psi_{ij}(t)}{\mathrm{d}t}\right|_{t=t_n}=\frac{\Psi_{ij}(t_{n+1})-\Psi_{ij}(t_{n-1})}{2h},\quad \Psi_{ij}(t)\big|_{t=t_n}=\Psi_{ij}(t_n),\qquad i=1,2,3\,. \tag{11.143}$$

Then Eq. 11.142 turns out to be

$$\Psi_{ij}(t_0)=\Psi_{ij}(t_0),\qquad \Psi_{ij}(t_1)=\Psi_{ij}(t_0)+h\dot{\Psi}_{ij}(t_0),\quad i=1,2,3\,.$$

$$\frac{\Psi_{ij}(t_{n+1})-2\Psi_{ij}(t_n)+\Psi_{ij}(t_{n-1})}{h^2}=$$
$$\sum_{k=1}^{3}\left(A_{ik}(t_n)\Psi_{kj}(t_n)+B_{ik}(t_n)\frac{\Psi_{kj}(t_{n+1})-\Psi_{kj}(t_{n-1})}{2h}\right)+G_{ij}(t_n),\quad i=1,2,3 \tag{11.144}$$

where $n=1, 2, \ldots, m-1$. For $i=1, 2, 3$ and the sequential number n, there are three equations and three unknowns of time t_{n+1}; so that the initial value problem has a set of unique solutions sequentially. Eqquation 11.144 can be rewritten as

$$\left(\frac{E}{h^2}-\frac{B(t_n)}{2h}\right)\begin{pmatrix}\Psi_{1j}(t_{n+1})\\ \Psi_{2j}(t_{n+1})\\ \Psi_{3j}(t_{n+1})\end{pmatrix}=\begin{pmatrix}R_1\\ R_2\\ R_3\end{pmatrix}, \tag{11.145}$$

(c) ketabton.com: The Digital Library

where

$$\begin{pmatrix} R_1 \\ R_2 \\ R_3 \end{pmatrix} = \left(\frac{2E}{h^2} + A(t_n)\right)\begin{pmatrix} \Psi_{1j}(t_n) \\ \Psi_{2j}(t_n) \\ \Psi_{3j}(t_n) \end{pmatrix} - \left(\frac{E}{h^2} + \frac{B(t_n)}{2h}\right)\begin{pmatrix} \Psi_{1j}(t_{n-1}) \\ \Psi_{2j}(t_{n-1}) \\ \Psi_{3j}(t_{n-1}) \end{pmatrix} + \begin{pmatrix} G_{1j}(t_n) \\ G_{2j}(t_n) \\ G_{3j}(t_n) \end{pmatrix}.$$

For n=1,…,m-1, above equation is solvable. It is notable that the three matrices

$$\left(\frac{E}{h^2} - \frac{B(t_n)}{2h}\right), \quad \left(\frac{2E}{h^2} + A(t_n)\right), \quad \left(\frac{E}{h^2} + \frac{B(t_n)}{2h}\right)$$

are independent from the column number j. The solutions of Eq. 11.145 are vectors

$$\begin{pmatrix} \Psi_{1j}(t_{n+1}) \\ \Psi_{2j}(t_{n+1}) \\ \Psi_{3j}(t_{n+1}) \end{pmatrix} \quad \text{and} \quad \begin{pmatrix} \dot{\Psi}_{1j}(t_{n+1}) \\ \dot{\Psi}_{2j}(t_{n+1}) \\ \dot{\Psi}_{3j}(t_{n+1}) \end{pmatrix}, \quad n = 1,...,m-1\,, \tag{11.146}$$

where the velocity vector can be computed using definition of Eq. 11.143. Solving the equations of all column j, the solutions of the initial value problem of Eqs. 11.140 and 11.141 can be obtained. It is notable that the needed values are the values of t_n and can be computed by averaging the values of t_{n+1} and t_{n-1}.

11.6 Numerical Integration and Interpolation Algorithms

The Runge-Kutta algorithm, Adams algorithm, Cowell algorithm and mixed algorithm as well as interpolation algorithms are discussed in this section (cf., e.g., Brouwer and Clemence 1961; Bate et al. 1971; Herrick 1972; Xu 1994; Liu et al. 1996; Press et al. 1992).

11.6.1 Runge-Kutta Algorithms

The Runge-Kutta algorithm is a method that can be used to solve the initial value problem of

$$\begin{aligned} &\frac{\mathrm{d}X}{\mathrm{d}t} = F(t, X) \\ &X(t_0) = X_0 \end{aligned}, \tag{11.147}$$

where X_0 is the initial value of variable X at time t_0, and F is the function of t and X. For step size h, the Runge-Kutta algorithm can be used to compute $X(t_0 + h)$. By repeating such process, a series of solutions can be obtained as $X(t_0 + h)$, $X(t_0 + 2h)$, …, $X(t_0 + nh)$, where n is an integer. Denoting $t_n = t_0 + nh$, $X(t_n + h)$ can be represented by the Taylor expansion at t_n by

(c) ketabton.com: The Digital Library

$$X(t_n+h)=X(t_n)+h\left.\frac{\mathrm{d}X}{\mathrm{d}t}\right|_{t=t_n}+\left.\frac{h^2}{2}\frac{\mathrm{d}^2X}{\mathrm{d}t^2}\right|_{t=t_n}+\ldots+\left.\frac{h^n}{n!}\frac{\mathrm{d}^nX}{\mathrm{d}t^n}\right|_{t=t_n}+\cdots, \tag{11.148}$$

where

$$\frac{\mathrm{d}X}{\mathrm{d}t}=F\,,$$

$$\frac{\mathrm{d}^2X}{\mathrm{d}t^2}=\frac{\mathrm{d}F(t,X)}{\mathrm{d}t}=\frac{\partial F}{\partial t}+\frac{\partial F}{\partial X}\frac{\partial X}{\partial t}=\frac{\partial F}{\partial t}+\frac{\partial F}{\partial X}F\,,$$

$$\frac{\mathrm{d}^3X}{\mathrm{d}t^3}=\frac{\partial^2F}{\partial t^2}+2\frac{\partial^2F}{\partial t\partial X}F+\frac{\partial^2F}{\partial t\partial X}+\frac{\partial^2F}{\partial X^2}F^2+\left(\frac{\partial F}{\partial X}\right)^2F \quad \text{and} \tag{11.149}$$

$$\frac{\mathrm{d}^4X}{\mathrm{d}t^4}=\frac{\partial^3F}{\partial t^3}+\frac{\partial^3F}{\partial t^2\partial X}(3F+1)+\frac{\partial^3F}{\partial t\partial X^2}(5F^2+2F)+2\frac{\partial^2F}{\partial t\partial X}\frac{\partial F}{\partial t}+4\frac{\partial^3F}{\partial X^3}F^3$$
$$+2\frac{\partial^2F}{\partial X^2}\frac{\partial F}{\partial t}F+4\frac{\partial F}{\partial X}\frac{\partial^2F}{\partial t\partial X}F+6\frac{\partial F}{\partial X}\frac{\partial^2F}{\partial X^2}F^2+\left(\frac{\partial F}{\partial X}\right)^2\frac{\partial F}{\partial t}+\left(\frac{\partial F}{\partial X}\right)^2\frac{\partial F}{\partial X}2F\,.$$

…

The principle of the Runge-Kutta algorithm is to use a set of combinations of the first order partial derivatives around the $(t_n, X(t_n))$ to replace the higher order derivatives in Eq. 11.148; that is,

$$X(t_{n+1})=X(t_n)+\sum_{i=1}^{L}w_iK_i\,, \tag{11.150}$$

where

$$K_1=hF(t_n,X(t_n)) \quad \text{and}$$

$$K_i=hF(t_n+\alpha_ih,X(t_n)+\sum_{j=1}^{i-1}\beta_{ij}K_j)\,,\quad (i=2,3,\ldots)\,, \tag{11.151}$$

where w_i, α_i, and β_{ij} are constants to be determined, and L is an integer. The Taylor expansions of K_i ($i = 2, 3, \ldots$) at $(t_n, X(t_n))$ to the first order are

$$K_i=hF(t_n,X(t_n))+h^2\alpha_i\frac{\partial F}{\partial t}+h\frac{\partial F}{\partial X}\sum_{j=1}^{i-1}\beta_{ij}K_j \quad \text{or} \tag{11.152}$$

$$K_2=hF(t_n,X(t_n))+h^2\left(\alpha_2\frac{\partial F}{\partial t}+\beta_{21}\frac{\partial F}{\partial X}F\right), \tag{11.153}$$

(c) ketabton.com: The Digital Library

$$K_3 = hF + h^2\left(\alpha_3\frac{\partial F}{\partial t} + (\beta_{31}+\beta_{32})\frac{\partial F}{\partial X}F\right) + h^3\beta_{32}\frac{\partial F}{\partial X}\left(\alpha_2\frac{\partial F}{\partial t} + \beta_{21}\frac{\partial F}{\partial X}F\right),$$

$$\begin{aligned} K_4 = {} & hF + h^2\left(\alpha_4\frac{\partial F}{\partial t} + (\beta_{41}+\beta_{42}+\beta_{43})\frac{\partial F}{\partial X}F\right) \\ & + h^3\left[(\beta_{42}\alpha_2+\beta_{43}\alpha_3)\frac{\partial F}{\partial X}\frac{\partial F}{\partial t} + (\beta_{42}\beta_{21}+\beta_{43}(\beta_{31}+\beta_{32}))\frac{\partial F}{\partial X}\frac{\partial F}{\partial X}F\right] \\ & + h^4\beta_{43}\beta_{32}\frac{\partial F}{\partial X}\frac{\partial F}{\partial X}\left(\alpha_2\frac{\partial F}{\partial t} + \beta_{21}\frac{\partial F}{\partial X}F\right), \end{aligned}$$

$$\begin{aligned} K_5 = {} & hF + h^2\left(\alpha_5\frac{\partial F}{\partial t} + (\beta_{51}+\beta_{52}+\beta_{53}+\beta_{54})\frac{\partial F}{\partial X}F\right) \\ & + h^3\frac{\partial F}{\partial X}\left(\begin{array}{l}\alpha_2\dfrac{\partial F}{\partial t} + \beta_{21}\dfrac{\partial F}{\partial X}F + \beta_{53}\left(\alpha_3\dfrac{\partial F}{\partial t} + (\beta_{31}+\beta_{32})\dfrac{\partial F}{\partial X}F\right) \\ + \beta_{54}\left(\alpha_4\dfrac{\partial F}{\partial t} + (\beta_{41}+\beta_{42}+\beta_{43})\dfrac{\partial F}{\partial X}F\right)\end{array}\right) \\ & + h^4\frac{\partial F}{\partial X}\left(\begin{array}{l}(\beta_{53}\beta_{32}\alpha_2 + \beta_{54}(\beta_{42}\alpha_2+\beta_{43}\alpha_3))\dfrac{\partial F}{\partial X}\dfrac{\partial F}{\partial t} \\ + (\beta_{54}(\beta_{42}\beta_{21}+\beta_{43}(\beta_{31}+\beta_{32})) + \beta_{32}\beta_{21})\dfrac{\partial F}{\partial X}\dfrac{\partial F}{\partial X}F\end{array}\right) \\ & + h^5\frac{\partial F}{\partial X}\beta_{54}\left(\beta_{43}\beta_{32}\frac{\partial F}{\partial X}\frac{\partial F}{\partial X}\left(\alpha_2\frac{\partial F}{\partial t} + \beta_{21}\frac{\partial F}{\partial X}F\right)\right) \end{aligned}$$

…

where F and the related partial derivatives have values at $(t_n, X(t_n))$. Substituting the above formulas into Eq. 11.150 and comparing the coefficients of h^n ($= 1/n!$) with Eq. 11.148, a group of equations of constants w_i, α_i and β_{ij} can be obtained by separating them through the partial derivative combinations. For example, for $L = 4$, one has

$$\begin{aligned} & w_1 + w_2 + w_3 + w_4 = 1, \\ & w_2\alpha_2 + w_3\alpha_3 + w_4\alpha_4 = \frac{1}{2}, \\ & w_2\beta_{21} + w_3(\beta_{31}+\beta_{32}) + w_4(\beta_{41}+\beta_{42}+\beta_{43}) = \frac{1}{2}, \\ & w_3\alpha_2\beta_{32} + w_4(\alpha_2\beta_{42} + \alpha_3\beta_{43}) = \frac{1}{6}, \\ & w_3\beta_{21}\beta_{32} + w_4(\beta_{21}\beta_{42} + \beta_{31}\beta_{43} + \beta_{32}\beta_{43}) = \frac{1}{6}, \end{aligned} \tag{11.154}$$

(c) ketabton.com: The Digital Library

$$w_4\alpha_2\beta_{43}\beta_{32}=\frac{1}{24} \quad \text{and}$$

$$w_4\beta_{21}\beta_{43}\beta_{32}=\frac{1}{24}.$$

There are 13 coefficients in the seven equations above, so the solution set of Eq. 11.154 is not a unique one. Considering w has the meaning of weight, and α is the step factor, one may set, e.g., $w_1 = w_2 = w_3 = w_4 = 1/4$, $\alpha_2 = 1/3$, $\alpha_3 = 2/3$, $\alpha_4 = 1$ into the above equations and have

$$\beta_{21}+\beta_{31}+\beta_{32}+\beta_{41}+\beta_{42}+\beta_{43}=2,$$

$$\beta_{32}+\beta_{42}+2\beta_{43}=2,$$

$$\beta_{21}\beta_{32}+\beta_{21}\beta_{42}+\beta_{31}\beta_{43}+\beta_{32}\beta_{43}=\frac{2}{3},$$

$$\beta_{43}\beta_{32}=\frac{1}{2}, \quad \text{and}$$

$$\beta_{21}\beta_{43}\beta_{32}=\frac{1}{6}.$$

Letting $\beta_{32} = 1$, one has $\beta_{42} = 0$, $\beta_{31} = -1/3$, and $\beta_{41} = 1/2$. Thus, a four-order Runge-Kutta formula is

$$X(t_{n+1})=X(t_n)+\frac{1}{4}\sum_{i=1}^{4}K_i, \tag{11.155}$$

where

$$K_1=hF(t_n,X(t_n)), \tag{11.156}$$

$$K_2=hF\left(t_n+\frac{1}{3}h,X(t_n)+\frac{1}{3}K_1\right),$$

$$K_3=hF\left(t_n+\frac{2}{3}h,X(t_n)-\frac{1}{3}K_1+K_2\right), \quad \text{and}$$

$$K_4=hF\left(t_n+h,X(t_n)+\frac{1}{2}K_1+\frac{1}{2}K_3\right).$$

Similarly, a commonly used eighth order Runge-Kutta formula can be derived. It is quoted as follows (cf. Xu 1994; Liu et al. 1996):

$$X(t_{n+1})=X_n+\frac{1}{840}(41K_1+27K_4+272K_5+27K_6+216K_7+216K_9+41K_{10}), \tag{11.157}$$

(c) ketabton.com: The Digital Library

where

$$K_1 = hF(t_n, X_n)\,, \quad X_n = X(t_n)\,, \tag{11.158}$$

$$K_2 = hF\left(t_n + \frac{4}{27}h, X_n + \frac{4}{27}K_1\right),$$

$$K_3 = hF\left(t_n + \frac{2}{9}h, X_n + \frac{1}{18}K_1 + \frac{1}{6}K_2\right),$$

$$K_4 = hF\left(t_n + \frac{1}{3}h, X_n + \frac{1}{12}K_1 + \frac{1}{4}K_3\right),$$

$$K_5 = hF\left(t_n + \frac{1}{2}h, X_n + \frac{1}{8}K_1 + \frac{3}{8}K_4\right),$$

$$K_6 = hF\left(t_n + \frac{2}{3}h, X_n + \frac{1}{54}(13K_1 - 27K_3 + 42K_4 + 8K_5)\right),$$

$$K_7 = hF\left(t_n + \frac{1}{6}h, X_n + \frac{1}{4320}(389K_1 - 54K_3 + 966K_4 - 824K_5 + 243K_6)\right),$$

$$K_8 = hF\left(t_n + h, X_n + \frac{1}{20}(-231K_1 + 81K_3 - 1164K_4 + 656K_5 - 122K_6 + 800K_7)\right),$$

$$K_9 = hF\left(t_n + \frac{5}{6}h, X_n + \frac{1}{288}(-127K_1 + 18K_3 - 678K_4 + 456K_5 - 9K_6 + 576K_7 + 4K_8)\right), \text{ and}$$

$$K_{10} = hF\left(t_n + h, X_n + \frac{1}{820}(1481K_1 - 81K_3 + 7104K_4 - 3376K_5 + 72K_6 - 5040K_7 - 60K_8 + 720K_9)\right).$$

From the derivation process, it is obvious that the Runge-Kutta algorithm is an approximation of the same order Taylor expansions. For every step of the solution, the function values of F have to be computed several times. The Runge-Kutta algorithm is also called the single step method and is commonly used for computing the start values for other multiple step methods.

Errors of the integration are dependent on the step size and the properties of function F. To ensure the needed accuracy of the orbit integration, a step size adaptive control is also meaningful in computing efficiency (cf. Press et al. 1992). Because of the periodical motion of the orbit, the step control just needs to be made in a few special cycles of the motion. A step doubling method is suggested by Press et al. (1992). Integration is taken twice for each step, first with a full step, then independently with two half steps. Through comparing the results, the step size can be adjusted to fit the accuracy requirement.

To apply the above formulas for solving the initial value problem of the equation of motion 11.134, Eq. 11.147 shall be rewritten as

(c) ketabton.com: The Digital Library

$$\begin{matrix} \dfrac{dX_k}{dt} = \dot{X}_k(t,X) \\ \dfrac{d\dot{X}_k}{dt} = f_k(t,X)/m \end{matrix}, \quad \begin{matrix} X_k(t_0) = X_{k0} \\ \dot{X}_k(t_0) = \dot{X}_{k0} \end{matrix}, \quad k=1,2,3\,,$$

where $X = (X_1, X_2, X_3, \dot{X}_1, \dot{X}_2, \dot{X}_3)$. Using the Runge-Kutta algorithm to solve the above problem, an additional index k shall be added to all X and K in Eq. 11.157:

$$X_k(t_{n+1}) = X_{kn} + \frac{1}{840}(41K_{k1} + 27K_{k4} + 272K_{k5} + 27K_{k6} + 216K_{k7} + 216K_{k9} + 41K_{k10})\,,$$

and the same index k shall be added to K on the left side and F on the right side of Eq. 11.158. For the last three equations, $F_k = f_k / m$, so $\dot{X}_k$ can be computed. For the first three equations, $F_k = \dot{X}_k$, so F_k can be computed through computing $\dot{X}_k$ at the needed coordinates t and X.

11.6.2 Adams Algorithms

For the initial value problem of

$$\begin{matrix} \dfrac{dX}{dt} = F(t,X) \\ X(t_0) = X_0 \end{matrix}, \tag{11.159}$$

there exists

$$X(t_{n+1}) = X(t_n) + \int_{t_n}^{t_{n+1}} F(t,X)dt\,. \tag{11.160}$$

The Adams algorithm uses the Newtonian backward differential interpolation formula to present the function F by

$$\begin{aligned} F(t,X) = F_n &+ \frac{t-t_n}{h}\nabla F_n + \frac{(t-t_n)(t-t_{n-1})}{2!h^2}\nabla^2 F_n + \cdots \\ &+ \frac{(t-t_n)(t-t_{n-1})\cdots(t-t_{n-k+1})}{k!h^k}\nabla^k F_n \end{aligned}, \tag{11.161}$$

where F_n is the value of F at the time t_n, h is the step size, $\nabla^k F$ is the k^{th} order backward numerical difference of F, and

$$\begin{aligned} &\nabla F_n = F_n - F_{n-1} \\ &\nabla^2 F_n = \nabla F_n - \nabla F_{n-1} = F_n - 2F_{n-1} + F_{n-2} \\ &\cdots \\ &\nabla^m F_n = \sum_{j=0}^{m} (-1)^j C_m^j F_{n-j}\,, \quad C_m^j = \frac{m!}{j!(m-j)!}\,, \end{aligned}, \tag{11.162}$$

(c) ketabton.com: The Digital Library

where C_{m}^{j} is the binomial coefficient. Letting $s = (t - t_n) / h$, then $\mathrm{d}t = h\mathrm{d}s$, $s = 0$ if $t = t_n$, $s = 1$ if $t = t_{n+1}$, so that Eqs. 11.161 and 11.160 turn out to be

$$F(t,X)=\sum_{m=0}^{k} C_{s+m-1}^{m}\nabla^{m}F_n \quad \text{and}$$

$$X(t_{n+1})=X(t_n)+\int_{t_n}^{t_{n+1}}\sum_{m=0}^{k} C_{s+m-1}^{m}\sum_{j=0}^{m}(-1)^{j}C_{m}^{j}F_{n-j}h\mathrm{d}s\,. \tag{11.163}$$

By denoting

$$\begin{aligned}\gamma_m &= \int_0^1 C_{s+m-1}^{m}\mathrm{d}s\\ \beta_j &= \sum_{m=j}^{k}(-1)^{j}C_{m}^{j}\gamma_m\end{aligned}\,, \tag{11.164}$$

one has

$$X(t_{n+1})=X(t_n)+h\sum_{j=0}^{k}\beta_j F_{n-j}\,, \tag{11.165}$$

where the sequences of the two sequential summations have been changed. For the first equation of 11.164, there is (cf. Xu 1994)

$$\gamma_0=1,\quad \gamma_m=1-\sum_{j=1}^{m}\frac{1}{j+1}\gamma_{m-j}\,,\quad (m\geq 1)\,. \tag{11.166}$$

Equation 11.165 is also called the Adams-Bashforth formula. It uses the function values of $\{F_{n-j}, j = 0, \ldots, k\}$ to compute the X_{n+1}. When the order of the algorithm is selected, the coefficients of β_j are constants. This makes the computation using Eq. 11.165 very simple. For every integration step, just one function value of F_n has to be computed. However, the Adams algorithm needs $\{F_{n-j}, j = 0, \ldots, k\}$ as initial values, whereas to compute those values, the states $\{X_{n-j}, j = 0, \ldots, k\}$ are needed. In other words, the Adams algorithm is not able to start the integration itself. The Runge-Kutta algorithm is usually used for computing the start values.

The Adams-Bashforth formula does not take the function value F_{n+1} into account. Using F_{n+1}, the Adams algorithm is expressed by the Adams-Moulton formula. Similar to the above discussions, function F can be represented by

$$\begin{aligned}F(t,X)=F_{n+1}&+\frac{t-t_{n+1}}{h}\nabla F_{n+1}+\frac{(t-t_{n+1})(t-t_n)}{2!h^2}\nabla^2F_{n+1}+\ldots\\&+\frac{(t-t_{n+1})(t-t_n)\cdots(t-t_{n-k+2})}{k!h^k}\nabla^kF_{n+1}\end{aligned}\,, \tag{11.167}$$

where

$$\nabla^{m}F_{n+1}=\sum_{j=0}^{m}(-1)^{j}C_{m}^{j}F_{n+1-j}\,. \tag{11.168}$$

(c) ketabton.com: The Digital Library

If one lets $s = (t - t_{n+1}) / h$, then $dt = hds$, $s = -1$ if $t = t_n$, and $s = 0$ if $t = t_{n+1}$; similar formulas of Eqs. 11.165 and 11.164 can be obtained:

$$X(t_{n+1}) = X(t_n) + h\sum_{j=0}^{k} \beta_j^* F_{n+1-j}\,, \tag{11.169}$$

$$\begin{aligned} \beta_j^* &= \sum_{m=j}^{k} (-1)^j C_m^j \gamma_m^* \\ \gamma_m^* &= \int_{-1}^{0} C_{s+m-1}^m \mathrm{d}s \end{aligned} \tag{11.170}$$

and (cf. Xu 1994)

$$\gamma_0^* = 1, \quad \gamma_m^* = -\sum_{j=1}^{m} \frac{1}{j+1} \gamma_{m-j}^*, \quad (m \geq 1)\,. \tag{11.171}$$

Because of the use of F_{n+1} to approximate F, the Adams-Moulton formula may reach a higher accuracy than that of the Adams-Bashforth formula. However, before X_{n+1} has been computed, F_{n+1} might not have been computed exactly. So an iterative process is needed to use the Adams-Moulton formula. A simplified way to use the Adams-Moulton formula is to use the Adams-Bashforth formula to compute X_{n+1} and F_{n+1}, and then to use the Adams-Moulton formula to compute the modified X_{n+1} using F_{n+1}. Experience shows that such a process will be accurate enough for many applications.

11.6.3 Cowell Algorithms

For the initial value problem of

$$\begin{aligned} &\frac{\mathrm{d}^2 X}{\mathrm{d}t^2} = F(t, X) \\ &\dot{X}(t_0) = \dot{X}_0 \\ &X(t_0) = X_0 \end{aligned}\,, \tag{11.172}$$

there is

$$\dot{X}(t) = \dot{X}(t_n) + \int_{t_n}^{t} F(t, X)\mathrm{d}t\,. \tag{11.173}$$

It is notable that here X is the position coordinate of the satellite. In other words, the disturbing force F is not the function of the velocity of the satellite.

By integrating Eq. 11.173 in areas of $[t_n, t_{n+1}]$ and $[t_n, t_{n-1}]$ respectively, one has

$$X(t_{n+1}) - X(t_n) - \dot{X}(t_n)(t_{n+1} - t_n) = \int_{t_n}^{t_{n+1}} \int_{t_n}^{t} F(t, X)\mathrm{d}t\mathrm{d}t \quad \text{and} \tag{11.174}$$

$$X(t_{n-1}) - X(t_n) - \dot{X}(t_n)(t_{n-1} - t_n) = \int_{t_n}^{t_{n-1}} \int_{t_n}^{t} F(t, X)\mathrm{d}t\mathrm{d}t\,, \tag{11.175}$$

(c) ketabton.com: The Digital Library

where $(t_{n+1} - t_n) = h = (t_n - t_{n-1})$. Adding both equations together, one has

$$X(t_{n+1}) - 2X(t_n) + X(t_{n-1}) = \int_{t_n}^{t_{n+1}} \int_{t_n}^{t} + \int_{t_n}^{t_{n-1}} \int_{t_n}^{t} F(t, X) \mathrm{d}t \mathrm{d}t. \tag{11.176}$$

Similar to the Adams-Bashforth formula, function F can be represented by

$$\begin{aligned} F(t, X) = F_n + \frac{t - t_n}{h} \nabla F_n + \frac{(t - t_n)(t - t_{n-1})}{2! h^2} \nabla^2 F_n + \dots \\ + \frac{(t - t_n)(t - t_{n-1}) \cdots (t - t_{n-k+1})}{k! h^k} \nabla^k F_n \end{aligned} . \tag{11.177}$$

Substituting Eq. 11.177 into Eq. 11.176, one has (similar to the derivation of Admas algorithms) (cf. Xu 1994)

$$X(t_{n+1}) = 2X(t_n) - X(t_{n-1}) + h^2 \sum_{j=0}^{k} \beta_j F_{n-j} , \tag{11.178}$$

where

$$\beta_j = \sum_{m=j}^{k} (-1)^j C_m^j \sigma_m , \tag{11.179}$$

$$\sigma_0 = 1, \quad \sigma_m = 1 - \sum_{j=1}^{m} \frac{2}{j+2} b_{j+1} \sigma_{m-j} , \ (m \geq 1) ,$$

$$b_j = \sum_{i=1}^{j} \frac{1}{i} .$$

Equation 11.178 is called the Stormer formula. Similar to the discussions in Adams algorithms, taking F_{n+1} into account, one has

$$\begin{aligned} F(t, X) = F_{n+1} + \frac{t - t_{n+1}}{h} \nabla F_{n+1} + \frac{(t - t_{n+1})(t - t_n)}{2! h^2} \nabla^2 F_{n+1} + \dots \\ + \frac{(t - t_{n+1})(t - t_n) \cdots (t - t_{n-k+2})}{k! h^k} \nabla^k F_{n+1} \end{aligned} \tag{11.180}$$

and (cf. Xu 1994)

$$X(t_{n+1}) = 2X(t_n) - X(t_{n-1}) + h^2 \sum_{j=0}^{k} \beta_j^* F_{n+1-j} , \tag{11.181}$$

where

$$\beta_j^* = \sum_{m=j}^{k} (-1)^j C_m^j \sigma_m^* , \tag{11.182}$$

(c) ketabton.com: The Digital Library

$$\sigma_0^* = 1 \ , \quad \sigma_m^* = -\sum_{j=1}^{m} \frac{2}{j+2} b_{j+1} \sigma_{m-j}^* \ , \quad (m \geq 1) \ , \quad \text{and}$$

$$b_j = \sum_{i=1}^{j} \frac{1}{i} \ .$$

Equation 11.181 is called the Cowell formula. Because of the use of F_{n+1} to approximate F, the Cowell formula may reach a higher accuracy than that of the Stormer formula. However, before X_{n+1} has been computed, F_{n+1} may not be computed exactly. So an iterative process is needed to use the Cowell formula. A simplified way to use the Cowell formula is to use the Stormer formula to compute X_{n+1} and F_{n+1}, and then to use the Cowell formula to compute the modified X_{n+1} using F_{n+1}. Experience shows that such a process will be accurate enough for many applications.

11.6.4 Mixed Algorithms and Discussions

Above we discussed three algorithms for solving the initial value problem of the orbit differential equation. The Runge-Kutta algorithm is a single step method. The formulas of different order Runge-Kutta algorithms do not have simple relationships, and even for a definite order the formulas are not unique. For every step of integration, several function values of F have to be computed for use. The most important property of the Runge-Kutta algorithm is that the method is a self-starting one. Generally, the Runge-Kutta algorithm is often used for providing the starting values for multiple-step algorithms.

Adams algorithms are multiple-step methods. The order of the formulas can be easily risen because of their sequential relationships. However, the Adams algorithms cannot start themselves. For every step of integration, only one function value has to be computed. The disturbing function is considered a function of time and the state of the satellite. So Adams methods can be used in orbit determination problems without any problem with the disturbing function. In the case of a higher accuracy requirement, a mixed Adams-Bashforth method and Adams-Moulton methods can be used in an iterative process.

Cowell algorithms are multiple-step methods too. The order can be changed easily. Cowell methods also need starting help from other methods. Analysis shows that Cowell algorithms have a higher accuracy than that of Adams algorithms when the same orders of formulas are used. However, Cowell formulas are only suitable for that kind of disturbing function F, which is the function of the time and the position of the satellite. It is well known that the atmospheric drag is a disturbing force, which is a function of the velocity of the satellite. Therefore Cowell algorithms can only be used for integrating a part of the disturbing forces. A mixed Cowell method still keeps such a property.

Obviously, the forces of the equation of motion have to be separated into two parts, one includes the forces that are functions of the velocity of the satellite, and the other includes all remaining forces. The first part can be integrated using Adams methods, and the other can be integrated using Cowell methods. The Runge-Kutta algorithm will be used for providing the needed starting values.

The selections of the order number and step size are dependent on the accuracy requirements and the orbit conditions. Usually the order and the step size are selectable input variables of the software, and can be properly selected after several test runs. Scheinert

(c) ketabton.com: The Digital Library

suggested using 8-order Runge-Kutta algorithms, as well as 12-order Adams and Cowell algorithms (cf. Scheinert 1996). It is notable that by order selection, it is not the higher the order is, the higher the accuracy will be. For the step size selection, it is not the smaller the step size is, the better the results will be.

11.6.5 Interpolation Algorithms

Orbits are given through integration at the step points $t_0 + nh$ ($n = 0, 1, \ldots$). For GPS satellites, h is usually selected as 300 seconds. However, GPS observations are made, usually in IGS, every 15 seconds. For linearisation and formation of the GPS observation equations, the orbit data sometimes have to be interpolated to the needed epochs. This is why we have to discuss the method of interpolation. The often-used Lagrange interpolation algorithm has been discussed in Sect. 3.4. A 5-order polynomial interpolation method has been given in Sect. 5.4.2. By deriving the Adams and Cowell algorithms, the Newtonian backward differentiation formula has been used to represent the disturbing function F. By simply considering F a function of t (t is any variable), then one has

$$F(t) = F(t_n) + \frac{t-t_n}{h}\nabla F_n + \frac{(t-t_n)(t-t_{n-1})}{2!h^2}\nabla^2 F_n + \ldots + \frac{(t-t_n)(t-t_{n-1})\cdots(t-t_{n-k+1})}{k!h^k}\nabla^k F_n \quad . \tag{11.183}$$

This is an interpolating formula of $F(t)$ using a set of function values of $\{F_{n-j}, j = 0, \ldots, k\}$.

11.7 Orbit-Related Partial Derivatives

As mentioned in Sect. 11.5.1 the partial derivatives of

$$\frac{\partial \vec{f}}{\partial \vec{r}}, \quad \frac{\partial \vec{f}}{\partial \dot{\vec{r}}} \quad \text{and} \quad \frac{\partial \vec{f}}{\partial \vec{Y}} \tag{11.184}$$

will be derived in this section in detail, where the force vector is a summated vector of all disturbing forces in the ECSF coordinate system. If the force vector is given in the ECEF coordinate system, there is

$$\left(\frac{\partial \vec{f}}{\partial \vec{r}}, \frac{\partial \vec{f}}{\partial \dot{\vec{r}}}\right) = R_P^{-1} R_N^{-1} R_S^{-1} R_M^{-1} \left(\frac{\partial \vec{f}_{ECEF}}{\partial \vec{r}}, \frac{\partial \vec{f}_{ECEF}}{\partial \dot{\vec{r}}}\right). \tag{11.185}$$

Because of

$$\vec{r} = R \cdot \vec{r}_{ECEF}$$
$$\vec{f} = R \cdot \vec{f}_{ECEF} \quad ,$$

one may have the velocity transformation formula

(c) ketabton.com: The Digital Library

$$\frac{\mathrm{d}\vec{r}}{\mathrm{d}t}=\frac{\mathrm{d}R}{\mathrm{d}t}\cdot\vec{r}_{\mathrm{ECEF}}+R\cdot\frac{\mathrm{d}\vec{r}_{\mathrm{ECEF}}}{\mathrm{d}t}\,,$$

where

$$R=R_{\mathrm{P}}^{-1}R_{\mathrm{N}}^{-1}R_{\mathrm{S}}^{-1}R_{\mathrm{M}}^{-1}\,.$$

Therefore one has

$$\frac{\partial\vec{r}_{\mathrm{ECEF}}}{\partial\vec{r}}=R^{-1}\,,$$

$$\frac{\partial\dot{\vec{r}}_{\mathrm{ECEF}}}{\partial\dot{\vec{r}}}=R^{-1}\,,$$

and

$$\frac{\partial\vec{f}_{\mathrm{ECEF}}}{\partial\vec{r}}=\frac{\partial\vec{f}_{\mathrm{ECEF}}}{\partial\vec{r}_{\mathrm{ECEF}}}\frac{\partial\vec{r}_{\mathrm{ECEF}}}{\partial\vec{r}}=\frac{\partial\vec{f}_{\mathrm{ECEF}}}{\partial\vec{r}_{\mathrm{ECEF}}}R^{-1}\,,$$

$$\frac{\partial\vec{f}_{\mathrm{ECEF}}}{\partial\dot{\vec{r}}}=\frac{\partial\vec{f}_{\mathrm{ECEF}}}{\partial\dot{\vec{r}}_{\mathrm{ECEF}}}\frac{\partial\dot{\vec{r}}_{\mathrm{ECEF}}}{\partial\dot{\vec{r}}}=\frac{\partial\vec{f}_{\mathrm{ECEF}}}{\partial\dot{\vec{r}}_{\mathrm{ECEF}}}R^{-1}\,.$$

1. *Geopotential Disturbing Force*

The geopotential disturbing force vector (cf. Sect. 11.2) has the form of

$$\vec{f}_{\mathrm{ECEF}}=\begin{pmatrix}f_{x'}\\f_{y'}\\f_{z'}\end{pmatrix}=\begin{pmatrix}b_{11}\dfrac{\partial V}{\partial r}+b_{21}\dfrac{\partial V}{\partial\varphi}+b_{31}\dfrac{\partial V}{\partial\lambda}\\[2ex] b_{12}\dfrac{\partial V}{\partial r}+b_{22}\dfrac{\partial V}{\partial\varphi}+b_{32}\dfrac{\partial V}{\partial\lambda}\\[2ex] b_{13}\dfrac{\partial V}{\partial r}+b_{23}\dfrac{\partial V}{\partial\varphi}\end{pmatrix},\tag{11.186}$$

where

$$\frac{\partial(r,\varphi,\lambda)}{\partial(x',y',z')}=\begin{pmatrix}b_{11}&b_{12}&b_{13}\\b_{21}&b_{22}&b_{23}\\b_{31}&b_{32}&b_{33}\end{pmatrix}=\begin{pmatrix}\cos\varphi\cos\lambda&\cos\varphi\sin\lambda&\sin\varphi\\[1ex] -\dfrac{1}{r}\sin\varphi\cos\lambda&-\dfrac{1}{r}\sin\varphi\sin\lambda&\dfrac{1}{r}\cos\varphi\\[2ex] -\dfrac{1}{r\cos\varphi}\sin\lambda&\dfrac{1}{r\cos\varphi}\cos\lambda&0\end{pmatrix},$$

and (x', y', z') are the three orthogonal Cartesian coordinates in the ECEF system. Thus,

(c) ketabton.com: The Digital Library

$$\frac{\partial \vec{f}_{\mathrm{ECEF}}}{\partial \vec{r}} = \begin{pmatrix} \dfrac{\partial f_{x'}}{\partial(x',y',z')} \\ \dfrac{\partial f_{y'}}{\partial(x',y',z')} \\ \dfrac{\partial f_{z'}}{\partial(x',y',z')} \end{pmatrix} = \left(\frac{\partial(f_{x'}, f_{y'}, f_{z'})}{\partial(r,\varphi,\lambda)} \frac{\partial(r,\varphi,\lambda)}{\partial(x',y',z')} \right)^T . \tag{11.187}$$

Using index j (= 1, 2, 3) to denote index (x', y', z'), one has

$$\frac{\partial f_j}{\partial(r,\varphi,\lambda)} = \begin{pmatrix} \dfrac{\partial b_{1j}}{\partial r}\dfrac{\partial V}{\partial r} + \dfrac{\partial b_{2j}}{\partial r}\dfrac{\partial V}{\partial \varphi} + \dfrac{\partial b_{3j}}{\partial r}\dfrac{\partial V}{\partial \lambda} + b_{1j}\dfrac{\partial^2 V}{\partial r^2} + b_{2j}\dfrac{\partial^2 V}{\partial r \partial \varphi} + b_{3j}\dfrac{\partial^2 V}{\partial r \partial \lambda} \\ \dfrac{\partial b_{1j}}{\partial \varphi}\dfrac{\partial V}{\partial r} + \dfrac{\partial b_{2j}}{\partial \varphi}\dfrac{\partial V}{\partial \varphi} + \dfrac{\partial b_{3j}}{\partial \varphi}\dfrac{\partial V}{\partial \lambda} + b_{1j}\dfrac{\partial^2 V}{\partial r \partial \varphi} + b_{2j}\dfrac{\partial^2 V}{\partial \varphi^2} + b_{3j}\dfrac{\partial^2 V}{\partial \varphi \partial \lambda} \\ \dfrac{\partial b_{1j}}{\partial \lambda}\dfrac{\partial V}{\partial r} + \dfrac{\partial b_{2j}}{\partial \lambda}\dfrac{\partial V}{\partial \varphi} + \dfrac{\partial b_{3j}}{\partial \lambda}\dfrac{\partial V}{\partial \lambda} + b_{1j}\dfrac{\partial^2 V}{\partial r \partial \lambda} + b_{2j}\dfrac{\partial^2 V}{\partial \varphi \partial \lambda} + b_{3j}\dfrac{\partial^2 V}{\partial \lambda^2} \end{pmatrix}^T , \tag{11.188}$$

where

$$\frac{\partial}{\partial r}\begin{pmatrix} b_{11} & b_{12} & b_{13} \\ b_{21} & b_{22} & b_{23} \\ b_{31} & b_{32} & b_{33} \end{pmatrix} = \begin{pmatrix} 0 & 0 & 0 \\ \dfrac{1}{r^2}\sin\varphi\cos\lambda & \dfrac{1}{r^2}\sin\varphi\sin\lambda & \dfrac{-1}{r^2}\cos\varphi \\ \dfrac{1}{r^2\cos\varphi}\sin\lambda & \dfrac{-1}{r^2\cos\varphi}\cos\lambda & 0 \end{pmatrix},$$

$$\frac{\partial}{\partial \varphi}\begin{pmatrix} b_{11} & b_{12} & b_{13} \\ b_{21} & b_{22} & b_{23} \\ b_{31} & b_{32} & b_{33} \end{pmatrix} = \begin{pmatrix} -\sin\varphi\cos\lambda & -\sin\varphi\sin\lambda & \cos\varphi \\ -\dfrac{1}{r}\cos\varphi\cos\lambda & -\dfrac{1}{r}\cos\varphi\sin\lambda & -\dfrac{1}{r}\sin\varphi \\ -\dfrac{\sin\varphi}{r\cos^2\varphi}\sin\lambda & \dfrac{\sin\varphi}{r\cos^2\varphi}\cos\lambda & 0 \end{pmatrix} \quad \text{and}$$

$$\frac{\partial}{\partial \lambda}\begin{pmatrix} b_{11} & b_{12} & b_{13} \\ b_{21} & b_{22} & b_{23} \\ b_{31} & b_{32} & b_{33} \end{pmatrix} = \begin{pmatrix} -\cos\varphi\sin\lambda & \cos\varphi\cos\lambda & 0 \\ \dfrac{1}{r}\sin\varphi\sin\lambda & -\dfrac{1}{r}\sin\varphi\cos\lambda & 0 \\ -\dfrac{1}{r\cos\varphi}\cos\lambda & -\dfrac{1}{r\cos\varphi}\sin\lambda & 0 \end{pmatrix} \tag{11.189}$$

(c) ketabton.com: The Digital Library

and

$$\frac{\partial^2 V}{\partial r^2} = \frac{\mu}{r^3}\left[2 + \sum_{l=2}^{\infty}\sum_{m=0}^{l}(l+1)(l+2)\left(\frac{a}{r}\right)^l \bar{P}_{lm}(\sin\varphi)[\bar{C}_{lm}\cos m\lambda + \bar{S}_{lm}\sin m\lambda]\right],$$

$$\frac{\partial^2 V}{\partial r\partial\varphi} = -\frac{\mu}{r^2}\sum_{l=2}^{\infty}\sum_{m=0}^{l}(l+1)\left(\frac{a}{r}\right)^l \frac{\mathrm{d}\bar{P}_{lm}(\sin\varphi)}{\mathrm{d}\varphi}[\bar{C}_{lm}\cos m\lambda + \bar{S}_{lm}\sin m\lambda],$$

$$\frac{\partial^2 V}{\partial r\partial\lambda} = -\frac{\mu}{r^2}\left[\sum_{l=2}^{\infty}\sum_{m=0}^{l}(l+1)\left(\frac{a}{r}\right)^l \bar{P}_{lm}(\sin\varphi)m[-\bar{C}_{lm}\sin m\lambda + \bar{S}_{lm}\cos m\lambda]\right],$$

$$\frac{\partial^2 V}{\partial\varphi^2} = \frac{\mu}{r}\sum_{l=2}^{\infty}\sum_{m=0}^{l}\left(\frac{a}{r}\right)^l \frac{\mathrm{d}^2\bar{P}_{lm}(\sin\varphi)}{\mathrm{d}\varphi^2}[\bar{C}_{lm}\cos m\lambda + \bar{S}_{lm}\sin m\lambda],$$

$$\frac{\partial^2 V}{\partial\varphi\partial\lambda} = \frac{\mu}{r}\sum_{l=2}^{\infty}\sum_{m=0}^{l}\left(\frac{a}{r}\right)^l \frac{\mathrm{d}\bar{P}_{lm}(\sin\varphi)}{\mathrm{d}\varphi}m[-\bar{C}_{lm}\sin m\lambda + \bar{S}_{lm}\cos m\lambda], \quad \text{and}$$

$$\frac{\partial^2 V}{\partial\lambda^2} = -\frac{\mu}{r}\sum_{l=2}^{\infty}\sum_{m=0}^{l} m^2\left(\frac{a}{r}\right)^l \bar{P}_{lm}(\sin\varphi)[\bar{C}_{lm}\cos m\lambda + \bar{S}_{lm}\sin m\lambda], \tag{11.190}$$

where

$$\frac{\mathrm{d}\bar{P}_{lm}(\sin\varphi)}{\mathrm{d}\varphi} = \beta(m)\bar{P}_{l(m+1)}(\sin\varphi) - m\tan\varphi\bar{P}_{lm}(\sin\varphi),$$

$$\begin{aligned}\frac{\mathrm{d}^2\bar{P}_{lm}(\sin\varphi)}{\mathrm{d}\varphi^2} &= \beta(m)\frac{\mathrm{d}\bar{P}_{l(m+1)}(\sin\varphi)}{\mathrm{d}\varphi} - m\frac{1}{\cos^2\varphi}\bar{P}_{lm}(\sin\varphi) - m\tan\varphi\frac{\mathrm{d}\bar{P}_{lm}(\sin\varphi)}{\mathrm{d}\varphi}\\ &= \beta(m)\beta(m+1)\bar{P}_{l(m+2)}(\sin\varphi) - \beta(m)\tan\varphi(2m+1)\bar{P}_{l(m+1)}(\sin\varphi)\\ &\quad + \left(m^2\tan^2\varphi - m\frac{1}{\cos^2\varphi}\right)\bar{P}_{lm}(\sin\varphi),\end{aligned}$$

$$\beta(m) = \left[\frac{1}{2}(2-\delta_{0m})(l-m)(l+m+1)\right]^{1/2} \quad \text{and}$$

$$\beta(m+1) = \left[\frac{1}{2}(l-m-1)(l+m+2)\right]^{1/2}. \tag{11.191}$$

(c) ketabton.com: The Digital Library

Other needed functions are already given in Sect. 11.1. Because the force is not a function of velocity, it is obvious that

$$\frac{\partial \vec{f}_{\mathrm{ECEF}}}{\partial \dot{\vec{r}}} = [0]_{3\times 3} \,. \tag{11.192}$$

Only non-zero partial derivatives will be given in later text.

Supposing the geopotential parameters $\overline{C}_{lm}^{N}, \overline{S}_{lm}^{N}$ are known (as initial values), $\overline{C}_{lm}, \overline{S}_{lm}$ are true values, and $\Delta\overline{C}_{lm}, \Delta\overline{S}_{lm}$ are searched corrections (unknowns), then the geopotential force is

$$\begin{aligned} \vec{f}_{\mathrm{ECEF}}(\overline{C}_{lm}, \overline{S}_{lm}) &= \vec{f}_{\mathrm{ECEF}}(\overline{C}_{lm}^{N}, \overline{S}_{lm}^{N}) + \vec{f}_{\mathrm{ECEF}}(\overline{C}_{lm}, \overline{S}_{lm}) - \vec{f}_{\mathrm{ECEF}}(\overline{C}_{lm}^{N}, \overline{S}_{lm}^{N}) \\ &= \vec{f}_{\mathrm{ECEF}}(\overline{C}_{lm}^{N}, \overline{S}_{lm}^{N}) + \vec{f}_{\mathrm{ECEF}}(\Delta\overline{C}_{lm}, \Delta\overline{S}_{lm}) \;, \end{aligned} \tag{11.193}$$

And

$$\frac{\partial \vec{f}_{\mathrm{ECEF}}}{\partial(\Delta\overline{C}_{lm}, \Delta\overline{S}_{lm})} = \begin{pmatrix} b_{11} & b_{12} & b_{13} \\ b_{21} & b_{22} & b_{23} \\ b_{31} & b_{32} & b_{33} \end{pmatrix}^{T} \frac{\partial}{\partial(\Delta\overline{C}_{lm}, \Delta\overline{S}_{lm})} \begin{pmatrix} \dfrac{\partial V}{\partial r} \\ \dfrac{\partial V}{\partial \varphi} \\ \dfrac{\partial V}{\partial \lambda} \end{pmatrix},$$

$$\frac{\partial}{\partial(\Delta\overline{C}_{lm}, \Delta\overline{S}_{lm})}\left(\frac{\partial V}{\partial r}\right) = -\frac{\mu}{r^2}(l+1)\left(\frac{a}{r}\right)^{l} \overline{P}_{lm}(\sin\varphi)\begin{pmatrix}\cos m\lambda & \sin m\lambda\end{pmatrix},$$

$$\frac{\partial}{\partial(\Delta\overline{C}_{lm}, \Delta\overline{S}_{lm})}\left(\frac{\partial V}{\partial \varphi}\right) = \frac{\mu}{r}\left(\frac{a}{r}\right)^{l} \frac{\mathrm{d}\overline{P}_{lm}(\sin\varphi)}{\mathrm{d}\varphi}\begin{pmatrix}\cos m\lambda & \sin m\lambda\end{pmatrix} \quad \text{and}$$

$$\frac{\partial}{\partial(\Delta\overline{C}_{lm}, \Delta\overline{S}_{lm})}\left(\frac{\partial V}{\partial \lambda}\right) = \frac{\mu}{r} m\left(\frac{a}{r}\right)^{l} \overline{P}_{lm}(\sin\varphi)\begin{pmatrix}-\sin m\lambda & \cos m\lambda\end{pmatrix}. \tag{11.194}$$

2. *Perturbation Forces of the Sun and the Moon as well as Planets*

The perturbation forces of the Sun, the Moon and the planets are given in Sect. 11.2.2 as (cf. Eq. 11.50)

$$\vec{f}_{m} = -m\sum_{j} \mathrm{Gm}(j)\left[\frac{\vec{r}-\vec{r}_{m(j)}}{\left|\vec{r}-\vec{r}_{m(j)}\right|^{3}} + \frac{\vec{r}_{m(j)}}{r_{m(j)}^{3}}\right], \tag{11.195}$$

where $\mathrm{Gm}(j)$ are the gravitational constants of the Sun and the Moon as well as the planets, and the vector with index $m(j)$ are the geocentric vector of the Sun, the Moon and the planets. The partial derivatives of the perturbation force with respect to the satellite vector are then

(c) ketabton.com: The Digital Library

$$\frac{\partial \vec{f}_m}{\partial \vec{r}} = -m \sum_j \frac{\mathrm{Gm}(j)}{\left|\vec{r} - \vec{r}_{m(j)}\right|^3} \left(E + \frac{3}{\left|\vec{r} - \vec{r}_{m(j)}\right|^2} \begin{pmatrix} x - x_{m(j)} \\ y - y_{m(j)} \\ z - z_{m(j)} \end{pmatrix} \begin{pmatrix} x - x_{m(j)} \\ y - y_{m(j)} \\ z - z_{m(j)} \end{pmatrix}^T \right), \tag{11.196}$$

where E is an identity matrix of size 3×3. The partial derivatives of the force vector with respect to the velocity vector of the satellite are zero. The disturbances of the Sun, Moon and planets are considered well-modelled; therefore, no parameters will be adjusted. In other words, the partial derivatives of the force vector with respect to the model parameters do not exist.

3. *Tidal Disturbing Forces*

Similar to the geopotential attracting force, the tidal force (cf. Sect. 11.2.3) has the form of

$$\vec{f}_{\mathrm{ECEF}} = \begin{pmatrix} f_{x'} \\ f_{y'} \\ f_{z'} \end{pmatrix} = \begin{pmatrix} b_{11} \dfrac{\partial V}{\partial r} + b_{21} \dfrac{\partial V}{\partial \varphi} + b_{31} \dfrac{\partial V}{\partial \lambda} \\ b_{12} \dfrac{\partial V}{\partial r} + b_{22} \dfrac{\partial V}{\partial \varphi} + b_{32} \dfrac{\partial V}{\partial \lambda} \\ b_{13} \dfrac{\partial V}{\partial r} + b_{23} \dfrac{\partial V}{\partial \varphi} \end{pmatrix}. \tag{11.197}$$

Where $V = \delta V + \delta V_1 + \delta V_2$, it is a summation of the Earth tide potential and the two parts of ocean loading tide potentials. The Eq. 11.188 is still valid for this case. Other higher order partial derivatives can be derived as follows:

$$\frac{\partial^2 \delta V}{\partial r^2} = \sum_{j=1}^{2} \mu_j \sum_{n=2}^{N} k_n \frac{(n+1)(n+2) a_e^{2n+1}}{r^{n+3} r_j^{n+1}} \left[\begin{array}{l} P_n(\sin\varphi) P_n(\sin\delta_j) \\ +2 \sum\limits_{k=1}^{n} \dfrac{(n-k)!}{(n+k)!} P_{nk}(\sin\varphi) P_{nk}(\sin\delta_j) \cos kh_j \end{array} \right],$$

$$\frac{\partial^2 \delta V}{\partial r \partial \varphi} = \sum_{j=1}^{2} \mu_j \sum_{n=2}^{N} -k_n \frac{(n+1) a_e^{2n+1}}{r^{n+2} r_j^{n+1}} \left[\begin{array}{l} \dfrac{\mathrm{d}P_n(\sin\varphi)}{\mathrm{d}\varphi} P_n(\sin\delta_j) \\ +2 \sum\limits_{k=1}^{n} \dfrac{(n-k)!}{(n+k)!} \dfrac{\mathrm{d}P_{nk}(\sin\varphi)}{\mathrm{d}\varphi} P_{nk}(\sin\delta_j) \cos kh_j \end{array} \right],$$

$$\frac{\partial^2 \delta V}{\partial r \partial \lambda} = \sum_{j=1}^{2} \mu_j \sum_{n=2}^{N} -k_n \frac{(n+1) a_e^{2n+1}}{r^{n+2} r_j^{n+1}} \left[2 \sum_{k=1}^{n} \frac{(n-k)!}{(n+k)!} P_{nk}(\sin\varphi) P_{nk}(\sin\delta_j) k \sin kh_j \right],$$

$$\frac{\partial^2 \delta V}{\partial \varphi^2} = \sum_{j=1}^{2} \mu_j \sum_{n=2}^{N} k_n \frac{a_e^{2n+1}}{r^{n+1} r_j^{n+1}} \left[\begin{array}{l} \dfrac{\mathrm{d}^2 P_n(\sin\varphi)}{\mathrm{d}\varphi^2} P_n(\sin\delta_j) \\ +2 \sum\limits_{k=1}^{n} \dfrac{(n-k)!}{(n+k)!} \dfrac{\mathrm{d}^2 P_{nk}(\sin\varphi)}{\mathrm{d}\varphi^2} P_{nk}(\sin\delta_j) \cos kh_j \end{array} \right],$$

(c) ketabton.com: The Digital Library

$$\frac{\partial^2 \delta V}{\partial \varphi \partial \lambda} = \sum_{j=1}^{2} \mu_j \sum_{n=2}^{N} k_n \frac{a_e^{2n+1}}{r^{n+1} r_j^{n+1}} \left[2 \sum_{k=1}^{n} \frac{(n-k)!}{(n+k)!} \frac{\mathrm{d}P_{nk}(\sin\varphi)}{\mathrm{d}\varphi} P_{nk}(\sin\delta_j) k \sin k h_j \right],$$

$$\frac{\partial^2 \delta V}{\partial \lambda^2} = \sum_{j=1}^{2} \mu_j \sum_{n=2}^{N} -k_n \frac{a_e^{2n+1}}{r^{n+1} r_j^{n+1}} \left[2 \sum_{k=1}^{n} \frac{(n-k)!}{(n+k)!} k^2 P_{nk}(\sin\varphi) P_{nk}(\sin\delta_j) \cos k h_j \right],$$

$$\frac{\partial^2 \delta V_1}{\partial r^2} = \iint_O G\sigma H \sum_{n=0}^{\infty} (1+k_n') \frac{(n+1)(n+2) a_e^n}{r^{n+3}} \left[\begin{array}{l} P_n(\sin\varphi) P_n(\sin\varphi_s) + (2-\delta_{0n}) \\ \sum_{k=0}^{n} \frac{(n-k)!}{(n+k)!} P_{nk}(\sin\varphi) P_{nk}(\sin\varphi_s) \cos k(\lambda_s - \lambda) \end{array} \right] \mathrm{d}s,$$

$$\frac{\partial^2 \delta V_1}{\partial r \partial \varphi} = \iint_O G\sigma H \sum_{n=0}^{\infty} (1+k_n') \frac{-(n+1) a_e^n}{r^{n+2}} \left[\begin{array}{l} \frac{\mathrm{d}P_n(\sin\varphi)}{\mathrm{d}\varphi} P_n(\sin\varphi_s) + (2-\delta_{0n}) \cdot \\ \sum_{k=0}^{n} \frac{(n-k)!}{(n+k)!} \frac{\mathrm{d}P_{nk}(\sin\varphi)}{\mathrm{d}\varphi} P_{nk}(\sin\varphi_s) \cos k(\lambda_s - \lambda) \end{array} \right] \mathrm{d}s,$$

$$\frac{\partial^2 \delta V_1}{\partial r \partial \lambda} = \iint_O G\sigma H \sum_{n=0}^{\infty} (1+k_n') \frac{-(n+1) a_e^n}{r^{n+2}} \left[\begin{array}{l} (2-\delta_{0n}) \cdot \\ \sum_{k=0}^{n} \frac{(n-k)!}{(n+k)!} P_{nk}(\sin\varphi) P_{nk}(\sin\varphi_s) k \sin k(\lambda_s - \lambda) \end{array} \right] \mathrm{d}s,$$

$$\frac{\partial^2 \delta V_1}{\partial \varphi^2} = \iint_O G\sigma H \sum_{n=0}^{\infty} (1+k_n') \frac{a_e^n}{r^{n+1}} \left[\begin{array}{l} \frac{\mathrm{d}^2 P_n(\sin\varphi)}{\mathrm{d}\varphi^2} P_n(\sin\varphi_s) + (2-\delta_{0n}) \cdot \\ \sum_{k=0}^{n} \frac{(n-k)!}{(n+k)!} \frac{\mathrm{d}^2 P_{nk}(\sin\varphi)}{\mathrm{d}\varphi^2} P_{nk}(\sin\varphi_s) \cos k(\lambda_s - \lambda) \end{array} \right] \mathrm{d}s,$$

$$\frac{\partial^2 \delta V_1}{\partial \varphi \partial \lambda} = \iint_O G\sigma H \sum_{n=0}^{\infty} (1+k_n') \frac{a_e^n}{r^{n+1}} \left[\begin{array}{l} (2-\delta_{0n}) \cdot \\ \sum_{k=0}^{n} \frac{(n-k)!}{(n+k)!} \frac{\mathrm{d}P_{nk}(\sin\varphi)}{\mathrm{d}\varphi} P_{nk}(\sin\varphi_s) k \sin k(\lambda_s - \lambda) \end{array} \right] \mathrm{d}s,$$

$$\frac{\partial^2 \delta V_1}{\partial \lambda^2} = \iint_O G\sigma H \sum_{n=0}^{\infty} (1+k_n') \frac{a_e^n}{r^{n+1}} \left[\begin{array}{l} -(2-\delta_{0n}) \cdot \\ \sum_{k=0}^{n} \frac{(n-k)!}{(n+k)!} P_{nk}(\sin\varphi) P_{nk}(\sin\varphi_s) k^2 \cos k(\lambda_s - \lambda) \end{array} \right] \mathrm{d}s,$$

(c) ketabton.com: The Digital Library

$$\frac{\partial^2 \delta V_2}{\partial r^2} = \oiint_C G\sigma_e u_r \sum_{n=0}^{\infty} \frac{(n+1)(n+2)a_e^n}{r^{n+3}} \left[P_n(\sin\varphi) P_n(\sin\varphi_s) + (2-\delta_{0n}) \cdot \sum_{k=0}^{n} \frac{(n-k)!}{(n+k)!} P_{nk}(\sin\varphi) P_{nk}(\sin\varphi_s) \cos k(\lambda_s - \lambda) \right] \mathrm{d}s \,,$$

$$\frac{\partial^2 \delta V_2}{\partial r \partial \varphi} = \oiint_C G\sigma_e u_r \sum_{n=0}^{\infty} \frac{-(n+1)a_e^n}{r^{n+2}} \left[\frac{\mathrm{d}P_n(\sin\varphi)}{\mathrm{d}\varphi} P_n(\sin\varphi_s) + (2-\delta_{0n}) \cdot \sum_{k=0}^{n} \frac{(n-k)!}{(n+k)!} \frac{\mathrm{d}P_{nk}(\sin\varphi)}{\mathrm{d}\varphi} P_{nk}(\sin\varphi_s) \cos k(\lambda_s - \lambda) \right] \mathrm{d}s \,,$$

$$\frac{\partial^2 \delta V_2}{\partial r \partial \lambda} = \oiint_C G\sigma_e u_r \sum_{n=0}^{\infty} \frac{-(n+1)a_e^n}{r^{n+2}} \left[(2-\delta_{0n}) \cdot \sum_{k=0}^{n} \frac{(n-k)!}{(n+k)!} P_{nk}(\sin\varphi) P_{nk}(\sin\varphi_s) k \sin k(\lambda_s - \lambda) \right] \mathrm{d}s \,,$$

$$\frac{\partial^2 \delta V_2}{\partial \varphi^2} = \oiint_C G\sigma_e u_r \sum_{n=0}^{\infty} \frac{a_e^n}{r^{n+1}} \left[\frac{\mathrm{d}^2 P_n(\sin\varphi)}{\mathrm{d}\varphi^2} P_n(\sin\varphi_s) + (2-\delta_{0n}) \cdot \sum_{k=0}^{n} \frac{(n-k)!}{(n+k)!} \frac{\mathrm{d}^2 P_{nk}(\sin\varphi)}{\mathrm{d}\varphi^2} P_{nk}(\sin\varphi_s) \cos k(\lambda_s - \lambda) \right] \mathrm{d}s \,,$$

$$\frac{\partial^2 \delta V_2}{\partial \varphi \partial \lambda} = \oiint_C G\sigma_e u_r \sum_{n=0}^{\infty} \frac{a_e^n}{r^{n+1}} \left[(2-\delta_{0n}) \cdot \sum_{k=0}^{n} \frac{(n-k)!}{(n+k)!} \frac{\mathrm{d}P_{nk}(\sin\varphi)}{\mathrm{d}\varphi} P_{nk}(\sin\varphi_s) k \sin k(\lambda_s - \lambda) \right] \mathrm{d}s \quad \text{and}$$

$$\frac{\partial^2 \delta V_2}{\partial \lambda^2} = \oiint_C G\sigma_e u_r \sum_{n=0}^{\infty} \frac{a_e^n}{r^{n+1}} \left[-(2-\delta_{0n}) \cdot \sum_{k=0}^{n} \frac{(n-k)!}{(n+k)!} P_{nk}(\sin\varphi) P_{nk}(\sin\varphi_s) k^2 \cos k(\lambda_s - \lambda) \right] \mathrm{d}s \,, \qquad (11.198)$$

where

$$\frac{\mathrm{d}P_n(\sin\varphi)}{\mathrm{d}\varphi} = \frac{n}{\cos\varphi} (P_{n-1}(\sin\varphi) - \sin\varphi P_n(\sin\varphi)) \quad \text{and}$$

$$\frac{\mathrm{d}P_{nk}(\sin\varphi)}{\mathrm{d}\varphi} = P_{n(k+1)}(\sin\varphi) - k\tan\varphi P_{nk}(\sin\varphi) \,. \qquad (11.199)$$

(c) ketabton.com: The Digital Library

4. *Solar Radiation Pressure*

Solar radiation force acting on the satellite's surface is (cf. Sect. 11.2.4)

$$\vec{f}_{\text{solar}} = m\gamma P_s C_r r_{\text{sun}}^2 \frac{S}{m} \frac{\vec{r} - \vec{r}_{\text{sun}}}{\left|\vec{r} - \vec{r}_{\text{sun}}\right|^3} ; \tag{11.200}$$

the partial derivatives of the perturbation force with respect to the satellite vector are then

$$\frac{\partial \vec{f}_{\text{solar}}}{\partial \vec{r}} = m\gamma P_s C_r r_{\text{sun}}^2 \frac{S}{m} \frac{1}{\left|\vec{r} - \vec{r}_{\text{sun}}\right|^3} \left(E - \frac{3}{\left|\vec{r} - \vec{r}_{\text{sun}}\right|^2} \begin{pmatrix} x - x_{\text{sun}} \\ y - y_{\text{sun}} \\ z - z_{\text{sun}} \end{pmatrix} \begin{pmatrix} x - x_{\text{sun}} \\ y - y_{\text{sun}} \\ z - z_{\text{sun}} \end{pmatrix}^T \right), \tag{11.201}$$

where E is an identity matrix of size 3×3. The partial derivatives of the force vector with respect to the velocity vector of the satellite are zero. The disturbance of the solar radiation is considered not well-modelled; therefore, unknown parameters will also be adjusted. The total model is (cf. Sect. 11.2)

$$\vec{f}_{\text{solar-force}} = \vec{f}_{\text{solar}} + \begin{pmatrix} a_{11} & a_{12} & a_{13} \\ a_{21} & a_{22} & a_{23} \\ a_{31} & a_{32} & a_{33} \end{pmatrix} \begin{pmatrix} 1 \\ \cos u \\ \sin u \end{pmatrix}. \tag{11.202}$$

Thus,

$$\frac{\partial \vec{f}_{\text{solar-force}}}{\partial \vec{r}} = \frac{\partial \vec{f}_{\text{solar}}}{\partial \vec{r}} + \begin{pmatrix} a_{11} & a_{12} & a_{13} \\ a_{21} & a_{22} & a_{23} \\ a_{31} & a_{32} & a_{33} \end{pmatrix} \begin{pmatrix} 0 \\ -\sin u \\ \cos u \end{pmatrix} \frac{\partial u}{\partial \vec{r}} , \tag{11.203}$$

where

$$\frac{\partial u}{\partial \vec{r}} = \frac{\partial u}{\partial(\Omega, i, \omega, a, e, M)} \frac{\partial(\Omega, i, \omega, a, e, M)}{\partial(\vec{r}, \dot{\vec{r}})} \frac{\partial(\vec{r}, \dot{\vec{r}})}{\partial \vec{r}} . \tag{11.204}$$

On the right-hand side of above equation there are three matrices, the first one is a 1×6 matrix (vector) and is given in Sect. 11.1.2 (cf. Eq. 11.24), the second one is given as its inverse in Sect. 11.4 (cf. Eqs. 11.130 and 11.132), and the third one is a 6×3 matrix, or

$$\frac{\partial u}{\partial(\Omega, i, \omega, a, e, M)} = (0, 0, 1, 0, \frac{2 + e\cos f}{1 - e^2} \sin f, \left(\frac{a}{r}\right)^2 \sqrt{1 - e^2}) ,$$

$$\frac{\partial(\Omega, i, \omega, a, e, M)}{\partial(\vec{r}, \dot{\vec{r}})} = \left(\frac{\partial(\vec{r}, \dot{\vec{r}})}{\partial(\Omega, i, \omega, a, e, M)} \right)^{-1} = \begin{pmatrix} \dfrac{\partial R}{\partial(\Omega, i, \omega)} \vec{q} & R \dfrac{\partial \vec{q}}{\partial(a, e, M)} \\ \dfrac{\partial R}{\partial(\Omega, i, \omega)} \dot{\vec{q}} & R \dfrac{\partial \dot{\vec{q}}}{\partial(a, e, M)} \end{pmatrix}^{-1} \quad \text{and}$$

(c) ketabton.com: The Digital Library

$$\frac{\partial(\vec{r},\dot{\vec{r}})}{\partial\vec{r}}=\begin{pmatrix}E_{3\times3}\\0_{3\times3}\end{pmatrix}. \tag{11.205}$$

$$\frac{\partial u}{\partial\dot{\vec{r}}}=\frac{\partial u}{\partial(\Omega,i,\omega,a,e,M)}\frac{\partial(\Omega,i,\omega,a,e,M)}{\partial(\vec{r},\dot{\vec{r}})}\frac{\partial(\vec{r},\dot{\vec{r}})}{\partial\dot{\vec{r}}} \quad \text{and}$$

$$\frac{\partial(\vec{r},\dot{\vec{r}})}{\partial\dot{\vec{r}}}=\begin{pmatrix}0_{3\times3}\\E_{3\times3}\end{pmatrix}. \tag{11.206}$$

The partial derivatives of the force vector with respect to the model parameters are (for $i=1, 2, 3$)

$$\frac{\partial\vec{f}_{\text{solar}-\text{force}}}{\partial a_{ij}}=\begin{cases}1 & \text{if } j=1\\ \cos u & \text{if } j=2\\ \sin u & \text{if } j=3\end{cases}. \tag{11.207}$$

If the Model 11.74

$$\alpha\vec{f}_{\text{solar}}=\begin{pmatrix}a_1 & b_1\\ a_2 & b_2\\ a_3 & b_3\end{pmatrix}\begin{pmatrix}1\\ t\end{pmatrix} \tag{11.208}$$

is used, then one has

$$\frac{\partial\vec{f}_{\text{solar}-\text{force}}}{\partial(a_i,b_i)}=(1,t),\quad i=1,2,3. \tag{11.209}$$

5. *Atmospheric Drag*

Atmospheric drag force has a form of (cf. Sect. 11.2.5)

$$\vec{f}_{\text{drag}}=-m\frac{1}{2}\left(\frac{C_dS}{m}\right)\sigma\left|\dot{\vec{r}}-\dot{\vec{r}}_{\text{air}}\right|\left(\dot{\vec{r}}-\dot{\vec{r}}_{\text{air}}\right), \tag{11.210}$$

and the air drag force model is

$$\vec{f}_{\text{air}-\text{drag}}=\vec{f}_{\text{drag}}+(1+q)\Delta\vec{f}_{\text{drag}}, \tag{11.211}$$

where (cf. Eqs. 11.84 and 11.85)

$$\Delta\vec{f}_{\text{drag}}=\left[a+b\varphi(2\omega)\cos(2f)+c\varphi(3\omega)\cos(3f)+d\varphi(\omega)\cos f\right]\vec{p}, \tag{11.212}$$

$$\varphi(k\omega)=\begin{cases}\sin k\omega & \text{if} \quad \cos k\omega=0\\ \dfrac{1}{\cos k\omega} & \text{if} \quad \cos k\omega\neq0\end{cases},\quad k=1, 2, 3 \tag{11.213}$$

(c) ketabton.com: The Digital Library

It is obvious that the partial derivatives of the air drag force with respect to the satellite position vector are zero, and

$$\frac{\partial \vec{f}_{\text{drag}}}{\partial \dot{\vec{r}}} = -m\frac{1}{2}\left(\frac{C_{\text{d}}S}{m}\right)\sigma\left(\left|\dot{\vec{r}}-\dot{\vec{r}}_{\text{air}}\right|E+\frac{1}{\left|\dot{\vec{r}}-\dot{\vec{r}}_{\text{air}}\right|}\begin{pmatrix}\dot{x}-\dot{x}_{\text{air}}\\ \dot{y}-\dot{y}_{\text{air}}\\ \dot{z}-\dot{z}_{\text{air}}\end{pmatrix}\begin{pmatrix}\dot{x}-\dot{x}_{\text{air}}\\ \dot{y}-\dot{y}_{\text{air}}\\ \dot{z}-\dot{z}_{\text{air}}\end{pmatrix}^{T}\right), \tag{11.214}$$

$$\frac{\partial \Delta\vec{f}_{\text{drag}}}{\partial f} = \left[-2b\varphi(2\omega)\sin(2f)-c\varphi(3\omega)\sin(3f)-d\varphi(\omega)\sin f\right]\vec{p}\,, \tag{11.215}$$

$$\frac{\partial \Delta\vec{f}_{\text{drag}}}{\partial \omega} = \left[b\cos(2f)\frac{\partial\varphi(2\omega)}{\partial\omega}+c\cos(3f)\frac{\partial\varphi(3\omega)}{\partial\omega}+d\cos f\frac{\partial\varphi(\omega)}{\partial\omega}\right]\vec{p}\,, \tag{11.216}$$

$$\frac{\partial\varphi(k\omega)}{\partial\omega} = \begin{cases} k\cos k\omega & \text{if} \quad \cos k\omega = 0 \\ \dfrac{k\tan k\omega}{\cos k\omega} & \text{if} \quad \cos k\omega \neq 0 \end{cases}, \quad k=1,2,3 \tag{11.217}$$

$$\frac{\partial \Delta\vec{f}_{\text{drag}}}{\partial(\vec{r},\dot{\vec{r}})} = \frac{\partial \Delta\vec{f}_{\text{drag}}}{\partial(\omega,f)}\frac{\partial(\omega,f)}{\partial(\Omega,i,\omega,a,e,M)}\frac{\partial(\Omega,i,\omega,a,e,M)}{\partial(\vec{r},\dot{\vec{r}})}\frac{\partial(\vec{r},\dot{\vec{r}})}{\partial(\vec{r},\dot{\vec{r}})}, \tag{11.218}$$

where

$$\frac{\partial\omega}{\partial(\Omega,i,\omega,a,e,M)} = (0,0,1,0,0,0)\,,$$

$$\frac{\partial f}{\partial(\Omega,i,\omega,a,e,M)} = \left(0,0,0,0,\frac{2+e\cos f}{1-e^2}\sin f,\left(\frac{a}{r}\right)^2\sqrt{1-e^2}\right)$$

Some of the formulas have been derived before in this subsection. The partial derivatives of the force vector with respect to the model parameters can be obtained from Eq. 11.215.

(c) ketabton.com: The Digital Library

Chapter 12

Discussions

The previous chapters of this book covered the most important contents of static and kinematic as well as dynamic GPS, including theory, algorithms, and applications. At the end of this book, the author will emphasize, discuss and comment on some important topics and remaining problems with GPS.

12.1 Independent Parameterisation and A Priori Information

A Priori Information

As already discussed in the parameterisation of the GPS observation model (Sects. 9.1 and 9.2), clock errors and instrumental biases as well as ambiguities are partially over-parameterised or linearly correlated (related to themselves and between them). Cancelling the over-parameterised unknowns out of the equation or modelling them first and then keeping them fixed using the a priori method (Sect. 7.8) is, generally speaking, equivalent. As long as one knows which parameters should be kept fixed, the a priori information used is true one and is just used as a tool for fixing the parameters to zero. If the model is not parameterised regularly and one does not exactly know which parameters are over-parameterised, then the normal equation will be singular and cannot be solved. Again, using a priori information may make the equation solvable. However, in this case, the a priori information has the meaning of the direct "measures" on the related parameters. Therefore the a priori information used must be a true and reasonable one; otherwise, the given a priori information will affect the solution in some unreasonable ways. If different a priori information is given, different results will be obtained. Therefore, the a priori information used should be based on true information.

Independent Parameterisation of the Observation Model

A priori information can be obtained from external surveys or from the experiences of long term data processing that does not use a priori information. A regular (independent) parameterisation of the GPS observation model is a precondition for a stable solution of the normal equation without using a priori information. As mentioned above, to parameterise the model independently or to fix the over-parameterised unknowns are equivalent. However, in order to keep some parameters fixed one has to know which parameters are over-parameterised and have to be fixed. Therefore, in any case, one has to know how to parameterise the GPS observation model regularly. Fixing the over-

(c) ketabton.com: The Digital Library

parameterised unknowns after a general parameterisation is equivalent to a direct independent parameterisation. Therefore, the parameterisation of the GPS observation model should be regular.

Inseparability of Some of the Bias Effects

Independent parameterisation is necessary because of the linear correlation of some parameters. The linear correlation partially merges the different effects together so that these effects cannot be separated exactly from each other. The constant parts of the different effects are nearly impossible to be separated without precise physical models, whereas many model parameters are presented in the GPS observation equation and have to be codetermined. The inseparability of the bias effects comes partially from the physics of the surveys and depends on strategy of the surveys. Understanding the inseparability of the bias effects is important for designing surveys. The physical models have to be determined more precisely in order to separate the constant parts of the effects.

Changing of the Physical Meanings of the Parameters

Because of the linear correlation and inseparability of some parameters, the parameters that are to be adjusted may sometimes change their physical meanings. For example, the instrumental biases of the reference frequency and channel are linearly correlated with the clock errors. This indicates that the mentioned biases cannot be modeled separately so that the clock error parameters represent the summation of the clock errors and the related instrumental biases. They may only be separated through extra surveys or alternative models. If the clock errors of the reference satellite and receiver are not adjusted, then the other clock errors represent the relative errors between the other clocks and the reference ones. If the other instrumental biases are not modelled, then they will be absorbed partly into the ambiguities. In such a case the ambiguities represent not only the ambiguities but also parts of instrumental biases so that the ambiguities are not integers anymore. The double difference may eliminate the instrumental biases so that the double differenced ambiguities are free from the effects of instrumental biases, whereas the un-differenced ambiguities include those biases. If the instrumental errors are not modeled, the un-differenced ambiguities are not integers anymore, whereas the double differenced ambiguities are integers (no data combinations are considered here).

Zero Setting and Fixing of the Parameters

Setting a parameter to zero or fixing the parameter to a definite value must be done carefully. Any incorrect setting or fixing is similar to a linear transformation (translation) of the linearly correlated parameters. For example, the clock errors and instrumental biases of the reference station and satellite generally are not zero. Keeping the clock errors and instrumental biases of the reference as zero is similar to making a time system translation with an unknown amount, and such a translation is an inhomogeneous one, because the orbit data are given in the GPS time system. External surveys may help for a correct zero setting.

(c) ketabton.com: The Digital Library

Independent Parameterisation of Physical Models

Independent parameterisation of the bias parameters of the GPS observation model indicates the necessity of further study of the parameterisation problem. As long as the parameters of the physical models should be codetermined by the GPS observation equations, how to parameterise the physical models should be investigated with great care.

12.2 Equivalence of the GPS Data Processing Algorithms

Equivalence Principle

For definitive measures and parameterisation of the observation model, the uncombined und combining algorithms, undifferenced and differencing algorithms, as well as their mixtures are equivalent. The results must be identical and the precisions are equivalent. The practical results should obey this principle.

The equivalence comes from the definite information contents of the surveys and the definitive parameterisation of the observation model. For better results or better precisions of the results, better measures should be made.

Traditional Combinations

Under the traditional parameterisation, the combinations are equivalent. Under the independent parameterisation, the combinations are equivalent, too. However, the combinations under the traditional parameterisation and independent parameterisation are not equivalent. Due to the inexactness of the traditional parameterisation, traditional combinations will lead to inexact results.

Traditional Differencing Algorithms

Traditional differencing algorithms usually only take the differencing equations into account and leave the undifferenced part aside. In this way, the differencing part of equations includes fewer parameters and the systematic effects are reduced. Meanwhile, however, the information contents of the observables are also reduced proportionally. The results of the interested parameters remain the same.

Equivalent Algorithms

Equivalent algorithms are general forms of undifferenced and differencing algorithms. The observation equation can be separated into two diagonal parts, respectively. Each part uses the original observation vector (therefore the original weight matrix); however, the equation owns only a part of the unknown parameters. The normal equation of the original observation equation can be separated into two parts, too. This indicates that any solvable adjustment problem can be separated into two sub-problems.

(c) ketabton.com: The Digital Library

Appendix 1

IAU 1980 Theory of Nutation

Table A.1. The units of A_i and B_i are 0."0001, units of A_i' and B_i' are 0."00001 (cf. McCarthy 1996)

Coefficents of					Values of			
l	l'	F	D	Ω	A_i	A_i'	B_i	B_i'
0	0	0	0	1	−171 996	−1 742	92 025	89
0	0	2	−2	2	−13 187	16	5 736	−31
0	0	2	0	2	−2 274	−2	977	−5
0	0	0	0	2	2 062	2	−895	5
0	−1	0	0	0	−1 426	34	54	−1
1	0	0	0	0	712	1	−7	0
0	1	2	−2	2	−517	12	224	−6
0	0	2	0	1	−386	−4	200	0
1	0	2	0	2	−301	0	129	−1
0	−1	2	−2	2	217	−5	−95	3
−1	0	0	−2	0	158	0	−1	0
0	0	2	−2	1	129	1	−70	0
−1	0	2	0	2	123	0	−53	0
1	0	0	0	1	63	1	−33	0
0	0	0	2	0	63	0	−2	0
−1	0	2	2	2	−59	0	26	0
−1	0	0	0	1	−58	−1	32	0
1	0	2	0	1	−51	0	27	0
−2	0	0	2	0	−48	0	1	0
−2	0	2	0	1	46	0	−24	0
0	0	2	2	2	−38	0	16	0
2	0	2	0	2	−31	0	13	0
1	0	2	−2	2	29	0	−12	0
2	0	0	0	0	29	0	−1	0
0	0	2	0	0	26	0	−1	0
0	0	2	−2	0	−22	0	0	0
−1	0	2	0	1	21	0	−10	0
0	2	0	0	0	17	−1	0	0
−1	0	0	2	1	16	0	−8	0
0	2	2	−2	2	−16	1	7	0
0	1	0	0	1	−15	0	9	0
1	0	0	−2	1	−13	0	7	0
0	−1	0	0	1	−12	0	6	0
2	0	−2	0	0	11	0	0	0
−1	0	2	2	1	−10	0	5	0
1	0	2	2	2	−8	0	3	0
0	0	2	2	1	−7	0	3	0
0	−1	2	0	2	−7	0	3	0
0	1	2	0	2	7	0	−3	0
1	1	0	−2	0	−7	0	0	0
1	0	2	−2	1	6	0	−3	0
0	0	0	2	1	−6	0	3	0
2	0	2	−2	2	6	0	−3	0
1	0	0	2	0	6	0	0	0
−2	0	0	2	1	−6	0	3	0

(c) ketabton.com: The Digital Library

Table A.1. *Continued*

Coefficents of					Values of			
l	l'	F	D	Ω	A_i	A_i'	B_i	B_i'
2	0	2	0	1	−5	0	3	0
1	−1	0	0	0	5	0	0	0
0	0	0	−2	1	−5	0	3	0
0	−1	2	−2	1	−5	0	3	0
0	0	0	1	0	−4	0	0	0
1	0	−2	0	0	4	0	0	0
0	1	0	−2	0	−4	0	0	0
1	0	0	−1	0	−4	0	0	0
0	1	2	−2	1	4	0	−2	0
2	0	0	−2	1	4	0	−2	0
0	−1	2	2	2	−3	0	1	0
3	0	2	0	2	−3	0	1	0
−1	−1	2	2	2	−3	0	1	0
1	−1	2	0	2	−3	0	1	0
1	0	2	0	0	3	0	0	0
1	1	0	0	0	−3	0	0	0
1	−1	0	−1	0	−3	0	0	0
−2	0	2	0	2	−3	0	1	0
−1	0	2	4	2	−2	0	1	0
0	0	2	1	2	2	0	−1	0
3	0	0	0	0	2	0	0	0
1	0	0	0	2	−2	0	1	0
2	0	0	0	1	2	0	−1	0
−1	0	2	−2	1	−2	0	1	0
1	1	2	0	2	2	0	−1	0
−2	0	0	0	1	−2	0	1	0
0	−2	2	−2	1	−2	0	1	0
0	1	0	1	0	1	0	0	0
0	0	2	4	2	−1	0	0	0
2	0	0	2	0	1	0	0	0
1	0	−2	2	0	−1	0	0	0
1	1	0	−2	1	−1	0	0	0
0	−1	2	0	1	−1	0	0	0
1	0	−2	−2	0	−1	0	0	0
0	1	0	2	0	−1	0	0	0
0	0	2	−1	2	−1	0	0	0
0	0	−2	0	1	−1	0	0	0
−1	−1	0	2	1	1	0	0	0
0	1	2	0	1	1	0	0	0
1	0	2	−2	0	−1	0	0	0
3	0	2	−2	2	1	0	0	0
0	0	4	−2	2	1	0	0	0
1	0	0	2	1	−1	0	0	0
2	0	2	2	2	−1	0	0	0
2	0	2	−2	1	1	0	−1	0
1	−1	0	−2	0	1	0	0	0
−1	0	4	0	2	1	0	0	0
−2	0	2	4	2	−1	0	1	0
1	0	2	2	1	−1	0	1	0
1	1	2	−2	2	1	0	−1	0
2	0	0	−4	0	−1	0	0	0
−2	0	2	2	2	1	0	−1	0
1	0	0	−4	0	−1	0	0	0
−1	0	0	0	2	1	0	−1	0
0	1	2	−2	0	−1	0	0	0
−1	0	0	1	1	1	0	0	0
0	1	0	0	2	1	0	0	0
0	1	−2	2	0	−1	0	0	0
0	0	−2	2	1	1	0	0	0
2	1	0	−2	0	1	0	0	0
2	0	−2	0	1	1	0	0	0

(c) ketabton.com: The Digital Library

Appendix 2

Numerical Examples of the Diagonalisation of the Equations

As discussed in Sect. 8.3.7, a normal equation can be diagonalised and the related observation equation can be formed.

For the linearised observation equation (cf. Eq. 8.38)

$$V = L - \begin{pmatrix} A_1 & A_2 \end{pmatrix} \begin{pmatrix} X_1 \\ X_2 \end{pmatrix}, \quad P, \tag{a2.1}$$

the least squares normal equation can be written as (cf. Eqs. 8.39 and 8.40)

$$\begin{pmatrix} M_{11} & M_{12} \\ M_{21} & M_{22} \end{pmatrix} \begin{pmatrix} X_1 \\ X_2 \end{pmatrix} = \begin{pmatrix} W_1 \\ W_2 \end{pmatrix}, \tag{a2.2}$$

where

$$\begin{pmatrix} A_1^T P A_1 & A_1^T P A_2 \\ A_2^T P A_1 & A_2^T P A_2 \end{pmatrix} = \begin{pmatrix} M_{11} & M_{12} \\ M_{21} & M_{22} \end{pmatrix} = M, \quad \mathrm{Inv}(M) = Q = \begin{pmatrix} Q_{11} & Q_{12} \\ Q_{21} & Q_{22} \end{pmatrix},$$

$$W_1 = A_1^T P L, \quad W_2 = A_2^T P L, \tag{a2.3}$$

The normal Eq. a2.2 can be diagonalised as (cf. Eq. 8.41)

$$\begin{pmatrix} M_1 & 0 \\ 0 & M_2 \end{pmatrix} \begin{pmatrix} X_1 \\ X_2 \end{pmatrix} = \begin{pmatrix} B_1 \\ B_2 \end{pmatrix} \tag{a2.4}$$

where

$$\begin{aligned} M_1 &= M_{11} - M_{12}\mathrm{Inv}(M_{22})M_{21} \\ B_1 &= W_1 - M_{12}\mathrm{Inv}(M_{22})W_2 \end{aligned} \quad \text{and} \tag{a2.5}$$

$$\begin{aligned} M_2 &= M_{22} - M_{21}\mathrm{Inv}(M_{11})M_{12} \\ B_2 &= W_2 - M_{21}\mathrm{Inv}(M_{11})W_1 \end{aligned}, \tag{a2.6}$$

The above diagonalisation process can be repeated $r - 1$ times to the second normal equation of Eq. a2.4, so that the second equation of Eq. a2.4 can be fully diagonalised and Eq. a2.4 can be represented as:

(c) ketabton.com: The Digital Library

$$\begin{pmatrix} M_1 & 0 \\ 0 & M_2^{'} \end{pmatrix}\begin{pmatrix} X_1 \\ X_2 \end{pmatrix}=\begin{pmatrix} B_1 \\ B_2^{'} \end{pmatrix}, \tag{a2.7}$$

where $M_2^{'}$ is a diagonal matrix, r is the dimension of X_2, and $B_2^{'}$ is a vector.

Normal Eq. a2.4 related observation equation is (cf. Eq. 8.43)

$$\begin{pmatrix} U_1 \\ U_2 \end{pmatrix}=\begin{pmatrix} L \\ L \end{pmatrix}-\begin{pmatrix} D_1 & 0 \\ 0 & D_2 \end{pmatrix}\begin{pmatrix} X_1 \\ X_2 \end{pmatrix}, \quad \begin{pmatrix} P & 0 \\ 0 & P \end{pmatrix}, \tag{a2.8}$$

where

$$D_1=(E-I)A_1, \quad D_2=(E-J)A_2 \quad \text{and} \tag{a2.9}$$

$$I=A_2M_{22}^{-1}A_2^TP, \quad J=A_1M_{11}^{-1}A_1^TP, \tag{a2.10}$$

where E is an identity matrix, and U_1 and U_2 are residual vectors, which have the same property as V in Eq. a2.1.

By similarly repeating the above process $r-1$ times to the observation equation of X_2 (i.e., the second equation of Eq. a2.8), then Eq. a2.8 turns out to have a form of

$$\begin{pmatrix} U_1 \\ U_2^{'} \end{pmatrix}=\begin{pmatrix} L \\ L^{'} \end{pmatrix}-\begin{pmatrix} D_1 & 0 \\ 0 & D_2^{'} \end{pmatrix}\begin{pmatrix} X_1 \\ X_2 \end{pmatrix}, \quad \begin{pmatrix} P & 0 \\ 0 & P^{'} \end{pmatrix}, \tag{a2.11}$$

where $D_2^{'}$ is in a form of a diagonal matrix where all elements are vectors of dimension r, $P^{'}$ is a diagonal matrix of P, $L^{'}$ is a vector of L, and $U_2^{'}$ is a residual vector that has the same property as V in Eq. a2.1. Equation a2.11 is the observation equation of normal Eq. a2.7.

Numerical examples to illustrate the diagonalisation process of the normal equation and observation equation are given below.

1. *The Case of Two Variables*

For the observation equation (where σ is set to 1, which does not affect all results)

$$\begin{pmatrix} V_1 \\ V_2 \end{pmatrix}=\begin{pmatrix} 1 \\ 2 \\ -1 \end{pmatrix}-\begin{pmatrix} 1 & 1 \\ 1 & 2 \\ 1 & 1 \end{pmatrix}\begin{pmatrix} X_1 \\ X_2 \end{pmatrix}, \quad P=\frac{1}{\sigma^2}\begin{pmatrix} 1 & 0 & 0 \\ 0 & 1 & 0 \\ 0 & 0 & 1 \end{pmatrix}, \tag{a2.12}$$

the least squares normal equation is

$$\begin{pmatrix} 3 & 4 \\ 4 & 6 \end{pmatrix}\begin{pmatrix} X_1 \\ X_2 \end{pmatrix}=\begin{pmatrix} 2 \\ 4 \end{pmatrix}. \tag{a2.13}$$

Because

$$M_1=3-4(1/6)4=1/3, \quad B_1=2-4(1/6)4=-2/3 \quad \text{and}$$

$$M_2=6-4(1/3)4=2/3, \quad B_2=4-4(1/3)2=4/3,$$

Eq. a2.13 is diagonalised as

(c) ketabton.com: The Digital Library

$$\begin{pmatrix} 1/3 & 0 \\ 0 & 2/3 \end{pmatrix}\begin{pmatrix} X_1 \\ X_2 \end{pmatrix}=\begin{pmatrix} -2/3 \\ 4/3 \end{pmatrix}. \tag{a2.14}$$

The solution ($X_1 = -2, X_2 = 2$) of Eq. a2.14 is the same as that of Eq. a2.13. Furthermore, to form the equivalent observation equation, there are

$$M_{11} = A_1^T A_1 = \begin{pmatrix} 1 & 1 & 1 \end{pmatrix}\begin{pmatrix} 1 \\ 1 \\ 1 \end{pmatrix} = 3, \quad M_{22} = A_2^T A_2 = \begin{pmatrix} 1 & 2 & 1 \end{pmatrix}\begin{pmatrix} 1 \\ 2 \\ 1 \end{pmatrix} = 6,$$

$$I = \begin{pmatrix} 1 \\ 2 \\ 1 \end{pmatrix}\frac{1}{6}\begin{pmatrix} 1 & 2 & 1 \end{pmatrix} = \frac{1}{6}\begin{pmatrix} 1 & 2 & 1 \\ 2 & 4 & 2 \\ 1 & 2 & 1 \end{pmatrix}, \quad J = \begin{pmatrix} 1 \\ 1 \\ 1 \end{pmatrix}\frac{1}{3}\begin{pmatrix} 1 & 1 & 1 \end{pmatrix} = \frac{1}{3}\begin{pmatrix} 1 & 1 & 1 \\ 1 & 1 & 1 \\ 1 & 1 & 1 \end{pmatrix},$$

$$D_1 = (E-I)A_1 = \frac{1}{6}\begin{pmatrix} 5 & -2 & -1 \\ -2 & 2 & -2 \\ -1 & -2 & 5 \end{pmatrix}\begin{pmatrix} 1 \\ 1 \\ 1 \end{pmatrix} = \frac{1}{3}\begin{pmatrix} 1 \\ -1 \\ 1 \end{pmatrix} \quad \text{and}$$

$$D_2 = (E-J)A_2 = \frac{1}{3}\begin{pmatrix} 2 & -1 & -1 \\ -1 & 2 & -1 \\ -1 & -1 & 2 \end{pmatrix}\begin{pmatrix} 1 \\ 2 \\ 1 \end{pmatrix} = \frac{1}{3}\begin{pmatrix} -1 \\ 2 \\ -1 \end{pmatrix};$$

thus, the observation equation related to Eq. a2.14 is

$$\begin{pmatrix} U_1 \\ U_2 \end{pmatrix} = \begin{pmatrix} \begin{pmatrix} 1 \\ 2 \\ -1 \end{pmatrix} \\ \begin{pmatrix} 1 \\ 2 \\ -1 \end{pmatrix} \end{pmatrix} - \begin{pmatrix} \frac{1}{3}\begin{pmatrix} 1 \\ -1 \\ 1 \end{pmatrix} & 0_{3\times 1} \\ 0_{3\times 1} & \frac{1}{3}\begin{pmatrix} -1 \\ 2 \\ -1 \end{pmatrix} \end{pmatrix}\begin{pmatrix} X_1 \\ X_2 \end{pmatrix}, \quad \begin{pmatrix} P & 0 \\ 0 & P \end{pmatrix}. \tag{a2.15}$$

The normal equation of the observation Eq. a2.15 is exactly the same as Eq. a2.14. This numerical example shows that the normal equation and the related observation equation can be diagonalised.

2. *The Case of Three Variables*

For the observation equation (where σ is set to 1, which does not affect all results)

$$\begin{pmatrix} V_1 \\ V_2 \\ V_3 \end{pmatrix} = \begin{pmatrix} 2 \\ 1 \\ 0 \\ -2 \end{pmatrix} - \begin{pmatrix} 1 & 1 & 1 \\ 2 & 1 & 1 \\ 1 & 1 & 2 \\ 1 & 1 & 1 \end{pmatrix}\begin{pmatrix} X_1 \\ X_2 \\ X_3 \end{pmatrix}, \quad P = \frac{1}{\sigma^2}E_{4\times 4}, \tag{a2.16}$$

(c) ketabton.com: The Digital Library

the least squares normal equation is

$$\begin{pmatrix} 7 & 5 & 6 \\ 5 & 4 & 5 \\ 6 & 5 & 7 \end{pmatrix}\begin{pmatrix} X_1 \\ X_2 \\ X_3 \end{pmatrix}=\begin{pmatrix} 2 \\ 1 \\ 1 \end{pmatrix}. \tag{a2.17}$$

Because

$$M_{22}^{-1}=\begin{pmatrix} 4 & 5 \\ 5 & 7 \end{pmatrix}^{-1}=\frac{1}{3}\begin{pmatrix} 7 & -5 \\ -5 & 4 \end{pmatrix}, \quad M_{11}^{-1}=\frac{1}{7},$$

$$M_1=7-\begin{pmatrix} 5 & 6 \end{pmatrix}\frac{1}{3}\begin{pmatrix} 7 & -5 \\ -5 & 4 \end{pmatrix}\begin{pmatrix} 5 \\ 6 \end{pmatrix}=\frac{2}{3}, \quad B_1=2-\begin{pmatrix} 5 & 6 \end{pmatrix}\frac{1}{3}\begin{pmatrix} 7 & -5 \\ -5 & 4 \end{pmatrix}\begin{pmatrix} 1 \\ 1 \end{pmatrix}=\frac{2}{3},$$

$$M_2=\begin{pmatrix} 4 & 5 \\ 5 & 7 \end{pmatrix}-\begin{pmatrix} 5 \\ 6 \end{pmatrix}\frac{1}{7}\begin{pmatrix} 5 & 6 \end{pmatrix}=\frac{1}{7}\begin{pmatrix} 3 & 5 \\ 5 & 13 \end{pmatrix} \quad \text{and} \quad B_2=\begin{pmatrix} 1 \\ 1 \end{pmatrix}-\begin{pmatrix} 5 \\ 6 \end{pmatrix}\frac{1}{7}\cdot 2=\frac{1}{7}\begin{pmatrix} 3 \\ 5 \end{pmatrix}, \tag{a2.18}$$

Eq. a2.17 is diagonalised as

$$\begin{pmatrix} 2/3 & 0 & 0 \\ 0 & 3/7 & 5/7 \\ 0 & 5/7 & 13/7 \end{pmatrix}\begin{pmatrix} X_1 \\ X_2 \\ X_3 \end{pmatrix}=\begin{pmatrix} 2/3 \\ -3/7 \\ -5/7 \end{pmatrix}. \tag{a2.19}$$

The X_2 and X_3 related normal equation can be further diagonalised. Because of

$$M_1^{'}=3/7-5(1/13)(5/7)=2/13, \quad B_1^{'}=-3/7-5(1/13)(-5/7)=-2/13,$$

$$M_2^{'}=13/7-5(1/3)(5/7)=2/3, \quad B_2^{'}=-5/7-5(1/3)(-3/7)=0,$$

Eq. a2.19 is further diagonalised as

$$\begin{pmatrix} 2/3 & 0 & 0 \\ 0 & 2/13 & 0 \\ 0 & 0 & 2/3 \end{pmatrix}\begin{pmatrix} X_1 \\ X_2 \\ X_3 \end{pmatrix}=\begin{pmatrix} 2/3 \\ -2/13 \\ 0 \end{pmatrix}. \tag{a2.20}$$

The solution ($X_1 = 1, X_2 = -1, X_3 = 0$) of Eq. a2.20 is the same as that of Eqs. a2.17 and a2.19. Furthermore, to form the equivalent observation equation of Eq. a2.19, there are

$$I=\begin{pmatrix} 1 & 1 \\ 1 & 1 \\ 1 & 2 \\ 1 & 1 \end{pmatrix}\frac{1}{3}\begin{pmatrix} 7 & -5 \\ -5 & 4 \end{pmatrix}\begin{pmatrix} 1 & 1 & 1 & 1 \\ 1 & 1 & 2 & 1 \end{pmatrix}=\frac{1}{3}\begin{pmatrix} 1 & 1 & 0 & 1 \\ 1 & 1 & 0 & 1 \\ 0 & 0 & 3 & 0 \\ 1 & 1 & 0 & 1 \end{pmatrix},$$

(c) ketabton.com: The Digital Library

$$J=\begin{pmatrix}1\\2\\1\\1\end{pmatrix}\frac{1}{7}\begin{pmatrix}1&2&1&1\end{pmatrix}=\frac{1}{7}\begin{pmatrix}1&2&1&1\\2&4&2&2\\1&2&1&1\\1&2&1&1\end{pmatrix},$$

$$D_1=(E-I)A_1=\frac{1}{3}\begin{pmatrix}-1\\2\\0\\-1\end{pmatrix}\quad\text{and}\quad D_2=(E-J)A_2=\frac{1}{7}\begin{pmatrix}2&1\\-3&-5\\2&8\\2&1\end{pmatrix};$$

thus, the observation equation related to Eq. a2.19 is

$$\begin{pmatrix}U_1\\U_2\end{pmatrix}=\begin{pmatrix}L\\L\end{pmatrix}-\begin{pmatrix}D_1&0\\0&D_2\end{pmatrix}\begin{pmatrix}X_1\\X_2\\X_3\end{pmatrix},\quad\begin{pmatrix}P&0\\0&P\end{pmatrix},\quad\text{where}\quad L=\begin{pmatrix}2\\1\\0\\-2\end{pmatrix}.\tag{a2.21}$$

The X_2 and X_3 related observation equation can be further diagonalised as follows. Because

$$I'=\frac{1}{7}\begin{pmatrix}1\\-5\\8\\1\end{pmatrix}\frac{7}{13}\cdot\frac{1}{7}\begin{pmatrix}1&-5&8&1\end{pmatrix}=\frac{1}{91}\begin{pmatrix}1&-5&8&1\\-5&25&-40&-5\\8&-40&64&8\\1&-5&8&1\end{pmatrix},$$

$$J'=\frac{1}{7}\begin{pmatrix}2\\-3\\2\\2\end{pmatrix}\frac{7}{3}\cdot\frac{1}{7}\begin{pmatrix}2&-3&2&2\end{pmatrix}=\frac{1}{21}\begin{pmatrix}4&-6&4&4\\-6&9&-6&-6\\4&-6&4&4\\4&-6&4&4\end{pmatrix},$$

$$D'_{21}=A'_1-I'A'_1=\frac{1}{7}\begin{pmatrix}2\\-3\\2\\2\end{pmatrix}-\frac{1}{7\cdot91}\begin{pmatrix}35\\-175\\280\\35\end{pmatrix}=\frac{1}{13}\begin{pmatrix}3\\-2\\-2\\3\end{pmatrix}\quad\text{and}$$

$$D'_{22}=A'_2-J'A'_2=\frac{1}{7}\begin{pmatrix}1\\-5\\8\\1\end{pmatrix}-\frac{1}{21\cdot7}\begin{pmatrix}70\\-105\\70\\70\end{pmatrix}=\frac{1}{3}\begin{pmatrix}-1\\0\\2\\-1\end{pmatrix},$$

(c) ketabton.com: The Digital Library

the observation equation related to Eq. a2.20 is

$$\begin{pmatrix} U_1 \\ U_2^{'} \\ U_3^{'} \end{pmatrix} = \begin{pmatrix} L \\ L \\ L \end{pmatrix} - \begin{pmatrix} D_1 & 0 & 0 \\ 0 & D_{21}^{'} & 0 \\ 0 & 0 & D_{22}^{'} \end{pmatrix} \begin{pmatrix} X_1 \\ X_2 \\ X_3 \end{pmatrix}, \quad \begin{pmatrix} P & 0 & 0 \\ 0 & P & 0 \\ 0 & 0 & P \end{pmatrix}. \tag{a2.22}$$

The normal Eq. a2.17 and its related observation Eq. a2.16 are fully diagonalised as Eqs. a2.20 and a2.22, respectively. These numerical examples show that the normal equation and the related observation equation can be diagonalised as described in Sect. 8.3.7.

(c) ketabton.com: The Digital Library

References

Abidin HZ (1995) GPS and hydro-oceanographic surveying in Indonesia. Int J Geomatics 9(4):35–37

Abidin HZ, et al. (2004) The deformation of Bromo Volcano as detected by GPS surveys method. J GPS 3(1–2):16–24

Abramowitz M, Stegun IA (1965) Handbook of mathematical functions. Dover Publications, Inc., New York

Adami D, Garroppo RG, Giordano S, Lucetti S (2003) On synchronization techniques: Performance and impact on time metrics monitoring. Int J Comm Syst 16(4):273–290

Afraimovich EL, Kosogorov EA, Leonovich LA (2000) The use of the international GPS network as the global detector (GLOBDET) simultaneously observing sudden ionospheric disturbance. Earth Planets Space 52(11):1077–1082

Akos DM (2003) The role of Global Navigation Satellite System (GNSS) software radios in embedded systems. GPS Solutions 7(1):1–4

Al-Haifi Y, Corbett S, Cross P (1997) Performance evaluation of GPS single-epoch on-the-fly ambigu-ity resolution. J Inst Navig 44,4:479–487

Albertella A, Sacerdote F (1995) Spectral analysis of block averaged data in geopotential global model determination. J Geodesy 70,3:166–175

Andersen OB (1994) M,2, and S,2, ocean tide models for the North Atlantic Ocean and adjacent seas from ERS-1 altimetry, Space at the service of our environment. In: Proceedings of the second ERS-1 symposium, Hamburg, 11–14 October 1993, Vol. 2., January 1994, Noordwijk, pp 789–794

Andersen PH, Kristiansen O, Zarraoa N (1995) Analysis of data from the VLBI-GPS collocation experiment CONT94. In: GPS Trends in Precise Terrestrial, Airborne, and Spaceborne Applications: 21st IUGG General Assembly, IAG Symposium No. 115, Boulder, USA, July 3–4, 1995, Springer-Verlag, Berlin, pp 315–319

Angermann D, Becker M (2000) Untersuchungen zu Genauigkeit und systematischen Effekten in großräumigen GPS-Netzen am Beispiel von GEODYSSEA. ZfV 125(3):88–95

Angermann D, Baustert G, Klotz J (1995) The impact of IGS on the analysis of regional GPS-network. In: GPS Trends in Precise Terrestrial Airborne, and Spaceborne Applications: 21st IUGG General Assembly, IAG Symposium No. 115, Boulder, USA, July 3–4, 1995, Springer-Verlag, Berlin, pp 35–41

Arikan F, Erol CB, Arikan O (2003) Regularized estimation of vertical total electron content from Global Positioning System data. J Geophys Res 108(A12):SIA20/1–12

Artese G, Cefalo R, Vettore A (1997) Real time kinematic GPS to bathymetry. Rep Geod 5(28):77–87

Ashby N, Spilker JJ (1996) Introduction to relativistic effects on the Global Positioning System. In: Parkinson BW, Spilker JJ (eds) Global Positioning System: Theory and applications, Vol. I, Chapter 18

Ashkenazi V, Beamson G, Bingley R (1995) Monitoring absolute changes in mean sea level. In: Proceedings of the First Turkish International Symposium on Deformations "Istanbul-94", Istanbul, September 5–9, pp 40–46

Ashkenazi V, Park D, Dumville M (2000) Robot positioning and the global navigation satellite system. Ind Robot 27(6):419–426

Aw York Bin, Goh Pong Chai (1996) Improving cadastral survey controls using GPS surveying in Singapore. Survey rev 33:488–495

Axelsson O (1994) Iterative Solution Methods. Cambridge University Press

Ayres F (1975) Differential- und Integralrechnung, Schaum's Outline. McGraw-Hill Book

Babu R (2005) Web-based resources on software GPS receivers. GPS Solutions 9(3):240–242

Baertlein H, Carlson B, Eckels R, Lyle S, Wilson S (2000) A high-performance, high-accuracy RTK GPS machine guidance system. GPS Solutions 3(3):4–11

Baldi P, Bonvalot S, Briole P, Marsella M (2000) Digital photogrammetry and kinematic GPS applied to the monitoring of Vulcano Island, Aeolian Arc, Italy. Geophys J Int 142(3):801–811

(c) ketabton.com: The Digital Library

Balmino G, Schrama E, Sneeuw N (1996) Compatibility of first-order circular orbit perturbations theories: Consequences for cross-track inclination functions. J Geodesy 70,9:554–561
Banyai L, Gianniou M (1997) Comparison of Turbo-Rogue and Trimble SSI GPS receivers for ionospheric investigation under anti-spoofing. ZfV 3:136–142
Bar-Sever YE (1996) A new model for GPS yaw attitude. J Geodesy 70:714–723
Barthelmes F (1996) Die Wavelet-Transformation zur Zeitreihenanalyse. Erste Geodätische Woche, Stuttgart, 7.–12. Oktober 1996, 15 Blatt
Bastos L, Landau H(1988) Fixing cycle slips in dual-frequency kinematic GPS-application using Kalman filtering. Manuscr Geodaet 13:249–256
Bastos L, Osorio J, Hein G (1995) GPS derived displacements in the Azores Triple Junction Region. In: GPS Trends in Precise Terrestrial Airborne, and Spaceborne Applications: 21st IUGG General Assembly, IAG Symposium No. 115, Boulder, USA, July 3–4, 1995, Springer-Verlag, Berlin, pp 99–104
Bate RR, Mueller DD, White JE (1971) Fundamentals of astrodynamics. Dover, New York
Bauer M (1994) Vermessung und Ortung mit Satelliten. Wichmann Verlag, Karslruhe
Bause F, Toelle W (1993) Programmieren mit C++, Version 3. Vieweg & Sohn, Verlagsgesellschaft mbH, Braunschweig
Becker M, Angermann D, Nordin S, Reigber C, Reinhart E (2000) Das Geschwindigkeitsfeld in Südostasien aus einer kombinierten GPS Lösung der drei GEODYSSEA Kampagnen von 1994 bis 1998. ZfV 125(3):74–80
Berrocoso M, Garate J, Martin J (1996) Improving the local geoid with GPS. In: Proceedings of the Techniques for local geoid determination, session G7 European Geophysical Society XXIst General Assembly The Hague, The Netherlands, 6–10 May, 1996, Masala, pp 91–96
Beutler G (1994) GPS trends in precise terrestrial, airborne, and space borne applications. Springer-Verlag, Heidelberg
Beutler G (1996) GPS satellite orbits. In Kleusberg A, Teunissen PJG (eds) GPS for geodesy. Springer-Verlag, Berlin
Beutler G (1996) The GPS as a tool in global geodynamics. In: Kleusberg A, Teunissen PJG (eds) GPS for geodesy. Springer-Verlag, Berlin
Beutler G, Brockmann E, Gurtner W, Hugentobler U, Mervart L, Rothacher M, Verdun A (1994) Extended orbit modelling techniques at the CODE Processing Center of the IGS: Theory and initial results. Manuscr Geodaet 19:367–386
Beutler G, Brockmann E, Hugentobler U (1996) Combining consecutive short arcs into long arcs for precise and efficient GPS orbit determination. J Geodesy 70,5:287–299
Beutler G, Schildknecht T, Hugentobler U, Gurtner W (2003) Orbit determination in satellite geodesy. Adv Space Res 31(8):1853–1868
Beyerle G, Wickert J, Schmidt T, Reigber C (2004) Atmos. sounding by global navigation satellite system radio occultation: An analysis of the negative refractivity bias using CHAMP observations. J Geophys Res 109(D01106):1–8
Bian S (1996) Topography supported GPS leveling. ZfV 121(3):109–113
Bian S, Jin J, Fang Z (2005) The Beidou satellite positioning system and its positioning accuracy. Navigation 52(3):123–129
Bisnath S, Wells D, Howden S, Dodd D, Wiesenburg D (2004) Development of an operational RTK GPS-equipped buoy for tidal datum determination. Int Hydrogr Rev 5(1):54–64
Blewitt G (1998) GPS data processing methodology. In: Teunissen PJG, Kleusberg A (eds) GPS for Geodesy. Springer-Verlag, Berlin Heidelberg New York, pp 231–270
Blomenhofer H (1996) Untersuchungen zu hochpräzisen kinematischen DGPS-Echtzeitverfahren mit besonderer Berücksichtigung atmosphärischer Fehlereinflüsse. Neubiberg, 166 S
Bock Y (1996) Reference systems. In: Kleusberg A, Teunissen PJG (eds) GPS for geodesy. Springer-Verlag, Berlin
Bock Y (1996) Medium distance GPS measurements. In: Kleusberg A, Teunissen PJG (eds) GPS for geodesy. Springer-Verlag, Berlin
Bock Y, Beutler G, Schaer S, Springer TA, Rothacher M (2000) Processing aspects related to permanent GPS arrays. Earth Planets Space 52(10):657–662
Bock Y, Prawirodirdjo L, Melbourne TI (2004) Detection of arbitrarily large dynamic ground motions with a dense high-rate GPS network. Geophys Res Lett 31(L06604):1–4
Boey SS, Coombe LJ, Gerdan GP (1996) Assessing the accuracy of real time kinematic GPS positions for the purposes of cadastral surveying. Aust Surveyor 41,2:109–120
Bona P (2000) Precision, cross correlation, and time correlation of GPS phase and code observations. GPS Solutions 4(2):3–13
Boomkamp H, Dow J (2005) Use of double difference observations in combined orbit solutions for LEO and GPS satellites. Adv Space Res 36(3):382–391

(c) ketabton.com: The Digital Library

Borge TK, Forssell B (1994) A new real time ambiguity resolution strategy based on polynomial indentification, In: Proceedings of the International Symposium on Kinematic Systems in Geodesy, Geomatics and Navigation, Banff, Canada, 30 August–2 September, pp 233–240
Borre K (2003) The GPS Easy Suit-Matlab code for the GPS newcomer. GPS Solutions 7(1):47–51
Bouin M-N, Vigny C (2000) New constraints on Antarctic plate motion and deformation from GPS data. J Geophys Res 105(B12):28279–28293
Braasch MS (1996) Multipath effects. Parkinson BW, Spilker JJ (eds) Global Positioning System: Theory and applications, Vol. I
Brodin G, Cooper J, Walsh D, Stevens J (2005) The effect of helicopter rotors on GPS signal reception. J Navig 58(3):433–450
Broederbauer V, Weber R (2003) Results of modelling GPS satellite clocks. Österr Z Vermess Geoinf 91(1):38–47
Bronstein IN, Semendjajew KA (1987) Taschenbuch der Mathematik. B.G. Teubner Verlagsgesellschaft, Leipzig, ISBN 3-322-00259-4
Brouwer D, Clemence GM (1961) Methods of celestial mechanics. Academic Press, New York
Brunner FK (1998) Advances in positioning and reference frames. Springer-Verlag, Heidelberg
Brunner FK, Gu M (1991) An improved model for the dual frequency ionospheric correction of GPS observations. Manuscr Geodaet 16:205–214
Brunner FK, Welsch WM (1993) Effect of the troposphere on GPS measurements. GPS World 4:42–51
Bust GS, Coco D, Makela JJ (2000) Combined Ionospheric Campaign 1: Ionospheric tomography and GPS total electron content (TEC) depletions. Geophys Res Lett 27(18):2849–2852
Campbell J, Goerres B, Siemens M, Wirsch J, Becker M (2004) Zur Genauigkeit der GPS Antennenkalibrierung auf der Grundlage von Labormessungen und deren Vergleich mit anderen Verfahren. Allgemeine Vermessungs-Nachrichten 111(1):2–11
Campos MA, Krueger CP (1995) GPS kinematic real-time applications in rivers and train. In: GPS Trends in Precise Terrestrial, Airborne, and Spaceborne Applications: 21st IUGG General Assem-bly, IAG Symposium No. 115, Boulder, USA, July 3–4, 1995. Springer-Verlag, Berlin, pp 222–225
Cangahuala L, Muellerschoen R, Yuan D-N (1995) TOPEX/Poseidon precision orbit determination with SLR and GPS anti-spoofing data. In: GPS Trends in Precise Terrestrial Airborne, and Spaceborne Applications: 21st IUGG General Assembly, IAG Symposium No. 115, Boulder, USA, July 3–4, 1995. Springer-Verlag, Berlin, pp 123–127
Cannon E, Weisenburger S (2000) The use of multiple receivers for constraining GPS carrier phase ambiguity resolution. Lighthouse 57:7–18
Cannon ME, Lachapelle G, Goddard TW (1997) Development and results of a precision farming system using GPS and GIS technologies. Geomatica 51,1:9–19
Cannon ME, Lachapelle G, Szarmes M, Herbert J, Keith J, Jokerst S (1997) DGPS kinematic carrier phase signal simulation analysis for precise velocity and position determination. Proceedings of ION NTM 97, Santa Monica, CA
Cannon ME, Skone S, Karunanayake MD, Kassam A (2004) Performance analysis of the real-time Canada-wide DGPS Service (CDGPS). Geomatica 58(2):95–105
Cardellach E, Behrend D, Ruffini G, Rius R (2000) The use of GPS buoys in the determination of oceanic variables. Earth Planets Space 52(11):1113–1116
Casotto S, Zin A (2000) An assessment of the benefits of including GLONASS data in GPS-based precise orbit determination – I: S/A analysis. Advances in the Astronautical Sciences 105(1):237–256
Castleden, et al. (2004) First results from Virtual Reference Station (VRS) and precise point positioning (PPP) GPS research at the Western Australian Centre for Geodesy. J GPS 3(1–2):79–84
Celebi M (2000) GPS in dynamic monitoring of long-period structures. Soil Dyn Earthq Eng 20(5–8): 477–483
Chang C-C (2000) Estimation of local subsidence using GPS and leveling data. Surveying and Land Information Systems 60(2):85–94
Chang C-C, Sun Y-D (2004) Application of a GPS-based method to tidal datum transfer. Hydrogr J 112:15–20
Chen D (1994) Development of a fast ambiguity search filtering (FASF) method for GPS carrier phase ambiguity resolution. Reports of the Department of Geomatics Engineering of the University of Calgary, Vol. 20071
Chen D, Lachapelle G (1994) A comparison of the FASF and least-squares search algorithms for ambiguity resolution on the fly. In: Proceedings of the International Symposium on Kinematic Systems in Geodesy, Geomatics and Navigation, Banff, Canada, August 30–September 2, pp 241–253
Chen Y-Q, Wang J-L (1996) Reliability measures for correlated observations. ZfV 121,5:211–219
Chen X, Langley RB, Dragert H (1995) The Western Canada Deformation Array: An update on GPS solutions and error analysis. In: GPS Trends in Precise Terrestrial Airborne, and Spaceborne Applications: 21st IUGG General Assembly, IAG Symposium No. 115, Boulder, USA, July 3–4, 1995. Springer-Verlag, Berlin, pp 70–74

(c) ketabton.com: The Digital Library

Chen CS, Chen Y-J, Yeh T-K (2000a) The impact of GPS antenna phase center offset and variation on the positioning accuracy. Bull Geod Sci Affini 59(1):73–94
Chen Y-Q, Ding XL, Huang DF, Zhu JJ (2000b) A multi-antenna GPS system for local area deformation. Earth Planets Space 52(10):873–876
Chen W, et al. (2004) Kinematic GPS precise point positioning for sea level monitoring with GPS buoy. J GPS 3(1–2):302–307
Chen H, Dai L, Rizos C, Han S (2005) Ambiguity recovery using the triple-differenced carrier phase type approach for long-range GPS kinematic positioning. Mar Geod 28(2):119–135
Chobotov VA (ed) (1991) Orbital mechanics. Published by AIAA, Washington
Clark TA (1995) Low-cost GPS time synchronization: The "Totally Accurate Clock". In: GPS Trends in Precise Terrestrial,Airborne, and Spaceborne Applications: 21st IUGG General Assembly,IAG Symposium No. 115, Boulder, USA, July 3–4, 1995. Springer-Verlag, Berlin, pp 325–327
Cohen CE (1996) Altitude determination. Parkinson BW, Spilker JJ (eds) Global Positioning System: Theory and applications, Vol. II
Colombo OL (1984) Altimetry, orbits and tides. NASA Technical Memorandum 86180
Colombo OL (1984) The global mapping of gravity with two satellites. Netherlands Geodetic Commission, Publications on Geodesy, Vol. 7, No. 3
Colombo OL, Rizos C, Hirsch B (1995) Testing high-accuracy, long-range carrier phase DGPS in Australasia. In: GPS Trends in Precise Terrestrial,Airborne, and Spaceborne Applications: 21st IUGG General Assembly, IAG Symposium No. 115, Boulder, USA, July 3–4, 1995. Springer-Verlag, Berlin, pp 226–230
Colombo OL, Hernández-Pajares M, Juan JM, Sanz J, Talaya J (1999) Resolving carrier-phase ambiguities on the fly, at more than 100 km from nearest reference site, with the help of ionospheric topography. ION GPS 99 14–17, September 1999, pp 1635–1642
Corbett SJ, Cross PA (1995) GPS single epoch ambiguity resolution. Survey rev 33(257):149–160
Cross PA, Ramjattan AN (1995) A Kalman filter model for an integrated land vehicle navigation system. In: Proceedings of the 3rd international workshop on high precision navigation: High precision navigation 95. University of Stuttgart, April 1995, Bonn, pp 423–434
Cui C (1990) Die Bewegung künstlicher Satelliten im anisotropen Gravitationsfeld einer gleichmässig rotierenden starren Modellerde. Deutsche Geodätische Kommission, Reihe C: Dissertationen, Heft Nr. 357
Cui C (1997) Satellite orbit integration based on canonical transformations with special regard to the resonance and coupling effects. München, 128 S
Cui C, Lelgemann D (1995) Analytical dynamic orbit improvement for the evaluation of geodetic-geodynamic satellite data. J Geodesy 70:83–97
Cui X, Yu Z, Tao B, Liu D (1982) Adjustment in surveying. Surveying Press, Peking, (in Chinese)
Dach R, Dietrich R (2000) Influence of the ocean loading effect on GPS derived precipitable water vapor. Geophys Res Lett 27(18):2953–2956
Dam T van, Larson KM, Wahr J, Gross S, Francis O (2000) Using GPS and gravity to infer ice mass changes in Greenland. EOS Trans. AGU 81(37):421, 426–427
Davis PJ (1963) Interpolation and approximation. Dover Publications Inc., New York
Davis J, Herring T (1984) New atmospheric mapping function. Center of Astrophysics, Cambridge, Mass., Manuscript July 1984
Davis P, Rabinowitz P (1984) Methods of numerical integration, 2nd Ed. Academic Press, INC
Davis JL, Cosmo ML, Elgered G (1995) Using the Global Positioning System to study the atmosphere of the Earth: Overview and prospects. In: GPS Trends in Precise Terrestrial, Airborne, and Spaceborne Applications: 21st IUGG General Assembly, IAG Symposium No. 115, Boulder, USA, July 3–4, 1995. Springer-Verlag, Berlin, pp 233–242
Denker H (1995) Grossräumige Höhenbestimmung mit GPS- und Schwerefelddaten. Schriftenreihe des Deutschen Vereins für Vermessungswesen, Bd. 18, Stuttgart, pp 233–258
Desai SD, Haines BJ (2003) Near-real-time GPS-based orbit determination and sea surface height observations from The Jason-1 mission. Mar Geod 26(3–4):383–397
Dick G (1997) Nutzung von GPS zur Bahnbestimmung niedrigfliegender Satelliten. GPS-Anwendungen und Ergebnisse '96: Beiträge zum 41. DVW-Fortbildungsseminar vom 7. bis 8. November 1996 am Geo-Forschungszentrum Potsdam, pp 241–249
Dick G, Gendt G (1997) GPS-Anwendungen und Ergebnisse '96: Beiträge zum 41. DVW-Fortbildungsseminar vom 7. bis 8. November 1996 am Geo-Forschungszentrum Potsdam. Geodesia: Nederl. geod. t., Stuttgart
Dierendonck AJ Van, Hegarty C (2000) The new L5 civil GPS signal. GPS World 11(9):64–71
Dietrich R (1997) Untersuchung von vertikalen Krustendeformationen wegen wechselnder Eislauflasten in Grönland. GPS-Anwendungen und Ergebnisse '96: Beiträge zum 41. DVW-Fortbildungsseminar vom 7. bis 8. November 1996 am Geo-Forschungszentrum Potsdam, pp 94–102

(c) ketabton.com: The Digital Library

Dietrich R, Rulke A, Scheinert M (2005) Present-day vertical crustal deformations in West Greenland from repeated GPS observations. Geophys J Int 163(3):865–874
Diggelen F (1998) GPS accuracy: Lies, damm lies, and statistics. GPS World 9,1:41–44 Diggelen F, Martin W (1997) GPS + GLONASS RTK: A quantum leap in RTK performance. Int J Geomatics 11(11):69–71
Ding X, Coleman R (1996) Multiple outlier detection by evaluating redundancy contributions of observations. J Geodesy 708:489–498
Ding X, Coleman R (1996) Adjustment of precision metrology networks in three dimension. Survey rev 33,259:305–315
Ding XL, et al. (2005) Seasonal and secular positional variations at eight co-located GPS and VLBI stations. J Geod 79(1–3):71–81
Dittrich J, Kuehmstedt E, Richter B, Reinhart E (1997) Accurate positioning by low frequency (ALF) and other services for emission of DGPS correction data in Germany. Rep Geod 6(29):97–108
Dodson AH, Shardlow PJ, Hubbard LCM (1995) Wet tropospheric effects on precise relative GPS height determination. J Geodesy 70(4):188–202
Doodson AT (1928) The analysis of tidal observations. Philos Tr R Soc S-A 227:223–279
Douša J (2004) Precise orbits for ground-based GPS meteorology: processing strategy and quality assessment of the orbits determined at geodetic observatory Pecny. J Meteor Soc Japan 82(1B): 371–380
Dow JM (1988) Ocean tides and tectonic plate motions from Lageos. Deutsche Geodätische Kommission, Rheihe C, Dissertation, Heft Nr. 344
Dow JM, Romay-Merino MM, Piriz R (1993) High precision orbits for ERS-1: 3-day and 35-day repeat cycles. In: Proceedings of the Second ERS-1 symposium: Space at the service of our environment, Hamburg, 11–14 October 1993, Vol. 2, Jan. 1994, Noordwijk, pp 1349–1354
Dragert H, James TS, Lambert A (2000) Ocean loading corrections for continuous GPS: A case study at the Canadian coastal site Holberg. Geophys Res Lett 27(14):2045–2048
Drewes H (1996) Kinematische Referenzsysteme für die Landesvermessung. ZfV 121(6):277–285
Drewes H (1997) Realisierung des geozentrischen Referenzsystems für Südamerika (SIRGAS). GPS-Anwendungen und Ergebnisse '96: Beiträge zum 41. DVW-Fortbildungsseminar vom 7. bis 8. November 1996 am Geo-Forschungszentrum Potsdam, pp 54–63
Du RL, Qiao XJ, Wang Q, Xing CF, You XZ (2005) Deformation in the Three Gorges Reservoir after the first impoundment determined by GPS measurements. Progress Natural Sci 15(6):515–522
Eissfeller B, Teuber A, Zucker P (2005) Untersuchungen zum GPS-Satellitenempfang in Gebäuden. Allgemeine Vermessungs-Nachrichten 112(4):137–145
Elosequi P, Davis JL, Jaldehag RTK (1995) Geodesy using the global positioning system: The effects of signal scattering on estimates of site position. J Geophys Res 100(B6):9921–9934
Emardson TR, Jarlemark POJ (1999) Atmospheric modelling in GPS analysis and its effect on the estimated geodetic parameters. J Geodesy 73:322–331
Engel F, Heiser G, Mumford P, Parkinson K, Rizos C (2004) An open GNSS receiver platform architecture. J GPS 3(1–2):63–69
Engelhardt G, Mikolaiski H (1996) Concepts and results of the GPS data processing with Bernese and GIPSY Software. In: German Contributions to the SCAR 95 Epoch Campaign, 1996: The Geodetic Antarctic Project GAP95, Muenchen, pp 37–51
Ephishov II, Baran LW, Shagimuratov II, Yakimova GA (2000) Comparison of total electron content obtained from GPS with IRI. Phys Chem Earth 25C(4):339–342
Euler H-J (1995) Statische/Kinematische Echtzeitvermessung mit GPS. Schriftenreihe des Deutschen Vereins für Vermessungswesen, Bd. 18, Stuttgart, pp 271–286
Euler H-J, Landau H (1992) Fast GPS ambiguity resolution on-the-fly for real-time applications. In: Proceedings of 6th Int. Geod. Symp. on Satellite Positioning. Columbus, Ohio, pp 17–20
Euler H-J, Seeger S, Takac F (2004) Analysis of biases influencing successful rover positioning with GNSS-network RTK. J GPS 3(1–2):70–78
Even-Tzur G, Agmon E (2005) Monitoring vertical movements in Mount Carmel by means of GPS and precise leveling. Surv Rev 38(296):146–157
Exertier P, Bonnefond P (1997) Analytical solution of perturbed circular motion: Application to satellite geodesy. J Geodesy 71(3):149–159
Farrell WE (1972) Deformation of the Earth by surface loads. Rev Geophys Space Ge 10(3):761–797
Faruqi FA, Turner KJ (2000) Extended Kalman filter synthesis for integrated global positioning/inertial navigation systems. Appl Math Comput 115(2–3):213–227
Featherstone WE (2004) Evidence of a north-south trend between AUSGeoid98 and the Australian height datum in southwest Australia. Survey Rev. 37(291):334–343
Featherstone W, Dentith M, Kirby J (1998) Strategies for the accurate determination of orthometric heights from GPS. Survey rev 34(267):278–296

(c) ketabton.com: The Digital Library

Feltens J (1991) Nicht gravitative Störeinflüsse bei der Modellierungen von GPS-Erdumlaufbahnen. DGK, Reihe C, Heft 371, Verlag der Bayerischen Akademie der Wissenschaften
Feng Y (2005) Future GNSS performance. Predictions using GPS with a virtual Galileo constellation. GPS World 16(3):46–52
Feng Y, Kubik K (1997) On the internal stability of GPS solutions. J Geodesy 72:1–10
Fliegel HF, Gallini TE, Swift ER (1992) Global Positioning System radiation force model for geodetic applications. J Geophys Res 97(B1):559–568
Flores A, Escudero A, Sedo MJ, Rius A (2000) A near real time system for tropospheric monitoring using GPS hourly data. Earth Planets Space 52(10):681–684
Forsberg R, Olesen AV, Timmen L, Xu GC, Bastos L, Hehl K, Solheim D (1998) Airborne gravity in Skagerrak and elsewhere: The AGMASCO project and a nordic outlook. In: Proceedings NKG meeting Gvle, May 1998
Forsberg R, Keller K, Nielsen CS, Gundestrup N, Tscherning CC, Madsen SN, Dall J (2000) Elevation change measurements of the Greenland Ice Sheet. Earth Planets Space 52(11):1049–1053
Fotopoulos G, Kotsakis C, Sideris MG (2003) How accurately can we determine orthometric height differences from GPS and geoid data? J Surv Eng ASCE 129(1):1–10
Fry WG (1997) GPS flies high in Midwest flood study: The Mississippi River Project demonstrates viability of large-area airborne GPS-controlled mapping. EOM: mag. geogr, mapp, Earth inf 6(1):28–31
Gabor MJ, Nerem RS (2004) Characteristics of satellite-satellite single difference widelane fractional carrier-phase biases. Navigation 51(1):77–92
Galas R, Reigber C (1997) Status of the IGS stations provided by GFZ. International GPS Service for Geodynamics: 1996 annual report, Pasadena, pp 393–396
Galas R, Reigber C, Baustert G (1995) Permanent betriebene GPS-Stationen in globalen und regionalen Netzen. ZfV 1209:431–438
Gallimore J, Maini A (2000) Galileo: The public-private partnership. GPS World 11(9):58–63
Gao Y, McLellan J, Schleppe J (1998) Integrating GPS with barometry for high-precision real-time kinematic seismic survey, Survey. Land Inf Syst 58(2):115–119
Gao Y, Wojciechowski, Chen K (2005) Airborne kinematic positioning using precise point positioning methodology. Geomatica 59(1):29–36
Garrison JL, Katzberg SJ (2000) The application of reflected GPS signals to ocean remote sensing. Remote Sens Environ 73(2):175–187
Ge L (2003) Integration of GPS and radar interferometry. GPS Solutions 7(1):52–54
Ge LL, Han SW, Rizos C (2000) Multipath mitigation of continuous GPS measurements using an adaptive filter. GPS Solutions 4(2):19–30
Ge M, Calais E, Haase J (2000) Reducing satellite orbit error effects in near real-time GPS zenith tropospheric delay estimation for meteorology. Geophys Res Lett 27(13):1915–1918
Ge M, Gendt G, Dick G, Zhang FP, Reigber C (2005) Impact of GPS satellite antenna offsets on scale changes in global network solutions. Geophys Res Lett 32(L06310):1–4
Gehlich U, Lelgemann D (1997) Zur Parametrisierung von GPS-Phasenmessungen. ZfV 6:262–270
Geiger A, Hirter H, Cocard M (1995) Mitigation of tropospheric effects in local and regional GPS networks. In: GPS Trends in Precise Terrestrial, Airborne, and Spaceborne Applications: 21st IUGG General As-sembly, IAG Symposium No. 115, Boulder, USA, July 3–4, 1995. Springer-Verlag, Berlin, pp 263–267
Gendt G (1997) Analysen der IGS-Daten und Ergebnisse, GPS-Anwendungen und Ergebnisse '96: Beiträge zum 41. DVW-Fortbildungsseminar vom 7. bis 8. November 1996 am Geo-Forschungs-zentrum Potsdam, 1997, Stuttgart, pp 43–53
Gendt G, Dick G, Reigber C (1995) Global plate kinematics estimated by GPS data of the IGS core network. In: GPS Trends in Precise Terrestrial, Airborne, and Spaceborne Applications: 21st IUGG General As-sembly, IAG Symposium No. 115, Boulder, USA, July 3–4, 1995. Springer-Verlag, Berlin, pp 30–34
Georgiadou Y, Doucet KD (1990) The issue of selective availability. GPS World 1(5):53–56
Gianniou M (1996) Genauigkeitssteigerung bei kurzzeit-statischen und kinematischen Satellitenmessungen bis hin zur Echtzeitanwendung. DGK, Reihe C, Heft 458, Verlag der Bayerischen Akademie der Wissenschaften
Gili JA, Corominas J, Rius J (2000) Using Global Positioning System techniques in landslide monitoring. Eng Geol 55(3):167–192
Gleason DM (1996) Avoiding numerical stability problems of long duration DGPS/INS Kalman filters. J Geodesy 70(5):263–275
Goad C (1996) Single-site GPS models. In: Kleusberg A, Teunissen PJG (eds) GPS for geodesy. Springer-Verlag, Berlin
Goad C (1996) Short distance GPS models. In: Kleusberg A, Teunissen PJG (eds) GPS for geodesy. Springer-Verlag, Berlin

(c) ketabton.com: The Digital Library

Goad C, Yang M (1997) A new approach to precision airborne GPS positioning for photogrammetry. Photogramm Eng Rem S 63(9):1067–1077
Goad C, Dorota A, Brzezinska G, Yang M (1996) Determination of high-precision GPS orbits using triple differencing technique. J Geodesy 70:655–662
Goerres B, Campbell J (1998) Bestimmung vertikaler Punktbewegungen mit GPS. ZfV 123(7):222–230
Goodhue J (1997) Experiments aloft: Balloon-borne payloads reach near space. GPS World 8(9):34–42
Gotthardt E (1978) Einführung in die Ausgleichungsrechnung. Herbert Wichmann Verlag, Karlsruhe
Graas FV, Braasch MS (1996) Selective availability. In: Parkinson BW, Spilker JJ (eds) Global Positioning System: Theory and applications, Vol. I, Chapter 17
Grafarend EW (2000) Mixed integer-real valued adjustment (IRA) problems: GPS initial cycle ambiguity resolution by means of the LLL algorithm. GPS Solutions 4(2):31–44
Grafarend E, Ardalan AW (1997) An estimate in the Finnish Height Datum N60, epoch 1993.4, from twenty-five GPS points of the Baltic Sea Level Project. J Geodesy 71(11):673–679
Grejner-Brzezinska DA, et al. (2004) An analysis of the effects of different network-based ionosphere estimation models on rover positioning accuracy. J GPS 3(1–2):115–131
Grejner-Brzezinska D, Toth C, Yi YD (2005) On improving navigation accuracy of GPS/INS systems. Photogramm. Eng Remot Sens 71(4):377–389
Grewal MS, Weill LR, Andrews AP (2001) Global Positioning System, Inertial Navigation, and Integration. John Wiley & Sons, Inc., New York, 392 p
Groten E (1979) Geodesy and the Earth's gravity field, Vol. I: Principles and conventional methods. Dümmler-Verlag, Bonn
Groten E (1980) Geodesy and the Earth's gravity field, Vol. II: Geodynamics and advanced methods. Dümmler-Verlag, Bonn
Guinn J, Muellerschoen R, Cangahuala L (1995) TOPEX/Poseidon precision orbit determination us-ing combined GPS, SLR and DORIS.In: GPS Trends in Precise Terrestrial,Airborne, and Spaceborne Applications: 21st IUGG General Assembly, IAG Symposium No. 115, Boulder, USA, July 3–4, 1995. Springer-Verlag, Berlin, pp 128–132
Guo JF, Ou JK, Ren C (2005) Partial continuation model and its application in mitigating systematic errors of doubled-differenced GPS measurements. Progress in Natural Sci. 15(3):246–251
Gurtner W (1994) RINEX: The receiver independent exchange format. GPS World 5(7):48–52
Gurtner W, Mader G (1990) Receiver independent exchange format version 2. GPS Bulletin 3(3):1–8
Gurtner W, Boucher C, Bruyninx C (1997) The use of the IGS/EUREF permanent network for EUREF densification campaigns. In: Symposium of the IAG Subcommission for Europe (EUREF), Sofia, Bulgaria, June 4–7, 1997, 3 pp
Haines BJ, Christensen EJ, Guinn JR (1995) Observations of TOPEX/Poseidon orbit errors due to gravitational and tidal modeling errors using the Global Positioning System. In: GPS Trends in Precise Terrestrial,Airborne, and Spaceborne Applications: 21st IUGG General Assembly,IAG Sym-posium No. 115, Boulder, USA, July 3–4, 1995. Springer-Verlag, Berlin, pp 133–138
Haines B, Bar-Server Y, Bertiger W, Desai S, Willis P (2004) One-centimeter orbit determination for Jason-1: New GPS-based strategies. Mar Geod 27(1–2):299–318
Hajj GA, Kursinski ER, Bertiger WI (1995) Initial results of GPS-LEO occultation measurements of Earth's atmosphere obtained with the GPS-MET experiment. In: GPS Trends in Precise Terrestrial, Airborne, and Spaceborne Applications: 21st IUGG General Assembly, IAG Symposium No. 115, Boulder, USA, July 3–4, 1995. Springer-Verlag, Berlin, pp 144–153
Hamilton GS, Whillans IA (2000) Point measurements of mass balance of the Greenland Ice Sheet using precision vertical Global Positioning System (GPS) surveys. J Geophys Res 105(B7):16295–16301
Han S (1997) Quality-control issues relating to instantaneous ambiguity resolution for real-time GPS kinematic positioning. J Geodesy 71(6):351–361
Han S, Rizos C (1996) Validation and rejection criteria for integer least-squares estimation. Survey rev 33(260):375–382
Han S, Rizos C (1997) Comparing GPS ambiguity resolution techniques. GPS World 8(10):54–61
Han S, Rizos C (2000a) GPS multipath mitigation using FIR filters. Survey rev 35(277):487–498
Han S, Rizos C (2000b) An instantaneous ambiguity resolution technique for medium-range GPS kinematic positioning. J Inst Navig 47(1):17–31
Han S, Rizos C (2000c) Airborne GPS kinematic positioning and its application to oceanographic mapping. Earth Planets Space 52(10):819–824
Hariharan R, Krumm J, Horvitz E (2005) Web-enhanced GPS. Lect Notes Comput Sci 3479:95–104
Hatanaka Y, Tsuji H, Iimura Y, Kobayashi K, Morishita H (1995) Application of GPS kinematic method for detection of crustal movements with high temporal resolution. In: GPS Trends in Precise Terrestrial, Airborne, and Spaceborne Applications: 21st IUGG General Assembly, IAG Symposium No. 115, Boulder, USA, July 3–4, 1995. Springer-Verlag, Berlin, pp 105–112
Hatch RR (1996) The promise of a third frequency, GPS World, 7(1996)5, 55–58

(c) ketabton.com: The Digital Library

Hatch RR (2004) Those scandalous clocks. GPS Solutions 8(2):67–73
Hatch RR, Sharpe RT (2004) Recent improvements to the SDtar Fire global DGPS navigation software. J GPS 3(1–2):143–153
Hay C, Wong J (2000) Enhancing GPS: Tropospheric delay prediction at the Master control Station. GPS World 11(1):56–62
He JK, Cai DS, Li YX, Gong ZS (2004a) Active extension of the Shanxi rift, north China: does it result from anticlockwise block rotations? Terra Nova 16(1):38–42
He XF, Guang Y, Ding XL, Chen YQ (2004b) Application and evaluation of a GPS-multi-antenna system for dam deformation monitoring. Earth Planets and Space 56(11):1035–1039
Heck B (1995) Grundlagen der SatellitenGeodaesie. Schriftenreihe des Deutschen Vereins für Vermessungswesen, Bd. 18, Stuttgart, pp 10–31
Heck B (1995) Grundlagen der erd- und himmelsfesten Referenzsysteme. Schriftenreihe des Deutschen Vereins für Vermessungswesen, Bd. 18, Stuttgart, pp 138–153
Hefty J, Rothacher M, Springer T, Weber R, Beutler G (2000) Analysis of the first year of Earth rotation parameters with a sub-daily resolution gained at the CODE processing center of the IGS. J Geodesy 74(6):479–487
Hehl K, Xu G, Fritsch J (1995) Results from field tests of an airborne gravity meter system. In:Proceedings of IUGG XXI General Assembly, IAG meeting at Boulder,Colorado, USA,July 1995, IAG Symposium G4, pp 169–174
Hein GW (2000) From GPS and GLONASS via EGNOS to Galileo. Position and navigation in the third millennium. GPS Solutions 3(4):39–47
Hein GW, Riedl B (1995) High precision deformation monitoring using differential GPS. In: GPS Trends in Precise Terrestrial,Airborne, and Spaceborne Applications: 21st IUGG General Assembly, IAG Symposium No. 115, Boulder, USA, July 3–4, 1995. Springer-Verlag, Berlin, pp 180–184
Hein GW, Eisfeller B, Pielmeier J (1995) Developments in airborne "high precision" digital photo flight navigation in "realtime". In: GPS Trends in Precise Terrestrial, Airborne, and Spaceborne Applications: 21st IUGG General Assembly, IAG Symposium No. 115, Boulder, USA, July 3–4, 1995. Springer-Verlag, Berlin, pp 175–179
Hein GW, et al. (2003) Galileo frequency and signal design. GPS World 14(6):30–37
Heinrich G, et al. (2004) HIGAPS. A highly integrated Galileo/GPS chipset for consumer applications. GPS World 15(9):38–47
Heiskanen WA, Moritz H (1967) Physical geodesy. W. H. Freeman and company, San Francisco and London
Heitz S (1988) Coordinates in geodesy. Springer-Verlag, Berlin
Hernández-Pajares M, Juan JM, Sanz J, Colombo OL (2000) Application of ionospheric tomography to real-time GPS carrier-phase ambiguities resolution, at scales of 400–1 000 km and with high geomagnetic activity. Geophys Res Lett 27(13):2009–2012
Hernández-Pajares M, Juan JM, Sanz J, Colombo OL (2003) Impact of real-time ionospheric determination on improving precise navigation with GALILEO and next-generation GPS. Navigation 50(3):205–218
Herrick S (1972) Astrodynamics, Vol. II. Van Nostrand Reinhold, London
Herring T (2003) MATLAB Tools for viewing GPS velocities and time series. GPS Solutions 7(3):194–199
Hess D, Keller W (1999) Gradiometrie mit GRACE Teil I, Fehleranalyse künstlicher Gradiometerdaten. ZfV 5:137–144
Hess D, Keller W (1999) Gradiometrie mit GRACE Teil II, Simulationsstudie. ZfV 7:205–211
Highsmith D, Axelrad P (1999) Relative state estimation using GPS flight data from co-orbiting spacecraft. ION GPS '99, 14–17 September 1999, pp 401–409
Hilla S (2004) Plotting pseudorange multipath with respect to satellite azimuth and elevation. GPS Solutions 8(1):44–48
Hiller W, Lauterbach P, Wlaka M (1997) Seeking sovereignty: A European navigation satellite system. GPS World 8(9):56–60
Hirahara K (2000) Local GPS tropospheric tomography. Earth Planets Space 52(11):935–939
Hofmann-Wellenhof B, Lichtenegger H, Collins J (1997, 2001) GPS theory and practice. Springer-Press, Wien
Hofmann-Wellenhof B, Legat K, Weiser M (2003) Navigation, Principles of Positioning Guidance. Springer-Verlag, New York, NY, xxix+427p
Holdridge DB (1967) An alternate expression for light time using general relativity. JPL Space Pro-gram Summary 37–48, III, pp 2–4
Hong Y, Ou JK (2006) Algebraic solution of the variation equation and its numerical validation. (In Chinese, in review)
Hopfield HS (1969) Two-quartic tropospheric refractivity profile for correcting satellite data. J Geophys Res 74(18):4487–4499

(c) ketabton.com: The Digital Library

Hopfield HS (1970) Tropospheric effect on electromagnetically measured ranges: Prediction from surface weather data. Applied Physics Laboratory, Johns Hopkins University, Baltimore, MD, July 1970
Hopfield HS (1972) Tropospheric range error parameters – further studies. Applied Physics Laboratory, Johns Hopkins University, Baltimore, MD, June 1972
Horvath I, Essex EA (2000) Using observations from the GPS and TOPEX satellites to investigate nighttime TEC enhancements at mid-latitudes in the southern hemisphere during a low sunspot number period. J Atmos Sol-Terr Phy 62(5):371–391
Hostetter GH (1987) Handbook of digital signal processing. Engineering Applications, Academic Press, Inc.
Hotine M (1991) Differential geodesy. Springer-Verlag, Berlin
Hsu R, Li S (2004) Decomposition of deformation primitives of horizontal geodetic networks: application to Taiwan's GPS network. J Geod 78(4–5):251–262
Hu GR, Khoo HS, Goh PC, Law CL (2003) Development and assessment of GPS virtual reference station for RTK positioning. J Geod 77(5–6):292–302
Huber PJ (1964) Robust estimation of a location parameter. Ann Math Stat 35:73–101
Hugentobler U, Schaer S, Fridez P (2001) Bernese GPS Software: Version 4.2. Astronomical Inst. Univ. of Berne
Hugentobler U, Ineichen D, Beutler G (2003) GPS satellites: Radiation pressure, attitude and resonance. Adv Space Res 31(8):1917–1926
Hünerbein K von, Hamann HJ, Rüter E, Wiltschko W (2000) A GPS-based system for recording the flight paths of birds. Naturwissenschaften 87(6):278–279
Ifadis IM (2000) A new approach to mapping the atmospheric effects for GPS. Earth Planets Space 52(10):703–708
Ihde J (1996) Geoidbestimmung unter Nutzung von GPS und Nivellement. Erste Geodätische Woche, Stuttgart, 7.–12. Oktober 1996, 6 Blatt
Ince CD, Sahin M (2000) Real-time deformation monitoring with GPS and Kalman Filter. Earth Plan-ets Space 52(10):837–840
ION, The Institute of Navigation. Proceedings of ION GPS-91, -92, -93, -94, -95, -96, -97, -98, -99, -00, -01, -02, -03, -04, -05
Jaggi A, Beutler G, Hugentobler U (2005) Reduced-dynamic orbit determination and the use of accelerometer data. Adv Space Res 36(3):438–444
Jakowski N, Sardon E, Engler E (1995) About the use of GPS measurements for ionospheric studies. In: GPS Trends in Precise Terrestrial, Airborne, and Spaceborne Applications: 21st IUGG General Assembly, IAG Symposium No. 115, Boulder, USA, July 3–4, 1995. Springer-Verlag, Berlin, pp 248–252
Jazwinski AH (1970) Stochastic processes and filtering theory. In: Mathematics in science and engineering, Vol. 64. Academic Press, New York and London
Jekeli C, Garcia R (1997) GPS phase accelerations for moving – base vector gravimetry. J Geodesy 71:630–639
Jensen A (1999) Influences of references on precise static/kinematic GPS positioning.
Jerde CL, Visscher DR (2005) GPS measurement error influences on movement model parameterization. Ecological Appl 15(3):806–810
Jeyapalan K (2004) Local geoid determination using global positioning systems. Surv Land Information Sci 64(1):65–75
Jin X-X (1995) A recursive procedure for computation and quality control of GPS differential corrections. Delft University of Technology, Faculty Geod. Engin., Delft Geodetic Computing Centre, Delft, 83 S
Jin SG, Zhu WY (2003) Active motion of tectonic blocks in East Asia: Evidence from GPS measurements. Acta Geologica Sinica 77(1):59–63
Jin X-X, Jong K de, Cees D (1996) Relationship between satellite elevation and precision of GPS code observations. Leipzig, 13 S
Jong PJ de (1998) A processing strategy of the application of the GPS in networks. PhD theis, Netherlands Geodetic Commision, Delft, The Netherland
Jong K de (1999) The Influence of Code Multipath on the Estimated Parameters of the Geometry-Free GPS Model. GPS Solutions 3(2):11–18
Jong K de (2000) Minimal detectable biases of cross-correlated GPS observations. GPS Solutions 3(3): 12–18
Jong K de, Teunissen PJG (2000) Minimal detectable biases of GPS observations for a weighted ionosphere. Earth Planets Space 52(10):857–862
Jonkman NF, Jong K de (2000) Integrity monitoring of IGEX-98 data, Part I: Availability. GPS Solu-tions 3(4):10–23
Jonkman NF, Jong K de (2000) Integrity monitoring of IGEX-98 data, Part II: Cycle slip and outlier detection. GPS Solutions 3(4):24–34

(c) ketabton.com: The Digital Library

Jonkman NF, Jong K de (2000) Integrity monitoring of IGEX-98 data, Part III: Broadcast navigation message validation. GPS Solutions 4(2):45–53
Joosten J (2000) The GPS integer least-squares statistics. Phys Chem Earth 25(A9–A11):687–692
Joosten P, Tiberius C (2000) Fixing the ambiguities. Are you sure they're right? GPS World 11(5):46–51
Kaczorowski M (1995) Calculation of the Green's loading functions. Part 1: Theory. Artificial Satellites, Journal of Planetary Geodesy 30(1):77–93
Kälber S, Jäger R, Schwäble R (2000) A GPS-based online control and alarm system. GPS Solutions 3(3):19–25
Kammeyer P (2000) A UT1-like quantity from analysis of GPS orbit planes. Celest Mech Dyn Astr 77(4):241–272
Kamp PD van (1967) Principles of astrometry. W. H. Freemann and Company, San Francisco and London
Kang Z (1998) Präzise Bahnbestimmung niedrigfliegender Satelliten mittels GPS und die Nutzung für die globale Schwerefeldmodellierung. Scientific Technical Report STR 98/25, GFZ Potsdam
Kang Z, Nagel P, Pastor R (2003) Precise orbit determination for GRACE. Adv Space Res 31(8):1875–1881
Kaniuth K, Kleuren D, Tremel H (1998) Sensitivity of GPS height estimates to tropospheric delay modelling. Allgemeine Vermessungsnachrichten 105(6):200–207
Kaniuth K, Kleuren D, Tremel H, Schlueter W (1998) Elevationabhängige Phasenzentrums-variationen geodätischer GPS-Antennen. ZfV 10:320–325
Karslioglu MO (2005) An interactive program for GPS-based dynamic orbit determination of small satellites. Comput Geosci 31(3):309–317
Kashani I, Wielgosz P, Grejner-Brzezinska D (2003) Datum definition in the long-range instantaneous RTK GPS network solution. J GPS 2(2):100–108
Katzberg SJ, Garrison JL (1996) Utilizing GPS to determine ionospheric delay over the ocean. NASA Technical Mernorandum TM-4750, NASA Langley Research Center
Kaula WM (1966) Theory of satellite geodesy. Blaisdell Publishing Company
Kechine MO, Tiberius CCJM, van der Marel H (2004) An experimental performance analysis of real-time kinematic positioning with NASA's Internet-based Global Differential GPS. GPS Solutions 8(1):9–22
Kelley K, Bologlu A (1995) DGPS on the waterfront: tracking cargo and equipment in maritime terminals. GPS World 6(9):62–71
Keong J, Lachapelle G (2000) Heading and pitch determination using GPS/GLONASS. GPS Solutions 3(3):26–36
Keshin MO (2004) Directional statistics of satellite-satellite single-difference widelane phases biases. Artificial Satellites 39(4):305–324
Khan SA (1999) Ocean loading tide effects on GPS positioning. MSc. thesis, Copenhagen University
Khan SA, Scherneck HG (2003) The M-2 ocean tide loading wave in Alaska: vertical and horizontal displacements, modeled and observed. J Geod 77(3-4):117–127
Khan SA, Tscherning CC (2001) Determination of semi-diurnal ocean tide loading constituents us-ing GPS in Alaska. Geophys Res Lett 28(11):2249–2252
Khazaradze G, Klotz J (2003) Short- and long-term effects of GPS measured crustal deformation rates along the south central Andes. J Geophys Res 108(B6):ETG5/1–15
Kim D, Langley RB (2000) A search space optimization technique for improving ambiguity resolution and computational efficiency. Earth Planets Space 52(10):807–812
Kim D, Langley RB (2003) On ultrahigh-precision GPS positioning and navigation. Navigation 50(2): 103–116
King RW, Masters EG, Rizos C, Stolz A, Collins J (1987) Surveying with Global Positioning System. Dümmler-Verlag, Bonn
King M, Coleman R, Morgan P (2000) Treatment of horizontal and vertical tidal signals in GPS data: A case study on a floating ice shelf. Earth Planets Space 52(11):1043–1047
King MA, Penna NT, Clarke PJ, King EC (2005) Validation of ocean tide models around Antarctica using onshore GPS and gravity data. J Geophys Res 110(B08401):1–21
Kistler M, Geiger A (2000) GPS am Seil herunterlassen: das Global Positioning System im Dienste des Seilbahnwesen. Vermess Photogramm Kulturtech 98(7):441–445
Kleusberg A (1995) Mathematics of attitude determination with GPS. GPS World, 6(9):72–78
Kleusberg A, Teunissen PJG (eds) (1996) GPS for geodesy. Springer-Verlag, Berlin
Klobuchar JA (1996) Ionospheric effects on GPS. In: Parkinson BW, Spilker JJ (eds) Global Position-ing System: Theory and applications, Vol. I, Chapter 12
Klotz J, Angermann D, Reinking J (1995) Großräumige GPS-Netze zur Bestimmung der rezenten Kinematik der Erde. ZfV 120(9):449–460
Knickmeyer ET, Knickmeyer EH, Nitschke M (1996) Zur Auswertung kinematischer Messungen mit dem Kalman-Filter. Schriftenreihe des Deutschen Vereins für Vermessungswesen, Bd. 22, Stuttgart, pp 141–166

(c) ketabton.com: The Digital Library

Knudsen P, Andersen O (1997) Global marine gravity and mean sea surface from multi mission satellite altimetry. Scientific Assembly of the International Association of Geodesy in conjunction with 28th Brazilian Congress of Cartography; Rio de Janeiro, 3–9 September 1997, 4 pp
Knudsen P, Olsen H, Xu G (1999) GPS-altimetry tests – Measuring GPS signal reflected from the Earth surface. Poster on the 22st IUGG General Assembly, IAG Symposium
Knudsen P, Andersen O, Khan SA, Hoeyer JL (2000) Ocean tide effects on GRACE gravimetry. IAG Symposia, (in press)
Koch KR (1980) Parameterschätzung und Hypothesentests in linearen Modellen. Dümmler-Verlag,Bonn
Koch KR (1988) Parameter estimation and hypothesis testing in linear models. Springer-Verlag, Berlin
Koch KR (1996) Robuste Parameterschätzung. Allgemeine Vermessungsnachrichten 103(1):1–18
Koch KR, Yang Y (1998) Konfidenzbereiche und Hypothesentests für robuste Parameterschätzungen. ZfV 123(1):20–26
Koch KR, Yang Y (1998) Robust Kalman filter for rank deficient observation model. J Geodesy 72: 436–441
Komjathy A, Langley RB, Vejrazka F (1995) Assessment of two methods to provide ionospheric range error corrections for single-frequency GPS users. In: GPS Trends in Precise Terrestrial, Airborne, and Spaceborne Applications: 21st IUGG General Assembly, IAG Symposium No. 115, Boulder, USA, July 3–4, 1995. Springer-Verlag, Berlin, pp 253–257
Komjathy A, Garrison J, Zavorotny V (1999) GPS: A new tool for ocean science. GPS World 10(4):50–56
Komjathy A, Zavorotny VU, Axelrad P, Born GH, Garrison JL (2000) GPS signal scattering from sea surface: Wind speed retrieval using experimental data and theoretical model. Remote Sens Environ 73(2):162–174
Konig R, Schwintzer P, Bode A (1996) GFZ-1: A small laser satellite mission for gravity field model improvement. Geophys Res Lett 23(22):3143–3146
Konig R, Reigber C, Zhu SY (2005) Dynamic model orbits and earth system parameters from combined GPS and LEO data. Adv Space Res 36(3):431–437
Kouba J, Heroux P (2001) Precise point positioning using IGS orbit and clock products. GPS Solutions 5(2):12–28
Kraus JD (1966) Radio astronomy. McGraw-Hill Book Company
Kristiansen O (1995) Experiences with high precision GPS processing in Norway. Rep Finnish Geod Inst 4:77–84
Kroes R, Montenbruck O (2004) Spacecraft formation flying: Relative positioning using dual-frequency carrier phase. GPS World 15(7):37–42
Kroes R, Montenbruck O, Bertiger W, Visser P (2005) Precise GRACE baseline determination using GPS. GPS Solutions 9(1):21–31
Kuang D, Rim HJ, Schutz BE (1996) Modeling GPS satellite attitude variation for precise orbit determination. J Geodesy 70(9):572–580
Kuang D, Rim HJ, Schutz BE, Abusali PAM (1996) Modeling GPS satellite attitude variation for precise orbit determination. J Geodesy 70:572–580
Kumar M (1997) Time-invariant bathymetry: A new concept to define and survey it using GPS. In: Proceedings of Fourteenth United Nations Regional Cartografic Conference for Asia and the Pacific, Bangkok, 3–7 February 1997. Bangkok, 4 pp
Kwon JH, Grejner-Brzezinska D, Bae TS, Hong CK (2003) A triple difference approach to Low Earth Orbiter precision orbit determination. J Navig 56(3):457–473
Lachapelle G (1995) Post-mission GPS absolute kinematic positioning at one-metre accuracy level. Int J Geomatics 9(1):37–39
Lachapelle G (2004) GNSS indoor location technologies. J GPS 3(1-2):2–11
Lachapelle G, Cannon ME, Qiu W, Varner C (1996) Precise aircraft single-point positioning using GPS post-mission orbits and satellite clock corrections. J Geodesy 70:562–571
Lachapelle G, Kuusniemi H, Dao DTH, Macgougan G, Cannon ME (2004) HSGPS signal analysis and performance under various indoor conditions. Navigation 51(1):29–43
Lambeck K (1988) Geophysical geodesy – The slow deformations of the Earth. Oxford Science Publications
Lambert A, Pagiatakis SD, Billyard AP, Dragert H (1988) Improved ocean tide loading correction for gravity and displacement: Canada and northern United States. J Geophys Res 103(B12):30231–30244
Landau H (1988) Zur Nutzung des Global Positioning Systems in Geodaesie und Geodynamik: Modellbildung, Software-Entwicklung und Analyse. Universität der Bundeswehr Müchen, Studiengang Vermessungswesen, Schriftenreihe, Heft 36
Landspersky D, Mervart L (1997) A contribution to the study of modelling of the troposphere biases of GPS observations with high accuracy. In: Proceedings of the EGS symposium G14 'Geodetic and Geodynamic programmes of the CEI': 22 General Assembly of the EGS, Vienna, Austria, 21– 25 April 1997. Warszawa, pp 207–211
Langley RB (1997a) GLONASS: Review and update. GPS World 8(7):46–51

(c) ketabton.com: The Digital Library

Langley RB (1997b) The GPS error budget. GPS World 8(3):51–56
Langley RB (1998a) Propagation of the GPS signals. In: Kleusberg A, Teunissen PJG (eds) GPS for geodesy. Springer-Verlag, Berlin
Langley RB (1998b) GPS receivers and the observables. In: Kleusberg A, Teunissen PJG (eds) GPS for geodesy. Springer-Verlag, Berlin
Langley RB (2000) GPS, the ionosphere, and the solar maximum. GPS World 11(7):44–49
Langley RB (2003) Getting your bearings. The magnetic compass and GPS. GPS World 14(9):70+
Lapucha D (1994) Real-time centimeter-accuracy positioning with on-the-fly carrier phase ambiguity resolution. Rep Geod 1:52–59
Lechner W (1995) Telemetriekonzepte für die GPS-unterstützte Echtzeitvermessung. Schriftenreihe des Deutschen Vereins für Vermessungswesen, Bd. 18, pp 260–286
Lee J-T, Mezera DF (2000) Concerns related to GPS-derived geoid determination. Survey rev 35(276): 379–397
Lee YC, O'Laughlin DG (2000) Performance analysis of a tightly coupled GPS/Inertial system for two integrity monitoring methods. J Inst Navig 47(3):175–189
Lee HK, Hewitson S, Wang J (2004) Web-based resources on GPS/INS integration. GPS Solutions 8(3): 189–191
Leick A (1995) GPS satellite surveying. John Wiley & Sons Ltd., New York
Leick A (2004) GPS Satellite Surveying, 3rd ed. John Wiley, New York, xxiv+664 p
Leinen S (1997) Hochpräzise Positionierung über große Entfernungen und in Echtzeit mit dem Global Positioning System. DGK, Reihe C, Heft 472,Verlag der Bayerischen Akademie der Wissenschaften
Lelgemann D (1983) A linear solution of equation of motion of an Earth-orbiting satellite based on a Lie-series. Celestial Mech 30:309
Lelgemann D (1996) Geodaesie im Weltraumzeitalter. Dtsch Geod Komm 25:59–77
Lelgemann D (2002) Lecture notes of geodesy
Lelgemann D, Petrovic S (1997) Bemerkungen über den Höhenbegriff in der Geodaesie. ZfV 122(11): 503–509
Lelgemann D, Xu G (1991) Zur Helmert-Transformation von terrestrischen und GPS-Netzen. ZfV (1)
Lemmens R (2004) Book review: GPS – Theory, Algorithms and Applications. International J Applied Earth Observation and Geoinformation 5:165–166
Leroy E (1995) GPS real-time levelling on the world's longest suspension bridge. Int J Geomatics 9(8):6–8
Levine J (2001) GPS and the legal traceability of time. GPS World 12(1):52–58
Li X (2004) The advantage of an integrated RTK-GPS system in monitoring structural deformation. J GPS 3(1–2):191–199
Li H, Xu G, Xue H, Zhao H, Chen J,Wang G (1999) Design of GPS application program. Science Press, Peking, ISBN 7-03-007204-9/TP.1049, 337 p (in Chinese and in C)
Lightsey EG, Blackburn GC, Simpson JE (2000) Going up: A GPS receiver adapts to space. GPS World 11(9):30–34
Linkwitz K, Hangleiter U (eds) (1995) High precision navigation 95. Dümmler-Verlag, Bonn
Liu L, Zhao D (1979) Orbit theory of the Earth satellite. Nanjing University Press, (in Chinese)
Liu D, Liu J, Liu G (1993) The three-dimensional combined adjustment of GPS and terrestrial surveying data. Acta Geod Cartogr Sinica 41–54 (select. papers Engl. ed.)
Liu DJ, Shi YM, Guo JJ (1996) Principle of GPS and its data processing. TongJi University Press, Shanghai, (in Chinese)
Liu M, Yang Y, Stein S, Zhu S, Engeln J (2000) Crustal shortening in the Andes: Why do GPS rate differ from geological rates? Geophys Res Lett 27(18):3005–3008
Ludwig R (1969) Methoden der Fehler- und Ausgleichsrechnung. Vieweg & Sohn, Braunschweig
MacGougan G, Normark P-L, Ståhlberg C(2005) Satellitenavigation evolution.The software GNSS receiver. GPS World16(1):48–52
Mackenzie R, Moore P (1997) A geopotential error analysis for a non planar satellite to satellite tracking mission J Geodesy 71(5):262–272
Mackie JB (1985) The elements of astronomy for surveyors. Charles Griffin & Company Ltd.
Mader GL (1995) Kinematic and rapid static (KARS) GPS positioning: Techniques and recent experiences. In: GPS Trends in Precise Terrestrial, Airborne, and Spaceborne Applications: 21st IUGG General Assembly, IAG Symposium No. 115, Boulder, USA, July 3–4, 1995. Springer-Verlag, Berlin, pp 170–174
Madsen FB, Madsen F (1994) Realization of the EUREF89 reference frame in Denmark. Report on the Symposium of the IAG Subcommission for the European Reference Frame (EUREF) held in Warsaw 8–11 June 1994. Reports of the EUREF Technical Working Group, Muenchen, pp 270–274
Maleki L, Prestage J (2005) Applications of clocks and frequency standards: from the routine to tests of fundamental models. Metrologia42(3):S145–S153

(c) ketabton.com: The Digital Library

Manning J, Johnston G (1995) A fiducial GPS network to monitor the motion of the Australien plate. In: Proceedings of the First Turkish International Symposium on Deformations "Istanbul-94", Istanbul, Sept. 5–9, 1995, Istanbul, pp 85–89
Mansfeld W (2004) Satellitenortung und Navigation, 2nd edn., Wiesbanden: Vieweg Verlag, 352 p
Masreliez CJ, Martin RD (1977) Robust Bayesian estimation for the linear model and robustifying the Kalman filter. IEEE T Automat Contr AC-22:361–371
McCarthy DD (1996) International Earth Rotation Service. IERS conventions, Paris, 95 p
McCarthy DD, Luzum BJ (1995) Using GPS to determine Earth orientation. In: GPS Trends in Precise Terrestrial, Airborne, and Spaceborne Applications: 21st IUGG General Assembly, IAG Symposium No. 115, Boulder, USA, July 3–4, 1995. Springer-Verlag, Berlin, pp 52–58
Meeus J (1992) Astronomische Algorithmen. Johann Ambrosius Barth
Melchior P (1978) The tides of the planet Earth. Pergamon Press
Mertikas SP, Rizos C (1997) On-line detection of abrupt changes in the carrier-phase measurements of GPS. J Geodesy 71(8):469–482
Mervart L (1995) Ambiguity resolution techniques in geodetic and geodynamic applications of the Global Positioning System. Dissertation an der Philosophisch- naturwissenschaftlichen Fakultät der Universität Bern
Mervart L, Beutler G, Rothacher M (1995) The impact of ambiguity resolution on GPS orbit determination and on global geodynamics studies. In: GPS Trends in Precise Terrestrial, Airborne, and Spaceborne Applications: 21st IUGG General Assembly, IAG Symposium No. 115, Boulder, USA, July 3–4, 1995. Springer-Verlag, Berlin, pp 285–289
Michel GW, Becker M, Angermann D, Reigber C, Reinhart E (2000) Crustal motion in E- and SE-Asia from GPS measurements. Earth Planets Space 52(10):713–720
Mickler D, Axelrad P, Born G (2004) Using GPS reflections for satellite remote sensing. Acta Astronautica 55(1):39–49
Milbert D (2005a) Influence of pseudorange accuracy on phase ambiguity resolution invarious GPS modernization scenarios. Navigation 52(1):29–38
Milbert D (2005b) Correction to "Influence of pseudorange accuracy on phase ambiguity resolution in various GPS modernization scenarios". Navigation 52(3):121–121
Miller KM (2000) A review of GLONASS. Hydrographic Journal 98:15–21
Mireault Y, Kouba J, Lahaye F (1995) IGS combination of precise GPS satellite ephemerides and clock. In: GPS Trends in Precise Terrestrial, Airborne, and Spaceborne Applications: 21st IUGG General Assembly, IAG Symposium No. 115, Boulder, USA, July 3–4, 1995. Springer-Verlag, Berlin, pp 14–23
Mitchell S, Jackson B, Cubbedge S (1996) Navigation solution accuracy from a spaceborne GPS receiver, GPS World, 7(1996)6, 42, 44, 46–48, 50
Mohamed AH, Schwarz KP (1999) Adaptive Kalman filtering for INS/GPS. J Geodesy 73:193–203
Montenbruck O (1989) Practical Ephemeris calculations. Springer-Verlag, Heidelberg
Montenbruck O (2003) Kinematic GPS positioning of LEO satellites using ionospheric-free single frequency measurements. Aerospace Sci Technol 7(5):396–405
Montenbruck O, Gill E (2000) Satellite orbits: Models, methods and applications. Springer-Verlag, Heidelberg
Montenbruck O, Kroes R (2003) In-flight performance analysis of the CHAMP BlackJack GPS receiver. GPS Solutions 7(2):74–86
Montenbruck O, Gill E, Kroes R (2005a) Rapid orbit determination of LEO satellites using IGS clock and ephemeris products. GPS Solutions 9(3):226–235
Montenbruck O, van Helleputte T, Kroes R, Gill E (2005b) Reduced dynamic orbit determination using GPS code and carrier measurements. Aerospace Sci Technol 9(3):261–271
Moore T, Zhang K, Close G, Moore R (2000) Real-time river level monitoring using GPS heighting. GPS Solutions 4(2):63–67
Moreau MC, Axelrad P, Garrison JL, Long A (2000) GPS receiver architecture and expected performance for autonomous navigation in high earth orbits. J Inst Navig 47(3):191–204
Moritz H (1980) Advanced physical geodesy. Herbert Wichmann Verlag, Karlsruhe
Mostafa MMR (2005) Airborne GPS augmentation alternatives. Potogramm. Eng Remote Sens 71(5):545+
Mostafa MMR (2005) Direct georeferencing – Airborn GPS augmentation alternatives – Part II satellite-based correction service. Potogramm Eng Remote Sens 71(7):783–783
Mueller II (1964) Introduction to satellite geodesy. Frederick Ungar Publishing Co.
Murakami M (1996) Precise determination of the GPS satellite orbits and its new applications: GPS orbit determination at the Geographical Survey Institute. J Geod Soc Japan 42(1):1–14
Musman S (1995) Deriving ionospheric TEC from GPS observations. In: GPS Trends in Precise Terrestrial, Airborne, and Spaceborne Applications: 21st IUGG General Assembly, IAG Symposium No. 115, Boulder, USA, July 3–4, 1995. Springer-Verlag, Berlin, pp 258–262

(c) ketabton.com: The Digital Library

Niell AE (2000) Improved atmospheric mapping functions for VLBI and GPS. Earth Planets Space 52(10):703–708
O'Keefe K, Stephen J, Lachapelle G, Gonzales RA (2000) Effect of ice loading of a GPS antenna. Geomatica 54(1):63–74
Obana K, Katao H, Ando M (2000) Seafloor positioning system with GPS-acoustic link for crustal dynamics observations. A preliminary result from experiments in the sea. Earth Planets Space 52(6):415–423
Odijk D, Marel H van der, Song I (2000) Precise GPS positioning by applying ionospheric corrections from an active control network. GPS Solutions 3(3):49–57
Ou J (1995) On atmospheric effects on GPS surveying. In: GPS Trends in Precise Terrestrial, Air-borne, and Spaceborne Applications: 21st IUGG General Assembly, IAG Symposium No. 115, Boulder, USA, July 3–4, 1995. Springer-Verlag, Berlin, pp 243–247
Ou JK, Wang ZJ (2004) An improved regularization method to resolve integer ambiguity in rapid positioning using single frequency GPS receivers. Chinese Sci Bull 49(2):196–200
Pachelski W (1995) GPS phases: Single epoch ambiguity and slip resolution. In: GPS Trends in Precise Terrestrial, Airborne, and Spaceborne Applications: 21st IUGG General Assembly, IAG Symposium No. 115, Boulder, USA, July 3–4, 1995. Springer-Verlag, Berlin, pp 295–299
Pan M, Sjoeberg LE (1995) Unification of regional vertical datums using GPS. In: GPS Trends in Precise Terrestrial, Airborne, and Spaceborne Applications: 21st IUGG General Assembly, IAG Symposium No. 115, Boulder, USA, July 3–4, 1995. Springer-Verlag, Berlin, pp 94–98
Parkinson BW, Spilker JJ (eds) (1996) Global Positioning System: Theory and applications, Vol. I, II. American Institute of Aeronautics and Astronautics, Progress in Astronautics and Aeronautics, Vol. 163
Pavlis EC, Beard RL (1995) The Laser Retroreflector Experiment on GPS-35 and 36. In: GPS Trends in Precise Terrestrial,Airborne, and Spaceborne Applications: 21st IUGG General Assembly,IAG Symposium No. 115, Boulder, USA, July 3–4, 1995. Springer-Verlag, Berlin, pp 154–158
Petovello MG (2006) Narrowlane: is it worth it? GPS Solutions DOI 10.1007/s10291-006-0020-1
Petovello MG, Lachapelle G (2000) Estimation of clock stability using GPS. GPS Solutions 4(1):21–33
Plumb J, Larson KM, White J, Powers E (2005) Absolute calibration of a geodetic time transfer. IEEE Trans Ultrason Ferr Freq Contr 52(11):1904–1911
Poutanen M, Vermeer M, Maekinen J (1996) The permanent tide in GPS positioning. J Geodesy 70: 499–504
Press WH, Teukolsky SA, Vetterling WT, Flannery BP (1992) Numerical recipes in C, 2nd Ed. Cam-bridge University Press
Psiaki ML, Powell SP, Kintner PM Jr. (2000) Accuracy of the Global Positioning System-derived acceleration vector. J Guid Control Dynam 23(3):532–538
Puglisi G, Briole P, Bonforte A (2004) Twelve years of ground deformation studies on Mt. Etna volcano based on GPS surveys. Geophys Monogr 143:321–341
Rabaeijs A, Grosso D, Huang X, Qi D (2003) GPS receiver prototype for integration into system-on-chip. IEEE Trans on Consumer Electronics 49(1):48–58
Rajal BS, Madhwal HB (1997) Kinematic Global Positioning System survey as the solution for quick large scale mapping. Survey rev 34(265):159–162
Ramatschi M (1998) Untersuchung von Vertikalbewegungen durch Meeresgezeitenauflasten an Referenzstationen auf Grönland. Dissertation, Technische Universität Clausthal
Rapp RH (1986) Global geopotential solutions. In: Sunkel H (ed) Mathematical and numerical techniques in physical geodesy. Lecture Notes inEarth Sciences, Vol. 7, Springer-Verlag, Heidelberg
Reigber C (1997a) Geowissenschaftlicher Kleinsatellit CHAMP. GPS-Anwendungen und Ergebnisse '96: Beiträge zum 41. DVW-Fortbildungsseminar vom 7. bis 8. November 1996 am Geo-Forschungszentrum Potsdam, pp 266–273
Reigber C (1997b) IERS und IGS: Stand und Perspektiven. GPS-Anwendungen und Ergebnisse '96: Beitraege zum 41. DVW-Fortbildungsseminar vom 7. bis 8. November 1996 am Geo-Forschungszentrum Potsdam, pp 34–42
Reigber C, Feissel M (1997) IERS missions, present and future. International Earth Rotation Service (ed) Report on the 1996 IERS workshop, Paris, 50 p (IERS technical note 22)
Reigber C, Schwintzer P, Luehr H (1996) CHAMP – a challenging mini-satellite payload for geoscientific research and application. Erste Geodaetische Woche, Stuttgart, 7.-12. Oktober 1996, 4 p)
Reigber C, et al. (2003) Global gravity field recovery using solely GPS tracking and accelerometer data from CHAMP. Space Sci Reviews 108(1–2):55–66
Reigber C, et al. (2005) An Earth gravity field model complete to degree and order 150 from GRACE: EIGEN-GRACE25. J Geodyn 39(1):1–10
Reinhart E, Franke P, Habrich H, Schlueter W, Seeger H, Weber G (1997) Implications of permanent GPS-arrays for the monitoring of geodetic reference frames. Sixth United Regional Cartographic Conference for the America, New York, 2–6 June 1997, 10 pp

(c) ketabton.com: The Digital Library

Reinking J, Angermann D, Klotz J (1995) Zur Anlage und Beobachtung grossräumiger GPS-Netze für geodynamische Untersuchungen. Allgemeine Vermessungsnachrichten 102(6):221–231
Remondi B (1984) Using the Global Positioning System (GPS) phase observable for relative geodesy: Modelling, processing, and results. University of Texas at Austin, Center for Space Research
Remondi BW (2004) Computing satellite velocity using the broadcast ephemeris. GPS Solutions 8(3): 181–183
Remondi BW, Brown G (2000) Triple differencing with Kalman filtering: Making it work. GPS Solutions 3(3):58–64
Remondi BW, Brown RG (2004) A comparison of a Hi/Lo GPS constellation with a populated conventional GPS constellation in support of RTK: A covariance analysis. GPS Solutions 8(2):82–92
Retscher G, Chao CHJ (2000) Precise real-time positioning in WADGPS networks. GPS Solutions 4(2): 68–75
Rizos C, Han S, Chen HY (2000) Regional-scale multiple reference stations for carrier phase-based GPS positioning: A correction generation algorithm. Earth Planets Space 52(10):795–800
Rizos C, Han S, Ge L, Chen HY, Hatanaka Y, Abe K (2000) Low-cost densification of permanent GPS networks for natural hazard navigation: First tests on GSI's GEONET network. Earth Planets Space 52(10):867–871
Roberts GW, Dodson AH, Ashkenazi V (2000) Experimental plan guidance and control by kinematic GPS. Proc. Institution of Civil Engineers, Civil Engineering 138(1):19–25
Rothacher M, Mervart L (1996) Bernese GPS Software Version 4.0. Astronomical Institute of Univer-sity of Bern
Rothacher M, Schaer S (1995) GPS-Auswertetechniken. Schriftenreihe des Deutschen Vereins für Vermessungswesen, Bd. 18, pp 107–121
Rothacher M, Gurtner W, Schaer S (1995) Azimuth- and elevation-dependent phase center corrections for geodetic GPS antennas estimated from calibration campaigns. In: GPS Trends in Precise Terrestrial, Airborne, and Spaceborne Applications: 21st IUGG General Assembly, IAG Symposium No. 115, Boulder, USA, July 3–4, 1995. Springer-Verlag, Berlin, pp 333–338
Rummel R, Gelderen M van (1995) Meissl scheme: Spectral characteristics of physical geodesy.Manuscr Geodaet 20(5):379–385
Rummel R, Ilk KH (1995) Height datum connection – the ocean part. Allgemeine Vermessungsnachrichten 102(8/9):321–330
Rush J (2000) Current issues in the use of the global positioning system aboard satellites. Acta Astronaut 47(2–9):377–387
Rutten JAc (2004) Book review: GPS – Theory, Algorithms and Applications, Xu G 2003. European Journal of Navigation 2(1):94
Saastamoinen J (1972) Contribution to the theory of atmospheric refraction. B Geod 105–106
Saastamoinen J (1973) Contribution to the theory of atmospheric refraction. B Geod 107
Salzmann M (1995) Real-time adaptation for model errors in dynamic systems. B Geod 69:81–91
Sandlin A, McDonald K, Donahue A (1995) Selective availability: To be or not to be? GPS World 6(9): 44–51
Satirapod C, Wang J, Rizos C (2003) Comparing different Global Positioning System data processing techniques for modeling residual systematic errors. J Surv Eng ASCE 129(4):129–135
Schaal RE, Netto NP (2000) Quantifying multipath using MNR ratios. GPS Solutions 3(3):44–48
Schaffrin B (1991) Generating robustified Kalman filters for the integration of GPS and INS. Techni-cal Report, No. 15, Institute of Geodesy, University of Stuttgart
Schaffrin B (1995) On some alternative to Kalman filtering. In: Sanso F (ed) Geodetic theory today. Springer-Verlag, Berlin, pp 235–245
Schaffrin B, Grafarend E (1986) Generating classes of equivalent linear models by nuisance parameter elimination. Manuscr Geodaet 11:262–271
Scheinert M (1996) Zur Bahndynamik niedrigfliegender Satelliten. DGK, Reihe C, Heft 435, Verlag der Bayerischen Akademie der Wissenschaften
Scherrer R (1985) The WM GPS primer. WM Satellite Survey Company, Wild, Herrbrugg, Switzerland
Schildknecht T, Dudle G (2000) Time and frequency transfer: High precision using GPS phase measurements. GPS World 11(2):48–52
Schmid R, Rothacher M, Thaller D, Steigenberger P (2005) Absolute phase center corrections of satellite and receiver antennas. Impact of global GPS solutions and estimation of azimuthal phase center variations of the satellite antenna. GPS Solutions 9(4):283–293
Schneider M (1988) Satellitengeodaesie. Wissenschaftsverlag, Mannheim
Schoene T, Reigber C, Braun A (2003) GPS offshore buoys and continuous GPS control of tide gauges. Int Hydrogr Rev 4(3):64–70
Schutz BE (2000) Numerical studies in the vicinity of GPS deep resonance. Advances in the Astronautical Sciences 105(1):287–302

(c) ketabton.com: The Digital Library

Schwarz K-P, El-Sheimy N (1995) Multi-sensor arrays for mapping from moving vehicles. In: GPS Trends in Precise Terrestrial, Airborne, and Spaceborne Applications: 21st IUGG General Assembly, IAG Symposium No. 115, Boulder, USA, July 3–4, 1995. Springer-Verlag, Berlin, pp 185–189

Schwarz K-P, Cannon ME, Wong RVC (1989) A Comparison of GPS kinematic models for the determination of position and velocity along a trajectory. Manuscr Geodaet 14:345–353

Schwiderski EW (1978) Global ocean tide, I. A detailed hydrodynamical interpolation model. Rep. NSWC/DL TR 3866, Nav. Surf. Weapons Cent. Dahlgren, Va.

Schwiderski EW (1979) Ocean tide, II. The semidiurnal principal lunar tide (M2). Rep. NSWC TR 79–414, Nav. Surf. Weapons Cent. Dahlgren, Va.

Schwiderski EW (1980) On charting global ocean tide. Rev Geophys 18:243–268

Schwiderski EW (1981a) Ocean tide, III. The semidiurnal principal solar tide (S2). Rep. NSWC TR 81–122, Nav. Surf. Weapons Cent. Dahlgren, Va.

Schwiderski EW (1981b) Ocean tide, IV. The diurnal luni-solar declination tide (K1), Rep. NSWC TR 81–142, Nav. Surf. Weapons Cent. Dahlgren, Va.

Schwiderski EW (1981c) Ocean tide, V. The diurnal principal lunar tide (O1). Rep. NSWC TR 81–144, Nav. Surf. Weapons Cent. Dahlgren, Va.

Schwintzer P, Kang Z, Reigber C (1995) GPS satellite-to-satellite tracking for TOPEX/Poseidon precise orbit determination and gravity field model improvement. J Geodyn 20(2):155–166

Seeber G (1993) Satelliten-Geodaesie. Walter de Gruyter 1989

Seeber G (1996) Grundprinzipien zur Vermessung mit GPS. Vermessungsingenieur 47(2):53–64

Seeber G (2003) Satellite Geodesy: Foundations, Methods, and Applications, Berlin: Walter de Gruyter, xx+589

Seeger H, Franke P, Schlueter H, Weber G (1997) The significance and results of permanent GPS arrays. In: Proceedings Fourteenth United Nations Regional Cartografic Conference for Asia and the Pacific, Bangkok, 3–7 February 1997. 10 p

Seitz K, Urakawa MJ, Heck B, Krueger C (2005) Zu jeder Zeit an jedem Ort – Studie zur Verfügbarkeit und Genauigkeit von GPS-Echtzeitmessungen im SAPOS-Service HEPS. Z Geod Geoinf Landmanag 130(1):47–55

Shank C (1998) GPS navigation message enhancements. GPS World 7(4):38–44

Shen YZ, Chen Y, Zheng DH (2006) A Quaternion-based geodetic datum transformation algorithm. J Geodesy 80:233–239

Sien-Chong Wu, William GM (1993) An optimal GPS data processing technique for precise positioning. IEEE Transactions on Geoscience and Remote Sensing 31:146–152

Sigl R (1978) Geodätische Astronomie. Wichmann Verlag, Karlsruhe

Sigl R (1989) Einführung in die Potentialtheorie. Wichmann Verlag, Karlsruhe

Sjoeberg LE (1998) On the estimation of GPS phase ambiguities by triple frequency phase and code data. ZfV 1235:162–163

Sjoeberg LE (1999) Unbiased vs biased estimation of GPS phase ambiguities from dual-frequency code and phase observables. J Geodesy 73:118–124

Skaloud J, Schwarz KP (2000) Accurate orientation for airborne mapping systems. Photogramm Eng Rem S 66(4):393–401

Smith AJE, Hesper ET, Kuijper DC, Mets GJ, Visser PN, Ambrosius BAC, Wakker KF (1996) TOPEX/Poseidon orbit error assessment. J Geodesy 70:546–553

Snow KB, Schaffrin B (2003) Three-dimensional outlier detection for GPS networks and their densification via the BLIMPBE approach. GPS Solutions 7(2):130–139

Spilker JJ (1996) GPS navigation data. In: Parkinson BW, Spilker JJ (eds) Global Positioning System: Theory and applications, Vol. I, Chapter 4

Springer TA, Beutler G, Rothacher M (1999) Improving the orbit estimates of GPS satellites. J Geodesy 73:147–157

Stoew B, Elgered G (2004) Characterization of atmospheric parameters using a ground based GPS network in north Europe. J Meteor Soc Japan 82(1B):587–596

Stowers D, Moore A, Iijima B, Lindqwister U, Lockhart T, Marcin M, Khachikyan R (1996) JPL-supported permanent tracking stations. International GPS Service for Geodynamics: 1996 annual report, Nov. 1997, Pasadena, pp 409–420

Strang G, Borre K (1997) Linear algebra, geodesy, and GPS. Wellesley-Cambridge Press

Sun HP, Ducarme B, Dehant V (1995) Effect of the atmospheric pressure on surface displacements. J Geodesy 70:131–139

Syndergaard S (1999) Retrieval analysis and methodologies in atmospheric limb sounding using the GNSS radio occultation technique. Dissertation, Niels Bohr Institute for Astronomy, Physics and Geophysics, Faculty of Science, University of Copenhagen

(c) ketabton.com: The Digital Library

Tapley BD, Schutz BE, Eanes RJ, Ries JC, Watkins MM (1993) Lageos laser ranging contributions to geodynamics, geodesy, and orbital dynamics. In: Contributions of Space Geodesy to Geodynamics: Earth Dynamics, Geodyn. Ser. 24:147–174
Tetreault P, Kouba J, Heroux P, LegreeP (2005) CSRS-PPP: An Internet service for GPS user access to the Canadian Spatial reference Frame. Geomatica 59(1):17–28
Teunissen PJG (1995) The least-squares ambiguity decorrelation adjustment: A method for fast GPS integer ambiguity estimation. J Geodesy 70(1–2):65–82
Teunissen PJG (1996) An analytical study of ambiguity decorrelation using dual frequency code and carrier phase. J Geodesy 70(8):515–528
Teunissen PJG (1996) GPS carrier phase ambiguity fixing concepts. In: Kleusberg A, Teunissen PJG (eds) GPS for geodesy. Springer-Verlag, Berlin
Teunissen PJG (1997) Closed form expressions for the volume of the GPS ambiguity search spaces. Artificial Satellites, Journal of Planetary Geodesy 32(1):5–20
Teunissen PJG (1998) Minimal detectable biases of GPS data. J Geodesy 72:630–639
Teunissen PJG (2003) Towards a unified theory of GPS ambiguity resolution. J GPS 2(1):1–12
Teunissen PJG (2004) Penalized GNSS Ambiguity resolution. J Geod 78(4–5):235–244
Teunissen PJG (2005) GNSS ambiguity resolution with optimally controlled failure-rate. Artificial Satellites 40(4):219–227
Teunissen PJG, Kleusberg A (1996) GPS observation equations and positioning concepts. In: Kleusberg A, Teunissen PJG (eds) GPS for geodesy. Springer-Verlag, Berlin
Teunissen P, Jonge P, Tiberius C (1997) Performance of the LAMBDA method for fast GPS ambiguity resolution. J Inst Navig 44(3):373–383
Theakstone WH, Jacobsen FM, Knudsen NT (2000) Changes of snow cover thickness measured by conventional mass balance methods and by global positioning system surveying. Geografiska Annaler 81(A4):767–776
Tiberius C (2003) Standard Positioning Service: Handheld GPS receiver accuracy. GPS World 14(2):46–51
Tiberius CCJM, Kenselaar F (2000) Estimation of the stochastic model for GPS code and phase observables. Survey rev 35(277):441–454
Timmen L, Ye X (1997) SAR-Interferometrie unterstützt durch GPS zur Überwachung von Erdoberflächendeformationen. GPS-Anwendungen und Ergebnisse '96: Beiträge zum 41. DVW-Fortbildungsseminar vom 7. bis 8. November 1996 am GeoForschungszentrum Potsdam, pp 104–114
Timmen L, Bastos L, Boebel T, Cunha S, Forsberg R, Gidskehaug A, Hehl K, Meyer U, Nesemann M, Olesen AV, Rubek F, Xu G (1998) The European Airborne Geoid Mapping System for Coastal Oceanography (AGMASCO). Progress in Geodetic Science at GW 98. In: Proceedings of the Geodetic Week 1998. University of Kaiserslautern, Germany, Shaker press, Aachen
Torge W (1989) Gravimetrie. Walter de Gruyter, Berlin
Torge W (1991) Geodesy. Walter de Gruyter, Berlin
Tregoning P, van Dam T (2005) Atmospheric pressure loading corrections applied to GPS data at the observing level. Geophys Res Lett 32(L22310):1–4
Tsai C, Kurz L (1983) An adaptive robustifing approach to Kalman filtering. Automatica 19:279–288
Tscherning C, Rubek F, Forsberg R (1997) Combining airborne and ground gravity using collocation, Scientific Assembly of the International Association of Geodesy in conjunction with 28th Brazilian Congress of Cartography; Rio de Janeiro, 3–9 September 1997, 6 pp
Tsujii T, Harigae M, Inagaki T, Kanai T (2000) Flight tests of GPS/GLONASS precise positioning versus dual frequency KGPS profile. Earth Planets Space 52(10):825–829
Urschl C, Dach R, Hugentobler U, Schaer S, Beutler G (2005) Validating ocean tide loading models using GPS. J Geod 78(10):616–625
van Dam T, Francis O (eds) (2004) The state of GPS vertical positioning precision: Separation of Earth processes by space geodesy. Centre Europeen de Geodynamique et de Seismologie, Luxembourg, Cahiers 23, xxii+176 p
van Sickle J (2003) GPS for Land Surveyors, 2nd ed. Chelsea, MI, Sleeping Bear Press, xii+284 p
Verhagen S (2004) Integer ambiguity validation: An open problem? GPS Solutions 8(1):36–43
Visser PNAM, IJssel J van den (2000) GPS-based precise orbit determination of the very low Earth-orbiting gravity mission GOCE. J Geodesy 74(7/8):590–602
Vittorini LD, Robinson B (2003) Receiver frequency standards. Optimizing indoor GPS performance. GPS World 14(11):40–42, 44, 46–48
Wagner JF (2005) GNSS/INS integration: still an attractive candidate for automatic landing systems? GPS Solutions9(3):179–193
Wagner J, Bauer M (1997) GPS-Vermessung mit Echtzeitauswertung (RTK-Vermessung): ein Beitrag zur Einschätzung der Praxistauglichkeit und Praxisrelevanz. Vermessungsingenieur 48(2): 87–92

(c) ketabton.com: The Digital Library

Wagner C, Klokocnik J (2003) The value of ocean reflections of GPS signals to enhance satellite altimetry: data distribution and error analysis. J Geod 77(3–4):128–138
Wang JG (1997) Filtermethoden zur fehlertoleranten kinematischen Positionsbestimmung. Neubiberg, 135 S
Wang J (2000) An approach to GLONASS ambiguity resolution. J Geodesy 74(5):421–430
Wang LX, Fang ZD, Zhang MY, Lin GB, Gu LK, Zhong TD, Yang XA, She DP, Luo ZH, Xiao BQ, Chai H, Lin DX (1979) Mathematic handbook. Educational Press, Peking, ISBN 13012-0165
Wang G, Chen Z, Chen W, Xu G (1988) The principle of GPS precise positioning system. Surveying Press, Peking, ISBN 7-5030-0141-0/P.58, 345 p, (in Chinese)
Wang G, Wang H, Xu G (1995) The principle of the satellite altimetry. Science Press, Peking, ISBN 7-03-004499-1/P.797, 390 p, (in Chinese)
Wang J, Steward MP, Tsakiri M (1999) Adaptive Kalman filtering for integration of GPS with GLONASS and INS. Presentation in the XXIIth IUGG, Birmingham, England
Wang J, Stewart MP, Tsakiri M (2000) A comparative study of the integer ambiguity validation procedures. Earth Planets Space 52(10):813–817
Wang CM, Hajj G, Pi XQ, Rosen IG, Wilson B (2004) Development of the Global Assimilative Ionospheric Model. Radio Sci 39(1) RS1S06:1–11
Wanninger L (1995) Enhancing differential GPS using regional ionospheric models. B Geod 69:283–291
Wanninger L (1995) Einfluß ionosphärischer Störungen auf präzise GPS-Messungen in Mitteleuropa. Schriftenreihe des Deutschen Vereins für Vermessungswesen, Bd. 18, Stuttgart, pp 218–232
Wanninger L (1999) Der Einfluss ionosphärischer Störungen auf die präzise GPS-Positionierung mit Hilfe virtueller Referenzstationen. ZfV 10:322–330
Wanninger L (2003a) Permanent GPS-Stationen als Referenz für präzise kinematische Positionierung. Photogramm Fernerkund Geoinf 7(4):343–348
Wanninger L (2003b) Virtuelle GPS-Referenzstationen fuer großraeumige kinematische Anwendungen. Z f Vermessungswessen 128(3):196–202
Ware RH, Fulker DW, Stein SA, Anderson DN, Avery SK, Clark RD, Droegemeier KK, Kuettner JP, Minster J, Sorooshian S (2000) Real-time national GPS networks: Opportunities for atmospheric sensing. Earth Planets Space 52(11):901–905
Warnant R, Pottiaux E (2000) The increase of the ionospheric activity as measured by GPS. Earth Planets Space 52(11):1055–1060
Weber G (1994) Initial operational capability für das GPS: aktuelle Entwicklungen der US Satellitennavigation. SATNAV 94: Satellitennavigationssysteme – Grundlagen und Anwendungen, DGON-Seminar, Hamburg 24.–26. Oktober 1994, pp 1–14
Weber R (1996) Monitoring Earth orientation variations at the Center for Orbit Determination in Europe (CODE). Oesterr Z Vermess Geoinf 84(3):269–275
Wells D, Lindlohr W, Schaffrin B, Grafarend E (1987) GPS Design: Undifferenced Carrier Beat Phase Observations and the Fundamental Differencing Theorem, University of New Brunswick
Wenzel H-G (1985) Hochauflösende Kugelfunktionsmodelle für das Gravitationspotential der Erde. Wissenschaftliche Arbeiten der TU Hannover, Nr. 137
Wickert J, Schmidt T, Beyerle G, Konig R, Reigber C (2004) The radio occultation experiment aboard CHAMP: Operational data analysis and validation of vertical atmospheric profiles. J Meteor Soc Japan 82(1B):381–395
Wicki F (1998) Robuste Schätzverfahren für die Parameterschätzung in geodätischen Netzen. Technische Hochschule Zürich
Wieser A, Brunner FK (2000) An extended weight model for GPS phase observations. Earth Planets Space 52(10):777–782
Williams SDP (2003) Offsets in Global Positioning System time series. J Geophys Res 108(B6):ETG12/1-13
Witte TH, Wilson AM (2004) Accuracy of non-differential GPS for the determination of speed over ground. J Biomechanics 37(12):1891–1898
Won J-H,Lee J-S (2005) A note on the group delay and phase advance phenomenon associated with GPS signal propagation through theionosphere.Navigation 52(2):95–97
Wu J, Lin SG (1995) Height accuracy of one and a half centimetres by GPS rapid static surveying. Int J Remote Sens 16(15):2863–2874
Wu CC, Kuo HC, Hsu HH, Jou BJD (2000) Weather and climate research in Taiwan: Potential application of GPS/MET data. Terr Atmos Ocean Sci 11(1):211–234
Wuebbena G (1991) Zur Modellierung von GPS-Beobachtungen für die hochgenaue Positionsbestimmung. Unversität Hannover
Wuebbena G, Seeber G (1995) Developments in real-time precise DGPS applications: concepts and status. In: GPS Trends in Precise Terrestrial, Airborne, and Spaceborne Applications: 21st IUGG General Assembly, IAG Symposium No. 115, Boulder, USA, July 3–4, 1995. Springer-Verlag, Berlin, pp 212–216

(c) ketabton.com: The Digital Library

Xia Y, Michel GW, Reigber C, Klotz J, Kaufmann H (2003) Seismic unloading and loading in northern central Chile as observed by differential Synthetic Aperture Radar Interferometry (D-INSAR) and GPS. Int J Remote Sensing 24(22):4375–4391
Xu G (1984) Very long baseline interferometry and tidal theories. The Institute of Geodesy and Geophysics, Chinese Academy of Sciences, M.Sc. Thesis No. 84011, (in Chinese)
Xu G (1992) Spectral analysis and geopotential determination (Spektralanalyse und Erdschwerefeldbestimmung). Dissertation, DGK, Reihe C, Heft Nr. 397, Press of the Bavarian Academy of Sciences, ISBN 3–7696–9442–2, 100 p, (with very detailed summary in German)
Xu QF (1994) GPS navigation and precise positioning. Army Press, Peking, ISBN 7-5065-0855-9/P.4, (in Chinese)
Xu P (1995) Estimating the state vector in observable and singular hybrid INS/GPS systems without the knowledge of initial conditions. Bull Geod Sci Affini 54(4):389–406
Xu G (2000) A concept of precise kinematic positioning and flight-state monitoring from the AGMASCO practice. Earth Planets Space 52(10):831–836
Xu G (2002a) A general criterion of integer ambiguity search. J GPS 1(2):122–131
Xu G (2002b) GPS data processing with equivalent observation equations. GPS Solutions 6(1–2):6:28–33
Xu G (2003a) A diagonalization algorithm and its application in ambiguity search. J GPS 2(1):35–41
Xu G (2003b) GPS – Theory, Algorithms and Applications. Springer Verlag, Berlin Heidelberg, xix+315 p
Xu G (2004) MFGsoft – Multi-Functional GPS/(Galileo) Software – Software User Manual, (Version of 2004), Scientific Technical Report STR04/17 of GeoForschungsZentrum (GFZ) Potsdam, ISSN 1610-0956, 70 pages, www.gfz-potsdam.de/bib/pub/str0417/0417.pdf
Xu G, Knudsen P (2000) Earth tide effects on kinematic/static GPS positioning in Denmark and Greenland. Phys Chem Earth 25(A4):409–414
Xu G, Qian Z (1986) The application of block elimination adjustment method for processing of the VLBI Data. Crustal Deformation and Earthquake, Vol. 6, No. 4, (in Chinese)
Xu G, Timmen L (1997) Airborne gravimetry results of the AGMASCO test campaign in Braunschweig. Geodetic Week Berlin '97, Oct. 6–11, 1997, electronic version published in *http://www.geodesy.tu-berlin.de*
Xu G, Hehl K, Angermann D (1994) GPS software development for use in aerogravimetry: Strategy, realisation, and first results. In: Proceedings of ION GPS-94, pp 1637–1642
Xu G, Bastos L, Timmen L (1997a) GPS kinematic positioning in AGMASCO campaigns – Strategic goals and numerical results. In: Proceedings of ION GPS-97 meeting in Kansas City, September 16–19, 1997, pp 1173–1184
Xu G, Fritsch J, Hehl K (1997b) Results and conclusions of the carborne gravimetry campaign in northern Germany. Geodetic Week Berlin '97, Oct. 6–11, 1997, electronic version published in *http://www.geodesy.tu-berlin.de*
Xu G, Schwintzer P, Reigber Ch (1998) KSGSoft – Kinematic/Static GPS Software – Software user manual (version of 1998). Scientific Technical Report STR98/19 of GeoForschungsZentrum (GFZ) Potsdam
Xu CJ, Liu JN, Song CH, Jiang WP, Shi C (2000) GPS measurements of present-day uplift in the Southern Tibet. Earth Planets Space 52(10):735–739
Xu P, Ando M, Tadokoro K (2005) Precise, three-dimensional seafloor geodetic deformation measurements using differential techniques. Earth, Planetsand Space 57(9):795–808
Xu G, Guo J, Yeh TK (2006a) Equivalence of the uncombined and combining GPS algorithms. (In review)
Xu G, Sun H, Shen YZ (2006b) On the parameterisation of the GPS observation models (In review)
Xu G, Yang YX, Zhang Q (2006c) Equivalence of the GPS data processing algorithms (In review)
Yang Y (1991) Robust Bayesian estimation. B Geod 65:145–150
Yang Y (1993) Robust estimation and its applications. Bayi Publishing House, Peking
Yang Y (1994) Robust estimation for dependent observations. Manuscr Geodaet 19:10–17
Yang Y (1997a) Estimators of covariance matrix at robust estimation based on influence functions. ZfV 122(4):166–174
Yang Y (1997b) Robust Kalman filter for dynamic systems. Journal of Zhengzhou Institute of Surveying and Mapping 14:79–84
Yang Y (1999) Robust estimation of geodetic datum transformation. J Geodesy 73:268–274
Yang M (2005) Noniterative method of solving the GPS doubled-differenced pseudorange equations. J Surv Eng ASCE 131(4):130–134
Yang Y, Cui X (2006) Adaptively Robust Filter with Multi Adaptive Factors. J Surv Eng
Yang Y, Gao W (2005) Comparison of Adaptive Factors on Navigation Results. The J Navigation 58: 471–478
Yang Y, Gao W (2006) Optimal Adaptive Kalman Filter with Applications in Navigation. J Geodesy
Yang M, Tang CH, Yu TT (2000) Development and assessment of a medium-range real-time kinematic GPS algorithm using an ionospheric information filter. Earth Planets Space 52(10):783–788

(c) ketabton.com: The Digital Library

Yang Y, He H, Xu G (2001) Adaptively robust filtering for kinematic geodetic positioning. J Geodesy 75:109–116
Yang YX, Xu TH, Song LJ (2005a) Robust estimation of variance components with application in global positioning system network adjustment. J Surv Eng ASCE 131(4):107–112
Yang YX, et al. (2005b) Combined adjustment project of national astronomical geodetic networks and 2000' national GPS control network. Progress Natural Sci 15(5):435–441
Yang Y, Tang Y, Li Q, Zou Y (2006) Experiments of adaptive filters for kinemetic GPS positioning applied in road information updating in GIS. J Surv Eng (in press)
Yeh TK, Chen CS (2006) Clarifying the relationship between the clock errors and positioning precision of GPS receiver, VI Hotline-Marussi Symposium of Theoretical and Computational Geodesy Wuhan
Yeh TK, Chen CS, Lee CW (2004) Sensing of precipitable water vapor in atmosphere using GPS technology. Boll Geod Sci Affini 63(4):251–258
Yoon JC, Lee BS, Choi KH (2000) Spacecraft orbit determination using GPS navigation solutions. Aerosp Sci Technol 4(3):215–221
Yuan YB, Ou JK (1999) The effects of instrumental bias in GPS observations on determining ionospheric delays and the methods of its calibration. Acta Geod Cartogr Sinica 28(2)
Yuan YB, Ou JK (2003) Preliminary results and analyses of using IGS GPS data to determine global ionospheric TEC. Progress Natural Sci 13(6):446–450
Yuan YB, Ou JK (2004) Ionospheric eclipse factor method (IEFM) for determining the ionospheric delay using GPS data. Progress Natural Sci 14(9):800–804
Yunck TP, Melbourne WG (1995) Spaceborne GPS for earth science. In: GPS Trends in Precise Terrestrial, Airborne, and Spaceborne Applications: 21st IUGG General Assembly, IAG Symposium No. 115, Boulder, USA, July 3–4, 1995. Springer-Verlag, Berlin, pp 113–122
Zhang Q, Qiu H (2004) A dynamic path search algorithm for tractor automatic navigation. Trans ASAE 47(2):639–646
Zhang Q, Moore P, Hanley J, Martin S (2006) Auto-BAHN: Software for Near Real-time GPS Orbit and Clock Computation
Zhao CM, Ou JK, Yuan YB (2005) Positioning accuracy and reliability of GALILEO, integrated GPS-GALILEO system based on single positioning model. Chinese Sci Bull 50(12):1252–1260
Zhao CM, Yuan YB, Ou JK, Chen JP (2005) Variation properties of ionospheric eclipse factor and ionospheric influence factor. Progress Natural Sci 15(6):573–576
Zheng DW, Zhong P, Ding XL, Chen W (2005) Filtering GPS time-series using a Vondrak filter and cross-validation. J Geod 79(6–7):363–369
Zhou J (1985) On the Jie factor. Acta Geodaetica et Geophysica 5 (in Chinese)
Zhou J (1989) Classical theory of errors and robust estimation. Acta Geod Cartogr Sinica 18:115–120
Zhou J, Huang Y, Yang Y, Ou J (1997) Robust least squares method. Publishing House of Huazhong University of Science and Technology, Wuhan
Zhu J (1996) Robustness and the robust estimate. J Geodesy 70(9):586–590
Zhu SY (1997) GPS-Bahnfehler und ihre Auswirkung auf die Positionierung. GPS-Anwendungen und Ergebnisse '96: Beiträge zum 41. DVW-Fortbildungsseminar vom 7. bis 8. November 1996 am GeoForschungszentrum Potsdam, pp 219–226
Zhu SY (2001) Private communication and the source code of the EPOS-OC software
Zhu SY, Reigber Ch, Massmann FH (1996) The German PAF for ERS, ERS standards used at D-PAF. D-PAF/GFZ ERS-D-STD-31101
Zhu WY, Fu Y, Li Y (2003) Global elevation vibration and seasonal changes derived by the analysis of GPS height. Science in China D 46(8):765–778
Zhu S, Reigber C, Koenig (2004) Integrated adjustment of CHAMP, GRACE, and GPS data. J Geod 78(1–2): 103–108
Ziebart M, Cross P (2003) LEO GPS attitude determination algorithm for a micro-satellite using boom-arm deployed antennas. GPS Solutions 6(4):242–256
Zumberge JF, Heflin MB, Jefferson DC, Watkins MM, Webb FH (1997) Precise point positioning for the efficient and robust analysis of GPS data from large networks. J Geophys Res 102(B3):5005–5017

(c) ketabton.com: The Digital Library

Subject Index

A

a priori
  –, constraint 131, 160–161, 165
  –, datum 122–123, 131, 133, 160–161, 165, 212, 215
  –, information 159–160, 165, 189, 307
Adams algorithms 291, 295
adaptively robust Kalman filter 133, 155, 165
airborne 70, 72, 79, 219, 226, 230, 232, 237, 240
aircraft 164–165, 226, 232–235, 237, 241
altimetry 79–80, 232, 237
ambiguity
  –, fixing 122, 141, 169, 173, 178–182, 233
  –, function 88, 167, 169, 182–183, 185
  –, -ionospheric equation 100, 204, 207, 210
  –, resolution 167, 169–170, 182
  –, search 164, 167, 169–179, 181, 223, 233, 241
    –, criterion 176, 178–179, 233
antenna phase centre 82, 85
anti-spoofing AS 43, 82, 169
apogee 26
apparent sidereal time 13–14, 16
argument
  –, of latitude 3, 31–32
  –, of perigee 26–27, 32, 270
AS anti-spoofing 43, 82, 169
ascending node 2–4, 15–16, 23, 26–27, 31–33, 267, 270, 272
atmospheric
  –, drag 32, 88, 219, 264–265, 267, 295, 305
  –, pressure 56, 59
attraction 256
azimuth 12–13, 49–50, 53, 61–62, 74, 92–93, 234

B

Barycentre 18
Barycentric Dynamic Time TDB 18
block-wise least squares adjustment 133, 141, 143, 146, 164, 199, 208
broadcast
  –, ephemerides 2, 32, 35
  –, ionospheric model 48–50

C

carrier phase 5, 37, 39–40, 42, 46, 78, 82, 87, 112, 167, 207, 209
Cartesian coordinates 81, 246–247, 253, 298
Celestial Reference Frame CRF 13
central force 21, 23, 31–32, 245, 252, 256, 264, 269
CIO Conventional International Origin 7, 13, 17
clock
  –, bias 77, 86, 203
  –, drift 213–214
  –, frequency 65, 214–215
  –, offset 35, 66
  –, parameter 92, 189, 202, 212
code
  –, delay 43
  –, -phase combination 87, 133, 145, 164
  –, pseudorange 37, 87, 95, 112, 204, 209
  –, smoothing 104
cofactor matrix 134, 199
combining algorithms 111–112, 114, 122, 188, 198–199, 201
conditional least squares adjustment 133, 138, 140, 159, 164, 170–171
constrained adjustment 133, 159
Conventional International Origin CIO 7, 13, 17
coordinate transformation 17, 88, 106, 204, 234, 274
covariance propagation 87, 94–95, 123, 187, 202, 222
Cowell algorithms 293, 295–296
cycle slip detection 104, 167–168, 204, 222

D

data
  –, combination 1, 87, 95, 97, 209
  –, condition 194, 198, 200–202
  –, differentiation 87, 104
diagonalisation 149, 164, 222
differencing algorithms 87, 111, 122, 187, 198–199, 201, 222
differential
  –, Doppler 102–103, 214–216, 222
  –, equation 25, 73, 245, 284–285, 295
  –, GPS 72, 131, 131, 209–211, 229–230, 232
  –, phases 104, 168

(c) ketabton.com: The Digital Library

–, positioning 212, 229
disturbed satellite motion 31
disturbing
–, force 32, 257, 259, 293, 295–297, 301
–, potential 253, 267–268
Doppler
–, data 77, 168, 212–214, 222
–, effect 41
–, frequency shift 41–42
–, integration 87, 102–104, 168
double difference 107, 109–111, 123, 130, 129–130, 201, 212, 231, 308
dynamic time 17–18

E

Earth
–, rotation 10, 14, 16, 38–39, 205, 213, 268
–, tide displacement 67–68, 70
eccentric anomaly 28–29, 66, 270
eccentricity 26–27, 31–32, 53, 66, 265, 270–273
ecliptic 13, 15, 17, 270, 272
electronic density 44–45, 121
elevation 49–50, 55, 80, 234
ellipsoidal mapping function 54
emission time 37–40, 77, 79, 82, 87, 91, 204, 212
ephemerides 2–3, 19–20, 32, 34–35, 69–71, 82, 220, 245, 269, 271, 273
equatorial
–, plane 7, 17, 23, 26
–, system 14, 273
equivalence theorem 1, 198–199, 203
equivalent
–, criterion 169–170, 177–178, 180–181
–, observation equation 122–125, 133, 148–149, 164, 177, 188

F

fictitious observations 159
flight state monitoring 226, 234
float solution 171–172, 174–178, 181, 232
frequency
–, drift 214
–, effect 64
–, offset 35
fundamental frequency 64–65, 113

G

gain matrix 151–152
Galileo 1–2, 4–5, 11, 20, 219
general
–, criterion 164, 169–170, 175–178, 181, 233
–, relativity 62, 64–67, 245, 269
geocentric latitude 8, 53, 265
geometric
–, co-mapping function 60
–, mapping function 52, 54, 60
geometry-free combination 98–101, 115–117
GLONASS 1, 3–5, 10–11, 19–20, 35
GNSS 1, 3–5
GPS
–, altimetry 80
–, observation equation 87, 112, 120, 131, 168, 171, 176–177, 187–188, 198–199, 210–211, 222, 280, 282–284, 308
–, time GPST 18, 35, 50–51, 69–70, 76, 308
–, week 19
Greenwich
–, Apparent Sidereal Time GAST 13–14, 16
–, Mean Sidereal Time GMST 16
–, hour angle 17
–, meridian 7, 13, 17
–, sidereal 33
gravitational
–, constant 21–23, 33, 65–68, 73, 246, 249, 252, 256, 258, 273, 300
–, field 12, 18, 64, 88, 251–253, 255
–, force 251
–, potential 64–65, 269
group delay 50

H

HDOP Horizontal Dilution of Precision 218
Helmert transformation 11, 223
Hopfield model 58–59
hour angle 17, 257

I

IERS International Earth Rotation Service 10
IGS 3, 34–35, 38
initial
–, state 246, 283–284
–, value problem 284–286, 290–293, 295
International Terrestrial Reference Frame ITRF 10
instrumental bias 85–86, 169, 207, 307–308
integer ambiguity 79, 167, 169, 171–176, 178, 181, 233
International
–, Atomic Time TAI 18
–, Earth Rotation Service IERS 10
interpolation 34, 223, 245, 286, 291, 296
ionosphere-free combination 46–47, 97–98, 113–115, 204, 206, 208, 210, 232
ionospheric
–, effect 38, 40, 43, 45–51, 55, 79, 82, 85, 87, 97, 102, 183, 206–207, 209–210, 219, 232, 241
–, model 2, 48–50, 52–53, 55, 82–83, 99, 204, 206, 219
–, residual 87, 101–102, 167–168

J

JD Julian Date 13, 18–19, 24, 214–215

K

Kalman filter 103, 133, 150–156, 158, 165, 215–216, 223

(c) ketabton.com: The Digital Library

Keplerian
–, elements 30–32, 222, 247, 250, 268, 272, 274, 278–282
–, ellipse 246
–, equation 27, 29, 34
–, motion 21, 31–32, 269

L

Lagrange
–, polynomial 34
–, interpolation 34, 296
least squares
–, adjustment 133, 135, 137–138, 140–141, 143, 146, 148, 151, 153, 159, 163–165, 170–171, 199, 208, 223
–, ambiguity search criterion 233
LSAS criterion 180–181
linear
–, combination 46, 96–97
–, correlation 308
–, transformation 94–95, 99, 105, 107, 109, 122–123, 131, 187, 189, 192, 308
loading tide 38, 40, 43, 67, 72–76, 88, 94, 204, 219, 223, 230, 239–240, 245, 301
local coordinate system 11–12, 217, 219
loss of lock 104, 168–169

M

mapping function 45, 50–52, 54–61, 93, 99, 119–120, 220
mean anomaly 15, 28–29, 32, 34, 270
minimum spanning tree 200, 223
MJD modified Julian Date 19
multipath 38, 40, 42–43, 78–80, 88, 205
multiple static references 230, 233, 236–237

N

navigation message 32, 35, 38, 66, 82, 205, 213
numerical
–, differentiation 102–103, 285
–, eccentricity 32, 53
–, integration 168, 245, 283, 286
nutation 13–17, 269, 271

O

observational model 89
ocean
–, loading tide displacement 72, 75, 223
–, tide 32, 72–75, 230, 245, 257–259
optimal baseline 106, 200–201, 223
orbit
–, correction 32, 220, 224, 245, 279–280
–, determination 1–2, 32, 37, 83, 88, 151, 204, 210, 219–220, 224, 245, 263–264, 283–284, 295
orbital
–, coordinate system 30
–, plane 2–4, 23–24, 26–29, 32–33, 248, 281–282

P

P-code 78
parameterisation 1, 59, 61, 76, 121, 125, 167, 187, 189–191, 194–195, 197–204, 222, 283, 307–308
path
–, delay 52–53, 55–56, 58–61, 99
–, range effect 65
PDOP Position Dilution of Precision 217
perigee 26–27, 29–30, 32, 247, 267, 270
perturbation force 251, 253, 255, 269, 300, 304
perturbed
–, equation of satellite motion 245–246, 248
–, orbit 2, 245, 273, 276, 279–280, 283
phase
–, advance 43, 50
–, centre 43, 82, 85
–, combination 87, 99, 102, 133, 145, 164
–, difference 79
–, model 40, 77, 207
point positioning 3, 77, 80–81, 203–209, 212, 223–224
polar motion 8, 14, 16–18, 223, 269
pre-processing 203, 222–223
precession 13–14, 17, 269
precise ephemerides 3, 34–35
projection mapping function 52, 59
pseudorange 3, 37–40, 51, 78–79, 87, 95, 112, 204–205, 207, 209–210

Q

quasi-stable datum 133, 161–162, 165

R

radial velocity 41
range rate 42, 280–281, 283
receiver Independent Exchange Format RINEX 203
reference
–, frequency 4, 308
–, satellite 131, 165, 190–192, 194, 197, 212, 308
refractive index 44, 55
relative positioning 70, 204, 212, 224, 233
relativistic effect 13, 38, 40, 43, 62, 64–66, 77, 88, 204, 213, 219
right ascension 23, 27, 31–32, 265, 270, 274
robust Kalman filter 133, 152–153, 155, 165, 223
rotational matrix 11
Runge-Kutta algorithms 286, 295–296

S

SA selective availability 43, 77, 82
Saastamoinen model 56, 59
Sagnac effect 66
satellite
–, antenna 82, 85

(c) ketabton.com: The Digital Library

–, orbit 1, 21, 24, 26, 32, 35, 37, 66, 80, 88, 223, 246
selective availability SA 43, 77, 82
sequential least squares adjustment 133, 137, 151, 165
shadow 85, 260–263, 269
sidereal time 13–14, 16–18, 33, 274
single
–, difference 105–107, 125–126, 129–130, 129, 190, 192, 212, 231
–, point positioning 3, 77, 203–209, 212, 223–224
solar radiation 32, 83, 88, 204, 219, 245, 248, 251, 260, 263–264, 269, 304
special relativity 62–64
spherical
–, coordinate 8, 185, 246, 252, 254–255, 257–258
–, harmonics 252
standard deviation 76, 95–98, 112, 121, 139, 153, 163, 171, 174–176, 183, 217, 232, 237
static reference 70, 206, 214, 226, 229–233, 235–237, 240–241

T

Terrestrial
–, Dynamic Time TDT 18, 69
–, Time TT 18
tidal
–, deformation 69, 257
–, effect 70, 94, 104, 230
–, potential 67–69, 220, 257–258
time system 1, 4–5, 7, 14, 17–18, 20, 35, 223, 308
transition matrix 150–151, 284
transmitting time 2, 34, 37–39, 62, 65–66, 76, 81, 88
triple difference 87, 110–111, 122–123, 130–131, 190, 211
tropospheric
–, delay 55–56, 58–59, 61, 92
–, effect 1, 38, 40, 43, 55, 59, 61, 88, 92, 105, 107, 111, 219
–, model 56, 58, 61, 76, 92, 204, 219–220, 226, 232, 241
true anomaly 29, 247, 267, 270

U

uncombined algorithm 115–118, 199
undifferenced algorithm 189, 194, 197–198
unified equivalent algorithm 131
Universal Time UT 16–18
–, Coordinated UTC 5, 18–20, 35
UT Universal Time 16–18

V

velocity determination 212–213, 215, 223–224
vernal equinox 13, 23, 30

W

WGS, World Geodetic System 10

Z

zenith delay 52–53, 99

Get more e-books from www.ketabton.com
Ketabton.com: The Digital Library